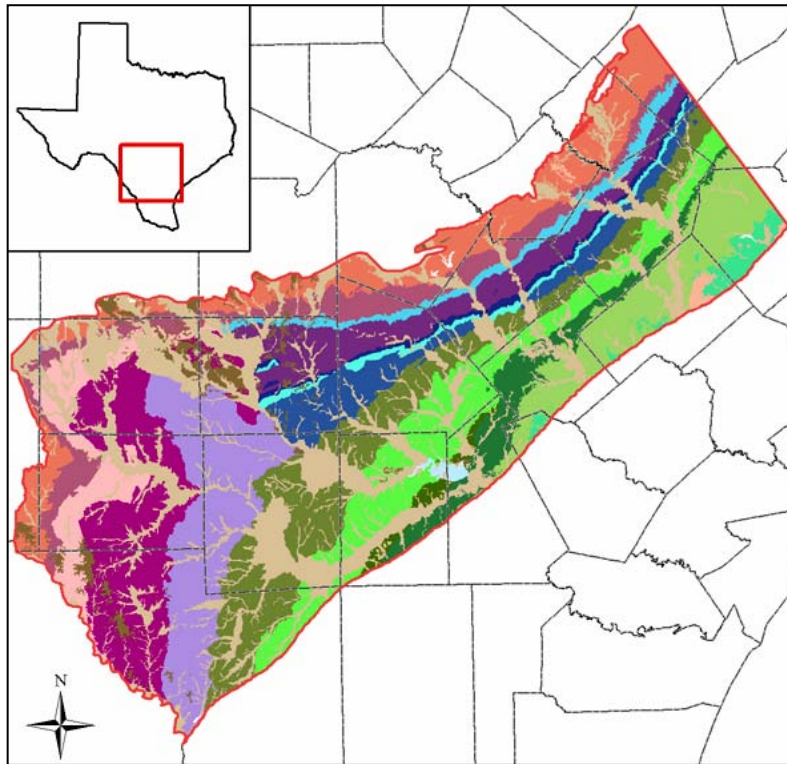


FINAL REPORT

Groundwater Availability Model for the Southern Carrizo-Wilcox Aquifer



Prepared for the:

Texas Water Development Board

Prepared by:

**Neil Deeds, Van Kelley,
Dennis Fryar, Toya Jones**



Art J. Whallon, and Kirk E. Dean

PARSONS

January 31, 2003

TABLE OF CONTENTS

ABSTRACT	xi
1.0 INTRODUCTION.....	1-1
2.0 STUDY AREA.....	2-1
2.1 Physiography and Climate.....	2-10
2.2 Geology	2-18
3.0 PREVIOUS INVESTIGATIONS	3-1
4.0 HYDROGEOLOGIC SETTING	4-1
4.1 Hydrostratigraphy	4-1
4.2 Structure	4-5
4.3 Hydraulic Properties.....	4-25
4.3.1 Processing of the Hydraulic Property Database	4-26
4.3.2 Statistical Analysis of the Hydraulic Property Data	4-27
4.3.3 Spatial Distribution of Hydraulic Property Data	4-27
4.3.4 Relationship between Hydraulic Property and Sand Distribution.....	4-30
4.3.5 Vertical Hydraulic Conductivity.....	4-32
4.3.6 Storativity	4-33
4.4 Water Levels and Regional Groundwater Flow	4-46
4.4.1 Predevelopment Conditions for the Carrizo Sand and the Wilcox Group....	4-47
4.4.2 Pressure versus Depth Analysis.....	4-49
4.4.3 Predevelopment Conditions in the Queen City/Bigford Formations.....	4-50
4.4.4 Transient Water Levels	4-50
4.4.5 Water-Level Elevations for Model Calibration and Verification.....	4-52
4.5 Recharge	4-86
4.6 Natural Aquifer Discharge.....	4-91
4.7 Aquifer Discharge Through Pumping	4-100
4.8 Water Quality.....	4-110
5.0 CONCEPTUAL MODEL OF GROUNDWATER FLOW IN THE AQUIFER.....	5-1
6.0 MODEL DESIGN	6-1
6.1 Code and Processor.....	6-1
6.2 Model Layers and Grid.....	6-2
6.3 Boundary Condition Implementation.....	6-5
6.3.1 Lateral Model Boundaries	6-6
6.3.2 Vertical Boundaries	6-6
6.3.3 Surface Water Implementation	6-7
6.3.4 Implementation of Recharge	6-9
6.3.5 Implementation of Pumping Discharge	6-11
6.4 Model Hydraulic Parameters	6-18
6.4.1 Hydraulic Conductivity	6-18
6.4.2 Storativity	6-21

TABLE OF CONTENTS (CONTINUED)

7.0	MODELING APPROACH.....	7-1
7.1	Calibration	7-1
7.2	Calibration Target Uncertainty	7-5
7.3	Sensitivity Analyses	7-6
7.4	Predictions	7-6
8.0	STEADY-STATE MODEL.....	8-1
8.1	Calibration	8-1
8.1.1	Horizontal and Vertical Hydraulic Conductivities	8-1
8.1.2	Recharge.....	8-3
8.1.3	Groundwater Evapotranspiration.....	8-3
8.1.4	General Head Boundaries.....	8-4
8.1.5	Streams	8-5
8.2	Results	8-17
8.2.1	Heads.....	8-17
8.2.2	Streams.....	8-18
8.2.3	Water Budget.....	8-18
8.3	Sensitivity Analysis.....	8-30
9.0	TRANSIENT MODEL.....	9-1
9.1	Calibration	9-1
9.2	Results	9-6
9.2.1	Hydraulic Heads	9-6
9.2.2	Stream-Aquifer Interaction.....	9-9
9.2.3	Water Budget.....	9-10
9.3	Sensitivity Analysis.....	9-31
10.0	MODEL PREDICTIVE SIMULATIONS.....	10-1
10.1	Drought of Record	10-1
10.2	Predictive Simulation Results.....	10-8
10.3	Predictive Simulation Water Budget.....	10-37
11.0	LIMITATIONS OF THE MODEL.....	11-1
11.1	Limitations of Supporting Data	11-1
11.2	Limiting Assumptions	11-3
11.3	Limits for Model Applicability.....	11-5
12.0	FUTURE IMPROVEMENTS.....	12-1
12.1	Supporting Data	12-1
12.2	Future Model Improvements	12-2
13.0	CONCLUSIONS.....	13-1
14.0	ACKNOWLEDGEMENTS	14-1
15.0	REFERENCES.....	15-1

LIST OF FIGURES

Figure 2.1	Location of the three Carrizo-Wilcox GAMs.....	2-4
Figure 2.2	Location of study area showing county boundaries, cities, lakes, and rivers.	2-5
Figure 2.3	Areal extent of the major aquifers in the study area.	2-6
Figure 2.4	Location of Regional Water Planning Groups in the study area.	2-7
Figure 2.5	Location of Groundwater Conservation Districts in the study area.....	2-8
Figure 2.6	Major river basins in the study area.	2-9
Figure 2.7	Topographic map of the study area.....	2-12
Figure 2.8	Ecological regions within the study area.....	2-13
Figure 2.9	Average annual net pan evaporation rate in inches per year.	2-14
Figure 2.10	Location of precipitation gages in the study area (Period of Record is 1900 to 1999).	2-15
Figure 2.11	Average annual precipitation (1961-1990) over the study area in inches per year (Source: Oregon Climate Service, Oregon State University, PRISM data set).	2-16
Figure 2.12	Annual precipitation time series for gages in Bexar, Fayette, Frio, Karnes, and Webb counties.....	2-17
Figure 2.13	Surface geology of the study area.....	2-20
Figure 2.14	Generalized stratigraphic section for the Carrizo-Wilcox aquifer in Texas (after Ayers and Lewis, 1985; Hamlin, 1988; Kaiser et al., 1978).	2-21
Figure 2.15	Structural cross-sections in the study area (after Hamlin, 1988).	2-22
Figure 3.1	Southern Carrizo-Wilcox GAM model boundary with previous modeling study boundaries which have included the Carrizo-Wilcox aquifer.	3-5
Figure 4.1.1	Hydrostratigraphy and model layers.	4-4
Figure 4.2.1	Structural setting of the study area.....	4-10
Figure 4.2.2	Structure contour map of the base of the Wilcox Group.....	4-11
Figure 4.2.3	Structure contour map of the top of the lower Wilcox.....	4-12
Figure 4.2.4	Structure contour map of the top of the middle Wilcox.....	4-13
Figure 4.2.5	Structure contour map of the top of the Wilcox Group.....	4-14
Figure 4.2.6	Structure contour map of the top of the Carrizo.	4-15
Figure 4.2.7	Structure contour map of the top of the Reklaw/Bigford formations.	4-16
Figure 4.2.8	Structure contour map of the top of the Queen City/El Pico.....	4-17
Figure 4.2.9	Thickness map of the lower Wilcox.....	4-18
Figure 4.2.10	Thickness map of the middle Wilcox.....	4-19
Figure 4.2.11	Thickness map of the upper Wilcox.....	4-20
Figure 4.2.12	Thickness map of the Carrizo.	4-21
Figure 4.2.13	Thickness map of the Reklaw/Bigford.....	4-22
Figure 4.2.14	Thickness map of the Queen City/El Pico.....	4-23
Figure 4.2.15	Thickness map of younger sediments overlying the Queen City.	4-24
Figure 4.3.1	Screening of hydraulic conductivity data.	4-35

LIST OF FIGURES (CONTINUED)

Figure 4.3.2	CDF curves of hydraulic conductivity for the modeled aquifer units.....	4-36
Figure 4.3.3	Variogram for hydraulic conductivity data for the lower Wilcox.	4-37
Figure 4.3.4	Variogram and kriged map of hydraulic conductivity for the lower Wilcox.....	4-38
Figure 4.3.5	Variogram and kriged map of hydraulic conductivity for the middle Wilcox.....	4-39
Figure 4.3.6	Variogram and kriged map of hydraulic conductivity for the Carrizo.....	4-40
Figure 4.3.7	Variogram and kriged map of hydraulic conductivity for the Queen- City.	4-41
Figure 4.3.8	Histogram of net-sand thickness for the Carrizo-upper Wilcox and maximum sand thickness of the Carrizo-upper Wilcox and hydraulic conductivity (Log K).	4-42
Figure 4.3.9	Histogram of sand percent for the Carrizo- upper Wilcox and the log of hydraulic conductivity (Log K).....	4-43
Figure 4.3.10	Percent sand for the Carrizo.	4-44
Figure 4.3.11	Percent sand for the upper Wilcox.	4-45
Figure 4.4.1	Water-level measurement locations for the Carrizo-Wilcox aquifer.	4-70
Figure 4.4.2	Predevelopment water-level elevations for the Carrizo-Wilcox aquifer.	4-71
Figure 4.4.3	Difference in predevelopment water-level elevation contours between adjusted and not adjusted water levels.....	4-72
Figure 4.4.4	Water-level measurement locations used for pressure-depth analysis.....	4-73
Figure 4.4.5	Pressure versus depth analysis results.	4-74
Figure 4.4.6	Predevelopment water-level elevation contours for the Queen City/Bigford formations.....	4-75
Figure 4.4.7	Water-level decline in the Carrizo –upper Wilcox from predevelopment to 1980.....	4-76
Figure 4.4.8	Model layer for locations with transient water-level data.	4-77
Figure 4.4.9	Example hydrographs for wells located in Bastrop, Caldwell, Gonzales, Guadalupe, and northern Wilson counties.....	4-78
Figure 4.4.10	Example hydrographs for wells in southern Wilson County and Karnes and Live Oak counties.	4-79
Figure 4.4.11	Example hydrographs for wells in the outcrop areas of Atascosa, Medina, Frio, Zavala, Maverick, and Dimmit counties.....	4-80
Figure 4.4.12	Example hydrographs for wells in the downdip areas of Atascosa, Frio, and Zavala counties.	4-81
Figure 4.4.13	Example hydrographs for wells in McMullen, La Salle, Webb, and the downdip area of Dimmit counties.....	4-82
Figure 4.4.14	Water-level elevation contours for the Carrizo-Wilcox aquifer at the start of model calibration (January 1980).	4-83
Figure 4.4.15	Water-level elevation contours for the Carrizo-Wilcox aquifer at the end model calibration (December 1989).	4-84
Figure 4.4.16	Water-level elevation contours for the Carrizo-Wilcox aquifer at the end model verification (December 1999).	4-85
Figure 4.5.1	Hydrographs for reservoirs in the Carrizo-Wilcox outcrop.....	4-90
Figure 4.6.1	Stream gain/loss studies in the study area (after Slade et al. 2002).....	4-98

LIST OF FIGURES (CONTINUED)

Figure 4.6.2	Documented spring locations in the study area.	4-99
Figure 4.7.1	Rural population density in the study area.	4-106
Figure 4.7.2	Younger (Layer 1) Pumpage, 1990 (AFY).....	4-107
Figure 4.7.3	Reklaw (Layer 2) Pumpage, 1990 (AFY).	4-107
Figure 4.7.4	Carrizo (Layer 3) Pumpage, 1990 (AFY).....	4-108
Figure 4.7.5	Upper Wilcox (Layer 4) Pumpage, 1990 (AFY).	4-108
Figure 4.7.6	Middle Wilcox (Layer 5) Pumpage, 1990 (AFY).....	4-109
Figure 4.7.7	Lower Wilcox (Layer 6) Pumpage, 1990 (AFY).....	4-109
Figure 5.1	Conceptual groundwater flow model for the Southern Carrizo- Wilcox GAM.	5-5
Figure 5.2	Schematic diagram of transient relationships between recharge rates, discharge rates, and withdrawal rates (from Freeze, 1971).	5-6
Figure 6.2.1	Southern Carrizo-Wilcox GAM model grid.	6-4
Figure 6.3.1	Layer 1 (Queen City) boundary conditions and active/inactive cells.	6-12
Figure 6.3.2	Layer 2 (Reklaw) boundary conditions and active/inactive cells.	6-13
Figure 6.3.3	Layer 3 (Carrizo) boundary conditions and active/inactive cells.	6-14
Figure 6.3.4	Layer 4 (upper Wilcox) boundary conditions and active/inactive cells.	6-15
Figure 6.3.5	Layer 5 (middle Wilcox) boundary conditions and active/inactive cells.	6-16
Figure 6.3.6	Layer 6 (lower Wilcox) boundary conditions and active/inactive cells.	6-17
Figure 8.1.1	Calibrated horizontal hydraulic conductivity field for the El Pico/Queen City (Layer 1).	8-7
Figure 8.1.2	Calibrated horizontal hydraulic conductivity field for Bigford/Reklaw (Layer 2).....	8-8
Figure 8.1.3	Calibrated horizontal hydraulic conductivity field for the Carrizo (Layer 3).....	8-9
Figure 8.1.4	Calibrated horizontal hydraulic conductivity field for the upper Wilcox (Layer 4).	8-10
Figure 8.1.5	Calibrated horizontal hydraulic conductivity field for middle Wilcox (Layer 5).....	8-11
Figure 8.1.6	Calibrated horizontal hydraulic conductivity field for the lower Wilcox (Layer 6).	8-12
Figure 8.1.7	Comparison between initial recharge and the calibrated recharge.	8-13
Figure 8.1.8	Steady-state calibrated recharge (in/year).	8-14
Figure 8.1.9	Steady-state groundwater ET maximum (in/year).	8-15
Figure 8.1.10	Steady-state calibrated GHB conductance.	8-16
Figure 8.2.1	Simulated steady-state head surface, residuals and scatterplot for the Queen City/El Pico (Layer 1).....	8-21
Figure 8.2.2	Simulated steady-state head surface and posted residuals for the Reklaw/Bigford (Layer 2).....	8-22
Figure 8.2.3	Simulated steady-state head surface, residuals and scatterplot for the Carrizo (Layer 3).	8-23
Figure 8.2.4	Simulated (a) and observed (b) steady-state head surfaces for the Carrizo (Layer 3).....	8-24

LIST OF FIGURES (CONTINUED)

Figure 8.2.5	Simulated steady-state head surface and posted residuals for the upper Wilcox (Layer 4).....	8-25
Figure 8.2.6	Simulated steady-state head surface and posted residuals for the middle Wilcox (Layer 5).....	8-26
Figure 8.2.7	Simulated steady-state head surface and posted residuals for the lower Wilcox (Layer 6).....	8-27
Figure 8.2.8	Steady-state model stream gain/loss (negative value denotes gaining stream).	8-28
Figure 8.2.9	Steady-state particle travel path and travel time (20,000 years) compared to the groundwater age dating study of Pearson and White (1967).....	8-29
Figure 8.3.1	Steady-state sensitivity results for the Carrizo (Layer 3) using target locations.	8-33
Figure 8.3.2	Steady-state sensitivity results for the Carrizo (Layer 3) using all active gridblocks.....	8-33
Figure 8.3.3	Steady-state sensitivity results for the Queen City/El Pico (Layer 1) using all active gridblocks.	8-34
Figure 8.3.4	Steady-state sensitivity results for the Reklaw/Bigford (Layer 2) using all active gridblocks.	8-34
Figure 8.3.5	Steady-state sensitivity results where GHB conductivity is varied.	8-35
Figure 8.3.6	Steady-state sensitivity results for the middle Wilcox (Layer 5) using all active gridblocks.....	8-35
Figure 8.3.7	Steady-state sensitivity results for the lower Wilcox (Layer 6) using all active gridblocks.....	8-36
Figure 8.3.8	Steady-state sensitivity results where recharge is varied.	8-36
Figure 9.1.1	Example of head sensitivity to Reklaw vertical hydraulic conductivity.....	9-4
Figure 9.1.2	Example of head sensitivity to specific storage.....	9-4
Figure 9.1.3	Storativity in the Carrizo Formation (Layer 3).....	9-5
Figure 9.2.1	Comparison between 1989 measured (a) and simulated (b) heads in the Carrizo formation (Layer 3).	9-16
Figure 9.2.2	Comparison between 1999 measured (a) and simulated (b) heads in the Carrizo formation (Layer 3).	9-17
Figure 9.2.3	Locations of hydrograph wells for the transient model.....	9-18
Figure 9.2.4	Calibration period (a) and verification period (b) crossplots for the Carrizo formation (Layer 3) in the calibrated transient model.	9-19
Figure 9.2.5	Calibration period crossplots for the calibrated transient model.	9-20
Figure 9.2.6	Verification period crossplots for the calibrated transient model.....	9-21
Figure 9.2.7	Transient model hydrographs from the Queen City/El Pico (Layer 1).....	9-22
Figure 9.2.8	Transient model hydrographs from the Carrizo (Layer 3), West.....	9-23
Figure 9.2.9	Transient model hydrographs from the Carrizo (Layer 3), Central.	9-24
Figure 9.2.10	Transient model hydrographs from the Carrizo (Layer 3), East.....	9-25
Figure 9.2.11	Transient model hydrographs from the upper Wilcox (Layer 4).....	9-26
Figure 9.2.12	Transient model hydrographs from the middle Wilcox (Layer 5).....	9-27
Figure 9.2.13	Transient model hydrographs from the lower Wilcox (Layer 6).....	9-28

LIST OF FIGURES (CONTINUED)

Figure 9.2.14	Average residuals for the verification period (1990-1999) in the Carrizo Formation (Layer 3).	9-29
Figure 9.2.15	Comparison of Slade et al. (2002) with average simulated stream gain/loss.	9-30
Figure 9.3.1	Transient sensitivity results for the Carrizo (Layer 3) using target locations.	9-34
Figure 9.3.2	Transient sensitivity results for the Carrizo (Layer 3) using all active gridblocks.	9-34
Figure 9.3.3	Transient sensitivity results for the Queen City/El Pico (Layer 1) using all active gridblocks.	9-35
Figure 9.3.4	Transient sensitivity results for the Reklaw/Bigford (Layer 2) using all active gridblocks.	9-35
Figure 9.3.5	Transient sensitivity results for the upper Wilcox (Layer 4) using all active gridblocks.	9-36
Figure 9.3.6	Transient sensitivity results for the middle Wilcox (Layer 5) using all active gridblocks.	9-36
Figure 9.3.7	Transient sensitivity results for the lower Wilcox (Layer 6) using all active gridblocks.	9-37
Figure 9.3.8	Transient sensitivity results where the horizontal hydraulic conductivities for all layers are varied.	9-37
Figure 9.3.9	Transient sensitivity results where recharge is varied.	9-38
Figure 9.3.10	Transient sensitivity results where specific yield is varied.	9-38
Figure 9.3.11	Transient sensitivity hydrographs from the Carrizo (Layer 3) where the horizontal hydraulic conductivities for all layers are varied.	9-39
Figure 9.3.12	Transient sensitivity hydrographs from the Carrizo (Layer 3) where pumping rate is varied.	9-40
Figure 10.1.1	Standard precipitation index (SPI) curves for the Dilley rain gage (#412458-Frio Co.) for 1 month, 1 year, 2 year, and 3 year time periods.	10-5
Figure 10.1.2	Standardized precipitation indices for precipitation gages in the region.	10-6
Figure 10.1.3	Standardized precipitation index averaged for all gages in the region from 1950-1960.	10-7
Figure 10.2.1	Simulated 2000 (a) and 2050 (b) head surfaces, Queen City/El Pico (Layer 1).	10-12
Figure 10.2.2	Difference between 2000 and 2050 simulated head surfaces, Queen City/El Pico (Layer 1).	10-13
Figure 10.2.3	Simulated 2000 (a) and 2050 (b) head surfaces, Carrizo (Layer 3).	10-14
Figure 10.2.4	Difference between 2000 and 2050 simulated head surfaces, Carrizo (Layer 3).	10-15
Figure 10.2.5	Simulated 2000 (a) and 2050 (b) head surfaces, upper Wilcox (Layer 4).	10-16
Figure 10.2.6	Difference between 2000 and 2050 simulated head surfaces, upper Wilcox (Layer 4).	10-17
Figure 10.2.7	Simulated 2000 (a) and 2050 (b) head surfaces, middle Wilcox (Layer 5).	10-18

LIST OF FIGURES (CONTINUED)

Figure 10.2.8	Difference between 2000 and 2050 simulated head surfaces, middle Wilcox (Layer 5).	10-19
Figure 10.2.9	Simulated 2000 (a) and 2050 (b) head surfaces, lower Wilcox (Layer 6).....	10-20
Figure 10.2.10	Difference between 2000 and 2050 simulated head surfaces, lower Wilcox (Layer 6).	10-21
Figure 10.2.11	Simulated 2010 head surface (a) and drawdown from 2000 (b) for the Carrizo (Layer 3).	10-22
Figure 10.2.12	Simulated 2020 head surface (a) and drawdown from 2000 (b) for the Carrizo (Layer 3).	10-23
Figure 10.2.13	Simulated 2030 head surface (a) and drawdown from 2000 (b) for the Carrizo (Layer 3).	10-24
Figure 10.2.14	Simulated 2040 head surface (a) and drawdown from 2000 (b) for the Carrizo (Layer 3).	10-25
Figure 10.2.15	Simulated 2010 (a) and 2020 (b) head surface, upper Wilcox (Layer 4).....	10-26
Figure 10.2.16	Simulated 2030 (a) and 2040 (b) head surface, upper Wilcox (Layer 4).....	10-27
Figure 10.2.17	Simulated 2010 (a) and 2020 (b) head surface, middle Wilcox (Layer 5).....	10-28
Figure 10.2.18	Simulated 2030 (a) and 2040 (b) head surface, middle Wilcox (Layer 5).....	10-29
Figure 10.2.19	Selected hydrographs from predictive simulation to 2050 with the DOR.....	10-30
Figure 10.2.20	Simulated difference in head surfaces for the Carrizo between the average condition 2050 simulation and the drought of record 2050 simulation.....	10-31
Figure 10.2.21	Simulated difference in head surfaces for the middle Wilcox between the average condition 2050 simulation and the drought of record 2050 simulation.	10-32
Figure 10.2.22	Simulated difference in head surfaces for the lower Wilcox between the average condition 2050 simulation and the drought of record 2050 simulation.	10-33
Figure 10.2.23	Simulated saturated thickness in the outcrop at year 2000.....	10-34
Figure 10.2.24	Simulated saturated thickness in the outcrop at year 2050.....	10-35
Figure 10.2.25	Difference between the 2010 base simulation and the 2010 simulation including the Twin Oaks Project in Bexar County.	10-36

LIST OF TABLES

Table 2.1	River basins in the Southern Carrizo-Wilcox GAM study area.....	2-3
Table 3.1	Previous groundwater models of the Carrizo-Wilcox aquifer in the study area.	3-2
Table 4.2.1	Data sources for layer elevations for the southern Carrizo-Wilcox model.	4-9
Table 4.3.1	Summary statistics for horizontal hydraulic conductivity	4-27
Table 4.3.2	Summary of literature estimates of Carrizo-Wilcox specific yield.	4-34
Table 4.4.1	Summary of data used to generate the predevelopment water-level elevation contours for the Carrizo Formation and the Wilcox Group.....	4-53
Table 4.4.2	Summary of data used to generate the predevelopment water-level elevation contours for the Queen City and Bigford formations.	4-54
Table 4.4.3	Data used to generate water-level elevation contours for the start of model calibration (January 1980).	4-55
Table 4.4.4	Data used to generate water-level elevation contours for the end of model calibration (December 1989).	4-61
Table 4.4.5	Data used to generate water-level elevation contours for the end of model verification (December 1999).	4-66
Table 4.5.1	Review of recharge rates for the Carrizo-Wilcox aquifer in Texas (after Scanlon et al., 2002).	4-88
Table 4.5.2	Potential recharge rates for the Carrizo-Wilcox (after LBG-Guyton and HDR, 1998).	4-89
Table 4.6.1	Stream flow gain/loss studies in the study area (after Slade et al., 2002, Table 1).	4-95
Table 4.6.2	Documented springs in the study area.	4-97
Table 4.7.1	Rate of groundwater withdrawal (AFY) from all model layers of the Carrizo-Wilcox aquifer for counties within the study area.....	4-105
Table 8.1.1	Calibrated hydraulic conductivity values for the steady-state model (ft/day).	8-6
Table 8.2.1	Steady-state head calibration statistics.	8-17
Table 8.2.2	Water budget for the steady-state model (AFY).	8-20
Table 8.2.3	Water budget for the steady-state model with values expressed as a percentage of inflow or outflow.	8-20
Table 9.2.1	Calibration statistics for the transient model for the calibration and verification periods.	9-12
Table 9.2.2	Calibration statistics for the hydrographs shown in Figures 9.2.7-9.2.13.	9-13
Table 9.2.3	Comparison of simulated stream leakance to LBG-Guyton and HDR (1998) simulated values (AFY per mile of stream).....	9-14
Table 9.2.4	Water budget for the transient model. All rates reported in AFY.	9-15
Table 10.1	SPI Precipitation Deficit Classification System (Hayes, 2001).	10-3
Table 10.3.1	Water budget for predictive simulations, AFY.	10-38

APPENDICES

Appendix A	Brief Summary of the Development of the Carrizo-Wilcox Aquifer in Each County and List of Reviewed Reports
Appendix B	Standard Operating Procedures (SOPs) for Processing Historical Pumpage Data TWDB Groundwater Availability Modeling (GAM) Projects
Appendix C	Standard Operating Procedures (SOPs) for Processing Predictive Pumpage Data TWDB Groundwater Availability Modeling (GAM) Projects
Appendix D1	Tabulated Groundwater Withdrawal Estimates for the Carrizo-Wilcox for 1980, 1990, 2000, 2010, 2020, 2030, 2040, and 2050
Appendix D2	Post Plots of Groundwater Withdrawal Estimates for the Carrizo-Wilcox for 1980, 1990, 2000, 2010, 2020, 2030, 2040, and 2050
Appendix D3	Carrizo-Wilcox Groundwater Withdrawal Distributions by County
Appendix E	Using SWAT with MODFLOW in a Decoupled Environment
Appendix F	Water Quality
Appendix G	Draft Report Comments and Responses

ABSTRACT

This report documents a three-dimensional groundwater model developed for the southern Carrizo-Wilcox aquifer in southwest and south-central Texas. The model was developed using MODFLOW and includes the Carrizo-Wilcox aquifer, the Reklaw/Bigford Formations, and the Queen City/El Pico Clay Formations. The purpose of this model is to provide a tool for making predictions of groundwater availability. The model has been calibrated to predevelopment conditions (prior to significant resource use) which are considered to be at steady state. The steady-state model reproduces the predevelopment aquifer heads well within the estimated head uncertainty. The model was also calibrated to transient aquifer conditions from 1980 through December 1989 reproducing aquifer heads and available estimates of aquifer-stream interaction. The transient-calibrated model was verified by simulating aquifer conditions from 1990 through December 1999 and comparing to observed aquifer heads and available estimates of aquifer-stream interaction for that time period.

The verified model was used to make predictions of aquifer conditions for the next 50 years based upon projected pumping demands as developed by the Regional Water Planning Groups. The pumping demand estimates developed from the regional water plans predicted a significant decline in Carrizo-Wilcox pumping demand starting in 2000. This decline is approximately 100,000 AFY. As a result of the predicted pumping declines, the model predicts that Carrizo-Wilcox water levels will rebound in the western model region where groundwater pumping was decreased. The eastern portion of the model shows gradual water-level decline as pumping demand generally increases in that part of the model. Pumping associated with potential future Laredo pumping (14,000 AFY) of the Carrizo-Wilcox in Northern Webb County created a local drawdown cone of over 100 feet by 2050.

This model provides an integrated tool for the assessment of water management strategies to directly benefit state planners, Regional Water Planning Groups (RWPGs), and Groundwater Conservation Districts (GCDs). The model is applicable for the assessment of groundwater availability on a regional scale (e.g., tens of miles). The model is not applicable for predicting conditions at an individual well and may not be applicable for determining operational details for particular water resource strategies without refinement. The model is ideally suited for refinement as it has been developed using a constant grid-block spacing of one square mile.

Surface-groundwater interaction has been modeled in a first-order analysis method and this GAM should not be used solely as a surface water assessment tool.

1.0 INTRODUCTION

The Carrizo-Wilcox aquifer is classified as a major aquifer in Texas (Ashworth and Hopkins, 1995) ranking third in the state for water use (430,000 acre-feet per year [AFY]) in 1997 behind the Gulf Coast aquifer and the Ogallala aquifer (TWDB, 2002). The aquifer extends from the Rio Grande in South Texas to East Texas and continues into Louisiana and Arkansas. The Carrizo-Wilcox aquifer provides water to all or parts of 60 Texas counties with the greatest historical use being in and around the Tyler, Lufkin-Nacogdoches, and Bryan-College Station metropolitan centers and in the Wintergarden region of South Texas (Ashworth and Hopkins, 1995).

The Texas Water Code codified the requirement for the development of a State Water Plan that allows for the development, management, and conservation of water resources and the preparation and response to drought, while maintaining sufficient water available for the citizens of Texas (TWDB, 2002). Senate Bill 1 and subsequent legislation directed the TWDB to coordinate regional water planning with a process based upon public participation. Also as a result of Senate Bill 1, the approach to water planning in the state of Texas has shifted from a water-demand based allocation approach to an availability-based approach.

Groundwater models provide a tool to estimate groundwater availability for various water use strategies and to determine the cumulative effects of increased water use and drought. A groundwater model is a numerical representation of the aquifer system capable of simulating historical and predicting future aquifer conditions. Inherent to the groundwater model, are a set of equations which are developed and applied to describe the physical processes considered to be controlling groundwater flow in the aquifer system. It can be argued that groundwater models are essential to performing complex analyses and in making informed predictions and related decisions (Anderson and Woessner, 1992). As a result, development of Groundwater Availability Models (GAMs) for the major Texas aquifers is integral to the state water planning process. The purpose of the GAM program is to provide a tool that can be used to develop reliable and timely information on groundwater availability for the citizens of Texas and to ensure adequate supplies or recognize inadequate supplies over a 50-year planning period.

The Southern Carrizo-Wilcox GAM has been developed using a modeling protocol which is standard to the groundwater model industry. This protocol includes; (1) the

development of a conceptual model for groundwater flow in the aquifer, (2) model design, (3) model calibration, (4) model verification, (5) sensitivity analysis, (6) model prediction, and (7) reporting. The conceptual model is a conceptual description of the physical processes which govern groundwater flow in the aquifer system. We reviewed the available data and reports for the model area in the conceptual model development stage. Model design is the process used to translate the conceptual model into a physical model, in this case a numerical model of groundwater flow. This involved organizing and distributing model parameters, developing a model grid and model boundary conditions, and determining the model integration time scale. Model calibration is the process of modifying model parameters so that observed field measurements (e.g., groundwater levels in wells) can be reproduced. The model was calibrated to predevelopment conditions (prior to significant resource use) which are considered to be at steady-state and to transient aquifer conditions from 1980 through 1990. Model verification is the process of using the calibrated model to reproduce observed field measurements not used in the calibration to test the model's predictive ability. The model was verified against measured aquifer conditions from 1990 through 1999. Sensitivity analyses were performed on both the steady-state and transient models to offer insight on the uniqueness of the model and the uncertainty in model parameter estimates. Model predictions were performed from 2000 to 2050 to estimate aquifer conditions for the next 50 years based upon projected pumping demands developed by the Regional Water Planning Groups. This report documents the modeling process and results from conceptual model development through predictions according to standard requirements specified by the TWDB in their Request for Qualifications. The model and associated data files are publicly available. These files, along with this report, are available at the TWDB GAM website at <http://www.twdb.state.tx.us/GAM>.

Consistent with state water planning policy, the Southern Carrizo-Wilcox GAM was developed with the support of stakeholders through quarterly stakeholder forums. The purpose of this GAM is to provide a tool for Regional Water Planning Groups, Groundwater Conservation Districts, River Authorities, and state planners for the evaluation of groundwater availability and to support the development of water management strategies and drought planning. The South Central Texas Regional Water Planning Group (Region L) area coincides with a large percent of the model area. Region L seeks to meet 25% of their water needs in 2050

by newly developed groundwater supplies with the bulk of these new supplies originating from the Carrizo-Wilcox aquifer. The GAM provides a tool for use in assessing these strategies.

2.0 STUDY AREA

The Carrizo-Wilcox aquifer is comprised of hydraulically connected sands from the Wilcox Group and the Carrizo Formation of the Claiborne Group (Ashworth and Hopkins, 1995). The Carrizo-Wilcox aquifer extends across Texas from the Rio Grande in the southwest to the Sabine River in the northeast and beyond into Louisiana and Arkansas. The Carrizo-Wilcox aquifer is classified as a major aquifer in Texas providing groundwater resources to all or part of 60 Texas counties (Ashworth and Hopkins, 1995).

Because of its large size, the Carrizo-Wilcox aquifer was divided by the TWDB for modeling purposes into three areas, with each being modeled separately. The three Carrizo-Wilcox GAMs are the Northern Carrizo-Wilcox GAM, the Central Carrizo-Wilcox GAM, and the Southern Carrizo-Wilcox GAM (Figure 2.1). These models have significant overlap areas as shown in Figure 2.1. This study documents the Southern Carrizo-Wilcox GAM. The model area is shown in Figure 2.2 and includes all or parts of Atascosa, Bastrop, Bee, Bexar, Caldwell, DeWitt, Dimmit, Duval, Fayette, Frio, Gonzales, Guadalupe, Karnes, La Salle, Lavaca, Live Oak, Maverick, McMullen, Medina, Uvalde, Webb, Wilson, and Zavala counties. Figure 2.3 shows the surface outcrop and downdip subcrop of the major aquifers in the study area.

Groundwater model boundaries are typically defined on the basis of surface or groundwater hydrologic boundaries. The model area for the Southern Carrizo-Wilcox GAM is bounded laterally on the northeast by the surface water basin divide between the Guadalupe and Colorado rivers and to the southwest by the Rio Grande. The basin divide serves as a model boundary in the outcrop (presumed groundwater flow divide) and was extended into the subsurface to the down-dip boundary of the model. The upper model boundary was defined by the ground surface in the outcrop of the Carrizo-Wilcox aquifer extending south to the extent of the Queen City/El Pico outcrop. The lower-model boundary is the base of the Wilcox Group representing the top of the Midway Formation. The down-dip boundary of the Carrizo-Wilcox aquifer extends past the limits of fresh water to the updip limit of the Wilcox growth fault zone (Bebout et al., 1982).

The study area encompasses all or part of five regional water-planning areas (Figure 2.4): (1) the Lower Colorado Region (Region K), (2) the South Central Texas Region (Region L), (3) the Rio Grande Region (Region M), (4) the Coastal Bend Region (Region N), and the

(5) Lavaca Region (Region P). The study area includes all or parts of the following Groundwater Conservation Districts (Figure 2.5): (1) the Bee Groundwater Conservation District, (2) the Edwards Aquifer Authority, (3) the Evergreen Underground Water Conservation District, (4) Fayette County Groundwater Conservation District, (5) the Gonzales County Underground Water Conservation District, (6) the Guadalupe County Groundwater Conservation District, (7) the Lavaca County Groundwater Conservation District, (8) the Live Oak Underground Water Conservation District, (9) the Lost Pines Groundwater Conservation District, (10) the McMullen Groundwater Conservation District, (11) the Medina County Groundwater Conservation District, (12) Pecan Valley Groundwater Conservation District, (13) the Plum Creek Conservation District, (14) the Uvalde County Underground Water Conservation District, and (15) the Wintergarden Groundwater Conservation District. The model study area also contains the southernmost extension of the Bexar Metropolitan Water District.

The study area also intersects six river authorities; (1) Lower Colorado River Authority, (2) Guadalupe-Blanco River Authority, (3) Lavaca-Navidad River Authority, (4) Nueces River Authority, (5) Rio Grande River Authority, and the (6) San Antonio River Authority. Figure 2.6 shows the major river basins in the study area.

The model area intersects six major river basins from west to east: (1) the Rio Grande, (2) the Nueces, (3) the San Antonio, (4) the Guadalupe, (5) the Colorado, and the Lavaca. Of these, the Rio Grande and the Colorado River originate outside of Texas. Climate is a major control on flow in rivers and streams. The primary climactic factors are precipitation and evaporation. In general flow in rivers in the western portion of the model area is episodic with extended periods of low flow, or no flow conditions. These rivers tend to lose water to the underlying formations on average. In contrast, in the eastern portion of the study area, rivers and streams are perennial and tend to gain flow from the underlying geology.

Table 2.1 provides a listing of the river basins in the study area along with the river length in Texas, the river basin area in Texas, and the number of major reservoirs within the river basin in Texas (BEG, 1976).

Table 2.1 River basins in the Southern Carrizo-Wilcox GAM study area.

River Basin	Texas River Length (mi)	Texas River Basin Drainage Area (square miles)	Number of Major Reservoirs
Rio Grande	1,250	48,259	3
Nueces	315	16,950	2
San Antonio	225	4,180	2
Guadalupe	250	6,070	2
Colorado	600	39,893	11
Lavaca	74	2,309	1

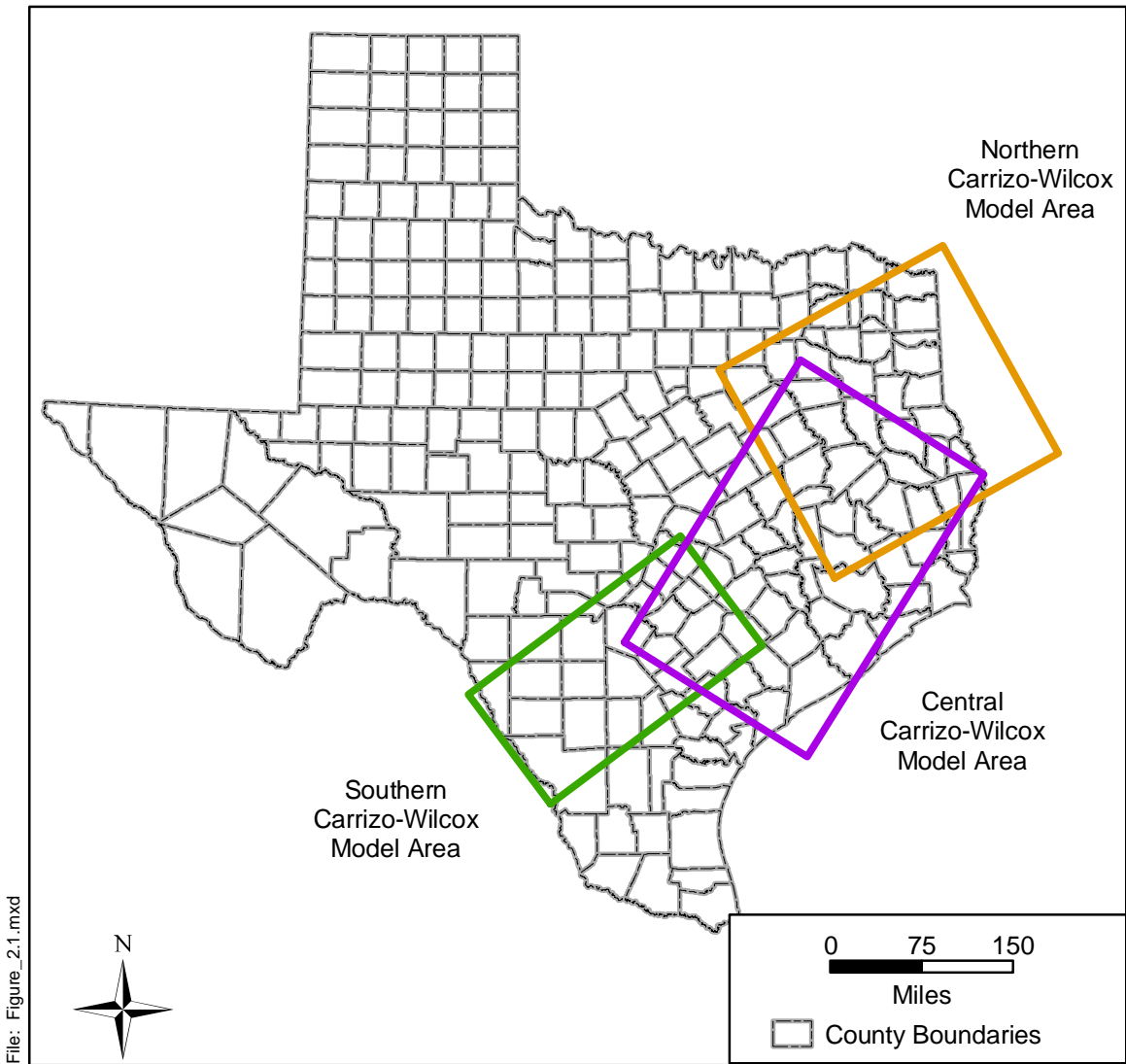


Figure 2.1 Location of the three Carrizo-Wilcox GAMs.

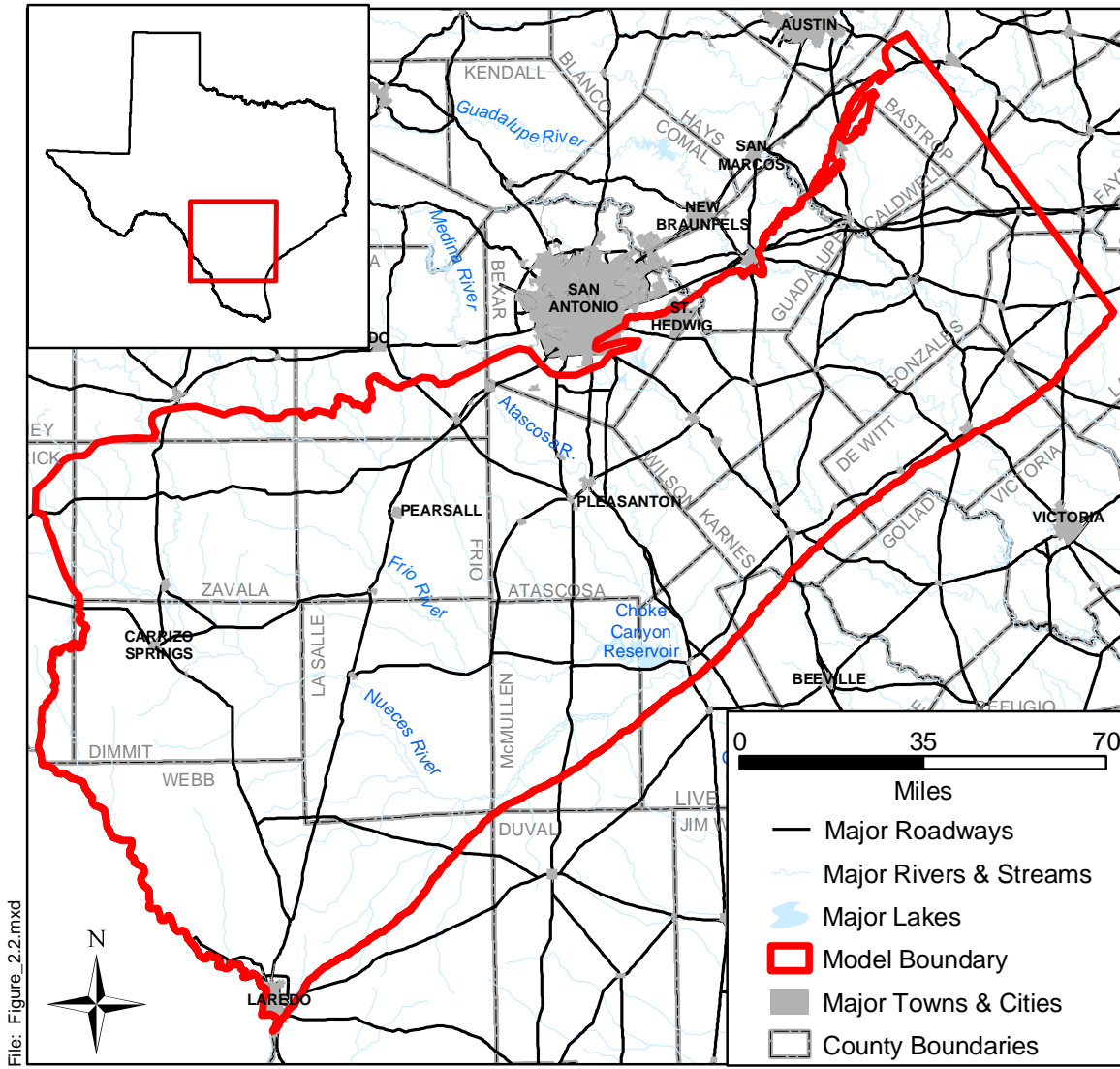


Figure 2.2 Location of study area showing county boundaries, cities, lakes, and rivers.

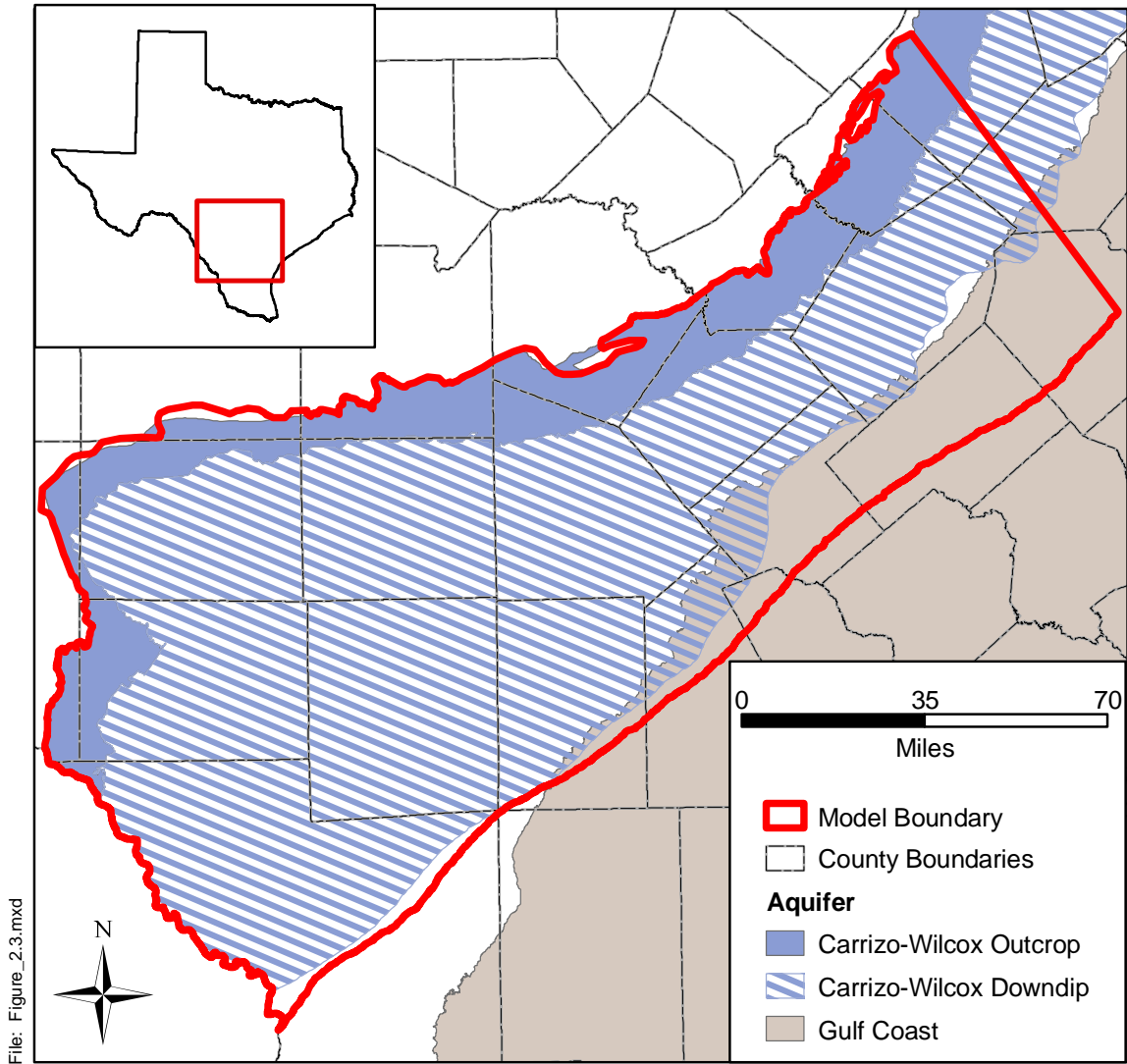
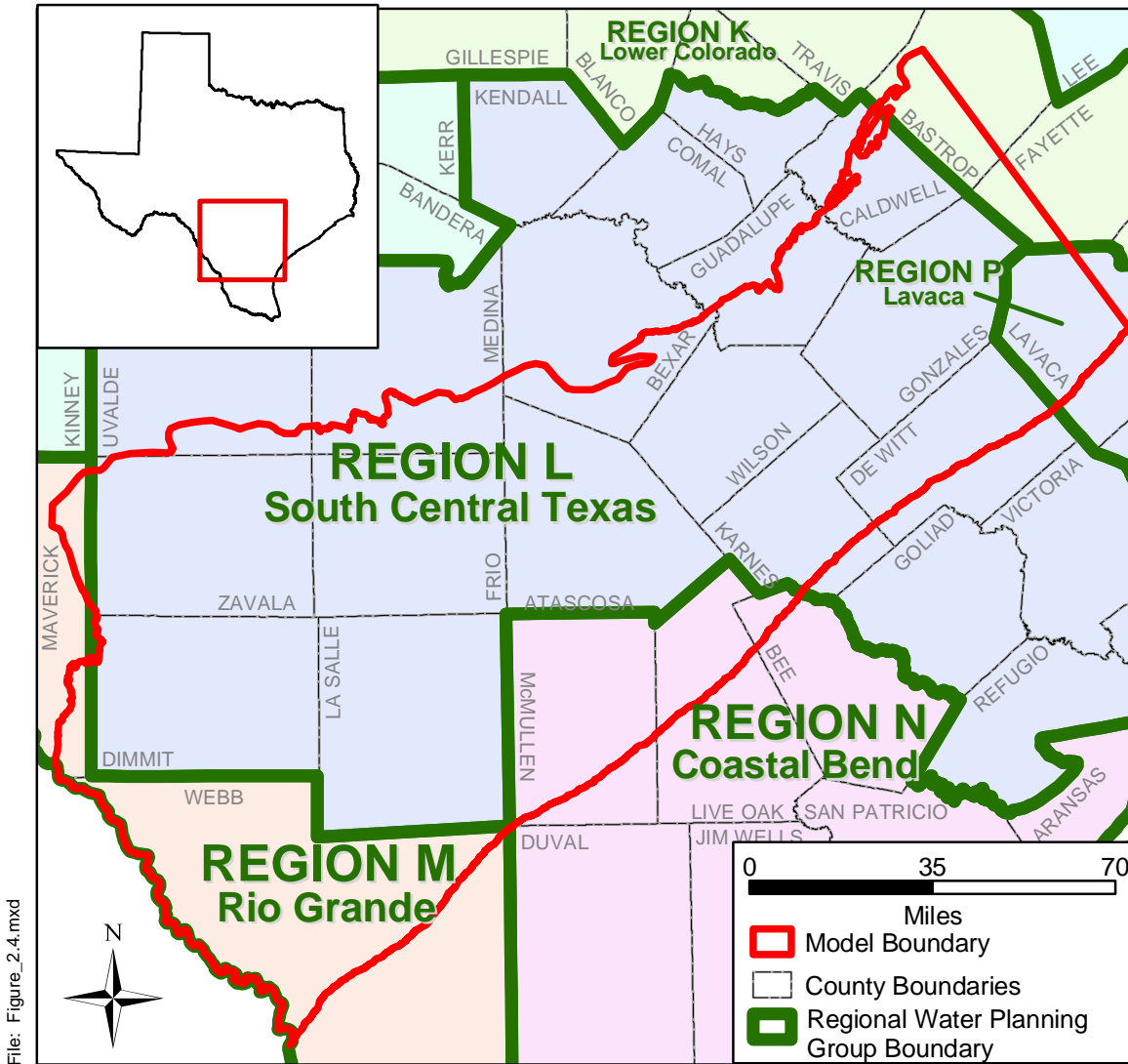


Figure 2.3 Areal extent of the major aquifers in the study area.



Source: Online: Texas Water Development Board, September 2002

Figure 2.4 Location of Regional Water Planning Groups in the study area.

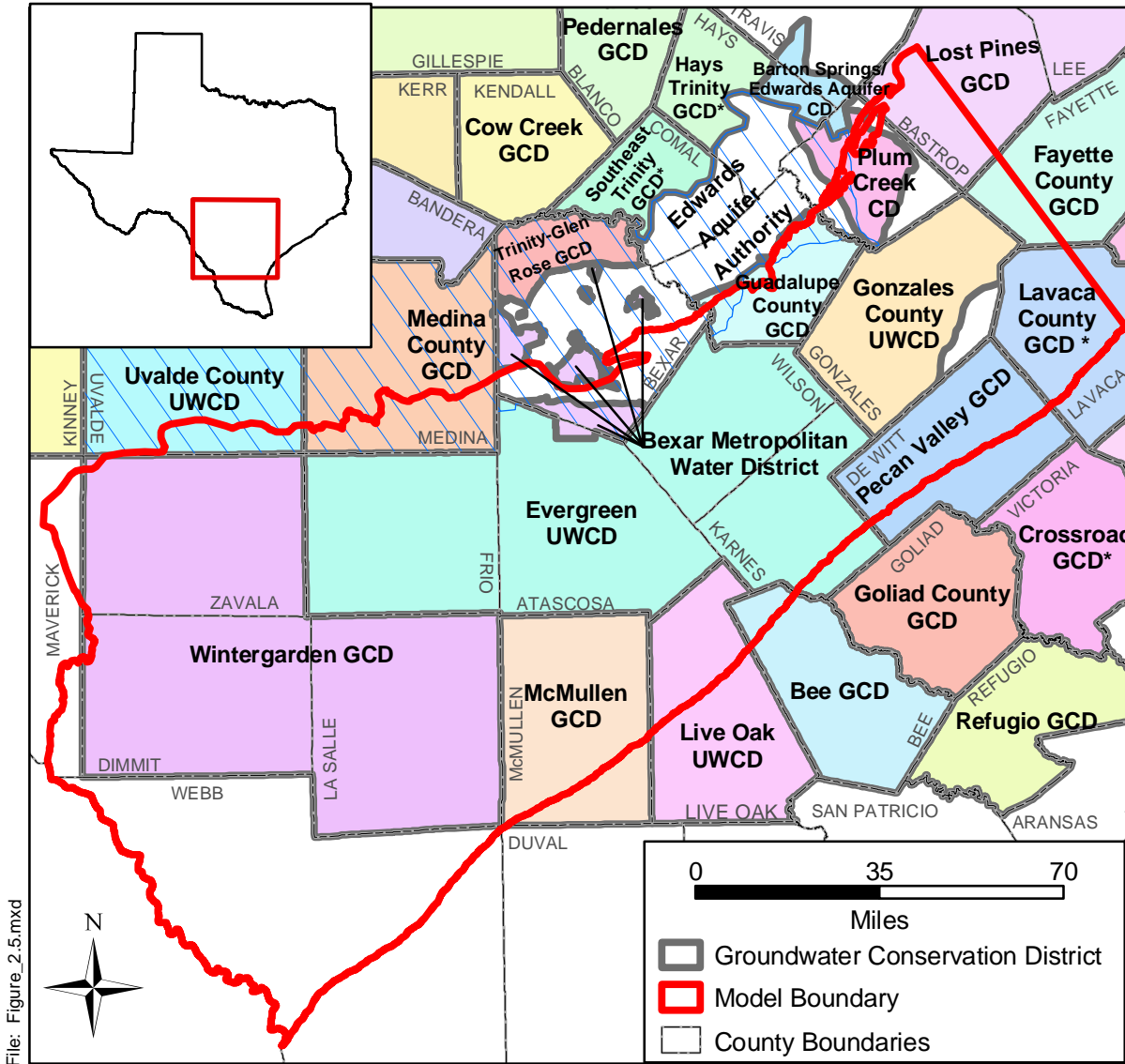


Figure 2.5 Location of Groundwater Conservation Districts in the study area.

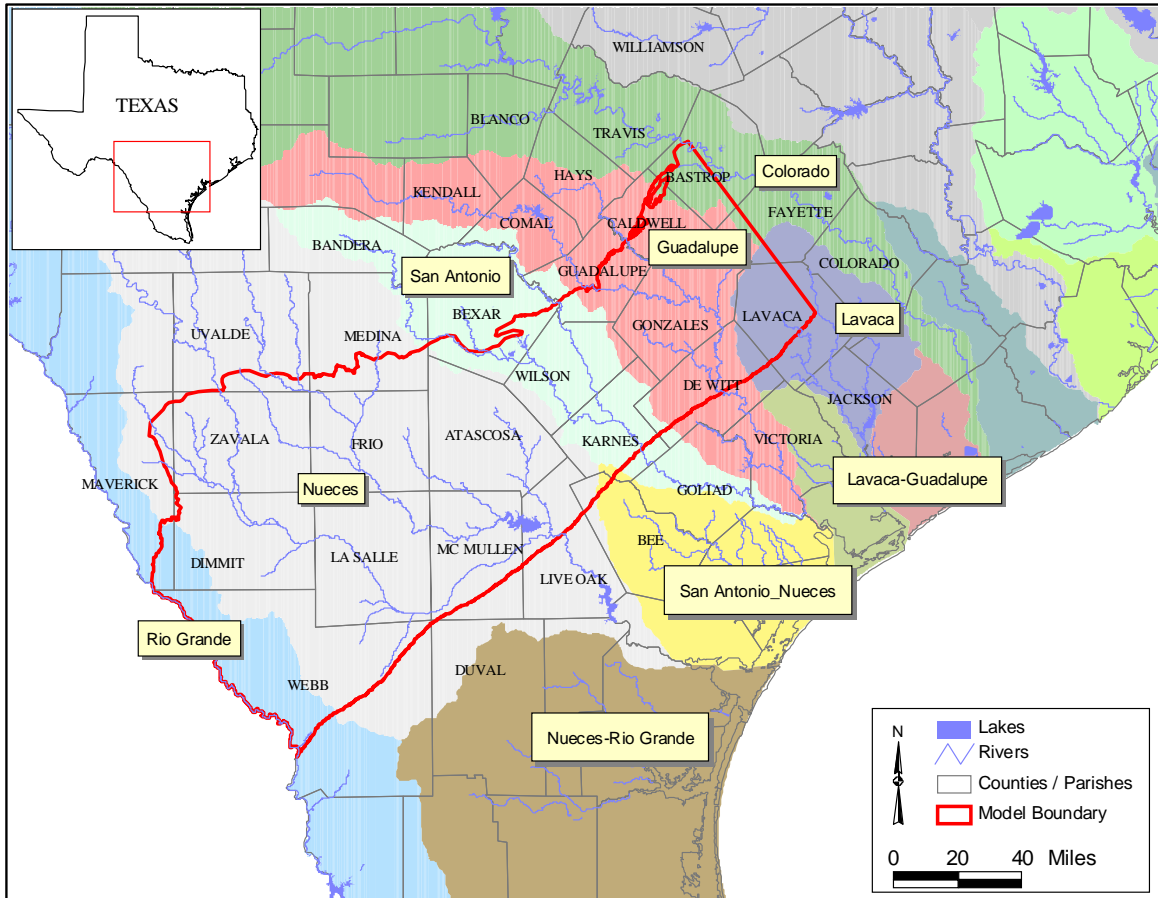


Figure 2.6 Major river basins in the study area.

2.1 Physiography and Climate

The study area is located in the Western Gulf Coastal Plain physiographic province (Alexander et al., 1964) in the Rio Grande Embayment of South Texas. The study area includes portions of the Rio Grande, Nueces, San Antonio, Guadalupe, Colorado, and Lavaca river basins. The region is characterized as having low relief with ground surface elevations gently decreasing from the southwest to the northeast and southeast. Figure 2.7 provides a topographic map of the study area. Ground surface elevation varies from nearly 300 feet above sea level in the western study area to less than 100 feet above sea level in river valleys and in the southeastern most regions of the study area. The gentle gulfward decrease in ground surface elevation is interrupted by resistant Tertiary sandstone outcrops, most prominently the Carrizo and the Catahoula-Oakville outcrops (Hamlin, 1988). The river valleys are broadly incised with terraced valleys that are hundreds of feet lower than the surface basin divide elevations (Hamlin, 1988). The model study area falls within the Gulf Coastal Plains, Blackland Prairies, and Coastal Prairies physiographic provinces. These physiographic provinces are further subdivided into ecological regions. Figure 2.8 shows the ecological regions which fall within the study area.

The study area intersects three climatic divisions in Texas: the Edwards Plateau division; the South Central division; and the South Texas division. The climate in the study area ranges from dry subhumid in the eastern part of the study area to semiarid in the west (Hamlin, 1988). Summers are usually hot and humid, while winters are often mild and dry. The hot weather persists from late May through September, accompanied by prevailing southeasterly winds (TWDB, 2002, Region L Plan). There is little change in the day-to-day summer weather except for the occasional thunderstorm, which produces much of the annual precipitation within the region. The cool season, beginning about the first of November and extending through March, is typically the driest season of the year as well. Winters are typically short and mild. Average daily temperature in the model region generally varies from a low in the low 40s to upper 30s in January to highs of the upper 90s in July (TWDB, 2002, Region L Plan). In the study region, the average annual temperature decreases from the south to the north from 73°F to 70°F (Hamlin, 1988).

The average annual net pan evaporation depth in the study area is high relative to available moisture ranging from a low of 49.9 inches per year in the far southeast portion of the model area to a high of 65.9 inches per year in the southwest corner of the model study area (Figure 2.9). For the study area, historical daily precipitation data is available at approximately 100 stations (Figure 2.10) from 1900 through 1999. The spatial distribution is relatively dense in the model domain across the period of record. However, the number of available gages in any given year is quite variable with a general chronological increase in the number of gages available. Most gages began measuring precipitation in the 1930s or 1940s. There are only eight precipitation gages in the study area that have records extending back to the first decade of the 1900's. Approximately 40 precipitation gages have records extending as far back as 1941.

Based upon the available precipitation records, the average annual precipitation in the study area is 29.4 inches. Historical average annual precipitation varies from a low of 20.9 inches at Eagle Pass to a high of 37.4 inches at Halletsville. The PRISM (Parameter-elevation Regressions on Independent Slopes Model) precipitation data set developed and presented online by the Oregon Climate Service at Oregon State University provides a good distribution of average annual precipitation across the model area based upon the period of record from 1961 to 1990. Figure 2.11 provides a raster data post plot of average annual precipitation across the model study area. Generally, the average annual precipitation is greater in the east and towards the coastal areas. Figure 2.12 shows annual precipitation recorded at five precipitation gages with long periods of record within the model area and located in San Antonio (Bexar Co.), Flatonia (Fayette, Co.), Dilley (Frio Co.), Runge (Karnes Co.), and Encinal (Webb Co.). Also plotted in these plots is the long-term period of record average annual precipitation depth for each gage.

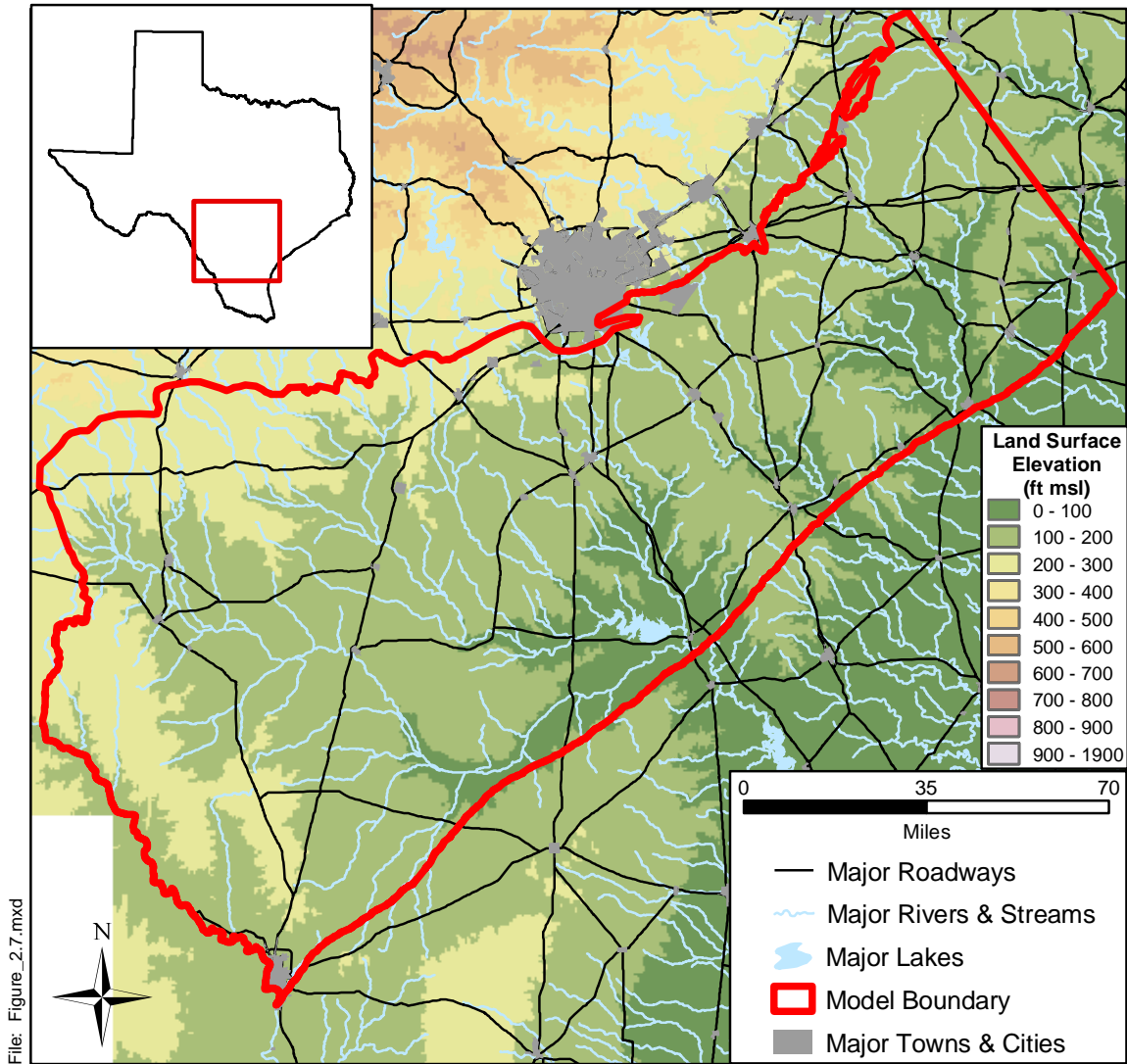


Figure 2.7 Topographic map of the study area.

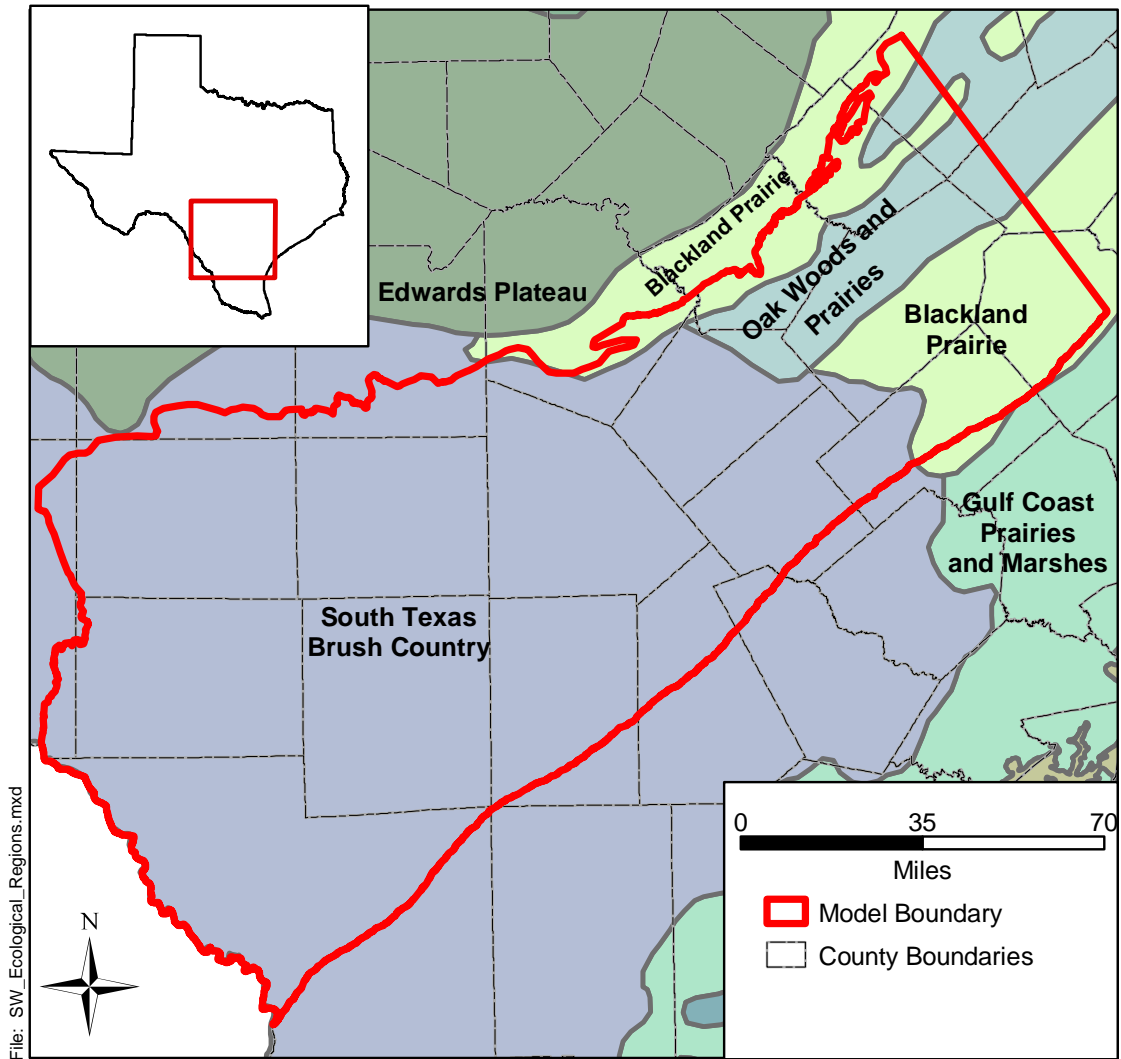
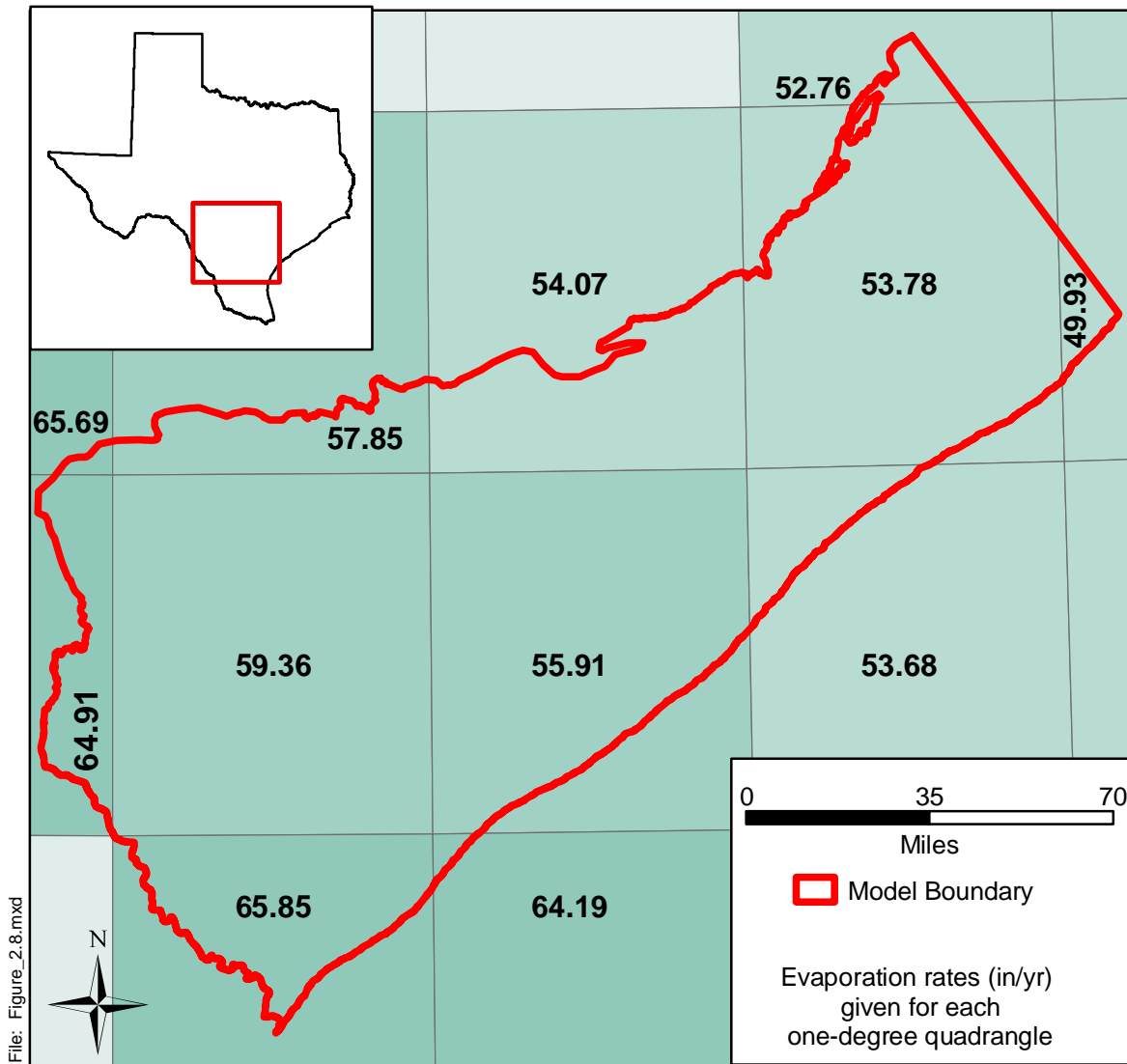


Figure 2.8 Ecological regions within the study area.



Source: Online: Texas Water Development Board, September 2002

Figure 2.9 Average annual net pan evaporation rate in inches per year.

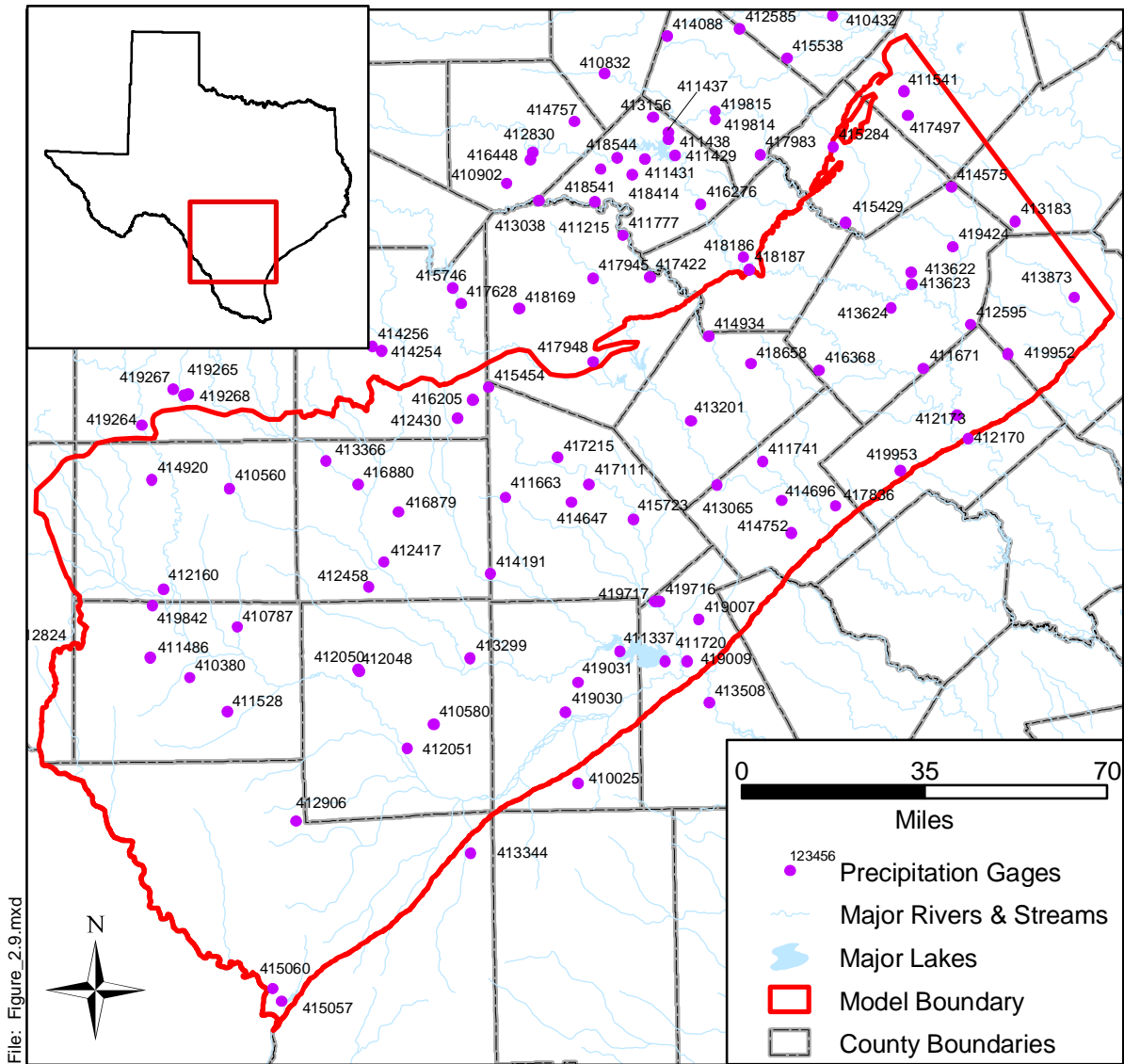
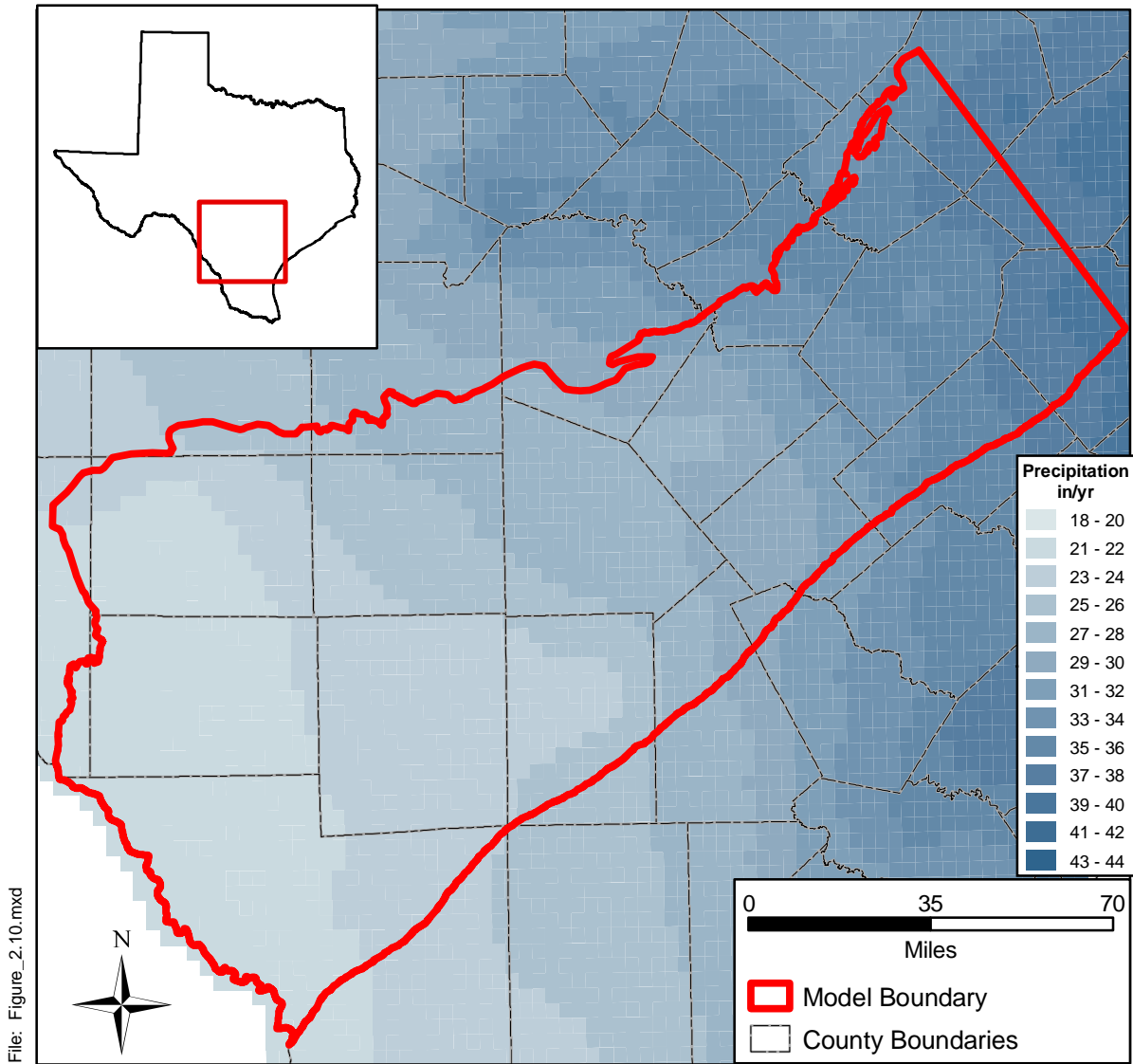


Figure 2.10 Location of precipitation gages in the study area (Period of Record is 1900 to 1999).



Source: Online: Oregon State University's Spatial Climate Analysis Service

Figure 2.11 Average annual precipitation (1961-1990) over the study area in inches per year (Source: Oregon Climate Service, Oregon State University, PRISM data set).

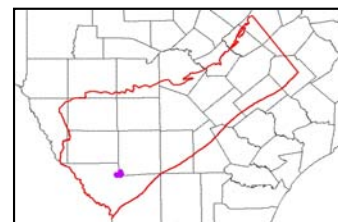
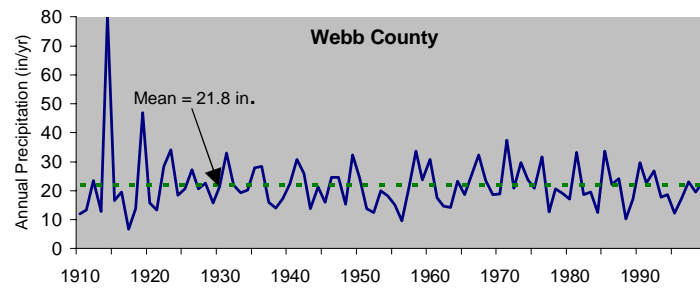
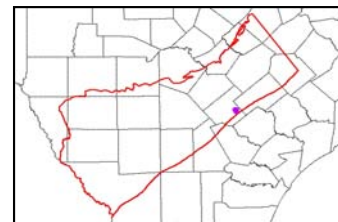
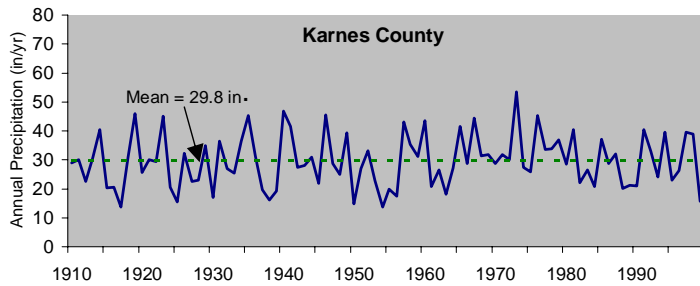
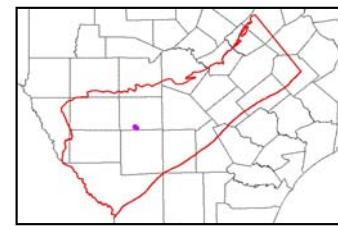
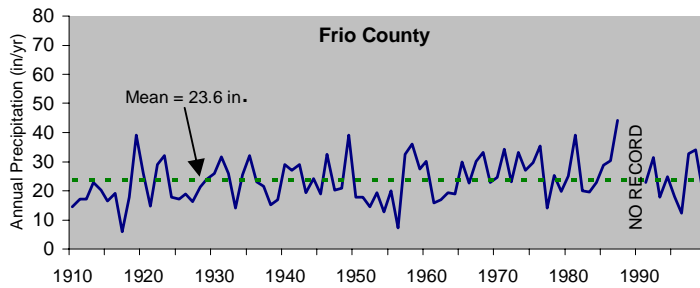
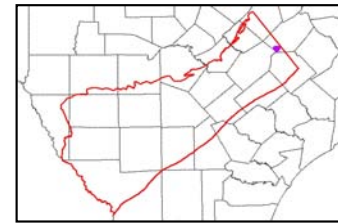
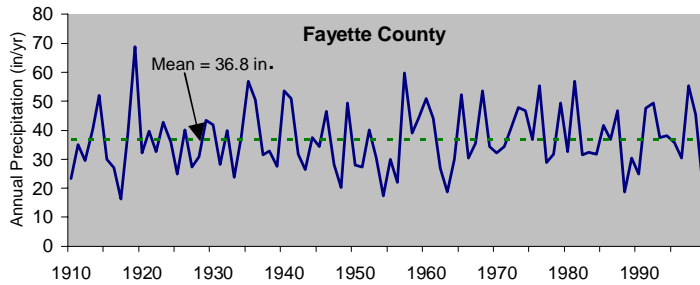
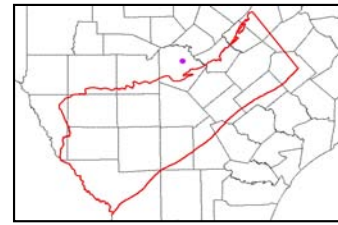
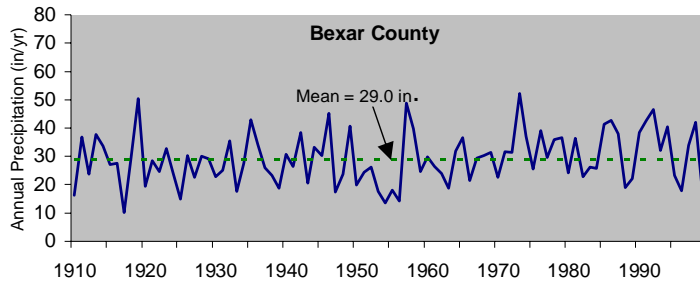


Figure 2.12 Annual precipitation time series for gages in Bexar, Fayette, Frio, Karnes, and Webb counties.

2.2 Geology

The sediments that form the aquifer in the study area are part of a gulfward thickening wedge of Cenozoic sediments deposited in the Rio Grande Embayment of the northwest Gulf Coast Basin. Deposition in the Rio Grande Embayment was influenced by regional crust subsidence, episodes of sediment inflow from areas outside of the Gulf Coastal Plain, and eustatic sea-level change (Grubb, 1997). Galloway et al. (1994) characterized Cenozoic sequences in the Gulf Coast in the following three ways. Deposition of Cenozoic sequences is characterized as an offlapping progression of successive, basinward thickening wedges. These depositional wedges aggraded the continental platform and prograded the shelf margin and continental slope from the Cretaceous shelf edge to the current Southwest Texas coastline. Deposition occurred along sand-rich, continental margin deltaic depocenters within embayments (Rio Grande, Houston, and Mississippi Embayments) and was modified by growth faults and salt dome development.

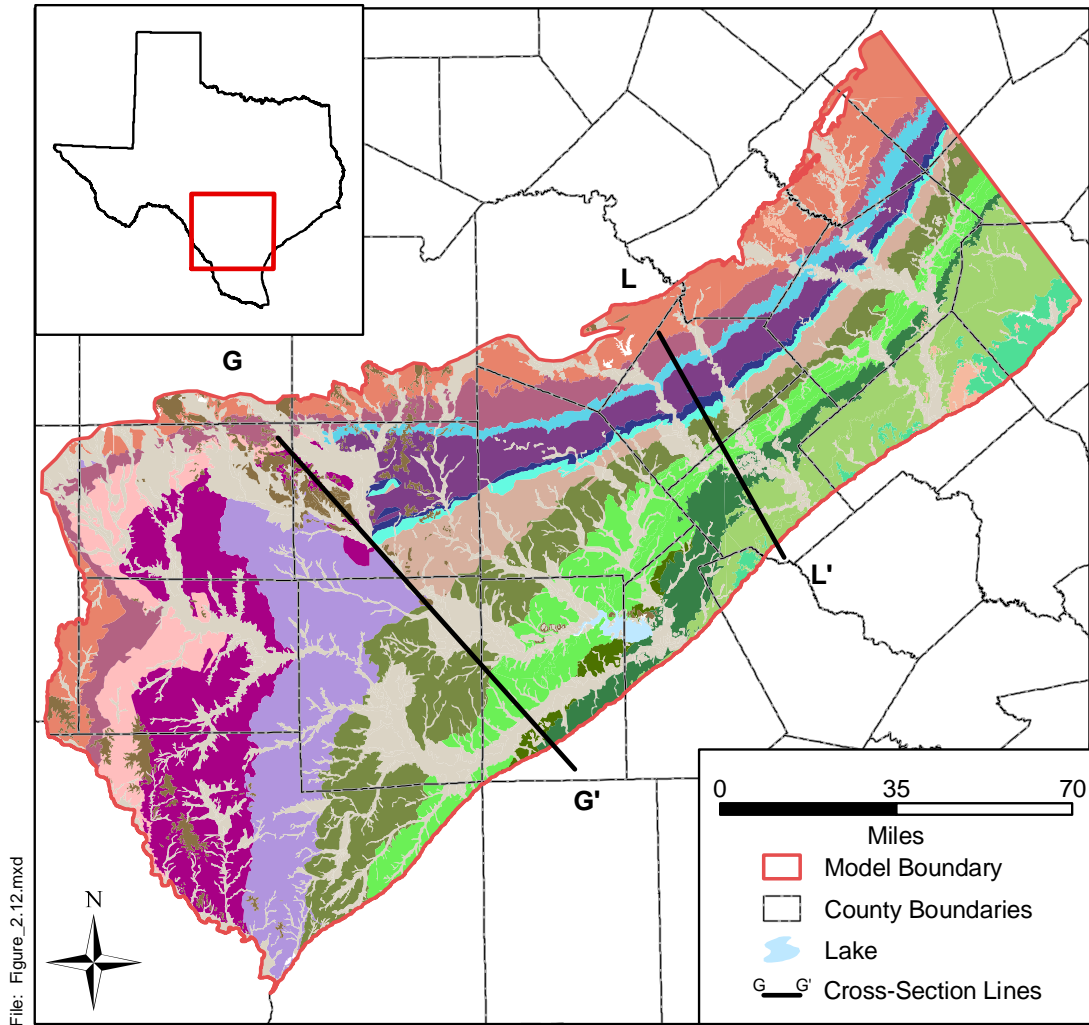
The primary Paleogene depositional sequences in ascending stratigraphic order are the lower Wilcox, the upper Wilcox, the Carrizo, the Queen City, the Sparta, the Yegua-Cockfield, the Jackson, and the Vicksburg-Frio (Galloway et al., 1994). Each of these depositional sequences is bounded by marine shales and finer grained sediments representing transgressions (e.g., Reklaw and Weches formations).

Figure 2.13 shows a geologic map of the area showing the Tertiary sediments comprising the aquifers of interest in this study as well as the Quaternary undivided sediments. Inspection of the surface geology shows the general outcrop pattern from southwest to northeast coincident with depositional strike, the Balcones Fault Zone, and normal to basin subsidence. Also important to note are the stratigraphic changes that occur from east of the Frio River to west of the Frio River. Many of the Tertiary formations change lithologic character in the vicinity of the Frio River coincident with the axis of the Rio Grande Embayment.

Figure 2.14 shows a representative stratigraphic section for the study area. The southern Carrizo-Wilcox aquifer overlies the Midway Group which is composed of marine clays. The southern Carrizo-Wilcox aquifer consists of fluvial-deltaic sediments of the upper Paleocene and lower Eocene Wilcox Group and Carrizo Sand. In the study area, the Wilcox Group is

subdivided into a lower, middle, and upper unit. The lower Wilcox is composed of sands and clays deposited in a barrier bar and lagoon-bay system (Fisher and McGowen, 1967). The middle Wilcox is not generally subdivided in the study area but is generally described as a lower energy depositional sequence representative of a minor transgression. The Carrizo Sand in the outcrop and shallow subsurface correlates with the upper part of the Wilcox Group in the deeper subsurface (Hamlin, 1988; Bebout et al., 1982). The Carrizo-upper Wilcox predominantly consists of a fluvial sand facies that grades into more deltaic and marine facies farther downdip (Bebout et al., 1982). South and west of the Frio River, the Wilcox is sometimes referred to as the Indio Formation and is composed of irregularly bedded sandstone and shale. Figure 2.15 shows two structural cross-sections (for location see Figure 2.13) after Hamlin (1988) in the study area. Cross-section G-G' of Hamlin shows that the Carrizo-Wilcox dips less in the southwestern portion of the study area and the fresh water line extends into McMullen County in the Carrizo. By contrast, section L-L' shows that the aquifer dips much more steeply in the east (Wilson & Karnes counties) with the extent of fresh water closer to the outcrop.

The Carrizo-Wilcox aquifer is bounded from above by the Reklaw Formation, representing a semi-confining unit between the Carrizo Sand and the shallow aquifer of the Queen City Formation. The Reklaw Formation consists of variable amounts of mud and sand and is considered the upper confining stratum of the Carrizo-upper Wilcox aquifer in the northeastern part of the study area. To the southwest in the study area, the Bigford Formation is the equivalent of the Reklaw, which consists mainly of sands, silts, and shales and is considered a minor aquifer compared to the underlying Carrizo-upper Wilcox aquifer. In the western part of the study area, the Bigford Formation is overlain by the El Pico Clay composed mainly of clays with few sand lenses. In the northeast portion of the study area, the Queen City Sand and clayey Weches Formation overlie the Reklaw and interfinger laterally with the El Pico Clay in the southwest. In the southwestern part of the model area, sands and sandstones of the Laredo aquifer overlie the El Pico Clay. The Laredo aquifer correlates with the interbedded sands and clays of the Sparta aquifer and with the clays and fine sands of the Cook Mountain Formation in the northeast. Both the Laredo and Sparta aquifers produce small to moderate quantities of water.



Source: Bureau of Economic Geology

West of Frio River	East of Frio River
	Quaternary Undivided
	Willis Formation
	Uvalde Gravel
	Goliad Formation
	Fleming Formation; Oakville Sandstone
	Catahoula Formation
	Frio Formation
	Jackson Group
	Yegua Formation
Laredo Formation	Cook Mountain Formation
El Pico Clay	Sparta Sand
Bigford Formation	Weches Formation
	Queen City Sand
	Reklaw Formation
	Carrizo Sand
	Wilcox Group
	Midway Group

Figure 2.13 Surface geology of the study area.

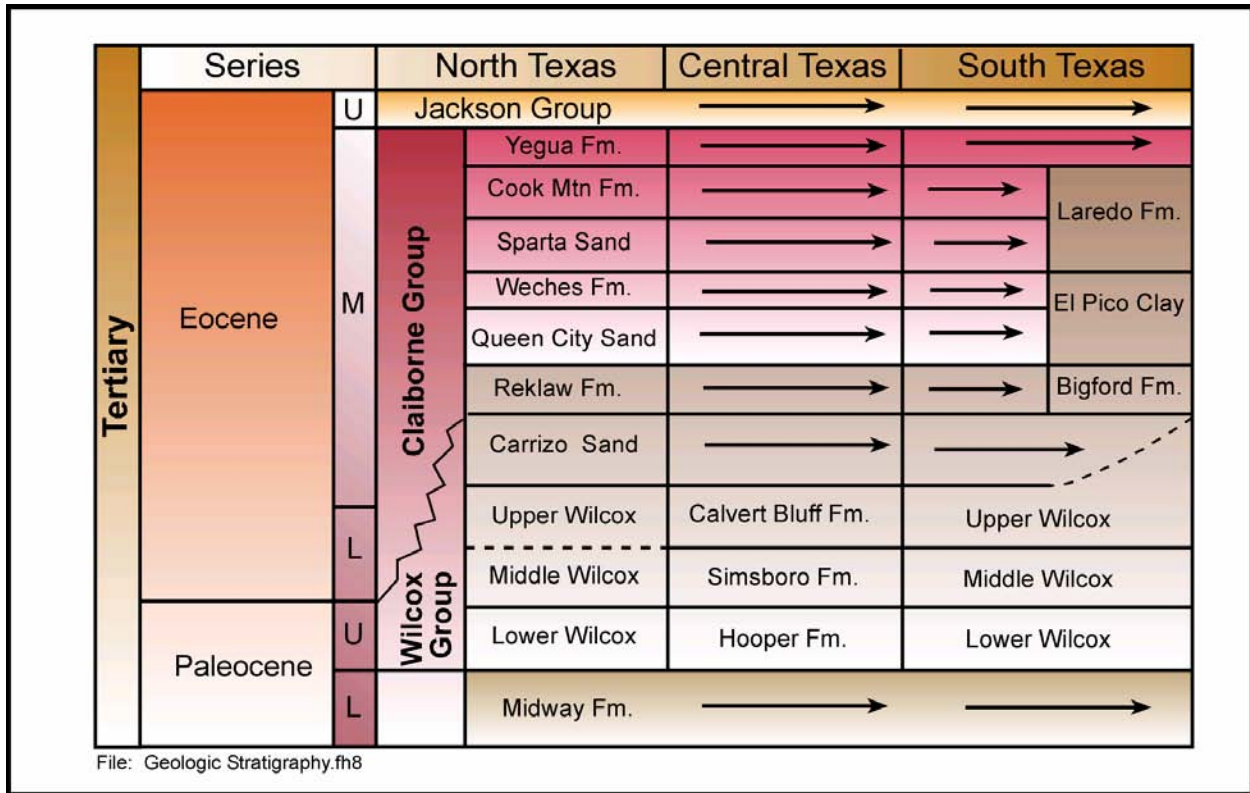


Figure 2.14 Generalized stratigraphic section for the Carrizo-Wilcox aquifer in Texas (after Ayers and Lewis, 1985; Hamlin, 1988; Kaiser et al., 1978).

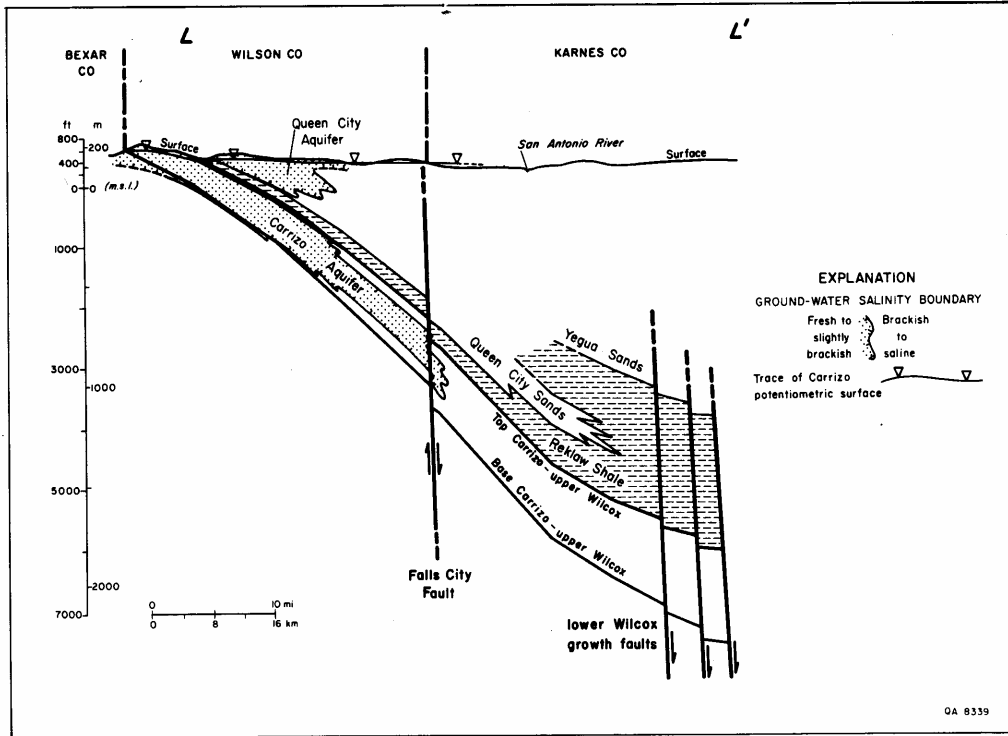
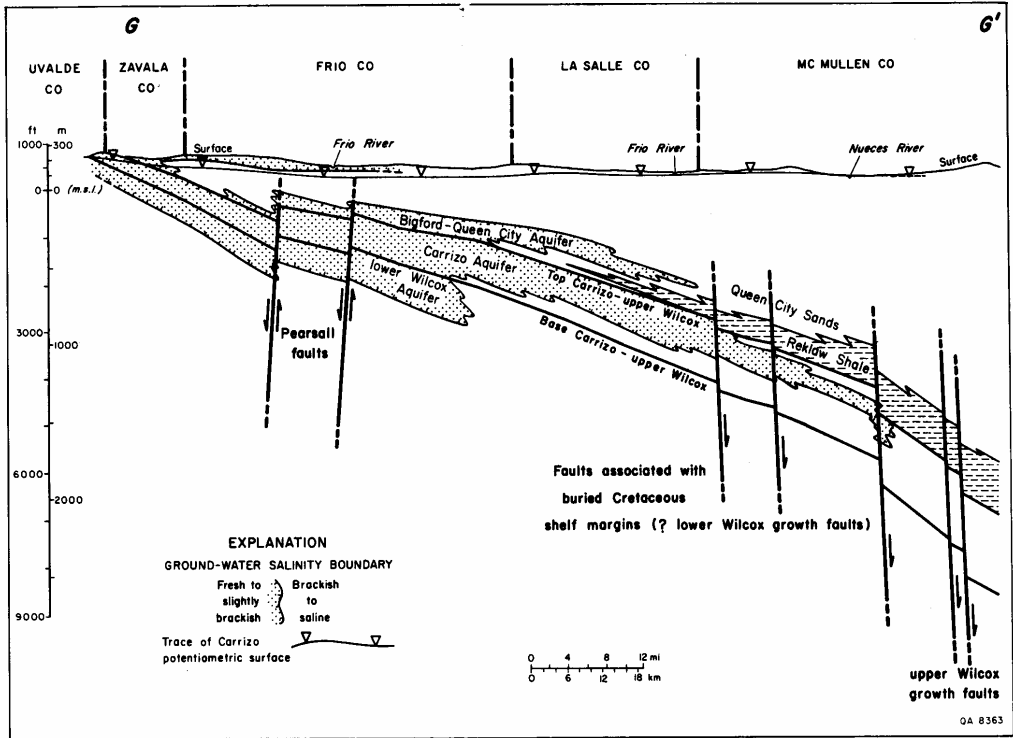


Figure 2.15 Structural cross-sections in the study area (after Hamlin, 1988).

3.0 PREVIOUS INVESTIGATIONS

The southern Carrizo-Wilcox aquifer has been studied by many investigators and numerous groundwater bulletins have been developed by the Texas Water Development Board for the counties in the study area. The two major hydrogeologic investigations in the model area are Klemt et al. (1976) and Hamlin (1988). Klemt et al. (1976) studied the groundwater resources of the Carrizo aquifer in the Wintergarden area. Klemt et al. (1976) included a comprehensive review of the available data concerning the aquifer including recharge, discharge, hydraulic conductivity, water quality, and groundwater availability. The study was a seminal study of groundwater in Texas because it included a groundwater model of the Carrizo aquifer in the Wintergarden region.

Hamlin (1988) focused on the depositional and sequence stratigraphy of the Carrizo and upper Wilcox in South Texas. Hamlin (1988) investigated the lithostratigraphy of the Carrizo and upper Wilcox and he mapped net sand thickness and sand percent within the study area which will be discussed further in Section 4 of this report. Hamlin (1988) also studied structure, hydraulic heads, flow patterns and geochemistry of the Carrizo and upper Wilcox in the study area. Both of these studies have been used and borrowed from extensively for the development of the Southern Carrizo-Wilcox GAM.

In addition to these groundwater flow studies, there have been several groundwater models developed with model domains that overlap this GAM study area. Figure 3.1 shows the model boundaries for the Southern Carrizo-Wilcox GAM as it relates to previous modeling study boundaries. Table 3.1 lists these previous investigations along with some basic model characteristics to provide a basis for the following discussion.

As previously mentioned, Klemt et al. (1976) developed a single-layer model of the Carrizo aquifer in the Wintergarden area to investigate future declines in water levels in the Carrizo aquifer. They performed three sets of simulations based on three criteria for future pumpage from the aquifer. The objective of the modeling was to assess the ability of the Carrizo aquifer to meet future demands. As one can see from Figure 3.1, the model area is nearly coincident with the GAM boundaries. From Table 3.1 it is important to note that the model was developed with a TWDB in-house simulator which was typical in the 1970s. The model was a single-layer model of the Carrizo and likely included much of the upper-Wilcox as it might be

defined by Hamlin (1988). The details regarding the calibration of this model are unknown. The model was used in a predictive mode to: (1) simulate regional water level declines 1970-2020, (2) determine the potential for Wilson County to provide up to 40,000 AFY of groundwater for municipal needs, and (3) see what pumping rate per unit area would be required to create a 400 foot decline in water levels throughout the Wintergarden area.

Table 3.1 Previous groundwater models of the Carrizo-Wilcox aquifer in the study area.

Model	Code	No. of Carrizo-Wilcox Layers	Calibration	Predictive Simulations
Klemt et al. (1976)	Research	1	unknown	1970 to 2020
Ryder (1988)	Research	2	Steady-state	No
Williamson et al. (1990)	Research	2	Steady-state (1980)	No
Thorkildsen et al. (1989)	MODFLOW	4	Steady-state (1985)	1985-2029
Ryder & Ardis (1991)	Research	2	Steady-state (1910) Transient (1910-1982)	Yes
Thorkildsen & Price (1991)	Unknown	4	Unknown	Unknown
LBG-Guyton & HDR (1998)	MODFLOW	2	Steady-state (1910); Transient (1910-1994)	1994-2050

Thorkildsen et al. (1989) modeled the Carrizo-Wilcox aquifer in the Colorado River Basin using MODFLOW. Their objective was to “provide a management tool for the Lower Colorado River Authority to evaluate the regional water-supply capabilities of the Carrizo-Wilcox aquifer within the Colorado River Basin”. Their three-dimensional model extended from the ground surface to the base of the Wilcox Group. The model was calibrated as a steady-state model to aquifer conditions in 1985. The model was used to predict future conditions in the aquifer from 1985 through 2029 based on estimated future pumping as documented in the TWDB 1984 State Water Plan.

Thorkildsen and Price (1991) report that a three-dimensional model of the Carrizo-Wilcox aquifer in central Texas was constructed as part of their study. Little is known regarding the details of this model, but it is expected that it was an extension of the 1989 model. The model was designed to evaluate the occurrence, availability, and quality of ground water in the Carrizo-Wilcox aquifer.

In 1998, LBG-Guyton Associates and HDR Engineering, Inc. developed a groundwater model with a focus on the interaction between surface water and groundwater in the

Wintergarden area (LBG-Guyton & HDR, 1998). The model was an extension of the Klemm et al. (1976) Carrizo model and modeled from the base of the Wilcox through the Yegua Formation. The model was developed with MODFLOW and results from the groundwater model were used to predict changes in surface water flows using proprietary surface water models of the area's river basins developed by HDR Engineering, Inc. Two model calibrations were performed: a steady-state calibration to predevelopment conditions (1910) and a transient calibration from 1910 through 1994. The calibrated model was then used to predict future conditions from 1994 through 2050 for three future pumping scenarios; (1) 1994 pumping (249,890 AFY), (2) 2050 pumping from 1994 through 2050 (264,715 AFY), and (3) 2050 plus (449,952 AFY including 185,237 additional AFY in Atascosa, Dimmit, Gonzales, and Wilson counties). Rick Hay at Texas A&M-Corpus Christi is currently (2002) using this model for the Evergreen Underground Water Conservation District to investigate future water resource strategies currently being considered by the Region L Planning Group and the San Antonio Water Supply.

In addition to these regional models, the United States Geological Survey (USGS) has developed super-regional models which incorporate the entire Carrizo-Wilcox aquifer in Texas (Ryder, 1988; Ryder and Ardis, 1991) and in the entire Gulf Coast Region (Williamson et al., 1990) as part of the RASA (Regional Aquifer-System Analysis) studies. Their analyses modeled from the Midway Formation through the Gulf Coast aquifer systems. The Carrizo-Wilcox aquifer was modeled as two layers, generally a lower and middle Wilcox aquifer and an upper Wilcox and Carrizo aquifer. Ryder (1988) reported that the model objectives were to define the hydrogeologic framework and hydraulic characteristics of the Texas coastal plain aquifer systems, delineate the extent of freshwater and density of saline water in the various hydrogeologic units, and describe the regional groundwater flow system. A steady-state calibration to predevelopment conditions was performed using a research code developed by Kuiper (1985).

The entire U.S. Gulf Coast aquifer system above the Midway Formation was modeled by Williamson et al. (1990) using the research code developed by Kuiper (1985). The model consisted of a steady-state calibration to predevelopment conditions, a steady-state calibration to 1980 water-level data, and transient simulations from 1935 to 1980. The model objectives were "to help in the development of quantitative appraisals of the major ground-water systems of the

United States, and to analyze and develop an understanding of the ground-water flow system on a regional scale, and to develop predictive capabilities that will contribute to effective management of the system”.

Ryder and Ardis (1991) extended the work performed by Ryder (1988) and developed another model of the coastal plain aquifers in Texas. The model, developed using the research code developed by Kuiper (1985), was calibrated to both steady-state predevelopment conditions and transient conditions from 1910 to 1982. In addition, transient predictive simulations were performed using the calibrated model. The objectives for the modeling study consisted of: (1) defining the hydrogeologic framework and hydraulic characteristics of the aquifer systems, (2) delineating the extent of fresh to slightly saline water in various hydrogeologic units, (3) describing and quantifying the groundwater flow system, (4) analyzing the hydrologic effects of man’s development on the flow system, and (5) assessing the potential of the aquifer systems for further development.

Each of these models provides information which is both relevant and useful to the study of groundwater availability in the southern Carrizo-Wilcox aquifer study area. However, many traits of the previous investigations have made development of the current GAM necessary to meet the GAM specifications defined by the TWDB. Specifically, GAM models are expected to (1) be well documented and publicly available, (2) utilize standard modeling tools which are non proprietary (MODFLOW), and (3) be calibrated both steady-state and transiently and capable of adequately simulating a verification period to a pre-defined calibration criteria.

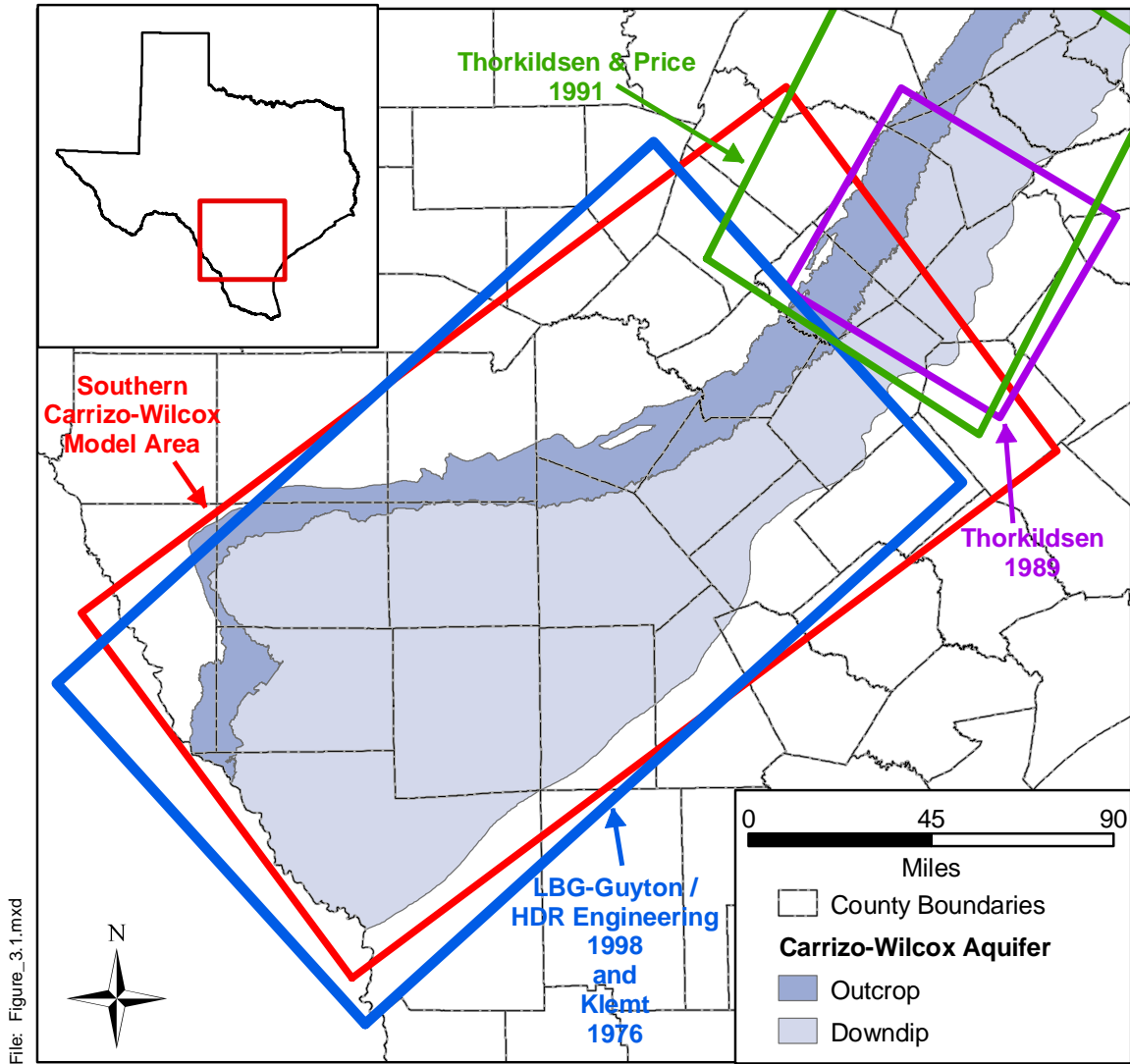


Figure 3.1 Southern Carrizo-Wilcox GAM model boundary with previous modeling study boundaries which have included the Carrizo-Wilcox aquifer.

4.0 HYDROGEOLOGIC SETTING

The hydrogeologic setting of the Carrizo-Wilcox aquifer is defined by the hydrostratigraphy, hydraulic properties, structure, regional groundwater flow, surface and groundwater interaction, and recharge and discharge. The characterization of the hydrogeologic setting is based on previous geologic and hydrologic studies in the area and a detailed compilation and analysis of structure maps, hydraulic properties, water-level data, spring and stream flow data, and climatic information.

4.1 Hydrostratigraphy

The Carrizo-Wilcox aquifer extends from South Texas northeastward through East Texas into Arkansas and Louisiana. The aquifer consists of fluvial-deltaic sediments of the upper Paleocene and lower Eocene Wilcox Group and Carrizo Sand. The aquifer is bounded below by marine deposits of the Midway Group and above by the Reklaw and Bigford formations, representing a semi-confining unit between the Carrizo Sand and the shallow aquifer, the Queen City Formation.

The Southern Carrizo-Wilcox GAM model area extends from the groundwater divide between the San Marcos and Colorado rivers to the Rio Grande to the south. In this area, the Wilcox Group is subdivided into a lower, middle, and upper Wilcox. The upper Wilcox in the deeper subsurface is correlated to the Carrizo Formation in the outcrop (Bebout et al., 1982; Hamlin, 1988). Bebout et al. (1982) mapped the lower contact of the upper Wilcox based on the lower regional marker identified in geophysical logs by Fisher and McGowen (1967). Hamlin (1988) also combined the Carrizo and upper Wilcox and mapped the base of the upper Wilcox as a distinct facies change from a fluvial (bed-load channel system) and mixed alluvial facies in the upper Wilcox to a predominantly marine facies (delta, prodelta) in the middle Wilcox.

In comparison, Klemt et al. (1976) lithologically picked the base of the Carrizo aquifer as the top of the Wilcox Group by identifying the base of the major sand units of the Carrizo Formation. Klemt's mapped Carrizo Formation correlates with the Carrizo, as mapped in central Texas (Ayers and Lewis, 1985), and was used as a layer for the southern model. However, the definition of the upper Wilcox required combining two different data sources having somewhat different interpretations. In order to discriminate the sand facies of the upper Wilcox from the

middle Wilcox, the thickness difference between the Carrizo Sand mapped by Klemt et al. (1976) and the Carrizo-upper Wilcox mapped by Hamlin (1988) was used as the upper Wilcox layer. In much of the updip section, Hamlin's base of the upper Wilcox intersects Klemt's base of Carrizo. For layer consistency, we assumed that in this area the upper Wilcox layer thins to a minimum thickness having the same characteristics as the underlying middle Wilcox.

The Carrizo-upper Wilcox in the southern GAM area is characterized by three distinct depositional systems, including a mixed alluvial system, a bed-load channel system, and a deltaic system (Hamlin, 1988). The bed-load channel system comprises the massive sand typically associated with the Carrizo aquifer, but also contains some sandy mud. The mixed alluvial system consists of interbedded sand and mud associated with channel sands and abandoned channel fill, levee and crevasse splay, floodplain, lacustrine, and delta plain sediments. The deltaic system consists of delta-front sand, which changes to prodelta mud basinward. This change to marine facies was considered the boundary between the upper and middle Wilcox (Hamlin, 1988). The middle Wilcox includes several transgressive flooding events and consists of various deltaic facies that form a partial hydrologic barrier between the fluvial-deltaic sediments of the lower Wilcox, and the predominant fluvial system of the Carrizo-upper Wilcox (Galloway et al., 1994).

The Reklaw Formation above the Carrizo corresponds to a more extensive transgressive flooding event and consists predominantly of marine mud, which grades in the southwestern part of the study area to non-marine mud and sands of the Bigford Formation.

The Queen City Formation represents another deltaic depositional system consisting of sands and clays and which is separated from the Sparta Sand by marine clays of the Weches Formation. In the southwest portion of the study area, the lower part of the Queen City grades into the Bigford Formation and the upper part into the El Pico clay. The overlying Sparta sand correlates to the basal sands of the Laredo Formation southwest of the Frio River.

The hydrostratigraphic layers of the Carrizo-Wilcox aquifer for the Southern Carrizo-Wilcox GAM (Figure 4.1.1) include the main depositional facies of the Wilcox Group and the Carrizo Sand. The Reklaw confining unit and Bigford Formation are represented by a single layer, accounting for variations in aquitard thickness and facies change from predominantly marine clay to mixed clay and sand in the southwestern portion of the study area. The Queen

City aquifer is included as the top layer of the model to better simulate the hydraulic gradient across the Reklaw confining unit. This allows for better determination of the leakage between the Carrizo and the shallow Queen City aquifer. Younger formations that lie above the Queen City in the southern part of the model are represented in the model by general head boundary conditions accounting for the hydraulic connection between the Queen City and the shallow water table.

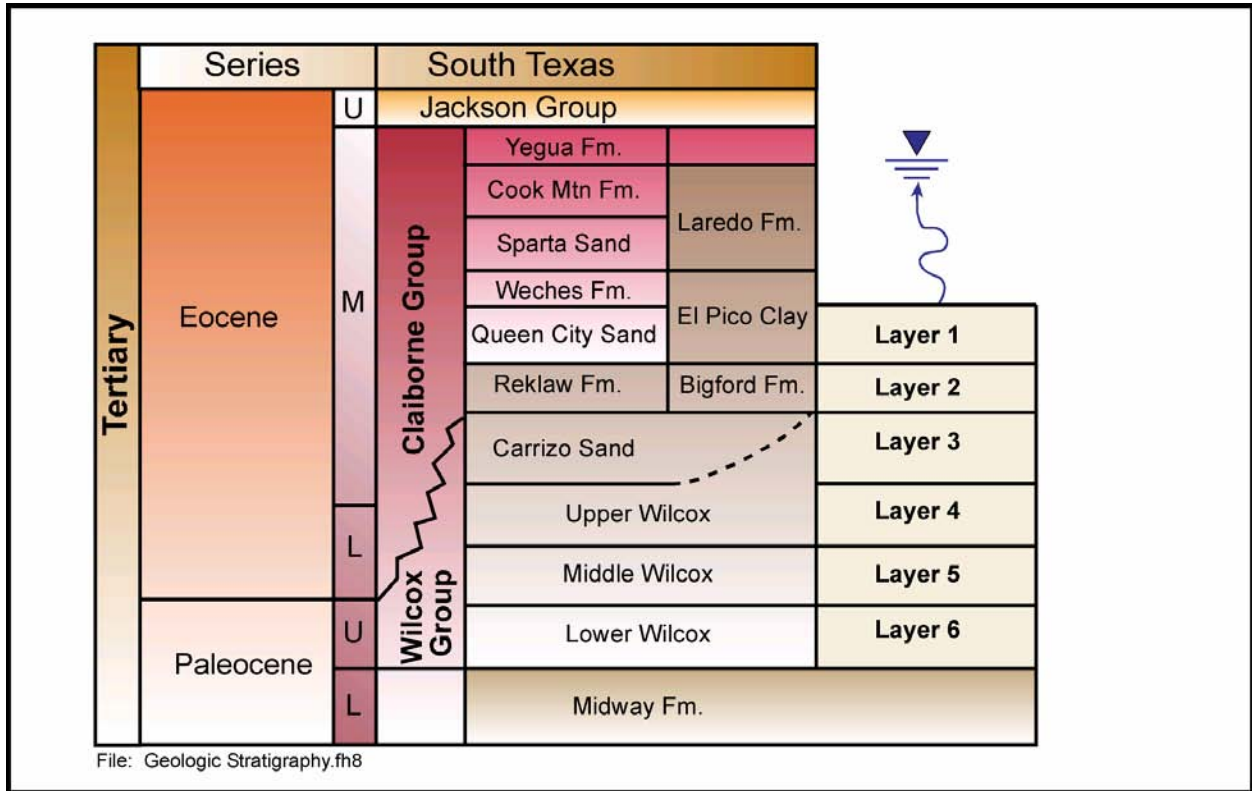


Figure 4.1.1 Hydrostratigraphy and model layers.

4.2 Structure

The structural setting for the Southern Carrizo-Wilcox GAM is dominated by the Rio Grande Embayment, the San Marcos Arch, and the growth faults along the downdip boundary of the model area. (Figure 4.2.1). The Wilcox Group and Carrizo Formation represent the earliest sand/mud sequence within the Gulf Coast Tertiary section. Cenozoic deposition is characterized by an offlapping progression of successive, basinward thickening wedges (Galloway et al., 1994). During deposition of each sediment wedge, deposition focused along sand-rich continental margin deltaic centers. The Rio Grande Embayment is the principal depocenter in the study area. Stable arches occupy the regions between embayments and are areas of lesser subsidence and deposition. In the study area, the San Marcos Arch separates the Rio Grande Embayment to the southwest from the Houston Embayment to the northeast. Growth fault trends exist within the Wilcox Group in areas where Wilcox deltas prograded basinward past the Cretaceous Stuart City Shelf Margin (Bebout et al., 1982). Displacement of sediments occurred across these faults during burial and loading, isolating pore fluids within sands and shales and preventing dissipation of pore fluids during compaction. As a result, pore fluids within the growth fault trends are at pressures above hydrostatic and are poorly connected to the up-dip portions of the aquifers.

Today the Carrizo-Wilcox aquifer outcrops in a band 10 to 20 miles wide that is sub parallel to the present-day coastline. The Carrizo-Wilcox aquifer dips into the subsurface at an average dip of 100 feet per mile. The structure surfaces of the different hydrostratigraphic units used for the Southern Carrizo-Wilcox GAM are based on many different sources, which are summarized in Table 4.2.1.

The processing of the structure data required several steps. The data from the different sources were digitized and converted to GAM coordinates and merged for the individual structure surfaces. The data were initially kriged to identify problems. Problems were solved through a combination of eliminating or adding source data or defining guide data points to constrain the kriging algorithm. The data were kriged again and delimited to the corresponding subcrop areas. The kriged and delimited data were then merged with the outcrop elevation grid, which was developed from U.S. Geological Survey digital elevation model (DEM) data. The

final kriged structure surfaces were then used to calculate layer thicknesses, which were checked to insure that layer thicknesses are not less than 20 ft throughout the model.

Figures 4.2.2 through 4.2.8 show the structure contour maps for the different hydrostratigraphic units. The structure maps identify the data control point locations and identify the data sources. The base of the Wilcox dips southeast toward the gulf coast. The overall dip of the structure surface generally increases from the south to the north (Figure 4.2.2). The top of the Lower Wilcox, shown in Figure 4.2.3, shows a similar structure as the base of the Wilcox. The data base for the bottom and top of the lower Wilcox is primarily from the USGS RASA study (Wilson and Hosman, 1987) and from Bebout et al. (1982), respectively, which both correlate with the structure surfaces in the Central Carrizo-Wilcox GAM area.

The top of the middle Wilcox is largely derived from the base of the upper Wilcox as mapped by Hamlin (1988), with additional data points from Bebout et al. (1982) in the northeastern part (Figure 4.2.4). This layer surface does not correlate with the central GAM area, because the middle Wilcox in the central GAM area is represented by the Simsboro Formation, which is mapped as the major sand layer of the Wilcox Group. South of the Colorado River, the sand thins and the Simsboro is not identifiable in geophysical logs. Figure 4.2.4 also shows the updip limit of the upper Wilcox, where the base of the upper Wilcox as mapped by Hamlin (1988) crosses the base of the Carrizo Formation as mapped by Klemt et al. (1976).

The top of the upper Wilcox corresponds to the base of the Carrizo Sand as mapped by Klemt et al. (1976), which is correlated to the top of the Wilcox in the central Carrizo Wilcox GAM (Figure 4.2.5). Similarly, the top of the Carrizo Sand is based on Klemt et al. (1976) and is correlated with the data from the Central Carrizo-Wilcox GAM (Figure 4.2.6). Additional data from TWDB (1972) were used in the downdip section. The top of the Reklaw and Bigford formations, shown in Figure 4.2.7, was based on multiple data sources (Table 4.2.1) and the top of the uppermost layer, representing the Queen City and El Pico formations (Figure 4.2.8) was based on data used in LBG-Guyton and HDR (1998).

The Gonzales County Underground Water Conservation District also provided structure data based upon boreholes in Gonzales County. Their data agreed well with the structure surfaces developed for the model on a regional basis.

The thickness maps of the various hydrostratigraphic units are shown in Figures 4.2.9 through 4.2.15, which were constructed based on the elevation difference in the structure contour maps (Figures 4.2.2 through 4.2.8). The thickness of the lower Wilcox generally increases downdip to as much as about 1800 ft (Figure 4.2.9). Note that actual data in the downdip section in the northeastern portion of the study area were limited (Figure 4.2.2 and 4.2.3) and the resulting thickness variation in this area is considered to be uncertain. The thickness of the middle Wilcox typically shows more variation reaching as much as 1000 ft in the southern part of the study area and increasing to as much as 1800 ft (Figure 4.2.10) in the northeastern part of the study area.

The upper Wilcox is comparatively thin (Figure 4.2.11) with a typical thickness range of 100 to 600 ft. As mentioned above, the updip limit is somewhat artificial because of the two different interpretations for the base of the Carrizo used by our data sources. In the model, the layer is extended beyond the updip limit with a uniform thickness of 20 ft, having properties identical to the middle Wilcox.

The thickness of the Carrizo Sand corresponds to that of Klemm et al. (1976) and is shown in Figure 4.2.12. The Carrizo is the main aquifer unit of the Southern Carrizo-Wilcox GAM. The thickness increases in the confined section to between 200 and 1100 ft, with a trend of greater thickness in the central and northeast areas as compared to the southwestern portion of the study area.

The thickness of the confining layer, represented by the Reklaw Formation in the northeast and the Bigford Formation in the southwest is shown in Figure 4.2.13. The thickness of the Reklaw is typically less than 300 ft; only toward the downdip boundary does the thickness increase significantly above 300 ft. The Bigford Formation southwest of the Frio River shows a somewhat higher thickness of about 500 ft increasing to over 800 ft near the downdip boundary (Figure 4.2.13). The uppermost model layer represents the Queen City Formation in the northeast and the El Pico Clay in the southwest (Figure 4.2.14). This layer ranges in thickness between 200 and 1500 ft in the confined section. Figure 4.2.15 provides a thickness map of the younger sediments overlying the Queen City. These units are not explicitly modeled in the GAM.

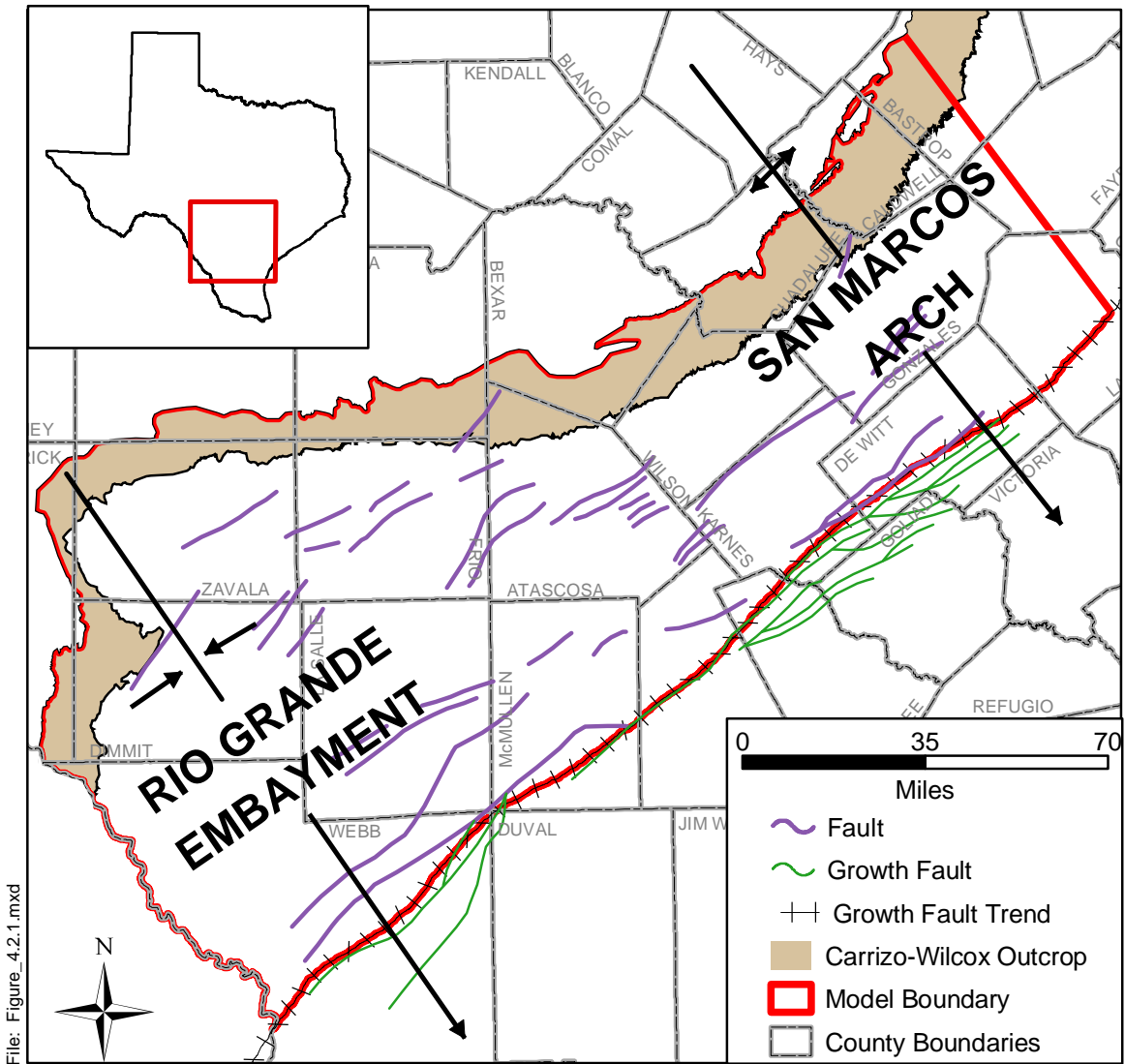
The major growth faults represent the downdip limit of the model area, where the different layers are displaced downward, effectively disconnecting downward flow paths. There are a number of smaller faults farther updip that are generally parallel to the growth fault trend (Figure 4.2.1). These faults may affect local groundwater flow pattern, but most of these faults are relatively small and do not offset the entire thickness of the modeled aquifers.

Table 4.2.1 Data sources for layer elevations for the southern Carrizo-Wilcox model.

Model Layer Boundary	LBG-Guyton and HDR (1998)	Klemt et al. (1976) (TWDB)	Wilson and Hosman (1988) (USGS RASA)	TWDB (1972)	Anders (1960) and Shafer (1965)	Hamlin (1988) (BEG)	Bebout et al. (1982) (BEG)	Central Carrizo-Wilcox GAM Model	Surface Elevations (USGS DEM)
Top of Queen City/El Pico	X								X
Top of Reklaw/Bigford	X		X		X			X	X
Top of Carrizo		X		X				X	X
Top of Wilcox		X						X	X
Top of Middle Wilcox						X	X		X
Top of Lower Wilcox							X	X	X
Base of Wilcox			X				X	X	X

Data format for the data sources:

Data Source	Report Number	Format
Klemt et al. (1976)	TWDB Report 210	Arc Info files of elevation contours provided by the Austin office of the USGS.
Wilson and Hosman (1988) - RASA	USGS Open-File Report 87-677	Printed tables.
TWDB (1972)	TWDB Report 157	Elevation contour map.
Shafer (1965) (Gonzales County)	TWDB Report 4	Geologic sections and a base map.
Anders (1960) (Karnes County)	TBWE Bulletin 6007	Geologic sections and a base map.
Hamlin (1988)	BEG RI No. 175	Elevation contour map and isopach map.
Bebout et al. (1982)	BEG RI No. 117	Geologic sections and a base map.
Central Carrizo-Wilcox GAM Model		Text files containing x, y, and elevation.
LBG-Guyton and HDR (1998)		MODFLOW input files
Surface Elevations		DEM files.



Source: Online: Texas Water Development Board, September 2002 and Hamlin, 1998

Figure 4.2.1 Structural setting of the study area.

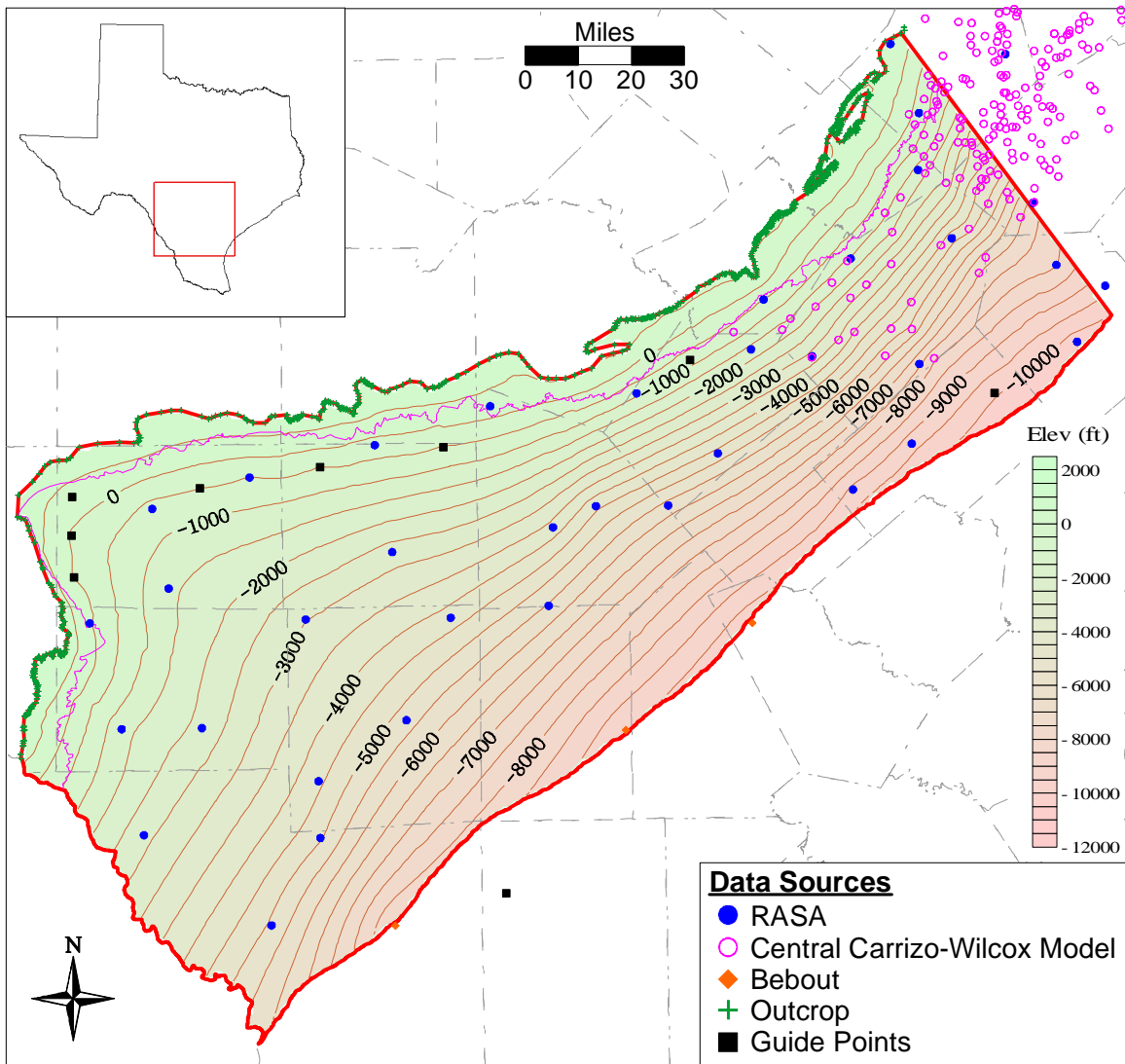


Figure 4.2.2 Structure contour map of the base of the Wilcox Group.

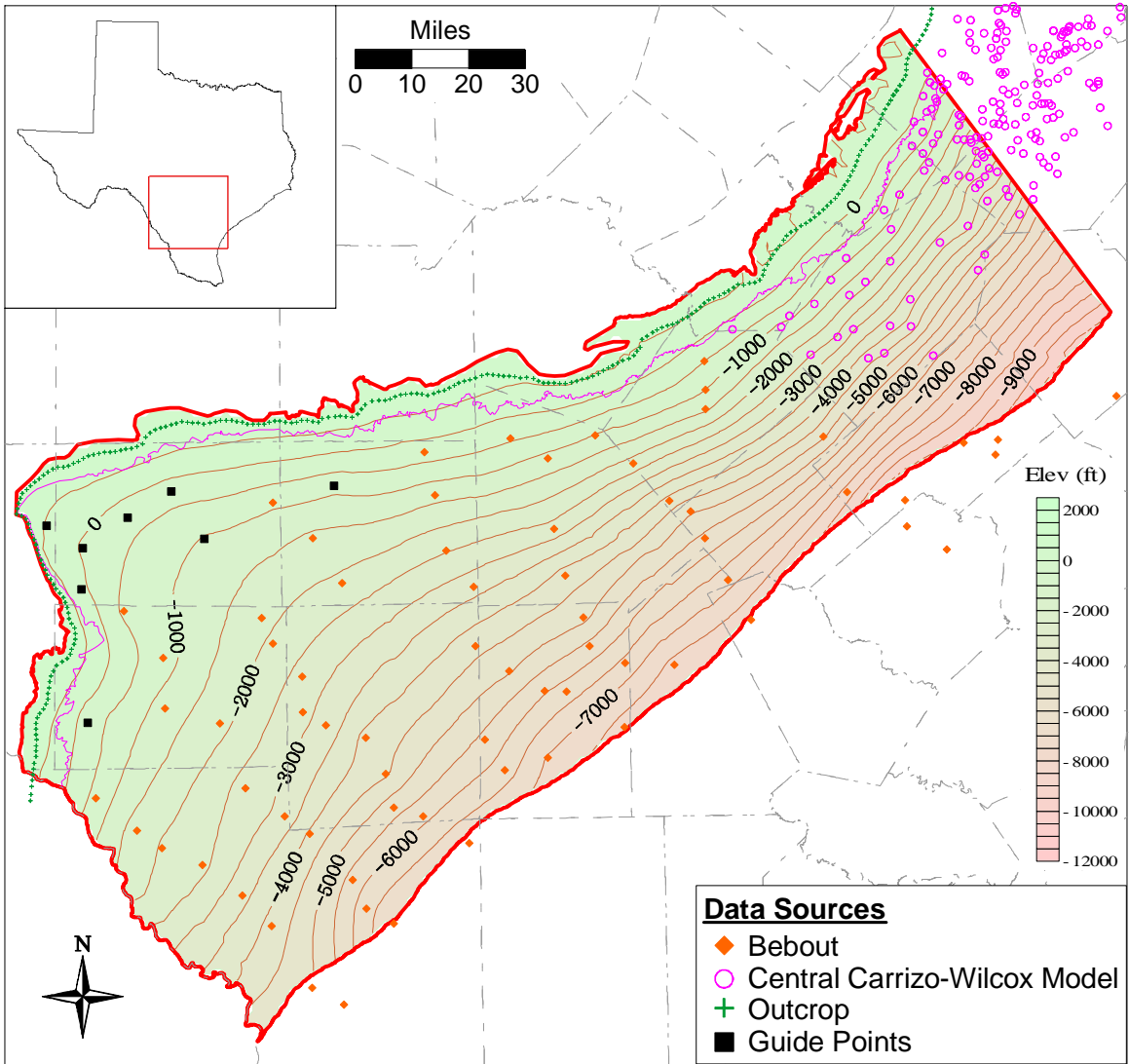


Figure 4.2.3 Structure contour map of the top of the lower Wilcox.

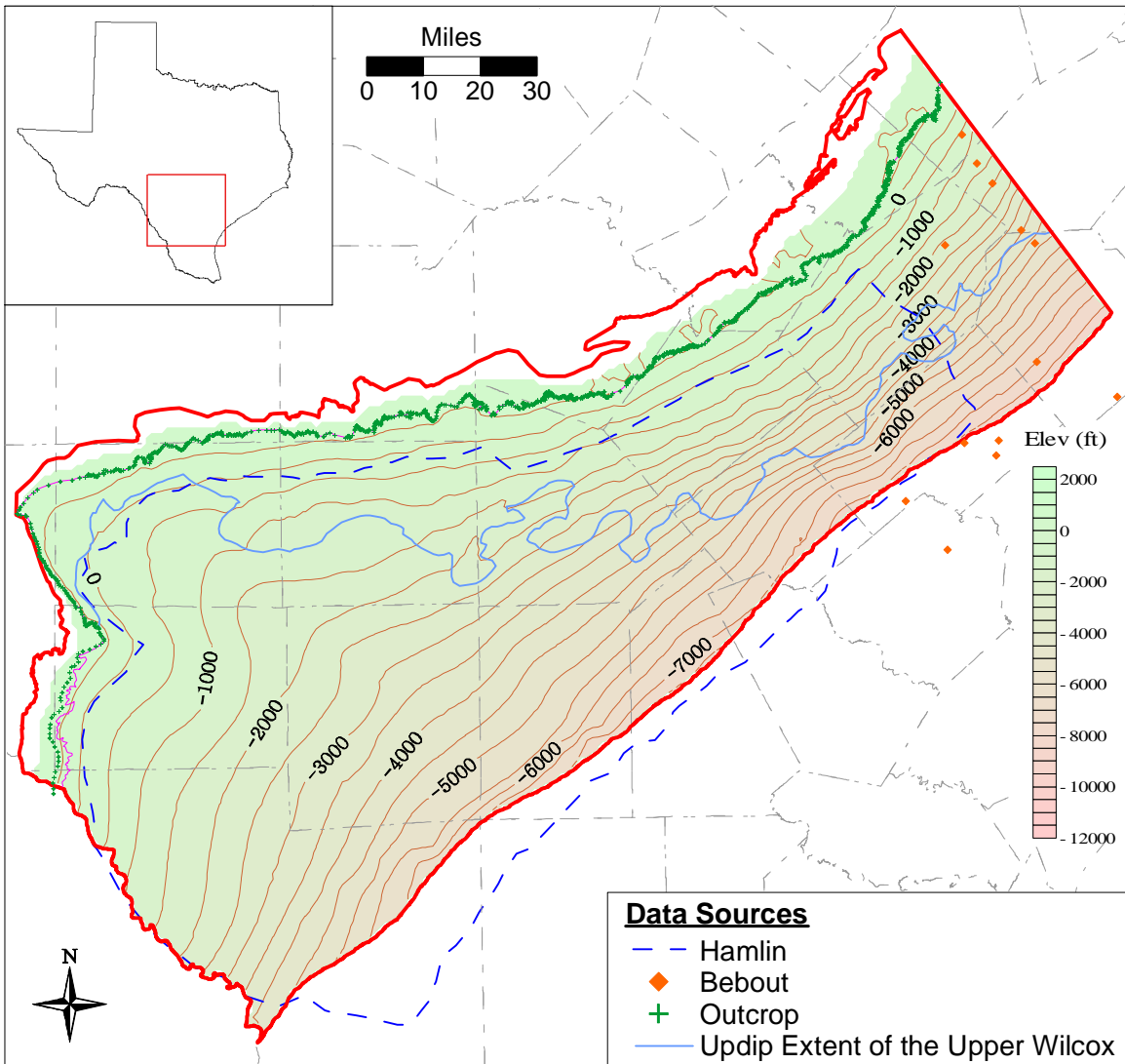


Figure 4.2.4 Structure contour map of the top of the middle Wilcox.

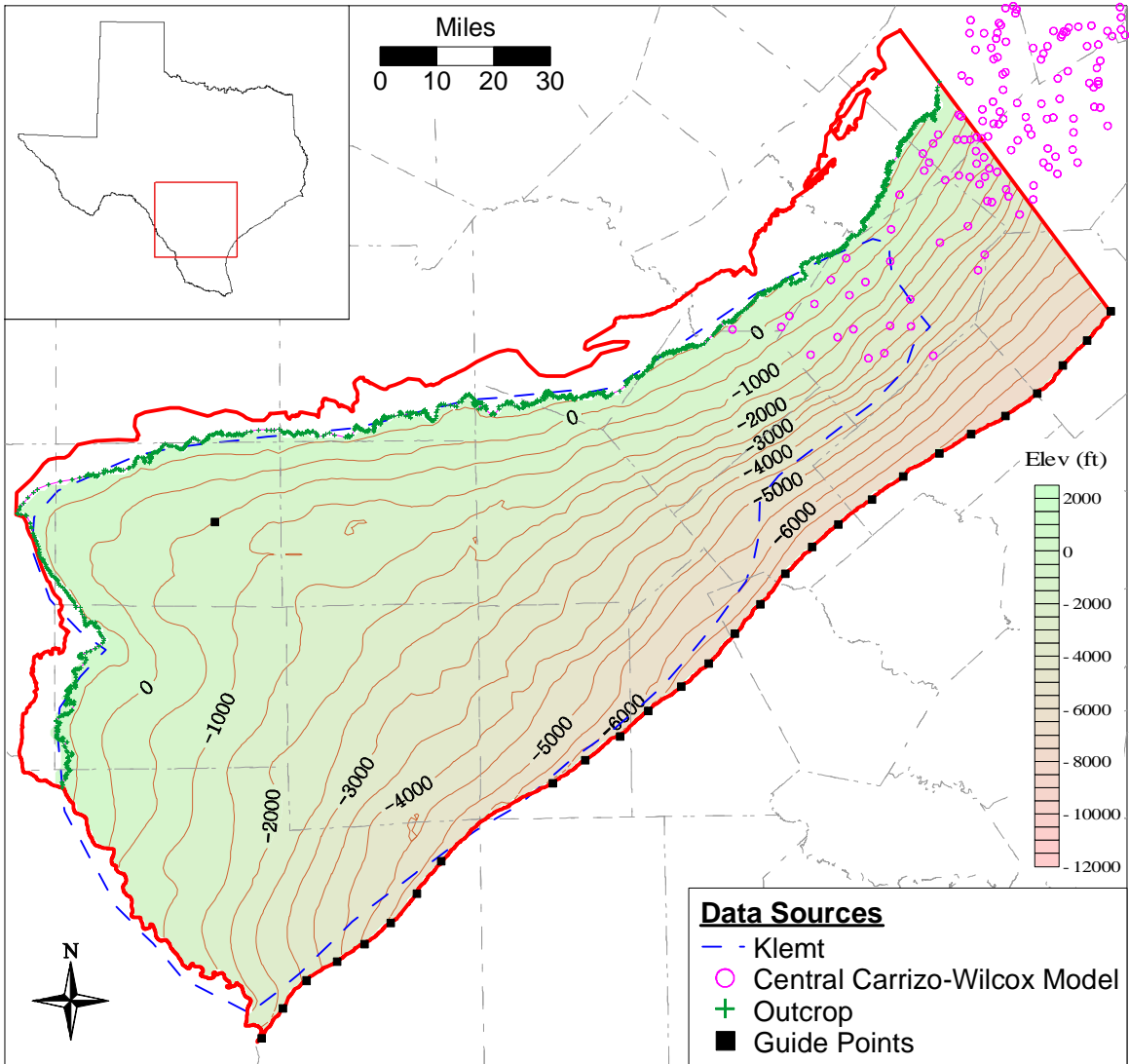


Figure 4.2.5 Structure contour map of the top of the Wilcox Group.

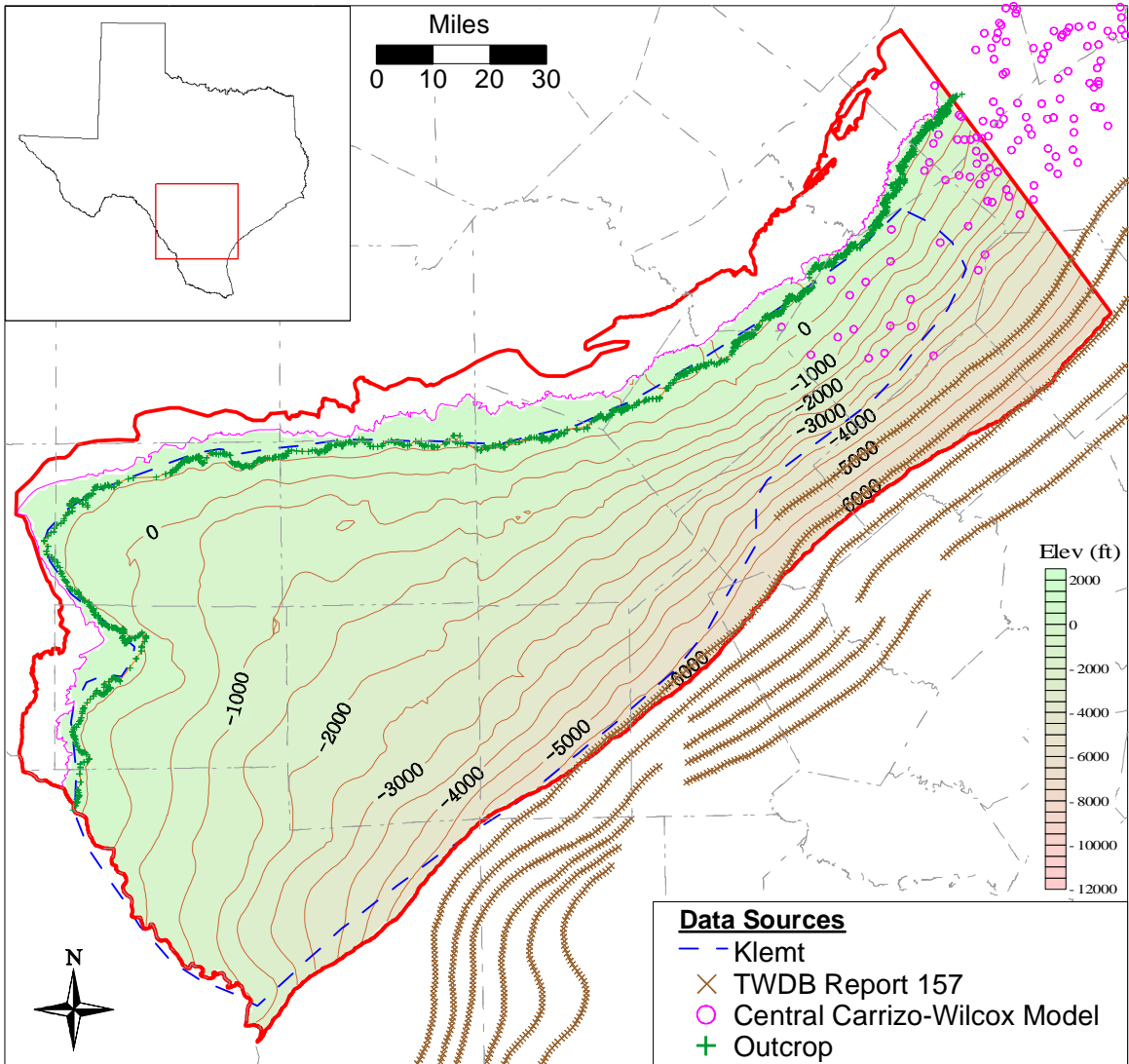


Figure 4.2.6 Structure contour map of the top of the Carrizo.

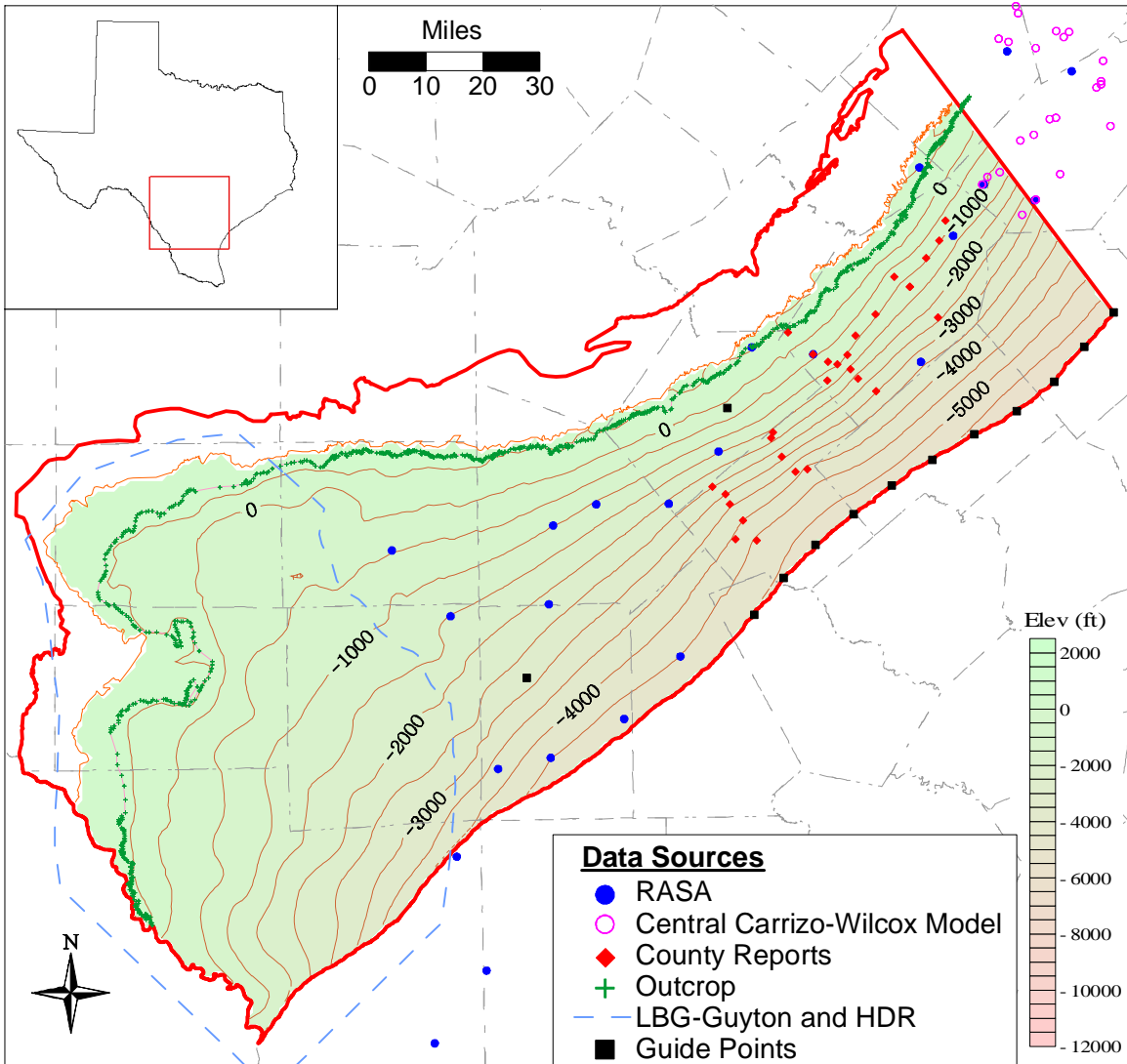


Figure 4.2.7 Structure contour map of the top of the Reklaw/Bigford formations.

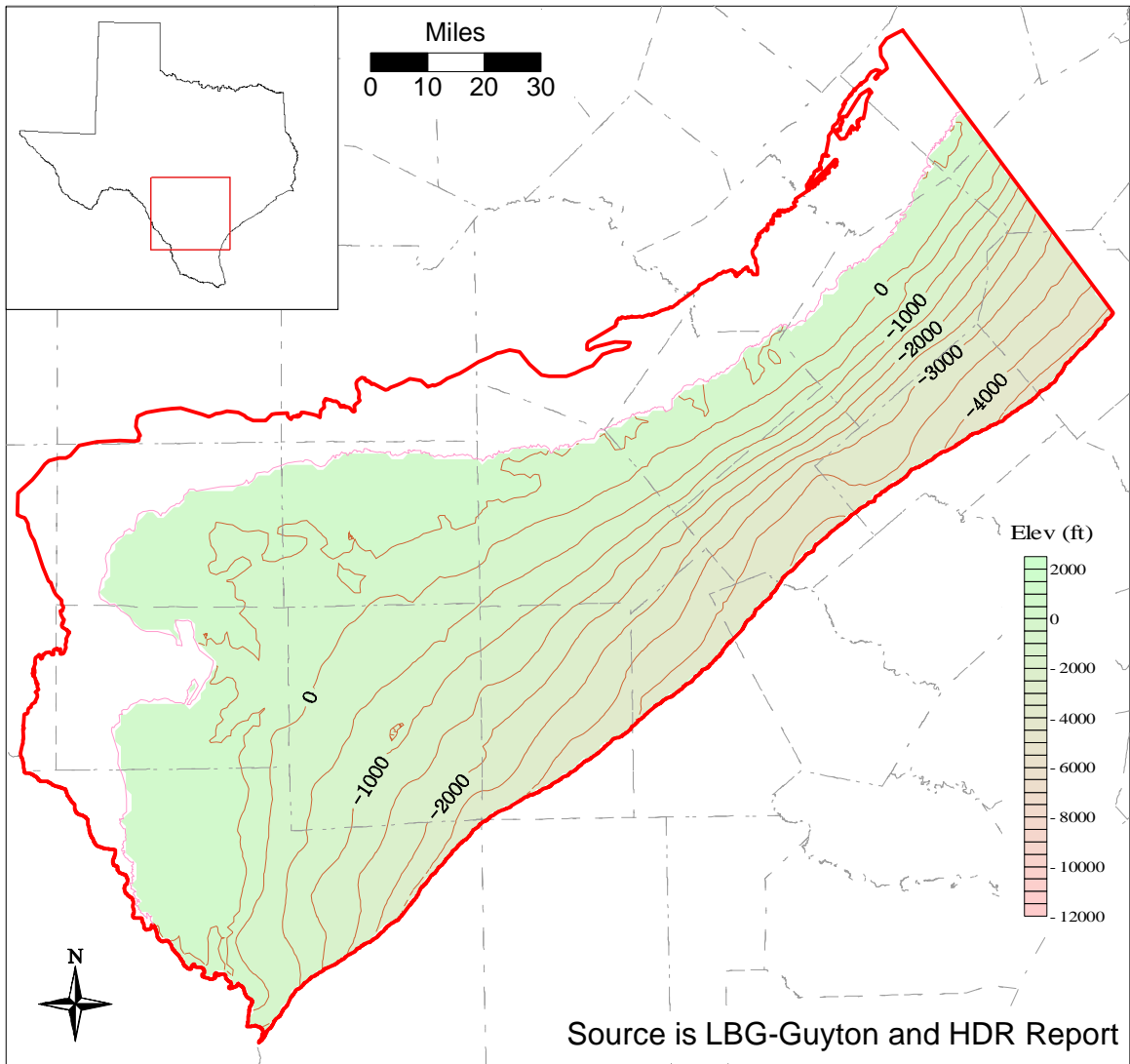


Figure 4.2.8 Structure contour map of the top of the Queen City/El Pico.

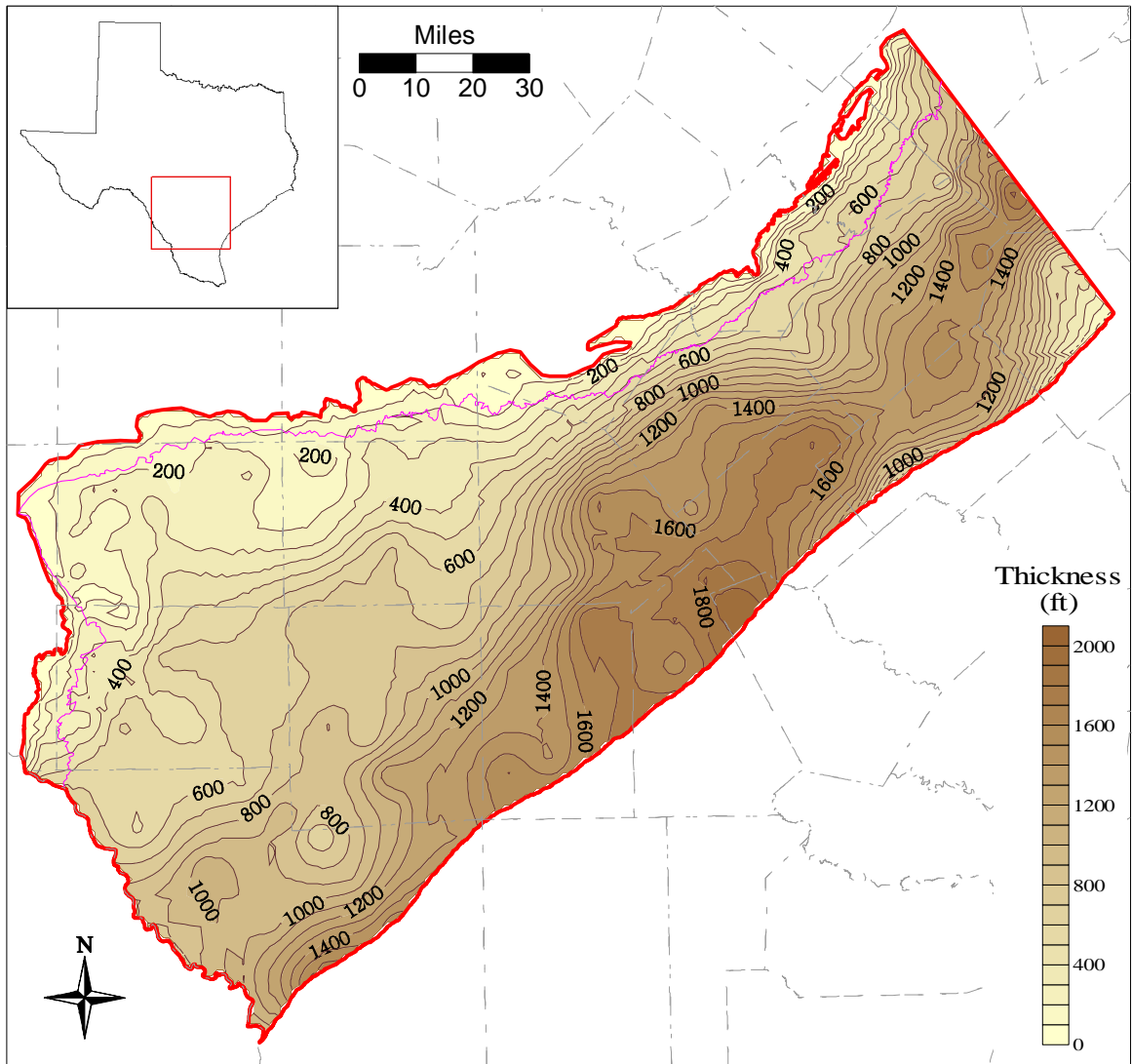


Figure 4.2.9 Thickness map of the lower Wilcox.

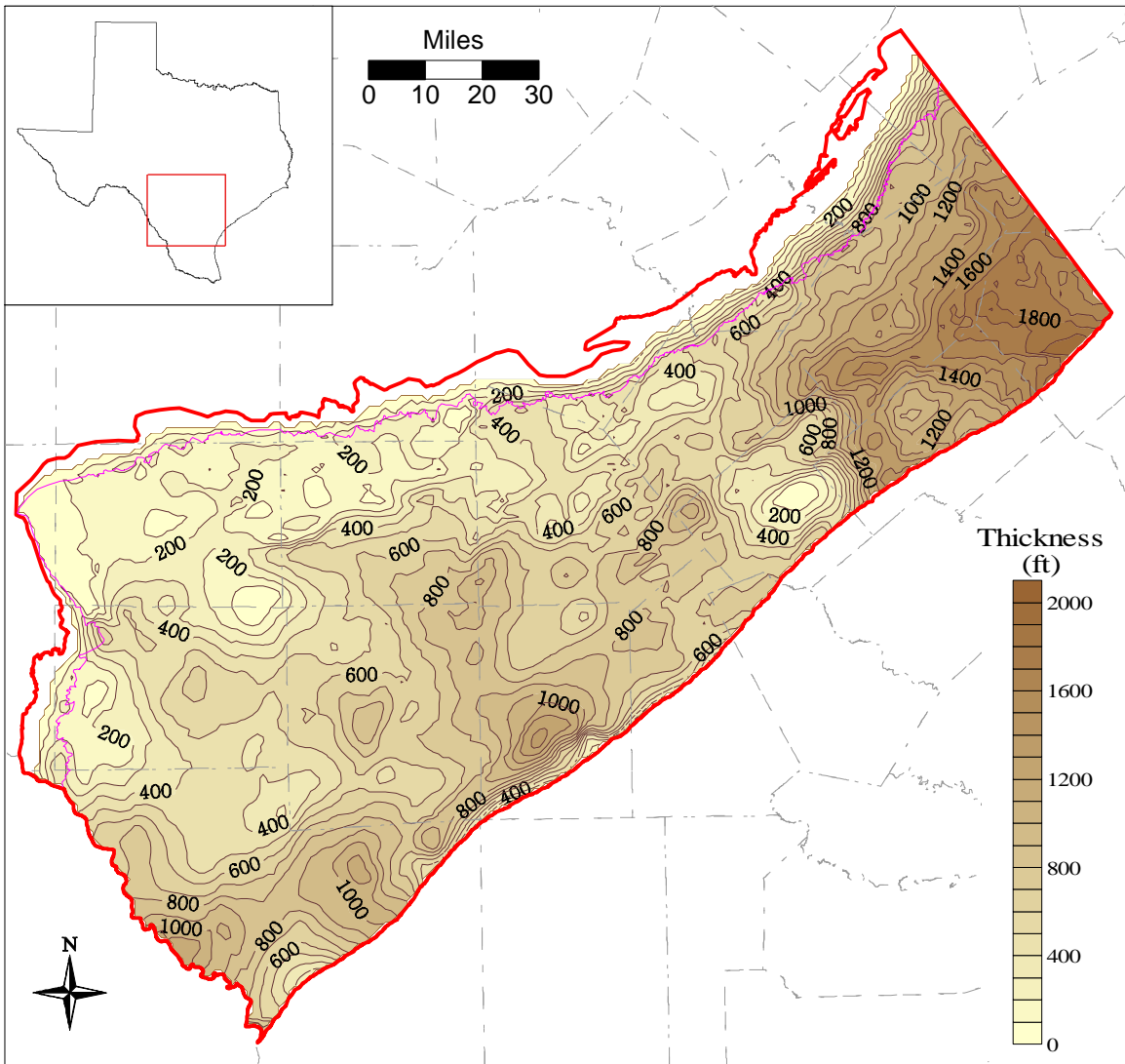


Figure 4.2.10 Thickness map of the middle Wilcox.

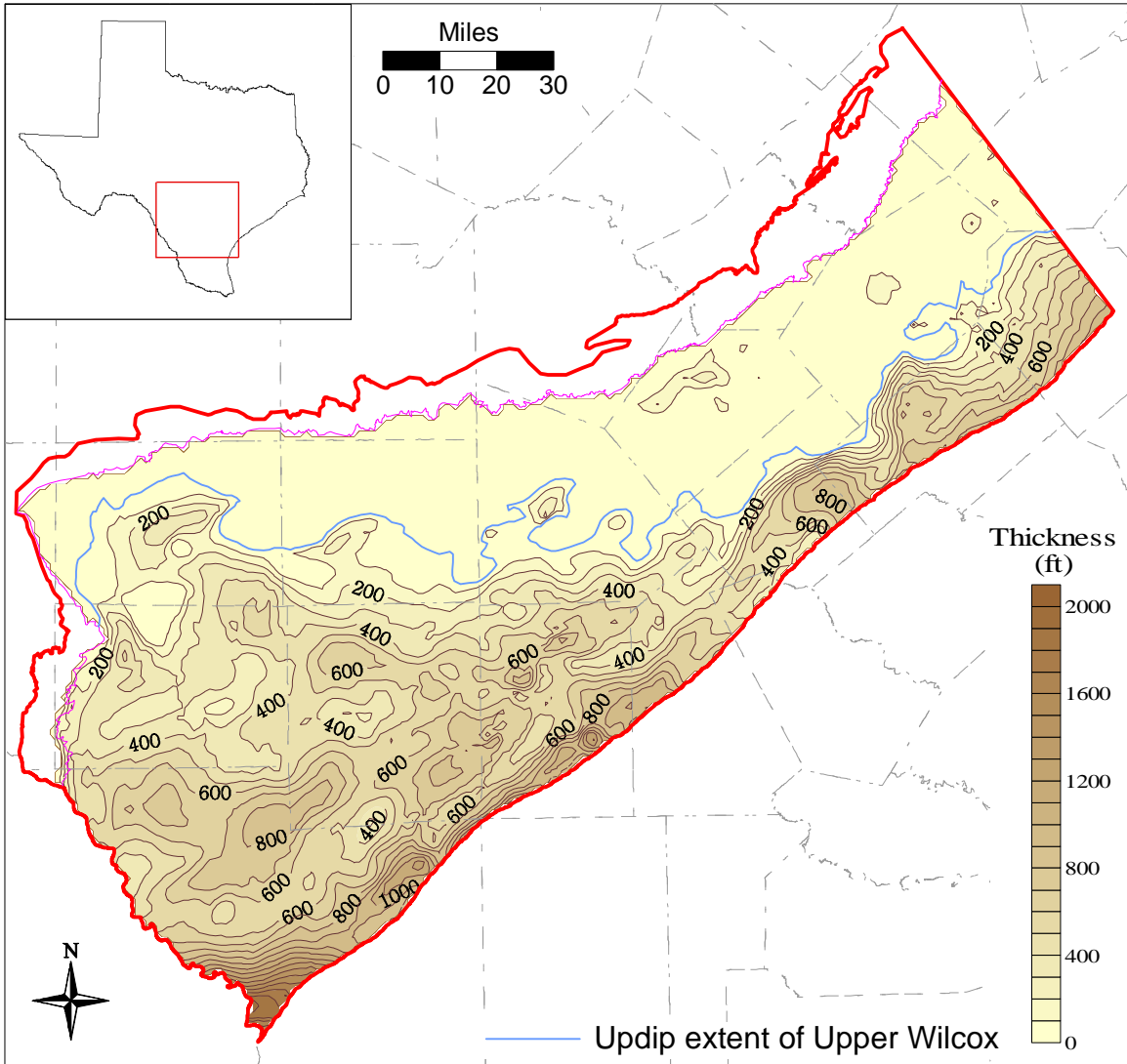


Figure 4.2.11 Thickness map of the upper Wilcox.

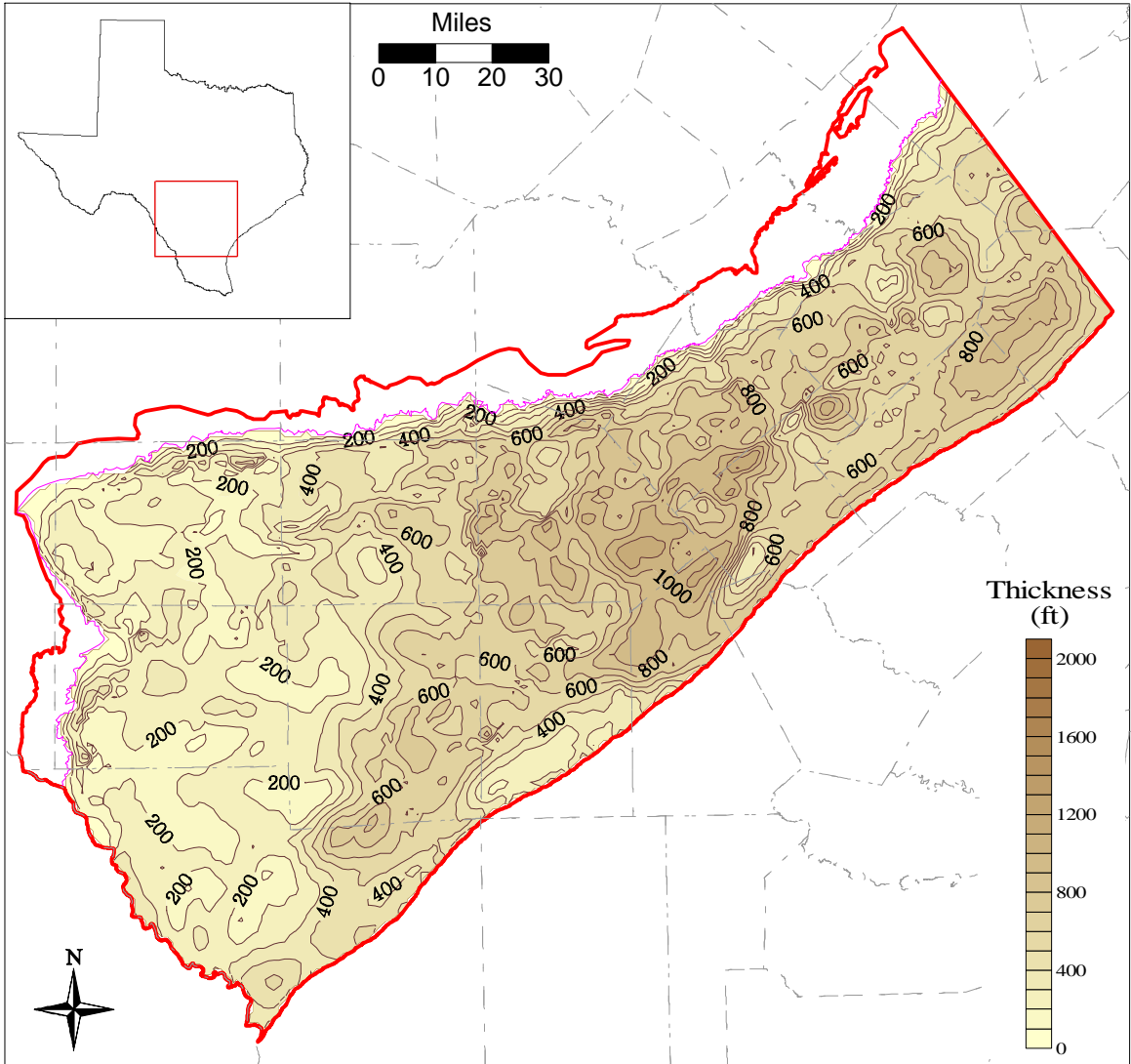


Figure 4.2.12 Thickness map of the Carrizo.

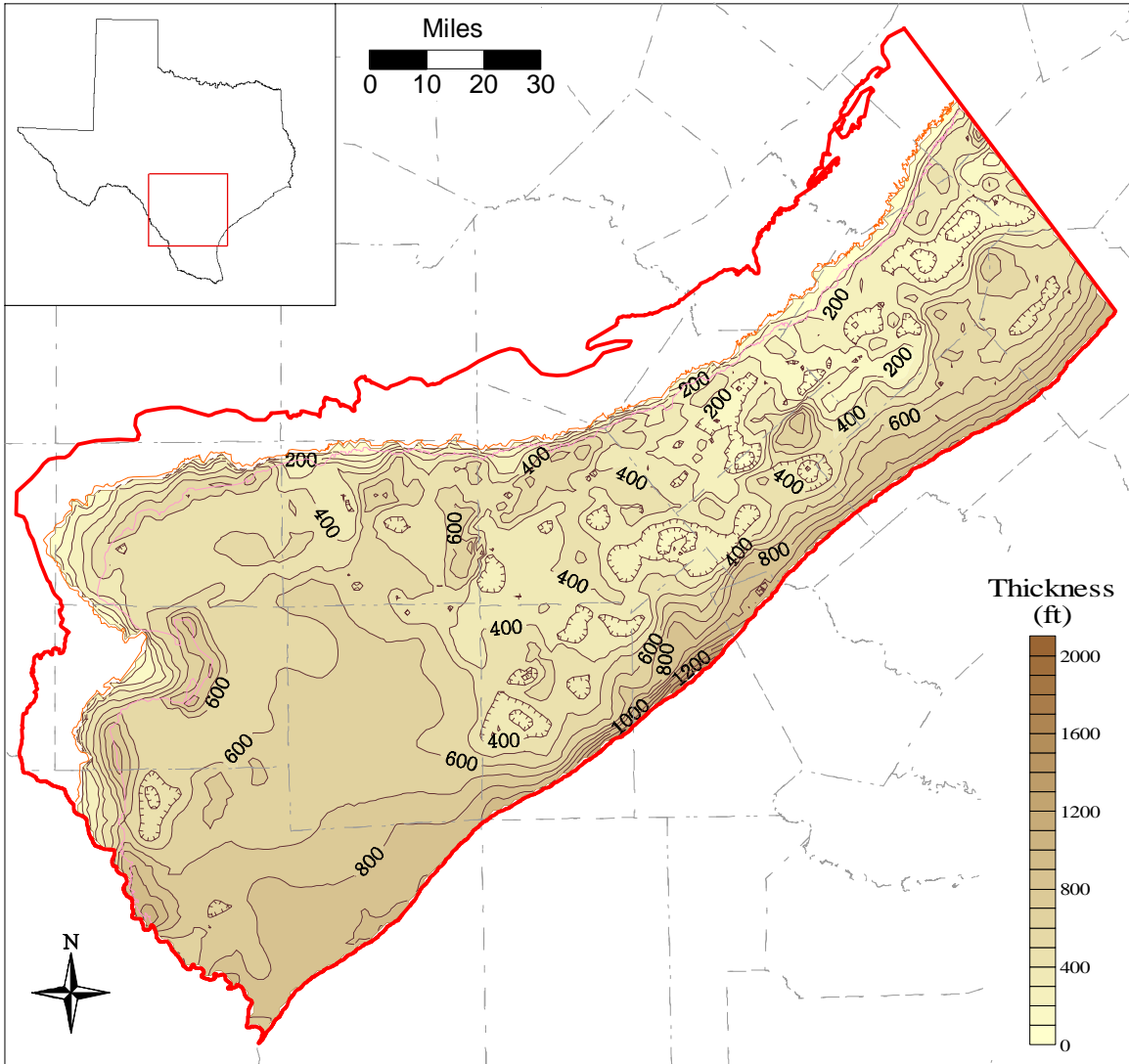


Figure 4.2.13 Thickness map of the Reklaw/Bigford.

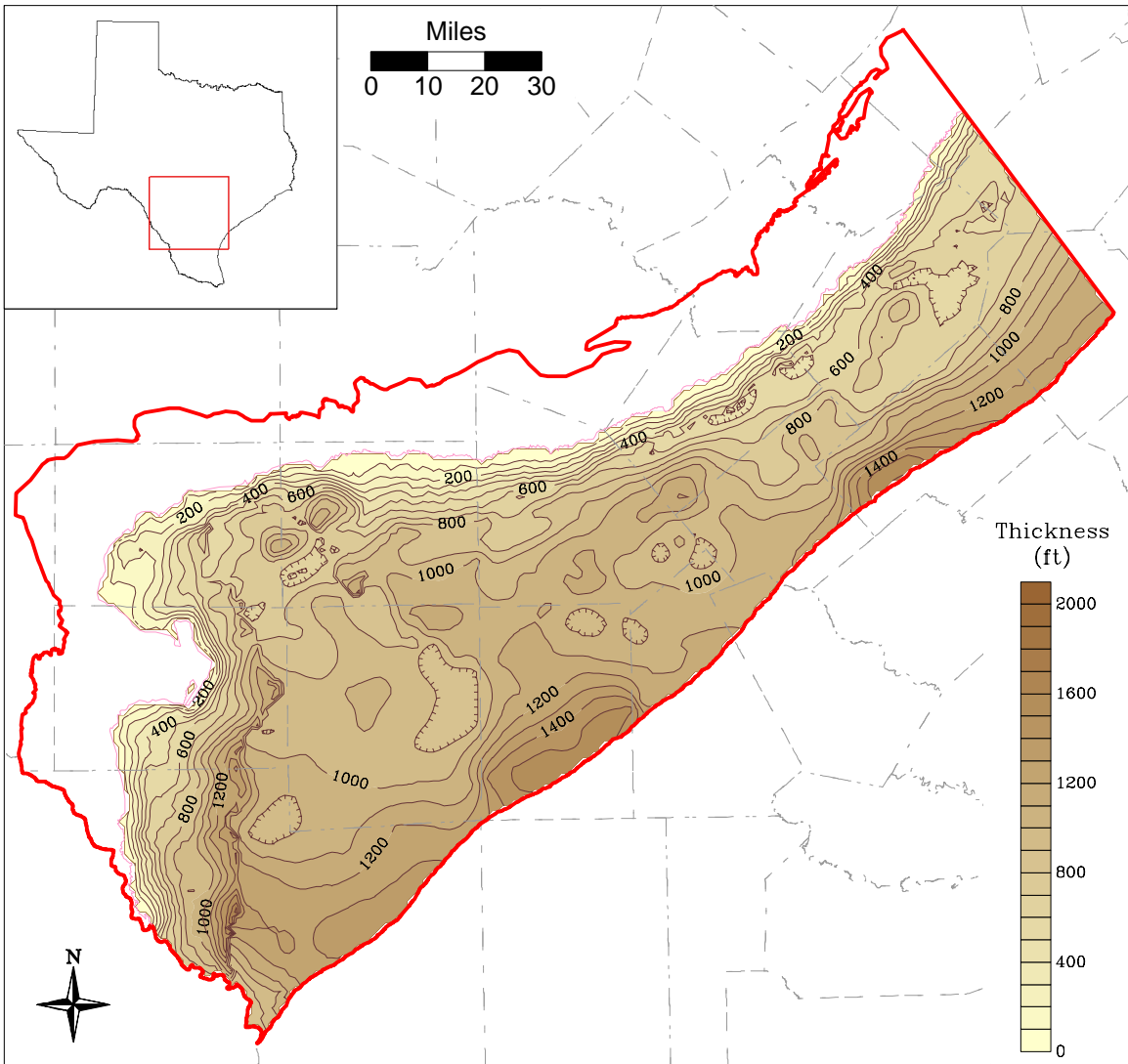


Figure 4.2.14 Thickness map of the Queen City/El Pico.

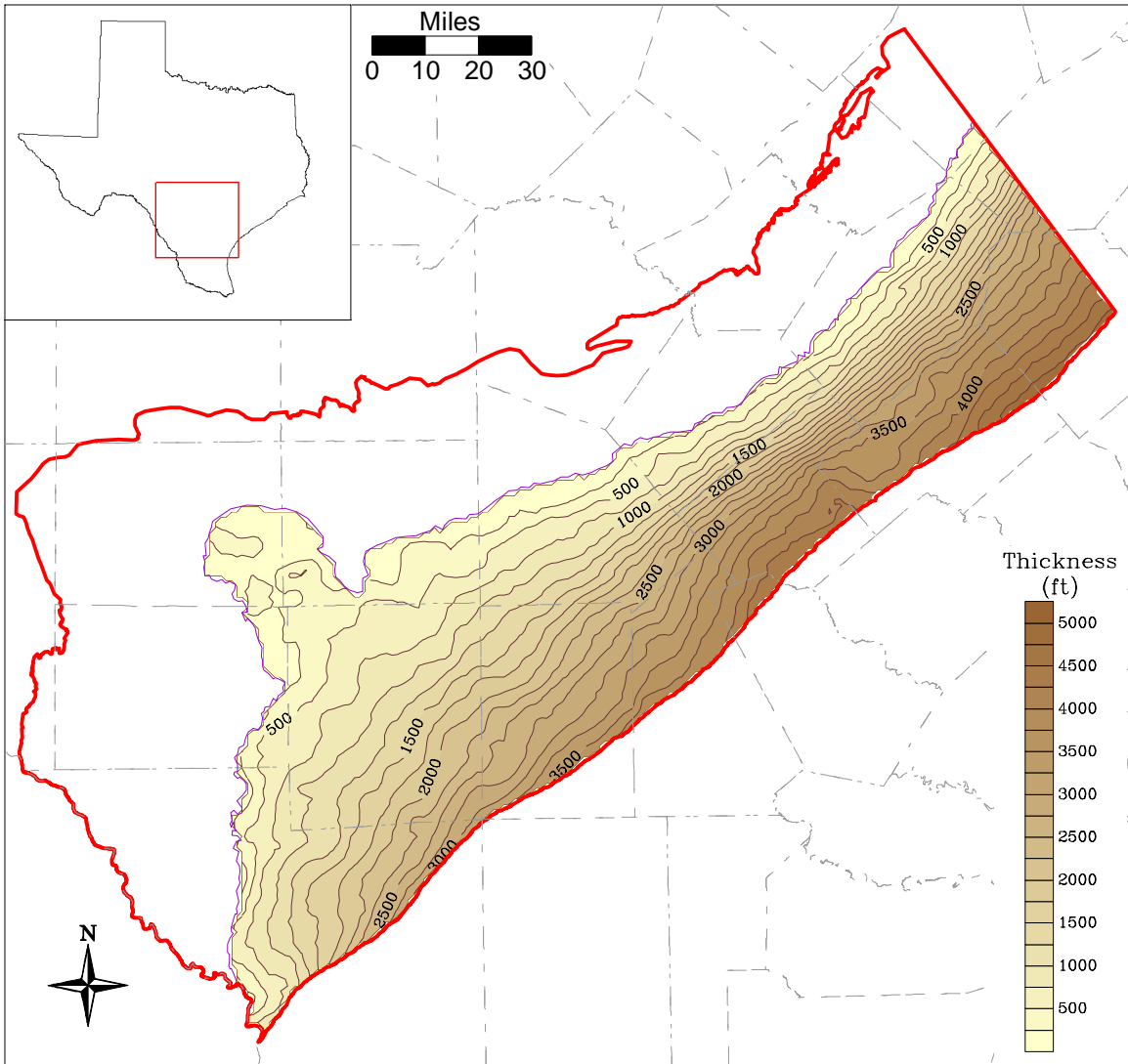


Figure 4.2.15 Thickness map of younger sediments overlying the Queen City.

4.3 Hydraulic Properties

Information on hydraulic properties of the Carrizo-Wilcox aquifer is based largely on data and sources provided by Mace et al. (2000a). INTERA also received aquifer test results for wells in Gonzales County and La Salle County from LBG-Guyton & Associates and URS Corporation, respectively. Mace et al. (2000a) compiled and statistically analyzed transmissivity, hydraulic conductivity, and storativity data from numerous sources for the entire Carrizo-Wilcox aquifer in Texas. They also analyzed spatial distributions of hydraulic properties in the Carrizo Sand and in the Wilcox Group, developing regional kriged maps of transmissivity and hydraulic conductivity. The uneven data coverage and relatively large local-scale variability, expressed in a high nugget in the semivariograms (Mace et al., 2000a), indicate significant uncertainty in the hydraulic properties of the Carrizo-Wilcox. A relationship between hydraulic properties and sand thickness (using sand maps from Bebout et al., 1982) could not be established. However, more detailed small-scale studies have determined correlations between different sand facies and hydraulic conductivities (e.g., Payne, 1975; Henry et al., 1980; Fogg, 1986; Thorkildsen and Price, 1991). The hydraulic conductivities determined through aquifer tests are biased towards higher permeability sands which tends to undermine the correlation of facies and hydraulic conductivity on a regional scale.

The Carrizo aquifer generally consists of fairly homogeneous fluvial sands overlying the multi-aquifer system of the Wilcox Group that is composed of fluvial and deltaic sands distributed among lower permeability interchannel sands and muds. Proper simulation of groundwater flow in such a complex depositional environment requires accurate description of both the subsurface arrangement of the various lithofacies (i.e., sand body distributions) and associated hydraulic properties. As pointed out by Fogg (1986), sensitivity of hydraulic head to heterogeneity or interconnectedness of sands in such a complex 3-D aquifer system is relatively low. This results in potential non-unique solutions in model calibrations and concomitant, inaccurate representations of simulated groundwater flow patterns. Moreover, hydraulic properties have to be representative for the hydrostratigraphic unit that is implemented as a model layer in the numerical model. That is, both the horizontal and vertical distributions of property measurements are important, so information on well locations and screen depths and/or well depths is required.

The evaluation of the hydraulic conductivity data was performed in several steps. Initially, the database from Mace et al. (2000a) was processed in terms of data location relative to the GAM region and to the hydrostratigraphic units. Next, a statistical analysis of the data was performed to evaluate variability between different data sources and different aquifers. A geostatistical analysis was then performed to characterize the spatial structure of the hydraulic conductivity data. Finally, trends in hydraulic properties were compared to depositional trends and/or sand-body distributions.

4.3.1 Processing of the Hydraulic Property Database

For the Southern Carrizo-Wilcox GAM, the original database from Mace et al. (2000a) was imported into an MS Access Database (file: cw_97_xp.mdb). A new data table that contains a link between the well BEG Number and the well location in GAM coordinates was added to the database (the coordinate conversion from decimal degrees to GAM coordinates was completed in ArcView). A new table was added titled “models” which identified the wells within the southern GAM region. This table was created in ArcView by intersecting the GAM outline with the point coverages of the wells. As recommended by Mace et al. (2000a), data from the Texas Railroad Commission (TRRC) and data from slug or bailing tests were excluded in this study, because of a bias toward lower values. The five aquifer tests obtained from URS and LBG-Guyton were also added to this database.

Figure 4.3.1 shows a flow diagram for the screening of hydraulic conductivity data. After discarding the TRRC, slug, and bailing test data, the remaining data were screened for the availability of a horizontal hydraulic conductivity measurement. Some data had a transmissivity measurement, but no estimate of effective thickness (e.g. screen length), and were discarded. If the top and bottom elevations of the well screen were recorded, these were compared to the model layer elevations. The hydraulic conductivity measurement was assigned to the layer that contained the largest fraction of the well screen. If the screen spanned more than three layers, the measurement was discarded. Those data without screen elevation information were checked for the presence of a layer-specific aquifer code. If this code was available, then the hydraulic conductivity measurement was assigned to that layer. Data marked only with general aquifer codes indicating multiple model layers (e.g. Wilcox Combined or Carrizo-Wilcox) were discarded.

4.3.2 Statistical Analysis of the Hydraulic Property Data

A summary of the statistical analysis of the hydraulic properties for the different hydrostratigraphic units is given in Table 4.3.1. The table summarizes the number of data measurements and the mean and median hydraulic conductivities. The hydraulic conductivities are summarized by layer with CDF curves in Figure 4.3.2. These distributions appear to be log-normal. The hydraulic conductivities for the different layers range between 0.1 ft/day to about 900 ft/day.

Table 4.3.1 Summary statistics for horizontal hydraulic conductivity

Layer	Unit	Count	Median K (ft/d)	Mean K (ft/d)
1	Queen City/El Pico	46	9.8	22.9
2	Reklaw/Bigford	74	9.9	16.3
3	Carrizo	605	31.5	55.8
4	Upper Wilcox	19	3.9	11.8
5	Middle Wilcox	215	8.1	28.2
6	Lower Wilcox	173	4.6	16.3

Figure 4.3.2 and Table 4.3.1 indicate that the Reklaw/Bigford Formation, which is considered the upper confining unit for the Carrizo-Wilcox aquifer, has relatively high horizontal hydraulic conductivity for a confining unit. The Reklaw Formation may contain extensive sand layers within muds and pumpage is reported from the Reklaw. However, some of the wells that are designated as Reklaw wells by aquifer code or by the structure data are probably completed in the adjacent Carrizo or Queen-City aquifer. Because the Reklaw is relatively thin, small errors in the structure surfaces can result in misplacement of screened intervals. West of the Frio River, the Bigford Formation is considered a minor aquifer with minor amounts of pumpage from sand layers within the muds. However, for both the Reklaw and Bigford, the more important hydraulic property is the vertical hydraulic conductivity, which is controlled by the hydraulic conductivity of the more continuous muds and shales within the Reklaw and Bigford. The vertical conductivity of the Reklaw/Bigford is not represented by the data set summarized in Table 4.3.1.

4.3.3 Spatial Distribution of Hydraulic Property Data

The spatial distribution of hydraulic properties was characterized by a variogram analysis to quantify spatial correlation and variability (for detailed background information on

geostatistics, refer to Isaaks and Srivastava, 1989). The variogram describes the degree of spatial variability between observation points as a function of distance. Typical hydrogeologic properties show some spatial correlation indicated by low variance for nearby measurements. As the distance between measurements increases, variance increases until it becomes constant, which corresponds to the ensemble variance of the entire data set. At the separation distance where the variance becomes constant, no correlation between measurements exists. The variogram quantifies the spatial variability in terms of the correlation length and variance, and provides information on spatial trends in the data. The variogram can also be used as a tool to characterize horizontal anisotropy in hydraulic conductivity. In an aquifer with horizontal anisotropy, hydraulic conductivity is a function of horizontal direction. We performed a directional-variogram analysis to detect any horizontal anisotropy in hydraulic conductivity. However, our analysis failed to identify anisotropy in horizontal hydraulic conductivity.

Figure 4.3.3 is a variogram for hydraulic conductivity of the lower Wilcox for the study area. The variogram indicates an increase in variance which levels off for distances greater than about 100,000 ft, though exhibiting large variations. A function was fit to the variogram data (experimental variogram), which shows an intercept of 0.22 at zero distance between measurements. The variance of the intercept is referred to as the “nugget”, indicating the local-scale variability of hydraulic conductivity. The nugget amounts to about half of the total variance of 0.42 of the ensemble data (“sill”), suggesting potentially large variability of hydraulic conductivity in nearby well locations and poor spatial correlation between measurements.

Once the model variogram has been developed, the spatial distribution of the hydraulic conductivity data is then produced by ordinary kriging, which uses the variogram information to estimate property values over the area of interest based on the limited number of data points available. Kriging results in some smoothing of the data by taking a weighted average of nearby measurement points. Using the hydraulic conductivity data points for the lower Wilcox, the variogram and corresponding kriged hydraulic conductivity distribution are shown in Figure 4.3.4. The kriged map of hydraulic conductivity shows that most of the data are along the outcrop and shallow confined section in the central and northeastern part of the study area. We did not krig properties past our data limits and past the correlation length. The hydraulic conductivities range from about 1 ft/day to about 30 ft/day.

The variogram for hydraulic conductivities of the middle Wilcox shows a correlation length of about 150,000 ft and a nugget of about 0.16 compared to a sill of about 0.42 (Figure 4.3.5). The hydraulic conductivity data are limited to the outcrop band and shallow subsurface similar to those of the lower Wilcox and showing a similar range in hydraulic conductivities (1 and 30 ft/day). Only 19 measurements were identified (Table 4.3.1) for the upper Wilcox located primarily in the southwestern part of the study area. We concluded that the data coverage was too sparse to construct a kriged map.

The variogram for the Carrizo Sand, shown in Figure 4.3.6, indicates a relatively small correlation length of about 25,000 ft compared to that in the lower and middle Wilcox (Figures 4.3.4 and 4.3.5). Again, the nugget is relatively high (0.16) compared to the sill (0.3), but the sill is significantly lower than those from the lower or middle Wilcox. That is, the overall variability of hydraulic conductivity in the Carrizo is lower than that of the Wilcox which is characterized by a sill of about 0.42. The kriged hydraulic conductivities range from about 1 ft/day to as much as 100 ft/day. Note that actual data coverage in the deeper confined section is limited; however, the kriged map for the Carrizo was extrapolated to the downdip boundary assuming a trend toward lower hydraulic conductivities, particularly in the southern part and the northeastern part of the study area.

The spatial distribution of hydraulic conductivity for the Reklaw and Bigford formations was not explicitly analyzed, because of limited data and uncertainty in the appropriate assignment of the data points to the Reklaw or to adjacent aquifer units. A preliminary evaluation of hydraulic property data for the Queen City Formation was performed, indicating a relatively small correlation length, a lower nugget (0.05), and a lower sill (0.2) as compared to the Carrizo-Wilcox (Figure 4.3.7). The kriged map indicates limited data distribution in the northern half of the area and very few data along the southwestern part of the area. For this particular map, the contours were limited to within a certain radius from the nearest observation point.

In general, the kriged maps of hydraulic conductivity indicate significant variability. These distributions represent horizontal permeabilities of sands within the different hydrostratigraphic units, because most wells tend to be completed and tested in sand intervals. In the Carrizo aquifer, which consists typically of 60 to over 90% sand, the spatial pattern

reflects lithologic variability and potentially depth of burial. The Carrizo kriged map was extended to the southern model boundary by including false data points to produce a decrease in hydraulic conductivity with depth toward the southern boundary consistent with interpretations by Klemm et al. (1976) and Prudic (1991). For the Wilcox, relatively large portions of the study area are not constrained by data. To incorporate the hydraulic property information into the numerical model, an approach is needed to assign properties where no data are available and to produce property values that are representative over the entire layer thickness. This is of particular importance, where the aquifer units consist of significant amounts of muds. In the following section, geologic information is examined for complementing the estimation of hydraulic properties.

4.3.4 Relationship between Hydraulic Property and Sand Distribution

The distribution of sand and muds not only affects the transmissivity of the aquifer but also the groundwater flow. Groundwater preferentially flows through more transmissive zones that consist of well connected sands of relatively high hydraulic conductivity. The hydraulic conductivity data presented in Section 4.3.3 were based on hydraulic tests performed at specific depth intervals which generally do not cover the entire thickness of the aquifer model layer. The data are also representative of the sand encountered in the interval rather than an average value over the entire screened section. The kriged hydraulic conductivity maps assume that the sands tested in adjacent wells at different depth intervals are laterally and vertically connected. This assumption is most likely valid for the Carrizo, which is dominantly sand. For the Wilcox Group, which typically consists of less than 50% sand in the lower and middle Wilcox, sand bodies are embedded in a fine-grained matrix and may not always be connected.

For the combined Carrizo-upper Wilcox unit, Hamlin (1988) produced detailed net-sand, sand-percent, and maximum sand thickness maps. The sand-percent maps by Hamlin (1988) indicated a range from 50 to over 90 percent for the Carrizo-upper Wilcox. The maximum sand thickness map identifies the thickest sand in the interval and shows spatial trends that are characteristic of high-energy bed-load sedimentation in major fluvial channels. The sand thickness is not only important to define the overall transmissivity of the aquifer but also can indicate zones of higher permeability. Intuitively, one would expect that sands in the major fluvial channels generally have higher conductivities than thinner, more isolated sands. Spatial information on sand distributions can be used as soft data to extrapolate the kriged permeability

maps to areas where no hydraulic conductivity data are available. Mace et al. (2000a) compared generalized net sand maps for the upper and lower Wilcox by Bebout et al. (1982) to transmissivity values for the Wilcox Group throughout Texas, but did not find a correlation between sand thickness and transmissivity. However, more local studies have shown relationships between sand thickness or specific channel sands and hydraulic conductivities (Payne, 1975; Fogg, 1986).

For the study area, we examined both the net sand thickness and maximum sands as well as the percent sand of the Carrizo-upper Wilcox (Hamlin, 1988) for comparison with hydraulic conductivity values. For this analysis, only hydraulic conductivity data with a Carrizo aquifer designation and with a known screen interval were used. Maximum sand maps are considered more indicative of the major channel sand, ignoring thinner and less continuous splay and overbank sands. However, the maximum sand maps show only a limited thickness range. Histograms of hydraulic conductivities (log-K) by maximum sand thickness and net sand thickness are shown in Figure 4.3.8. These two histograms show no clear relationships. The maximum sand histograms do not indicate a clear trend, whereas the net-sand histograms indicate generally lower median log-K values for thicker sands. This may be due to the fact that the net sand thickness increases downdip, where data are more limited. The kriged map for the Carrizo indicates that the highest observed conductivities are in the shallow confined section and in the outcrop, where net sand thickness is low. Figure 4.3.9 shows a correlation of increasing hydraulic conductivity with increasing sand percent. This suggests a trend to generally lower permeability downdip, where net-sand increases and sand-percent decreases. A similar trend of decreasing conductivities in the deeper section was indicated by the permeability map constructed by Klemm et al. (1976).

There are some limitations in the analysis. The sand thickness maps are manually contoured taking into account the depositional model. Furthermore, the hydraulic conductivity data points were assigned to the nearest sand thickness contour. For this study, the net-sand map was primarily used to estimate the transmissivity of the model layer. For the Carrizo, we did extrapolate the kriged hydraulic conductivities into the downdip section with limited data coverage, based on an inferred trend toward lower conductivity. This trend is apparent in the southern and northeastern part of the model areas (Figure 4.3.6).

For consistency with Carrizo structure, the net-sand map for the Carrizo was taken from Klemt et al. (1976) and using our total thickness map of the Carrizo, a sand-percent map was generated (Figure 4.3.10). The percent sand for the upper Wilcox (Figure 4.3.11) was derived by subtracting the sand thickness of Klemt et al. (1976) from the combined Carrizo-upper Wilcox sand thickness by Hamlin (1988) and dividing by our total thickness map of the upper Wilcox. Zones of hydraulic conductivity were based upon the derived sand percent map. Similarly, hydraulic properties for the middle and lower Wilcox were based on zones incorporating the kriged hydraulic conductivities in the outcrop and shallow confined section where data were available.

4.3.5 Vertical Hydraulic Conductivity

Specific data on vertical hydraulic conductivity within the Carrizo-Wilcox aquifer and for the Reklaw confining layer are not available at the scale of this study. Previous modeling studies of the Carrizo-Wilcox aquifer derived estimates of vertical permeability from model calibration. Stochastic modeling studies of a generic aquifer system consisting of two contrasting hydraulic conductivity facies (channel sands and finer grained interchannel sediments) having various degrees of vertical interconnection indicate effective vertical conductivities ranging between the geometric and harmonic mean conductivities (Fogg, 1989).

A lower bound estimate of vertical conductivity can be calculated as the lowest vertical conductivity value measured in a hydrostratigraphic section, assuming complete lateral continuity of the low-permeability zone. Measurements of hydraulic conductivity typically focus on high-permeability zones with a few core data available for low-permeability muds within the Wilcox Group (Bob Harden, personal communication). In the Region G model developed by Harden and Associates (2000), core estimates of clay hydraulic conductivity were used to represent clay strata within the Carrizo-Wilcox aquifer ($K = 5.35 \times 10^{-6}$ ft/day). The effective vertical conductivity for the different aquifer layers were estimated based on a harmonic mean of the individual proportions of sand, silt, and clay (Harden and Associates, 2000).

Fogg et al. (1983) inferred a maximum reasonable horizontal to vertical permeability ratio K_h/K_v (anisotropy ratio) on the order of 10,000 to 1,000 to reproduce the vertical head gradients within the Carrizo-Wilcox aquifer in a groundwater flow model near the Oakwood salt

dome in Freestone and Leon counties. A vertical to horizontal anisotropy ratio of 1,000,000 was considered too low to reproduce the general pressure-depth gradients across the model.

The vertical hydraulic conductivity of the Reklaw confining layer can be considered to be less than that of the Wilcox aquifer, because of more continuous fine-grained lithologies. In the southwestern portion of the study area, the Bigford contains more sand layers within the clays, which could increase the effective vertical hydraulic conductivity. On the other hand, the Bigford Formation is thicker, allowing for more continuous clay layers.

Fogg et al. (1983) used a vertical hydraulic conductivity of 2.6×10^{-4} ft/day for the Reklaw in their model, which they considered a maximum value. The USGS RASA model for the Texas Gulf Coast aquifer systems reported a vertical hydraulic conductivity of the lower Claiborne confining unit (equivalent to the Reklaw Formation) of 2×10^{-5} ft/day from their calibrated transient model (Ryder and Ardis, 1991). This value was lower than the calibrated value from an earlier steady-state model by Ryder (1988) of 1×10^{-4} ft/day.

The Carrizo Formation is generally considered to have much lower anisotropy ratios than the Wilcox, because of typically much higher sand content. However, the range in measured hydraulic conductivities for the Carrizo in the study area ranges over four orders of magnitude (Figure 4.3.2). Previous modeling studies reported Carrizo-upper Wilcox anisotropy ratios (K_v/K_h) of 2.5×10^{-3} based on a steady-state calibration (Ryder, 1988) and 8.7×10^{-5} based on a transient model calibration (Ryder and Ardis, 1991).

4.3.6 Storativity

The specific storage of a confined saturated aquifer can be defined as the volume of water that a unit volume of aquifer releases from storage under a unit decline in hydraulic head (Freeze and Cherry, 1979). The storativity is equal to the product of specific storage and aquifer thickness and is dimensionless. For unconfined conditions, the storativity is referred to as the specific yield and is defined as the volume of water an unconfined aquifer releases from storage per unit surface area of aquifer per unit decline in water table (Freeze and Cherry, 1979).

Mace et al. (2000a) compiled 107 estimates of storativity and calculated 64 estimates of specific storage from tests of the Carrizo-Wilcox aquifer where the screen length was known. Storativity ranged in magnitude from 1×10^{-6} to 0.1 with a geometric mean equal to 3×10^{-4} . Specific storage ranged from about 1×10^{-7} to 1×10^{-4} 1/m with a geometric mean of 4.6×10^{-6} 1/m.

The medians were essentially equal to the geometric mean for both distributions demonstrating the lognormal form of both distributions.

Specific yield estimates summarized in Table 4.3.2 are derived from aquifer tests and from model calibrated values. The range of specific yield is from 0.05 to 0.32. Perhaps the most direct estimate of specific yield is from Duffin and Elder (1979). They performed 20 seismic refraction profiles in the Carrizo Sand outcrop in areas west of Gonzales County.

Table 4.3.2 Summary of literature estimates of Carrizo-Wilcox specific yield.

Source	Specific Yield	Reference
TWDB Report 210	0.25 (average)	Klemt et al. (1976)
TDWR Report 229	0.16 to 0.32	Duffin and Elder (1979)
TWDB/LCRA model	0.05 to 0.3	Thorkildsen et al. (1989)
TWDB Report 332	0.1 to 0.3	Thorkildsen & Price (1991)
USGS OFR 91-64	0.15	Ryder & Ardis (1991)
BEG RI 256	0.29 (Simsboro)	Dutton (1999)
Region G Model	0.15	Harden & Assoc. (2000)

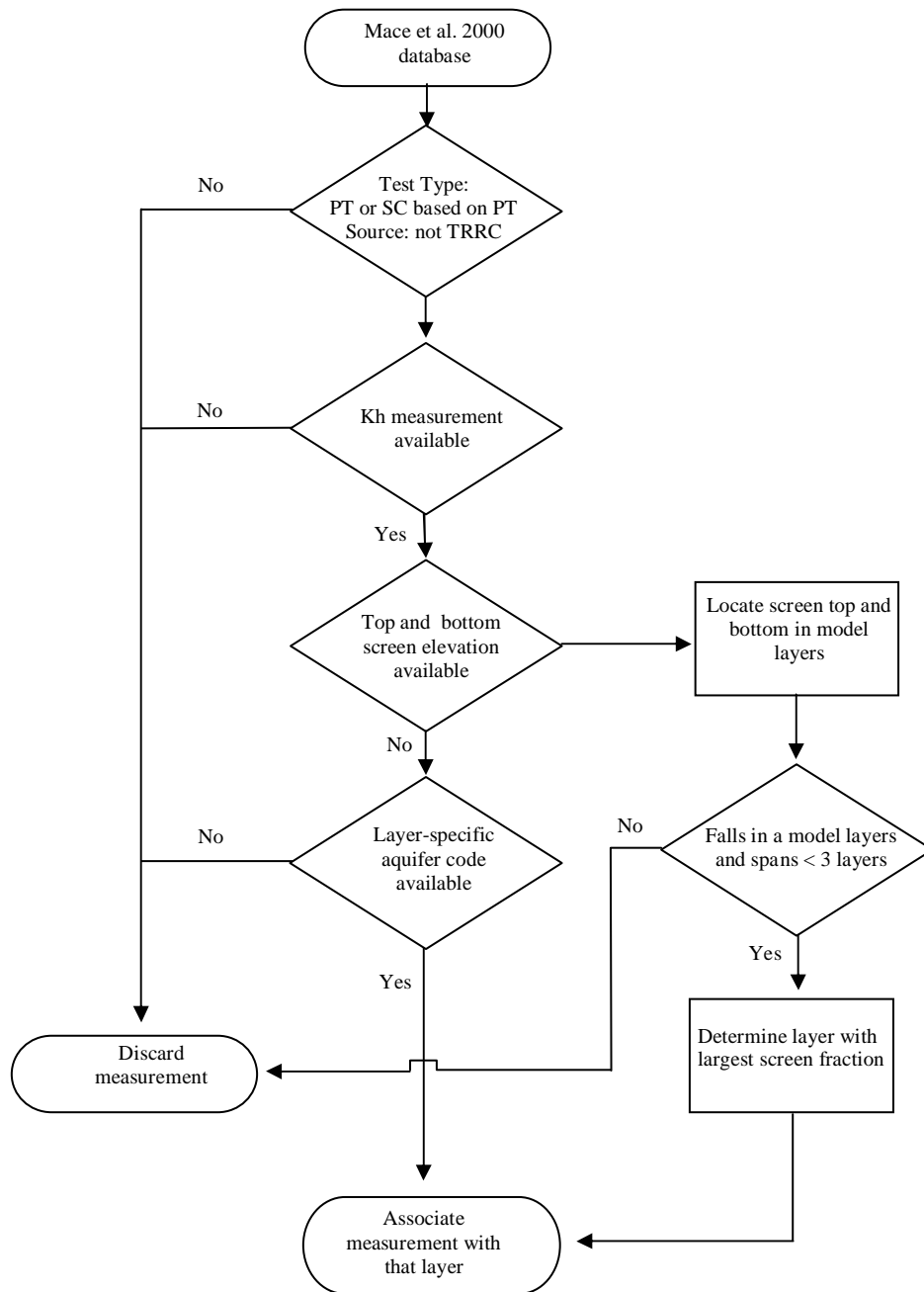


Figure 4.3.1 Screening of hydraulic conductivity data.

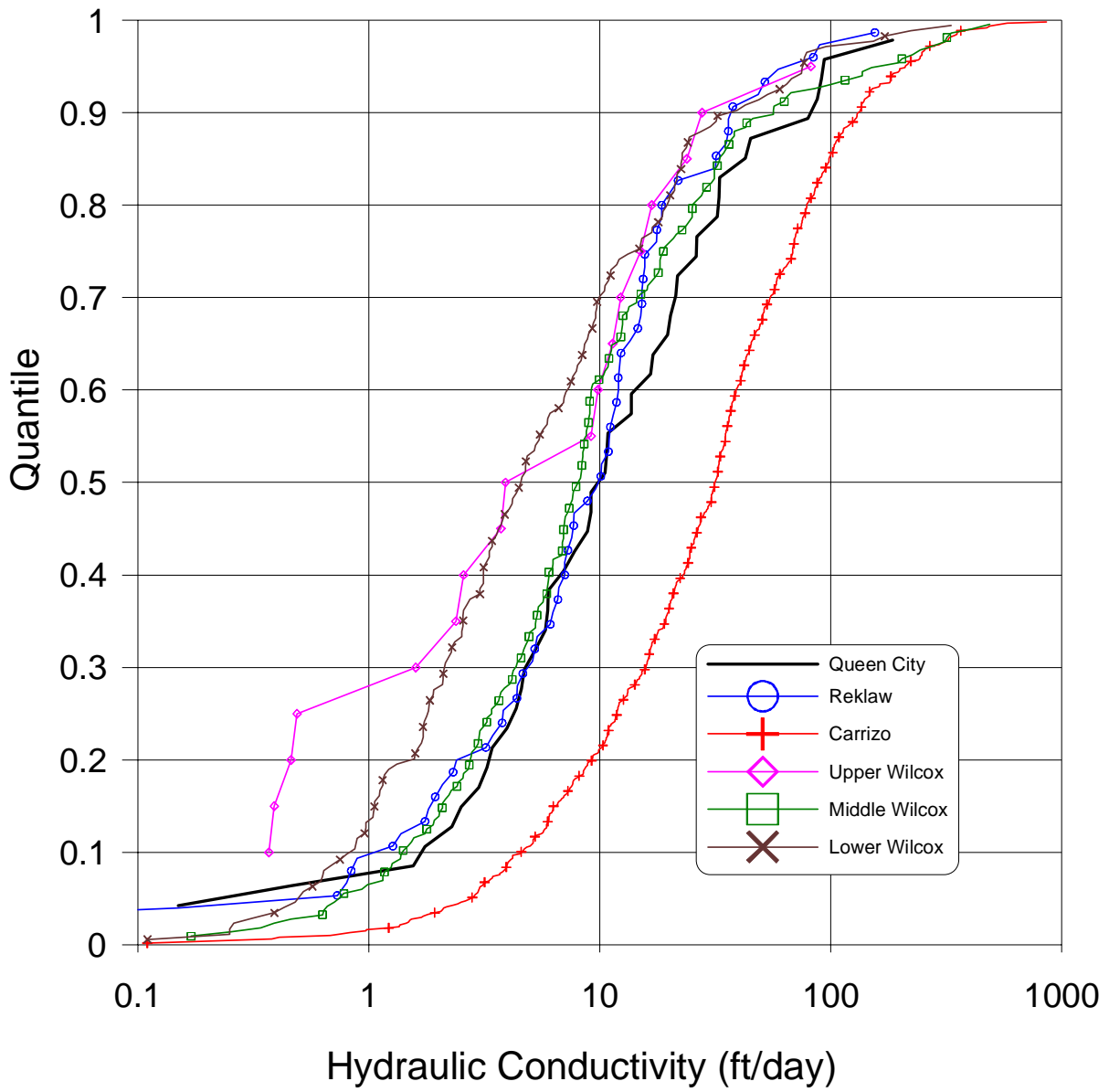


Figure 4.3.2 CDF curves of hydraulic conductivity for the modeled aquifer units.

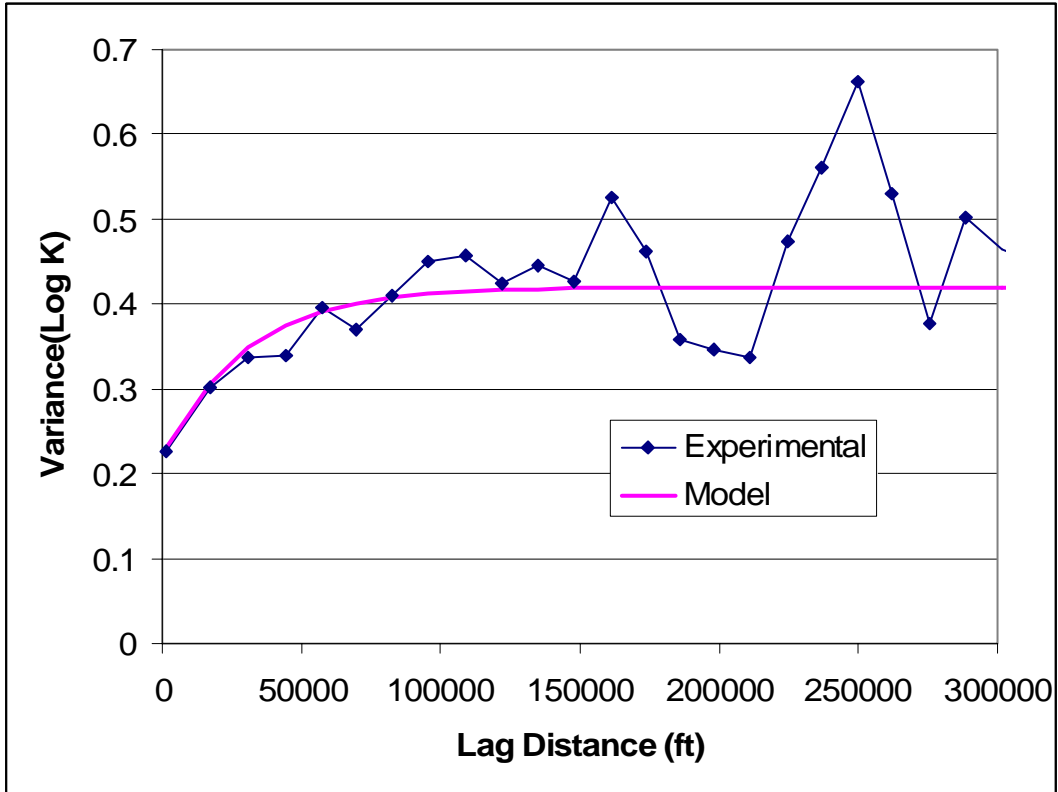


Figure 4.3.3 Variogram for hydraulic conductivity data for the lower Wilcox.

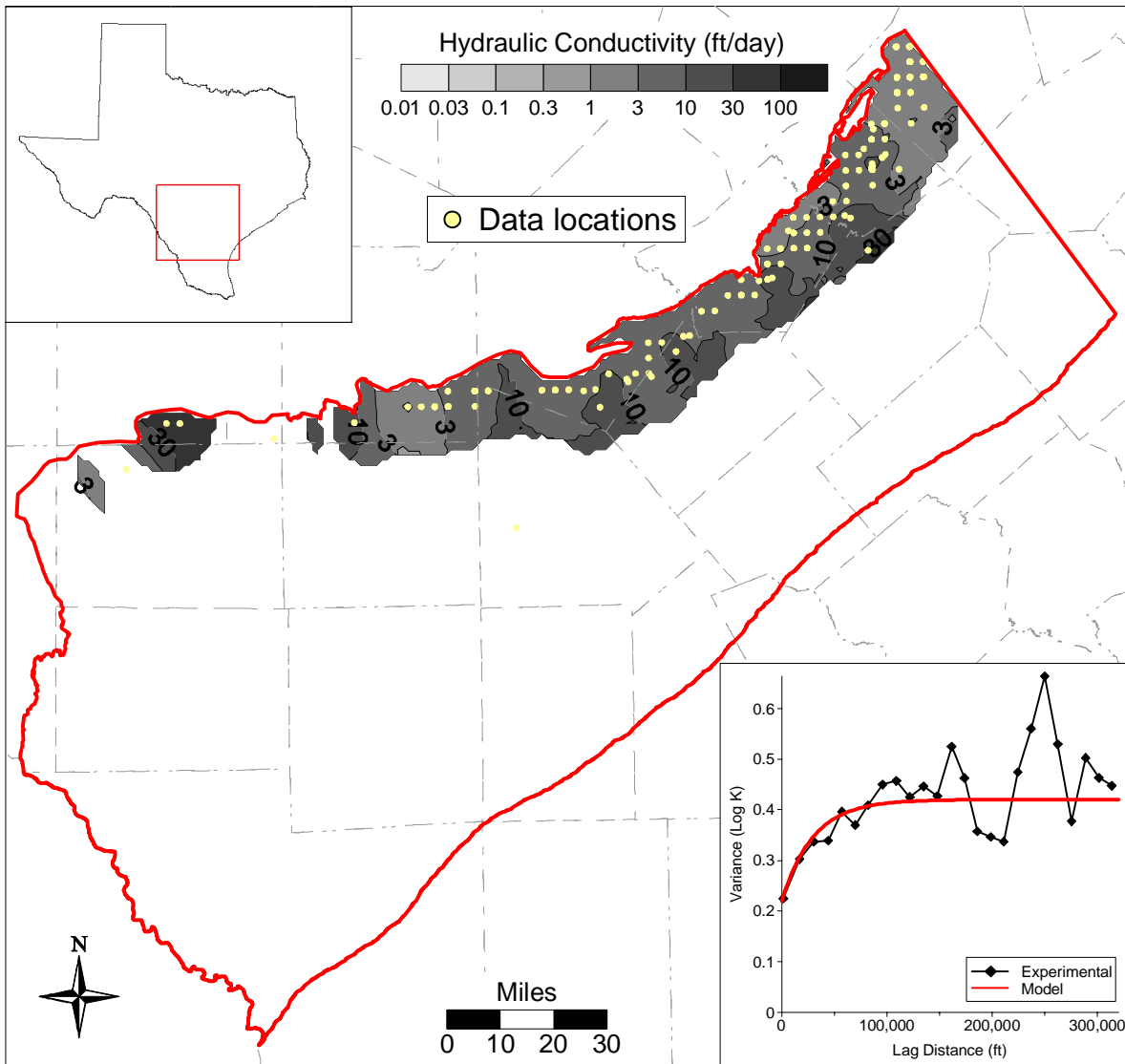


Figure 4.3.4 Variogram and kriged map of hydraulic conductivity for the lower Wilcox.

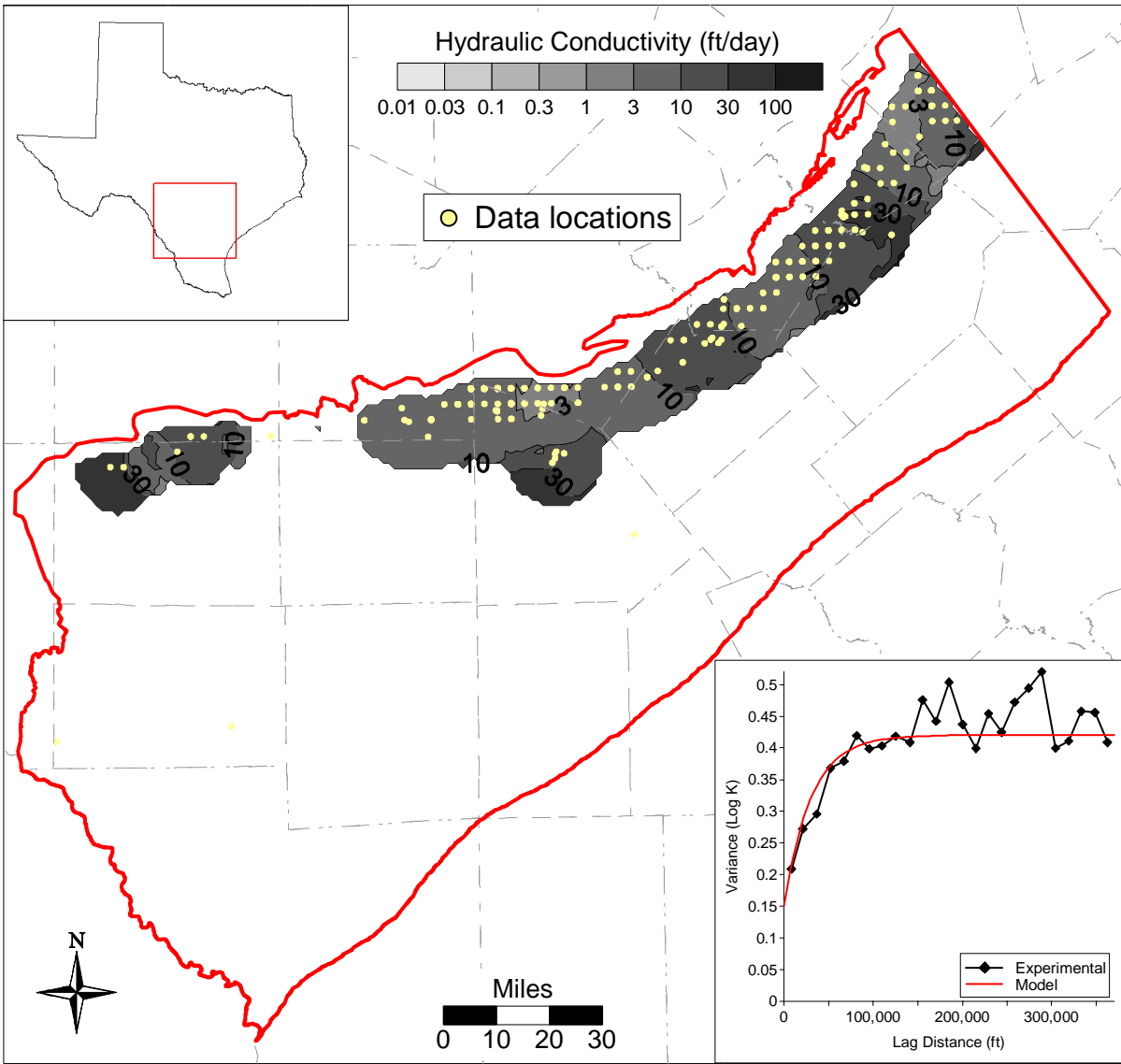


Figure 4.3.5 Variogram and kriged map of hydraulic conductivity for the middle Wilcox.

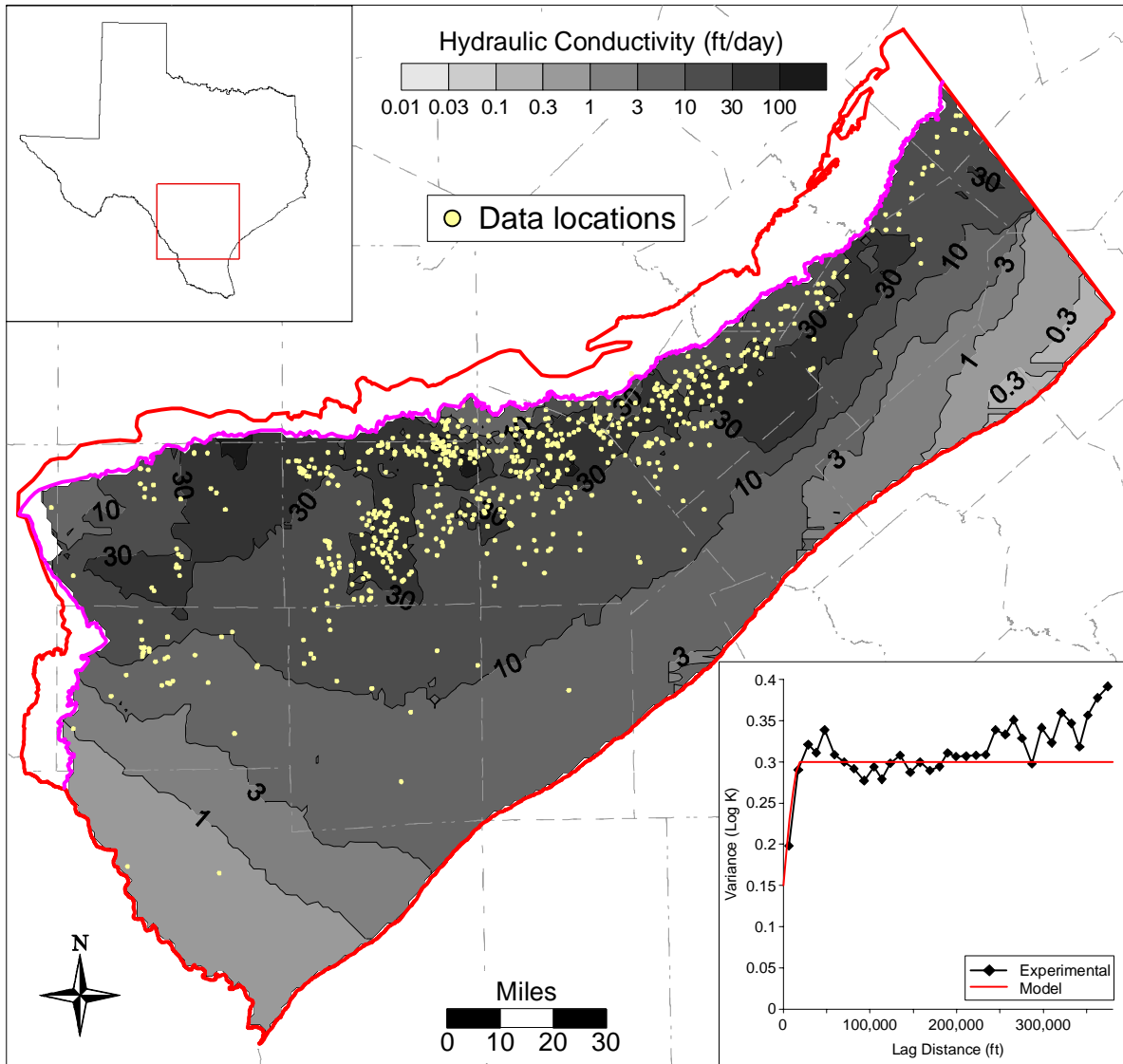


Figure 4.3.6 Variogram and kriged map of hydraulic conductivity for the Carrizo.

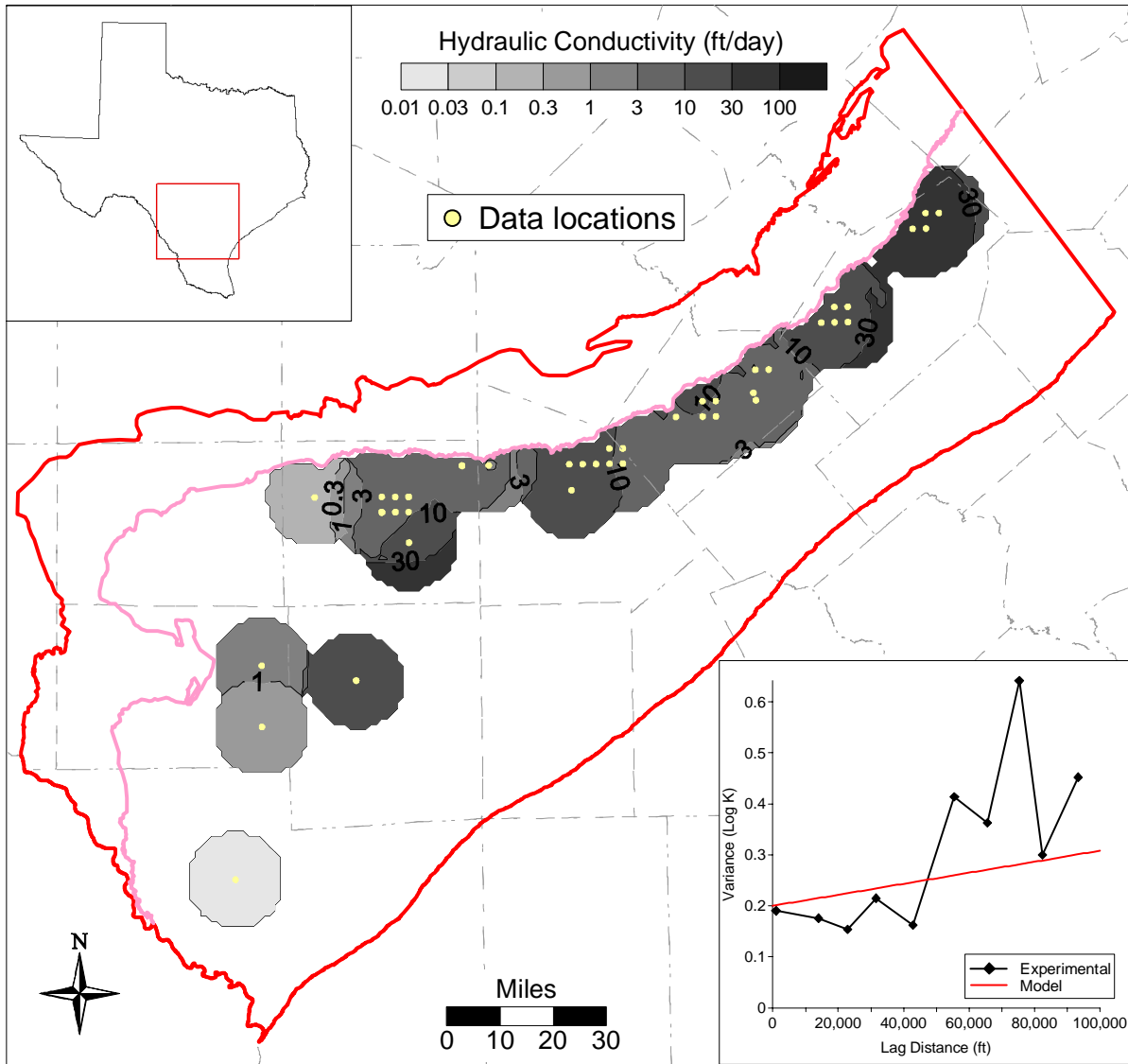


Figure 4.3.7 Variogram and kriged map of hydraulic conductivity for the Queen-City.

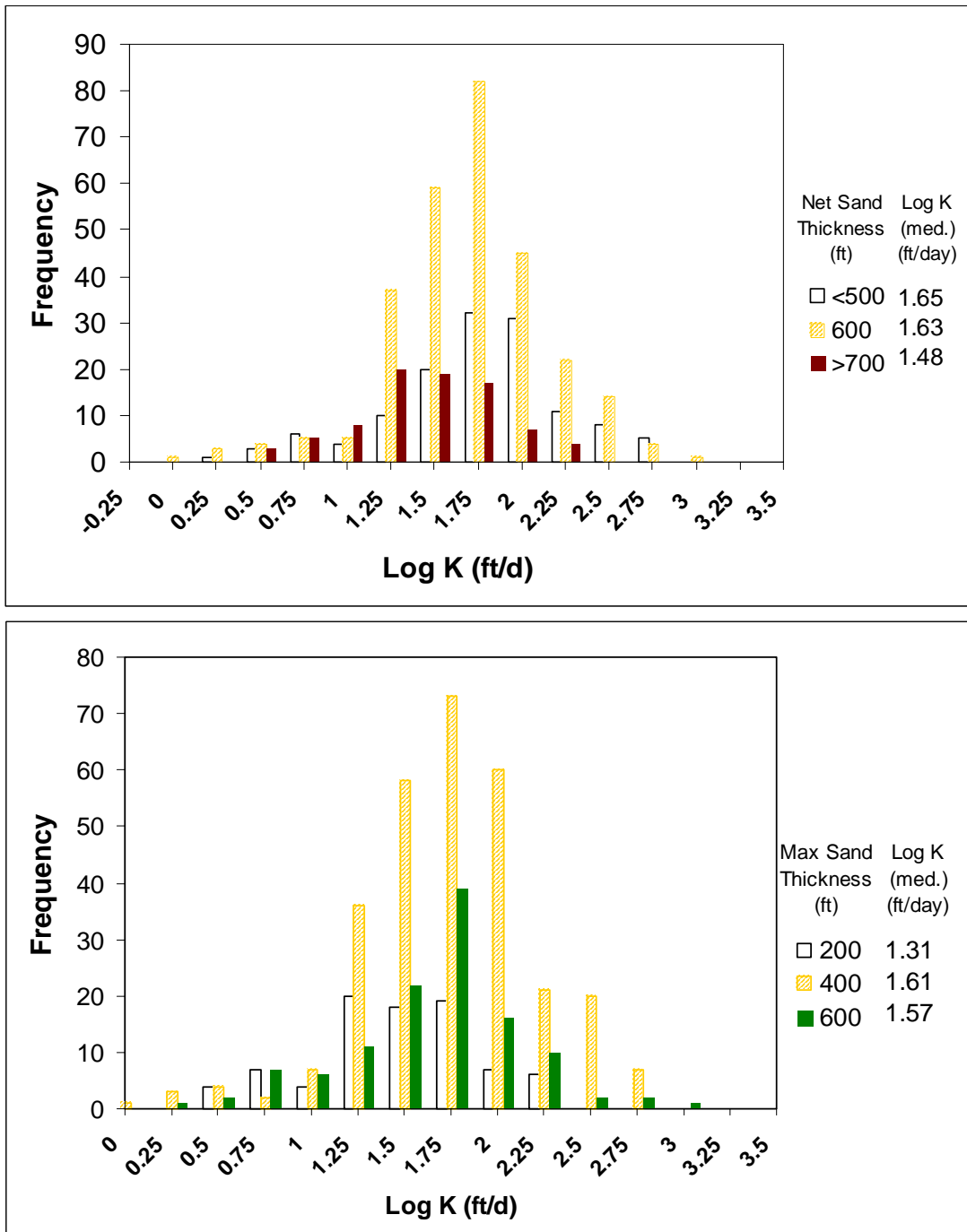


Figure 4.3.8 Histogram of net-sand thickness for the Carrizo-upper Wilcox and maximum sand thickness of the Carrizo-upper Wilcox and hydraulic conductivity (Log K).

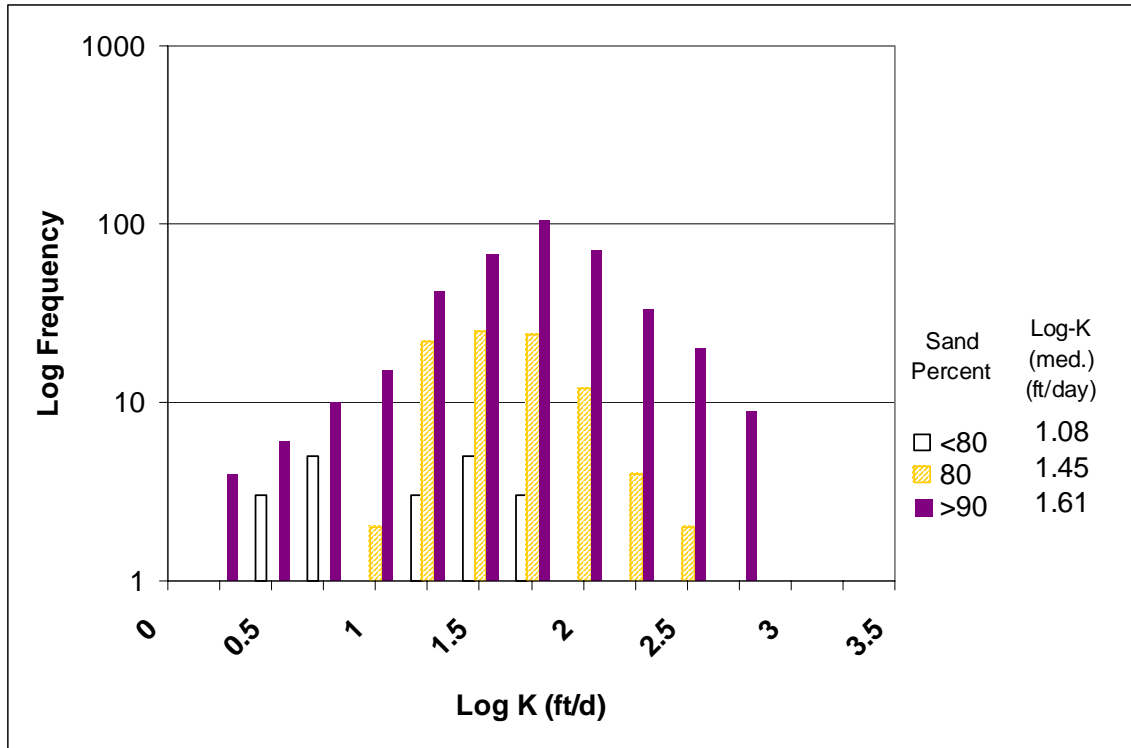


Figure 4.3.9 Histogram of sand percent for the Carrizo- upper Wilcox and the log of hydraulic conductivity (Log K).

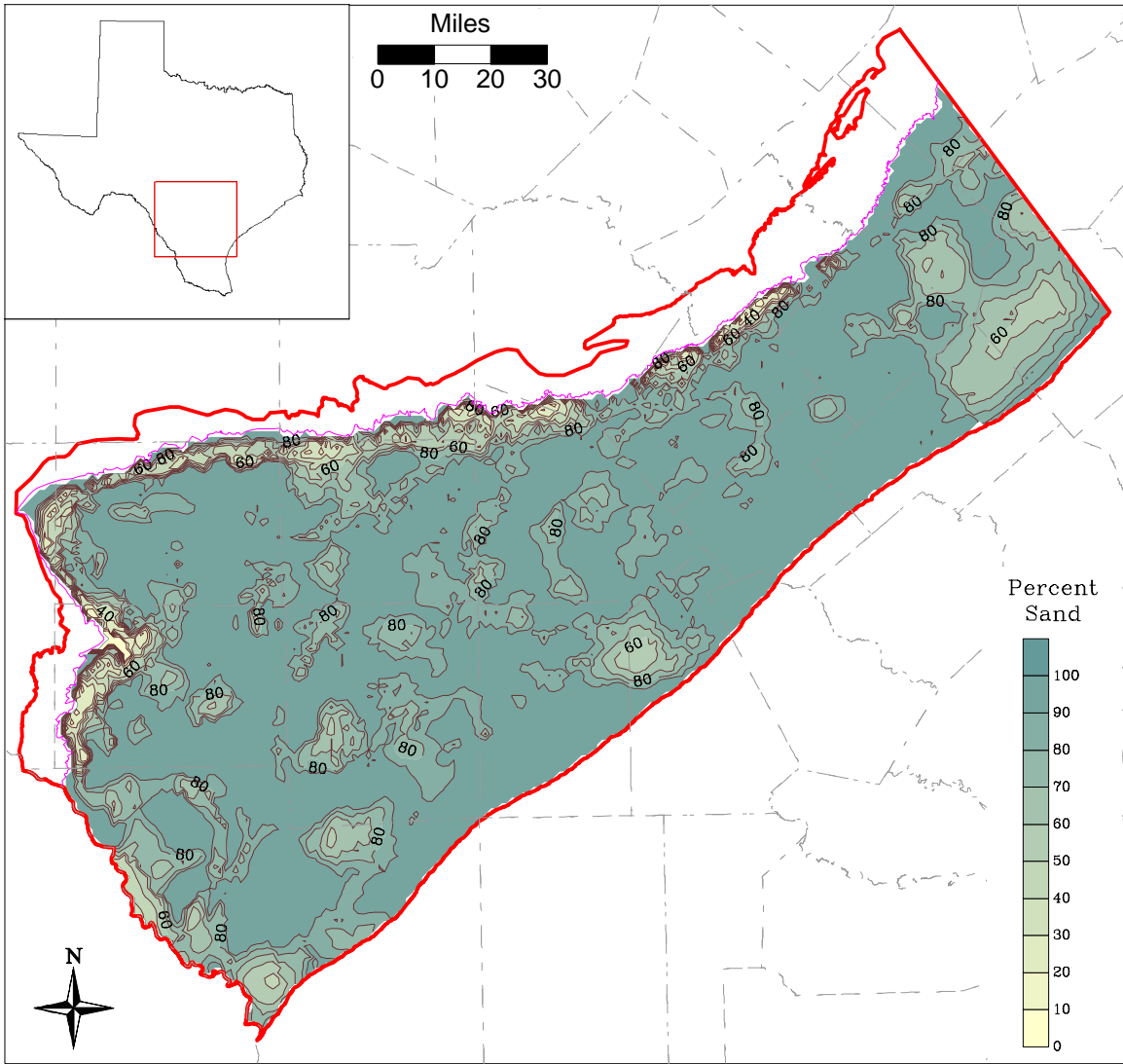


Figure 4.3.10 Percent sand for the Carrizo.

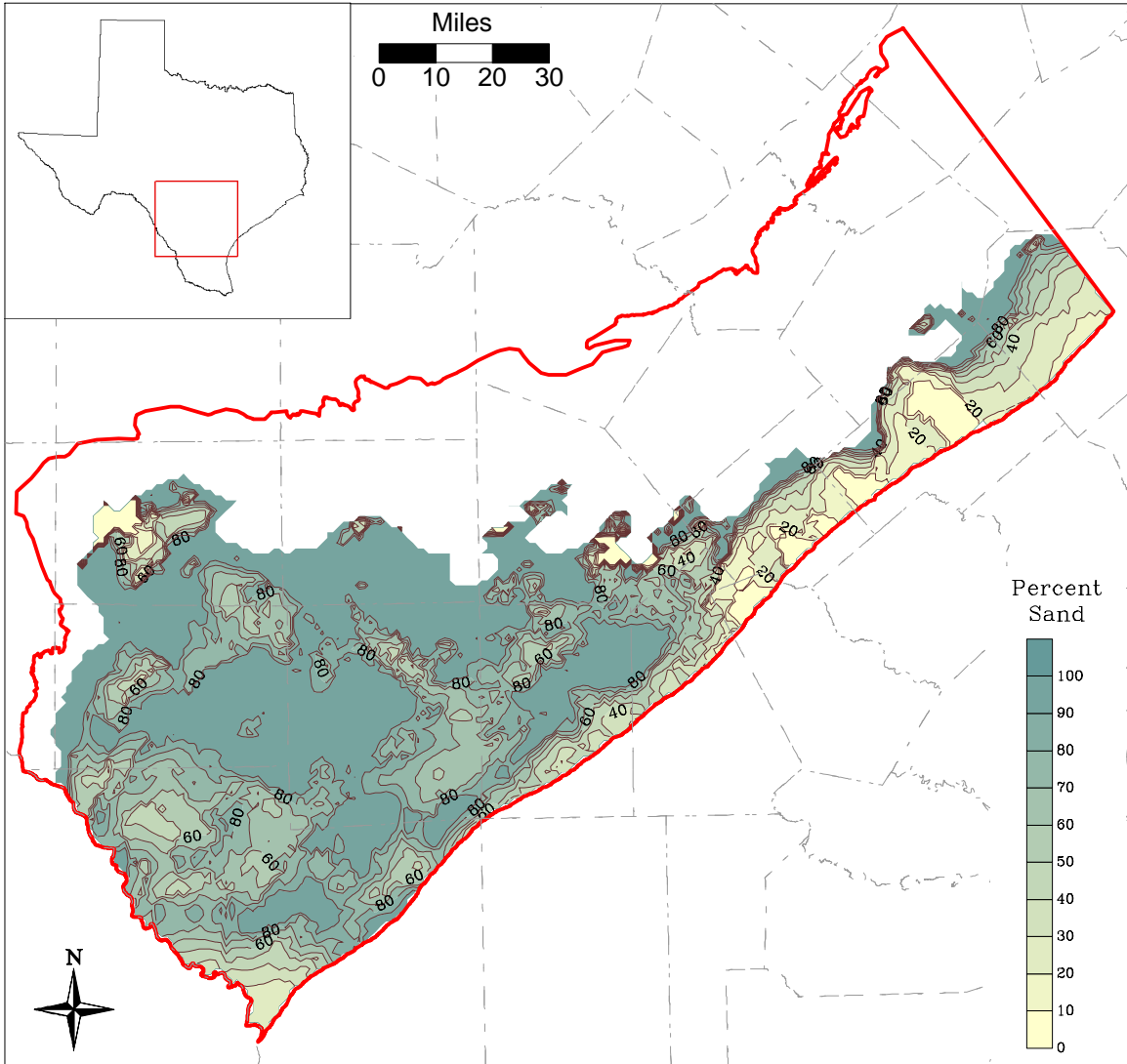


Figure 4.3.11 Percent sand for the upper Wilcox.

4.4 Water Levels and Regional Groundwater Flow

An extensive literature search was conducted to understand (1) regional groundwater flow in the Carrizo Sand and Wilcox Group prior to extensive development of groundwater resources in the area and (2) the history of groundwater usage from the Carrizo Sand and the Wilcox Group. The literature search included a review of the available county reports, historical USGS reports (predominately water-supply papers), and reports by the various Texas state agencies responsible for water resources (i.e., the Texas Board of Water Engineers, the Texas Water Commission, and the Texas Water Development Board). A summary of all reports reviewed can be found in Appendix A. In addition, water-level data provided by the Texas Water Development Board (TWDB) on their website¹ was used to (1) perform a pressure versus depth analysis, (2) investigate pseudo predevelopment conditions for the Queen City Sand/Bigford Formation, (3) investigate transient water level conditions, and (4) develop water-level elevation contours for the start of the calibration period (January 1980), the end of the calibration period (December 1989), and the end of the verification period (December 1999).

The Carrizo Sand is the principal aquifer in most of the Southern Carrizo-Wilcox GAM area. In general, the sands of the Wilcox Group provide fresh to slightly saline water only in and near the outcrop area. Sands of the Wilcox Group are not considered to be an aquifer in Karnes County due to the moderate to high salinity of the water (Anders, 1960). The Wilcox Group is "...not known to yield water..." in LaSalle and McMullen counties (Harris, 1965). The county report for Live Oak County (Anders and Baker, 1961) does not mention the Wilcox Group, suggesting that the sands of the Wilcox Group are not an aquifer in that county. In Caldwell and Bastrop counties, the sands of the Carrizo and Wilcox are hydraulically connected and are considered to act as a single aquifer (Follett, 1966 and Follett, 1970, respectively). Moulder (1957) states that the sands of the Carrizo and Wilcox are hydraulically connected to some extent in Zavala County. The water-level data available in the TWDB database indicates, in general, Carrizo and Wilcox wells in the outcrop areas and Carrizo wells concentrated downdip of the outcrop (Figure 4.4.1).

¹ Found on the web site:
rio.twdb.state.tx.us/publications/reports/GroundWaterReports/GWDatabaseReports/GWdatabaserpt.htm

Water within the Carrizo and Wilcox sands is under water-table conditions in the outcrop areas and under artesian conditions down dip of the outcrop. In many areas, artesian pressures within the aquifer were originally sufficient to drive water above ground surface (Moulder, 1957). Moulder (1957) estimates that the depth to water in the Wintergarden area (Zavala, Frio, Dimmit, La Salle, and Atascosa counties) was originally less than 100 ft.

4.4.1 Predevelopment Conditions for the Carrizo Sand and the Wilcox Group

Development of groundwater resources from the Carrizo Sand and Wilcox Group began in the early 1900s in parts of the study area. The first flowing well was drilled in 1884 at Carrizo Springs in Dimmit County (Turner et al., 1960). Successful crop growth and available transport to market via railroads resulted in the rapid development of Carrizo and Wilcox waters in parts of the Wintergarden District as early as 1910 (Moulder, 1957). Irrigation was greatest in Dimmit and Zavala counties. White and Meinzer (1931) investigated groundwater conditions in southwestern Texas and showed that the original extent of flowing wells was substantially reduced by 1930 in these two counties.

To develop an estimate of water-level conditions in the Carrizo Sand and Wilcox Group prior to significant pumpage, the history of well development and pumpage was compared to the dates of water-level measurements available from literature sources and the TWDB data for each county within the area of interest. In addition, maximum water-level elevations within the counties, regardless of time, were compared to maps showing the locations of originally flowing wells and to ground surface elevations. A brief summary of the development of the Carrizo Sand and the Wilcox Group in each county and the methodology for developing water-level elevations in that county representative of predevelopment conditions can be found in Appendix A.

Actual water-level measurements were used to generate the predevelopment contours for the Carrizo-Wilcox aquifer with the exception of measurements in Dimmit County, northwestern LaSalle County and southern Zavala County. For these locations, all available water-level measurements reflected the effects of pumpage. Map 3 in White and Meinzer (1931) shows the areas in these counties where wells completed to the Carrizo and Wilcox originally flowed. Based on that map, the values for selected water-level elevations measured in those three areas were increased by between 75 and 125 ft. This was done in order to obtain a measurement that was above ground surface and was consistent with the contour lines generated in the other areas

of the model using actual measured values. Water-level elevations in Zavala, Frio, and Atascosa counties used to generate the predevelopment contours were compared to the map from White and Meinzer (1931) to verify that they were higher than ground surface in the areas shown on the map as originally having flowing wells. The predevelopment water-level elevation contours indicate that, under undisturbed conditions, groundwater in the Carrizo Sand and Wilcox Group flows from topographic highs in and near the outcrop areas to topographic lows to the southeast.

The predevelopment water-level elevations represent a combined Carrizo-Wilcox aquifer in and near the outcrop areas and in Caldwell and Bastrop counties, and the Carrizo aquifer only in the remaining areas. The water-level elevation contours generated to represent predevelopment conditions in the Carrizo-Wilcox aquifer are shown in Figure 4.4.2. This figure also shows the ground-surface elevation based on USGS DEM elevations, and the location and value of water-level elevations used to generate the contours. The values shown in black indicate actual measured values, and the values shown in red indicate measured values that were increased as discussed above. Table 4.4.1 summarizes the water-level measurements used in generating the predevelopment water-level elevation contours.

To evaluate the acceptability of increasing the water-level elevations in Dimmit County, northwestern LaSalle County, and southern Zavala County, a comparison was made between contours generated with and without those values increased (Figure 4.4.3). As can be seen in the figure, the contours generated using the values that were not increased bend in northern LaSalle County and are lower than ground surface in areas of Dimmit, LaSalle, and Zavala counties known to originally have flowing wells.

The predevelopment contours were compared to the predevelopment contours of Ryder (1988). In general, the predevelopment contours shown here give the same flow direction but are (1) wider apart than those of Ryder (1988) indicating a shallower gradient, (2) about 50 ft higher than those of Ryder (1988) in the eastern portion of the model region (Wilson County east) and in northern Atascosa and Frio counties, and (3) about 100 ft higher than those of Ryder (1988) in southern Atascosa and Frio counties, and in LaSalle, Dimmit, and Zavala counties. Note, however, that the predevelopment contours of Ryder (1988) are below ground surface in northern LaSalle County, Dimmit County, and southern Zavala County, locations shown by White and Meinzer (1931) to be areas containing wells that originally flowed. Therefore, the

predevelopment contours presented here are considered to be consistent with historical information and data.

4.4.2 Pressure versus Depth Analysis

A study of pressure head versus screen-midpoint depth was conducted using wells having both water-level and screen-depth data on the TWDB website. The analyses used water-level measurements taken prior to 1950. The goal of the study was to evaluate vertical movement between the hydrostratigraphic units. The locations of the wells used and the unit in which they are completed are shown in Figure 4.4.4. This figure shows that most of the wells completed in the Wilcox are located in the outcrop area in Bastrop, Caldwell, and Guadalupe counties. The majority of the wells completed in the Carrizo are located downdip of the outcrop in the Wintergarden area.

Figure 4.4.5 shows the pressure-depth analysis results for water level measurements prior to 1950. The results by hydrostratigraphic unit are shown in the upper plot and the results by county are shown in the lower plot. The screen midpoints for wells completed in the Carrizo Sand range from very shallow depths to depths greater than 1600 ft. The range in screen midpoints is significantly less for the wells completed in the Wilcox Group. A fit through the data for the 44 wells completed in the Carrizo Sand gives a slope of 1.02 indicating near hydrostatic conditions. A fit through the data for the 44 wells analyzed in the Wilcox Group gives a slope of 0.86 indicating downward flow.

The difference in slope between the data for the Carrizo and Wilcox may suggest a lack of hydraulic communication. However, the spatial distribution of the data (Figure 4.4.4), with the Carrizo wells in the southwestern portion of the study area and the Wilcox wells in the northeastern part of the study area, may represent different regimes of the aquifer system. The pressure-depth Wilcox data are from the outcrop in Bastrop and Caldwell counties. Bastrop County data show a slope of 0.91 indicating downward flow in the outcrop area, though the data range is very limited and difficult to interpret. Caldwell County data indicate near hydrostatic conditions. Most of the data in Caldwell County are located in the outcrop near the San Marcos River, where an upward flow component would be expected.

Carrizo data in Zavala and Dimmit counties show pressure-depth slopes of 1.06 and 1.01, indicating upward flow to hydrostatic conditions. Data distributions within the two counties

extend from the outcrop, where a downward flow would be expected, into the confined section, where upward flow would be expected. Visual inspection of data for Dimmit County does suggest that shallow wells in the outcrop indicate a slope of less than 1, suggesting downward flow. By comparison, deeper wells in the confined section indicate a slope greater than 1 suggesting upward flow (Figure 4.4.5). Shallow wells in Zavala County also suggest a downward flow component as compared to deeper wells in that county which show more data scatter and do not indicate a clear upward trend.

4.4.3 Predevelopment Conditions in the Queen City/Bigford Formations

Water-level elevation contours representative of predevelopment conditions in the Queen City Sand/Bigford formations were estimated. Only water-level data on the TWDB website were used. Therefore, the level of detail considered in construction of predevelopment conditions in the Queen City/Bigford formations were less than that considered for the Carrizo and Wilcox. Generation of approximate predevelopment water-level elevations for the Queen City/Bigford formations consisted of investigating maximum water-level elevations in each county, regardless of time. Figure 4.4.6 shows the predevelopment water-level elevation contours estimated for the Queen City/Bigford formations. Water-level measurements in several wells were above ground surface indicating flowing conditions. In several instances, measured water levels were adjusted upward in order for the developed head map to honor the locations of flowing wells. Table 4.4.2 summarizes that water-level data used in generating the predevelopment water-level elevation contours for the Queen City and Bigford formations.

4.4.4 Transient Water Levels

Historically, the greatest water-level declines have occurred in the Wintergarden District. Figure 4.4.7 shows the decline in water level from predevelopment conditions to 1980. The largest drawdowns (exceeding 400 ft) are found in southern Zavala County and northern Dimmit County. Drawdowns of greater than 150 ft are observed throughout the Wintergarden District. Based on the available data, the rate of decline was fastest during the 1940s and 1950s. Outside of the area influenced by pumpage in the Wintergarden District, historical water-level declines have been relatively small (Figure 4.4.7). The drawdown in central Gonzales County could be an artifact of our predevelopment head surface. Historical head maps in central Gonzales County are usually depressed as a result of the Guadalupe River. Appendix A includes select

long-term hydrographs in the study area showing the magnitude of historical head declines. The remainder of this section will focus on the transient calibration period of record.

Figure 4.4.8 shows the locations for which transient water-level data (hydrographs) are available for the last 20 years based on data in the TWDB database. Also shown on the figure is either the model layer in which the midpoint of the well screen is located or, where screen data are not available, the model layer in which the bottom of the well is located. In general, hydrographs show that water levels have remained relatively constant (less than 20 to 30 ft fluctuation) in the eastern portion of the study area (Bastrop, Caldwell, Guadalupe, Gonzales, and middle to northern Wilson counties) (Figure 4.4.9). The water-level spike in the hydrograph for Guadalupe County shown on this figure is not considered to represent actual conditions. All hydrograph data for Guadalupe County for this time period (six wells) show a water-level spike on the same measurement date (December 1, 1993). The increase in water level indicated by the spikes ranges from 61 to 196 ft greater than preceding and subsequent water-level measurements. In Karnes, Live Oak, and southern Wilson counties, the hydrograph data indicate water-level declines ranging from 25 to 45 ft over the last 20 years (Figure 4.4.10). In the outcrop areas of Bexar, Atascosa, Medina, Frio, Zavala, Maverick, and Dimmit counties, water levels have, in general, remained constant or slightly decreased in the last 20 yrs with the exception of one well in Medina County which shows a slight increase (well 68-49-808) (Figure 4.4.11). Notice that the well showing the increase is completed in the Lower Wilcox whereas all of the other wells are completed in the Carrizo Sand.

Over the last 20 years, no consistent trend is observed in the water levels for wells in the downdip areas of Atascosa, McMullen, Frio, LaSalle, Zavala, Dimmit, and Webb counties. Example hydrographs for Atascosa, Frio, and Zavala counties are provided in Figure 4.4.12. In general, water levels have declined up to 50 ft in Atascosa County over this time period (well 78-20-101), but an increase of over 125 ft is observed in one well (well 78-15-805). Most of the wells in Frio County for which hydrograph data are available show an overall decrease in water level over the last 20 yrs (well 77-23-301). Water levels in many of the downdip wells in Zavala County have decreased over the last 20 yrs (well 77-04-431), several have remained constant or increased (well 77-18-516), and many have had large fluctuations (well 77-19-102). Example hydrographs for Dimmit, La Salle, McMullen, and Webb counties are provided in Figure 4.4.13. Water levels in many of the downdip wells in Dimmit County remained relatively

flat over the last 20 yrs, others declined up to 30 ft (well 77-35-601), while still others had an overall increase in water level (well 77-26-605). All of the wells in McMullen County for which hydrograph data are available show an overall decrease in water level over the last 20 yrs. The majority of the hydrographs for wells in La Salle County show declines in water levels in the past 20 yrs (well 77-48-301), but several show substantial increases in water levels (well 77-37-301). Hydrographs for wells in Webb County show, in general, water-level decreases over the past 20 yrs.

4.4.5 Water-Level Elevations for Model Calibration and Verification

Model calibration considered the time period from January 1, 1980 to December 31, 1989 and model verification considered the time period from January 1, 1990 to December 31, 1999. Water-level data found on the TWDB website were used to develop water-level elevation contours for the start of calibration, the end of calibration, and the end of verification. The contours for the start of calibration were used to initialize the transient model. The contours for the end of calibration and verification were used to evaluate the model's ability to reproduce measured water-level data across the model domain.

Water level data on the TWDB website is not available at regular time intervals in every well. Therefore, the coverage of water-level data for a particular month or even a year is very sparse. For example, water levels were measured in three wells in December, 1980, and in a total of eight wells during 1980. Because this is not enough data to develop contours across the entire model area, measured water levels were averaged across two years before the date of interest and two years after the date of interest. For example, the water-level elevation contours for the end of calibration (December 31, 1989) used an average of the water levels measured in 1988, 1989, 1990, and 1991. This provided a total of 227 measurements for use in contouring.

Recall from Figure 4.4.1 that little water-level data are available for wells completed in the Wilcox downdip of the outcrop. Therefore, the water-level elevation contours for model calibration and verification focused on the Carrizo. The water-level elevation contours for the start of calibration are shown in Figure 4.4.14 and tabulated in Table 4.4.3, for the end of calibration in Figure 4.4.15 and Table 4.4.4, and for the end of verification in Figure 4.4.16 and Table 4.4.5. These figures show that there is continued depressurization of the Carrizo Sand in Webb, La Salle, and McMullen counties throughout this time period.

Table 4.4.1 Summary of data used to generate the predevelopment water-level elevation contours for the Carrizo Formation and the Wilcox Group.

State Well Number ^(a)	County ^(a)	Aquifer Code ^(a)	Year of Measurement ^(a)	LSD Elevation ^(a) (ft)	Depth to Water ^(a) (ft)	Water Level Elevation ^(b) (ft)	Adjusted Water Level Elevation ^(c) (ft)	Amount of Adjust-ment ^(d) (ft)
6851802	Atascosa	124CRRZ	1909	637	108	529		
6859502	Atascosa	124CRRZ	1910	547	25	522		
7803401	Atascosa	124CRRZ	1908	555	38	517		
5854901	Bastrop	124CRRZ	1950	545	118	427		
6706701	Bastrop	124CRRZ	1925	515	90	425		
6713801	Caldwell	124CRRZ	1923	469	40	429		
7624903	Dimmit	124WLCX	1929	689	75	614	714	100
7725202	Dimmit	124CRRZ	1929	682	82	600	686	86
7726414	Dimmit	124CRRZ	1913	578	4	574	674	100
7743502	Dimmit	124CRRZ	1933	571	75	496	596	100
7744105	Dimmit	124CRRZ	1920	520	69	451	575	124
6716404	Fayette	124CRRZ	1966	348	-2	350		
6857701	Frio	124CRRZ	1929	578	10	568		
6961605	Frio	124CRRZ	1929	699	84	615		
7723801	Frio	124CRRZ	1928	541	17	524		
7818206	Frio	124CRRZ	1929	401	-80	481		
6737201	Gonzales	124CRRZ	1931	282	-104	386		
6742903	Gonzales	124CRRZ	1940	390	-21	411		
6718903	Guadalupe	124WLCX	1936	592	82	510		
6733206	Guadalupe	124WLCX	1936	555	27	528		
6733401	Guadalupe	124WLCX	1982	561	59	502		
6832801	Guadalupe	124WLCX	2000	625	62	563		
6840101	Guadalupe	124CZWX	1936	575	7	568		
7816601	Karnes	124CRRZ	1956	502	99	403		
7731703	La Salle	124CRRZ	1960	570	151	419	519	100
7850201	La Salle	124CRRZ	1959	395	-41	436		
7828603	McMullen	124CRRZ	1959	309	-114	423		
7836901	McMullen	124CZWX	1959	351	-66	417		
6849918	Medina	124CRRZ	1930	680	43	637		
6858111	Medina	124CRRZ	1930	641	75	566		
6733703	Wilson	124CRRZ	1910	567	110	457		
6958401	Zavala	124CRRZ	1931	770	31	739		
6958601	Zavala	124WLCX	1929	809	78	731		
6959601	Zavala	124CRRZ	1929	789	49	740		
6960501	Zavala	124CRRZ	1929	860	187	673		
7710603	Zavala	124CRRZ	1931	625	43	582	659	77

- (a) source is the TWDB website:
rio.twdb.state.tx.us/publications/reports/GroundWaterReports/GWDatabaseReports/GWdatabaserpt.htm
- (b) calculated as the LSD elevation minus the depth to water
- (c) determined based on scientific judgment
- (d) the difference between the adjusted and not adjusted water-level elevations

Table 4.4.2 Summary of data used to generate the predevelopment water-level elevation contours for the Queen City and Bigford formations.

State Well Number ^(a)	County ^(a)	Aquifer Code ^(a)	Year of Measurement ^(a)	LSD Elevation ^(a) (ft)	Depth to Water ^(a) (ft)	Water Level Elevation ^(b) (ft)	Adjusted Water Level Elevation ^(c) (ft)	Amount of Adjustment ^(d) (ft)
7805604	Atascosa	124QNCT	1944	350	-16	366	416	50
7812105	Atascosa	124QNCT	1944	408	-2	410	445	35
7813702	Atascosa	124QNCT	1971	330	-41	371	421	50
7814203	Atascosa	124QNCT	1944	350	-1	351	406	55
5855305	Bastrop	124QNCT	1965	570	17	553		
5855501	Bastrop	124QNCT	1941	500	3	497		
5855602	Bastrop	124QNCT	1939	585	54	531		
6707401	Bastrop	124QNCT	1964	500	33	467		
6714101	Bastrop	124QNCT	1952	490	30	460		
6714704	Caldwell	124QNCT	1964	520	26	494		
7727709	Dimmit	124BGDF	1977	525	9	516		
7749301	Dimmit	124BGDF	1961	700	161	539		
6708604	Fayette	124QNCT	1979	342	24	318		
6857702	Frio	124QNCT	1952	578	30	548		
6857908	Frio	124QNCT	1963	601	75	526		
7707403	Frio	124QNCT	1964	580	90	490	510	20
7708401	Frio	124QNCT	1958	660	104	556		
7708701	Frio	124QNCT	1956	602	38	564		
7708802	Frio	124QNCT	1932	640	50	590		
7715901	Frio	124QNCT	1932	508	45	463		
7716403	Frio	124QNCT	1932	569	58	511		
6721201	Gonzales	124QNCT	1977	415	5	410		
6728303	Gonzales	124QNCT	1938	365	56	309	409	100
6728702	Gonzales	124QNCT	1938	350	45	305	390	85
6729701	Gonzales	124QNCT	1963	300	-9	309	379	70
6734803	Gonzales	124QNCT	1981	442	39	403		
6735902	Gonzales	124QNCT	1962	374	50	324	364	40
6743401	Gonzales	124QNCT	1959	314	-25	339	379	40
6743406	Gonzales	124QNCT	1959	312	-14	326	376	50
7724801	La Salle	124BGDF	1959	434	0	434	484	50
7746804	La Salle	124BGDF	1942	450	-8	458		
7826502	McMullen	124QNCT	1971	373	-8	381	431	50
7827903	McMullen	124QNCT	1959	336	-36	372		
7828303	McMullen	124QNCT	1959	281	-110	391		
8519201	Webb	124QNCT	1977	543	38	505		
6854902	Wilson	124QNCT	1963	530	78	452	462	10
6856804	Wilson	124QNCT	1996	489	81	408	458	50
6862507	Wilson	124QNCT	1977	500	84	416	466	50
6960401	Zavala	124BGDF	1946	817	50	767		
7702401	Zavala	124BGDF	1952	732	109	623		
7703502	Zavala	124BGDF	1973	782	115	667		
7704207	Zavala	124BGDF	1976	725	45	680		

- (a) source is the TWDB website:
rio.twdb.state.tx.us/publications/reports/GroundWaterReports/GWDatabaseReports/GWdatabaserpt.htm
- (b) calculated as the LSD elevation minus the depth to water
- (c) determined based on scientific judgment
- (d) the difference between the adjusted and not adjusted water-level elevations

Table 4.4.3 Data used to generate water-level elevation contours for the start of model calibration (January 1980).

State Well Number ^(a)	County ^(a)	Aquifer Code ^(a)	LSD Elevation (ft) ^(a)	Average Depth to Water (ft) ^(b)	Average Water-Level Elevation (ft) ^(c)
6851602	Atascosa	124CRRZ	705	120	585
6851701	Atascosa	124CRRZ	610	55	555
6851801	Atascosa	124CRRZ	673	128	545
6852718	Atascosa	124CRRZ	665	195	470
6858204	Atascosa	124CRRZ	646	161	485
6858302	Atascosa	124CRRZ	650	162	488
6858602	Atascosa	124CRRZ	534	91	443
6859303	Atascosa	124CRRZ	580	123	457
6859501	Atascosa	124CRRZ	545	100	445
6859621	Atascosa	124CRRZ	483	50	433
6859804	Atascosa	124CRRZ	496	86	410
6860303	Atascosa	124CRRZ	550	124	426
6860312	Atascosa	124CRRZ	550	125	425
6860401	Atascosa	124CRRZ	515	102	413
6860610	Atascosa	124CRRZ	535	131	404
6860912	Atascosa	124CRRZ	446	61	385
6860913	Atascosa	124CRRZ	430	59	371
6861310	Atascosa	124CRRZ	520	115	405
6861501	Atascosa	124CRRZ	471	67	404
6861602	Atascosa	124CRRZ	475	74	401
6861905	Atascosa	124CRRZ	482	106	376
6862405	Atascosa	124CRRZ	492	118	374
7802303	Atascosa	124CRRZ	592	150	442
7802602	Atascosa	124CRRZ	530	168	362
7803302	Atascosa	124CRRZ	490	96	394
7803509	Atascosa	124CRRZ	575	205	370
7803601	Atascosa	124CRRZ	565	163	402
7804204	Atascosa	124CRRZ	430	53	377
7804803	Atascosa	124CRRZ	480	104	376
7804812	Atascosa	124CRRZ	421	67	354
7805104	Atascosa	124CRRZ	385	26	359
7805116	Atascosa	124CRRZ	373	13	360
7805501	Atascosa	124CRRZ	405	55	350
7806103	Atascosa	124CRRZ	422	56	366
7806503	Atascosa	124CRRZ	392	35	357
7806507	Atascosa	124CRRZ	350	11	339
7810303	Atascosa	124CRRZ	480	126	354
7810606	Atascosa	124CRRZ	450	111	339
7811202	Atascosa	124CRRZ	542	203	339
7811301	Atascosa	124CRRZ	479	107	372
7811501	Atascosa	124CRRZ	495	138	357
7811903	Atascosa	124CRRZ	400	92	308
7812701	Atascosa	124CRRZ	452	117	335
7814801	Atascosa	124CRRZ	241	-92	333
7814802	Atascosa	124CRRZ	233	-94	327
7815805	Atascosa	124CRRZ	469	116	353
7818601	Atascosa	124CRRZ	376	51	325
7820101	Atascosa	124CRRZ	464	144	320
7821106	Atascosa	124CRRZ	305	-20	325
7822201	Atascosa	124CRRZ	228	-96	324

Table 4.4.3 (continued)

State Well Number^(a)	County^(a)	Aquifer Code^(a)	LSD Elevation (ft)^(a)	Average Depth to Water (ft)^(b)	Average Water-Level Elevation (ft)^(c)
7822202	Atascosa	124CRRZ	242	-104	346
6706201	Bastrop	124CRRZ	480	117	363
6706501	Bastrop	124CRRZ	480	83	397
6706502	Bastrop	124CRRZ	460	91	369
6706609	Bastrop	124CRRZ	593	99	494
6706802	Bastrop	124CRRZ	593	97	496
6853703	Bexar	124CRRZ	570	137	433
6853805	Bexar	124CRRZ	535	121	414
6713201	Caldwell	124CRRZ	575	137	438
6713605	Caldwell	124CRRZ	490	75	415
6713801	Caldwell	124CRRZ	469	47	422
6721104	Caldwell	124CRRZ	475	68	407
7648801	Dimmit	124CRRZ	680	25	655
7718904	Dimmit	124CRRZ	573	320	253
7719703	Dimmit	124CRRZ	572	312	260
7726613	Dimmit	124CRRZ	534	221	313
7726708	Dimmit	124CRRZ	602	180	422
7726904	Dimmit	124CRRZ	525	238	287
7728503	Dimmit	124CRRZ	535	290	245
7733301	Dimmit	124CRRZ	705	165	540
7733611	Dimmit	124CRRZ	690	111	579
7734319	Dimmit	124CRRZ	520	223	297
7734402	Dimmit	124CRRZ	628	166	462
7734607	Dimmit	124CRRZ	565	203	362
7734702	Dimmit	124CRRZ	650	171	479
7737101	Dimmit	124CRRZ	475	212	263
7744103	Dimmit	124CRRZ	560	112	448
6716404	Fayette	124CRRZ	348	8	340
6857402	Frio	124CRRZ	667	192	475
6857505	Frio	124CRRZ	605	113	492
6857616	Frio	124CRRZ	660	196	464
6857701	Frio	124CRRZ	578	82	496
6857901	Frio	124CRRZ	631	125	506
6858506	Frio	124CRRZ	611	165	446
6962601	Frio	124CRRZ	698	206	492
6962902	Frio	124CRRZ	610	144	466
6963605	Frio	124CRRZ	632	134	498
6964501	Frio	124CRRZ	711	191	520
7706205	Frio	124CRRZ	660	259	401
7707201	Frio	124CRRZ	586	166	420
7707501	Frio	124CRRZ	555	175	380
7707901	Frio	124CRRZ	600	251	349
7708201	Frio	124CRRZ	700	290	410
7708409	Frio	124CRRZ	660	274	386
7708716	Frio	124CRRZ	618	269	349
7708803	Frio	124CRRZ	652	353	299
7708806	Frio	124CRRZ	642	292	350
7708812	Frio	124CRRZ	648	295	353
7714601	Frio	124CRRZ	510	231	279
7714904	Frio	124CRRZ	522	221	301
7715907	Frio	124CRRZ	485	176	309

Table 4.4.3 (continued)

State Well Number^(a)	County^(a)	Aquifer Code^(a)	LSD Elevation (ft)^(a)	Average Depth to Water (ft)^(b)	Average Water-Level Elevation (ft)^(c)
7716201	Frio	124CRRZ	652	318	334
7716603	Frio	124CRRZ	640	330	310
7716705	Frio	124CRRZ	532	222	310
7716801	Frio	124CRRZ	521	241	280
7722502	Frio	124CRRZ	610	348	262
7723106	Frio	124CRRZ	520	260	260
7723301	Frio	124CRRZ	515	242	273
7723509	Frio	124CRRZ	575	294	281
7723602	Frio	124CRRZ	500	240	260
7723701	Frio	124CRRZ	560	323	237
7723803	Frio	124CRRZ	562	288	274
7724202	Frio	124CRRZ	458	191	267
7801501	Frio	124CRRZ	525	133	392
7801801	Frio	124CRRZ	501	144	357
7802402	Frio	124CRRZ	582	192	390
7802701	Frio	124CRRZ	553	202	351
7802702	Frio	124CRRZ	522	153	369
7809305	Frio	124CRRZ	471	123	348
7809602	Frio	124CRRZ	491	160	331
7818206	Frio	124CRRZ	401	13	388
6721204	Gonzales	124QNCT	430	51	379
6721701	Gonzales	124CRRZ	430	57	373
6721703	Gonzales	124CRRZ	420	68	352
6721903	Gonzales	124CRRZ	390	12	378
6727502	Gonzales	124CRRZ	435	73	362
6727503	Gonzales	124WLCX	433	74	359
6727701	Gonzales	124CRRZ	392	13	379
6727703	Gonzales	124CRRZ	450	115	335
6727801	Gonzales	124CRRZ	429	55	374
6727805	Gonzales	124CRRZ	370	15	355
6727806	Gonzales	124CRRZ	400	39	361
6727903	Gonzales	124CRRZ	345	-3	348
6727909	Gonzales	124CRRZ	400	37	363
6728104	Gonzales	124CRRZ	321	1	320
6729201	Gonzales	124CRRZ	408	46	362
6729602	Gonzales	124CRRZ	375	28	347
6735701	Gonzales	124CRRZ	364	-13	377
6742202	Gonzales	124CRRZ	409	15	394
6742906	Gonzales	124CRRZ	390	29	361
6743104	Gonzales	124CRRZ	360	-18	378
6743901	Gonzales	124CRRZ	322	-43	365
6744201	Gonzales	124CRRZ	288	-62	350
6744701	Gonzales	124CRRZ	290	-107	397
6734302	Guadalupe	124CRRZ	495	58	437
6734402	Guadalupe	124CRRZ	620	176	444
6734704	Guadalupe	124CRRZ	470	35	435
7816601	Karnes	124CRRZ	502	163	339
7730502	La Salle	124CRRZ	580	349	231
7730801	La Salle	124CRRZ	516	295	221
7731703	La Salle	124CRRZ	570	241	329
7737301	La Salle	124CRRZ	448	174	274

Table 4.4.3 (continued)

State Well Number ^(a)	County ^(a)	Aquifer Code ^(a)	LSD Elevation (ft) ^(a)	Average Depth to Water (ft) ^(b)	Average Water-Level Elevation (ft) ^(c)
7738901	La Salle	124CRRZ	449	193	256
7739301	La Salle	124CRRZ	565	334	231
7739407	La Salle	124CRRZ	431	200	231
7739601	La Salle	124CRRZ	458	73	385
7740303	La Salle	124CRRZ	422	159	263
7748301	La Salle	124CRRZ	420	153	267
7764401	La Salle	124CRRZ	395	74	321
7825803	La Salle	124CRRZ	368	101	267
7841301	La Salle	124CRRZ	455	183	272
7823502	Live Oak	124CRRZ	358	27	331
7607901	Maverick	124CRRZ	703	76	627
7607919	Maverick	124CRRZ	700	75	625
7608401	Maverick	124CRRZ	700	61	639
7608704	Maverick	124CRRZ	701	50	651
7821801	McMullen	124CZWX	378	48	330
7826601	McMullen	124CRRZ	365	29	336
7826802	McMullen	124CRRZ	363	59	304
7827303	McMullen	124CRRZ	394	77	317
7827503	McMullen	124CRRZ	380	85	295
7828501	McMullen	124CRRZ	335	25	310
7828702	McMullen	124CRRZ	342	60	282
7836902	McMullen	124CRRZ	350	25	325
7842902	McMullen	124CRRZ	332	35	297
6849902	Medina	124CRRZ	655	72	583
6850702	Medina	124CRRZ	725	136	589
6857210	Medina	124CZWX	655	144	511
6857307	Medina	124CRRZ	643	106	537
6858101	Medina	124CRRZ	650	138	512
6858109	Medina	124CRRZ	620	113	507
6858110	Medina	124CRRZ	618	134	484
7749601	Webb	124CRRZ	795	272	523
7758701	Webb	124CRRZ	700	215	485
8504401	Webb	124CRRZ	620	177	443
8511302	Webb	124CRRZ	625	110	515
6741102	Wilson	124CRRZ	590	173	417
6741401	Wilson	124CRRZ	536	115	421
6741801	Wilson	124CRRZ	547	144	403
6749201	Wilson	124CRRZ	470	93	377
6750203	Wilson	124CRRZ	434	53	381
6847903	Wilson	124CRRZ	590	164	426
6848502	Wilson	124CRRZ	430	31	399
6848601	Wilson	124CRRZ	490	92	398
6848802	Wilson	124CRRZ	416	8	408
6848812	Wilson	124CRRZ	426	28	398
6848907	Wilson	124CRRZ	502	95	407
6854301	Wilson	124CRRZ	492	99	393
6854602	Wilson	124CRRZ	525	135	390
6854802	Wilson	124CRRZ	575	195	380
6854901	Wilson	124CRRZ	515	89	426
6855202	Wilson	124CRRZ	507	113	394
6855407	Wilson	124CRRZ	456	51	405

Table 4.4.3 (continued)

State Well Number^(a)	County^(a)	Aquifer Code^(a)	LSD Elevation (ft)^(a)	Average Depth to Water (ft)^(b)	Average Water-Level Elevation (ft)^(c)
6855601	Wilson	124CRRZ	513	123	390
6855704	Wilson	124CRRZ	430	37	393
6855706	Wilson	124CRRZ	440	60	380
6855901	Wilson	124CRRZ	396	24	372
6855902	Wilson	124CRRZ	390	44	346
6855903	Wilson	124CRRZ	390	24	366
6856101	Wilson	124CRRZ	490	85	405
6856201	Wilson	124CRRZ	428	32	396
6856302	Wilson	124CRRZ	431	33	398
6856401	Wilson	124CRRZ	565	175	390
6856704	Wilson	124CRRZ	489	113	376
6856902	Wilson	124CRRZ	460	78	382
6862104	Wilson	124CRRZ	590	209	381
6862202	Wilson	124CRRZ	496	102	394
6862205	Wilson	124CRRZ	532	149	383
6862902	Wilson	124CRRZ	437	72	365
6863101	Wilson	124CRRZ	448	66	382
6863302	Wilson	124CRRZ	430	66	364
6863802	Wilson	124CRRZ	456	105	351
6864401	Wilson	124CRRZ	400	32	368
6864402	Wilson	124CRRZ	403	26	377
6864902	Wilson	124CRRZ	358	28	330
6958701	Zavala	124CRRZ	772	131	641
6958704	Zavala	124CRRZ	784	164	620
6958707	Zavala	124CRRZ	789	154	635
6958715	Zavala	124CRRZ	768	83	685
6958801	Zavala	124CRRZ	750	58	692
6959911	Zavala	124CRRZ	765	249	516
6959913	Zavala	124CRRZ	811	280	531
6961502	Zavala	124CRRZ	717	194	523
6961525	Zavala	124CRRZ	719	178	541
6961818	Zavala	124CRRZ	703	225	478
7608406	Zavala	124CRRZ	712	67	645
7624201	Zavala	124CRRZ	608	129	479
7624906	Zavala	124CRRZ	631	231	400
7701101	Zavala	124CRRZ	762	113	649
7701311	Zavala	124CRRZ	776	89	687
7701404	Zavala	124CRRZ	735	110	625
7701501	Zavala	124CRRZ	771	299	472
7701605	Zavala	124CRRZ	739	291	448
7701702	Zavala	124CRRZ	698	103	595
7702103	Zavala	124CRRZ	757	297	460
7702403	Zavala	124CRRZ	748	347	401
7702606	Zavala	124CRRZ	688	280	408
7702706	Zavala	124CRRZ	729	340	389
7703401	Zavala	124CRRZ	731	322	409
7704431	Zavala	124CRRZ	708	291	417
7704601	Zavala	124CRRZ	704	310	394
7704706	Zavala	124CRRZ	680	292	389
7709201	Zavala	124CRRZ	679	375	304
7709704	Zavala	124CRRZ	621	278	343

Table 4.4.3 (continued)

State Well Number^(a)	County^(a)	Aquifer Code^(a)	LSD Elevation (ft)^(a)	Average Depth to Water (ft)^(b)	Average Water-Level Elevation (ft)^(c)
7710604	Zavala	124CRRZ	624	302	322
7711703	Zavala	124CRRZ	634	332	302
7711715	Zavala	124CRRZ	636	325	311
7711718	Zavala	124CRRZ	641	321	320
7717707	Zavala	124CZWX	603	216	387
7719102	Zavala	124CRRZ	614	326	288
Dummy-1 ^(d)					350
Dummy-2 ^(d)					350
Dummy-3 ^(d)					350

- (a) source is the TWDB website:
rio.twdb.state.tx.us/publications/reports/GroundWaterReports/GWDatabaseReports/GWdatabaserpt.htm
- (b) calculated as the LSD elevation minus the average water-level elevation
- (c) calculated from the 1978-1981 data on the TWDB website
- (d) included to define water level in areas with little data

Table 4.4.4 Data used to generate water-level elevation contours for the end of model calibration (December 1989).

State Well Number ^(a)	County ^(a)	Aquifer Code ^(a)	LSD Elevation (ft) ^(a)	Average Depth to Water (ft) ^(b)	Average Water-Level Elevation (ft) ^(c)
6851602	Atascosa	124CRRZ	705	122	583
6851701	Atascosa	124CRRZ	610	56	555
6852713	Atascosa	124CRRZ	665	179	486
6852718	Atascosa	124CRRZ	665	202	463
6858302	Atascosa	124CRRZ	650	177	473
6858602	Atascosa	124CRRZ	534	110	424
6859312	Atascosa	124CRRZ	580	129	451
6859501	Atascosa	124CRRZ	545	116	429
6859517	Atascosa	124CRRZ	578	177	401
6859633	Atascosa	124CRRZ	500	105	395
6859804	Atascosa	124CRRZ	496	107	389
6860312	Atascosa	124CRRZ	550	139	411
6861310	Atascosa	124CRRZ	520	139	381
6861602	Atascosa	124CRRZ	475	78	397
6861905	Atascosa	124CRRZ	482	124	359
6862405	Atascosa	124CRRZ	492	136	357
7802303	Atascosa	124CRRZ	592	187	405
7803509	Atascosa	124CRRZ	575	238	337
7803601	Atascosa	124CRRZ	565	186	379
7804204	Atascosa	124CRRZ	430	77	353
7804612	Atascosa	124CRRZ	420	95	325
7804812	Atascosa	124CRRZ	421	89	332
7805116	Atascosa	124CRRZ	373	34	339
7805501	Atascosa	124CRRZ	405	72	333
7806103	Atascosa	124CRRZ	422	84	339
7806507	Atascosa	124CRRZ	350	14	336
7810303	Atascosa	124CRRZ	480	147	333
7810606	Atascosa	124CRRZ	450	153	297
7811202	Atascosa	124CRRZ	542	229	313
7811218	Atascosa	124CRRZ	445	242	203
7811301	Atascosa	124CRRZ	479	148	331
7811903	Atascosa	124CRRZ	400	127	273
7814801	Atascosa	124CRRZ	241	-63	304
7814802	Atascosa	124CRRZ	233	-64	297
7815301	Atascosa	124CRRZ	475	113	363
7815805	Atascosa	124CRRZ	469	116	353
7820101	Atascosa	124CRRZ	464	170	294
7821106	Atascosa	124CRRZ	305	25	280
7822201	Atascosa	124CRRZ	228	-77	305
7822202	Atascosa	124CRRZ	242	-90	332
5863103	Bastrop	124CRRZ	370	15	355
5863606	Bastrop	124CRRZ	380	60	320
6706501	Bastrop	124CRRZ	480	92	389
6707204	Bastrop	124CRRZ	390	48	343
6852903	Bexar	124CRRZ	608	180	428
6852905	Bexar	124CRRZ	589	165	424
6853703	Bexar	124CRRZ	570	149	421
6854402	Bexar	124CRRZ	435	39	397
6713201	Caldwell	124CRRZ	575	136	439
6720603	Caldwell	124CRRZ	472	77	395

Table 4.4.4 (continued)

State Well Number^(a)	County^(a)	Aquifer Code^(a)	LSD Elevation (ft)^(a)	Average Depth to Water (ft)^(b)	Average Water-Level Elevation (ft)^(c)
6721104	Caldwell	124CRRZ	475	72	403
7624801	Dimmit	124CRRZ	665	110	556
7648801	Dimmit	124CRRZ	680	24	656
7718704	Dimmit	124CRRZ	580	271	309
7725604	Dimmit	124CRRZ	612	232	380
7726101	Dimmit	124CRRZ	590	250	340
7726605	Dimmit	124CRRZ	525	254	271
7726613	Dimmit	124CRRZ	534	212	322
7726708	Dimmit	124CRRZ	602	195	407
7728503	Dimmit	124CRRZ	535	273	262
7733301	Dimmit	124CRRZ	705	173	532
7733322	Dimmit	124CRRZ	665	101	565
7733611	Dimmit	124CRRZ	690	119	571
7733701	Dimmit	124CRRZ	810	229	581
7734606	Dimmit	124CRRZ	553	222	331
7734607	Dimmit	124CRRZ	565	194	371
7734702	Dimmit	124CRRZ	650	170	480
7735601	Dimmit	124CRRZ	540	235	305
7737101	Dimmit	124CRRZ	475	207	268
7737501	Dimmit	124CRRZ	485	225	260
7742801	Dimmit	124CRRZ	613	168	445
7744101	Dimmit	124CRRZ	480	180	300
6857402	Frio	124CRRZ	667	204	464
6857701	Frio	124CRRZ	578	101	478
6858506	Frio	124CRRZ	611	183	428
6962902	Frio	124CRRZ	610	171	439
6963605	Frio	124CRRZ	632	144	488
7706205	Frio	124CRRZ	660	273	387
7706301	Frio	124CRRZ	605	207	398
7707201	Frio	124CRRZ	586	214	372
7707501	Frio	124CRRZ	555	219	336
7707901	Frio	124CRRZ	600	278	322
7708201	Frio	124CRRZ	700	308	393
7708409	Frio	124CRRZ	660	310	351
7708716	Frio	124CRRZ	618	311	308
7708806	Frio	124CRRZ	642	321	321
7708812	Frio	124CRRZ	648	310	338
7714601	Frio	124CRRZ	510	245	265
7714904	Frio	124CRRZ	522	246	276
7715907	Frio	124CRRZ	485	153	333
7716603	Frio	124CRRZ	640	333	307
7716705	Frio	124CRRZ	532	243	289
7716801	Frio	124CRRZ	521	250	271
7721301	Frio	124CRRZ	620	370	250
7722502	Frio	124CRRZ	610	382	228
7723301	Frio	124CRRZ	515	253	263
7723602	Frio	124CRRZ	500	249	251
7723701	Frio	124CRRZ	560	318	242
7723807	Frio	124CRRZ	535	417	118
7723808	Frio	124CRRZ	561	329	232
7724202	Frio	124CRRZ	458	207	252

Table 4.4.4 (continued)

State Well Number ^(a)	County ^(a)	Aquifer Code ^(a)	LSD Elevation (ft) ^(a)	Average Depth to Water (ft) ^(b)	Average Water-Level Elevation (ft) ^(c)
7801501	Frio	124CRRZ	525	154	371
7801801	Frio	124CRRZ	501	161	340
7802402	Frio	124CRRZ	582	226	357
7802501	Frio	124CRRZ	572	182	391
7802701	Frio	124CRRZ	553	216	337
7802702	Frio	124CRRZ	522	187	336
7809305	Frio	124CRRZ	471	141	330
7809507	Frio	124CRRZ	490	165	325
7818206	Frio	124CRRZ	401	18	383
6721703	Gonzales	124CRRZ	420	73	347
6721903	Gonzales	124CRRZ	390	51	339
6727502	Gonzales	124CRRZ	435	76	359
6727805	Gonzales	124CRRZ	370	19	351
6728104	Gonzales	124CRRZ	321	3	319
6729303	Gonzales	124CRRZ	410	53	357
6729602	Gonzales	124CRRZ	375	34	341
6729603	Gonzales	124CRRZ	375	38	337
6742202	Gonzales	124CRRZ	409	20	390
6726311	Guadalupe	124CRRZ	490	90	400
6734402	Guadalupe	124CRRZ	620	181	439
6734406	Guadalupe	124CRRZ	540	85	455
6734704	Guadalupe	124CRRZ	470	39	431
7816601	Karnes	124CRRZ	502	173	329
7730502	La Salle	124CRRZ	580	349	231
7730801	La Salle	124CRRZ	516	274	242
7731703	La Salle	124CRRZ	570	182	388
7737301	La Salle	124CRRZ	448	52	396
7738201	La Salle	124CRRZ	468	232	236
7738901	La Salle	124CRRZ	449	207	242
7739301	La Salle	124CRRZ	565	337	228
7739407	La Salle	124CRRZ	431	205	226
7739408	La Salle	124CRRZ	415	189	226
7739601	La Salle	124CRRZ	458	72	386
7740303	La Salle	124CRRZ	422	155	268
7740305	La Salle	124CRRZ	402	70	332
7747802	La Salle	124CRRZ	398	37	361
7748301	La Salle	124CRRZ	420	160	260
7764401	La Salle	124CRRZ	395	88	307
7823502	Live Oak	124CRRZ	358	58	300
7607901	Maverick	124CRRZ	703	71	632
7607919	Maverick	124CRRZ	700	71	629
7608401	Maverick	124CRRZ	700	71	629
7615303	Maverick	124CRRZ	707	58	649
7826802	McMullen	124CRRZ	363	88	275
7827503	McMullen	124CRRZ	380	116	264
7828501	McMullen	124CRRZ	335	60	276
7828602	McMullen	124CRRZ	288	18	270
7828702	McMullen	124CRRZ	342	77	266
7837103	McMullen	124CRRZ	345	78	267
6849902	Medina	124CRRZ	655	75	580
6850717	Medina	124CRRZ	690	149	541

Table 4.4.4 (continued)

State Well Number^(a)	County^(a)	Aquifer Code^(a)	LSD Elevation (ft)^(a)	Average Depth to Water (ft)^(b)	Average Water-Level Elevation (ft)^(c)
6857307	Medina	124CRRZ	643	116	527
6858101	Medina	124CRRZ	650	146	504
6858110	Medina	124CRRZ	618	143	475
6956903	Medina	124CRRZ	750	120	630
6960201	Uvalde	124CRRZ	891	199	692
7749501	Webb	124CRRZ	862	310	552
7750601	Webb	124CRRZ	655	226	429
7750603	Webb	124CRRZ	655	199	457
7759401	Webb	124CRRZ	720	283	437
7760201	Webb	124CRRZ	668	365	303
8504401	Webb	124CRRZ	620	196	424
6741102	Wilson	124CRRZ	590	180	411
6741801	Wilson	124CRRZ	547	143	405
6749201	Wilson	124CRRZ	470	99	371
6846903	Wilson	124CRRZ	520	105	415
6846904	Wilson	124CRRZ	520	110	410
6847601	Wilson	124CRRZ	652	201	452
6847903	Wilson	124CRRZ	590	172	418
6848402	Wilson	124CRRZ	547	90	457
6848502	Wilson	124CRRZ	430	32	398
6848507	Wilson	124CRRZ	473	68	405
6848601	Wilson	124CRRZ	490	96	394
6848812	Wilson	124CRRZ	426	30	396
6848907	Wilson	124CRRZ	502	106	397
6854506	Wilson	124CRRZ	419	36	383
6854602	Wilson	124CRRZ	525	145	380
6854802	Wilson	124CRRZ	575	215	360
6854901	Wilson	124CRRZ	515	137	378
6855202	Wilson	124CRRZ	507	116	391
6855206	Wilson	124CRRZ	525	120	405
6855407	Wilson	124CRRZ	456	50	406
6855704	Wilson	124CRRZ	430	49	382
6855706	Wilson	124CRRZ	440	53	387
6856101	Wilson	124CRRZ	490	79	411
6856201	Wilson	124CRRZ	428	37	391
6856302	Wilson	124CRRZ	431	40	391
6856409	Wilson	124CRRZ	560	176	384
6856902	Wilson	124CRRZ	460	87	373
6862205	Wilson	124CRRZ	532	163	369
6862902	Wilson	124CRRZ	437	99	338
6862906	Wilson	124CRRZ	422	67	355
6863101	Wilson	124CRRZ	448	72	376
6863802	Wilson	124CRRZ	456	123	333
6864401	Wilson	124CRRZ	400	38	362
6958701	Zavala	124CRRZ	772	131	641
6958707	Zavala	124CRRZ	789	166	623
6958715	Zavala	124CRRZ	768	82	686
6958801	Zavala	124CRRZ	750	60	690
6959401	Zavala	124CRRZ	815	100	715
6959904	Zavala	124CRRZ	743	267	477
6961502	Zavala	124CRRZ	717	203	514

Table 4.4.4 (continued)

State Well Number ^(a)	County ^(a)	Aquifer Code ^(a)	LSD Elevation (ft) ^(a)	Average Depth to Water (ft) ^(b)	Average Water-Level Elevation (ft) ^(c)
6961525	Zavala	124CRRZ	719	183	536
7608406	Zavala	124CRRZ	712	70	642
7608503	Zavala	124CRRZ	728	92	636
7624906	Zavala	124CRRZ	631	233	398
7701311	Zavala	124CRRZ	776	88	689
7701404	Zavala	124CRRZ	735	117	619
7701501	Zavala	124CRRZ	771	300	471
7701702	Zavala	124CRRZ	698	121	577
7702103	Zavala	124CRRZ	757	305	452
7702414	Zavala	124CRRZ	747	338	409
7702606	Zavala	124CRRZ	688	290	399
7703401	Zavala	124CRRZ	731	311	420
7704202	Zavala	124CRRZ	751	304	447
7704431	Zavala	124CRRZ	708	338	370
7704603	Zavala	124CRRZ	688	282	406
7704718	Zavala	124CRRZ	686	327	359
7709101	Zavala	124CRRZ	668	275	393
7709704	Zavala	124CRRZ	621	244	377
7711703	Zavala	124CRRZ	634	300	334
7711718	Zavala	124CRRZ	641	306	335
7712702	Zavala	124CRRZ	641	325	317
7718516	Zavala	124CRRZ	574	278	296
7719102	Zavala	124CRRZ	614	328	286

- (a) source is the TWDB website:
rio.twdb.state.tx.us/publications/reports/GroundWaterReports/GWDatabaseReports/GWdatabaserpt.htm
- (b) calculated as the LSD elevation minus the average water-level elevation
- (c) calculated from the 1988-1991 data on the TWDB website

Table 4.4.5 Data used to generate water-level elevation contours for the end of model verification (December 1999).

State Well Number ^(a)	County ^(a)	Aquifer Code ^(a)	LSD Elevation (ft) ^(a)	Average Depth to Water (ft) ^(b)	Average Water-Level Elevation (ft) ^(c)
6851701	Atascosa	124CRRZ	610	59	552
6852713	Atascosa	124CRRZ	665	172	494
6852718	Atascosa	124CRRZ	665	199	466
6858302	Atascosa	124CRRZ	650	185	465
6858602	Atascosa	124CRRZ	534	116	419
6859212	Atascosa	124CRRZ	603	132	471
6859312	Atascosa	124CRRZ	580	139	441
6859316	Atascosa	124CRRZ	593	113	480
6859317	Atascosa	124CRRZ	565	137	428
6859501	Atascosa	124CRRZ	545	125	420
6859517	Atascosa	124CRRZ	578	158	420
6859633	Atascosa	124CRRZ	500	104	396
6859804	Atascosa	124CRRZ	496	105	391
6860852	Atascosa	124CRRZ	472	118	354
6860912	Atascosa	124CRRZ	446	101	345
6861602	Atascosa	124CRRZ	475	75	401
6861905	Atascosa	124CRRZ	482	136	346
6862405	Atascosa	124CRRZ	492	137	355
7804612	Atascosa	124CRRZ	420	95	326
7805116	Atascosa	124CRRZ	373	38	336
7805124	Atascosa	124CRRZ	385	54	331
7805212	Atascosa	124CRRZ	405	76	329
7805802	Atascosa	124CRRZ	410	85	325
7806103	Atascosa	124CRRZ	422	82	340
7810315	Atascosa	124CRRZ	489	192	297
7811202	Atascosa	124CRRZ	542	243	300
7811301	Atascosa	124CRRZ	479	173	306
7814801	Atascosa	124CRRZ	241	-13	254
7814802	Atascosa	124CRRZ	233	-17	250
7815805	Atascosa	124CRRZ	469	-18	487
7820101	Atascosa	124CRRZ	464	172	292
7822201	Atascosa	124CRRZ	228	-22	250
5863103	Bastrop	124CRRZ	370	13	358
5863606	Bastrop	124CRRZ	380	53	327
6706501	Bastrop	124CRRZ	480	89	391
6707204	Bastrop	124CRRZ	390	44	347
6853907	Bexar	124CRRZ	565	210	355
7624801	Dimmit	124CRRZ	665	108	557
7648801	Dimmit	124CRRZ	680	25	655
7718704	Dimmit	124CRRZ	580	276	304
7726605	Dimmit	124CRRZ	525	254	271
7726708	Dimmit	124CRRZ	602	195	407
7728503	Dimmit	124CRRZ	535	283	252
7733301	Dimmit	124CRRZ	705	176	529
7733309	Dimmit	124CRRZ	665	122	543
7733322	Dimmit	124CRRZ	665	107	558
7733611	Dimmit	124CRRZ	690	132	558
7733701	Dimmit	124CRRZ	810	236	574
7734607	Dimmit	124CRRZ	565	213	352
7734702	Dimmit	124CRRZ	650	175	475

Table 4.4.5 (continued)

State Well Number^(a)	County^(a)	Aquifer Code^(a)	LSD Elevation (ft)^(a)	Average Depth to Water (ft)^(b)	Average Water-Level Elevation (ft)^(c)
7737501	Dimmit	124CRRZ	485	183	302
7742801	Dimmit	124CRRZ	613	176	437
7744101	Dimmit	124CRRZ	480	202	278
6716404	Fayette	124CRRZ	348	0	348
6857701	Frio	124CRRZ	578	110	468
6858506	Frio	124CRRZ	611	214	397
6962902	Frio	124CRRZ	610	191	420
7707201	Frio	124CRRZ	586	215	372
7707501	Frio	124CRRZ	555	244	311
7707901	Frio	124CRRZ	600	318	282
7708409	Frio	124CRRZ	660	344	317
7708716	Frio	124CRRZ	618	304	314
7708803	Frio	124CRRZ	652	354	298
7708806	Frio	124CRRZ	642	269	373
7708812	Frio	124CRRZ	648	257	392
7714904	Frio	124CRRZ	522	361	161
7716603	Frio	124CRRZ	640	319	322
7716705	Frio	124CRRZ	532	257	276
7716801	Frio	124CRRZ	521	257	265
7721301	Frio	124CRRZ	620	320	300
7722401	Frio	124CRRZ	605	338	268
7723205	Frio	124CRRZ	553	370	183
7723301	Frio	124CRRZ	515	297	219
7723602	Frio	124CRRZ	500	312	188
7723807	Frio	124CRRZ	535	366	170
7724202	Frio	124CRRZ	458	210	248
7801501	Frio	124CRRZ	525	157	369
7802702	Frio	124CRRZ	522	186	336
7802815	Frio	124CRRZ	534	209	325
7809305	Frio	124CRRZ	471	163	308
7809506	Frio	124CRRZ	550	283	267
7809507	Frio	124CRRZ	490	206	285
7818206	Frio	124CRRZ	401	24	377
6721703	Gonzales	124CRRZ	420	75	345
6727502	Gonzales	124CRRZ	435	0	435
6727805	Gonzales	124CRRZ	370	22	349
6727903	Gonzales	124CRRZ	345	-2	347
6728104	Gonzales	124CRRZ	321	3	319
6729602	Gonzales	124CRRZ	375	40	336
6729603	Gonzales	124CRRZ	375	34	342
6742202	Gonzales	124CRRZ	409	22	387
6742906	Gonzales	124CRRZ	390	-44	434
6742913	Gonzales	124CRRZ	341	-9	350
6734704	Guadalupe	124CRRZ	470	40	430
6734706	Guadalupe	124CRRZ	515	98	417
7808301	Karnes	124CRRZ	330	-32	362
7808302	Karnes	124CRRZ	325	-40	365
7808306	Karnes	124CRRZ	315	-117	432
7816601	Karnes	124CRRZ	502	175	327
7729603	La Salle	124CRRZ	515	303	212
7730502	La Salle	124CRRZ	580	405	175

Table 4.4.5 (continued)

State Well Number^(a)	County^(a)	Aquifer Code^(a)	LSD Elevation (ft)^(a)	Average Depth to Water (ft)^(b)	Average Water-Level Elevation (ft)^(c)
7730801	La Salle	124CRRZ	516	330	186
7731703	La Salle	124CRRZ	570	189	381
7738201	La Salle	124CRRZ	468	266	202
7738901	La Salle	124CRRZ	449	117	332
7739301	La Salle	124CRRZ	565	364	201
7739407	La Salle	124CRRZ	431	253	178
7740303	La Salle	124CRRZ	422	195	227
7740305	La Salle	124CRRZ	402	66	337
7747802	La Salle	124CRRZ	398	23	375
7748301	La Salle	124CRRZ	420	195	225
7748801	La Salle	124CRRZ	345	106	239
7764401	La Salle	124CRRZ	395	115	280
7607901	Maverick	124CRRZ	703	72	631
7607919	Maverick	124CRRZ	700	70	630
7828501	McMullen	124CRRZ	335	81	254
7828602	McMullen	124CRRZ	288	37	252
7837103	McMullen	124CRRZ	345	106	239
6849902	Medina	124CRRZ	655	78	577
6857307	Medina	124CRRZ	643	126	517
6858101	Medina	124CRRZ	650	159	491
6960201	Uvalde	124CRRZ	891	200	691
7750603	Webb	124CRRZ	655	248	407
7759501	Webb	124CRRZ	714	280	434
8401601	Webb	124CRRZ	380	-60	440
8503905	Webb	124CRRZ	595	161	434
8504401	Webb	124CRRZ	620	211	409
6741102	Wilson	124CRRZ	590	178	412
6741304	Wilson	124CRRZ	519	118	401
6749201	Wilson	124CRRZ	470	100	371
6848401	Wilson	124CRRZ	547	73	474
6848502	Wilson	124CRRZ	430	31	399
6848509	Wilson	124CRRZ	430	32	398
6848601	Wilson	124CRRZ	490	93	398
6848812	Wilson	124CRRZ	426	33	393
6848907	Wilson	124CRRZ	502	114	388
6853902	Wilson	124CRRZ	585	211	375
6854506	Wilson	124CRRZ	419	42	377
6854602	Wilson	124CRRZ	525	154	372
6854901	Wilson	124CRRZ	515	111	404
6855111	Wilson	124CRRZ	483	116	367
6855407	Wilson	124CRRZ	456	46	410
6855505	Wilson	124CRRZ	450	73	377
6855704	Wilson	124CRRZ	430	60	370
6855901	Wilson	124CRRZ	396	40	356
6855902	Wilson	124CRRZ	390	108	282
6856101	Wilson	124CRRZ	490	94	396
6856201	Wilson	124CRRZ	428	41	387
6856302	Wilson	124CRRZ	431	43	388
6862108	Wilson	124CRRZ	572	220	352
6862902	Wilson	124CRRZ	437	104	333
6862906	Wilson	124CRRZ	422	62	360

Table 4.4.5 (continued)

State Well Number ^(a)	County ^(a)	Aquifer Code ^(a)	LSD Elevation (ft) ^(a)	Average Depth to Water (ft) ^(b)	Average Water-Level Elevation (ft) ^(c)
6863101	Wilson	124CRRZ	448	54	394
6863802	Wilson	124CRRZ	456	145	311
6864402	Wilson	124CRRZ	403	48	355
7806302	Wilson	124CRRZ	415	60	355
6958701	Zavala	124CRRZ	772	138	634
6958707	Zavala	124CRRZ	789	153	636
6958715	Zavala	124CRRZ	768	85	683
6958801	Zavala	124CRRZ	750	60	690
6959904	Zavala	124CRRZ	743	284	459
6961502	Zavala	124CRRZ	717	221	497
6961525	Zavala	124CRRZ	719	205	514
7608406	Zavala	124CRRZ	712	24	688
7624906	Zavala	124CRRZ	631	237	394
7701101	Zavala	124CRRZ	762	96	666
7701311	Zavala	124CRRZ	776	89	687
7701404	Zavala	124CRRZ	735	117	618
7701702	Zavala	124CRRZ	698	109	589
7702414	Zavala	124CRRZ	747	338	409
7702606	Zavala	124CRRZ	688	303	385
7703401	Zavala	124CRRZ	731	336	396
7704431	Zavala	124CRRZ	708	355	353
7704603	Zavala	124CRRZ	688	350	338
7709101	Zavala	124CRRZ	668	289	379
7711718	Zavala	124CRRZ	641	317	324
7712702	Zavala	124CRRZ	641	335	306
7718516	Zavala	124CRRZ	574	219	355
7719102	Zavala	124CRRZ	614	305	309

(a) source is the TWDB website:

rio.twdb.state.tx.us/publications/reports/GroundWaterReports/GWDatabaseReports/GWdatabaserpt.htm

(b) calculated as the LSD elevation minus the average water-level elevation

(c) calculated from the 1998-2001 data on the TWDB website

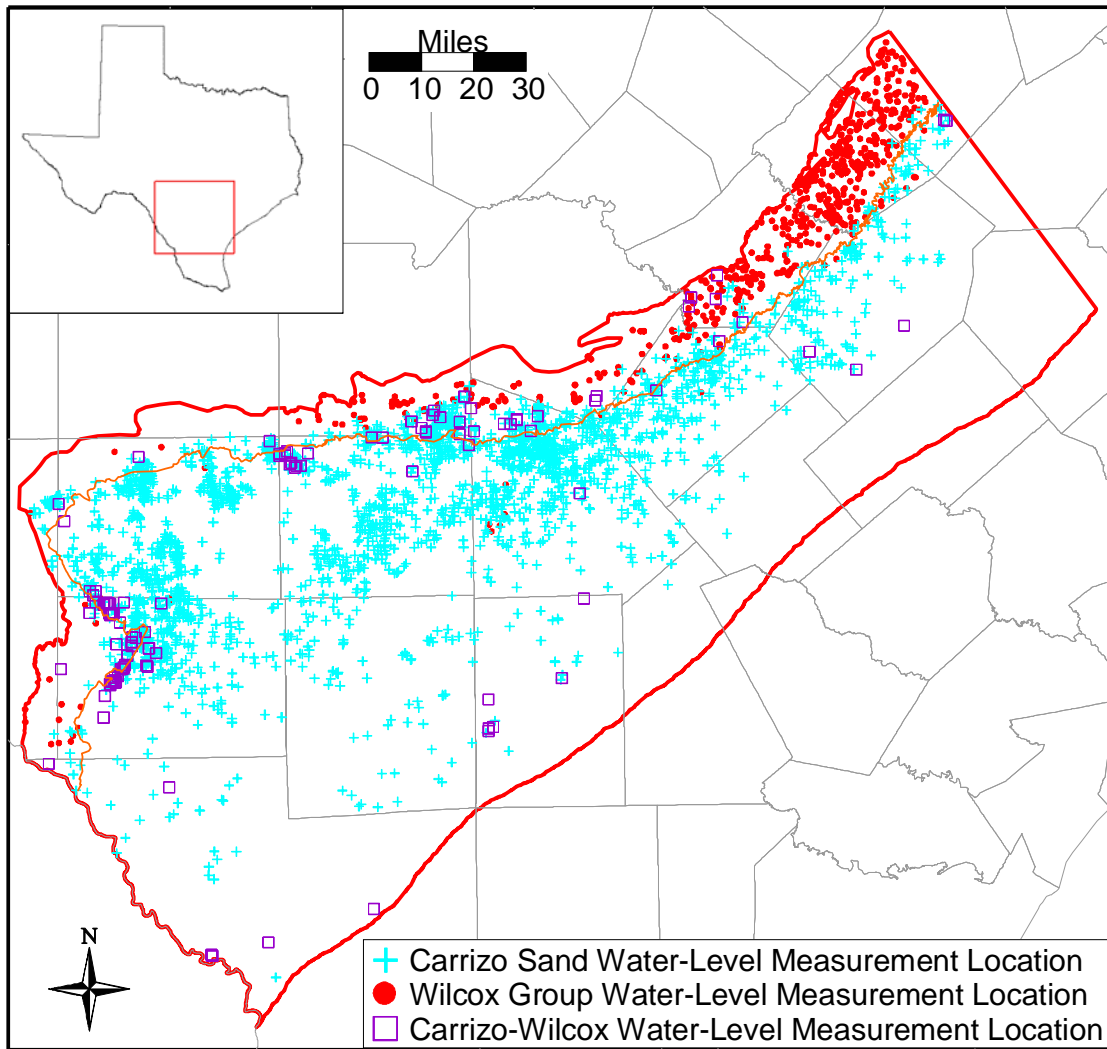


Figure 4.4.1 Water-level measurement locations for the Carrizo-Wilcox aquifer.

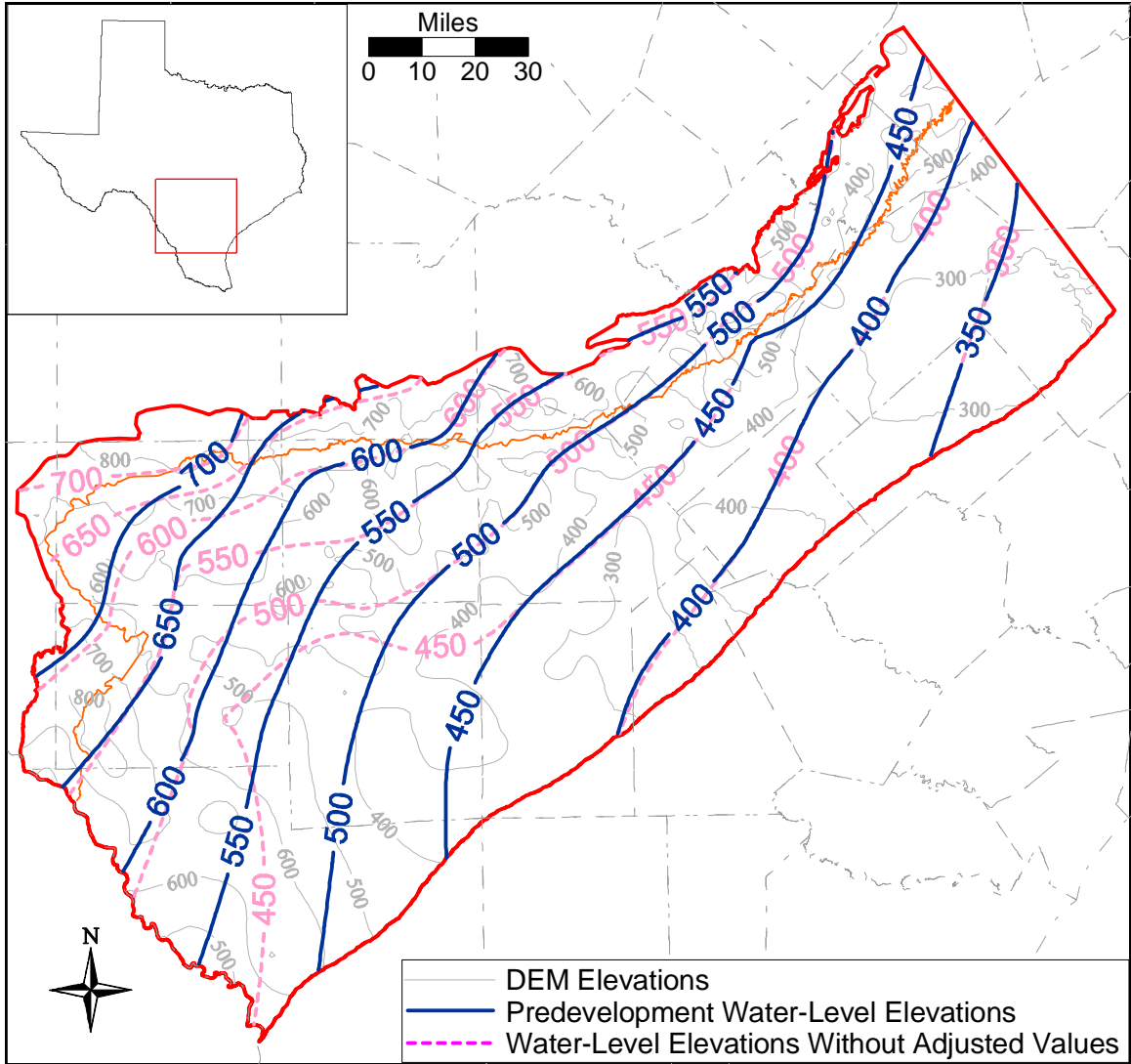


Figure 4.4.3 Difference in predevelopment water-level elevation contours between adjusted and not adjusted water levels.

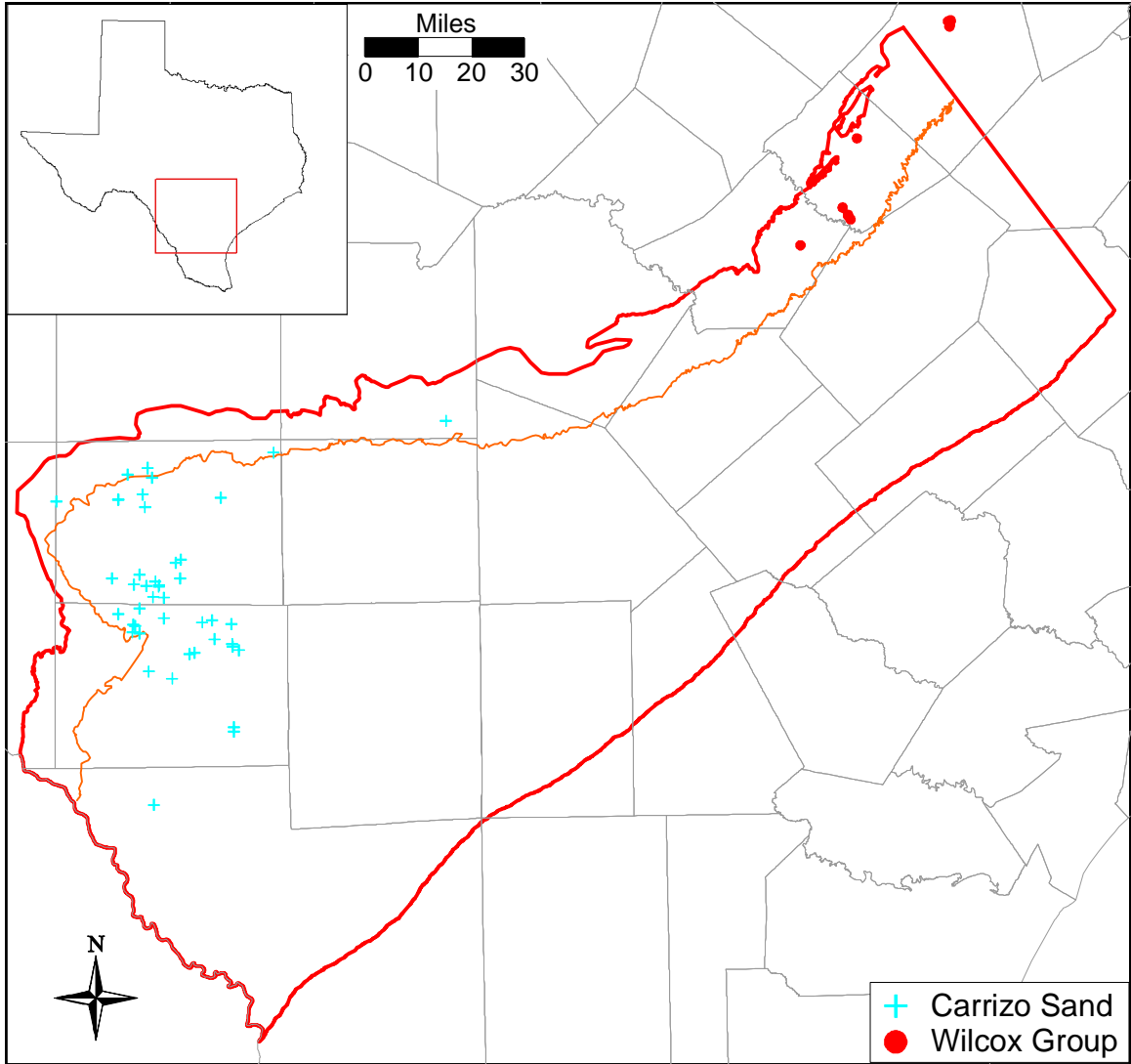


Figure 4.4.4 Water-level measurement locations used for pressure-depth analysis.

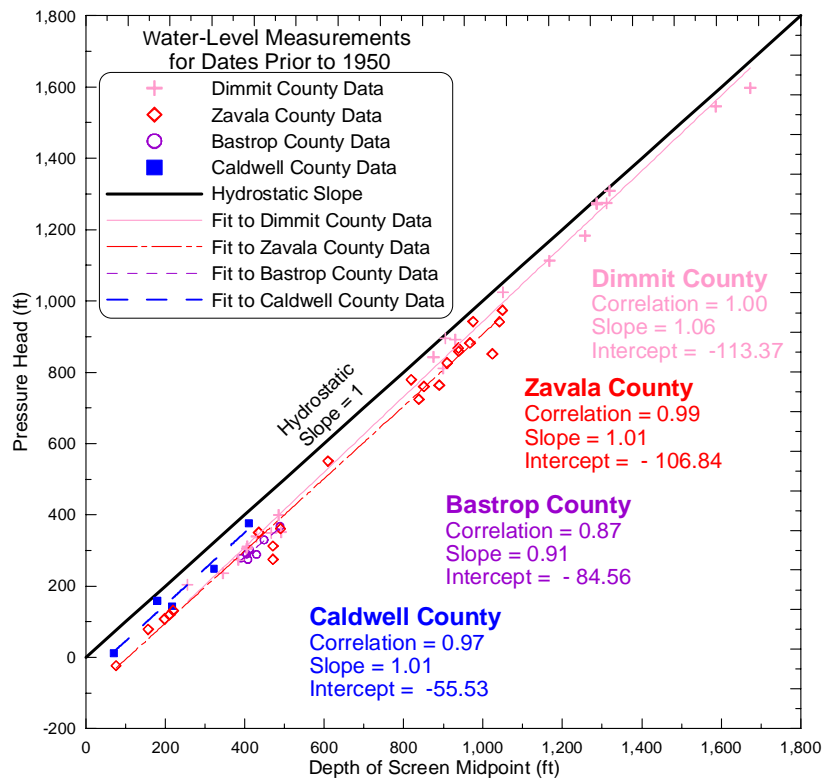
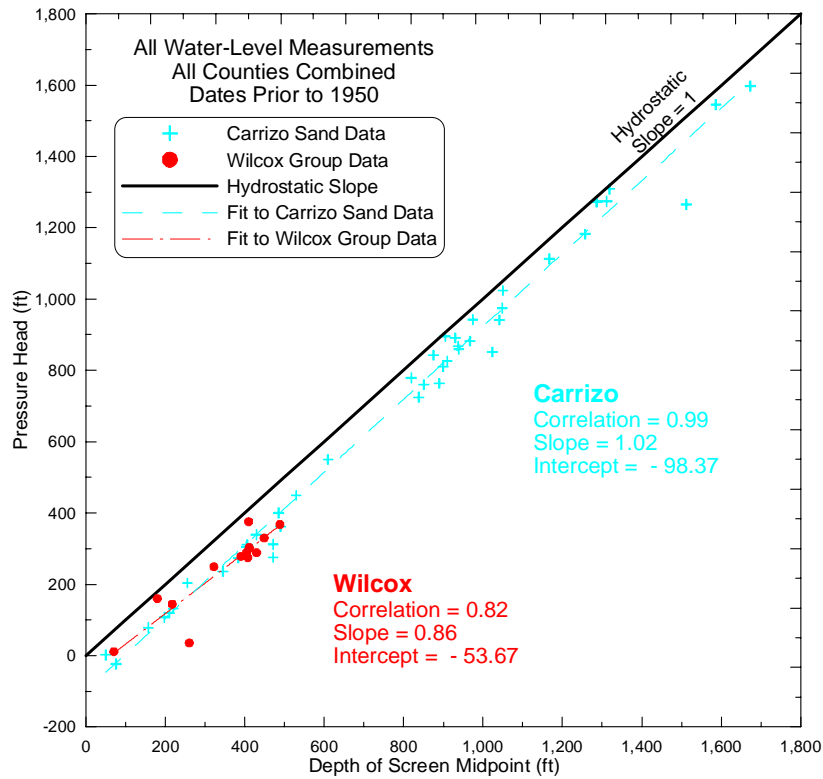


Figure 4.4.5 Pressure versus depth analysis results.

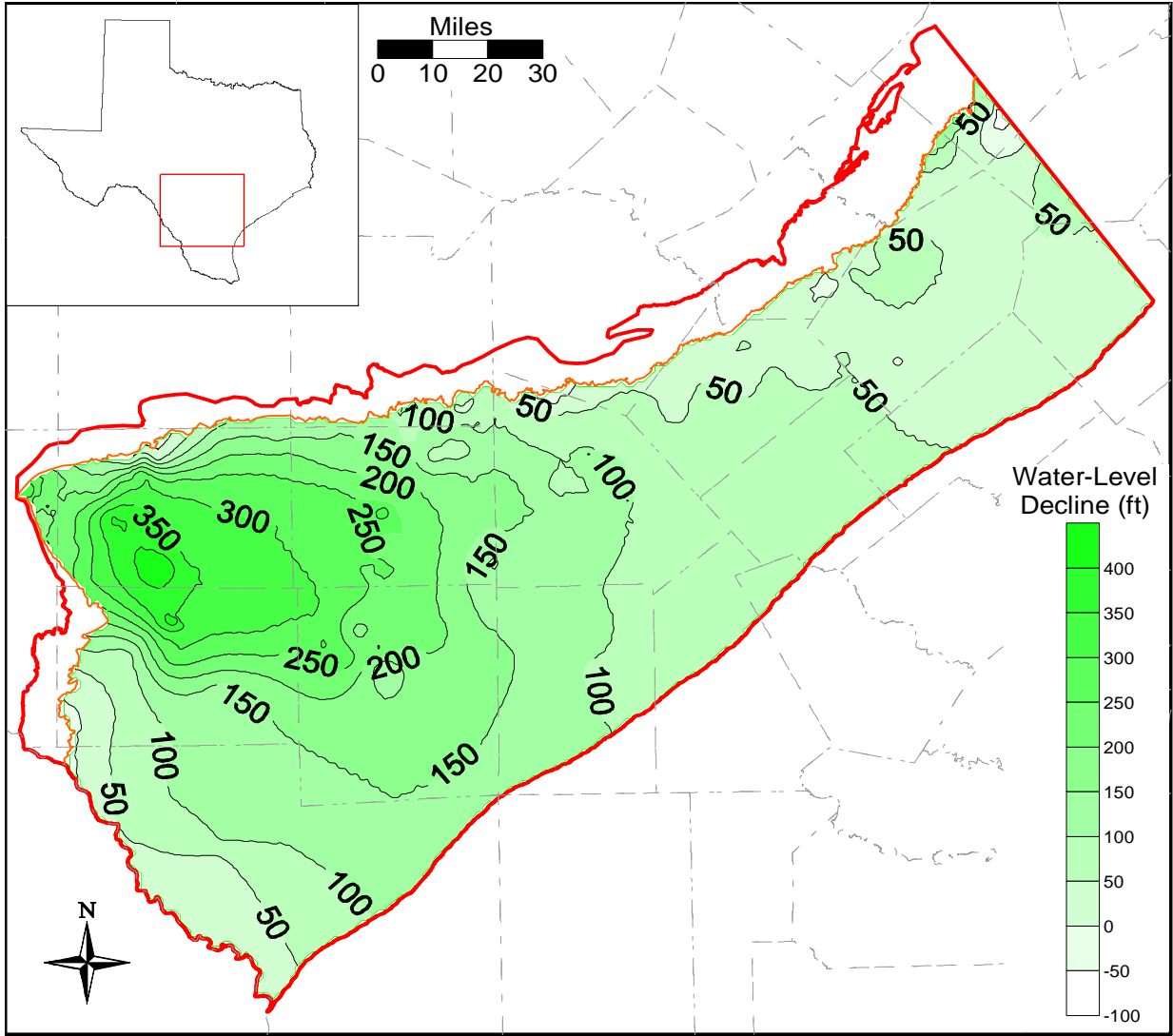


Figure 4.4.7 Water-level decline in the Carrizo –upper Wilcox from predevelopment to 1980.

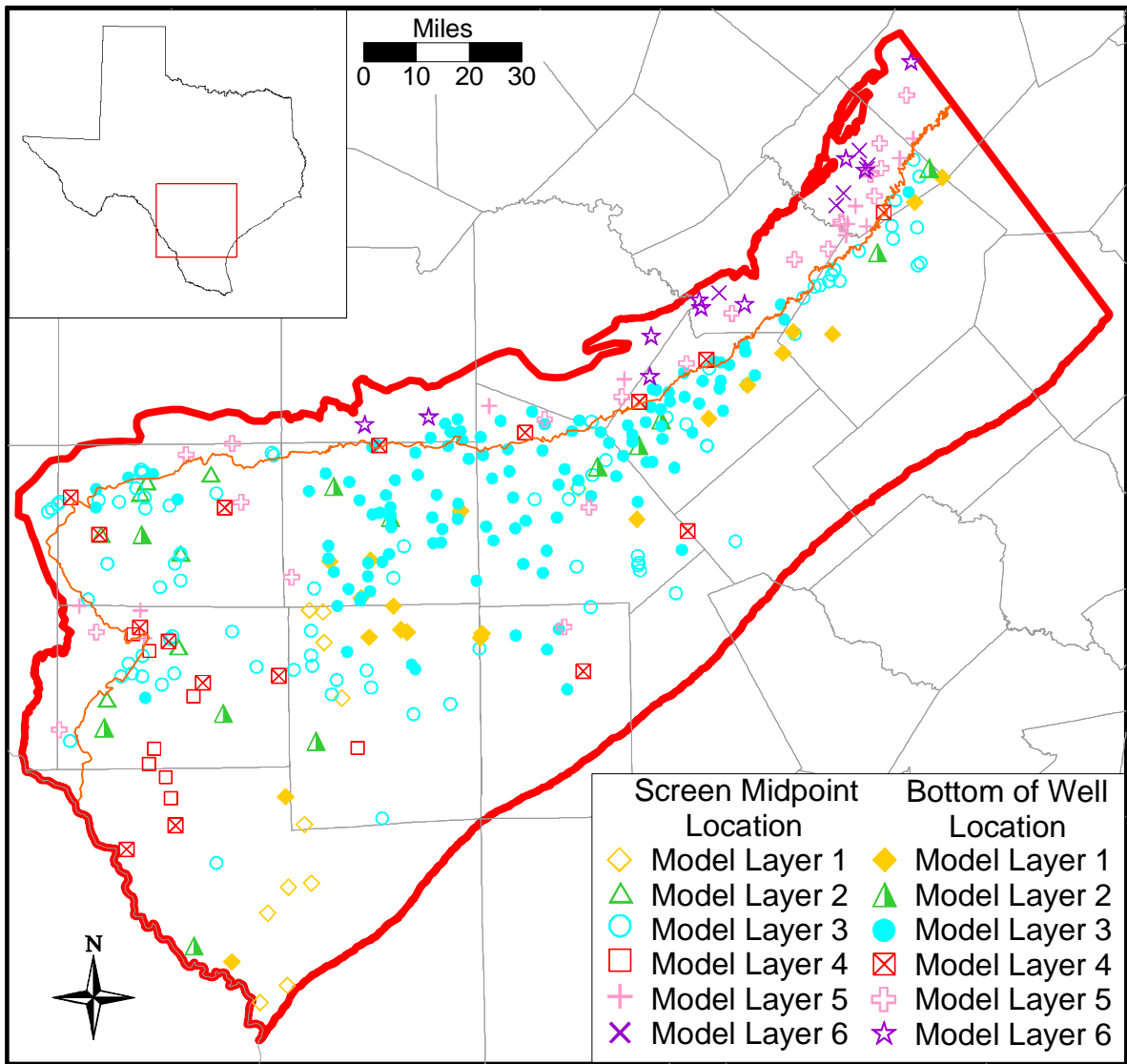


Figure 4.4.8 Model layer for locations with transient water-level data.

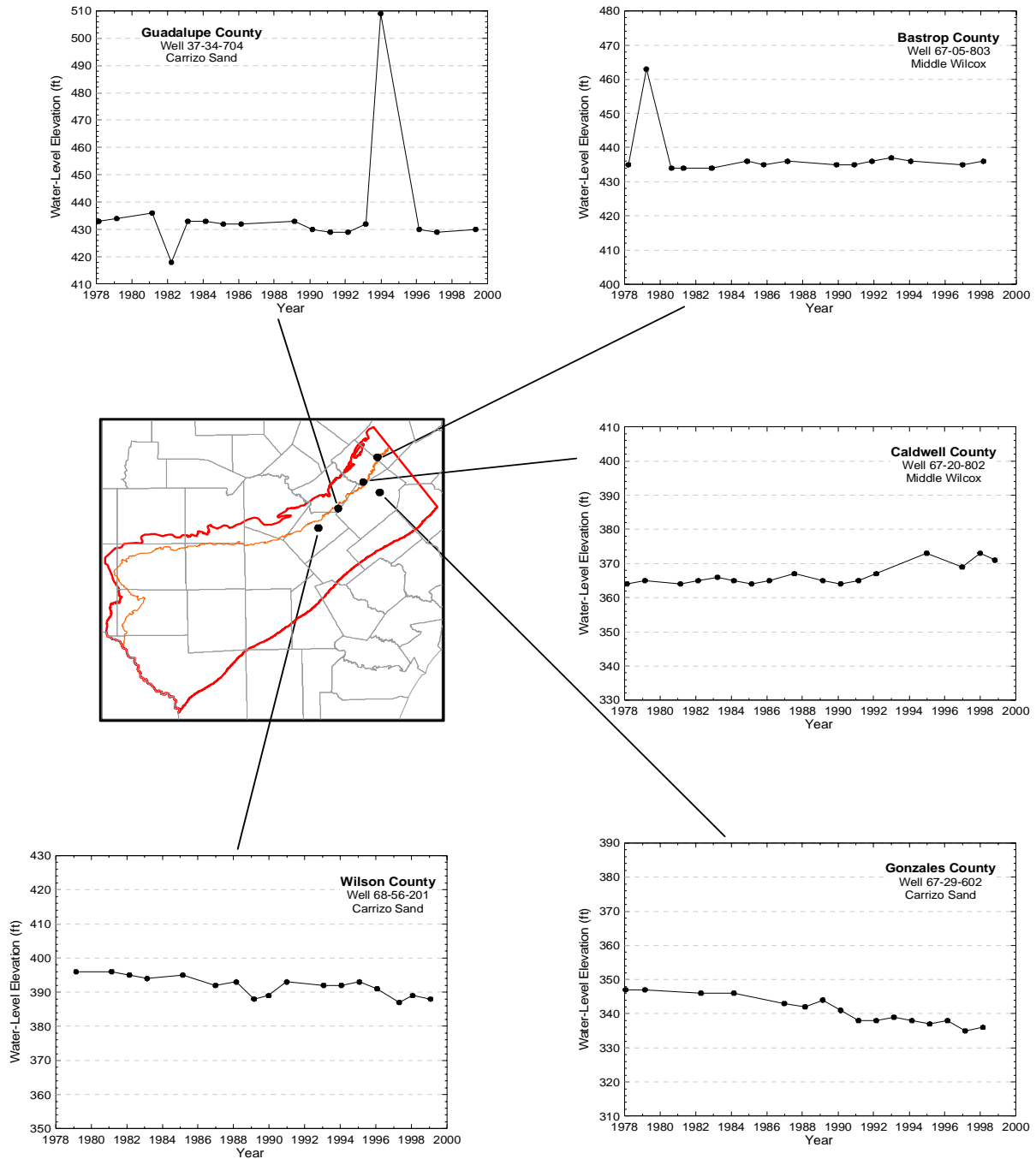


Figure 4.4.9 Example hydrographs for wells located in Bastrop, Caldwell, Gonzales, Guadalupe, and northern Wilson counties.

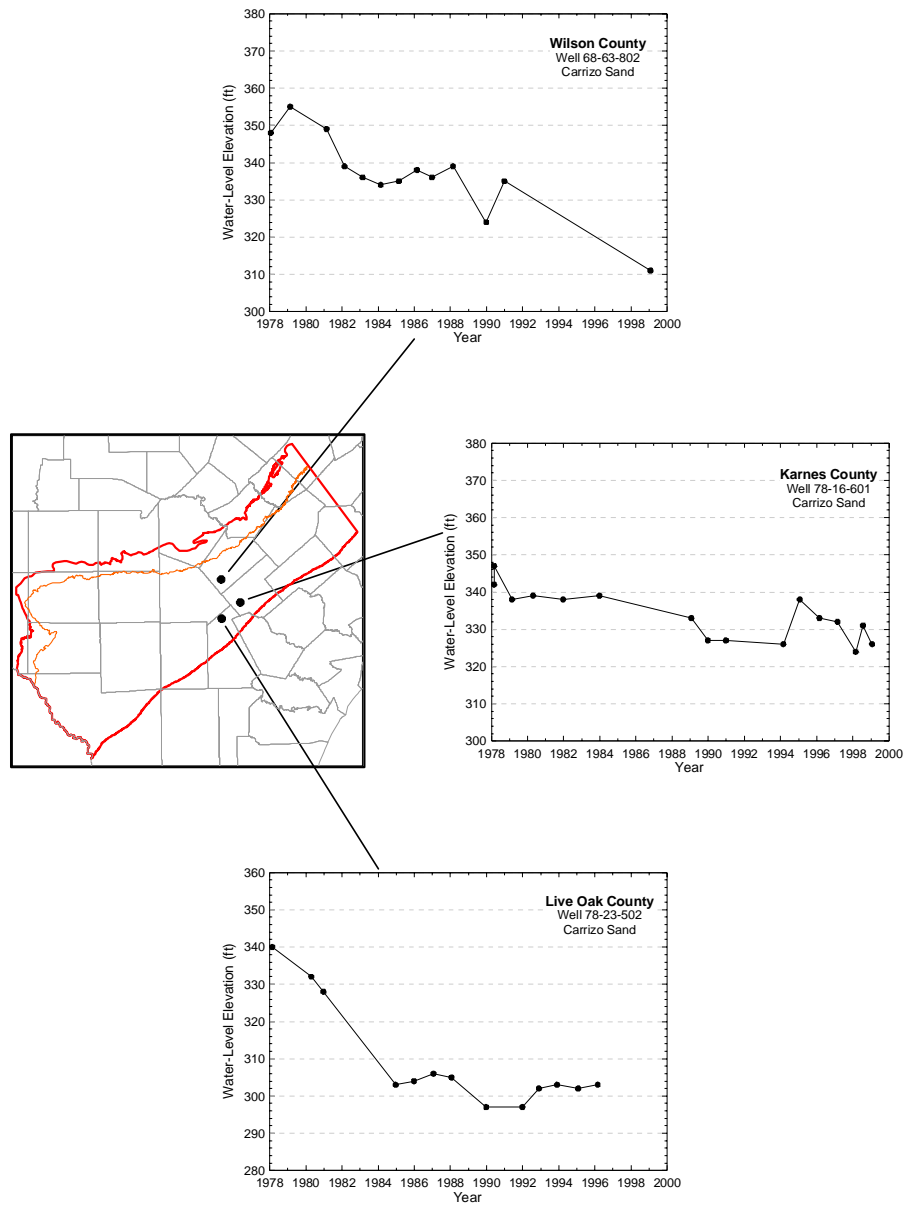


Figure 4.4.10 Example hydrographs for wells in southern Wilson County and Karnes and Live Oak counties.

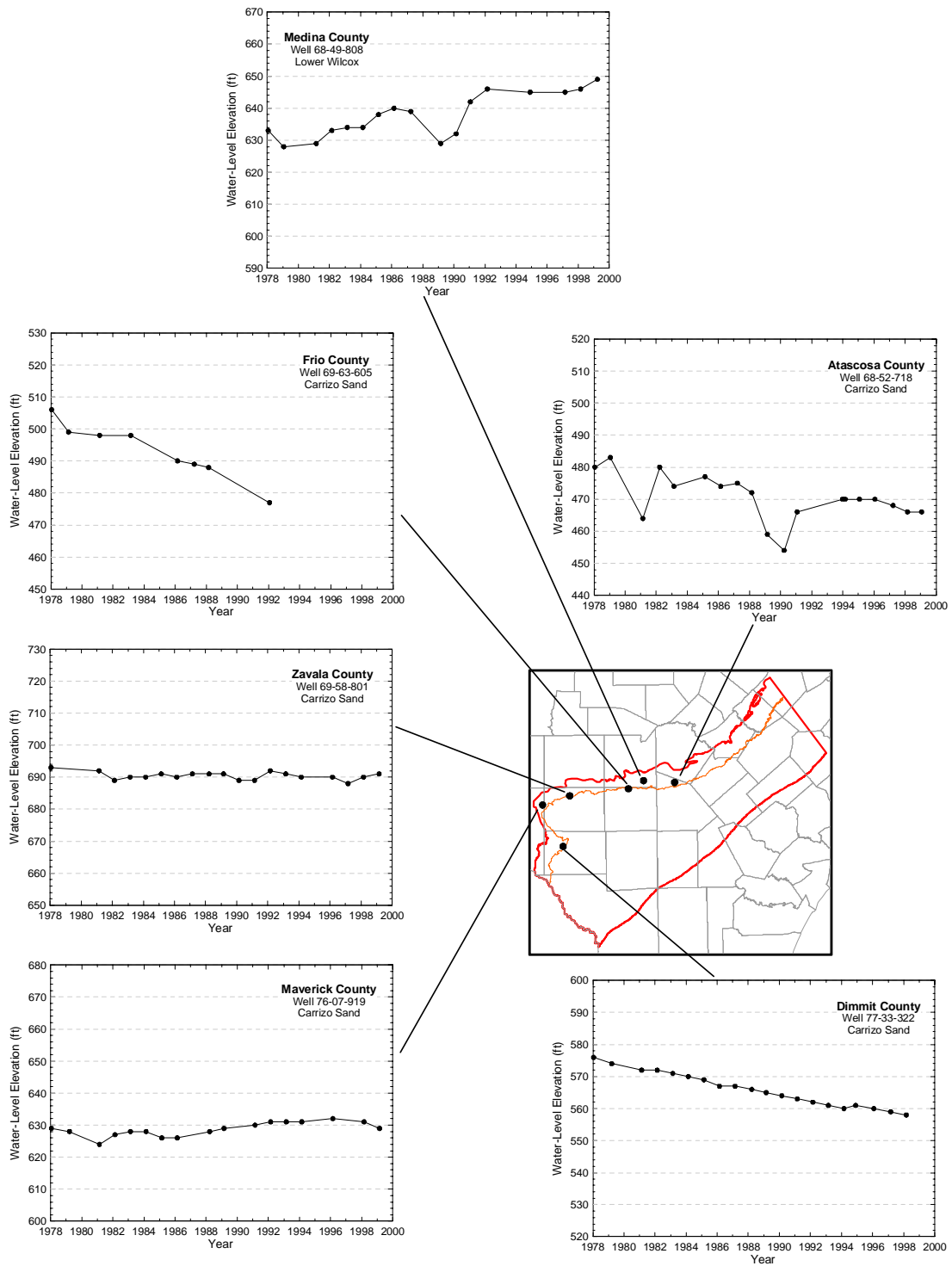


Figure 4.4.11 Example hydrographs for wells in the outcrop areas of Atascosa, Medina, Frio, Zavala, Maverick, and Dimmit counties.

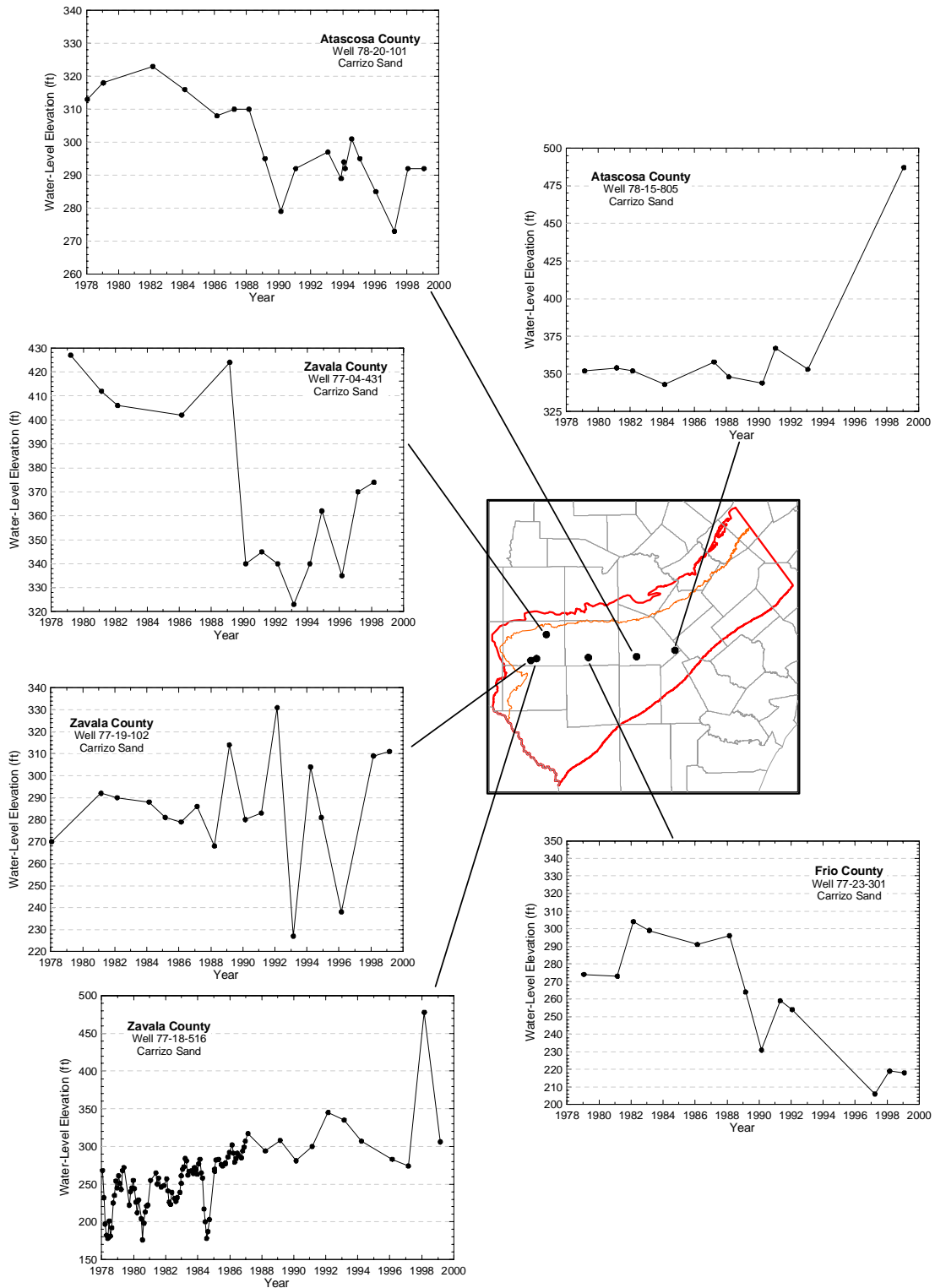


Figure 4.4.12 Example hydrographs for wells in the downdip areas of Atascosa, Frio, and Zavala counties.

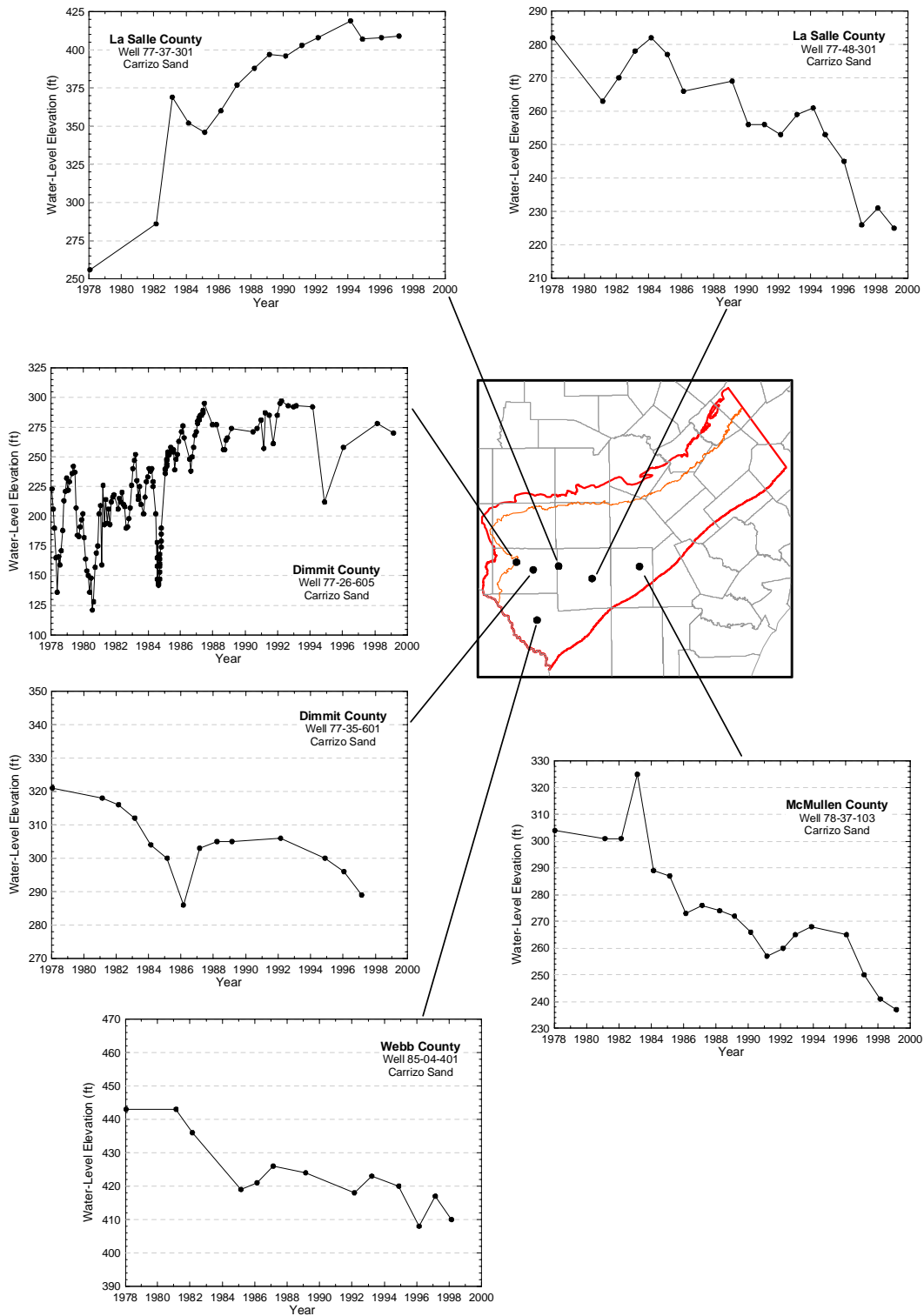


Figure 4.4.13 Example hydrographs for wells in McMullen, La Salle, Webb, and the downdip area of Dimmit counties.

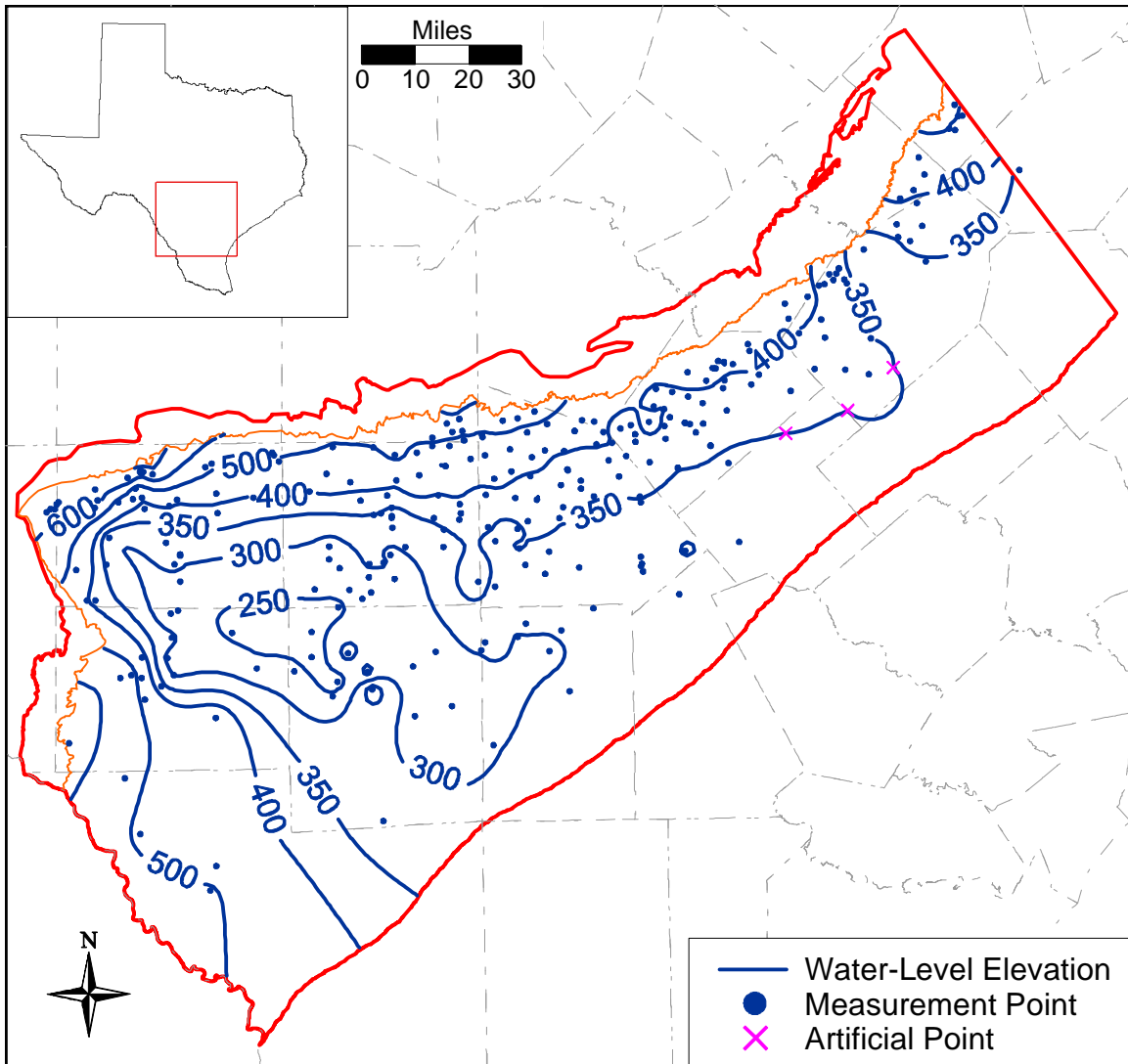


Figure 4.4.14 Water-level elevation contours for the Carrizo-Wilcox aquifer at the start of model calibration (January 1980).

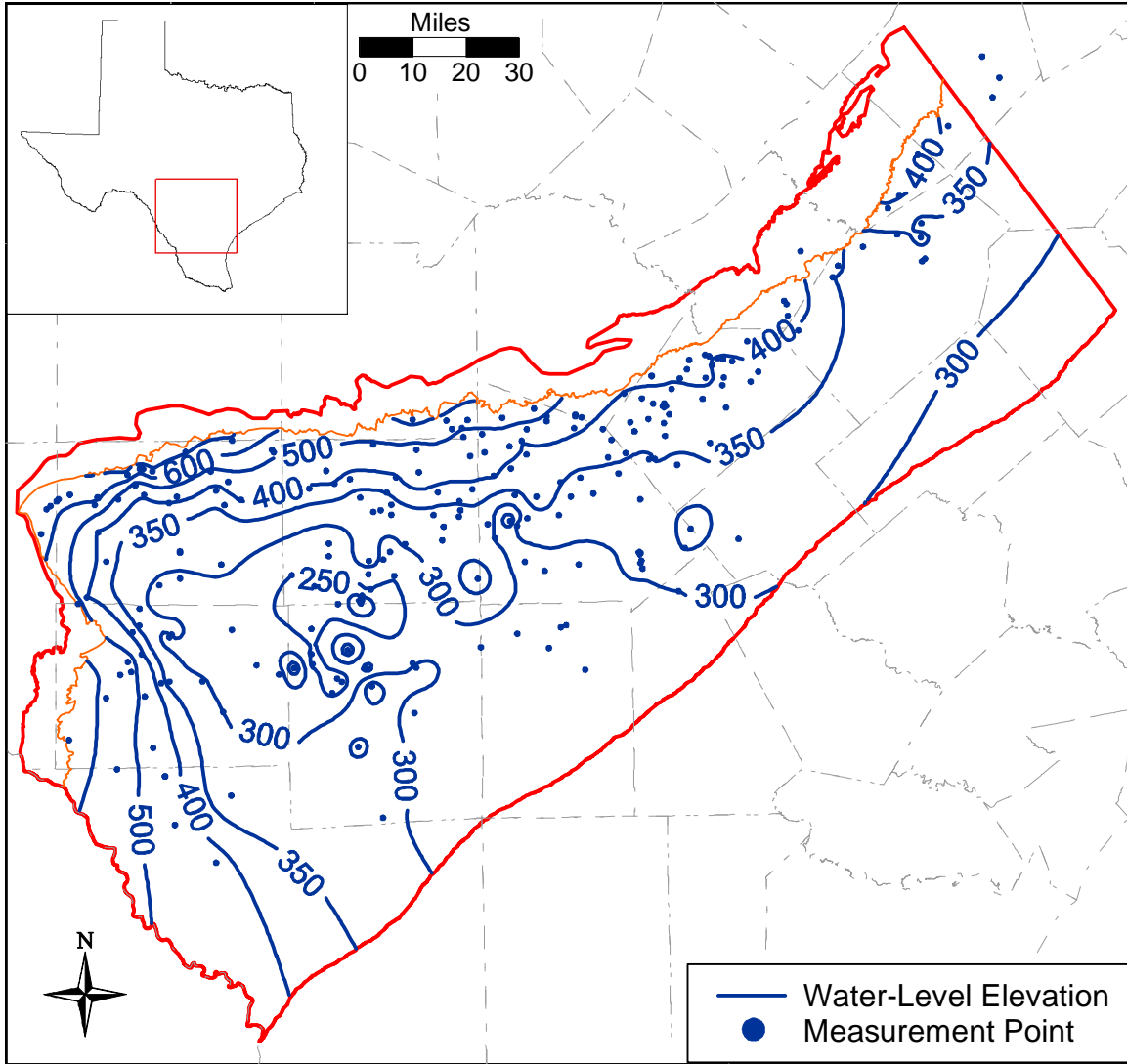


Figure 4.4.15 Water-level elevation contours for the Carrizo-Wilcox aquifer at the end model calibration (December 1989).

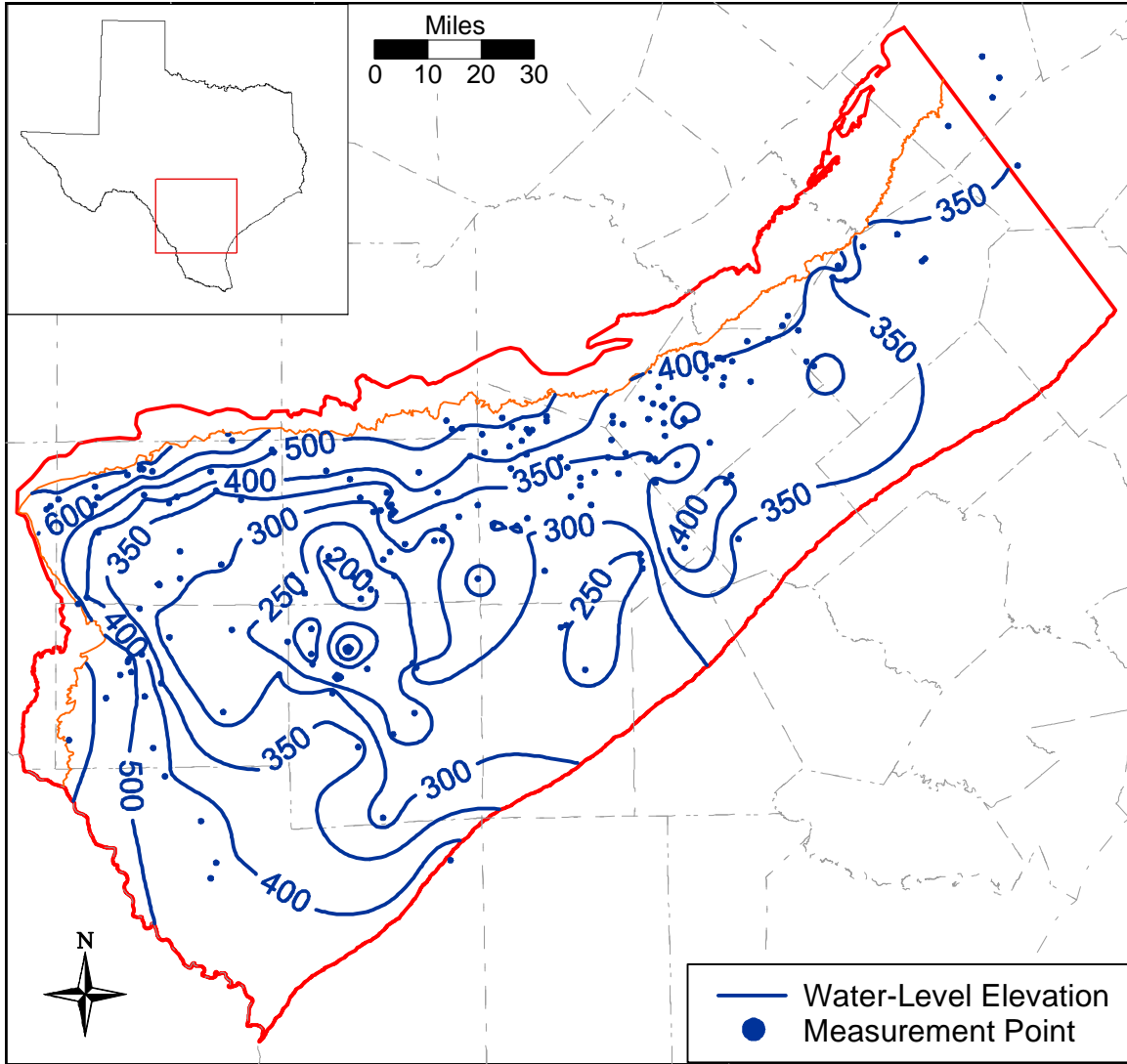


Figure 4.4.16 Water-level elevation contours for the Carrizo-Wilcox aquifer at the end model verification (December 1999).

4.5 Recharge

Recharge can be defined as water which enters the saturated zone at the water table (Freeze, 1969). Potential sources for recharge to the water table include precipitation, stream or reservoir leakage, or irrigation return flow. In the Southern Carrizo-Wilcox GAM area, recharge is conceptualized to occur as diffuse recharge in the inter-stream areas as a result of precipitation and irrigation return flow and as focused recharge in the stream valleys and in the vicinity of reservoirs (Scanlon et al, 2002). In the Southern Carrizo-Wilcox GAM region, the streams tend to be losing which makes them areas for potential recharge.

The cleaner and more massive sands of the Carrizo Formation have commonly been assumed to be the preferentially recharged unit in the Carrizo-Wilcox aquifer system. This is likely the result of the formation's increased ability to move water away from the water table (Freeze, 1969) relative to other hydrostratigraphic units adjacent to and within the Carrizo-Wilcox. However, recharge is a complex function of precipitation rate and volume, soil type, water level and soil moisture, topography, and evapotranspiration (ET) (Freeze, 1969). Because of its large outcrop area and relatively high sand content, the Wilcox Group also has a good potential for diffuse recharge in the study area. When recharge rates exceed the saturated hydraulic conductivity of the underlying soils and aquifer, then the transmission capability of the underlying formation becomes a limiting factor. These conditions may be expected to occur in locations of focused recharge near streams during high flow conditions and around reservoirs. Because precipitation, ET, and soil moisture vary as a function of time, recharge is also expected to vary as a function of time. Recharge will be highest in times of significant rainfall when soil moisture content is high. In drier times, redistribution and ET may effectively prevent significant recharge.

Several investigators have studied recharge in the Carrizo-Wilcox aquifer in Texas and these studies have been summarized by Scanlon et al. (2002) and are reproduced in Table 4.5.1. Those studies which are limited to the Southern Carrizo-Wilcox GAM model area are grouped as the top five entries in Table 4.5.1 because of their direct relevance to this study. For all studies, recharge rates range from a low of 0.1 inches estimated for Rains and Van Zandt counties (White, 1973) using a Darcy's Law approach to a high of 5.8 inches per year in Atascosa County (Opfel and Elder, 1978) using neutron probe measurements in the vadose zone. The range

specific to the study area is similar in magnitude ranging from a low of 0.2 inches per year (LBG-Guyton Associates and HDR 1998) in the Winter Garden Area to a high of 5.8 inches per year (Opfel and Elder, 1978) in Atascosa County as described above.

The most recent recharge study in the GAM model area is a groundwater model developed using MODFLOW and proprietary surface water models developed by HDR Engineering (LBG-Guyton and HDR, 1998). In that study, recharge was estimated for three components, diffuse recharge, main-channel stream recharge, and flood-flow recharge. The estimation of recharge was based upon an iterative methodology that partitioned the three types of recharge for each basin modeled based upon potential aquifer recharge estimates from unpublished TWDB transmission capacity estimates. The potential recharge estimates from LBG-Guyton and HDR (1998) are summarized in Table 4.5.2 for counties that intersect the Southern Carrizo-Wilcox GAM area. To estimate these recharge potentials in terms of inches per year, we intersected the Carrizo-Wilcox outcrop with the county boundaries to get a contributing recharge area per county.

Their range in recharge potential based upon transmission capacity ranged from 0.2 to 7.2 inches per year in the GAM model area. LBG-Guyton and HDR (1998) estimated that total recharge to their model (including the Queen City, Sparta and Younger units) partitioned into 66.7% diffuse recharge, 24.8% flood-flow recharge, and 8.5% main-channel stream recharge. There are no natural lakes in the model study area. There are two reservoirs that intersect one or more of the active outcrop grid cells in the GAM area, Calaveras Lake and Victor Braunig Lake, which are both located in Southern Bexar County. Figure 4.5.1 shows the locations of these two reservoirs and includes lake stage elevations for the historical simulation period from 1980 to 1999.

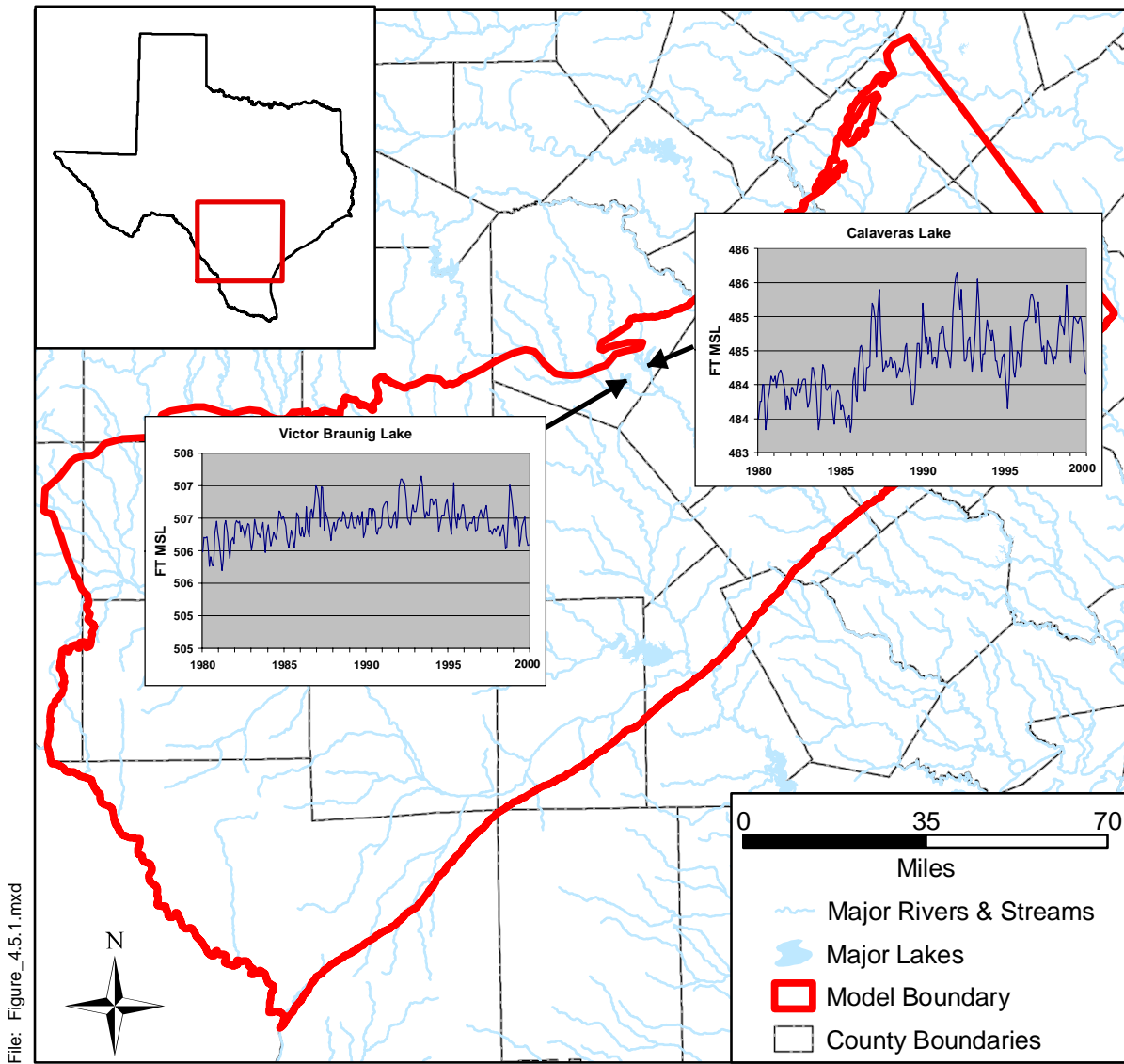
Table 4.5.1 Review of recharge rates for the Carrizo-Wilcox aquifer in Texas (after Scanlon et al., 2002).

Major Aquifer	Location (County/Area)	Aquifer	Recharge rate (mm/yr)	Recharge rate (in/yr)	Total recharge (af/yr)	Reference	Technique
Carrizo Wilcox	Atascosa, Frio	Carrizo sand	45.7	1.8		Alexander and White, 1966	¹⁴ C, Darcy's Law
	Winter Garden Area	undifferentiated	5-127	0.2-5		LBG-Guyton & Assoc. and HDR, 1998	modeling, water budget
	Bexar	Hooper, Simsboro, Calvert Bluff	45.7	1.8		HDR Engineering, 2000	groundwater modeling
	Atascosa	Carrizo	147	5.8		Opfel and Elder, 1978	neutron probe logging
	Atascosa, Bexar, Dimmit, Frio, Gonzales, Guadalupe, Medina, Uvalde, Wilson, Zavala	undifferentiated			25,000	Turner, et al., 1960	Darcy's Law
	Sabine, San Augustine	undifferentiated	50.8	2.0		Anders, 1967	Darcy's Law
	Sabine, San Augustine	undifferentiated	25.4	1.0		Anders, 1967	baseflow discharge
	Camp, Franklin, Morris, Titus	Carrizo Wilcox			12,000	Broom et al., 1965	baseflow discharge
	Harrison	Cypress	7.9	0.3	15,000	Broom and Myers, 1966	Darcy's Law
	Harrison	Cypress	7.9	0.3	40,000	Broom and Myers, 1966	baseflow discharge
	Wood	Carrizo	12.7	0.5	3,000	Broom, 1968	Darcy's Law
	Bastrop, Lee, Milam	Simsboro, Carrizo	51-102	2.0-4.0		Dutton, 1999	groundwater modeling
	Bastrop	Carrizo, Wilcox sand	38	1.5		Follett, 1970	Darcy's Law
	Bastrop, Lee, Milam, Robertson, Falls, Limestone, Freestone, Navarro	Carrizo, Simsboro	76-127	3.0-5.0		Harden and Associates, 2000	groundwater modeling
	Bastrop, Lee, Milam, Robertson, Falls, Limestone, Freestone, Navarro	Calvert Bluff, Hooper	12.7	0.5		Harden and Associates, 2000	groundwater modeling
	Winter Garden area	undifferentiated			100,000	Klemt et al., 1976	groundwater modeling
	Rusk	Carrizo	<25.4	<1.0		Sandeen, 1987	Darcy's Law
	Navarro	Carrizo Wilcox	12.7	0.5		Thompson, 1972	estimate
	Caldwell, Bastrop, Lee, Milam, Robertson, Limestone, Freestone	undifferentiated	25.4	1.0		Thorkildsen and Price, 1991	groundwater modeling
	Bastrop, Lee, Fayette	undifferentiated	25.4	1.0		Thorkildsen et al., 1989	groundwater modeling
Rains, Van Zandt	Carrizo Wilcox	3	0.1	5,000	White, 1973	Darcy's Law	

Table 4.5.2 Potential recharge rates for the Carrizo-Wilcox (after LBG-Guyton and HDR, 1998).

County	Recharge Potential (acre feet per year) ⁽¹⁾	Recharge Potential (inches per year) ⁽²⁾
Atascosa	21,582	2.65
Bexar	10,552	0.57
Caldwell	3,063	0.19
Dimmit	6,095	0.45
Frio	5,677	2.64 ⁽³⁾
Gonzales	9,840	7.15 ⁽³⁾
Guadalupe	19,947	1.04
Maverick	1,803	0.18
Medina	18,265	1.04
Uvalde	1,614	0.29
Wilson	33,551	4.05
Zavala	11,058	0.78
Total	143,047	1.06

- (1) As reported by LBG-HDR (1998)
- (2) Calculated by estimating outcrop areas by county
- (3) Small outcrop areas may lead to large error in calculated recharge



File: Figure_4.5.1.mxd

Source: City of San Antonio Public Service, 2001

Figure 4.5.1 Hydrographs for reservoirs in the Carrizo-Wilcox outcrop.

4.6 Natural Aquifer Discharge

Under steady-state conditions (predevelopment), groundwater flow in the aquifer is elevation driven from the higher elevation outcrops to the confined sections of the aquifer. In the predevelopment condition, recharge occurring as a result of diffuse and focused recharge is balanced by discharge in stream valleys and springs, and through cross-formational flow. Under predevelopment conditions, prior to 1900, western streams such as the Nueces and Frio rivers were likely gaining streams based upon historical occurrence of flowing wells. By 1904 there were thirty artesian wells in the Carrizo Springs area alone, with average flows ranging from 40 to 300 gallons per minute. From early times, the Dimmit County area was famous for spring fed creeks that supported travelers and wildlife. Within 40 years of the drilling of the first well, virtually all of the springs and creeks they fed were dry. By 1910, farmers in some areas had to pump their wells (<http://historicdistrict.com/Genealogy/Dimmit/history.htm>). Hamlin (1988) reports that, prior to significant production (before 1900), Carrizo wells flowed at elevations up to 700 ft amsl. By the 1930s, flowing wells were limited to elevations below 500 ft amsl and, by 1972, only certain wells flowed at elevations below 360 ft amsl. In the eastern portion of the model area, flowing Carrizo wells still exist in areas such as Gonzales County. Participants in the Southern Carrizo-Wilcox GAM Stakeholder Advisory Forums have indicated that portions of Cibolo Creek that run through their property in Wilson County have ceased to be perennial gaining streams in recent history.

As a result of precipitation rates, recharge rates, natural depth to water, and pumping induced water level declines, streams tend to change from being perennial and gaining to being non-perennial and losing from east to west across the model study area. LBG-Guyton and HDR (1998) performed an analysis of important stream segments within their model area which closely coincides with this GAM model area. They estimated base flow in summer and winter for stream segments having gages located above and below the Carrizo-Wilcox outcrop. Their analysis indicated that the Nueces and the Frio rivers are dominantly losing in both winter and summer. Cibolo Creek was found to be gaining in both winter and summer. The San Antonio River and the Guadalupe River were found to be gaining in the winter months and losing in the summer months when evapotranspiration was assumed to exceed base flow.

The LBG-Guyton-HDR (1998) model was calibrated to transient heads from 1910 through 1994. Their analysis predicted the gain/loss on a ten-year moving average basis for each major river in the model study area from 1942 through 1994. Their analysis predicted that San Miguel Creek, the Nueces River, and the Frio River were losing streams throughout their analysis period (1942-1994). Through the historical period of interest in this GAM, their results predicted that the Nueces and Frio rivers lose, on average, approximately 500 acre feet per year per mile of outcrop. Conversely, the San Marcos and Guadalupe rivers were shown to be gaining streams throughout the predictive period, gaining less than 100 acre feet per year per mile of outcrop from 1980 through 1994. The San Antonio River changed from strongly gaining (over 400 acre feet per year per mile) to losing greater than 400 acre feet per year per mile of outcrop by 1990. The change from gaining to losing occurred in the late 1960s. The Atascosa River also changed from gaining conditions to losing in the early 1970s to becoming slightly losing (less than 50 acre feet per year per mile) from 1980 through 1994. Cibolo Creek also changed from gaining 200 acre feet per year per mile in the 1940s to losing upwards of 100 acre feet per year per mile in the late 1970s through 1994.

Slade et al (2002) summarized the results of 366 gain/loss studies involving 249 unique reaches of streams throughout Texas since 1918. They documented 33 individual gain/loss studies in the model area in the Carrizo-Wilcox outcrop for the Rio Grande River, the Nueces River, the Leona River, the Medina River and Cibolo Creek. Figure 4.6.1 shows the locations and survey numbers of the gain/loss studies in the model area. Table 4.6.1 provides the characteristics of the gain/loss studies reported by Slade et al. (2002) in the study area. The survey numbers in Figure 4.6.1 correspond to the survey numbers in Table 4.6.1.

Most of the relevant gain/loss studies in the model area have been performed on the Nueces River. Studies 182 through 185 were performed on the same stretch of the Nueces in four surveys from April 1940 through September 1940. The average and median loss estimates for that time period were -814 and -898 (negative indicated a losing stream) acre feet per year per mile of stream, respectively. Studies 194-202 and 206, 207, and 210 were performed as early as 1925 and as late as 1933. The Nueces was predominantly losing during this period with average and median gain/loss estimates of -653 and -959 acre feet per year per mile, respectively. Studies 165 through 175 were performed on the Leona River in Zavala and Uvalde counties from as early as 1925 and as late as 1947. The Leona River was predominantly gaining

over this period with average and median gain/loss estimates of 221 and 50 acre feet per year per mile, respectively. There does seem to be a weak correlation between season and interaction with stream loss occurring more in summer and stream gain occurring more in winter. Study 104 investigated Cibolo Creek across a 62 mile length in September of 1949. The creek was found to be gaining at an average rate of 163 acre feet per year per mile. Study 130 on the Medina River in May of 1925 estimated an average loss rate of -42 acre feet per year per mile of stream. Three studies (325,327,328) were performed on the Rio Grande River yielding widely varying results from an average loss of -1453 to an average gain of 495 acre feet per year per mile.

Discharge also occurs in areas where the water table intersects the surface at springs or weeps. These springs usually occur in topographically low areas in river valleys or in areas of the outcrop where hydrogeologic conditions preferentially reject recharge. We performed a literature survey of springs with location and flow rate data available for the model area (Figure 4.6.2 and Table 4.6.2). The available measured spring flow rates range from a low of 0.01 cubic feet per second (7 acre feet per year) to a high of 3.5 cubic feet per second (2,534 acre feet per year) measured at Mitchell Lake Springs and representing reservoir leakage. Discarding this value as unrepresentative of natural springs in the area, the next highest measurement is at Martinez Springs in Bexar County which is 1.6 cubic feet per second (1,158 acre feet per year) representing a baseflow measurement in a stream. Carrizo Springs flowed constantly until 1929 (Brune, 1975). Because of free-flowing wells in Dimmit County from the late 1800s through the 1930s, Carrizo Springs quit flowing in 1929 and has flowed only intermittently since.

Cross-formational flow is also a natural mechanism for discharge of groundwater from the Carrizo-Wilcox aquifer. Investigators have determined that heads within the Carrizo-Wilcox aquifer of south Texas are higher than heads in the overlying younger strata (Harris, 1965; Kreitler, 1979). This is consistent with our own analysis which found that pre-development head differences between the Carrizo and the Queen City increase with depth of confinement to magnitudes as high as 60 feet. Water chemistry data support the proposed upward flow from the Carrizo Sand to overlying sands (Hamlin, 1988). Our analysis also found that the upward gradient continued between the Queen City aquifer and the estimated regional water table in the confined section. Cross-formational flow occurring in the Carrizo-Wilcox aquifer is not directly measurable and is best determined through modeling studies such as this GAM.

With development of the Carrizo-Wilcox aquifer system, the natural balance of deep section recharge and cross-formational flow has changed. In areas experiencing extensive groundwater pumping, hydraulic gradients between the Carrizo and the overlying units have reversed creating potential for cross-formation flow from younger units to the Carrizo (Hamlin, 1988; Klemt et al., 1976; Mason, 1960). Klemt et al. (1976) estimated that in the central and southwestern portions of the study area cross-formational flow recharging the Carrizo from younger units was approximately 10,000 acre feet per year.

Table 4.6.1 Stream flow gain/loss studies in the study area (after Slade et al., 2002, Table 1).

Streamflow Study No.	Major River Basin	Stream Name	Reach Identification	Date of Study	Reach Length (river mi)	Total No. of Measurement Sites	No. of Measurement Sites on Main Channel	Major Aquifer Outcrop(s) Intersected by Reach	Total Gain or Loss (-) In Reach (ft ³ /s)	Gain or Loss per Mile of Reach (ft ³ /s-mi)	Gain or Loss per AFY-mi
104	Guadalupe	Cibolo Cr	Schertz to San Antonio R near Falls City (08183500)	9/12-13/1949	62	10	7	Carrizo-Wilcox	13.95	0.225	163.0
130	Guadalupe	Medina R	Medina Co Irrigation Co. diversion dam to Losoya	5/26-28/1925	55.1	19	14	Carrizo-Wilcox, Edwards	-3.2	-0.058	-42.0
135	Lavaca	Lavaca R	East of Hallettsville (08163500) to southeast of Edna	12/14-17/1970	65.4	18	14	Gulf Coast	18.23	0.279	202.1
140	Nueces	Atascosa, Frio, and Nueces R	3 mi southwest of Poteet to near Mathis	1/23-26/1951	103.8	29	14	Gulf Coast	4.83	0.047	34.0
141	Nueces	Atascosa, Frio, and Nueces R	Campbellton to near Mathis	4/19-21/1951	60.2	30	15	Gulf Coast	1.13	0.019	13.8
142	Nueces	Atascosa, Frio, and Nueces R	Campbellton to near Mathis	4/27-5/1/1951	58.3	23	13	Gulf Coast	-0.22	-0.004	-2.9
154	Nueces	Frio R	Choke Canyon Reservoir to Shamrock Refinery	11/12-13/1991	8.59	5	4	Gulf Coast	0.12	0.014	10.1
159	Nueces	Frio R	near Fowlerton to mouth	12/18-21/1967	62.9	13	6	Gulf Coast	10.63	0.169	122.4
165	Nueces	Leona R	1.7 mi southeast of Uvalde to 0.2 mi east of Zavalla-Frio Co line	2/5-8/1946	49.4	35	32	Carrizo-Wilcox	2.0	0.04	29.0
166	Nueces	Leona R	1.7 mi southeast of Uvalde to 35 mi southeast of Uvalde	6/11-12/1931	37.5	15	12	Carrizo-Wilcox	-3.1	-0.083	-60.1
167	Nueces	Leona R	1.7 mi southeast of Uvalde to 7.1 mi southeast of Batesville	8/7-9/1946	36.3	22	21	Carrizo-Wilcox	0.3	0.008	5.8
168	Nueces	Leona R	1.7 mi southeast of Uvalde to 9.5 mi southeast of Uvalde	3/1/1947	9.8	5	5	Carrizo-Wilcox	14.91	1.521	1101.9
169	Nueces	Leona R	1.7 mi southeast of Uvalde to below Batesville	6/21-22/1934	34.6	13	10	Carrizo-Wilcox	-3.1	-0.09	-65.2
170	Nueces	Leona R	1.7 mi southeast of Uvalde to below Batesville	10/18-20/1934	34.6	14	11	Carrizo-Wilcox	2.4	0.069	50.0
171	Nueces	Leona R	1.7 mi southeast of Uvalde to below Batesville	7/5-6/1939	23	14	11	Carrizo-Wilcox	4.3	0.187	135.5
172	Nueces	Leona R	1.7 mi southeast of Uvalde to near Batesville	11/7/1932	17	6	4	Carrizo-Wilcox	21.2	1.247	903.4
173	Nueces	Leona R	10 mi below Uvalde to below Batesville	6/8-10/1939	26	10	8	Carrizo-Wilcox	-3.8	-0.146	-105.8
174	Nueces	Leona R	below Kincaid Dam to 9.5 mi southeast of Uvalde	2/19/1946	5.2	7	7	Carrizo-Wilcox	0.7	0.135	97.8
175	Nueces	Leona R	Uvalde-Friortown Hwy to near Batesville	4/25-28/1925	33.5	14	11	Carrizo-Wilcox	15.89	0.474	343.4
182	Nueces	Nueces R	above Laguna (08190000) to 4.8 mi southeast of La Pryor	5/2-3/1940	46.9	14	13	Carrizo-Wilcox, Edwards	-63.8	-1.36	-985.3
183	Nueces	Nueces R	above Laguna (08190000) to 4.8 mi southeast of La Pryor	7/9-10/1940	46.9	14	13	Carrizo-Wilcox, Edwards	-66.7	-1.422	-1030.2

Table 4.6.1 (continued)

Streamflow study no.	Major river basin	Stream name	Reach identification	Date of study	Reach length (river mi)	Total no. of measurement sites	No. of measurement sites on main channel	Major aquifer outcrop(s) intersected by reach	Total gain or loss (-) in reach (ft ³ /s)	Gain or loss per mile of reach (ft ³ /s-mi)	Gain or loss per AFY-mi
184	Nueces	Nueces R	above Laguna (08190000) to 4.8 mi southeast of La Pryor	8/28-29/1940	46.8	14	13	Carrizo-Wilcox, Edwards	-52.3	-1.118	-809.9
185	Nueces	Nueces R	above Laguna (08190000) to 4.8 mi southeast of La Pryor	9/26-27/1940	46.9	14	12	Carrizo-Wilcox, Edwards	-27.9	-0.595	-431.1
191	Nueces	Nueces R	below Odley Cr near Vance to La Pryor	3/17-26/1924	74.4	21	18	Carrizo-Wilcox, Edwards, Edwards-Trinity (Plateau)	19.8	0.266	192.7
192	Nueces	Nueces R	Cotulla (08194000) to Simmons (08194600)	7/28-30/1981	108.1	13	10	Gulf Coast	7.6	0.07	50.7
193	Nueces	Nueces R	Cotulla (08194000) to Simmons (08194600)	8/11-13/1981	108.1	13	10	Gulf Coast	9.29	0.086	62.3
194	Nueces	Nueces R	Laguna (08190000) to 3.8 mi southeast of Cinonia	6/14-30/1939	61.6	27	25	Carrizo-Wilcox, Edwards	-23.7	-0.385	-278.9
195	Nueces	Nueces R	Laguna (08190000) to 5 mi northeast of La Pryor	11/14-16/1931	39.6	10	10	Carrizo-Wilcox, Edwards	-60.2	-1.52	-1101.2
196	Nueces	Nueces R	Laguna (08190000) to 5 mi northeast of La Pryor	1/24-25/1932	39.6	11	11	Carrizo-Wilcox, Edwards	-59.5	-1.503	-1088.9
197	Nueces	Nueces R	Laguna (08190000) to Cinonia	4/30-5/8/1925	54.9	14	14	Carrizo-Wilcox, Edwards	-29.9	-0.545	-394.8
198	Nueces	Nueces R	Laguna (08190000) to Cinonia	5/16-17/1931	56.5	11	11	Carrizo-Wilcox, Edwards	-76.0	-1.345	-974.4
199	Nueces	Nueces R	Laguna (08190000) to Cinonia	6/4-6/1931	53	10	10	Carrizo-Wilcox, Edwards	-84.0	-1.585	-1148.3
200	Nueces	Nueces R	Laguna (08190000) to Cinonia	6/15-17/1931	56.5	12	12	Carrizo-Wilcox, Edwards	-73.6	-1.303	-944.0
201	Nueces	Nueces R	Laguna (08190000) to Cinonia	6/22-24/1931	56.5	12	12	Carrizo-Wilcox, Edwards	-91.9	-1.627	-1178.7
202	Nueces	Nueces R	Laguna (08190000) to Cinonia	7/2-4/1931	56.5	12	12	Carrizo-Wilcox, Edwards	-82.5	-1.46	-1057.7
206	Nueces	Nueces R	Laguna (08190000) to near Cinonia	11/1-4/1932	56.5	14	14	Carrizo-Wilcox, Edwards	28.0	0.496	359.3
207	Nueces	Nueces R	Laguna (08190000) to near Cinonia	7/23-25/1933	56.5	14	14	Carrizo-Wilcox, Edwards	-8.7	-0.154	-111.6
210	Nueces	Nueces R	Uvalde (08204000) to Cinonia	7/13/1931	33.8	7	7	Carrizo-Wilcox	4.0	0.118	85.5
211	Nueces	Nueces R	Miller's Ranch to Nueces R at Highway 59	11/12-13/1991	16.45	7	6	Gulf Coast	65.89	4.005	2901.5
219	Nueces	Nueces R	US 90 to near Crystal City	11/23-25/1964	52.2	19	10	Carrizo-Wilcox	13.4	0.257	186.2
325	Rio Grande	Rio Grande	Eagle Pass to Laredo	2/22-4/12/1928	128	6	6	--	-10.0	-0.078	-56.5
327	Rio Grande	Rio Grande	Eagle Pass to Laredo	4/3-22/1928	128	6	6	--	-75.0	-0.586	-424.5
328	Rio Grande	Rio Grande	Eagle Pass to San Ygnacio	2/12-22/1926	167.5	22	17	Carrizo-Wilcox	336.0	-2.006	-1453.3
349	San Antonio	Cibolo Cr	near Randolph AFB to mouth	3/5-7/1963	79.3	18	13	Carrizo-Wilcox, Gulf Coast	16.68	0.21	152.1
350	San Antonio	Cibolo Cr	Selma (08185000) to mouth	3/4-8/1968	87.1	52	27	Carrizo-Wilcox, Gulf Coast	59.53	0.683	494.8

Table 4.6.2 Documented springs in the study area.

ID	WELL ID	COUNTY	Spring	Aquifer	Flow Rate LPS	Flow Rate GPM	Flow rate CFS	Date of Measurement	Measurement	Notes and Historical Information	Source
1	-	Dimmit	Carrizo Springs	Carrizo Sands	7.36	116.70	0.26	1/1/1892	1 of 3	Flowed constantly until 1929	Brune (1975)
2	-	Dimmit	Carrizo Springs	Carrizo Sands	37.00	586.46	1.31	12/30/1901	2 of 3	Flowed constantly until 1929	Brune (1975)
3	-	Dimmit	Carrizo Springs	Carrizo Sands	0.32	5.07	0.01	1/1/1979	3 of 3	Flowed constantly until 1929	Brune (1975)
4	-	Bexar	Martinez Springs	Wilcox Sands	45.31	718.13	1.60	3/5/1963		Baseflow in gravel streambed	Brune (1975)
5	-	Bexar	Mitchell Lake Springs	Wilcox Sands	99.11	1570.91	3.50	5/28/1925		Represents seepage from reservoir	Brune (1975)
6	-	Wilson	Sutherland Springs	Carrizo Sands	42.48	673.25	1.50	1/1/1949	1 of 3	Includes White Sulphur, Cold, Sour and Alligator Springs. ~100 springs	Brune (1975)
7	-	Wilson	Sutherland Springs	Carrizo Sands	0.28	4.49	0.01	1/1/1954	2 of 3	Includes White Sulphur, Cold, Sour and Alligator Springs. ~100 springs	Brune (1975)
8	-	Wilson	Sutherland Springs	Carrizo Sands	4.25	67.32	0.15	3/6/1968	3 of 3	Includes White Sulphur, Cold, Sour and Alligator Springs. ~100 springs	Brune (1975)
9	6733905	Guadalupe	King Hill Spring	Carrizo Sands	0.63	10.00	0.02			Reported numerous openings in quick sand. Flows about 10 gpm into pond.	TWDB Well Database
10	-	Webb	Sullivan Springs	Tertiary Eocene Sand	0.32	5.07	0.01	2/8/1979			GNIS, Brune (1975)

1 cubic feet per second (cfs) = 724 acre feet per year (AFY)

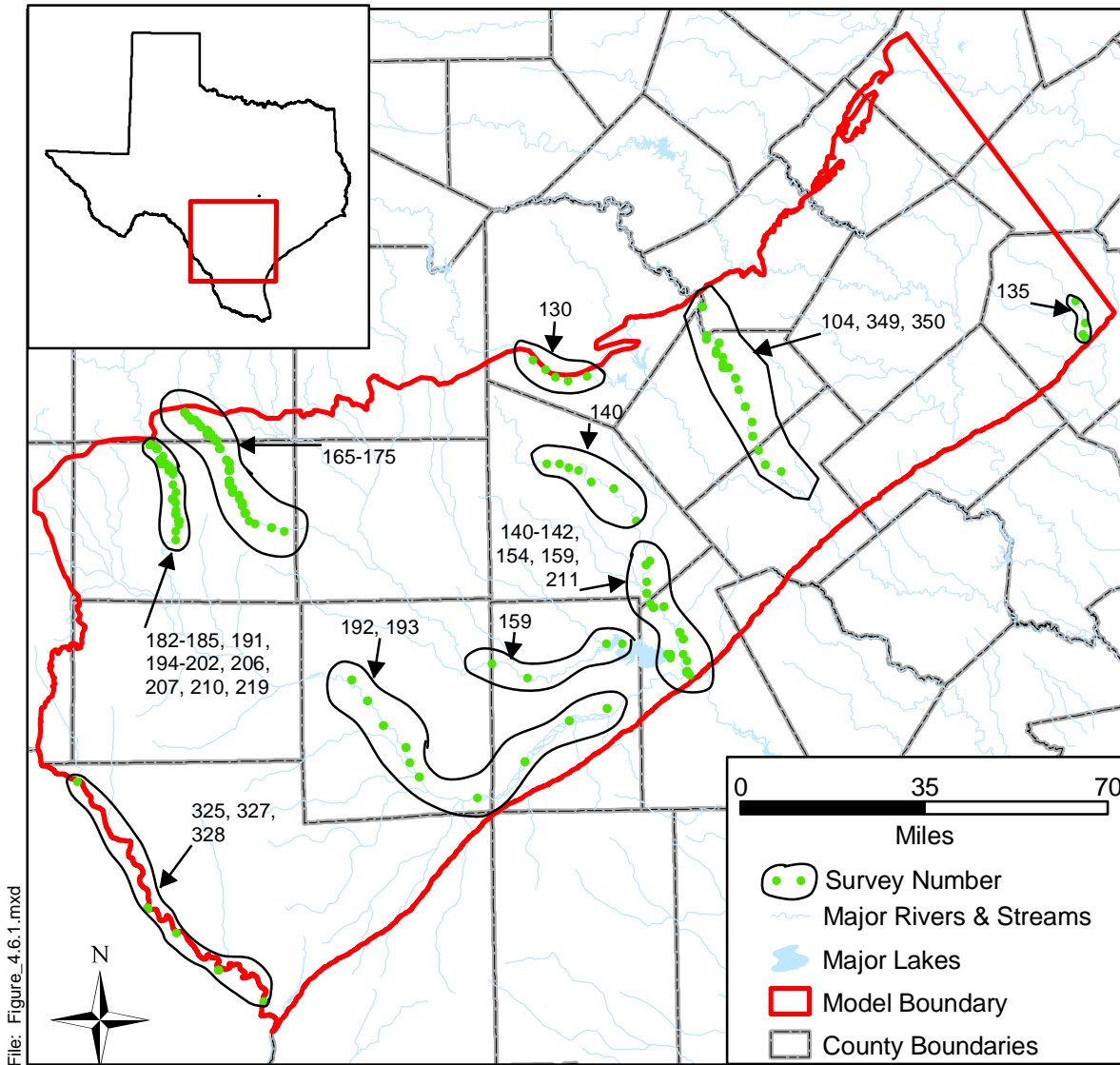


Figure 4.6.1 Stream gain/loss studies in the study area (after Slade et al. 2002).

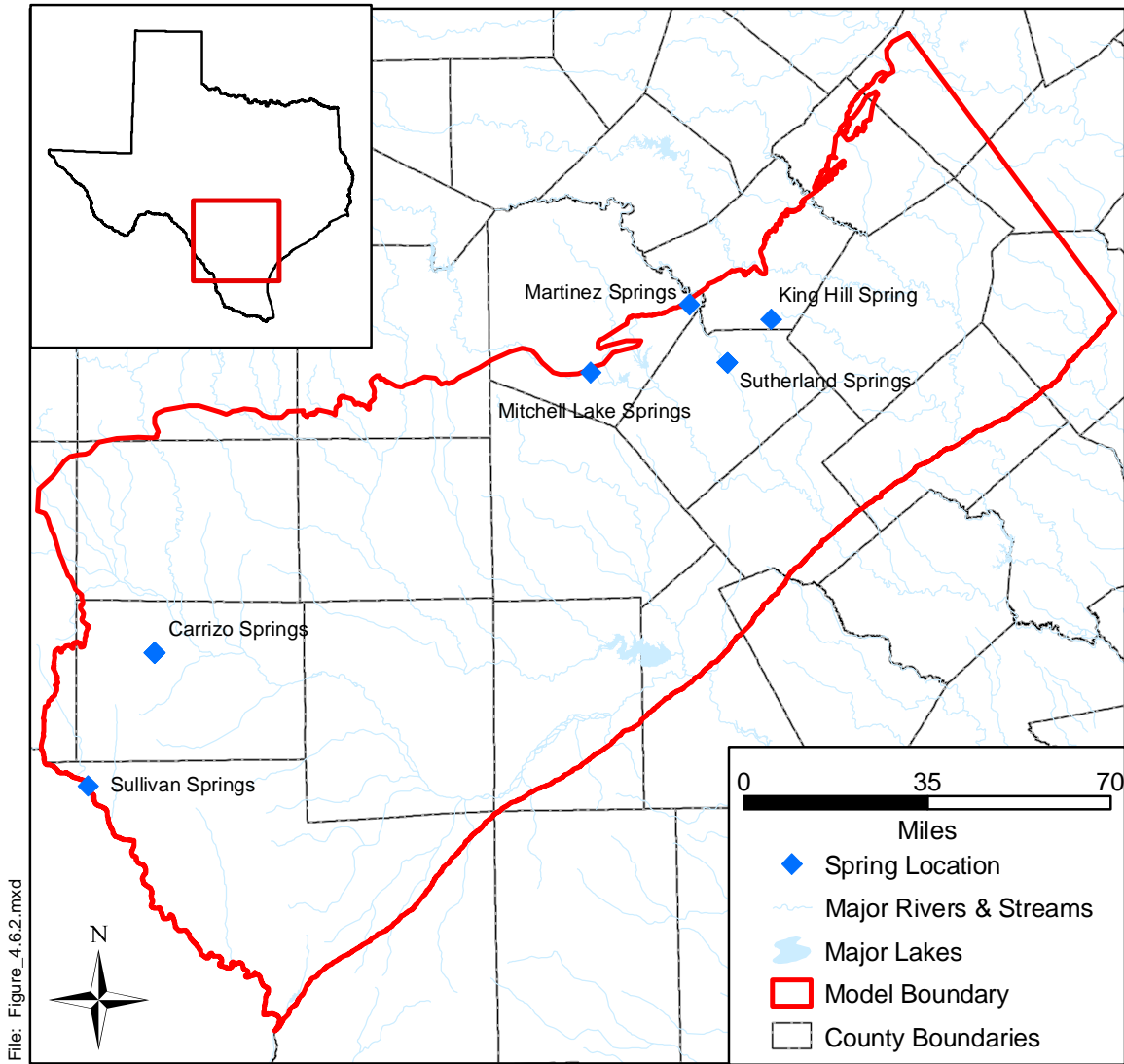


Figure 4.6.2 Documented spring locations in the study area.

4.7 Aquifer Discharge Through Pumping

Pumping discharge from the model required estimations for both the historical modeling period (1980 to 1999) and for the predictive period (2000 to 2050). Historical estimates of groundwater pumpage from the Carrizo-Wilcox aquifer were based on the water use survey database provided by the Texas Water Development Board. The seven water use categories utilized were municipal (MUN), manufacturing (MFG), power generation (PWR), mining (MIN), livestock (STK), irrigation (IRR), and county-other (C-O), which consists primarily of unreported domestic water use. The methodology used to distribute those pumpage estimates is described briefly below, and in detail in the “Standard Operating Procedure for Processing Historical Pumpage Data”, Appendix B to this report.

Municipal, manufacturing, mining, and power pumpage estimates were actual monthly water use records reported by the water user, which were available for 1980 through 1999. In cases where only the total annual pumpage was reported, the average monthly distribution of annual pumpage for the same water use category in the same county-basin, or an adjacent county-basin, was used. A county-basin is a geographic unit created by the intersection of county and river basin boundaries. For example, a county partly crossed by two river basins comprises two county-basins.

The water use survey also included historical annual pumpage estimates for livestock, irrigation, and county-other water use for the years 1980 and 1984 through 1997 for each county-basin. Annual pumpage estimates for the years 1981, 1982, 1983, 1998, and 1999 were developed by linear regression based on significant relationships between reported pumpage and (1) average annual temperature, (2) total annual rainfall measured at the nearest weather station, and (3) the year, for each water use category.

The monthly distribution of county-other water use was assumed to be similar to that of municipal use. The average monthly distribution of municipal water use for a given year within the same (if possible) or an adjacent county-basin was used to estimate how much of the annual total county-other usage was pumped in each month.

Annual livestock water use was distributed uniformly across all twelve months. While this may not accurately reflect seasonality of livestock use, it was not expected to have much impact because livestock is a relatively minor use in the study area.

The procedures for temporal distribution of annual irrigation water use differed for rice and non-rice crops. For rice, monthly irrigation pump electricity consumption use records were used to indicate how much water was pumped in each month for rice irrigation. For non-rice crops, annual irrigation water use was distributed among months using predicted monthly water deficits, based on the rainfall deficit and crop evapotranspiration estimates for each Texas Crop Reporting District, using the approach of Borrelli et al. (1998).

Reported historical pumpage for municipal, manufacturing, mining, and power water uses were matched to the specific wells from which it was pumped to identify the location in the aquifer from which it was drawn (latitude, longitude, and depth below mean sea level) based on the well's reported properties. The well properties were obtained by compiling data from the TWDB's state well database, the Texas Commission on Environmental Quality's Public Water System database, the U.S. Geological Survey's National Water Information System, the TWDB's follow up survey with water users, and various other minor sources as described in the "Standard Operating Procedure for Processing Historical Pumpage Data", Appendix B to this report. When more than one well was associated with a given water user, groundwater withdrawals were divided evenly among those wells.

Livestock pumpage totals within each county-basin were distributed uniformly over the rangeland within the county-basin, based on land use maps, using the categories "herbaceous rangeland", "shrub and brush rangeland", and "mixed rangeland". Vertical assignment of livestock pumpage to model flow layers was performed by interpolating an average well depth and screened interval for all Carrizo-Wilcox livestock watering wells in the TWDB state well database, using the inverse distance method to enhance the influence of nearby wells.

County-other pumpage was distributed within each county-basin based on population density (Figure 4.7.1), after excluding urban areas which would generally be served by municipal water suppliers, using the 1990 federal block-level census data for the years 1980-1990, and the 2000 census data for the years 1991-1999. Vertical assignment of county-other pumpage to model flow layers was performed by interpolating an average well depth and screened interval

for all Carrizo-Wilcox county-other wells in the TWDB state well database, using the inverse distance method to enhance the influence of nearby wells.

Irrigation pumpage within each county-basin was spatially distributed across the land use categories “row crops”, “orchard/vineyard”, and “small grains”. However, the pumpage was not uniformly distributed across these land uses, but weighted based on proximity to irrigated farms mapped from the irrigated farmlands surveys performed in 1989 and 1994 by the Natural Resource Conservation Service of the U.S. Department of Agriculture. The 1989 irrigation survey was used for pumpage between 1980 and 1989, while the 1994 survey was used for pumpage from 1990 to 1999. Further details of the procedure are available in the “Standard Operating Procedure for Processing Historical Pumpage Data”, Appendix B to this report. Vertical assignment of irrigation pumpage to model flow layers was performed by interpolating an average well depth and screened interval for all Carrizo-Wilcox irrigation wells in the TWDB state well database, using the inverse distance method to enhance the influence of nearby wells.

Predicted groundwater pumpage from the Carrizo-Wilcox aquifer for the period 2000 through 2050 was estimated based on projected water demand reported by Regional Water Planning Groups as part of Senate Bill 1 planning (TWDB, 2002). The methodology used to distribute pumpage estimates is described briefly here, and in detail in the “Standard Operating Procedure for Processing Predictive Pumpage Data”, Appendix C to this report. The RWPG water demand projections were available for the years 2000, 2010, 2020, 2030, 2040, and 2050; intervening year projections were developed by linear interpolation. In some cases, the RWPGs identified new well field locations for developing new water supplies. In such instances, the specific locations of the future well fields were used to spatially distribute the groundwater pumpage forecasts. However, in the absence of any data indicating otherwise, it was assumed that the most recent past spatial distribution of groundwater pumpage represented the best available estimate of the locations of future groundwater withdrawals.

Predicted municipal water use totals for each public water supplier were matched to the same wells used for that water user in 1999. Similarly for manufacturing, mining, and power generation, predicted future water pumpage totals by county-basin were distributed among the same wells and locations used by those water users in 1999. Irrigation, county-other, and

livestock pumpage estimates for each county-basin from 2000 to 2050 also utilized the same spatial distribution within county-basins as was used in 1999.

Groundwater withdrawal estimates from the Carrizo-Wilcox aquifer for the years 1980 and 1990, and predictions for 2000, 2010, 2020, 2030, 2040, and 2050 in those counties, or portions of counties, within the model area are provided in Tables D1.1 through D1.6 in Appendix D1. It should be noted that these estimates are the sums of model grid cells. Because the 1 square mile grid cells often cross county boundaries, and are added to that county total in which the center of the grid cell occurs, these county-level estimates are not exact. County-level estimates also may not match the original TWDB estimate because a portion of the county occurred outside the model domain or in inactive model cells, because the location of groundwater withdrawal could not be identified, or because the groundwater was found to have been pumped from a different aquifer based on well properties.

Based on this analysis, approximately 313,000 acre-feet of groundwater were withdrawn from the modeled portion of the Carrizo-Wilcox aquifer in 1980 (Table 4.7.1). The amount of groundwater withdrawn declined by approximately 10% to roughly 282,000 acre-feet by 1990. Based upon regional water planning databases, it is estimated that only approximately 181,000 acre-feet were withdrawn in the year 2000. Based upon the regional water plans, groundwater withdrawals from the modeled aquifers are expected to increase slightly through the year 2020, then decline through 2030. From 2030 to 2050, withdrawals are expected to increase with groundwater withdrawals in 2050 expected to total approximately 160,000 acre-feet, roughly half of the 1980 level. Figures 4.7.2 through 4.7.7 show the 1990 pumping demand for the six model layers. These figures show that the predominant aquifer being used in the model area is the Carrizo (layer 3). Moderate quantities of groundwater are produced from aquifers younger than the Carrizo-Wilcox in the study area (Figure 4.7.2). The pumping analysis indicates that there is some production from permeable sands in the Reklaw east of the Frio River and in the Bigford west of Frio River. The upper and middle Wilcox layers show their greatest use in the Wintergarden area. The lower Wilcox layer (Figure 4.7.7) only provides adequate supplies of potable water in the outcrop and the shallow confined section in Zavala County.

Historically, agricultural irrigation has been responsible for the largest withdrawals from the Carrizo-Wilcox aquifer in the study area, particularly in Atascosa, Zavala, and Frio counties.

However, irrigation water use from the Carrizo-Wilcox in this area is expected to decline substantially. Municipal use of water from the Carrizo-Wilcox is expected to continue to increase, particularly in Bexar, Atascosa, Guadalupe, and Webb counties.

Appendix D2 provides post plots for the pumping distribution in AFY for each model layer for years 1980, 1990, 2000, and 2050. Appendix D3 provides bar charts of total pumping in AFY by year from 1980 through 2050 organized by county.

Table 4.7.1 Rate of groundwater withdrawal (AFY) from all model layers of the Carrizo-Wilcox aquifer for counties within the study area.

COUNTY	1980	1990	2000	2010	2020	2030	2040	2050
ATASCOSA	72676	56463	18938	19388	19916	8905	11365	18926
BASTROP	830	1233	5612	6655	7698	8829	10259	12793
BEE	0	0	80	81	80	82	84	88
BEXAR	7658	6681	36709	37699	37688	32316	32882	31340
CALDWELL	2184	3163	7245	7608	7972	8312	8363	8390
DEWITT	9	10	0	0	0	0	0	0
DIMITT	22321	9350	10360	10070	10111	10476	10562	10704
FAYETTE	87	105	8	8	7	7	6	6
FRIO	77550	83623	20587	20680	20736	5614	5723	5808
GONZALES	3516	4589	3174	2998	2837	2688	2640	2607
GUADALUPE	2060	2680	12761	14176	15769	18001	19879	21254
KARNES	1650	841	3266	2932	2782	2591	2556	2532
LA SALLE	9068	7320	4922	4752	4552	4116	3979	3839
LAVACA	4	2	0	0	0	0	0	0
LIVE OAK	115	80	171	171	171	171	171	171
MAVERICK	1203	3625	576	1061	1601	1505	1367	1244
MCMULLEN	433	1560	578	510	470	440	414	395
MEDINA	8433	1630	6556	6612	6650	2422	2476	2570
UVALDE	4740	366	4442	4388	4345	1544	1533	1512
WEBB	347	712	2580	7430	9096	12597	12599	12628
WILSON	10031	15879	13679	13570	12370	11276	11901	12613
ZAVALA	85741	80449	26771	26789	26744	7465	7704	8005
Total	312636	282351	181015	189588	193615	141387	148503	159475

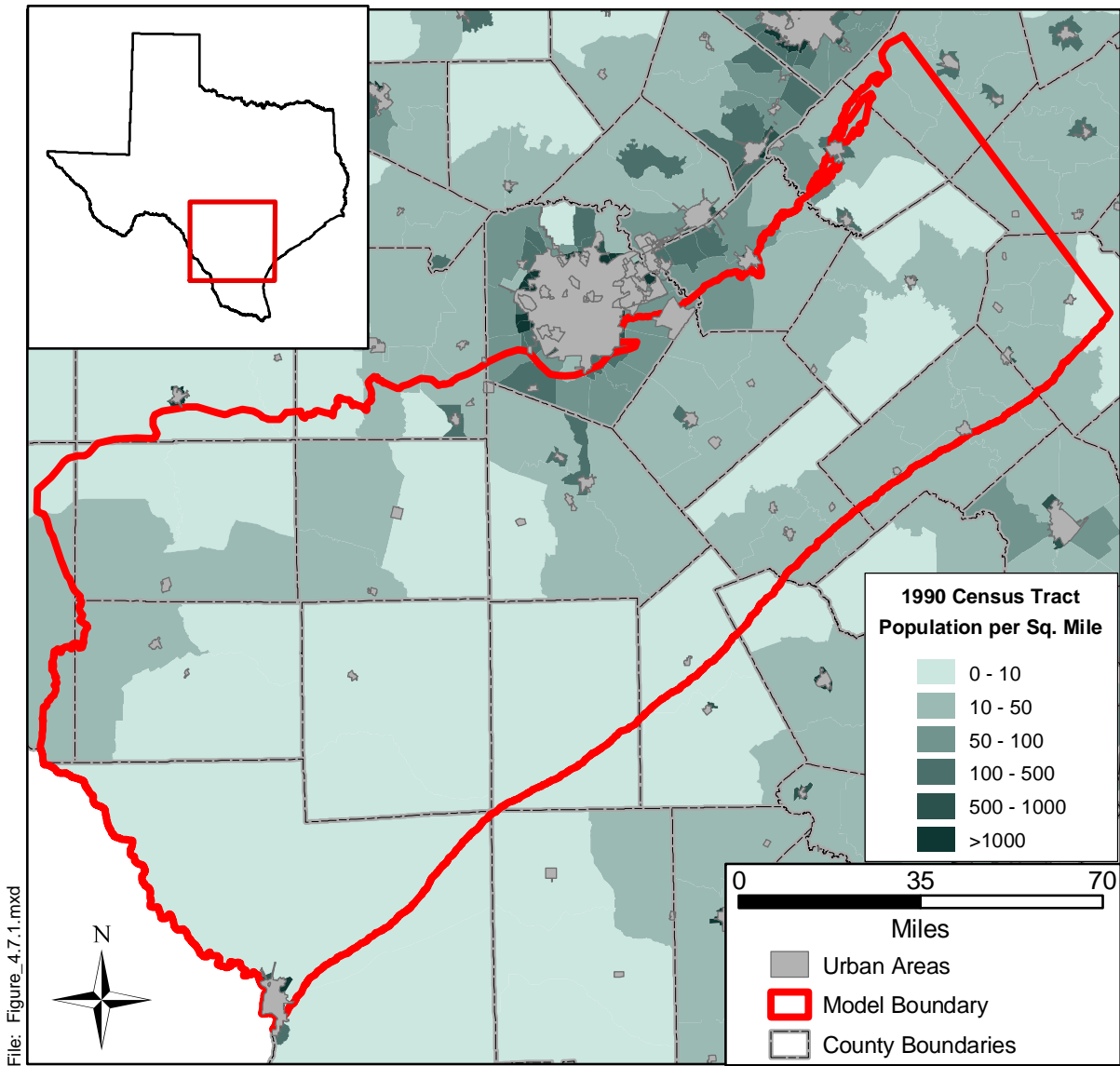


Figure 4.7.1 Rural population density in the study area.

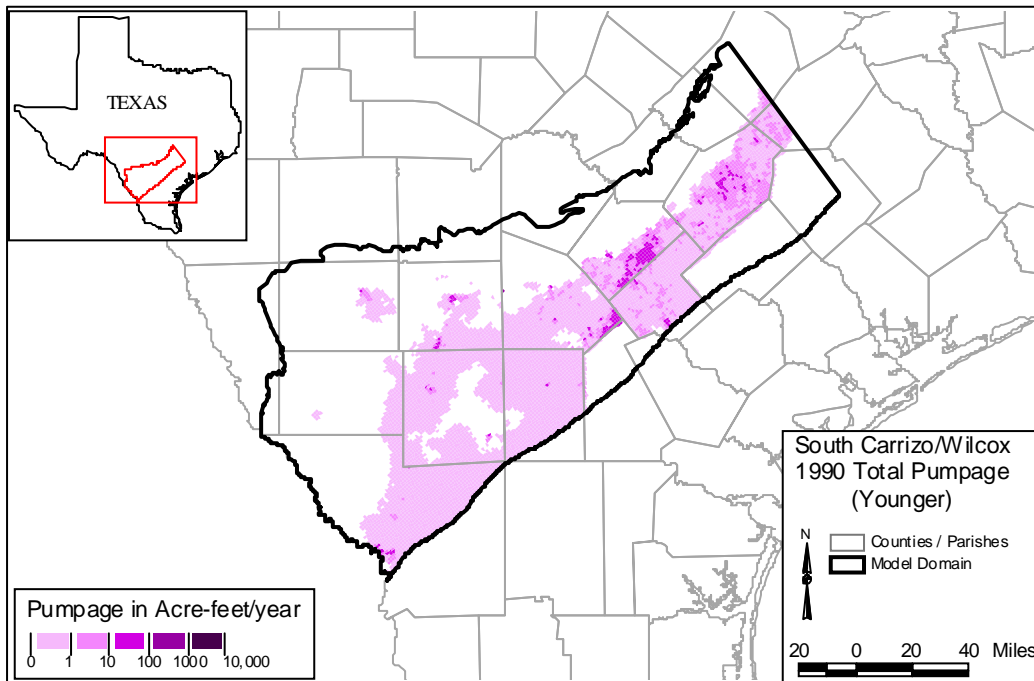


Figure 4.7.2 Younger (Layer 1) Pumpage, 1990 (AFY).

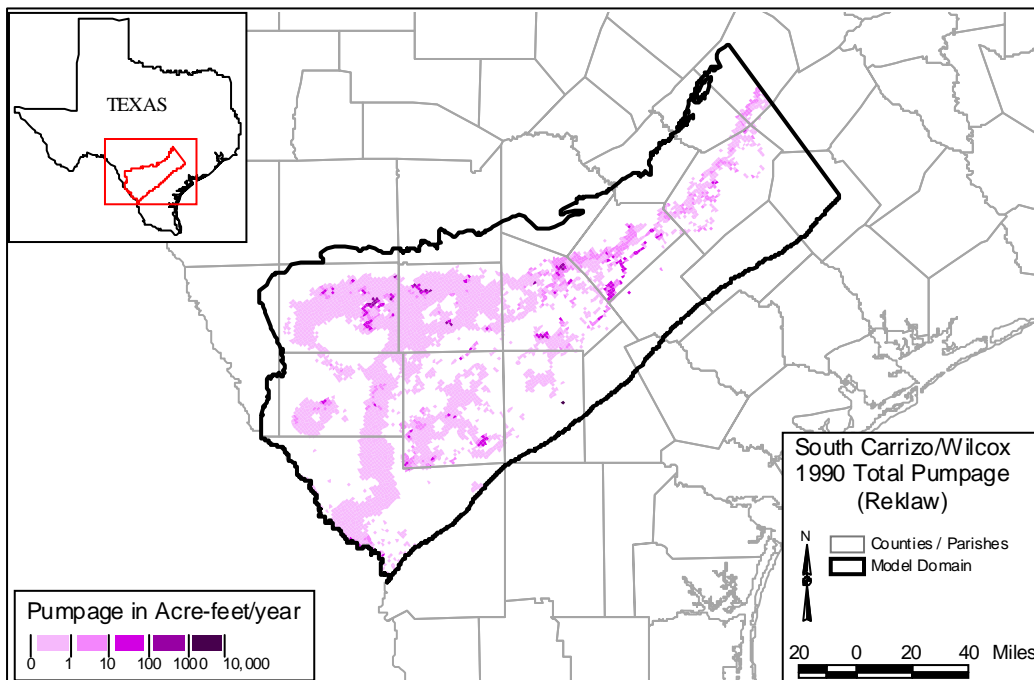


Figure 4.7.3 Reklaw (Layer 2) Pumpage, 1990 (AFY).

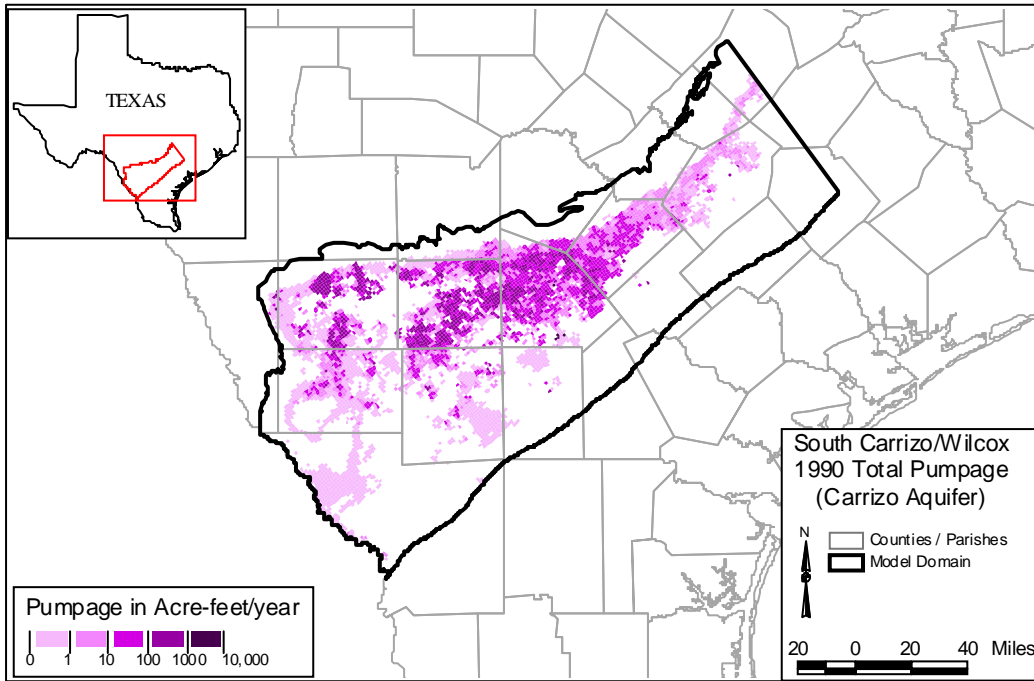


Figure 4.7.4 Carrizo (Layer 3) Pumpage, 1990 (AFY).

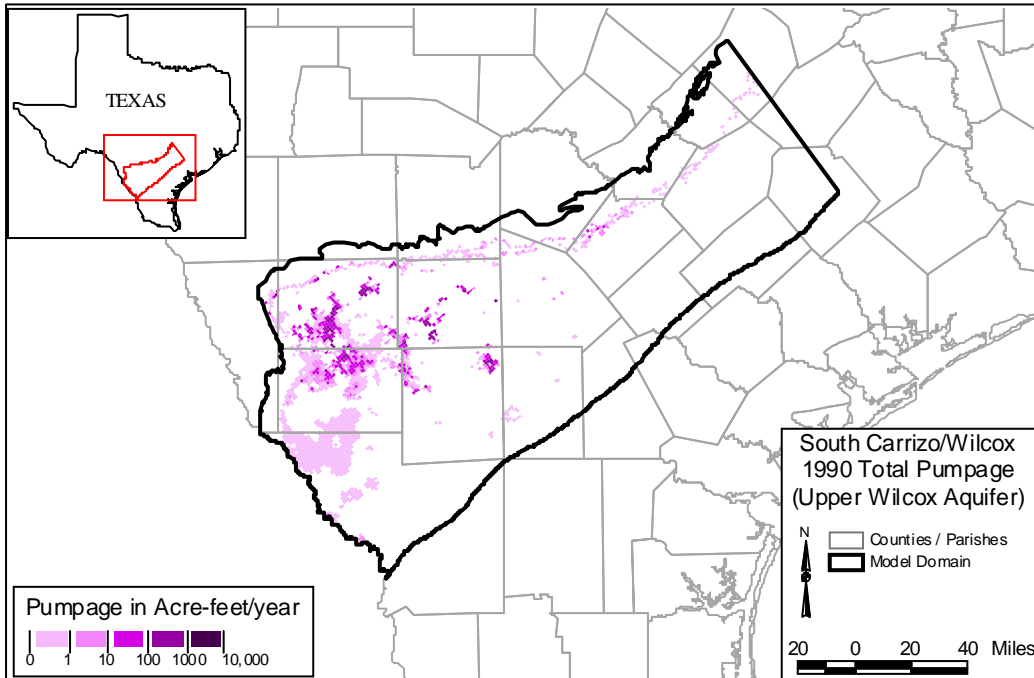


Figure 4.7.5 Upper Wilcox (Layer 4) Pumpage, 1990 (AFY).

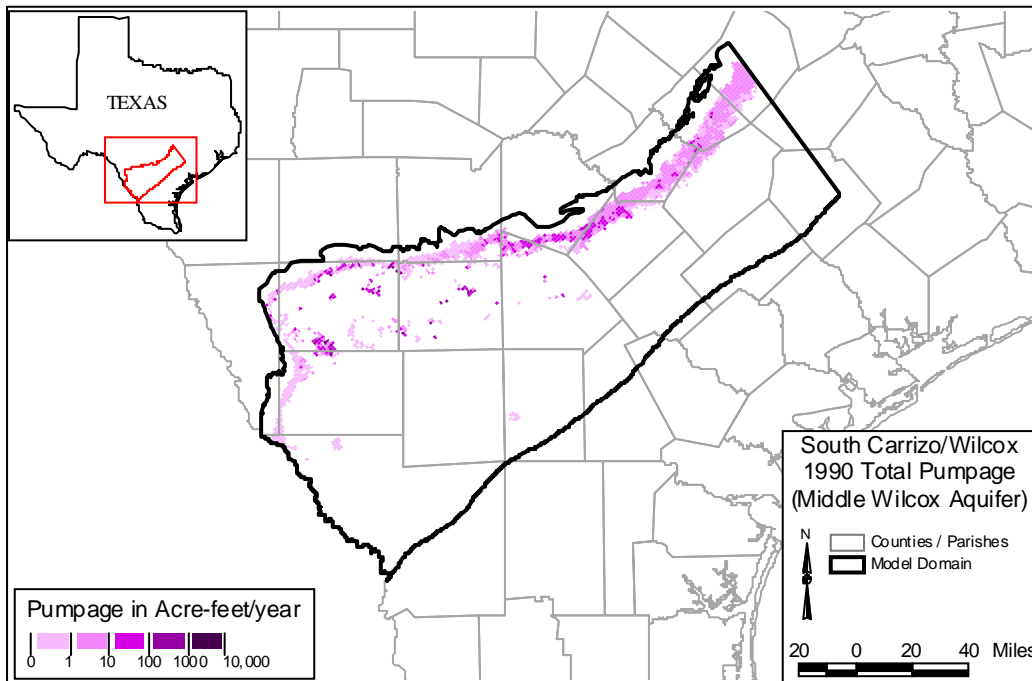


Figure 4.7.6 Middle Wilcox (Layer 5) Pumpage, 1990 (AFY).

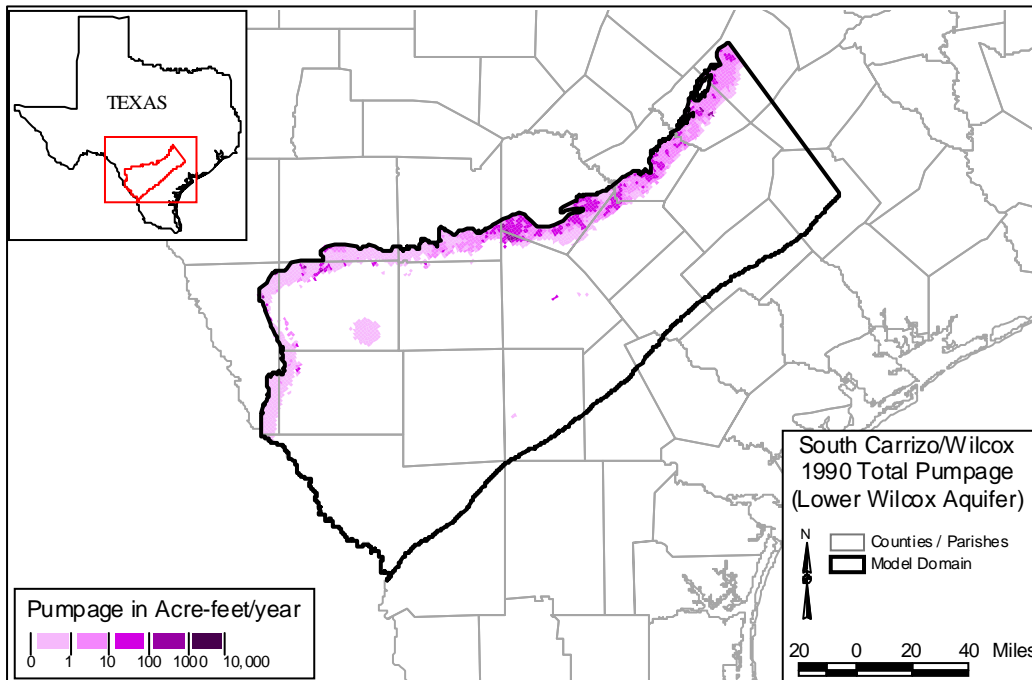


Figure 4.7.7 Lower Wilcox (Layer 6) Pumpage, 1990 (AFY).

4.8 Water Quality

Water quality data for the southern Carrizo-Wilcox aquifer were examined in terms of drinking water quality, irrigation water quality, and industrial water quality, which are described in detail in Appendix F. For the water-quality assessment, available water quality measurements derived from various databases were compared to screening levels for specific constituents (Table F.1 and F.2). Screening levels for drinking water supply are based on the maximum contaminant levels (MCLs) established in National Primary and Secondary Drinking Water Regulations. Irrigation water quality is evaluated based on the concentrations of specific constituents, such as boron, chloride, and TDS, as well as the salinity hazard, owing to their limited tolerance for crop irrigation. Groundwater suitability for industrial purposes is indicated by the content of dissolved solids, as well as its corrosiveness and tendency to form scale and sediments (Table F.1 and F.2). Table F.1 indicates for each constituent the percent of wells in the Carrizo-Wilcox aquifer exceeding the screening levels, and Table F.2 list the percentage of wells in individual counties exceeding one or more screening levels. The spatial concentration distributions of selected constituents in the southern Carrizo-Wilcox aquifer are shown in Figures F.1 through F.7. Note that these water quality data have been reported to the different state agencies and are typically from operational wells. Wells that were drilled and subsequently abandoned due to insufficient yield or unsuitable water quality are typically not reported and may not be included in the available databases.

5.0 CONCEPTUAL MODEL OF GROUNDWATER FLOW IN THE AQUIFER

The conceptual model for groundwater flow in the Southern Carrizo-Wilcox GAM area is based on the hydrogeologic setting, described in Section 4. The conceptual model is a simplified representation of the hydrogeological features which govern groundwater flow in the aquifer. These include the hydrostratigraphy, hydraulic properties, and stresses such as pumping and recharge, and the boundaries. Each of the elements of our conceptual model is described below. The schematic diagram in Figure 5.1 depicts the conceptual hydrogeologic model of groundwater flow in the Carrizo-Wilcox aquifer. Figure 5.1 represents the aquifer under predevelopment conditions. With the addition of pumping as the resource is developed, an additional discharge from each aquifer layer would occur. The pumping discharge would be depicted by an additional arrow from each pumped layer in Figure 5.1.

The conceptual model distinguishes four layers in the Carrizo-Wilcox aquifer, consisting of the lower, middle, and upper Wilcox layers in addition to the Carrizo Sand. These layers tie in with the subdivision of the aquifer in the Central Carrizo-Wilcox GAM, except for the top of the middle Wilcox. The Carrizo-Wilcox aquifer is overlain by the Reklaw Formation, representing the confining unit downdip of the Carrizo outcrop, separating the major Carrizo-Wilcox aquifer from the shallower Queen City and Sparta minor aquifers. For the Southern Carrizo-Wilcox GAM, the Reklaw confining unit and the overlying Queen City aquifer unit are represented as separate layers in the model to properly account for vertical flow across the Reklaw. Southeast, and down dip of the Queen City outcrop, a wedge of younger sediments overly the aquifer. In this part of the study area, vertical flow between the Queen City aquifer and the water table is approximated using general-head boundary conditions.

In addition to identifying the hydrostratigraphic layers of the aquifer, the conceptual model also defines the mechanisms of recharge and discharge, as well as groundwater flow through the aquifer. Recharge occurs mainly in the outcrop areas of the Carrizo-Wilcox layers along the northwestern edge of the study area. Similarly, recharge to the shallow Queen City aquifer occurs through infiltration in the outcrop area. Additional recharge to the Carrizo-Wilcox aquifer may occur by cross-formational flow from the Queen City aquifer through the Reklaw confining unit (Figure 5.1) in areas where the vertical gradient has been reversed by Carrizo

pumping. However, in the confined section, vertical gradients are naturally upward from the Carrizo-Wilcox aquifer to the overlying Queen City. Cross-formational flow between the different layers within the Carrizo-Wilcox aquifer may redistribute groundwater, recharged in the outcrops, into different aquifer layers as a result of variations in hydraulic properties and topography (Figure 5.1).

Most of the precipitation falling on the outcrop runs off into the small creeks, which discharge through major streams out of the model area. In addition to runoff, a significant portion of the precipitation is lost by evapotranspiration (ET), leaving only a small fraction of the precipitation to infiltrate into the subsurface and recharge the aquifer. Diffuse recharge occurs preferentially in topographically higher interstream areas within the outcrops. Focused recharge along streams can occur when the water table in the aquifer is below the stream-level elevation. If stream levels are lower than surrounding groundwater levels, groundwater discharges to the streams resulting in gaining streams. In this case, water levels in the valley are typically close to land surface and some of the shallow groundwater in this area can be lost to evapotranspiration.

Recharge is a complex function of precipitation, soil type, geology, water level and soil moisture, topography, and ET. Precipitation, ET, water-table elevation, and soil moisture vary spatially and temporally, whereas soil type, geology, and topography vary spatially. In addition to natural phenomena, water levels are affected by pumping and man-made surface-water reservoirs, which may in turn affect recharge. Under undisturbed conditions (e.g., prior to pumping), groundwater recharge is balanced by natural discharge of groundwater. To maintain a state of dynamic equilibrium, groundwater withdrawal by pumping must be balanced by (1) an increase in recharge, (2) a decrease in natural discharge, (3) a loss of storage, (4) or a combination of these factors. Balancing pumping by increased recharge implies that recharge was rejected prior to the onset of pumpage (Theis, 1940; Domenico and Schwartz, 1990). This occurs primarily in outcrop areas of aquifers where the water table is near land surface.

The onset of pumpage and the concomitant water-level decline induces an increase in recharge, because less water is captured by evapotranspiration as the water table declines below the root zone and vertical gradients in the recharge zone increase. Freeze (1971) showed for an unconfined aquifer that the increase in recharge occurs initially without affecting the natural discharge even though pumpage continues to increase (Figure 5.2a). After some time, the

recharge stabilizes as the increased pumpage is offset by a decrease in the natural discharge (i.e., gaining streams). With continued increase in pumpage and concomitant decrease in basin discharge, the conditions could become 'unstable', whereby the decrease in natural discharge can no longer feed the increased pumpage (Figure 5.2b). Water levels decline to a depth below which the maximum recharge rate can no longer be sustained, because of consistently drier conditions in the unsaturated zone and increased evapotranspiration during redistribution (Freeze, 1969). Compared to the hypothetical system described by Freeze (1971), the unconfined-confined system of the Carrizo-Wilcox aquifer will exhibit a more complex response, whereby the water-table response in the outcrop to pumpage in the confined section would be delayed.

Our conceptual model for the southern Carrizo-Wilcox aquifer is considered to represent a stable groundwater basin, as indicated in Figure 5.2b, though with a limited rejected recharge potential particularly toward the southwest. That is, depth to water during predevelopment conditions is typically at or below the root zone and a further water-level decline due to pumpage does not decrease evapotranspiration. This implies that effective recharge during predevelopment conditions is expected to be at or slightly less than current average recharge as a result of pumpage over the last several decades.

In the eastern portion of the study area, groundwater from the aquifer discharges to local creeks and major streams throughout the area, contributing to the baseflow of the major streams. In addition, discharge from the Carrizo-Wilcox aquifer occurs by cross-formational flow through the overlying Reklaw Formation into the Queen City. Similarly, discharge from the Queen City aquifer is to the streams in the Queen City outcrop area or through leakage across the younger formations above the Queen City aquifer in the downdip section of the aquifer.

Groundwater flow within the aquifers is controlled by the topography, the structure, and the permeability variation within the different layers. The available data suggest that the Carrizo has the highest average hydraulic conductivity, whereas the underlying Wilcox layers have significantly lower conductivities. Groundwater flow in the Carrizo-Wilcox aquifer is generally downdip to the southeast turning more to the east farther downdip owing to the lower topographic elevations in the northeastern part of the model.

The heterogeneity and structure of the aquifer affect the water quality. The structural dip of the aquifer layers affects the extent of the fresh-water section, which is greater in the southern part compared to the northeastern part, where the dip of the strata increase (Hamlin, 1988). Fault zones may limit downdip flow of fresh groundwater, as indicated by higher total dissolved solids (TDS) southeast of the strike-oriented faults updip of the growth fault zone (Hamlin, 1988). Even though delineating high-TDS groundwater is important for water availability determinations, water quality assessment is not an explicit requirement of the current GAM. However, a preliminary characterization of water quality for the Carrizo-Wilcox aquifer in the study area is given in Appendix F.

The vertical boundary along the southern edge of the model corresponds to the updip limit of the growth faults, displacing mainly Wilcox and deeper strata downward (Figure 5.1). This boundary is represented by a no-flow boundary in the model, representing the stagnant zone associated with the overall downdip hydraulic gradient of the Carrizo-Wilcox aquifer system and the general updip gradient of the geopressured zone southeast of the growth fault zone. As a result, discharge from the confined section of the Carrizo-Wilcox aquifer is through upward cross-formational flow or pumping.

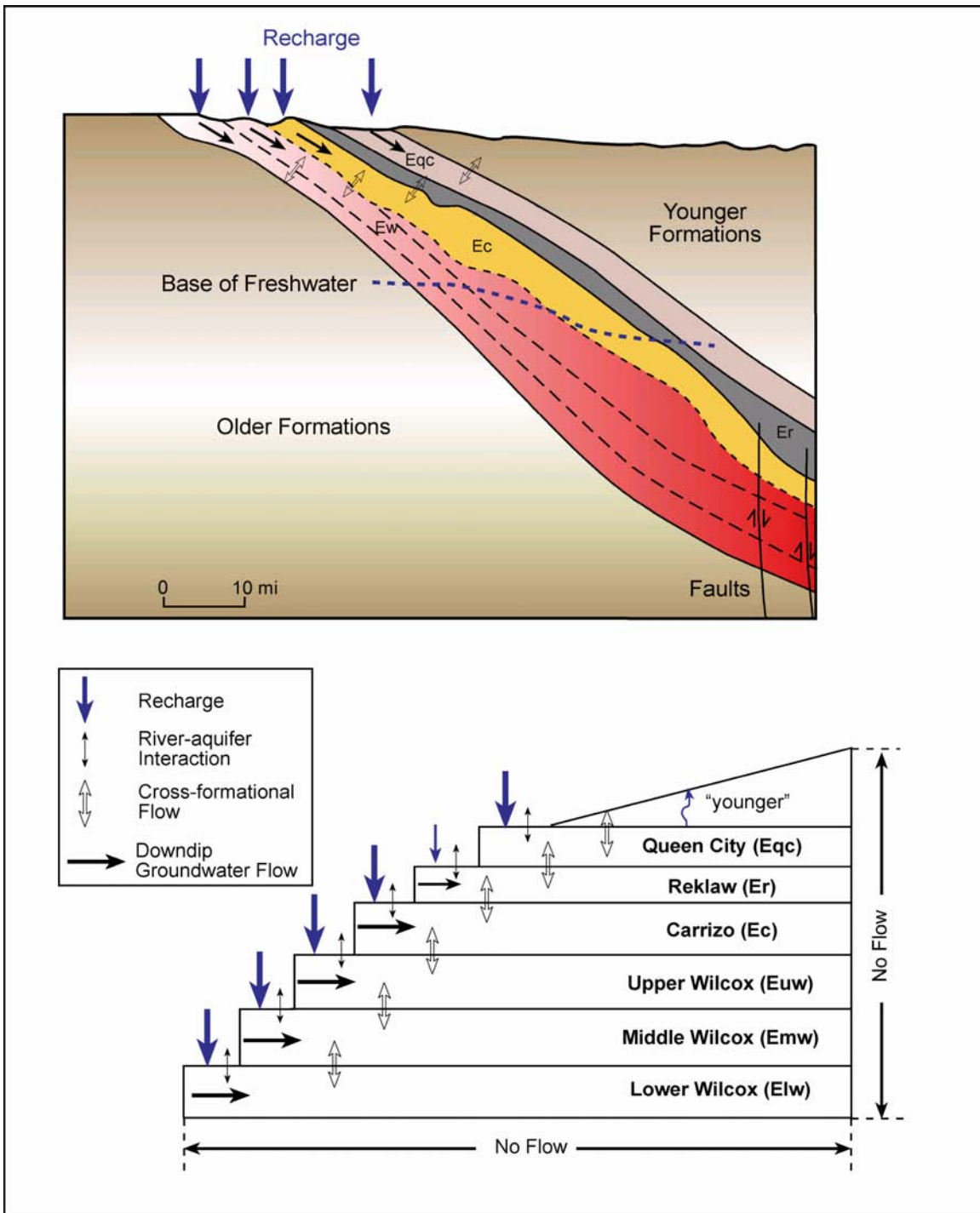


Figure 5.1 Conceptual groundwater flow model for the Southern Carrizo-Wilcox GAM.

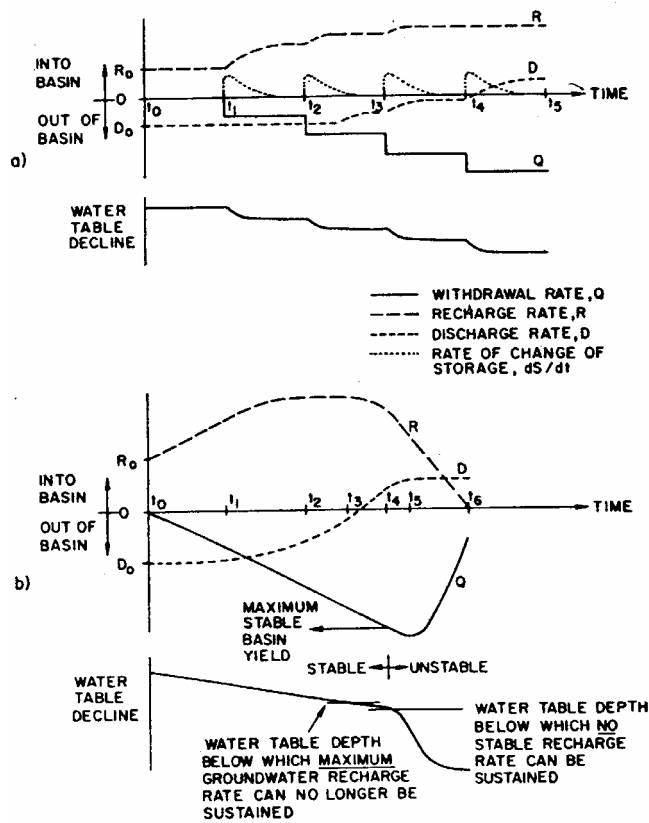


Figure 5.2 Schematic diagram of transient relationships between recharge rates, discharge rates, and withdrawal rates (from Freeze, 1971).

6.0 MODEL DESIGN

Model design represents the process of translating the conceptual model for groundwater flow in the aquifer (Section 5) into a numerical representation which is generally described as the model. The conceptual model for flow defines the required processes and attributes for the code to be used. In addition to selection of the appropriate code, model design includes definition of the model grid and layer structure, the model boundary conditions, and the model hydraulic parameters. Each of these elements of model design and their implementation are described in this section.

6.1 Code and Processor

The code selected for the Southern Carrizo-Wilcox GAM and for all GAMs developed by or for the TWDB is MODFLOW-96 (Harbaugh and McDonald, 1996). MODFLOW-96 is a multi-dimensional, finite-difference, block-centered, saturated groundwater flow code which is supported by enhanced boundary condition packages to handle recharge, ET, streams (Prudic, 1988), and reservoirs (Fenske et al., 1996).

The benefits of using MODFLOW for the Southern Carrizo-Wilcox GAM include; (1) MODFLOW incorporates the necessary physics represented in the conceptual model for flow described in Section 5 of this report, (2) MODFLOW is the most widely accepted groundwater flow code in use today, (3) MODFLOW was written and is supported by the United States Geological Survey (USGS) and is public domain, (4) MODFLOW is well documented (McDonald and Harbaugh, 1988; Harbaugh and McDonald, 1996), (5) MODFLOW has a large user group, and (6) there are a plethora of graphical user interface programs written for use with MODFLOW.

To the extent possible, we have developed the MODFLOW data sets to be compatible with Processing MODFLOW for Windows (PMWIN) Version 5.3 (Chiang and Kinzelbach, 1998). The size of the GAM and the complexity of our application precludes 100-percent compatibility with PMWIN, as well as many other interfaces.

We have executed the model on x86 compatible (i.e. Pentium or Athlon) computers equipped with the Windows 2000 operating system. MODFLOW is not typically a memory-

intensive application in its executable form. However, if any preprocessor (such as PMWIN) is used for this size and complexity of model, at least 256MB of RAM is recommended.

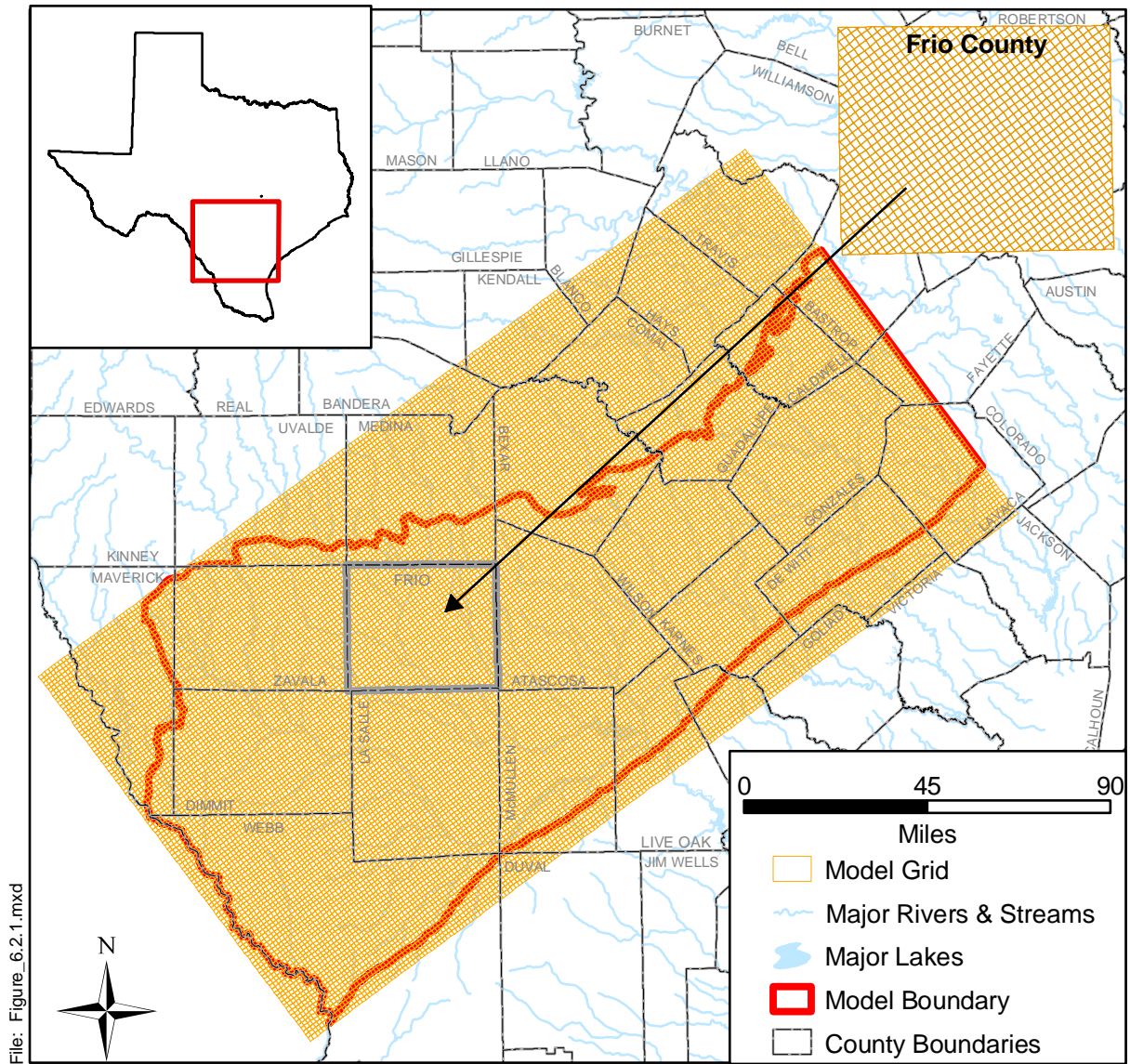
6.2 Model Layers and Grid

Consistent with the model hydrostratigraphy described in Section 4.1 and the conceptual flow model detailed in Section 5, we have divided the Southern Carrizo-Wilcox GAM into six model layers. MODFLOW-96 numbers layers from top (nearest to ground surface) to bottom and this is the order by which each layer will be introduced. Layer 1 is the Queen City Formation east of the Frio River and the El Pico Clay west of the Frio River. Layer 2 is the Reklaw Formation east of the Frio River and the equivalent Bigford Formation west of the Frio River. Layer 3 is the Carrizo Sand, the primary aquifer in the study area (Klemt et al., 1976). Layer 4 is the upper Wilcox, which is present only in the confined portion of the aquifer. Layer 5 is the middle Wilcox and Layer 6 is the lower Wilcox. The middle and lower Wilcox are primarily used as a water resource in their outcrops. The model layers are shown with the model hydrostratigraphy in Figures 4.1.1 and 5.1.

The Southern Carrizo-Wilcox GAM model area is bounded laterally on the northeast by the surface water basin divide between the Guadalupe and Colorado rivers and to the southwest by the Rio Grande. The updip limit of the model is defined by the outcrop of the Carrizo-Wilcox aquifer at the contact with the Midway Formation. The southern boundary of the model is defined by the updip limit of the Wilcox growth fault zone (Bebout et al., 1982). MODFLOW-96 requires a rectilinear grid and also requires an equal number of rows for all columns. As a result, the model area is constrained to being a rectangular grid. Typically, one axis of the model grid is aligned parallel to the primary direction of flow (this is to the southeast for the Southern Carrizo-Wilcox GAM). The model area was determined by imposing the preceding constraints with the additional constraint of minimizing the number of model grid cells. The model grid origin is located at GAM Coordinates (5,062,000, 18,280,000), with the x-axis rotated positive 0.641 radians (E 36.727° N). The GAM standard requires that grid cells be square of a uniform dimension of 1 mile (area of 1 square mile). The model has 217 columns and 112 rows for a total number of grid cells per layer of 24,304. As discussed below, not all of these grid cells are active in the model. Figure 6.2.1 shows the entire model grid. Included on

this figure is an inset with an enlargement of Frio County to show the model grid at the county scale.

Not all model grid cells are active grid cells. We defined the active area of each model layer by intersecting the layer grid with the geologic map and the growth fault boundaries to the south. Cells extending past the outcrop or downdip of the growth fault boundary were defined as inactive in the IBOUND array. If a cell was 50% or more in the outcrop, it was defined as active. Cells west of the Rio Grande on the southwestern boundary of the model were also made inactive on the assumption that the Rio Grande is a regional sink for the aquifer being modeled. After clipping the layers to their proper dimensions, Layers 1 through 6 had the following number of grid cell respectively, 11682, 12848, 13781, 13911, 14910, and 15674. The total number of active grid cells in the model grid is 82896.



File: Figure_6.2.1.mxd

Figure 6.2.1 Southern Carrizo-Wilcox GAM model grid.

6.3 Boundary Condition Implementation

A boundary condition can be defined as a constraint put on the active model grid to characterize the interaction between the active simulation grid domain and the surrounding environment. There are generally three types of boundary conditions; specified head (First Type or Dirichlet), specified flow (Second Type or Neumann), and head-dependent flow (Third Type or Cauchy). The no-flow boundary condition is a special case of the specified flow boundary condition.

Boundaries can be defined as being time independent or time dependent. An example of a time dependent boundary might be a pumping flow boundary or a reservoir stage elevation. Because many boundaries require time dependent (transient) specification, the stress periods used by MODFLOW must be specified. A stress period in MODFLOW defines the minimum time period over which a boundary or model stress may remain constant. Each stress period may have a number of computational time steps which are some fraction of the stress period but over which boundaries remain constant. For this model, the stress periods have been set at one month. Therefore, all transient boundaries in the model cannot change over a period of less than one month.

Boundaries requiring specification include: layer lateral and vertical boundaries, surface water boundaries, recharge boundaries, and discharge boundaries caused by pumping. Lateral and vertical boundaries will be a combination of specified flow (no-flow, Second Type) or head-dependent flow boundaries (general head boundaries, Third Type). Surface water boundaries are head-dependent flow boundaries (Third Type). Recharge is a specified flow boundary (Second Type). Evapotranspiration (ET) is a head-dependent flow boundary (Third Type). Pumping discharge is a specified flow boundary (Second Type).

Figures 6.3.1 through 6.3.6 show the active and inactive grid cells along with the model boundary conditions for each of the six model layers, respectively. Implementation of the boundary conditions for the Southern Carrizo-Wilcox GAM is described below. Unless otherwise specified below, the boundary between the active and inactive cells is a no-flow boundary.

6.3.1 Lateral Model Boundaries

The lateral model boundaries have been defined to occur on the northeast at the drainage divide between the Guadalupe and Colorado rivers and to the southwest along the Rio Grande. Both of these boundaries are assumed to be groundwater divides which are equivalent to no-flow boundaries (Second Type). From a review of the predevelopment hydraulic head map, we concluded that the eastern model boundary is coincident with the groundwater flow direction and reasonably mimics a no-flow boundary. A no-flow boundary was also assigned to the southwestern model boundary with the assumption of insignificant underflow of the Rio Grande in the model area.

The applicability of no-flow boundaries was investigated further for the simulated historical period (1980 through 1999). A no-flow boundary was maintained at the Rio Grande during the transient and predictive model periods (1980-2050). For the northeastern model boundary, water levels were reviewed for the period from 1980 through 1999. Water levels were found to be reasonably constant given the scale of the model with a head decrease observed from a few feet up to 30 feet. Because specification of boundary heads across the northeastern model boundary is inherently uncertain, and because head decreases along the boundary are within the model head error, the northeastern boundary was maintained as a no-flow boundary throughout the transient historical simulation period. If pumping east of the boundary is equal or less than pumping west of the boundary, the assumed boundary is conservative. The northeastern boundary was also investigated for the predictive simulation period (2000-2050). Preliminary maps of drawdown provided by the Central Carrizo-Wilcox GAM team indicated that drawdowns over the predictive period were on the order of historical drawdowns and the no-flow boundary was maintained.

6.3.2 Vertical Boundaries

The model has a no flow boundary on the bottom of Layer 6 (the lower Wilcox) representing the marine shales of the Midway Formation. The upper model boundary is the free-water surface calculated in the outcrops of Layers 1 through 6. In downdip portions of the model where younger sediments overlie the Queen City, these sediments are represented by a general head boundary condition (Third Type). The initial vertical conductances of the general head boundaries were based upon a harmonic average of the hydraulic conductivities of the overlying units. The 1998 model of LBG-Guyton and HDR (1998) was used to estimate the hydraulic

conductances of the overlying younger units. The hydraulic heads associated with the general head boundaries were set equal to the water table as estimated using the regression equations of Williams and Williamson (1989).

6.3.3 Surface Water Implementation

Surface water acts as a head-dependent flow (Third Type) boundary condition for the top boundary of the active model grid cells (outcrop). The stream package (Prudic, 1988) and reservoir package (Fenske et al., 1996) are head-dependent flow boundary conditions that offer a first-order approximation of surface water/groundwater interaction. The stream-routing package will allow for stream-related recharge to be rejected during gaining conditions and for stream-related recharge to be induced during losing conditions. When pumping affects water levels near stream/aquifer connections, recharge will be included through stream loss.

The stream routing package requires designation of segments and reaches. A reach is the smallest division of the stream network and is comprised of an individual grid cell. A segment is a collection of reaches which are contiguous and do not have contributing or diverting tributaries. In MODFLOW, physical properties must be defined describing the hydraulic connection (conductance) between the stream and the aquifer. Stream flow rates are defined at the beginning of each segment for each stress period.

INTERA developed a GIS-based method for developing the reach and segment data coverages for MODFLOW. Figures 6.3.1 through 6.3.6 show the model grid cells which contain stream reaches in the model domain. Required physical properties of the reaches including stream width, bed thickness, and roughness are taken from the EPA River Reach data set (<http://www.epa.gov/region02/gis/atlas/rf1.htm>). The hydraulic conductivity used to define the hydraulic conductance between the aquifer and the stream was initially approximated based on the hydraulic conductivity of the underlying formation. Hibbs and Sharp, (1991) studied the hydraulic connection between the Colorado River and the alluvium and Carrizo-Wilcox aquifer near a Bastrop well field. They concluded that the connection between the river and the aquifer was very good and did not see hydraulic evidence for a low permeability river bed. Our initial approach was to keep the hydraulic conductivity of the stream bed high and relatively constant and allow the stream width taken from the EPA River Reach data set (RFI) to control the streambed conductance.

The stream routing package also requires specification of stream flow rate for each starting reach at each stress period. For predevelopment conditions, and for the historical period, no representative stream gage data exist for the majority of the stream segments. To handle this for the pre-development simulation, we have used mean flow rates from the EPA RF1 data set to specify the flow rate entering each model segment. The EPA RF1 data set contains mean flow rates estimated along the entire stream and coinciding with all of the modeled stream segments.

For the transient simulations, stream flows were based on historical records. However, because the stream gage coverage is sparse, stream flow rates required estimation at the majority of stream segments. The approach we employed to develop ungaged stream segment flow rates has the following assumptions: (1) gages in close proximity behave similarly, (2) the RF1 average stream segment stream flow estimates are accurate, (3) a gage's distribution of monthly stream flow is lognormal, and (4) the standard deviation of the log of monthly flow rate at an ungaged location is equal to the standard deviation of the log of monthly flow rate at a nearby ungaged location. We have checked assumptions 1 through 3 and have found they generally do hold for the model region. Assumption 4 cannot be definitively established in the current domain, due to lack of data for cross-validation.

To calculate the ungaged stream segment flow rates at each monthly stress period, we first constructed the monthly distribution of log flow rate at our gaged stream locations and calculated the standard deviation of that distribution. From the EPA RF1 data set we have the mean flow rates for all segments. For example, if for a given stress period the gaged monthly stream flow was equal to the 75th percentile of the distribution, we would use the mean flow rate from the EPA RF1 data set with the standard deviation borrowed from the actual gaged flow distribution to estimate the 75th percentile flow rate at the ungaged segment. This technique maintains the proper magnitude of flows at ungaged locations as constrained by the EPA RF1 mean flow estimates while superposing the flow variability based upon the nearest gaged data.

The MODFLOW reservoir package (Fenske et al., 1996) has been used to model reservoirs and lakes. Modeled reservoir properties include the hydraulic conductance between the lake and the aquifer and the reservoir stage as a function of stress period. Because reservoirs are in river valleys, the reservoir package must be integrated with the stream routing package. This is done by starting a new segment at the downstream side of each reservoir. The hydraulic

conductivity used to estimate the reservoir/aquifer hydraulic conductance was initially set to a constant, approximately based on the hydraulic conductivity of the underlying formation. Lake stage records were developed by reviewing records in the literature and by contacting various river authorities in the study area. These stage histories are provided in the data model delivered with this modeling report. Only two reservoirs were modeled in the GAM, Calaveras Lake and Victor Braunig Lake, both located in southern Bexar County.

Spring discharge records were reviewed for application in the Southern Carrizo-Wilcox GAM as drain boundary conditions (Type 3). However, as discussed in Section 4 of this report, there are no significant springs still flowing in the model area that are not coincident with stream reach cells (which provide a sufficiently similar boundary condition).

6.3.4 Implementation of Recharge

Because an evaluation of groundwater availability is largely dependent upon recharge (Freeze, 1971), it is an important model input parameter warranting careful examination and meaningful implementation. In typical model applications, recharge is either homogeneously defined as a percentage of the yearly average precipitation or calibrated as an unknown parameter. Unfortunately, recharge and hydraulic conductivity can be correlated parameters preventing independent estimation when using only head data constraints. Another compounding problem is that recharge is a complex function of precipitation rate and volume, soil type, water level and soil moisture, topography, and ET (Freeze, 1969). Precipitation, ET, water table elevation, and soil moisture are areally and temporally variable. Soil type, geology, and topography are spatially variable. For the GAM, recharge requires specification for steady-state conditions, for transient conditions from 1980 until 2000, for the transient drought of record, and for average conditions. Reliable tools for specification of recharge at watershed scale, or the regional model scale (1000s of square miles for the GAMs) do not currently exist.

As a tractable approach to dealing with recharge at the scale of this model, we have used SWAT (Soil Water Assessment Tool) to estimate diffuse recharge rates. SWAT was developed for the USDA Agricultural Research Service by the Blacklands Research Center in Temple, Texas. SWAT is a public-domain model. The SWAT Website where downloads and code-specific documentation can be found is <http://www.brc.tamus.edu/swat/>. SWAT provides a GIS-driven, watershed scale tool to estimate regional soil water balances, incorporating soils data

(USDA/NRCS STATSGO) with the USGS Multi-Resolution Land Characteristics (MRLC) data. SWAT uses standard techniques to track water after it reaches the ground as precipitation. SWAT uses the NRCS Curve Number Method (accounting for antecedent moisture conditions) to partition precipitation into runoff and infiltration. Infiltrating water either increases the soil moisture, is lost through ET, or continues down to the water table. We used the Hargreaves Method for estimating potential ET because it only requires estimates of monthly mean minimum and maximum temperatures which are available for the study area. Average daily net radiation is available within SWAT for month and degrees of latitude. The Hargreaves method is considered accurate for simulation periods that are equal to, or larger than, one month. This is consistent with one month stress periods and the assumptions underlying the NRCS curve-number method for estimating runoff. The potential ET is converted to an actual ET based on the vegetation size and type (determines maximum ET) and soil water availability (determines actual ET).

SWAT is used in an uncoupled mode to estimate several model inputs for MODFLOW. Consistent with the transient MODFLOW stress periods of one month, SWAT results were output in one month increments. However, SWAT simulations were carried out using daily time steps and precipitation/temperature data. Daily time steps (or less) are necessary for approximating runoff during precipitation events. SWAT was simulated for the time period from 1975 through 1999 to coincide with the spinup, calibration and transient model simulation periods.

For each MODFLOW stress period, SWAT calculates: (1) the recharge rate for the recharge package, (2) the ET max for the ET package, and (3) the extinction depth for the ET package. The SWAT estimate of shallow recharge is used as a recharge flux in MODFLOW. SWAT accounts for ET which may occur in the vadose zone. However, in our method of application, SWAT does not account for groundwater transpiration. To account for groundwater ET, the “surplus” ET from SWAT ($ET_{max} - ET_{actual}$) was applied as ET max in the groundwater ET package in MODFLOW. For each month simulated, SWAT calculates a rooting depth representative of the season, vegetative cover, and soil type. This rooting depth is passed through to MODFLOW as the extinction depth required by the MODFLOW ET Package. As a result, ET from groundwater will occur when the water table (as simulated by MODFLOW) is above the extinction depth and there is surplus ET potential for that particular stress period.

Appendix E provides a more detailed explanation of our use of SWAT in an uncoupled mode with MODFLOW.

For the predevelopment model, the SWAT estimates for recharge were averaged values taken from the 1975 to 1999 simulation. The ET max estimates were also averaged for this same time period for input into the MODFLOW ET package. The maximum soil rooting depth was used for the predevelopment model. In the transient simulation, recharge varies as a function of time as well as location.

SWAT was also used for implementing recharge in the predictive simulation period (2000-2050). Recharge was varied seasonally in the predictive simulations based upon monthly average recharge from the 1975 to 1999 simulation. For example, all of the January outputs for the period from 1975 through 1999 were averaged, all of the February outputs were averaged, etc. Predictive simulations end with a drought-of-record. Recharge conditions for the drought-of-record were developed by running SWAT through the drought-of-record climatic conditions. A discussion of the drought-of-record will be held until discussion of the predictive simulations in Section 10.

6.3.5 Implementation of Pumping Discharge

Pumping discharge is not considered in the predevelopment model because the model is meant to be representative of times prior to significant resource use. However, pumping discharge is the primary stress on the model during the historical (1980-1999) and the predictive (2000-2050) model periods. Pumping discharge is a cell dependent specified flow boundary.

The procedural techniques used to estimate and allocate pumping are provided in Section 4.7 and Appendices B and C. For details of how the historical or predictive pumping was derived, the reader is referred to those appendices. Once the pumping had been estimated for each of the seven user groups, it was summed across all user groups for a given model cell (row, column) and a given model layer. This process was repeated for all active model cells in the model domain for each transient stress period. As discussed above, the stress period used in the transient simulations is 1 month. Therefore, the MODFLOW well-package data set has a specified flow boundary condition for each month of simulation, for each active grid cell within which pumping is occurring.

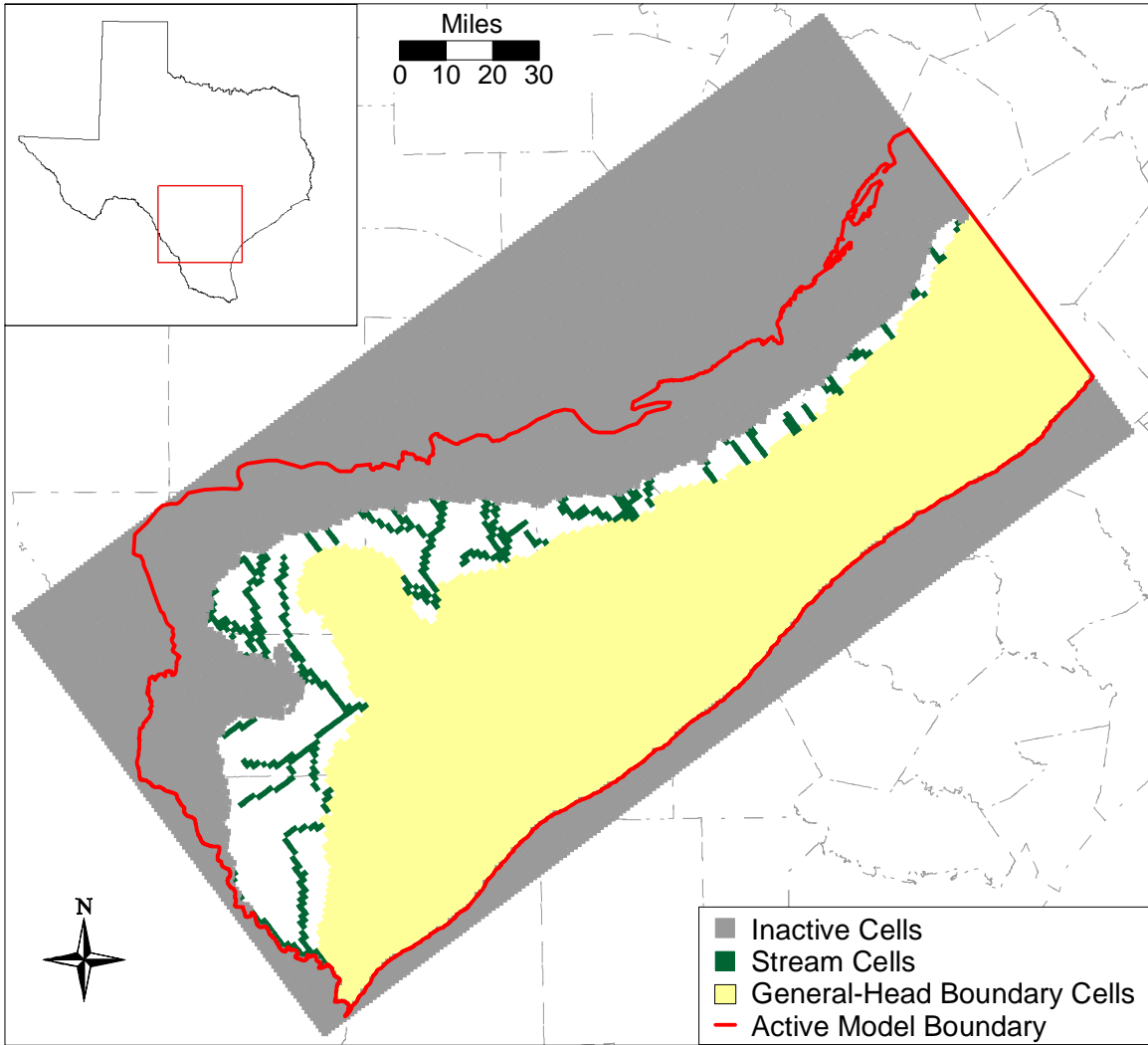


Figure 6.3.1 Layer 1 (Queen City) boundary conditions and active/inactive cells.

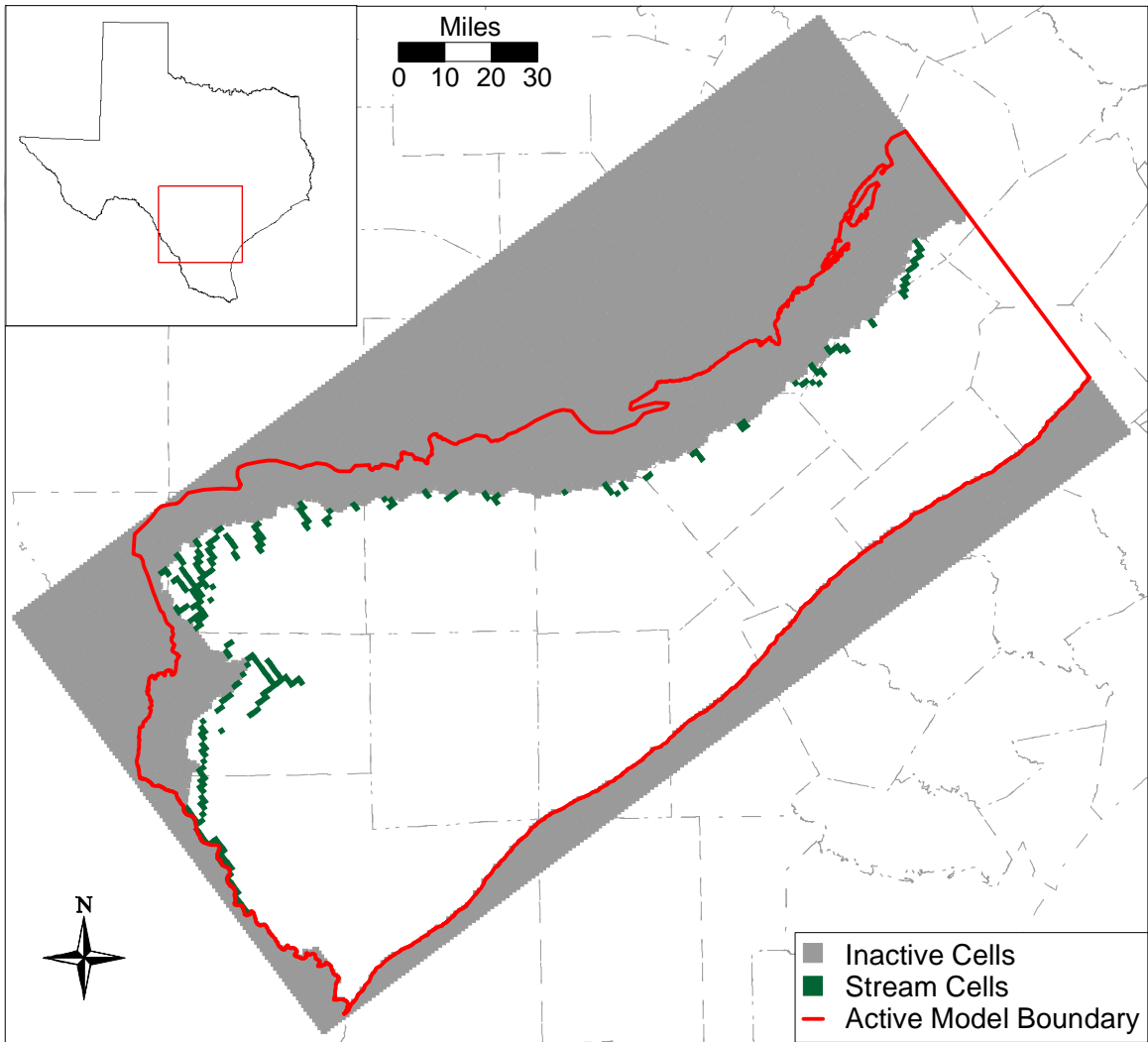


Figure 6.3.2 Layer 2 (Reklaw) boundary conditions and active/inactive cells.

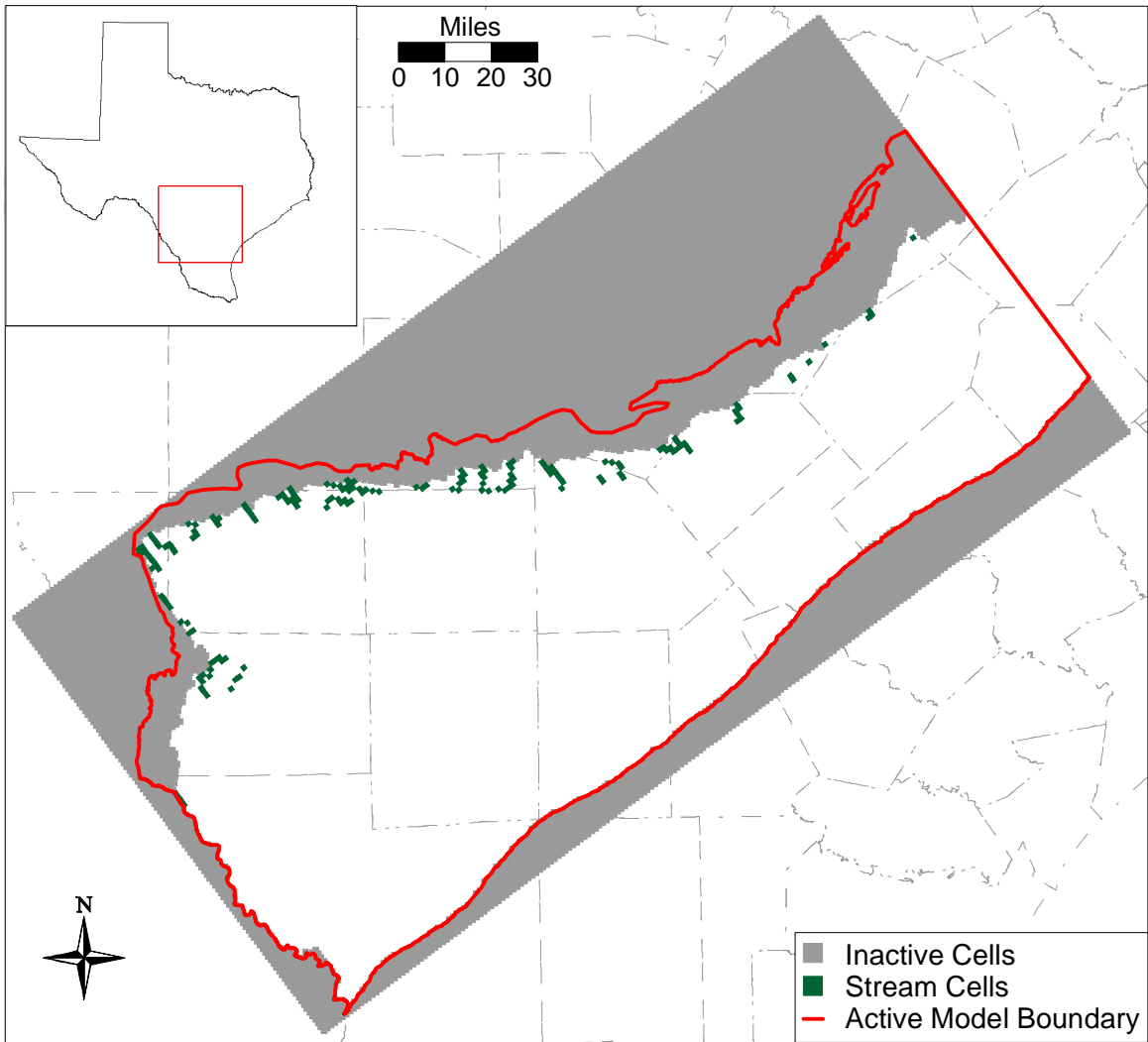


Figure 6.3.3 Layer 3 (Carrizo) boundary conditions and active/inactive cells.

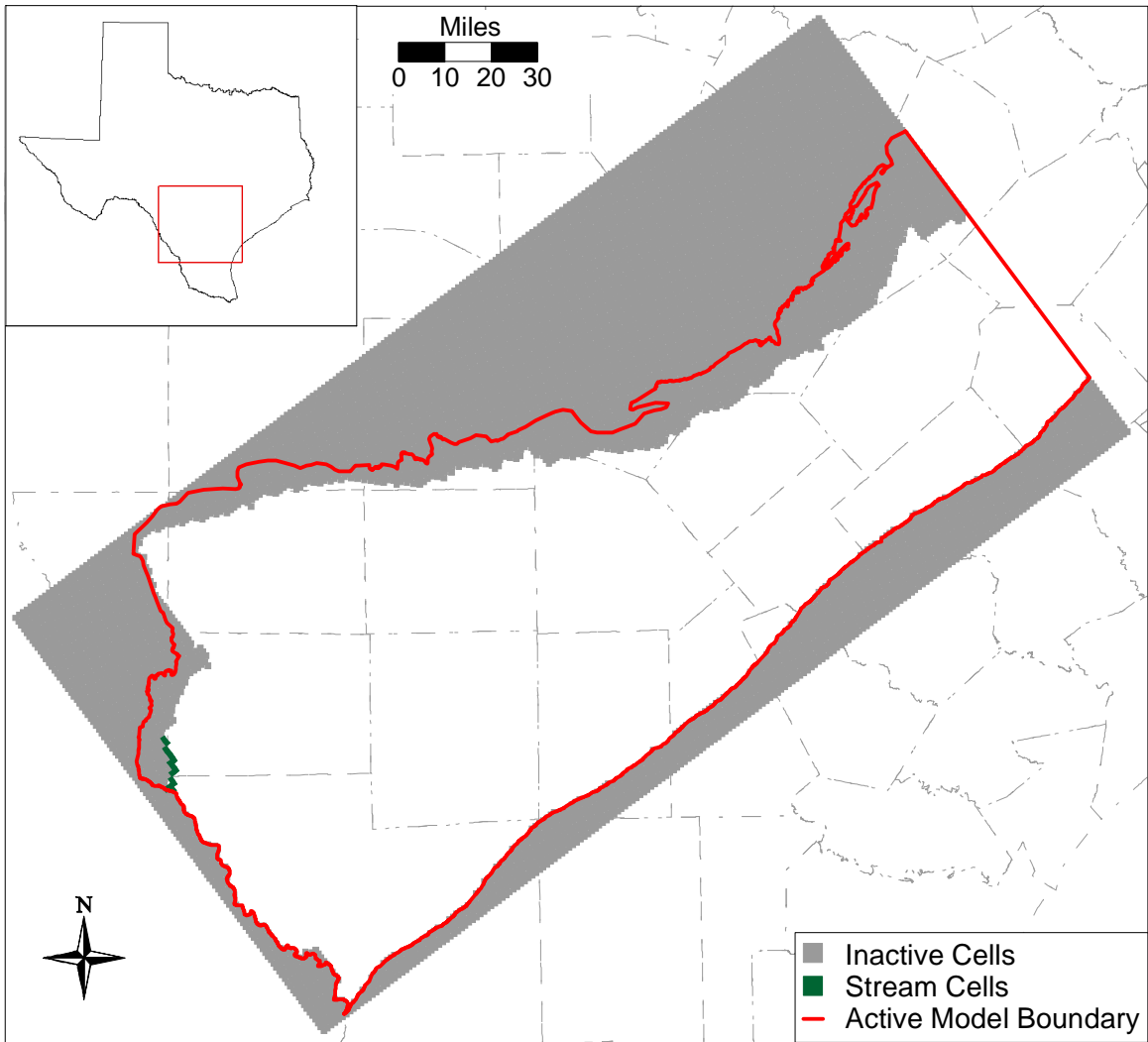


Figure 6.3.4 Layer 4 (upper Wilcox) boundary conditions and active/inactive cells.

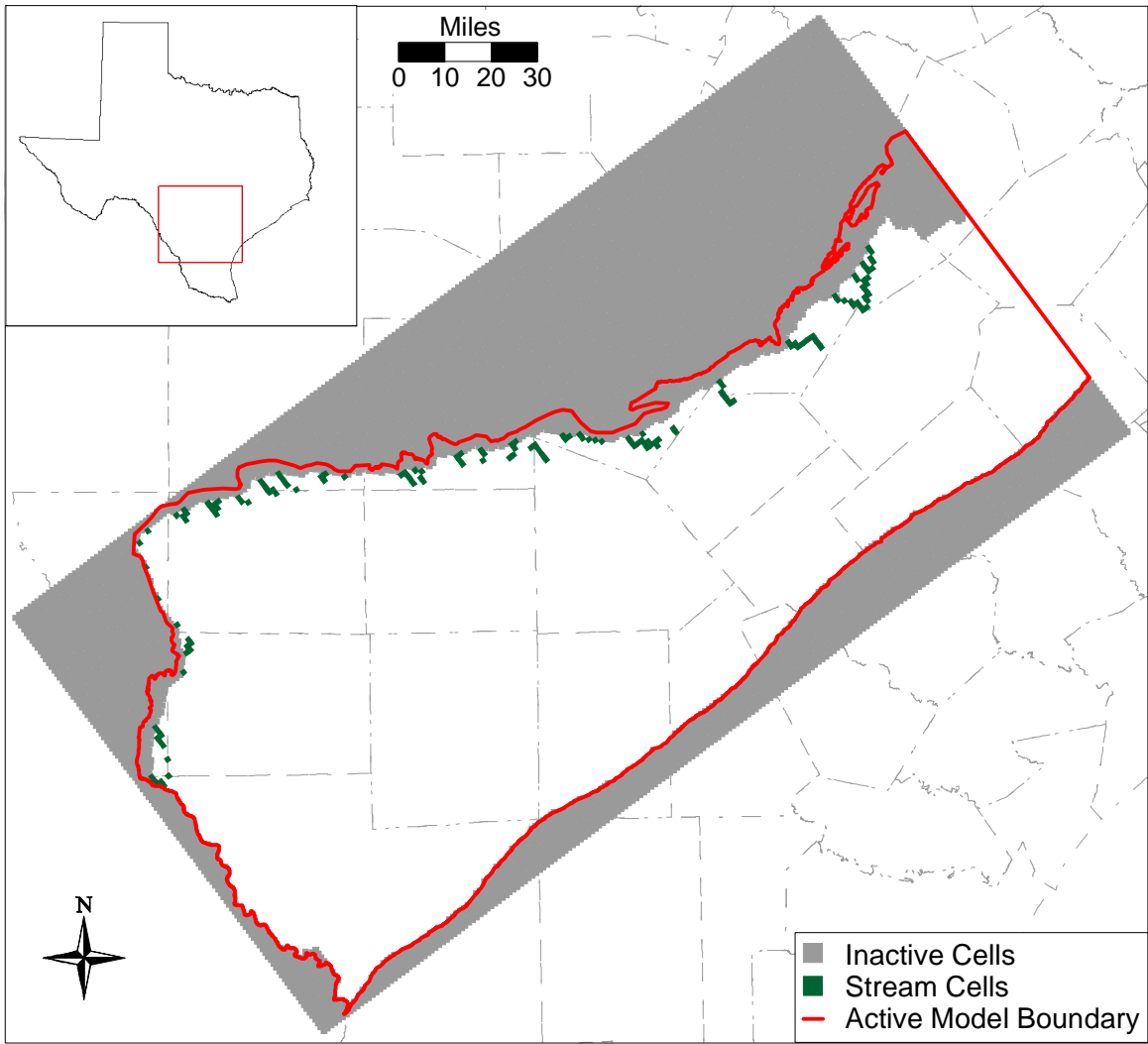


Figure 6.3.5 Layer 5 (middle Wilcox) boundary conditions and active/inactive cells.

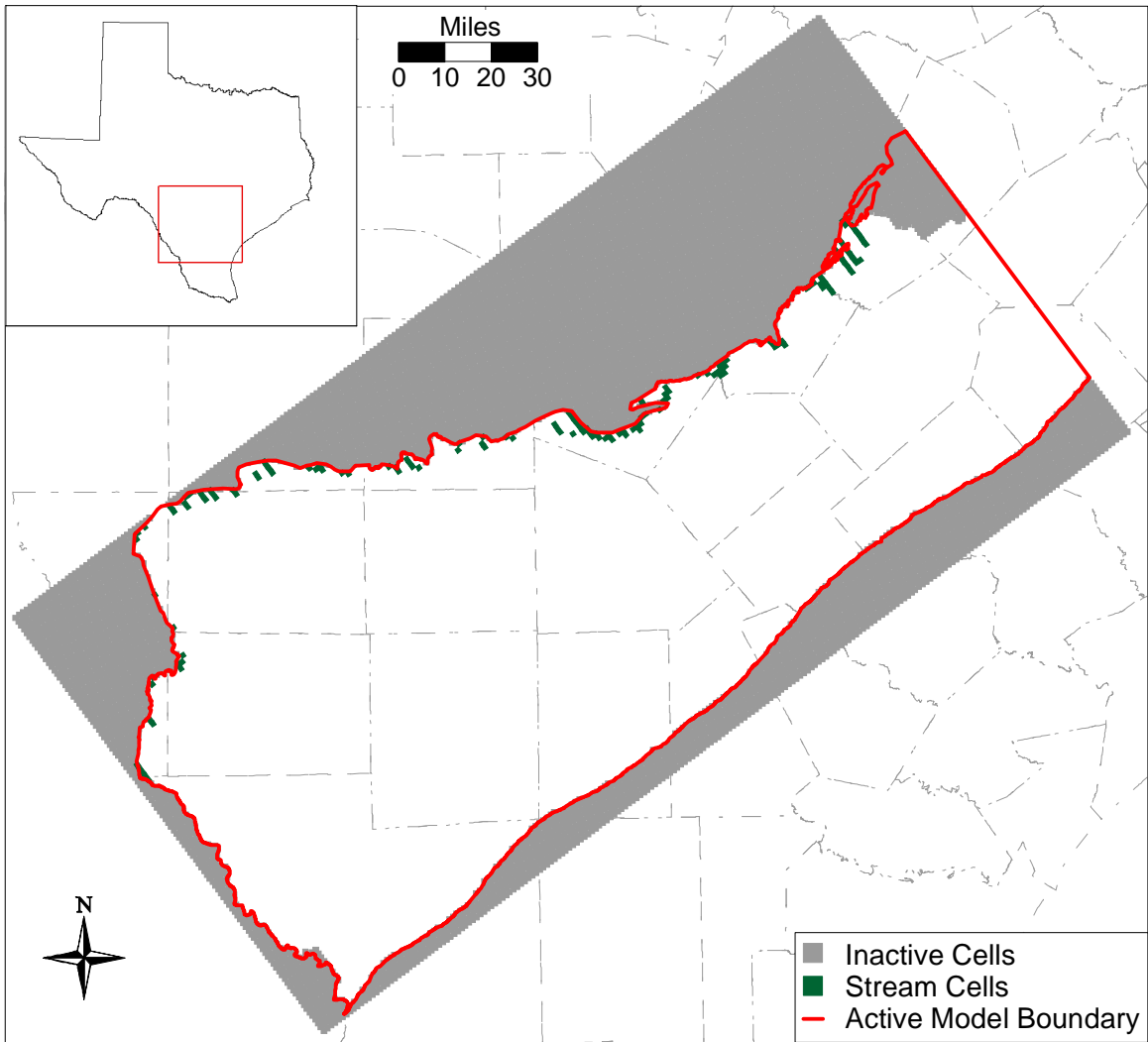


Figure 6.3.6 Layer 6 (lower Wilcox) boundary conditions and active/inactive cells.

6.4 Model Hydraulic Parameters

For the steady state model, the primary parameter to be estimated and distributed across the model grid is hydraulic conductivity. For the transient model, the storage coefficient becomes important. The method used for distributing hydraulic conductivity and storage in the model domain is described in the following.

6.4.1 Hydraulic Conductivity

In the GAM, model properties are constant within a given grid block which is one square mile in area and varies in thickness from a minimum of 20 feet to hundreds of feet. The challenge in constructing a regional model at this scale is in the development of an accurate “effective” hydraulic conductivity that is representative of the grid block scale, and thus represents the different lithologies present in each grid cell. The effective hydraulic conductivity depends on the geometry, hydraulic conductivity, and the correlation scale relative to the grid scale and simulation scale of the various lithologies present in the grid cell (Freeze, 1975).

There have been many investigations on estimating an average effective hydraulic conductivity given assumptions for flow dimension, layer geometry, and correlation scales (Warren and Price, 1961; Gutjahr et al., 1978, Fogg, 1989). For one-dimensional flow in lithologies combined in parallel (i e., layered), the appropriate effective hydraulic conductivity would be the weighted arithmetic mean. For one-dimensional flow in lithologies combined in series, the effective hydraulic conductivity is the harmonic mean. Hydraulic conductivity has been found to be a log-normally distributed parameter. In two-dimensional uniform flow, assuming that the hydraulic conductivity is log-normally distributed and randomly juxtaposed, the effective-hydraulic conductivity is exactly the geometric mean (deMarsily, 1986). Fogg (1989) has studied effective hydraulic conductivity for a model of the Carrizo-Wilcox aquifer in Freestone and Anderson counties in East Texas. His study concluded that for the case when the individual lithologic layers vary in dimension from smaller and larger than the model grid scale, the effective hydraulic conductivity in the horizontal dimension is between the geometric mean and the arithmetic mean. In the vertical dimension, he found that the effective hydraulic conductivity should vary from the geometric to the harmonic mean.

In Section 4.3 we discussed the distribution of hydraulic conductivities available for the Carrizo-Wilcox aquifer in Mace et al. (2000a). Hydraulic parameterization of coastal plain

sediments is often correlated to sand body thickness, geometry, and depositional facies (e.g., Payne, 1975; Henry et al., 1980; Fogg, 1986; Thorkildsen and Price, 1991). From the analysis provided in Section 4.3 of this report, hydraulic conductivity has been distributed within the model regions where data were available. Likewise, sand thickness and sand fraction (%) distributions for the modeled aquifers were developed where data were available. However, as discussed earlier in Section 4.3, correlations between sand thickness (sand fraction) and hydraulic conductivity were not successful.

There are two key assumptions that underlie the method which we used to estimate horizontal and vertical hydraulic conductivity. First, it was assumed that the available transmissivity data, or interpreted hydraulic conductivity data, are representative of the higher permeability strata encountered in the borehole. The higher permeability strata were also assumed to be dominated by a sand lithology. Second, it was assumed that the measured hydraulic conductivities are representative of horizontal hydraulic conductivity, not vertical hydraulic conductivity. Vertical hydraulic conductivity data at a scale representative of this model were not available. Based upon these assumptions, the method we used to distribute horizontal and vertical hydraulic conductivity is discussed below.

The model used the geostatistical analysis (kriging) presented in Section 4.3 as the initial sand hydraulic conductivities for a given block. In areas lacking hydraulic conductivity measurements, we used depositional models, lithofacies zones, and sparse hydraulic data to estimate hydraulic conductivity within zones. Data tends to be biased towards the outcrop and shallow subcrop. Previous investigators have found, both theoretically and empirically, that the hydraulic conductivity of unconsolidated sediments decreases with depth (Helm, 1976; Prudic, 1991). This is thought to be a result of sediment compaction with increased overburden pressure. In the Texas Gulf Coastal Plain, this could also be a result of low-energy depositional environments as one moves downdip towards the depocenter. Regardless, we considered decreasing hydraulic conductivity as a function of overburden when data were not available.

With the sand hydraulic conductivity estimated at the grid scale by kriging, we used the sand fraction to estimate an effective horizontal hydraulic conductivity adjusted for the percent of the formation that is not sand (i.e., silt or clay). That is:

$$K_h \text{ effective} = K_{\text{sand}} \times (\text{net sand } b / \text{layer } b) \quad (6.1)$$

where: K_h effective is the effective grid block horizontal hydraulic conductivity, K_{sand} is the hydraulic conductivity of the sand as interpreted from hydraulic test data and interpolated to the grid scale, net sand b is the net sand thickness in feet in a given layer, and layer b is the total layer thickness. This equation assumes horizontal flow and also assumes that the horizontal hydraulic conductivity of the non-sand lithologies is unimportant to grid-scale horizontal flow relative to the sands. MODFLOW combines total layer thickness (layer b) and the effective horizontal hydraulic conductivity to calculate grid block transmissibilities which govern flow rates within the model. Equation 6.1 above essentially corrects MODFLOW's calculation of transmissibility to account for the lower permeability strata in the individual layers.

As noted in Section 4.3, the model layers had varying amounts of available supporting data for assigning effective horizontal hydraulic conductivity to model grid cells in the layer. The Carrizo layer (Layer 3) had the most data available. The kriged horizontal hydraulic conductivity field shown in Figure 4.3.6 and the percent sand map shown in Figure 4.3.10 were combined using equation 6.1 to yield an effective horizontal hydraulic conductivity field. This field was then sampled at model grid cell centers to yield effective horizontal hydraulic conductivity for each cell.

Data coverage was far less complete for the remaining layers. Effective hydraulic conductivity was estimated for cells in these layers by dividing each layer into large zones of constant effective horizontal hydraulic conductivity, based on "soft" data -- depositional models, lithofacies zones, etc. as noted above. The properties in these zones could then be scaled during calibration if necessary. In the Queen City/El Pico (Layer 1), four main zones were created. The area was divided first by the outcrop and downdip sections, and then further subdivided at the facies change along the Frio River. Note that in the eastern outcrop zone, the effective horizontal hydraulic conductivity varies according to the kriged data shown in Figure 4.3.7. The Bigford/Reklaw (Layer 2) was also subdivided into four zones. The upper Wilcox (Layer 4) was zoned in the southern downdip portion according to net sand maps from Hamlin (1988) and Klemm et al. (1976). Three downdip zones were created based on cuts in sand fraction of 0.33 and 0.66. In the updip portion where the upper Wilcox has pinched out, this layer takes on the properties (and thus zonation) of the middle Wilcox. The middle Wilcox (Layer 5) was divided into three zones. The outcrop was the first zone and it took on the properties from the kriged data shown in Figure 4.3.5. The downdip section was divided into two large zones of constant

effective horizontal hydraulic conductivity, with the expectation that hydraulic conductivity should decrease moving downdip. The lower Wilcox (Layer 6) was divided into three zones. The outcrop was the first zone and it took on the properties from the kriged data shown in Figure 4.3.4. The downdip section was divided into two large zones of constant effective horizontal hydraulic conductivity, based on the net sand map of Bebout et al. (1982). The calibrated conductivity fields with the zonation discussed above are further discussed in Section 8.1 and shown in Figures 8.1.1 through 8.1.6.

Vertical hydraulic conductivity is not measurable on a model grid scale and is therefore generally a calibrated parameter. Typical vertical anisotropy ratios are on the order of 1 to 1000 determined from model applications (Anderson and Woessner, 1992). However, Williamson et al. (1990) reported that vertical resistance to flow could be significant in the Gulf Coast Aquifer system in Texas and Louisiana which is composed of similar types of coastal plain sediments as encountered in the Carrizo-Wilcox aquifer. Previous regional modeling studies in the Carrizo-Wilcox aquifer have documented vertical anisotropy ratios as high as 50,000 (Williamson et al., 1990).

Because vertical hydraulic conductivity of an aquifer is expected to be controlled by depositional environment and lithofacies, we used percent sand, maximum sand, depositional environment, lithofacies, and depth of burial in zoning vertical hydraulic conductivity to the degree practical.

The final calibrated property values (both effective hydraulic conductivity and anisotropy ratio) for each zone can be found in Section 8: Calibration.

6.4.2 Storativity

For unconfined aquifer conditions, the storativity was assigned homogeneously equal to a value of 0.25. Grid cells which represented outcrop (land surface), are modeled as either confined or unconfined depending upon the elevation of the simulated water table in that grid cell. The confined storativity assigned to outcrop cells was one to account for the condition of ponding water on the ground surface and to help prevent non-physical heads from being computed and used in the equations governing groundwater flow.

For confined aquifer conditions, the storativity was calculated as a function of aquifer thickness based upon a constant specific storage of 3×10^{-6} 1/ft. This results in a potential range in storativity from 2×10^{-4} to 2×10^{-3} in the downdip portions of the Carrizo-Wilcox aquifer.

7.0 MODELING APPROACH

In the context of groundwater modeling, model calibration can be defined as the process of producing agreement between model simulated water levels and aquifer discharge, and field measured water levels and aquifer discharge through the adjustment of independent variables (typically hydraulic conductivity, storativity, and recharge). Generally accepted practice for groundwater calibration usually includes performance of a sensitivity analysis and, if the model is going to be used for predictive purposes, a verification analysis. A sensitivity analysis entails a systematic variation of the calibrated parameters and stresses and the re-simulation of the aquifer conditions. Those parameters which strongly change the simulated aquifer heads and discharges would be important parameters to the calibration. It is important to note, that the “one-off” standard sensitivity analysis does not estimate parameter uncertainty as limited parameter space is investigated and parameter correlation is not accounted for. A verification analysis is a test to determine if the model is suitable for use as a predictive tool. This is performed by using the model to predict aquifer conditions during a period which was not used in the model calibration. Consistent with the approach outlined above, we calibrated the model, verified the model, performed sensitivity analyses, and performed predictive simulations.

7.1 Calibration

Groundwater models are inherently non-unique, meaning that multiple combinations of hydraulic parameters and aquifer stresses can reproduce measured aquifer water levels. To reduce the impact of non-uniqueness, we employed a method described by Ritchey and Rumbaugh (1996). This method includes (1) calibrating the model using parameter values (i.e., hydraulic conductivity, storativity, recharge) that are consistent with measured values, (2) calibrating to multiple hydrologic conditions, and (3) using multiple calibration performance measures such as hydraulic heads and discharge rate to assess calibration. Each of these elements is discussed below.

We used measured hydraulic conductivity and storativity data to initially estimate our parameters. The analysis of hydraulic parameters in Section 4.3 of this report indicates that there is a large amount of hydraulic conductivity data that is available for use as initial model values. Vertical hydraulic conductivity is not measurable at the model scale and thus cannot be well

constrained. Storativity is a parameter which is not well defined on the scale of the model. However, storativity is estimated from measured specific storage data in combination with the aquifer thickness. Recharge has not been directly measured in the study area and is arguably not measurable at the model scale. As described earlier in the report, we used SWAT to provide an initial estimate of shallow recharge. Adjustment of all model parameters were held to within plausible ranges based upon the available data and relevant literature. Adjustments to aquifer parameters from initial estimates were minimized to the extent possible to meet the calibration criteria. As a general rule, parameters that have few measurements were adjusted preferentially as compared to properties that have a good supporting database.

The model was calibrated over two time periods, one representing steady-state conditions and the other representing transient conditions. Because the confined section of the Carrizo-Wilcox aquifer in south Texas has been extensively developed since the turn of the century, portions of the aquifer have not been at steady-state conditions through most of the historical record. Therefore, we have chosen to use “predevelopment” conditions as our steady-state model. Section 4.4.1 describes the process used to estimate aquifer water levels for the steady-state predevelopment model. No pumping stresses were applied to the predevelopment model consistent with the assumption of steady-state conditions prior to significant resource development. The transient model was started in 1975 to allow any initialization effects to dampen by 1980, the start of the calibration period. This period from 1975 to 1980 was considered a “ramp up” period, and was not used for calibration. The transient calibration period ran from 1980 through 1989 consistent with the GAM model requirements. The initial heads used for the transient model were based upon 1980 observations (see Section 4.4.4). Section 4.4.4 describes the aquifer water levels and how they were derived to be used for the transient calibration period. Pumping estimates based upon historical records were applied on a monthly time scale in the transient calibration period. Likewise, recharge, stream flow, and reservoir stage were estimated on a monthly time basis and set as input through the transient calibration period. The time period from 1990 until 1999 was used as the verification period to assess the predictive ability of the model. Like the calibration period, transient stresses or boundary conditions were determined on a monthly time step. Unlike the calibration period, parameters were not adjusted in the verification process.

The model was calibrated through a wide range of hydrological conditions. The steady-state predevelopment model represents a period of equilibrium where recharge and aquifer discharge through streams and cross-formational flow are in balance. Under these conditions, the aquifer rejects the maximum amount of recharge and, as was detailed in Section 5, a minimum amount of recharge is expected under stable basin conditions (Freeze, 1971). The steady-state model is sensitive to recharge. The calibration and verification period (1980 through 1999) represents a significantly different period. By this time, portions of the aquifer have been extensively developed resulting in loss of storage and declining heads. Some of the recharge being rejected under steady-state predevelopment conditions may be captured as a result of losing streams and increased vertical gradients. The calibration and verification period also helps constrain the model parameterization because a wide variety of hydrologic conditions are encountered and simulated. The transient model may be sensitive to parameters that are not sensitive parameters for the steady-state model.

Calibration requires development of calibration targets and specification of calibration measures. To address the issue of non-uniqueness, it is best to use as many types of calibration targets as possible. The primary type of calibration target is hydraulic head (water level). However, we also used stream flows and gain-loss estimates. Simulated heads were compared to measured heads at specific observation points through time (hydrographs) and head distributions (maps) for select time periods (see Section 4.4) to ensure that model head distributions are consistent with hydrogeologic interpretations and accepted conceptual models for flow within the aquifer.

Stream calibration targets were derived from two types of data. First, we compared model simulated stream flow rates to observed flow rates at key stream gages in the model area. Because stream flow rates greatly exceed aquifer/stream fluxes for local cells, available gain/loss estimates were also used for the major streams crossing the outcrop.

Traditional calibration measures (Anderson and Woessner, 1992) such as the mean error, the mean absolute error, and the root mean square error quantify the average error in the calibration process. The mean error (ME) is the mean of the differences between measured heads (h_m) and simulated heads (h_s):

$$ME = \frac{1}{n} \sum_{i=1}^n (h_m - h_s)_i \quad (7.1)$$

where n is the number of calibration measurements. The mean absolute error (MAE) is the mean of the absolute value of the differences between measured heads (h_m) and simulated heads (h_s):

$$MAE = \frac{1}{n} \sum_{i=1}^n |(h_m - h_s)_i| \quad (7.2)$$

where n is the number of calibration measurements. The root mean square (RMS) error is the square root of the average of the squared differences between measured heads (h_m) and simulated heads (h_s):

$$RMS = \left[\frac{1}{n} \sum_{i=1}^n (h_m - h_s)_i^2 \right]^{0.5} \quad (7.3)$$

where n is the number of calibration measurements. The difference between the measured hydraulic head and the simulated hydraulic head is termed a residual.

We used the RMS as the basic measure of calibration for heads. The required calibration criterion for heads is an RMS that is equal to or less than 10 percent of the observed head range in the aquifer being simulated. To provide information on model performance with time, the RMS was calculated for the calibration period (1980-1989) and the verification period (1990-1999). The RMS is useful for describing model error on an average basis but, as a single measure, it does not provide insight into spatial trends in the distribution of the residuals.

An examination of the distribution of residuals is necessary to determine if they are randomly distributed over the model grid and not spatially biased. Post plots of head residuals were used to check for spatial bias by indicating the magnitude and direction of mis-match between observed and simulated heads. Simulated head distributions were also compared to the head distributions developed from the field measurements. Finally, scatter plots were used to determine if the head residuals are biased based on the magnitude of the observed head surface.

For streams, the calibration criteria were defined to be within 10% of the measured values where uncertainty in these targets is proven to be acceptable for such a criteria.

7.2 Calibration Target Uncertainty

Calibration targets are uncertain. In order to not “over-calibrate” a model, which is a stated desire for the GAM models, calibration criteria should be defined consistent with the uncertainty in calibration targets. The primary calibration target in groundwater modeling is hydraulic head. Uncertainty in head measurements can be the result of many factors including, measurement error, scale errors, and various types of averaging errors, both spatial and temporal. The calibration criteria for head is an RMS less than or equal to 10% of head variation within the aquifer being modeled. Head differences across the aquifers in the study area are on the order of 400 to 500 feet. This leads to an acceptable RMS of between 40 and 50 feet. We can compare this RMS to an estimate of the head target errors and see what level of calibration the underlying head targets can support.

Measurement errors are typically on the order of tenths of feet, and at the GAM scale can be insignificant. However, measuring point elevation errors can be significant. Our analysis of differences between the reported land-surface datum (LSD) and the ground surface elevation as determined from a digital elevation map determined that the average difference was -5 feet with a standard deviation of 28 feet. Add to this error in averaging ground surface elevations available on a 30 m grid to a one mile grid, and the resulting errors can average 10 to 20 feet and may greatly exceed 20 feet in areas with higher topographic slopes. Additional error is caused by combining multiple lithologies into a single grid block representing one simulated head. Horizontal to vertical hydraulic conductivity ratios have been proven to be high in the Coastal Plain aquifers of Texas (Fogg et al., 1983; Williamson et al., 1990). As a result, significant vertical gradients can occur within individual model layers. Vertical gradients near pumping centers are quite large and approach 0.1 (Williamson et al., 1990). This implies that portions of the aquifer can have head variations within a single model layer on the order of 10 to 50 feet. On average, in areas away from large pumping centers, this scale effect is expected to be on the order of 10 to 20 feet. Horizontal gradients relative to the grid scale also account for an additional one to five feet error with even greater errors near pumping centers. When these errors are added up, the average error in model heads could easily equal our calibration criteria of 40 to 50 feet. The nugget observed on kriged head maps within the modeled aquifers equals from 20 to 30 feet. This nugget captures both uncertainty and variability in the observed heads being rationalized above. Calibrating to RMS values significantly less than 30 feet would

constitute over calibration of the model and parameter adjustments to reach that RMS are not supported by the hydraulic head uncertainty.

7.3 Sensitivity Analyses

A sensitivity analysis was performed on the steady-state and transient calibrated models to determine the impact of changes in a calibrated parameter on the predictions of the calibrated model. A standard “one-off” sensitivity analysis was performed. This means that hydraulic parameters or stresses were adjusted from their calibrated “base case” values one by one while all other hydraulic parameters were unperturbed.

7.4 Predictions

Once the model satisfied the calibration criteria for both the calibration and verification periods, the model was used to make predictive simulations. The predictive simulations have different simulation periods. Simulations were run from 1999 to 2010, 2020, 2030, 2040, and 2050. Average climatic conditions were applied for each predictive simulation with the simulation ending with a drought of record. Stream flow rates and recharge were applied with seasonal variation in the average conditions period. Pumping stresses were based upon the Regional Water Plans as described in Section 4.7 and Appendix C.

8.0 STEADY-STATE MODEL

The steady-state model is representative of predevelopment conditions. In predevelopment, aquifer inflow from recharge and streams is balanced by groundwater to surface-water discharge and cross-formational flow from the Carrizo-Wilcox aquifer upwards to the younger overlying units. This section provides the details of the calibration of the steady-state model and presents the steady-state model results. This section also describes the results of a sensitivity analysis identifying the model parameters to which the steady-state model calibration is most sensitive.

8.1 Calibration

As was discussed in Section 7, calibration is the process of adjusting model parameters to produce agreement between model simulated water levels and aquifer discharges and measured water levels and aquifer discharges. The calibration process for the steady-state model is described below.

8.1.1 Horizontal and Vertical Hydraulic Conductivities

Section 6.4.1 describes the determination of initial horizontal and vertical hydraulic conductivities for the model. Figures 8.1.1-8.1.6 show the final calibrated effective horizontal hydraulic conductivity fields for the steady-state model. Table 8.1.1 includes the calibrated range of horizontal hydraulic conductivity for each model layer. The horizontal hydraulic conductivities did not require modification from their initial estimates. Queen City (Layer 1) heads were relatively insensitive to changes in horizontal hydraulic conductivity, partially due to the general head boundary that is attached to this layer in the downdip (confined) section. This insensitivity is also the result of the large number of stream cells which act as head boundaries in the Queen City/El Pico outcrop. The Reklaw and Bigford formations (Layer 2) are aquitards in the model area and as a result horizontal hydraulic conductivity had little importance for flow. The Carrizo (Layer 3) has relatively good data coverage for horizontal hydraulic conductivity based upon aquifer tests. We did not have to alter this initial distribution to calibrate. The Wilcox Group (Layers 4-6) lacked significant targets, and horizontal hydraulic conductivity in these layers did not affect heads in the Carrizo, or the model in general, to a significant degree.

Table 8.1.1 shows the calibrated anisotropy ratios (K_h/K_v) for the steady-state model. Downdip heads in the Carrizo (Layer 3) were sensitive to the vertical hydraulic conductivity in the Reklaw (Layer 2, east of the Frio River), due to the change in head gradient across the Reklaw. This sensitivity was consistent with the conceptual model which predicts that groundwater in the Carrizo discharges through cross-formational flow across the Reklaw to the Queen City Formation in the downdip confined portions of the aquifer. Decreasing the vertical hydraulic conductivity of the Reklaw resulted in less groundwater discharge across the Reklaw. The decreased discharge results in increased heads in the downdip portions of the Carrizo.

The anisotropy ratio for the Bigford Formation (Layer 2, west of the Frio River) had much less effect on downdip heads in the Carrizo than did the ratio for the Reklaw east of the Frio River. This difference could result from the fact that lateral downdip flow in the Carrizo extends over a much larger model area in the west than in the east, providing greater surface area for cross-formational flow in the west relative to the east. Hamlin (1988) noted that, as a result of the dip of the Carrizo-Wilcox aquifer, the bad water line encroaches much closer to the outcrop in the eastern model area than in the west. The steady-state model was also insensitive to changes in the anisotropy ratio in the Wilcox layers. This is likely because the Wilcox head targets were confined to the outcrop portions of the model with no predevelopment downdip targets available in these layers. For these reasons, the steady-state model could be calibrated with several different anisotropy ratios for the Bigford Formation and the Wilcox Group.

As a result of the steady-state model's insensitivity to vertical hydraulic conductivity in the Bigford and the Wilcox, these parameters are poorly constrained by the steady-state model. Our initial estimates of anisotropy for these formations during steady-state model calibration were much lower than the final calibrated values. For example, our initial estimate of vertical anisotropy for the Bigford Formation was 300, while the value after transient calibration (and steady-state recalibration) was 10,000. The initial estimate of anisotropy for the upper Wilcox was 100, while the final value after transient calibration was 1,000. These examples illustrate the value of calibrating to multiple hydrologic conditions as discussed in Section 7. We were able to greatly improve the uniqueness of the calibrated parameters by iteratively calibrating between steady-state and transient models.

8.1.2 Recharge

Recharge estimates were based upon forward simulations using SWAT for the time period 1975 through 1999 (see Section 6.3.4). For the steady-state model, recharge was input as an average recharge rate estimated over the transient simulation period. Some modifications were required to the recharge estimates calculated from SWAT. The transient recharge results were adjusted slightly from the SWAT outputs in the eastern model region, due to anomalously high recharge rates estimated by SWAT in this area (Section 9.1). In the steady-state model, recharge was reduced at a few outcrop cells where heads were rising significantly above ground surface. These cells usually had the combined characteristics of high recharge and low hydraulic conductivity or they were thin edge cells with no flow boundaries both below and to the east or west. Figure 8.1.7 shows a histogram comparison of steady-state recharge, before and after calibration. Note that the number of high values of recharge is reduced. The median recharge rate decreased from 0.64 inches per year to 0.51 inches per year. Figure 8.1.8 shows a post plot of the calibrated recharge rates over the modeled outcrop. The spatial variation of recharge did not change significantly during steady-state calibration. In general, Figure 8.1.8 shows recharge increasing from the western portion of the model to the eastern portion. This trend is consistent with the overall trend of increasing precipitation from the west to the east across the model area.

The steady-state model is sensitive to recharge for two reasons: (1) recharge is the primary input source for water and (2) the model is at steady-state where inflow balances outflow with no change in storage or time dependence. In a transient model, recharge to the outcrop can be added to storage over decades without significantly affecting downdip heads. In a steady-state model, where there is no net change in storage, a balance must be found between the input recharge and all other flows in the model. This implies that the behavior of the whole model will be sensitive to the input recharge rate. We believe that SWAT performed well in generating an overall average recharge distribution for the Southern Carrizo-Wilcox GAM because we had to make only minor adjustments to recharge during calibration of the steady-state model.

8.1.3 Groundwater Evapotranspiration

Steady-state groundwater evapotranspiration (ET) was averaged from SWAT transient results and applied as ET maximum in the MODFLOW ET package (see Section 6.3.4). Naturally, ET occurs above the ground surface, within the vadose zone, and within the saturated

zone. Note that the ET maximum taken from SWAT and applied in MODFLOW is groundwater ET, not vadose zone ET (which was already considered in the SWAT recharge results). Appendix E provides further details regarding the application of SWAT with MODFLOW. The maximum rooting depths were taken from the SWAT results and input as the extinction depth in the MODFLOW ET package. The ET surface was set to ground surface, so groundwater ET varied linearly starting from a maximum at ground surface and going down to the root depth. These parameters were fixed during calibration. Figure 8.1.9 shows how the average groundwater ET maximum varies across the model region. The median groundwater ET maximum for the region was 1.2 inches/year. The median rooting depth for the region was 6 feet.

The ET package in MODFLOW added considerable instability to the steady-state model. A model that would previously converge in several minutes without the ET package, would either take much longer or diverge completely when ET was activated. The final calibrated model with ET has a relatively slow convergence for a steady-state model, but is stable for the calibrated parameter set.

8.1.4 General Head Boundaries

The heads assigned to the general head boundaries (GHBs) were estimated from the surficial water table (Section 6.3.2). The initial hydraulic conductances of the GHBs were estimated from the vertical conductivities of the LBG-Guyton and HDR (1998) model “Younger” layers. Heads in the El Pico/Queen City Formation (Layer 1) were very sensitive to the conductance of the GHBs. The heads in the El Pico/Queen City Formation affect the gradient across the Reklaw Formation (Layer 2) to the underlying Carrizo, and therefore affect heads in the Carrizo. As a result, conductance of the GHBs was significant to steady-state calibration in Layers 1 and 3. Figure 8.1.10 shows the conductances for the calibrated GHBs. During calibration, hydraulic conductances of the GHBs were adjusted from their initial estimates by decreasing the conductance west of the Frio River, and slightly increasing the conductance east of the Frio River. These changes are in agreement with the adjustments made to the vertical hydraulic conductivity of Layer 2, where vertical hydraulic conductivity in the Bigford Formation (west of the Frio River) was decreased relative to the vertical hydraulic conductivity of the Reklaw Formation (east of the Frio River). In the process of calibration, heads in the Queen City/El Pico were calibrated through adjustments to the GHBs. When

satisfactory heads were simulated, the vertical hydraulic conductivity of the Reklaw was varied until heads in the Carrizo were close to calibration. Modifications to the GHB conductance and the Reklaw vertical conductivity were made iteratively until the gradient across the Reklaw was matched.

8.1.5 Streams

Our initial approach for the estimation of streambed conductance was to calculate them based upon the hydraulic conductivity of the underlying formation. However, we had some difficulty with this approach because the stream segments could cross multiple outcrops, and the conductivities within the outcrops were widely varying. To simplify the initial estimates, we set a constant streambed conductivity of 1 ft/day and let the overall streambed conductance vary with the streambed width as specified in the EPA RF1 dataset (Section 6.3.3). During the initial steady-state calibration, the streambed conductances were decreased in the western portion of the model (including the Rio Grande, Nueces, and Frio rivers) in order to match heads in the Carrizo outcrop. This resulted in heads increasing in the outcrop with water exiting less freely from the unconfined section to the streams. However, after transient calibration the vertical hydraulic conductivity of the Bigford Formation (Layer 2, west of the Frio River) was decreased (Section 8.1.1 above), increasing heads in the Carrizo and necessitating a return to the original streambed conductivities. Therefore in the final calibration, the streambed conductivities were not modified from their initial estimates.

Table 8.1.1 Calibrated hydraulic conductivity values for the steady-state model (ft/day).

Horizontal Hydraulic Conductivity (ft/day)	Outcrop		Downdip	
	<i>West of Frio River</i>	<i>East of Frio River</i>	<i>West of Frio River</i>	<i>East of Frio River</i>
El Pico / Queen City	0.5	1 – 30*	0.5	2
Bigford / Reklaw	2	3	2	1
Carrizo	0.3 – 100*			
Upper Wilcox	--		0.3 – 3	
Middle Wilcox	1 – 30*		0.3 - 1	
Lower Wilcox	1 – 30*		1 - 3	
Anisotropy (Kh/Kv)				
El Pico / Queen City	30	30	300	30
Bigford / Reklaw	10000	1000	10000	1000
Carrizo	30			
Upper Wilcox	--		1000	
Middle Wilcox	10000			
Lower Wilcox	3000			

* These ranges are approximate – the Kh in these areas was kriged from well tests. Please see Figure 8.1.1 - 8.1.6 for specific values.

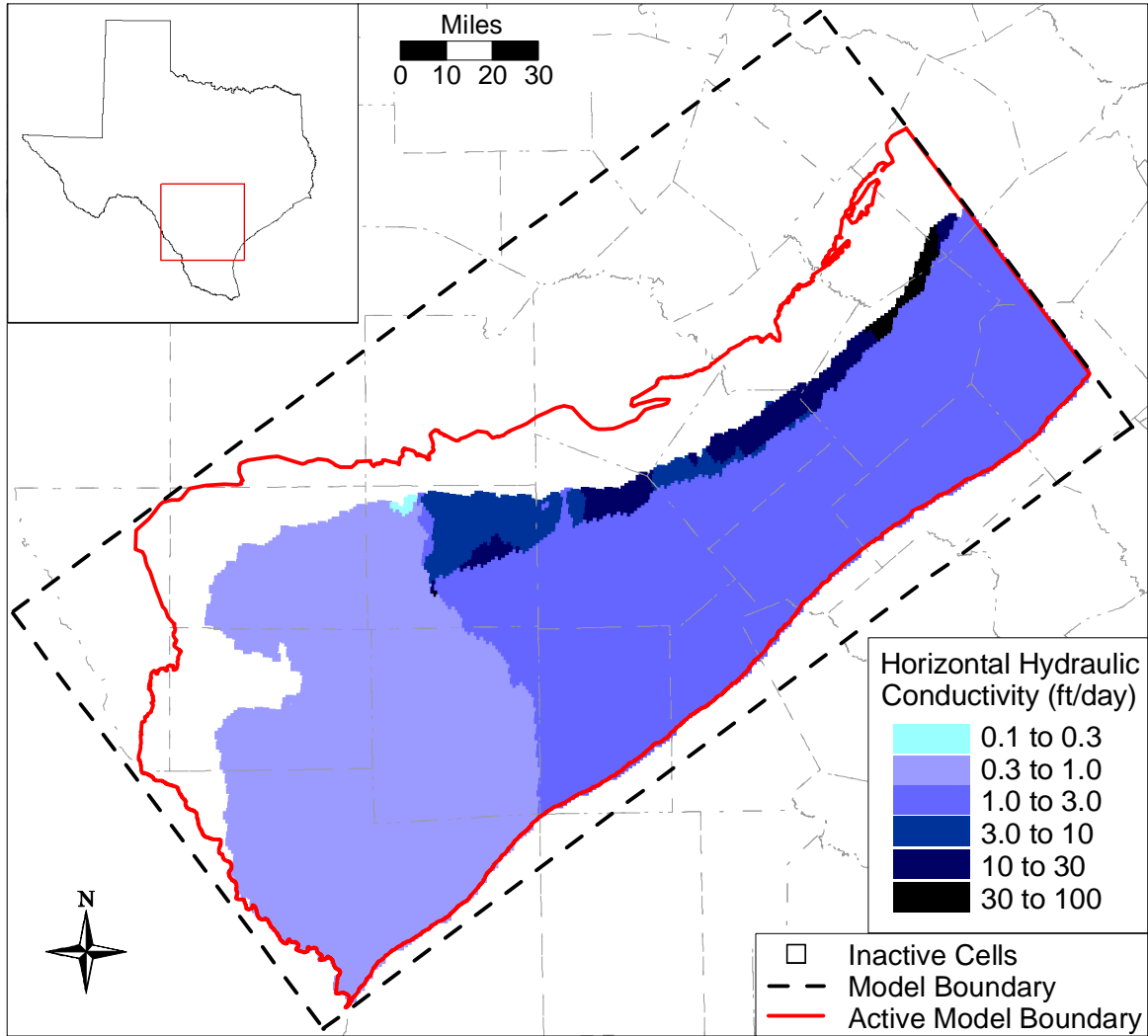


Figure 8.1.1 Calibrated horizontal hydraulic conductivity field for the El Pico/Queen City (Layer 1).

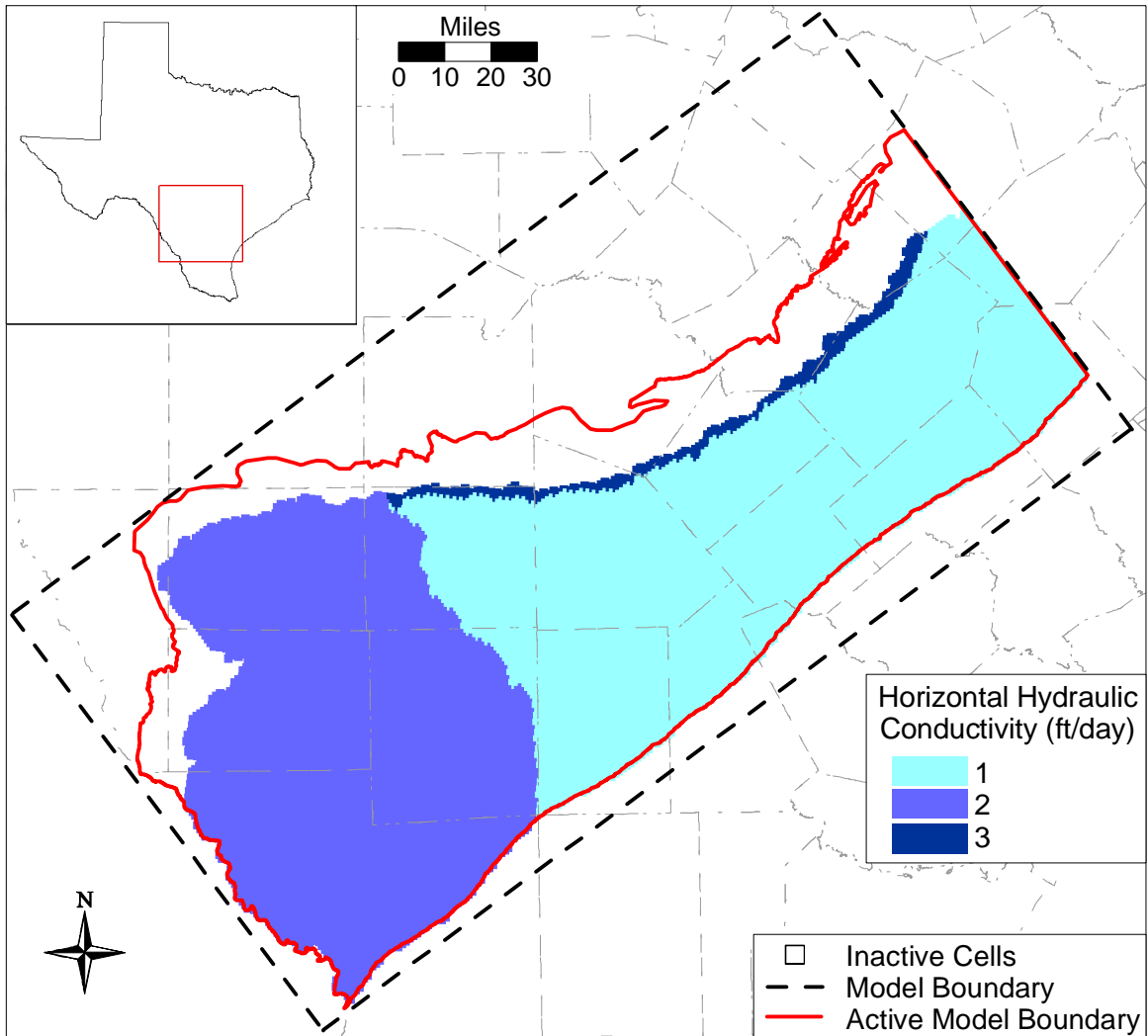


Figure 8.1.2 Calibrated horizontal hydraulic conductivity field for Bigford/Reklaw (Layer 2).

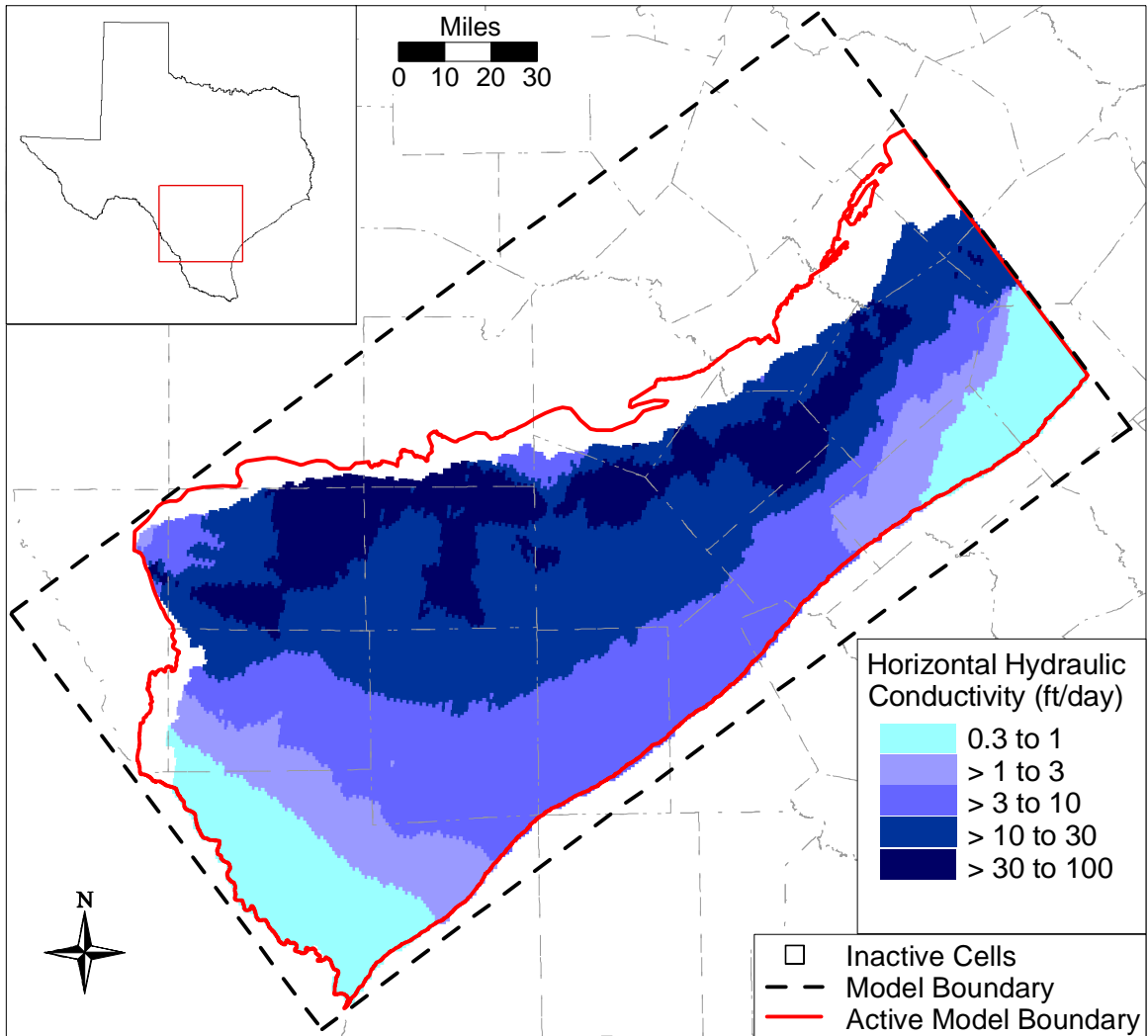


Figure 8.1.3 Calibrated horizontal hydraulic conductivity field for the Carrizo (Layer 3).

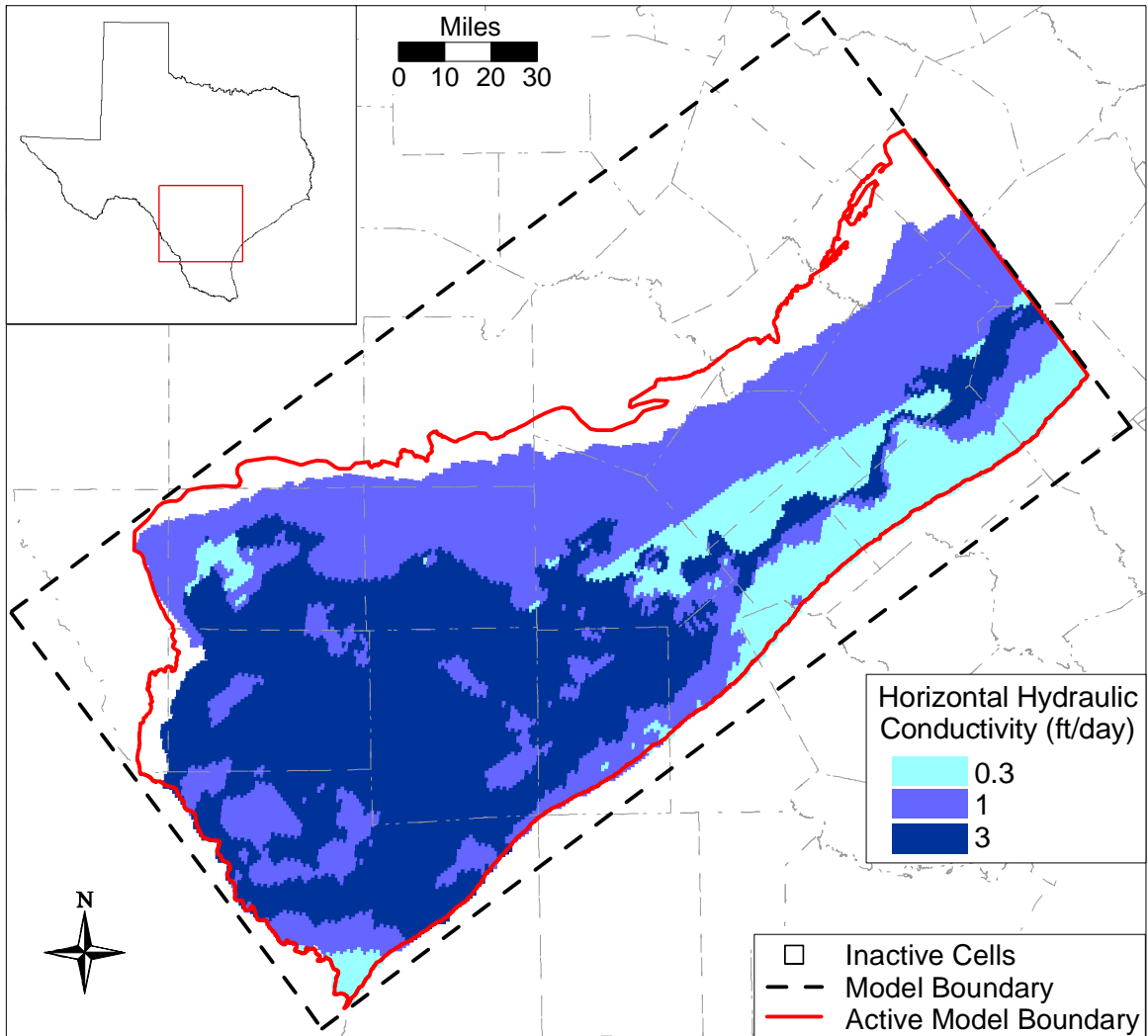


Figure 8.1.4 Calibrated horizontal hydraulic conductivity field for the upper Wilcox (Layer 4).

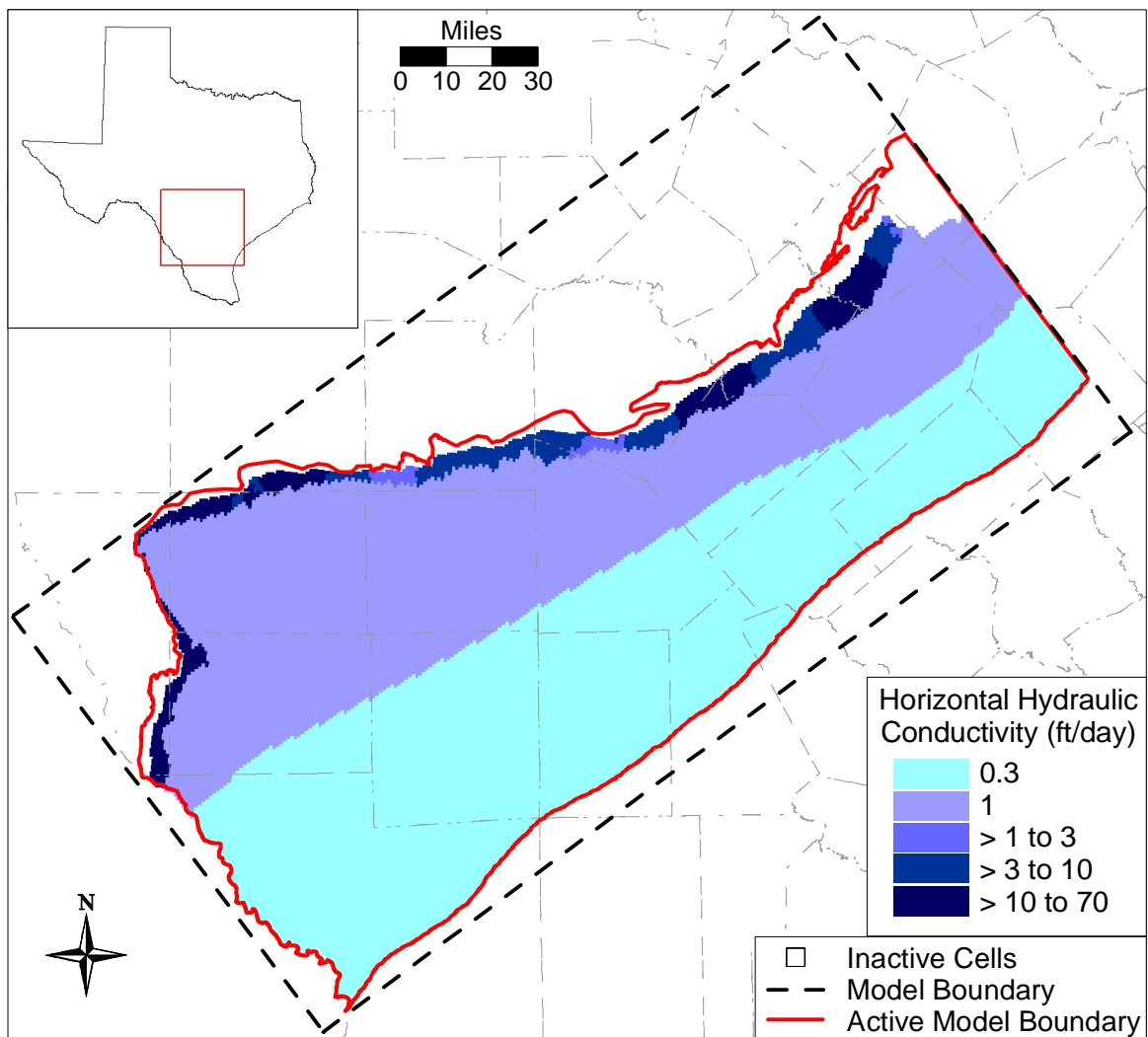


Figure 8.1.5 Calibrated horizontal hydraulic conductivity field for middle Wilcox (Layer 5).

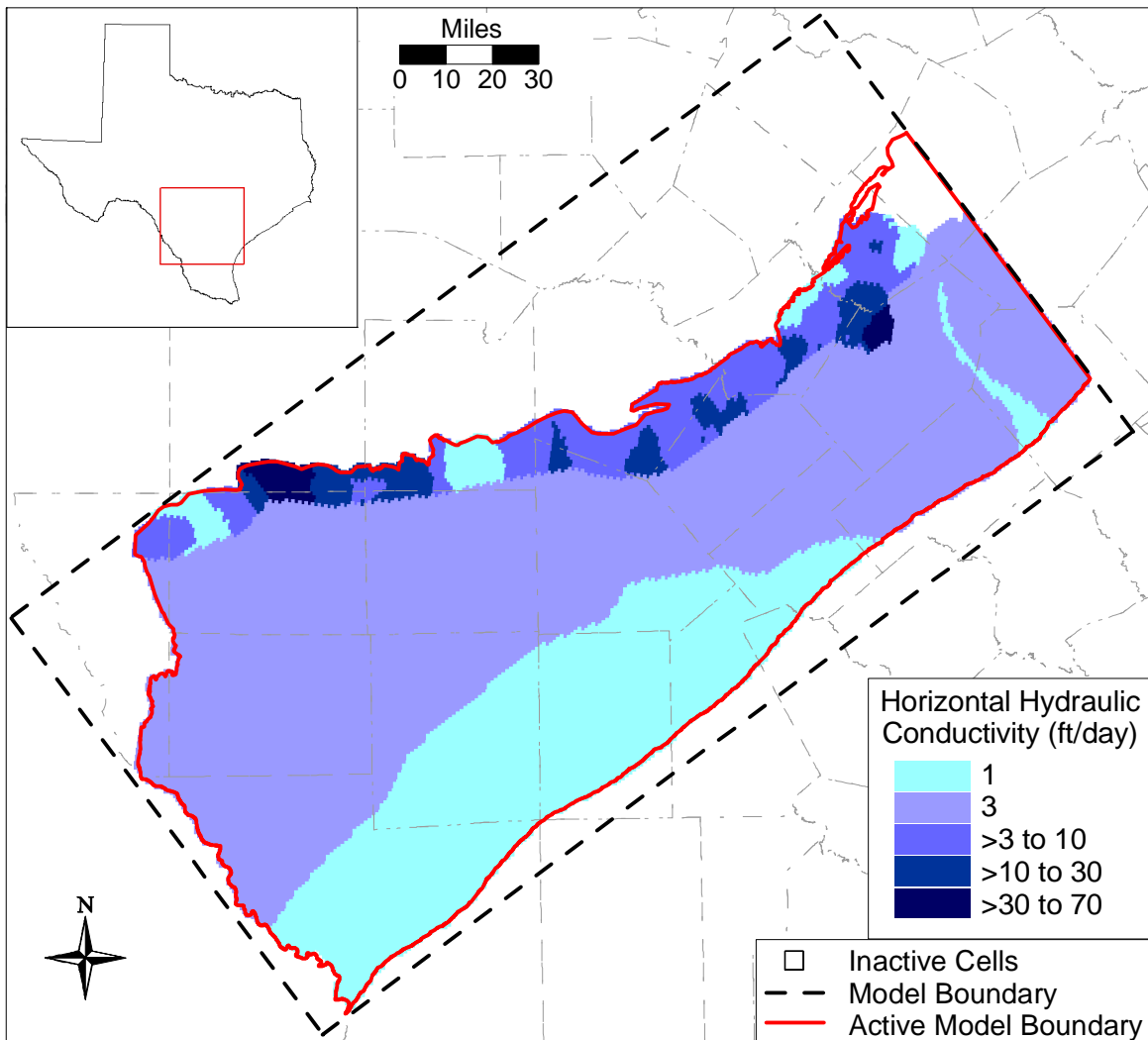


Figure 8.1.6 Calibrated horizontal hydraulic conductivity field for the lower Wilcox (Layer 6).

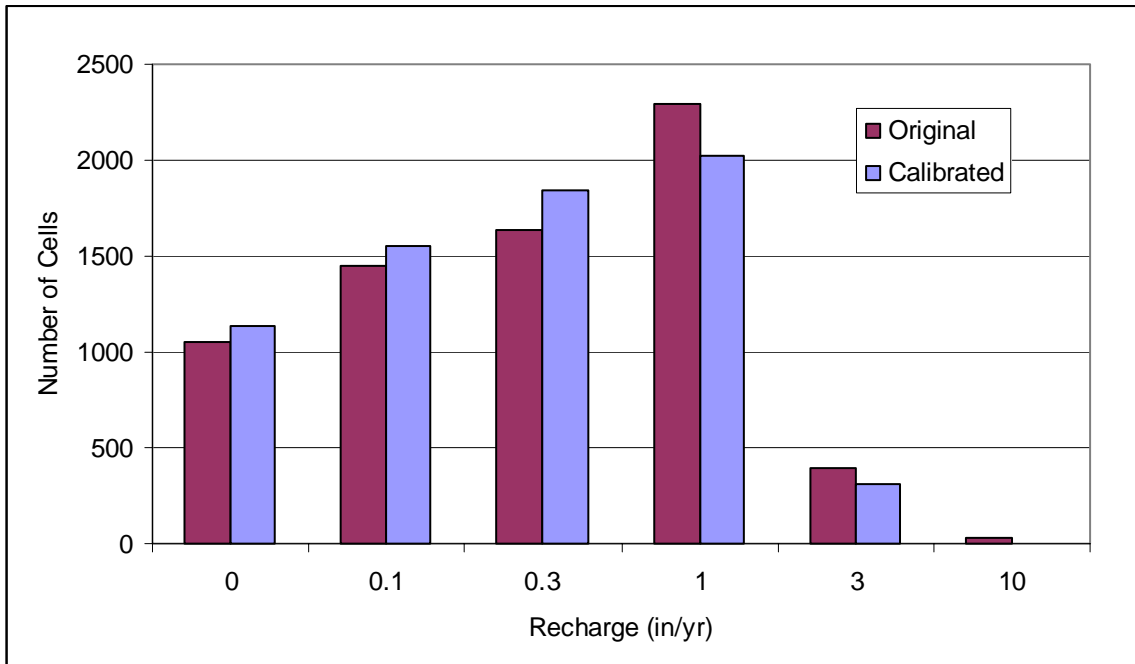


Figure 8.1.7 Comparison between initial recharge and the calibrated recharge.

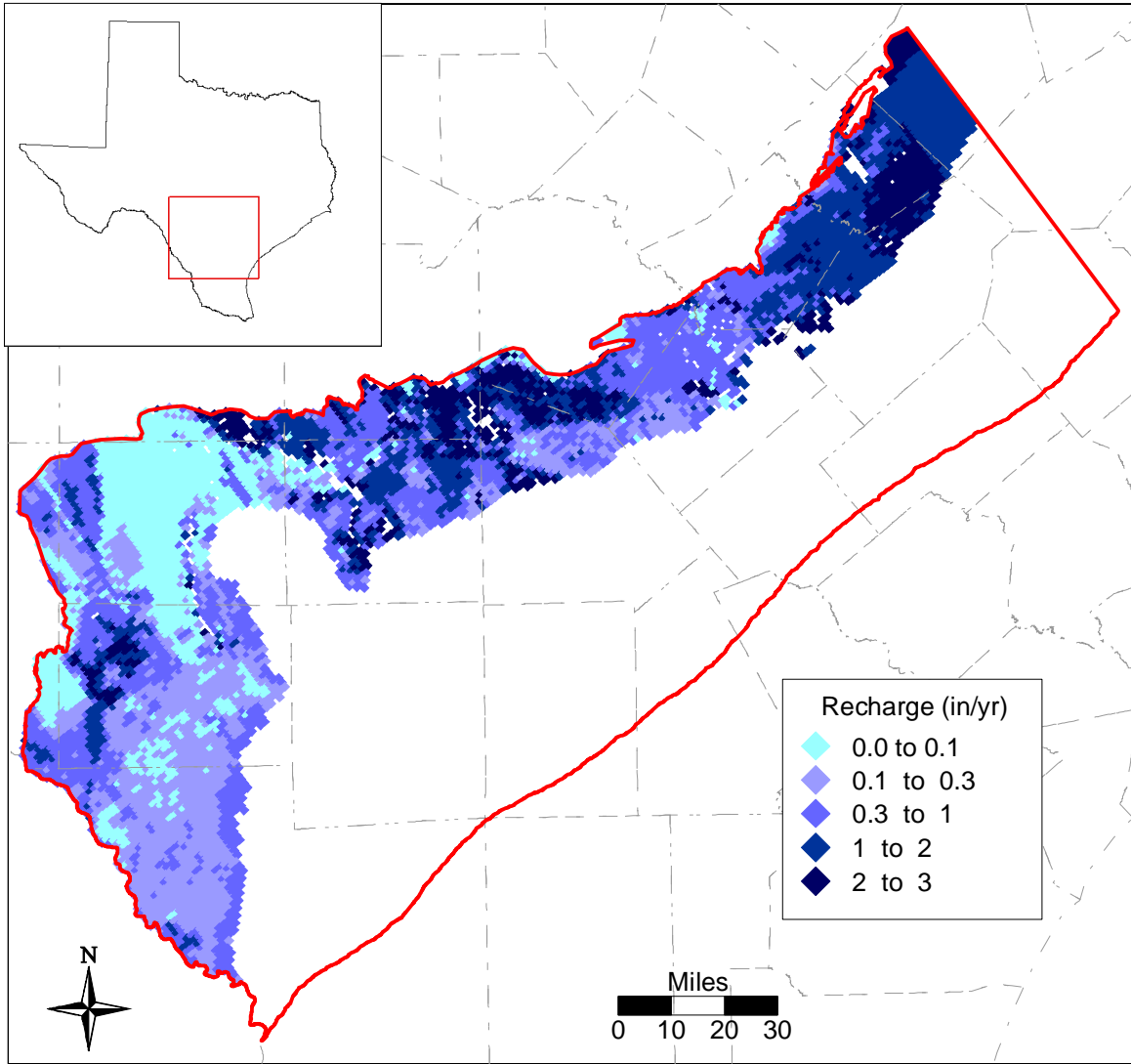


Figure 8.1.8 Steady-state calibrated recharge (in/year).

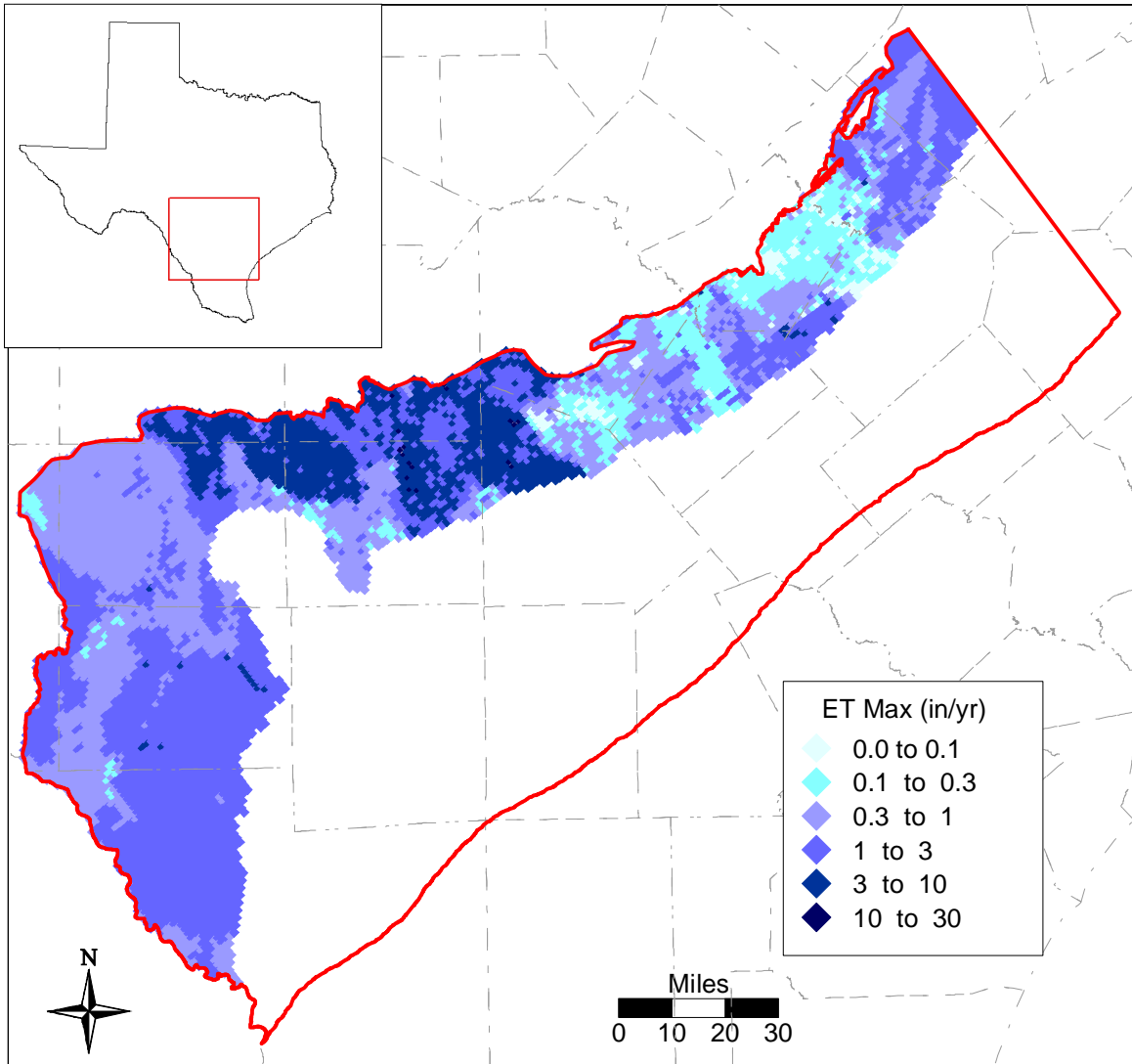


Figure 8.1.9 Steady-state groundwater ET maximum (in/yr).

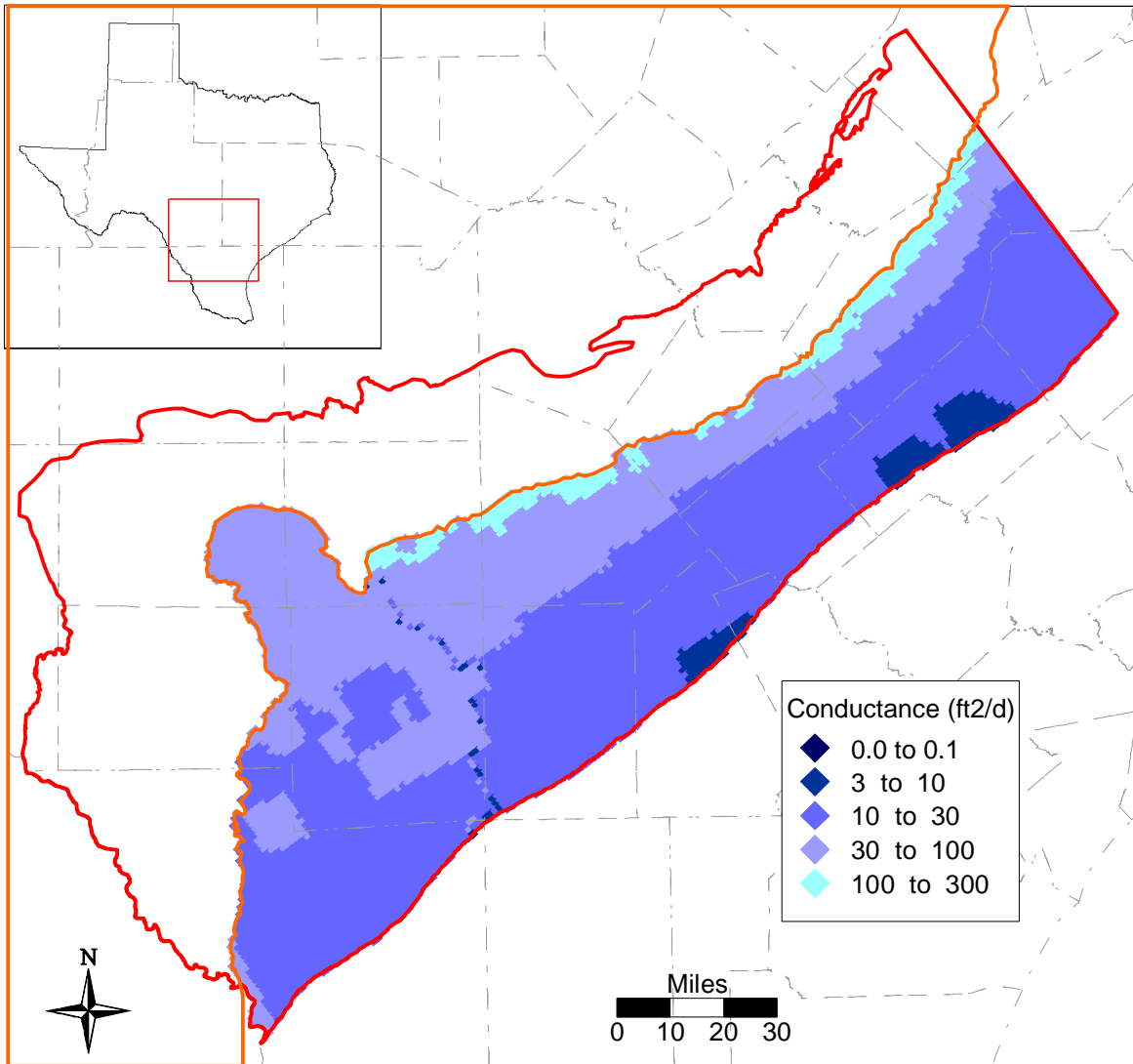


Figure 8.1.10 Steady-state calibrated GHB conductance.

8.2 Results

Steady-state model results are discussed in this section in terms of heads, stream flows, and the model water budget.

8.2.1 Heads

Figures 8.2.1-8.2.7 show the head surface results for the calibrated steady-state model. The residuals are plotted on the same figures, where residuals are defined as:

$$residual = head_{measured} - head_{simulated} \quad (8.1)$$

The RMS (Equation 7.3) for Layer 1 (Queen City/El Pico) in the steady-state model is 34.5 ft. The head range in this layer was 306 ft, giving an RMS/range of 0.11. The RMS in Layer 3 (Carrizo) was 26.9 ft and the range in head was 353.4 ft, giving an RMS/range of 0.076. The head calibration statistics are summarized in the Table 8.2.1.

Table 8.2.1 Steady-state head calibration statistics.

Layer	Count	ME (ft)	MAE (ft)	RMS (ft)	Range (ft)	RMS/Range
1	30	8.6	28.6	34.6	306.6	0.11
3	23	6.9	19.7	26.9	353.4	0.076

Figures 8.2.1 and 8.2.3 support these statistics where slightly more variation is evident in the scatter plot (Figure 8.2.1) for Layer 1 than in the scatter plot (Figure 8.2.3) for Layer 3. The scatter plots show a good distribution of residuals around zero. Figure 8.2.4 shows a comparison of the simulated steady-state Carrizo head surface and the estimated predevelopment Carrizo-Wilcox head surface (Section 4.4.1). Note that statistics could not be calculated for layers 2, 4, 5, and 6 where only one or two predevelopment targets were available. The simulated head surface for the Reklaw/Bigford (Layer 2) is included in Figure 8.2.2. The simulated head surfaces for the upper, middle, and lower Wilcox layers are included in Figures 8.2.5-8.2.7.

The Carrizo head surface in Figure 8.2.3 indicates that the gradient in the steady-state model is mostly east-southeast, moving downdip consistent with the observed heads. In the eastern portion of the model, there is a depression in the head surface in Gonzales County. This depression is considered the result of a large number of streams running through that area. The

Wilcox layers show similar trends in head distribution to the Carrizo (Figures 8.2.5 – 8.2.7), with gradients decreasing in the lower Wilcox layers. Heads increase in the lower layers for a given horizontal location, indicating an upward gradient in the downdip portion of the model. This upward gradient is consistent with the conceptual model discussed in Section 5.

Some cells went dry in the steady-state simulation. The rewetting option was not used in the steady-state, because it was unstable when combined with the ET package. Out of 6,892 outcrop cells, 259 were dry, or 3.7%. These dry cells can be indicative of model instability or actual subsurface conditions. Because no obvious discontinuities exist in the model predicted outcrop water table, these cells are likely indicative of actual subsurface conditions (i.e., small cell thickness, low water table). The small number of dry cells does not have a significant impact on model results.

8.2.2 Streams

We have no defined calibration targets for the streams for the predevelopment model because no gain/loss estimates are available for the modeled streams in the applicable time period (turn of the century or before). Based upon historical occurrence of flowing wells across the model area, intuitively we would expect the major streams to be gaining. This is consistent with the analysis performed in LBG-Guyton and HDR (1998).

Figure 8.2.8 shows the gain/loss values for the stream reaches in the steady-state model. As would be expected, the larger stream segments are more likely to be gaining than the smaller tributaries which are typically higher in shallower channels and higher in overall elevation. The streams in the eastern portion of the model are more gaining than those in the west, partially due to the higher amount of recharge in that region and the shallower water table.

8.2.3 Water Budget

Table 8.2.2 summarizes the water budget for the model. The mass balance error for the steady-state model was 0.71 percent. As would be expected, the predominant input source is recharge. Water discharging from the model is split between the streams, ET, and the GHBs in descending order. Groundwater ET removes about 36% of the recharge that goes into the model under predevelopment conditions. The majority of the water exiting the Carrizo leaves by cross-formational flow through the bottom of the Reklaw Formation which is consistent with our conceptual model detailed in Section 5. This rate is approximately equal to that leaving the

Reklaw through the top, and is also similar to the rate exiting Layer 1 through the GHBs. This indicates that most of the water that is flowing in the Carrizo in the confined section exits upward through the Reklaw and Queen City formations. Also, the Carrizo has groundwater flowing in through the bottom of the formation, although it is small in comparison to the amount coming in through recharge. The accuracy of this component of flow into the Carrizo from below is unknown because there were very few Wilcox wells in the confined section in historical times. However, it is hydraulically correct that flow is diverted towards higher permeability layers from less permeable layers.

Table 8.2.3 gives the various sources and sinks as percentages of the total water entering or leaving the model. The highest percentage of recharge occurs in the Queen City, due to its large outcrop. The highest percentage of ET occurs in this same layer, for the same reason. Recharge makes up 87% of the inflow to the model, with streams contributing 11%. Forty-three percent of the water leaving the aquifer exits through the streams, while 31% and 27% exit through groundwater ET and GHBs, respectively. Approximately two-thirds of the water that enters the model through recharge and losing streams ends up moving downdip and exiting the Carrizo-Wilcox via cross-formational flow.

In Atascosa County there is a study that allows us to check the Carrizo flow rates from the outcrop to the confined section. Pearson and White (1967) performed a groundwater age dating study in Atascosa County using Carbon-14 age dating techniques. Figure 8.2.9 shows their estimate of groundwater travel times from the outcrop to the confined section. Also included in Figure 8.2.9 is a particle track from the steady-state model run for 20,000 years. The model travel path and time of travel shows good agreement with the results of Pearson and White (1967) providing a good validation measure for flow in that portion of the model. Consistent with our conceptual model, the particle moves from the Carrizo and into the Reklaw in southern Atascosa County.

Table 8.2.2 Water budget for the steady-state model (AFY).

IN	Layer	GHBs	Recharge	Streams	Top	Bottom
	1	7,892	125,096	16,681		95,491
	2		37,677	11,341	18,610	99,316
	3		71,137	6,544	30,852	23,118
	4		893	105	9,350	16,390
	5		58,061	3,922	1,981	19,841
	6		33,852	3,607	8,683	
	Sum	7,892	326,716	42,199	69,477	254,156
OUT						
OUT	Layer					
	1	100,523	57,496	68,937		18,610
	2		17,958	22,757	95,491	30,852
	3		7,200	17,256	99,316	9,350
	4		896	935	23,118	1,981
	5		19,934	38,736	16,390	8,683
	6		14,054	12,810	19,841	
	Sum	100,523	117,539	161,431	254,156	69,477

Table 8.2.3 Water budget for the steady-state model with values expressed as a percentage of inflow or outflow.

IN	Layer	GHBs	Recharge	Streams
	1	2.1	33.2	4.4
	2		10.0	3.0
	3		18.9	1.7
	4		0.2	0.0
	5		15.4	1.0
	6		9.0	1.0
	Sum	2.1	86.7	11.2

OUT	Layer	GHBs	ET	Streams
	1	26.5	15.2	18.2
	2		4.7	6.0
	3		1.9	4.5
	4		0.2	0.2
	5		5.3	10.2
	6		3.7	3.4
	Sum	26.5	31.0	42.5

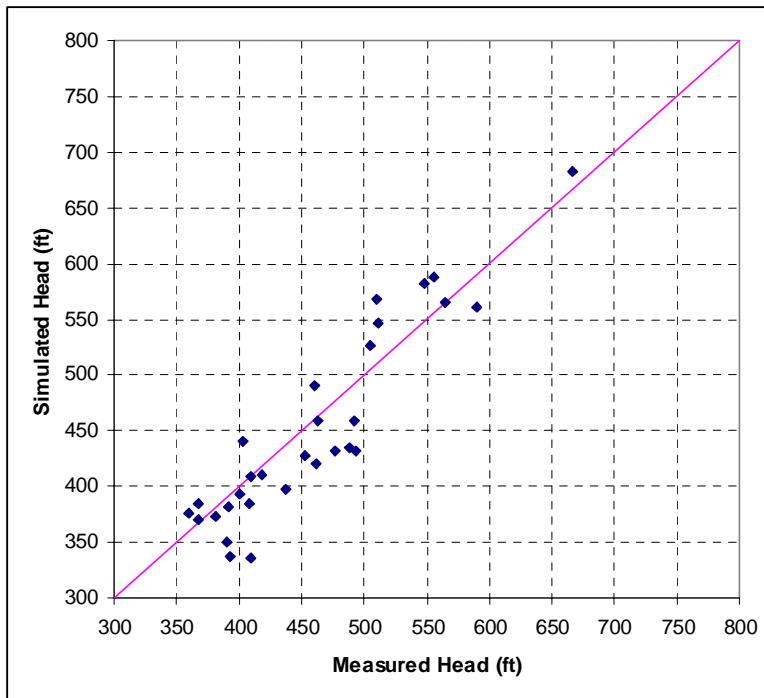
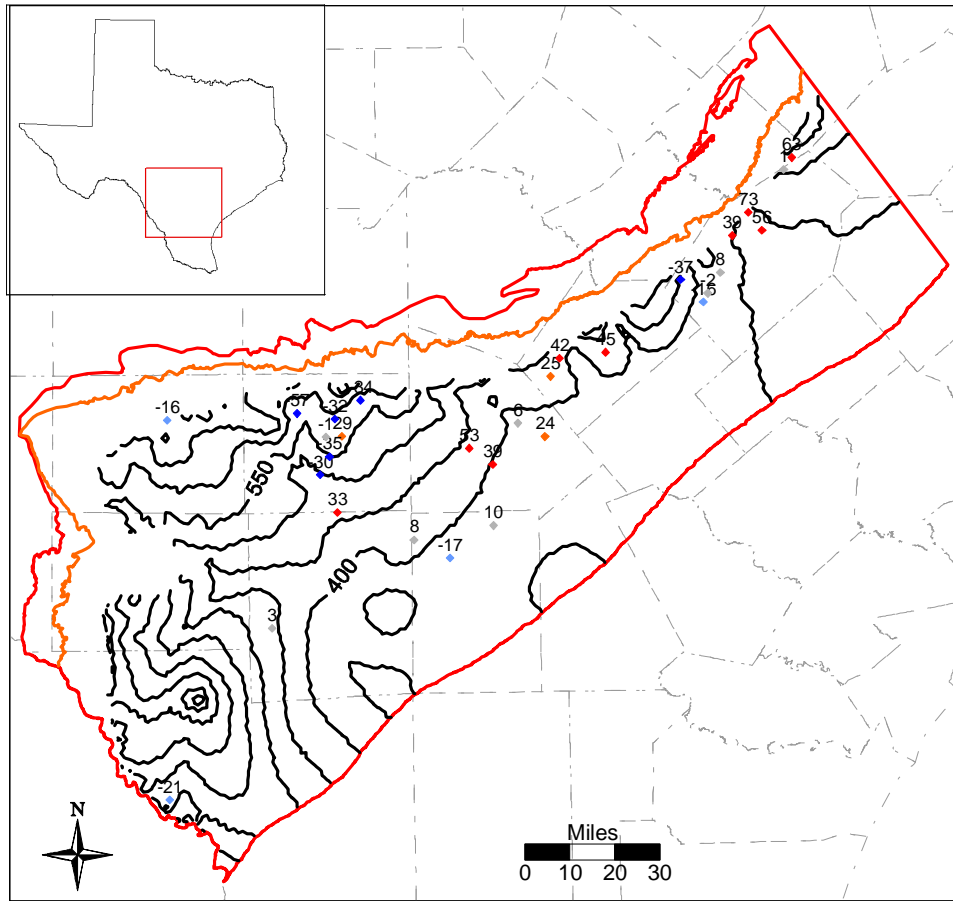


Figure 8.2.1 Simulated steady-state head surface, residuals and scatterplot for the Queen City/El Pico (Layer 1).

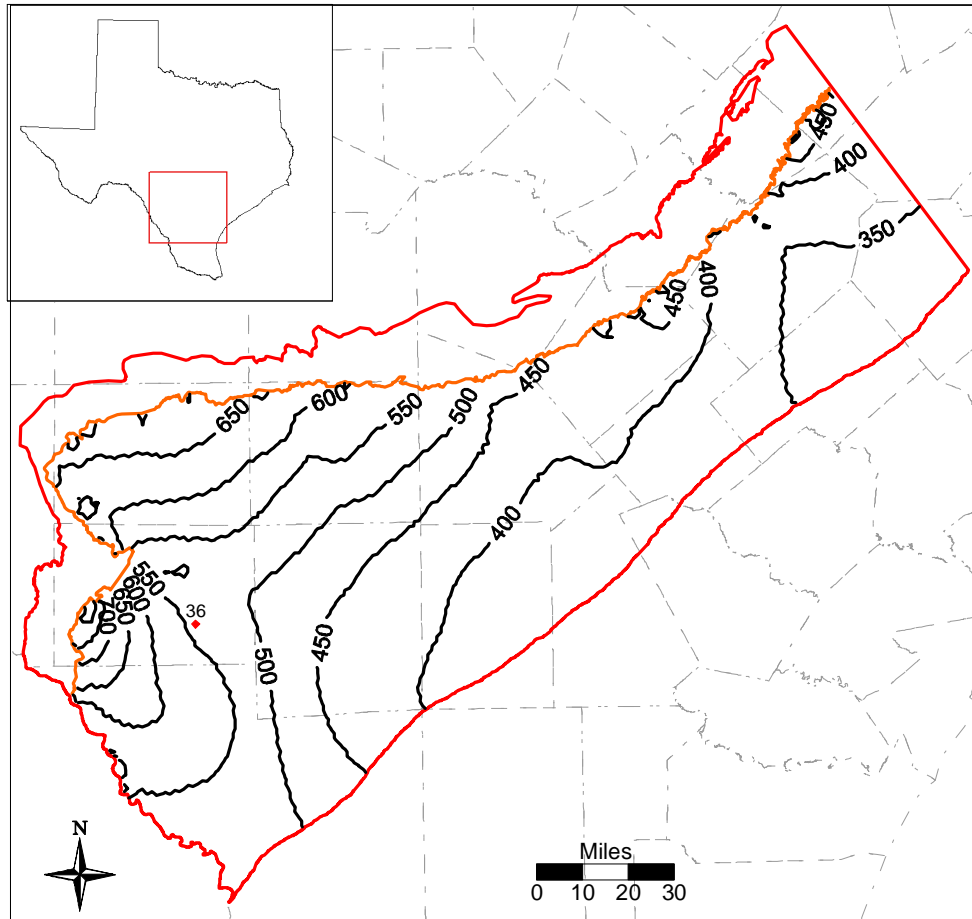


Figure 8.2.2 Simulated steady-state head surface and posted residuals for the Reklaw/Bigford (Layer 2).

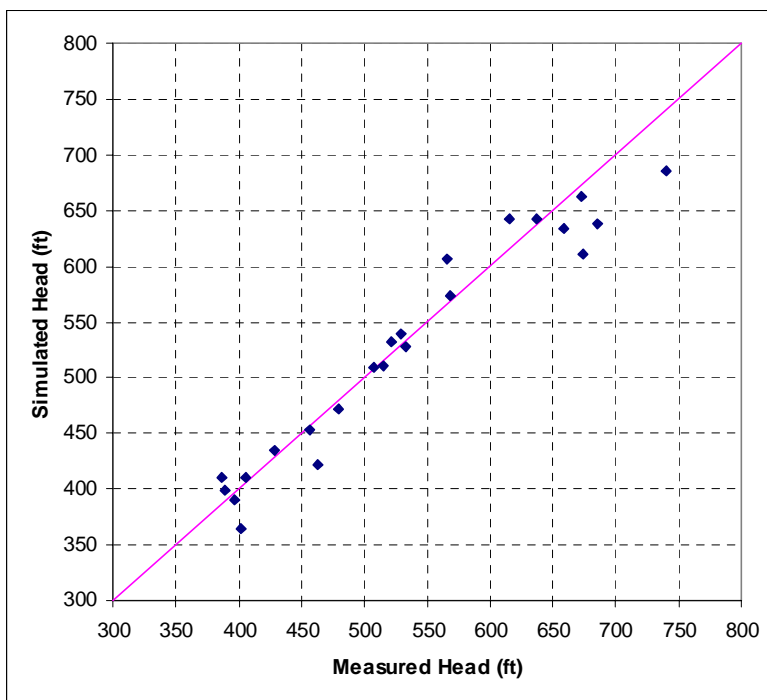
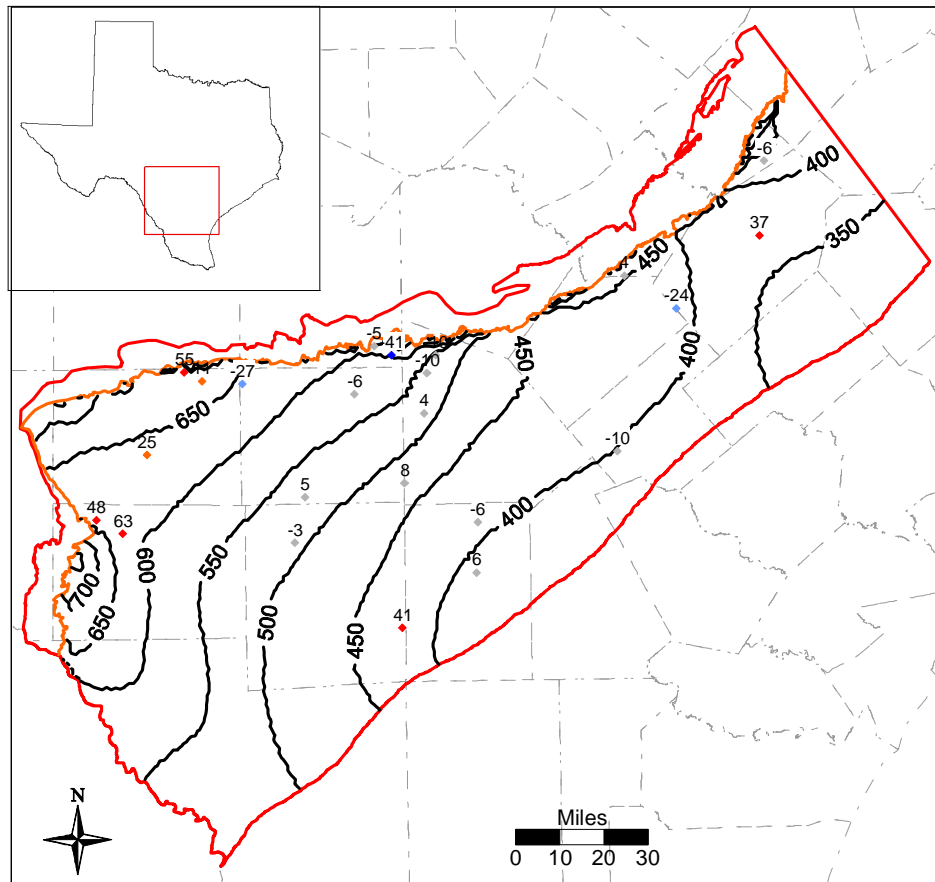


Figure 8.2.3 Simulated steady-state head surface, residuals and scatterplot for the Carrizo (Layer 3).

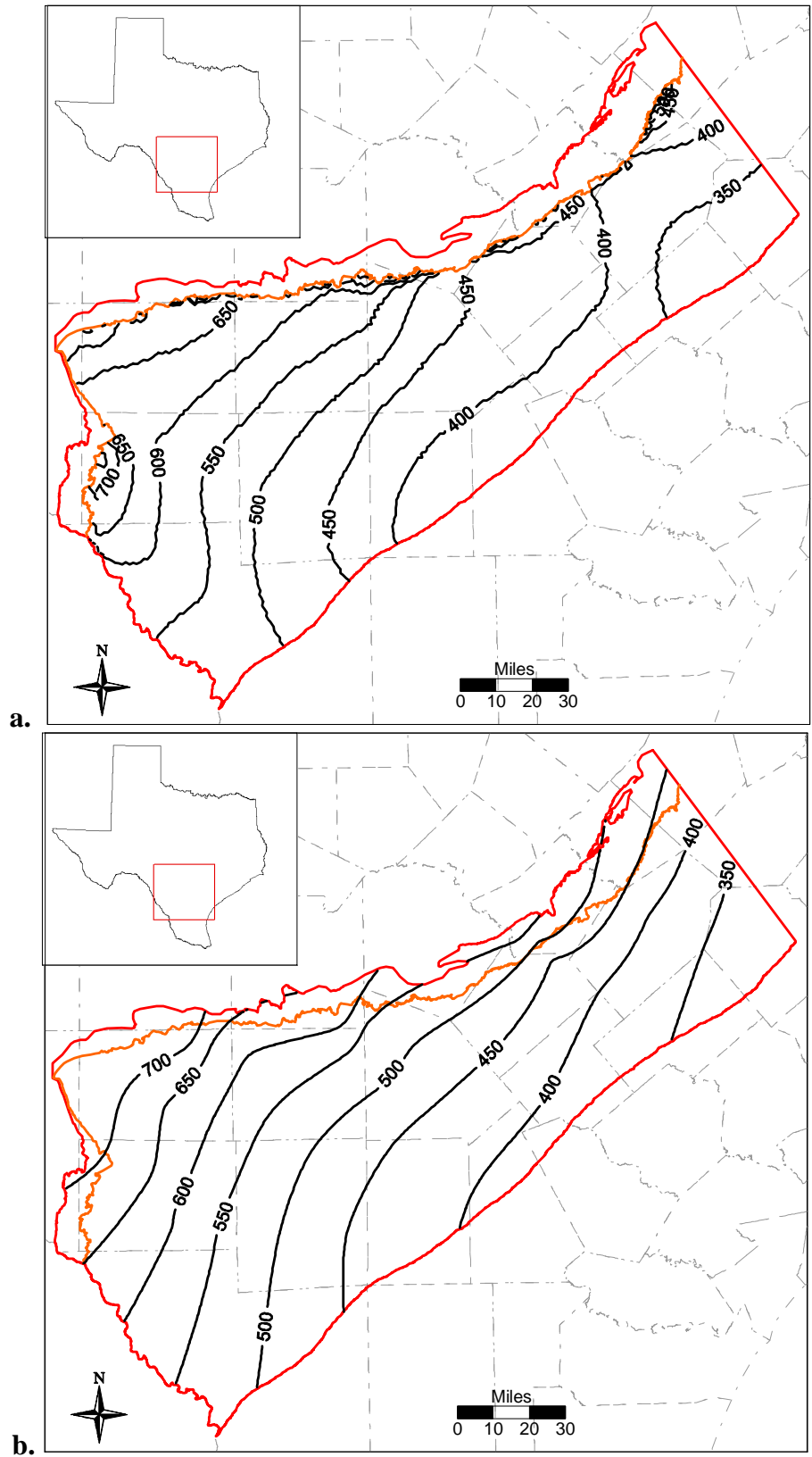


Figure 8.2.4 Simulated (a) and observed (b) steady-state head surfaces for the Carrizo (Layer 3).

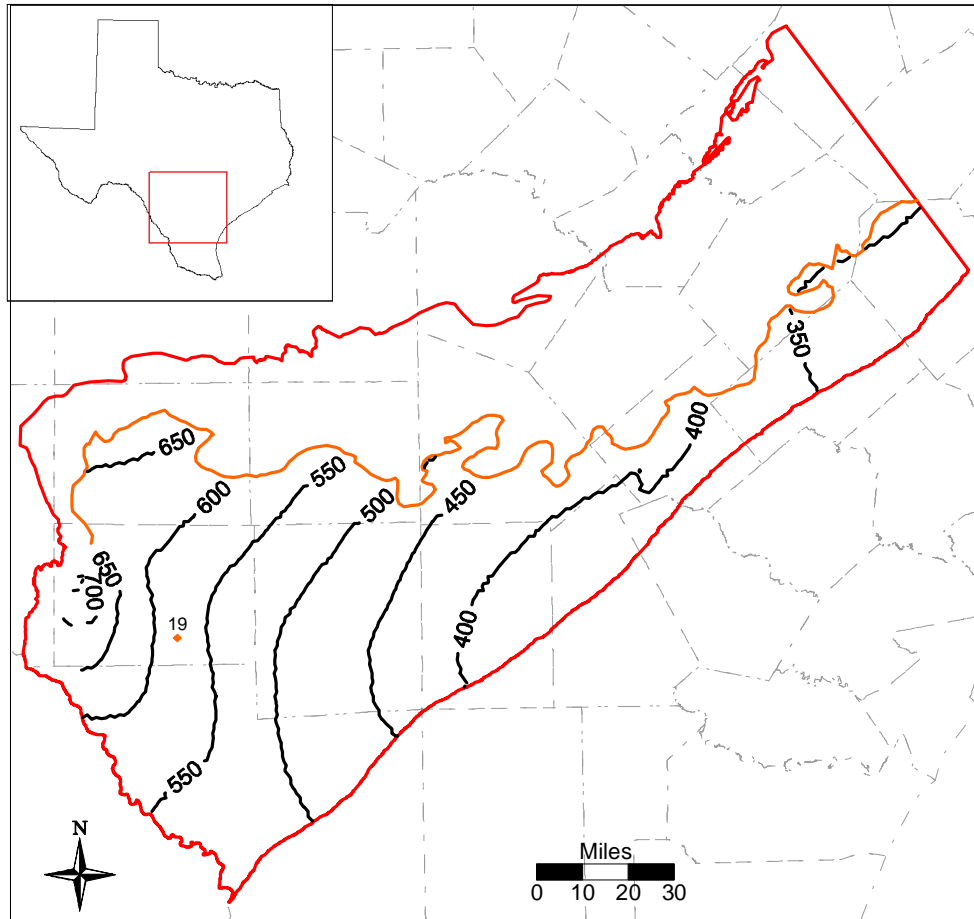


Figure 8.2.5 Simulated steady-state head surface and posted residuals for the upper Wilcox (Layer 4).

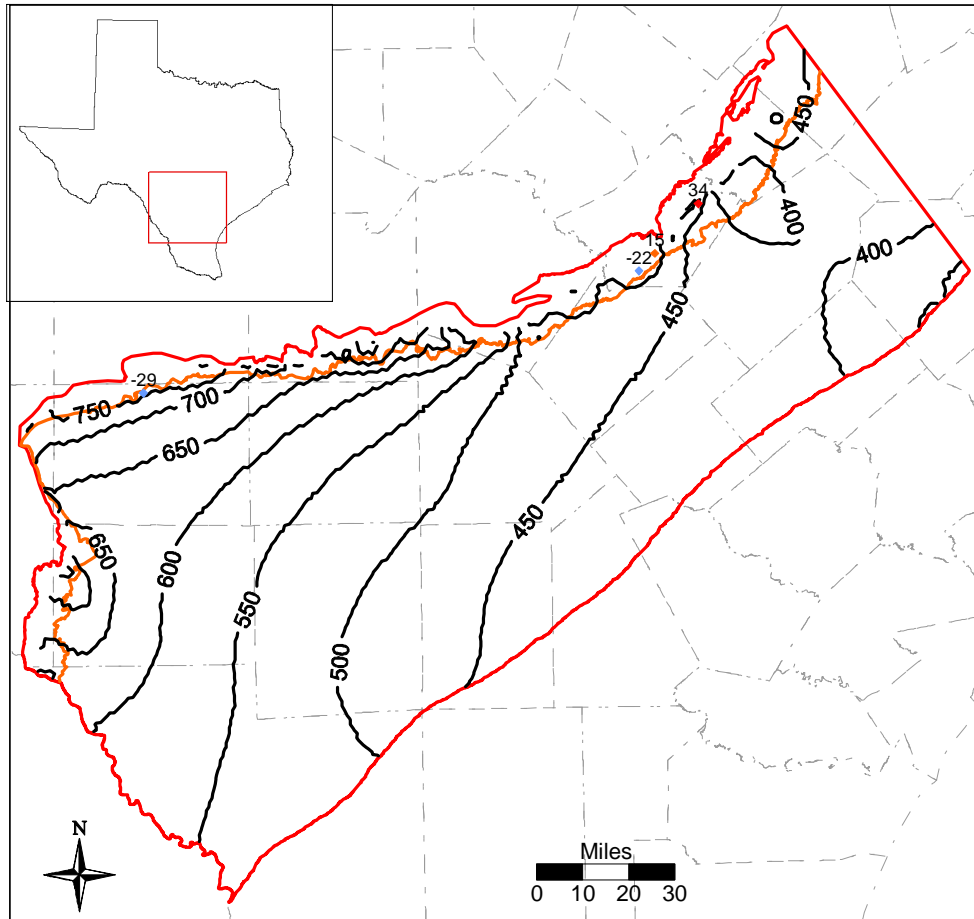


Figure 8.2.6 Simulated steady-state head surface and posted residuals for the middle Wilcox (Layer 5).

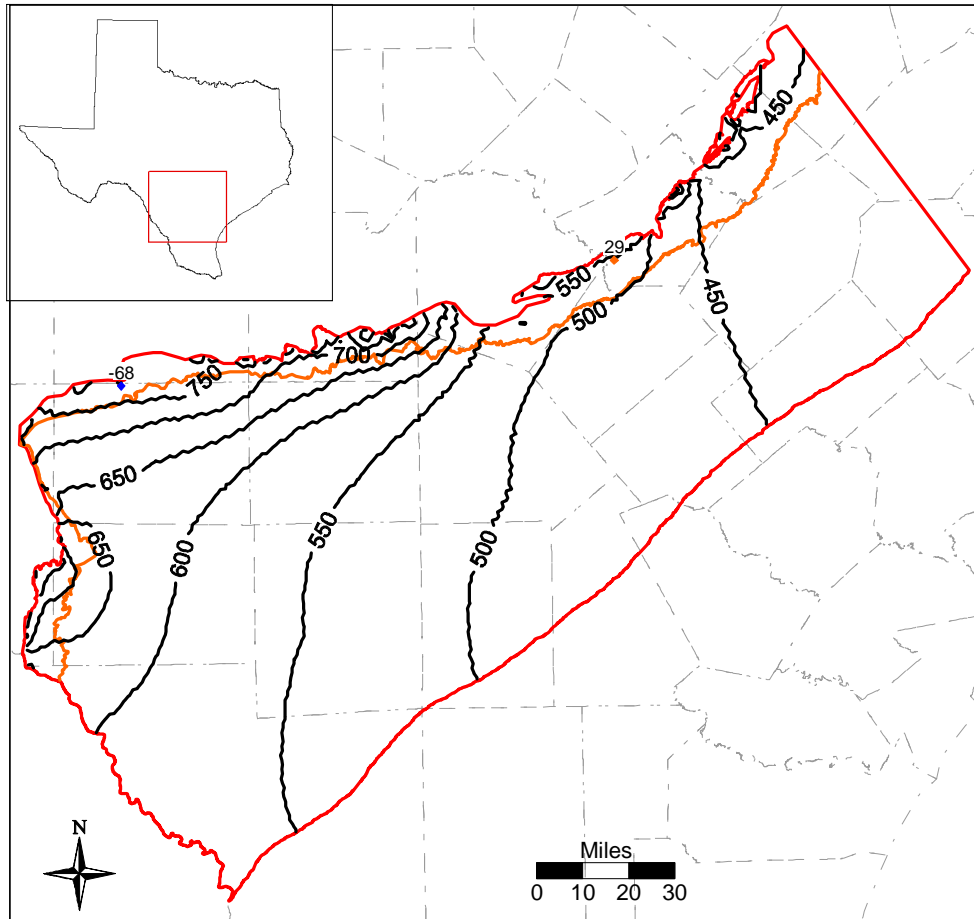


Figure 8.2.7 Simulated steady-state head surface and posted residuals for the lower Wilcox (Layer 6).

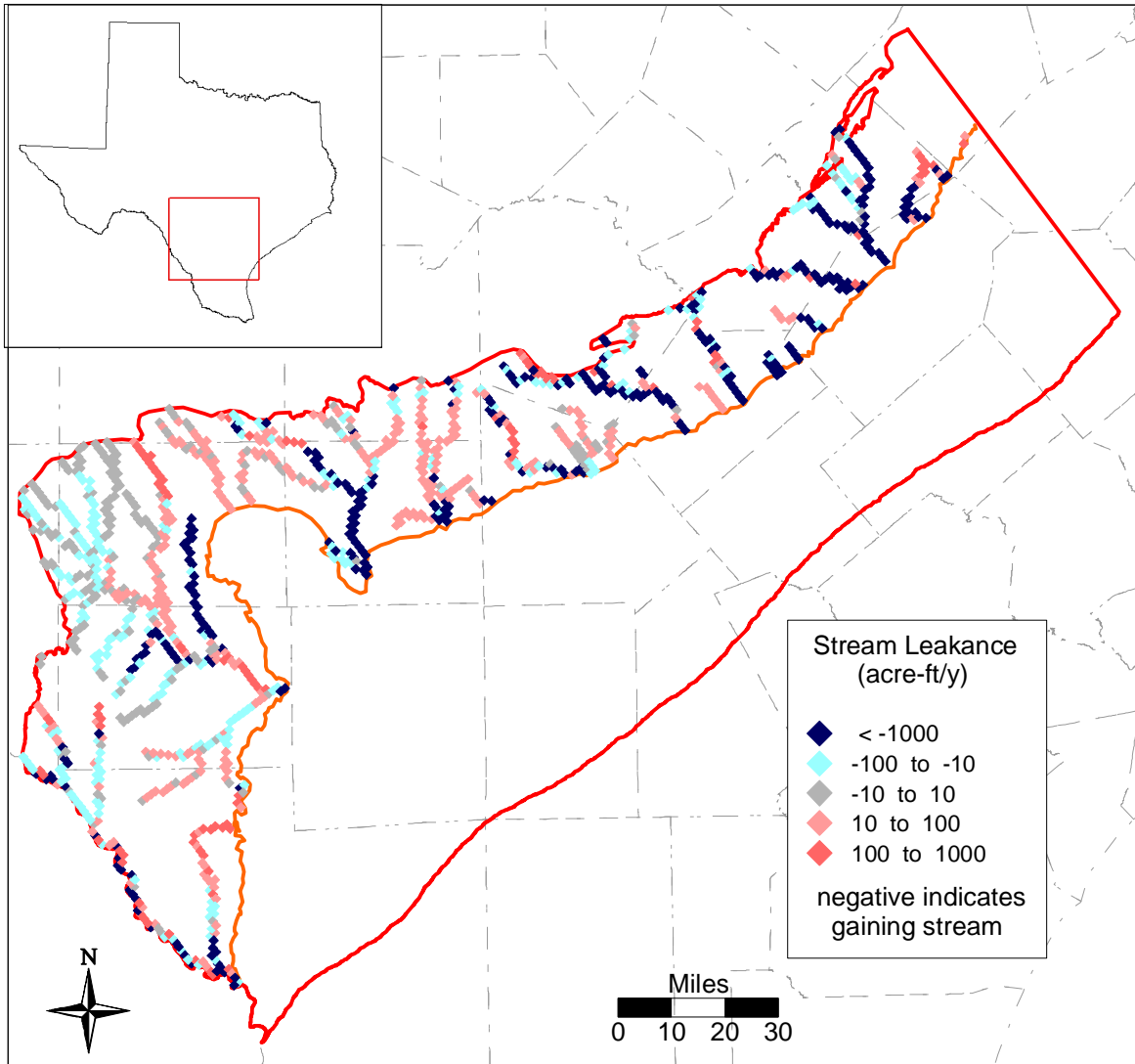


Figure 8.2.8 Steady-state model stream gain/loss (negative value denotes gaining stream).

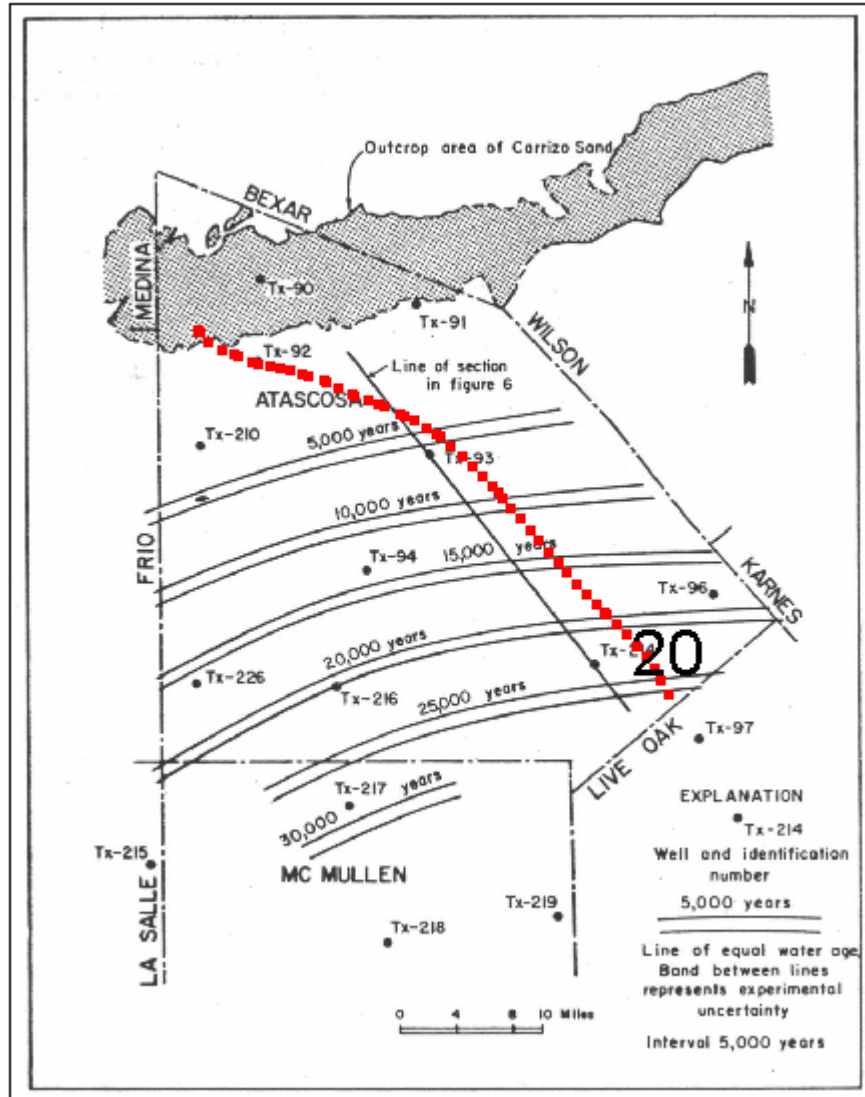


Figure 8.2.9 Steady-state particle travel path and travel time (20,000 years) compared to the groundwater age dating study of Pearson and White (1967).

8.3 Sensitivity Analysis

A sensitivity analysis was performed for the calibrated steady-state model. A sensitivity analysis provides a means of formally describing the impact of varying specific parameters or groups of parameters on model outputs. In this sensitivity analysis, input parameters were systematically increased and decreased from their calibrated values while the change in head was recorded. Four simulations were completed for each parameter varied, where the input parameters were varied either according to:

$$\text{sensitivity value} = (\text{calibrated value})(\text{factor}) \quad (8-2)$$

$$\text{sensitivity value} = (\text{calibrated value})(10^{\text{factor}-1}) \quad (8-3)$$

and the factors were 0.75, 0.9, 1.1, and 1.25. For parameters such as hydraulic conductivity, which typically vary by orders of magnitude and are usually lognormally distributed, equation (8-3) was used. Parameters such as recharge were varied linearly using equation (8-2). For the output variable, we calculated the mean difference (*MD*) between the base simulated head and the simulated head calculated for the sensitivity simulation for each layer. The equation for calculating the *MD* is:

$$MD = \frac{1}{n} \sum_{i=1}^n (h_{sens,i} - h_{cal,i}) \quad (8-4)$$

where

$h_{sens,i}$ = sensitivity simulation head at active grid block i

$h_{cal,i}$ = calibrated simulation head at active grid block i

n = number of grid blocks compared

We considered two approaches to applying Equation 8-4 to the sensitivity of output heads. First, we compared the heads in all active grid blocks between the sensitivity output and the calibrated output. Second, we compared the heads only at grid blocks where measured targets were available (i.e., n = number of targets in that layer). A comparison between these two methods can provide information about the bias in the target locations, i.e. a similar result indicates adequate target coverage. However, a drawback to the second method is that sensitivity results will not be available in layers containing an insufficient number of targets.

For the steady-state analysis, we completed 6 parameter sensitivities:

1. Horizontal hydraulic conductivity, model-wide (K_h)
2. Vertical hydraulic conductivity in Layer 2 (K_v -Reklaw, model leakance between layers 2-3)
3. Vertical hydraulic conductivity in Layers 4-6 (K_v -Wilcox, model leakance between layers 3-4, 4-5, and 5-6)
4. Recharge, model-wide
5. Streambed conductance, model-wide (K-Stream)
6. GHB conductance, model-wide (K-GHB)

Equation 8-2 was used for sensitivity to recharge (4), and Equation 8-3 was used for the remainder. Note that the head values assigned to the GHBs were not varied in the sensitivity analysis. These heads were estimated as water table elevations (Section 6.3.2), and variation would result in water levels above ground surface.

Figure 8.3.1 shows the sensitivity results for the Carrizo (Layer 3), with *MDs* calculated from just the gridblocks where targets were available. Figure 8.3.2 shows the sensitivity results for the Carrizo, with *MDs* calculated from all active cells in the layer. Note that the two figures indicate similar trends in sensitivities at 0.75 for the two most positive *MDs* [hydraulic conductivity of the GHBs (K-GHB) and vertical hydraulic conductivity of the Reklaw (K_v -Reklaw)] and the most negative *MD* (recharge). The two figures are less consistent for the *MDs* that were close to zero. However, the good agreement for the significant *MD* values indicates adequate target coverage in the Carrizo.

Figure 8.3.1 indicates that change in head in the Carrizo for the steady-state model is most positively correlated with recharge and most negatively correlated with the conductance of the GHBs. Also, the figure indicates that decreasing the Reklaw vertical hydraulic conductivity increases heads in the Carrizo, as would be expected given the upward cross-formational flow from the Carrizo to the Reklaw. Figures 8.3.3 and 8.3.4 show that Layers 1 and 2 are strongly influenced by the conductivity of the GHBs. Because the GHBs are present in a large portion of Layer 1, they have a large effect. This effect propagates through to the Carrizo (Layer 3), since the gradient between Layers 1 and 3 is important to determining Carrizo heads downdip. This effect is illustrated in Figure 8.3.5, which gives the sensitivity results for all layers when the

GHB conductivity was varied. The sensitivity decreases in order with increasing layer depth. A significant drop in sensitivity occurs between the Carrizo and middle Wilcox layers. Because of the low vertical conductivity of the middle Wilcox (Layer 5), the effect is dampened. This is illustrated again in Figure 8.3.6, where the sensitivity of the middle Wilcox to both recharge and vertical hydraulic conductivity is on the same order as the sensitivity to GHB conductance. Heads in the lower Wilcox (Layer 6) are most sensitive to the vertical hydraulic conductivity of the Wilcox, as shown in Figure 8.3.7. Because this layer is modeled as impermeable at the bottom, its connection to the rest of the model is through the middle Wilcox, or through recharge in the outcrop, which is the second most important factor. Recharge is an interesting sensitivity, because the relative *MD* for a layer appears to be dependent on the elevation of the outcrop. Figure 8.3.8 illustrates this, with the lower Wilcox (Layer 6) being most sensitive and the Queen City/El Pico (Layer 1) being least sensitive, even though Layer 1 has the largest outcrop. However, this could be due to the higher calibrated head values in Layer 6. Stated otherwise, a similar percent change in head leads to higher *MDs* in Layer 6 as compared to Layer 1 because *MD* is not scaled by calibrated head.

The sensitivity analysis determined that the two most important parameters to predicting heads in the Carrizo in the steady-state model are recharge and the vertical conductivity of the formations overlying the Carrizo (vertical hydraulic conductivity of the Reklaw and the GHBs).

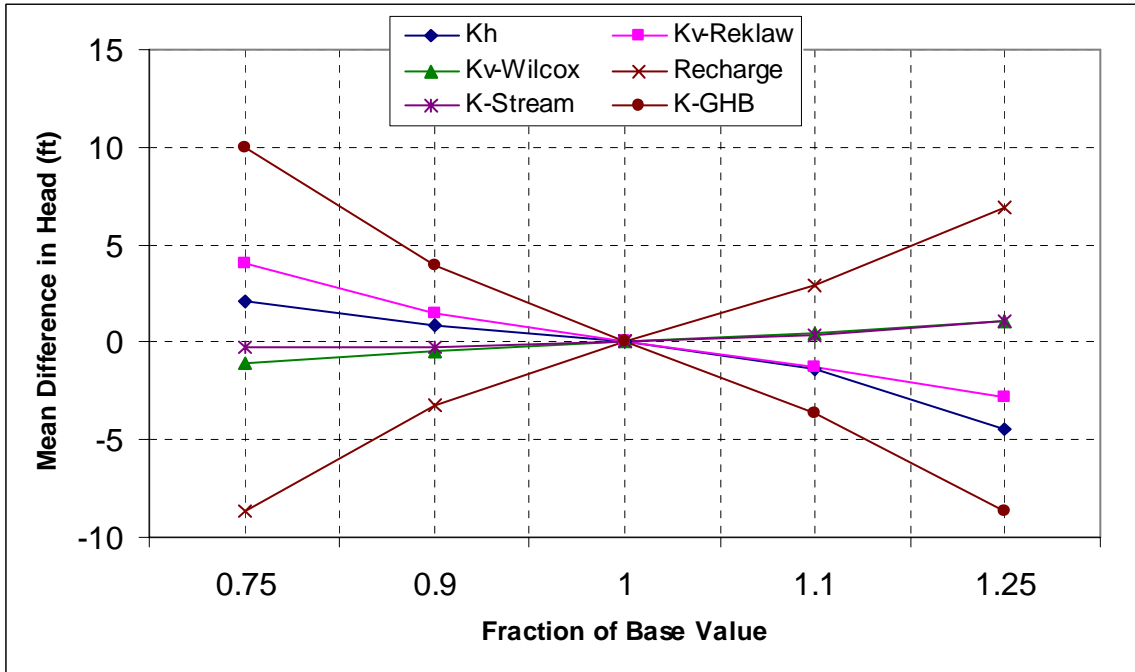


Figure 8.3.1 Steady-state sensitivity results for the Carrizo (Layer 3) using target locations.

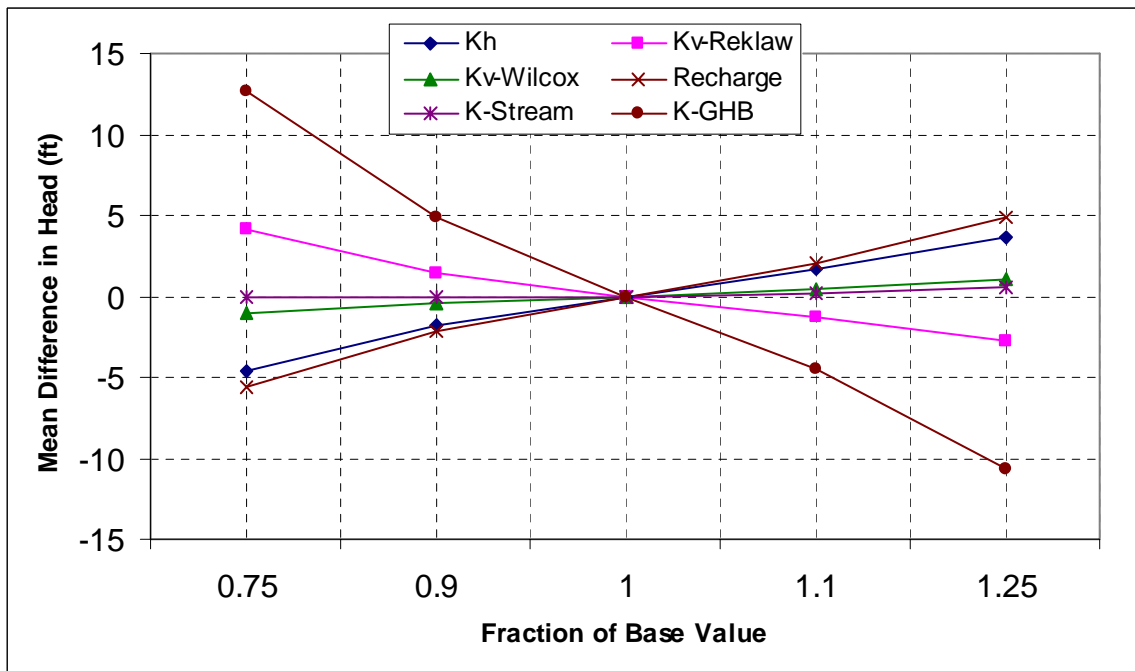


Figure 8.3.2 Steady-state sensitivity results for the Carrizo (Layer 3) using all active gridblocks.

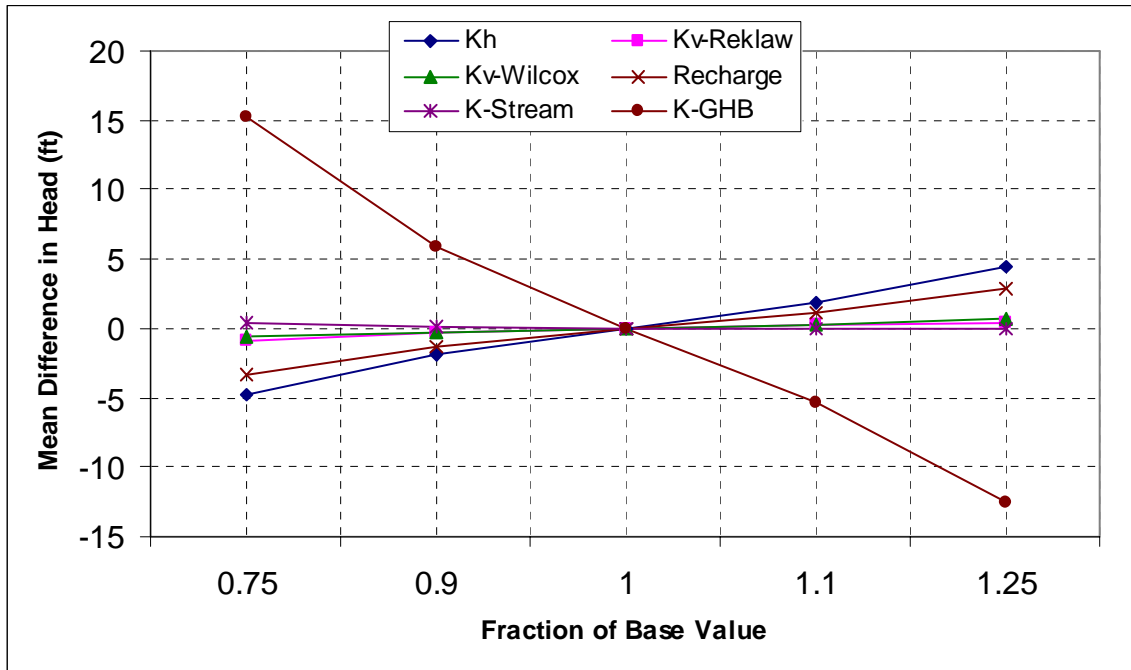


Figure 8.3.3 Steady-state sensitivity results for the Queen City/El Pico (Layer 1) using all active gridblocks.

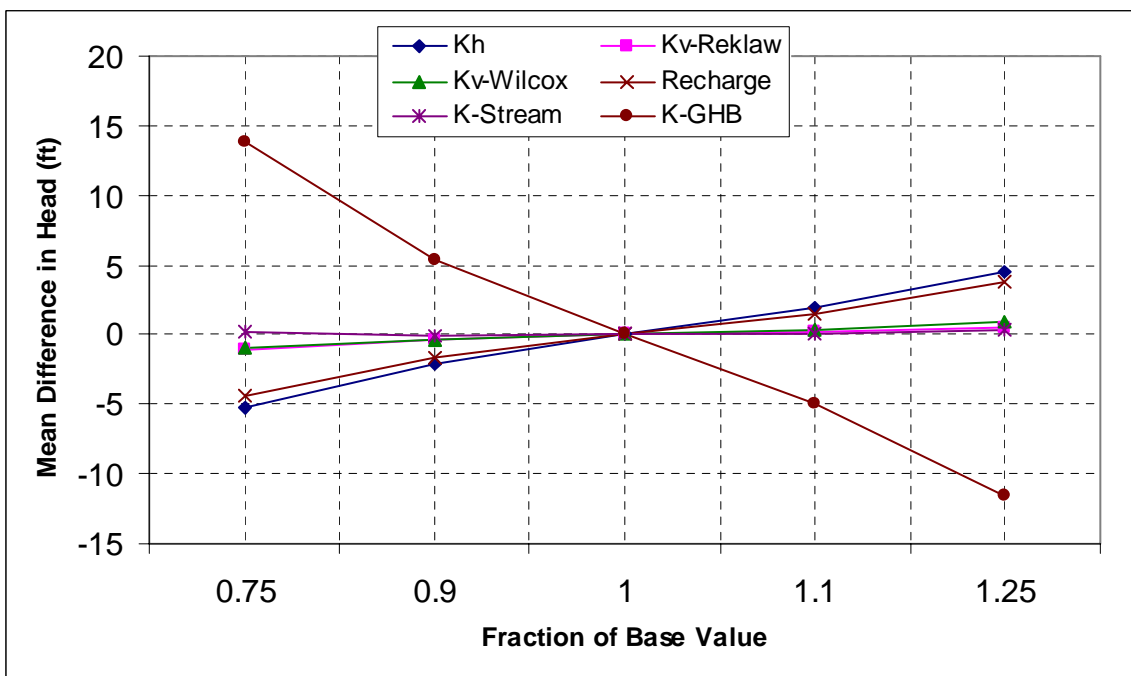


Figure 8.3.4 Steady-state sensitivity results for the Reklaw/Bigford (Layer 2) using all active gridblocks.

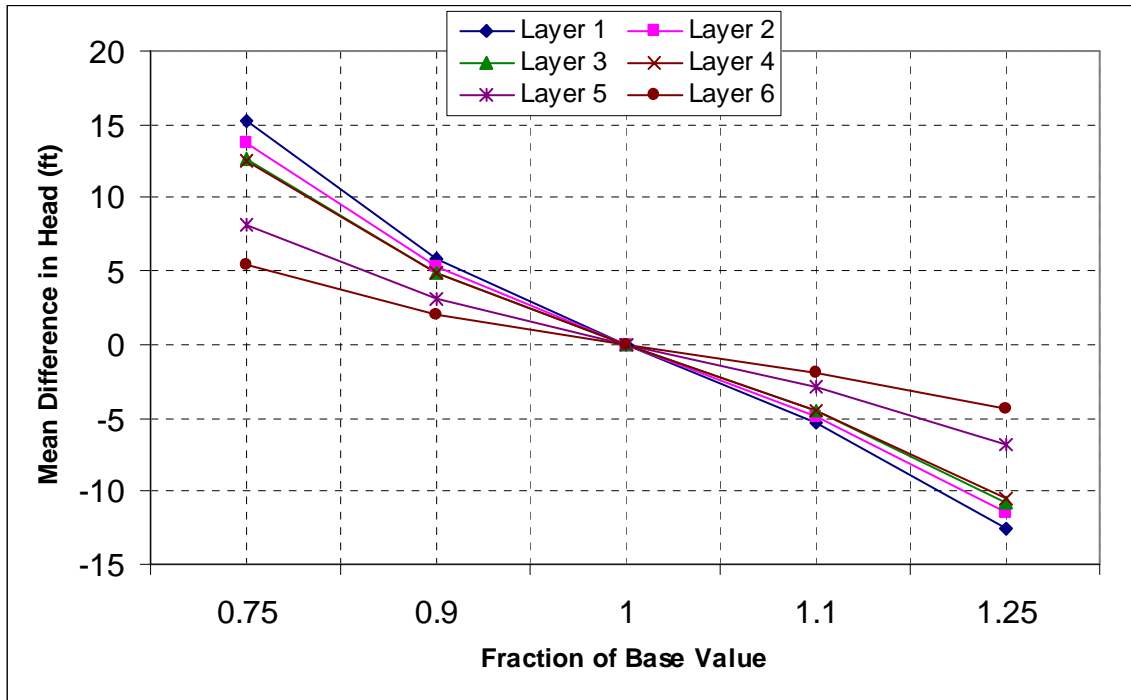


Figure 8.3.5 Steady-state sensitivity results where GHB conductivity is varied.

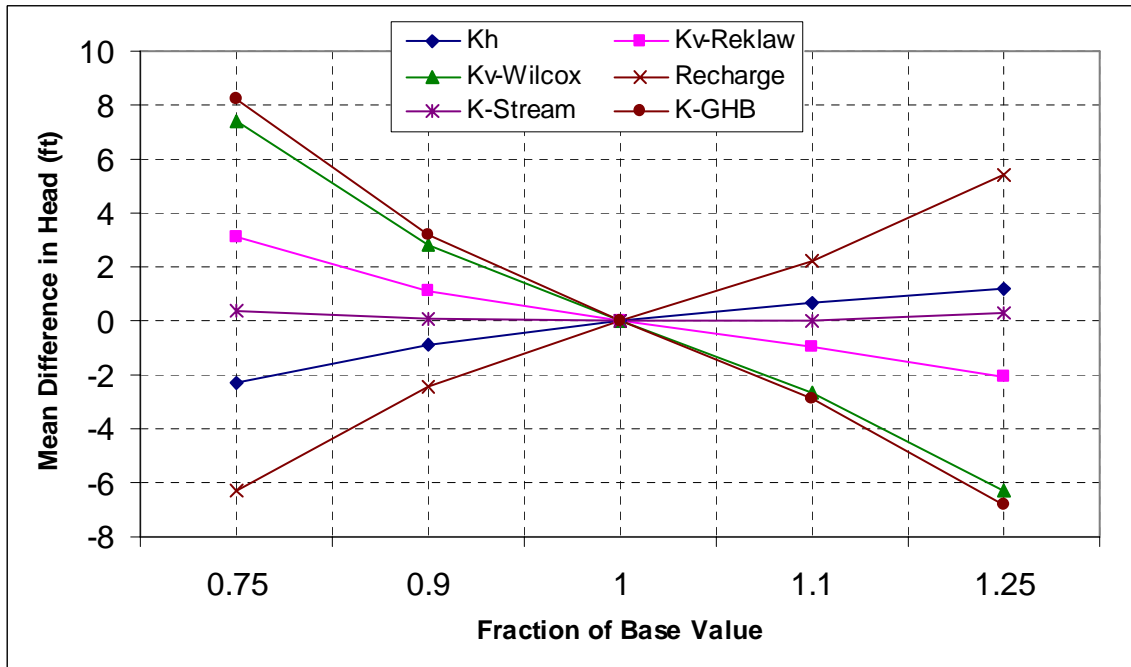


Figure 8.3.6 Steady-state sensitivity results for the middle Wilcox (Layer 5) using all active gridblocks.

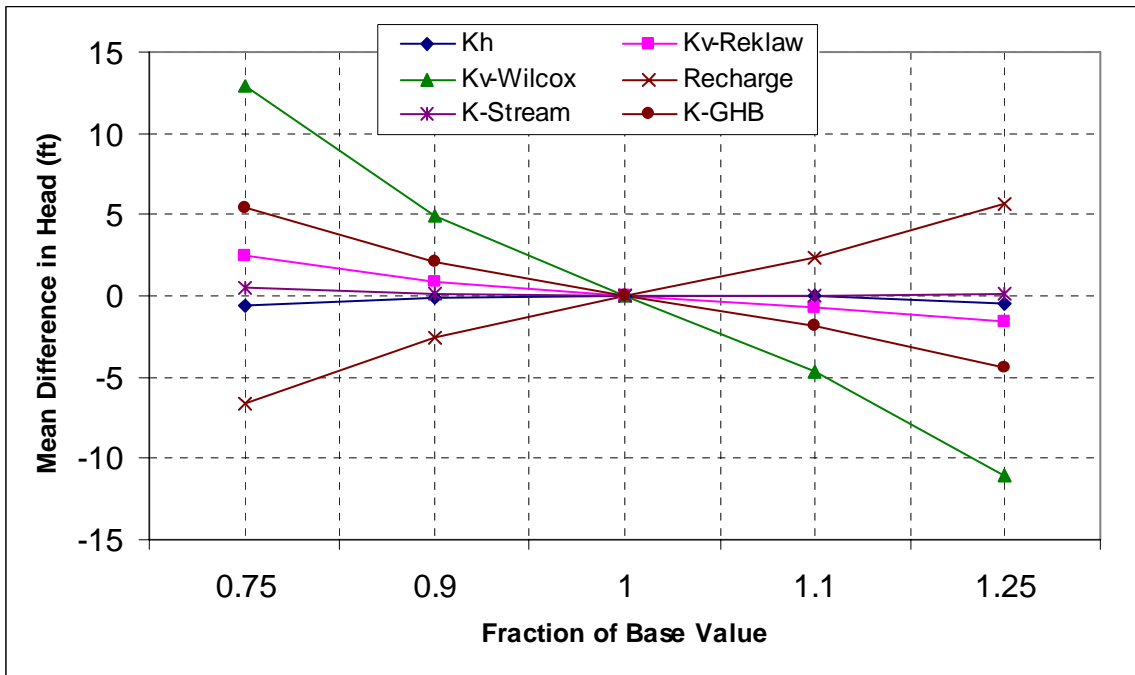


Figure 8.3.7 Steady-state sensitivity results for the lower Wilcox (Layer 6) using all active gridblocks.

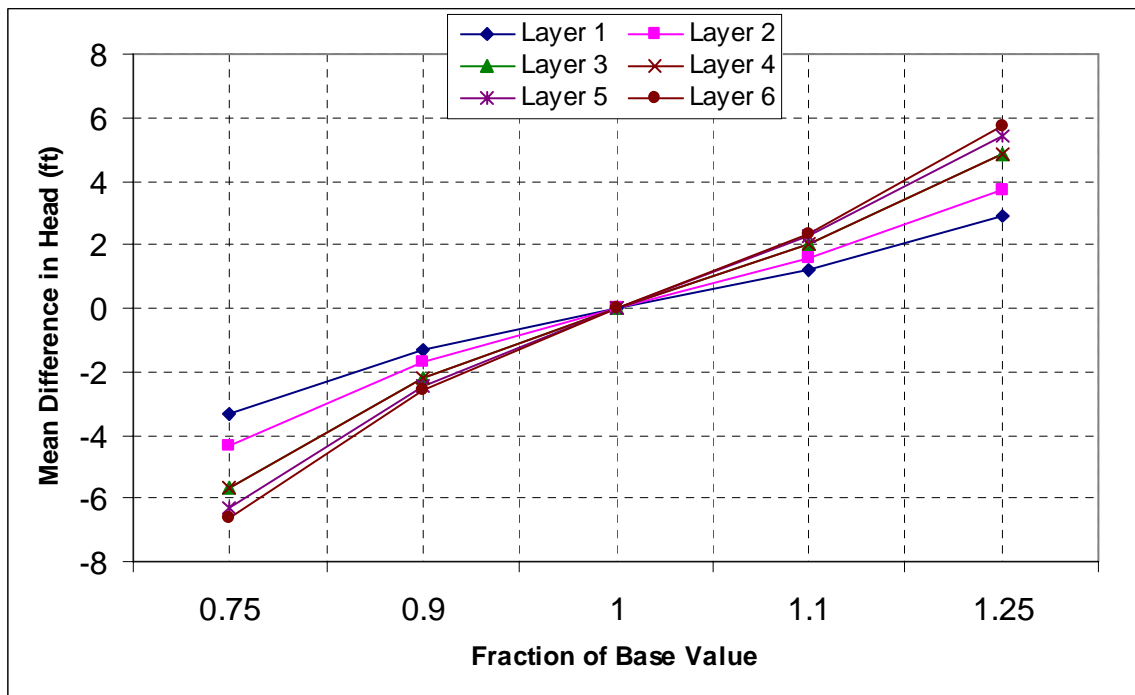


Figure 8.3.8 Steady-state sensitivity results where recharge is varied.

9.0 TRANSIENT MODEL

This section describes the calibration and verification of the transient model and presents the transient model results. This section also describes a sensitivity analysis for the transient model. The transient model was started in 1975 to allow any initialization effects to dampen by 1980, the start of the calibration period. This period from 1975 to 1980 was considered a “ramp up” period, and was not used for calibration. The model was calibrated for the time period from 1980 through 1989. The model was verified for the time period from 1990 through 1999. The model calibration is discussed in Section 9.1. The results from the calibration period and the verification period are discussed together in Section 9.2. A formal sensitivity analysis with the calibrated transient model is presented in Section 9.3.

9.1 Calibration

Because the groundwater model must be calibrated to steady-state and transient conditions using the same physical hydraulic properties, calibration is an iterative process between the conditions. As a result, the physical properties which are common between the steady-state model and the transient model are the same, as presented in Section 8.1. In addition, a transient model requires storage estimates for the aquifers and these are discussed in this section. Also, the calibration process is further discussed in light of the transient model.

The transient model played an important part in setting vertical anisotropy ratios (K_h/K_v) for the model. We initially set the anisotropy ratios of the Reklaw/Bigford (Layer 2) and the Wilcox Group (Layers 4-6) to values on the order of 100 to 1,000. However, during initial transient calibration, we found that water was flowing between the formations so freely that drawdowns resulting from pumping centers could not be maintained at the estimated pumping rates. Water was moving into the Carrizo from storage in the Wilcox and Reklaw/Bigford layers (or from storage in the El Pico/Queen City through the Reklaw/Bigford) due to the high vertical gradients initialized in pumping centers, especially in the Wintergarden area. We tried increasing the anisotropy ratios by decreasing the vertical hydraulic conductivity in the Reklaw/Bigford and the Wilcox to near the extremes of published values. This increase in anisotropy mitigated the “rebound” effect considerably in these areas. Figure 9.1.1 illustrates the impact in Wilson County of half an order of magnitude change in anisotropy in the Reklaw.

Figure 9.1.1 shows that the water level trend changes from basically flat to downward during the calibration period. During calibration, we reduced the vertical hydraulic conductivity (e.g. increased anisotropy) until an optimum match was attained. The final vertical hydraulic conductivities resulting from the calibrated anisotropy ratios (Table 8.1.1) are within published limits for these formation materials, but are lower in magnitude than we expected for a regional scale model.

Primary and secondary storage (also called storativity and specific yield) are properties of a transient model that are not required in a steady-state model. Specific storage was defined as 3.0×10^{-6} (1/ft) in all layers based upon a review of published data, prior models, and considering the materials of the formation. Specific storage was then multiplied by layer thickness to provide the storativity at each grid cell. Storativity has an impact upon the amplitude of head variation due to pumping. However, we did not find overall hydrograph trends to be strongly sensitive to storativity, and therefore did not make areal changes in storativity during calibration. Figure 9.1.2 is a hydrograph that illustrates the effect of an order of magnitude increase in storativity in Frio County. Note that the seasonal effect of pumping is dampened, but the overall trend of the hydrograph is very similar. When we reduced the storativity further, the response of simulated heads to seasonal variations in pumping increased to unreasonable levels. Figure 9.1.3 shows the variation of storativity in the Carrizo. The storativity of the Carrizo is generally less than 0.003 except for a thick portion of the aquifer in south Atascosa County and in the outcrop where it was set to one. A storativity of one in the outcrop overcomes the numerical limitation of MODFLOW when it calculates heads above ground surface in an unconfined section.

Because there are only two reservoirs in the model area, reservoirs did not play a significant role in the calibration. We initially assumed a hydraulic conductivity of 1 foot per day in the reservoir conductance calculation. This value resulted in too much aquifer-reservoir interaction, so we decreased the conductivity until a more reasonable amount of water passed between the reservoirs and the aquifer.

Because we lacked good targets for stream leakance, we made only coarse adjustments to streambed conductivity during the calibration. The streams exchange significant volumes of water with the aquifer, so they are important in the outcrop area. However, in the transient

model, the hydrology of the outcrop has little effect on downdip regions during the simulation period. We made comparisons between simulated stream leakances and some general reported estimates (Section 9.2.2).

As noted in the steady-state calibration Section 8.1.2, SWAT-predicted recharge was decreased in the eastern portion of the model so that recharge in that area was more consistent with the rest of the model. Recharge is still highest in the east, reaching values in excess of 3 inches per year.

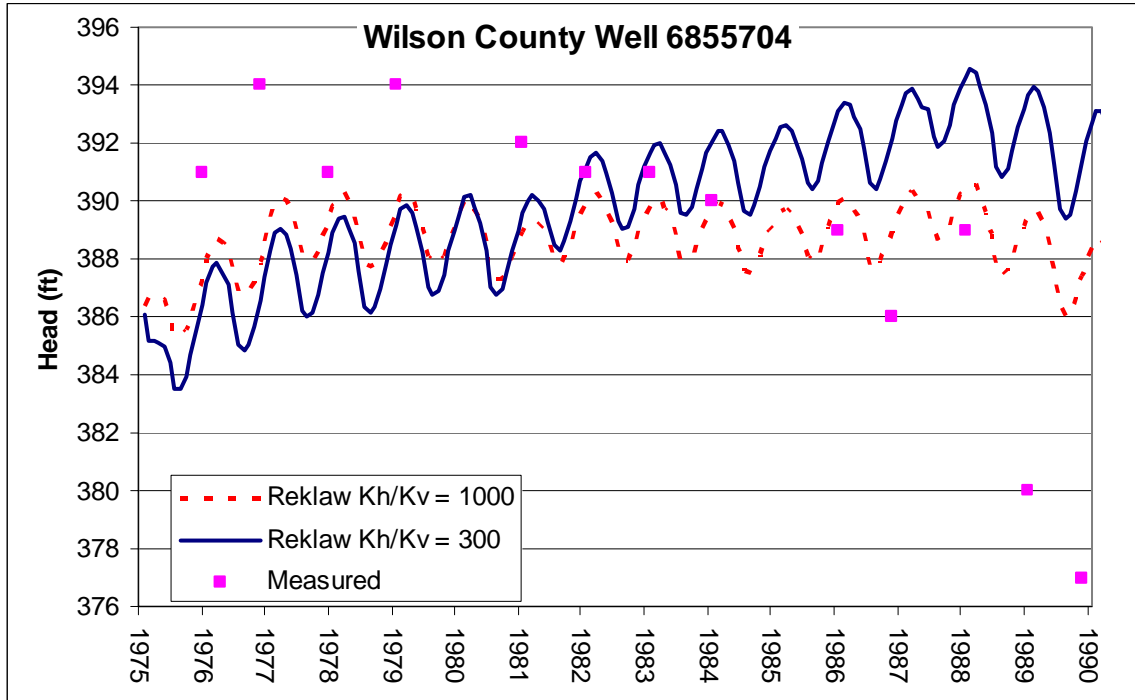


Figure 9.1.1 Example of head sensitivity to Reklaw vertical hydraulic conductivity.

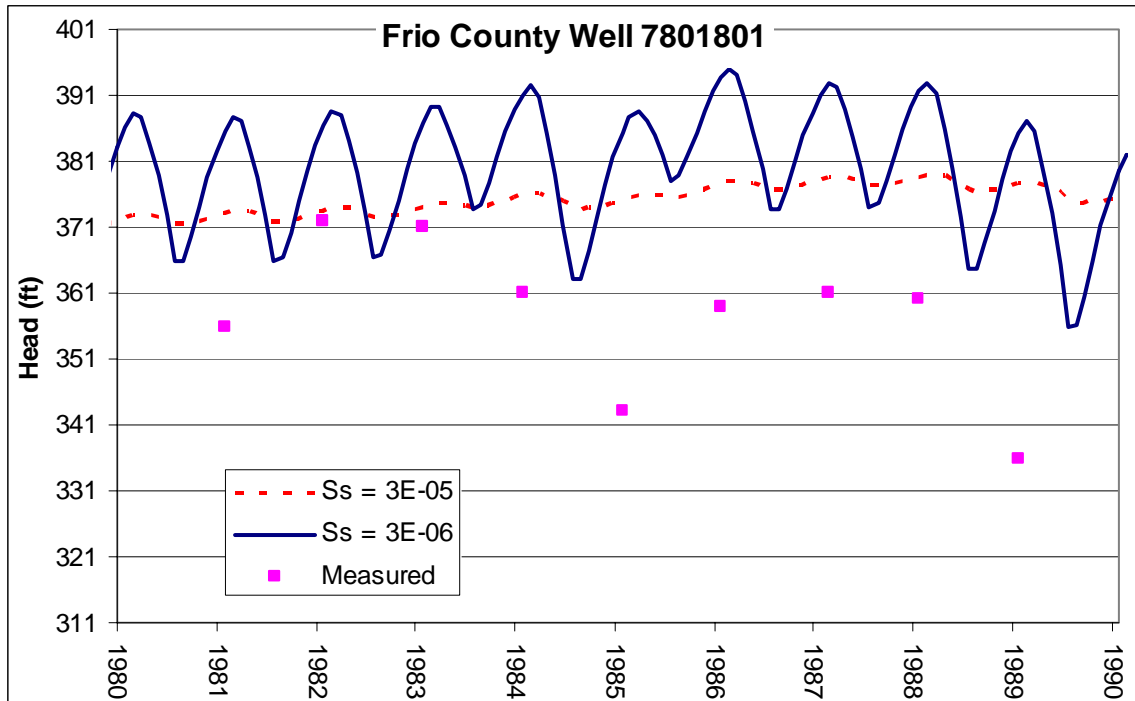


Figure 9.1.2 Example of head sensitivity to specific storage.

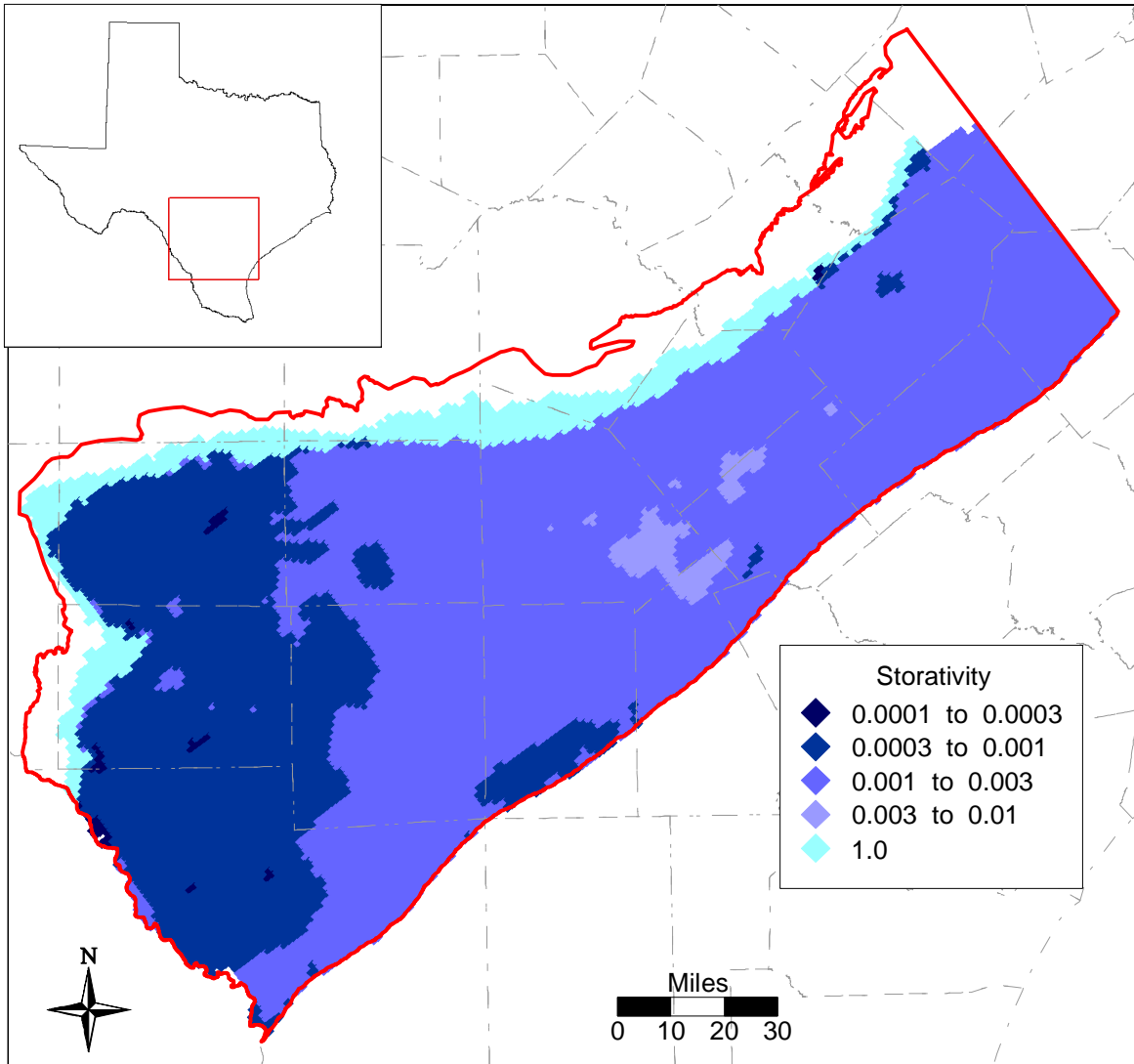


Figure 9.1.3 Storativity in the Carrizo Formation (Layer 3).

9.2 Results

The results of the transient calibrated model are compared to the available calibration targets in this section. The calibration measures were also applied to the verification period to provide an indication of the model's predictive capability.

9.2.1 Hydraulic Heads

Figures 9.2.1 and 9.2.2 show simulated head surfaces at the end of the transient calibration period (1989) and at the end of the verification period (1999) respectively. The measured and predicted heads are representative of December of those years. The general trends of the simulated and measured data are the same. However, the simulated heads do not show as pronounced a drawdown in portions of the western model region where significant water level declines have been observed. As noted in the previous section, during calibration we decreased the vertical hydraulic conductivity of the model layers above and below the Carrizo to help maintain drawdowns in the western portion of the model. However, without modifying either horizontal hydraulic conductivity or pumping, we were not able to sustain the largest drawdowns. Because well-distributed well test data exist for the Carrizo throughout most of the problem area, we did not feel that we could arbitrarily modify horizontal hydraulic conductivity. Similarly, we could not find objective evidence for re-distributing our pumping, even though we know that the distribution of pumping is uncertain. This problem with insufficient drawdowns in the largest drawdown centers in the Wintergarden area was also experienced by LBG-Guyton and HDR (1998). The fit in the west-central part of the model should be further investigated as discussed in the future improvements section of this report.

Figure 9.2.3 shows the distribution of available transient head targets for the model layers. The majority of the targets are in the Carrizo layer. Most of the targets had incomplete records over the simulated time period. As a result, calibration statistics have been calculated using all of the available data in time and space for the calibration and verification periods. Table 9.2.1 shows the mean error (ME), mean absolute error (MAE), root mean square error (RMS), range, and RMS/range for aquifer layers in the transient model for the calibration and verification periods. The RMS/range for the Carrizo (Layer 3) was 0.059 for the calibration period. The RMS/range increases to 0.092 in the verification period, which is still within the calibration criteria of 0.10. The increase in RMS during the verification period is largely due to

the aforementioned non-sustained drawdowns in the western portion of the model. This is evident in Figure 9.2.4 which shows a crossplot comparison for the Carrizo (Layer 3) between the calibration and verification periods. These crossplots compare all of the measured heads through each time period to their corresponding simulated heads. The tailing in the lower part of the verification period crossplot is a result of the inability of the model to maintain the largest drawdowns in the western region. Figures 9.2.5 and 9.2.6 show the crossplots for the calibration and verification periods, respectively, for the remainder of the model layers. Note the general scarcity of data in these layers compared to the Carrizo. In all cases where significant data are available, the crossplots show a good correlation between the measured and simulated heads.

Figures 9.2.7 – 9.2.13 show selected hydrographs by layer for the transient model. Table 9.2.2 provides the calibration statistics for these hydrographs. All hydrographs in this section are shown on a 100 ft vertical scale for consistency, unless the data range exceeds 100 ft. Figure 9.2.7 shows hydrographs for the Queen City/El Pico (Layer 1). In general, both the simulated and measured heads stay at nearly the same level throughout the simulation. Figure 9.2.8 shows the hydrographs for the Carrizo (Layer 3) in the western region of the model. Some of the hydrographs in Zavala and Dimmitt counties show considerable fluctuation with seasonal pumping. The measured data for these hydrographs typically show scatter in a similar range. This region is very difficult to simulate because some proximal hydrographs show opposite trends, as illustrated in Figure 9.2.8. Examples of both declining and recovering heads are shown for Zavala and Dimmitt counties. These trends emphasize the importance of having correct pumping, not only in magnitude but also in location. Figure 9.2.9 shows the hydrographs for the Carrizo (Layer 3) in the central region of the model. The figure shows declining hydrographs in Bexar and Atascosa counties that are matched well by the simulated heads. The recovering heads in LaSalle County are not matched as well, with the simulated heads flattening out while the measured heads continue to recover. Figure 9.2.10 shows the hydrographs for the Carrizo (Layer 3) in the eastern region of the model. The counties in this region generally do not have much pumping stress, and both the measured and simulated hydrographs are relatively flat. The exception is the hydrograph from Guadalupe County in which both the simulated and measured data are slowly declining over the course of the simulation. Figure 9.2.11 shows the few hydrographs in the upper Wilcox Formation. The measured data from Webb County and from one of the Dimmitt County hydrographs are erratic, making it difficult to judge the trend.

The Atascosa County hydrograph shows declining heads with a good fit for the simulated heads. The southern Dimmitt County measured hydrograph appears flat, while the simulated hydrograph is rising, resulting in a poor fit. Figure 9.2.12 shows transient hydrographs from the middle Wilcox formation. The simulated heads in both Wilson and Gonzales County hydrographs are increasing slightly over the course of the simulation. While this trend is not reflected in the measured data, the increase is less than 10 feet over the entire simulated time period. Given the scale of the model, and the model error discussed in Section 7.2, this trend is not significant. The Uvalde and Atascosa County graphs show stable simulated and measured heads. The Zavala County hydrograph is somewhat erratic, although the range of the scatter is similar to the amplitude of the simulated head, possibly indicating a good estimate of storativity for that region. Figure 9.2.13 shows transient hydrographs for the lower Wilcox. The measured and simulated heads in these hydrographs remain relatively stable throughout the simulated period.

Figure 9.2.14 shows the head residuals averaged for the verification period. In the figure, the blue indicates over prediction of heads, and orange or red indicates under prediction of heads. In general, there is a good mix of over and under prediction throughout the model. The area between Atascosa and Frio counties appears to have consistent over prediction which we were unable to correct during calibration, without modifying horizontal hydraulic conductivity or pumping.

More cells go dry in the transient simulation than in the steady-state simulation. This increase is expected since the transient simulation includes pumping, and also includes years where recharge is much lower than average. Dry cells are typically thin cells located at the farthest updip edge of layer outcrops. Because some of these cells are only 20 ft thick, the cells go dry if the water table is more than 20 ft below ground surface. The MODFLOW rewetting package is active, allowing these cells to resaturate given a subsequent increase of the water table elevation. Out of 6,892 outcrop cells, between 1400 and 1550 (20-22%) are dry during the transient simulation. The drying of these thin edge cells is a physically correct condition and we do not expect it to have an adverse impact on model results.

9.2.2 Stream-Aquifer Interaction

We performed direct comparisons of simulated streamflow to stream gages in the model area, and these compared well. However, this is expected because we defined headwater streamflow rates based upon the available gage data. The more important metric for aquifer-stream interaction is the gain/loss estimate. Therefore, we used two data sources for comparison to simulated stream gain or loss; (1) the Slade et al. (2002) study of stream gains and losses in Texas and (2) the average stream gain/loss estimates reported in LBG-Guyton and HDR (1998). Unfortunately, the Slade (2002) report does not contain measurements made within the simulated time period for our model area. The report contained several studies in the area (shown in Figure 4.6.1) completed earlier than the simulated period. The results of these studies are shown in Figure 9.2.15, represented by the solid circles. In addition, the 10th, 50th, and 90th percentile average (1980-1999) simulated stream gain or loss for the same river reaches is shown on the plot, represented by the horizontal lines. Note that reach statistics are based on all stream cells in each reach, for all stress periods in the duration. So, this figure compares the simulated gain/loss estimates to those reported by Slade et al. (2002). The gain/loss studies are referenced by study number on the bottom horizontal axis consistent with Table 4.6.1 of this report and Slade et al. (2002). Studies 104, 349, and 350 were performed on Cibolo Creek. As would be expected, the measured data are predominantly gaining and consistent with the simulated results. Studies 325, 327, and 328 are on the Rio Grande. All of the measured data fall within the simulated data. However, the median of the simulated data is gaining, while all of the measured data are losing. The middle group of studies shown on Figure 9.2.15 were performed on the Nueces River. Most of the measured data fall within the simulated data, showing losing conditions. However, there are two studies that indicated gaining conditions which were not well represented by the model. Studies 165 through 175 are on the Leona River. The magnitude of variation in the measured data is larger than that of the simulated data. The measured data are also both losing and gaining, while the simulated data do not show significant gaining values. In study 130, on the Medina River, the one measurement is within the simulated data and very near the median.

We also compared the stream gain/loss to average estimates reported by LBG-Guyton and HDR (1998) for the period of time when the two models overlap (1980-1990). Table 9.2.3 shows the values taken from Figure 7-7 of LBG-Guyton and HDR (1998) compared to the simulated values. The simulated values are taken from the Carrizo-Wilcox outcrop. In all cases,

the current simulated values show gaining or losing concurrent with the reported simulated values. The largest difference is in the Frio River results, where LGB-Guyton and HDR (1998) simulated the Frio as more strongly losing by 400 acre-ft/yr-mi.

9.2.3 Water Budget

Table 9.2.4 shows the water budget for the transient model totaled for years 1980, 1988 (lowest annual precipitation in the calibration period), 1990, and 1999. In the overall model, the greatest influx of water consistently occurs from recharge, and the greatest outflow of water consistently occurs from pumping. Stream leakance accounts for a large amount of influx or outflow, depending on climatic conditions for the model. In 1980, pumping accounts for approximately 300,000 acre-feet of water extracted from the model, while recharge adds 193,000 acre-feet of water and 303,000 acre-feet of water is lost through the streams. Secondary to these are groundwater evapotranspiration, which removes 62,000 acre-feet and the GHBs, which add 38,000 acre-feet to the Queen City/El Pico. If we consider the outcrop only, 109,000 acre-feet discharge through the streams from storage in the outcrop. The remaining decrease in storage occurs downdip due to pumping. It is important to note when looking at the water budget that the majority of pumping occurs downdip, so most of the water being removed from storage by pumping will not be replenished during the simulation by recharge. The outcrop and downdip sections operate nearly independently over the simulation time period. The streams, recharge and, to a lesser extent, groundwater ET and pumping dominate outcrop hydrogeology. Pumping and storage are the main components of downdip hydrogeology.

The water budget for 1990 illustrates the effect of a wet year on the water budget in this model. Not only does recharge increase significantly, but the streams contain higher flows and higher stages (rising faster than groundwater levels), which leads to greater leakance into the aquifer from losing streams, and less leakance out of the aquifer in gaining streams. Note that if recharge increases groundwater heads above a previously losing stream stage, then the effect will be mitigated by the stream going from losing to gaining. In 1999, dry conditions lead to less recharge and less water in the streams, so the net stream leakance returns to negative.

The Carrizo layer as a single unit is most affected by pumping. Pumping in the Carrizo draws water from storage in the layer and from cross-formational flow from above and below. The net flow of water from the Reklaw to the Carrizo indicates that some of the gradients seen in

the steady-state model, where water was flowing up and out of the Carrizo through the Reklaw, have been reversed by pumping in the Carrizo.

Table 9.2.1 Calibration statistics for the transient model for the calibration and verification periods.

Calibration period (1980-1989)						
Layer	Count	ME (ft)	MAE (ft)	RMS (ft)	Range (ft)	RMS/Range
1	112	-5.1	15.5	19.0	142	0.13
3	1644	-6.8	25.5	33.7	571	0.059
4	95	-13.8	29.3	34.9	300	0.12
5	251	-0.2	18.7	25.5	471	0.054
6	77	4.0	16.1	22.5	303	0.074
Verification period (1990-1999)						
Layer	Count	ME (ft)	MAE (ft)	RMS (ft)	Range (ft)	RMS/Range
1	76	-10.5	23.1	28.9	112	0.26
3	1141	-11.8	38.3	50.8	553	0.092
4	69	-14.6	25.4	30.9	279	0.11
5	205	-1.1	17.4	24.4	465	0.052
6	72	2.2	20.4	25.7	299	0.086

Table 9.2.2 Calibration statistics for the hydrographs shown in Figures 9.2.7-9.2.13.

Well	Layer	Count	ME (ft)	MAE (ft)	RMS (ft)	Figure
7814203	1	9	15.6	15.6	15.9	9.2.7
7732501	1	11	3.5	3.7	4.7	9.2.7
6856804	1	17	-12.3	12.3	12.4	9.2.7
6721201	1	13	1.5	2.7	2.9	9.2.7
7715903	1	11	-6.7	6.7	7.1	9.2.7
6714801	1	17	3.9	3.9	4.0	9.2.7
7726605	3	108	-46.2	47.6	56.5	9.2.8
7608406	3	11	6.0	6.0	6.2	9.2.8
7722502	3	9	-47.3	47.3	52.1	9.2.8
6857402	3	12	-2.7	7.9	10.2	9.2.8
7733611	3	17	9.1	9.2	10.0	9.2.8
7711703	3	13	-11.0	19.6	23.5	9.2.8
6858302	3	14	-1.0	4.9	5.3	9.2.9
7826802	3	7	-32.8	32.8	35.3	9.2.9
7740305	3	12	12.4	12.4	12.7	9.2.9
7737301	3	15	64.9	66.3	69.8	9.2.9
7806507	3	7	-16.1	16.1	17.0	9.2.9
6853703	3	12	11.3	11.3	13.1	9.2.9
6721104	3	9	0.6	4.5	5.6	9.2.10
6727502	3	15	1.4	2.7	3.1	9.2.10
6856302	3	18	-2.4	3.9	4.5	9.2.10
6863101	3	16	2.2	8.1	9.8	9.2.10
6734402	3	8	10.3	10.3	10.3	9.2.10
7816601	3	13	-1.2	7.9	9.1	9.2.10
7737501	4	19	-49.4	49.4	53.6	9.2.11
7758301	4	5	7.5	21.4	22.4	9.2.11
7742801	4	17	-33.1	33.1	33.7	9.2.11
6859312	4	9	4.4	4.4	4.8	9.2.11
7704603	5	14	-36.4	41.8	50.4	9.2.12
6960201	5	13	4.0	5.0	5.6	9.2.12
6719608	5	16	1.8	3.1	3.6	9.2.12
6852713	5	26	10.2	10.3	11.7	9.2.12
6847601	5	11	9.0	9.1	9.7	9.2.12
6727806	5	33	-19.6	19.6	19.6	9.2.12
6733407	6	10	-17.9	17.9	18.4	9.2.13
6846902	6	6	-27.0	27.0	27.1	9.2.13
6712111	6	17	4.3	4.3	4.8	9.2.13
6955901	6	19	4.5	4.5	5.1	9.2.13

Table 9.2.3 Comparison of simulated stream leakance to LBG-Guyton and HDR (1998) simulated values (AFY per mile of stream)

Stream	LBG-Guyton / HDR		GAM	
	<i>Gaining</i>	<i>Losing</i>	<i>Gaining</i>	<i>Losing</i>
Cibolo Creek		100		31
Guadalupe River	50		62	
Nueces River		500		209
San Antonio River		325		108
San Marcos River	100		350	
San Miguel River		100		72
Frio River		500		104
Atascosa River		50		103

Table 9.2.4 Water budget for the transient model. All rates reported in AFY.

Year	Layer	GHBs	Reserv.	Wells	ET	Top	Bottom	Rech.	Streams	Storage
1980	1	37,679	0	-7,142	-51,703	0	-54,293	115,689	-193,735	152,555
	2	0	0	-13,264	-3,325	54,293	-30,954	18,379	-60,455	33,974
	3	0	0	-215,491	-76	30,954	-27,502	20,912	932	190,281
	4	0	0	-32,896	-139	27,502	2,797	1,055	-3,635	5,245
	5	0	3,050	-16,833	-2,761	-2,797	1,659	22,499	-23,679	18,851
	6	0	0	-14,748	-4,269	-1,659	0	14,476	-22,301	28,500
	Sum	37,679	3,050	-300,373	-62,272	108,293	-108,293	193,009	-302,872	429,407
1988	1	22,622	0	-6,604	-40,312	0	-50,983	55,416	-443,820	462,699
	2	0	0	-11,986	-2,913	50,983	-38,183	10,469	-484,424	475,007
	3	0	0	-191,034	-65	38,183	-18,667	17,914	-39,595	193,276
	4	0	0	-26,784	-12	18,667	4,099	3,413	-36,959	37,512
	5	0	3,196	-15,913	-3,339	-4,099	1,247	19,490	-92,135	91,535
	6	0	0	-10,219	-3,272	-1,247	0	13,838	-90,785	91,679
	Sum	22,622	3,196	-262,540	-49,914	102,487	-102,487	120,539	-1,187,718	1,351,707
1990	1	21,253	0	-8,335	-6,683	0	-56,068	171,951	171,766	-294,074
	2	0	0	-12,570	-680	56,068	-50,911	81,838	297,279	-371,279
	3	0	0	-199,913	-11	50,911	-18,423	91,366	15,830	60,249
	4	0	0	-25,799	0	18,423	7,067	20,882	21,287	-41,871
	5	0	4,065	-16,131	-2,337	-7,067	3,196	54,406	15,526	-51,679
	6	0	0	-10,944	-1,591	-3,196	0	38,095	41,684	-64,060
	Sum	21,253	4,065	-273,693	-11,302	115,138	-115,138	458,539	563,372	-762,713
1999	1	16,219	0	-7,963	-24,002	0	-60,527	78,495	-285,584	283,289
	2	0	0	-10,184	-3,339	60,527	-61,059	14,684	-303,657	302,899
	3	0	0	-201,371	-119	61,059	-8,445	16,206	-49,437	182,117
	4	0	0	-19,319	-36	8,445	9,695	1,922	-24,294	23,583
	5	0	1,742	-13,936	-2,193	-9,695	2,920	11,188	-65,572	75,528
	6	0	0	-10,788	-1,654	-2,920	0	8,517	-55,197	62,032
	Sum	16,219	1,742	-263,560	-31,342	117,416	-117,416	131,013	-783,740	929,448

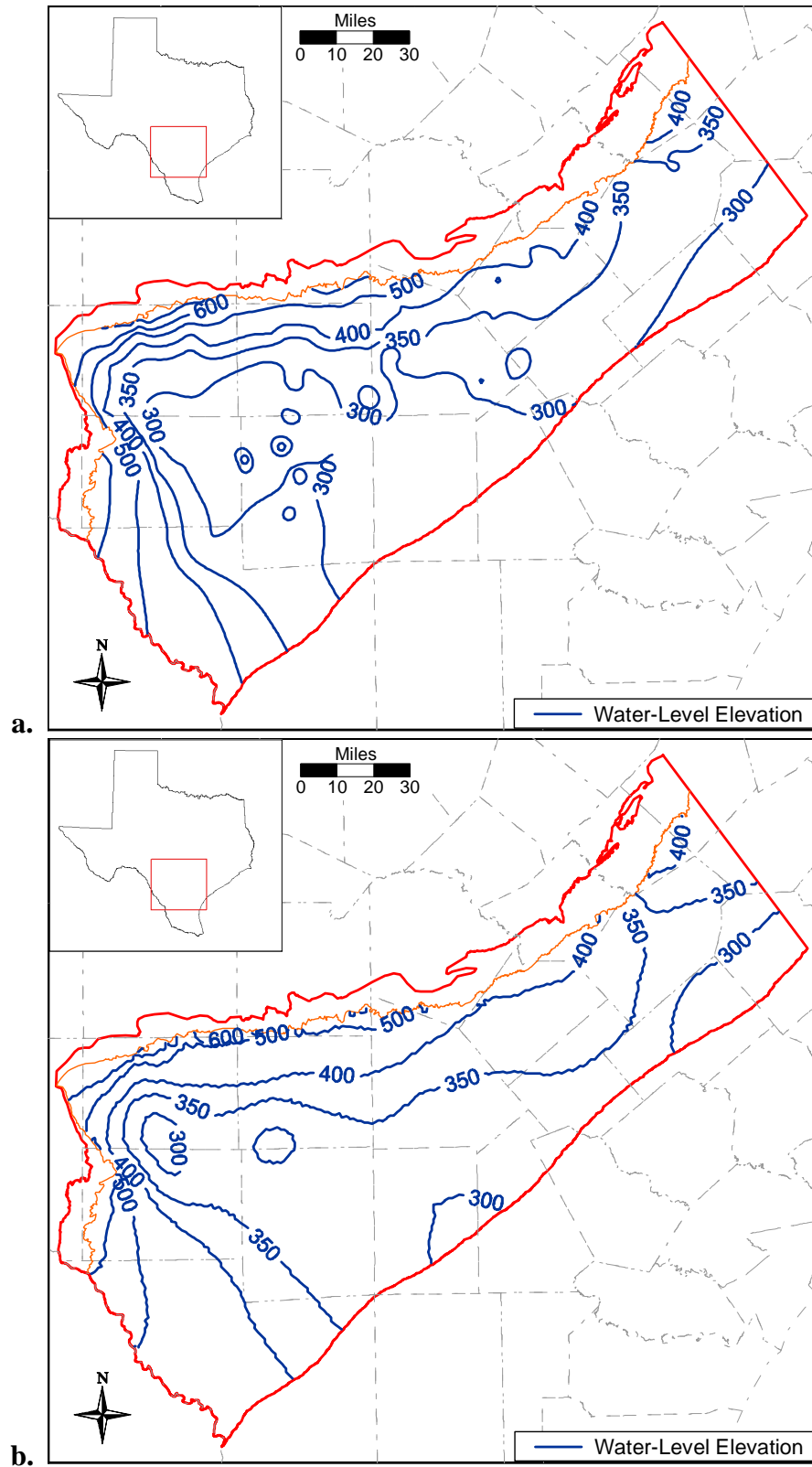


Figure 9.2.1 Comparison between 1989 measured (a) and simulated (b) heads in the Carrizo formation (Layer 3).

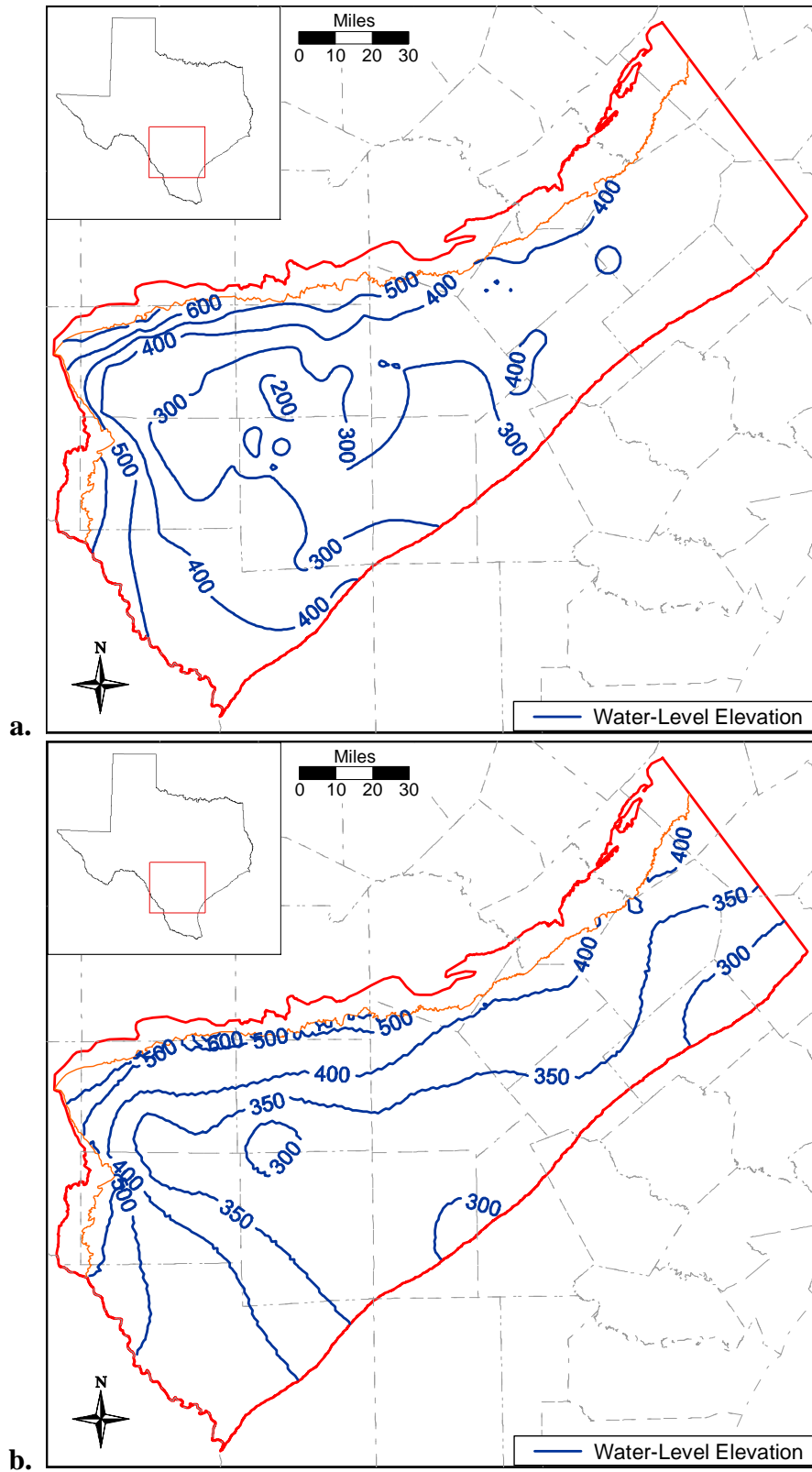


Figure 9.2.2 Comparison between 1999 measured (a) and simulated (b) heads in the Carrizo formation (Layer 3).

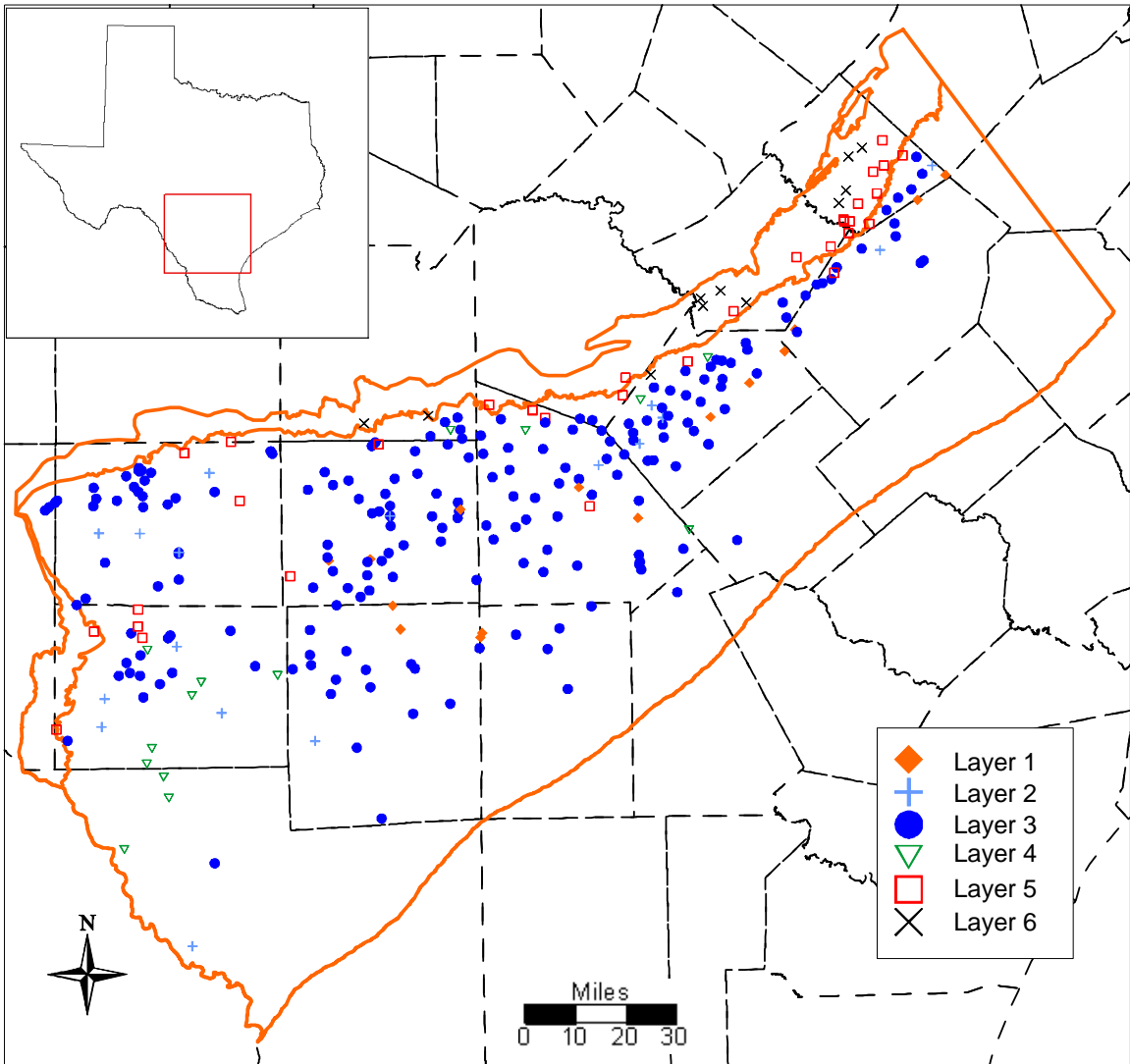


Figure 9.2.3 Locations of hydrograph wells for the transient model.

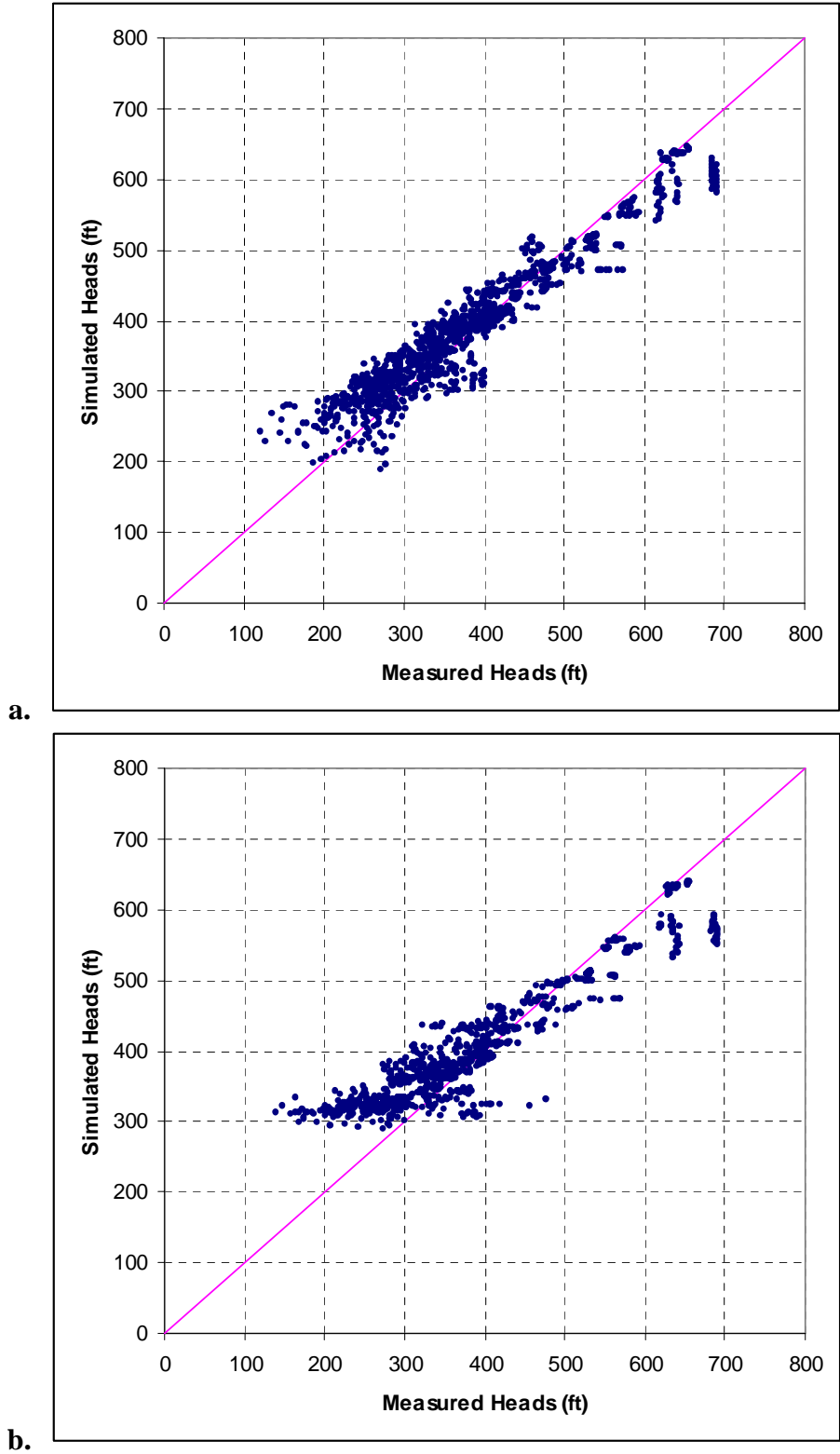
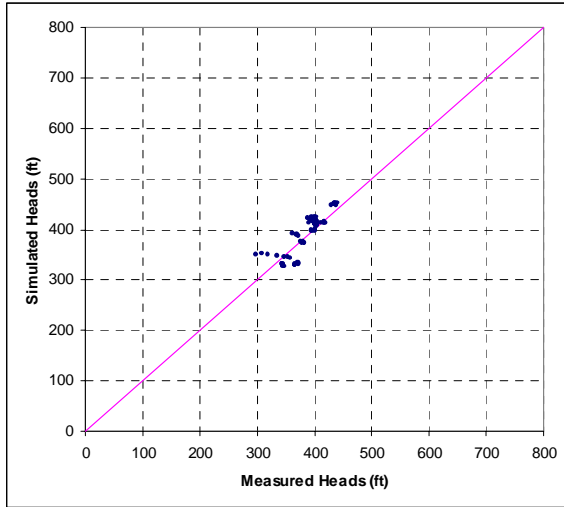
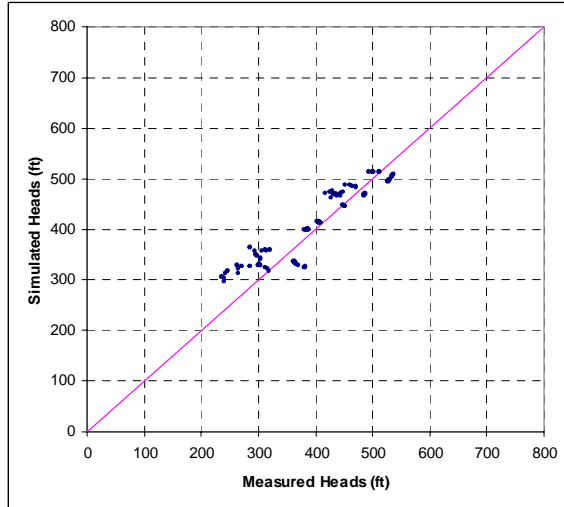


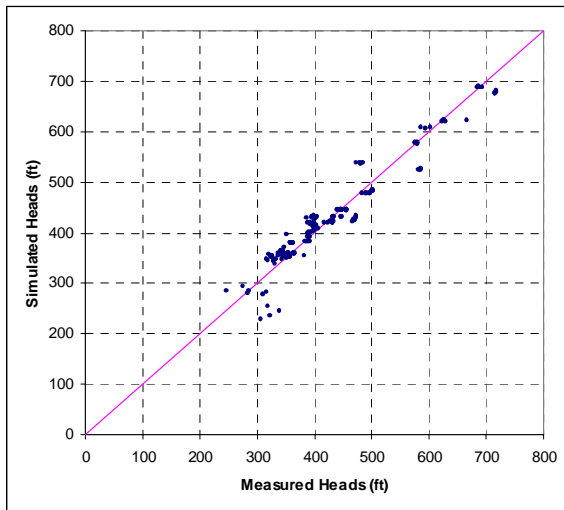
Figure 9.2.4 Calibration period (a) and verification period (b) crossplots for the Carrizo formation (Layer 3) in the calibrated transient model.



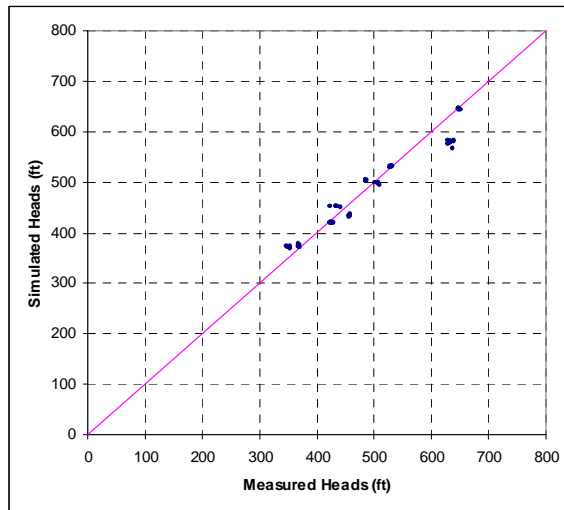
El Pico/Queen City



Upper Wilcox

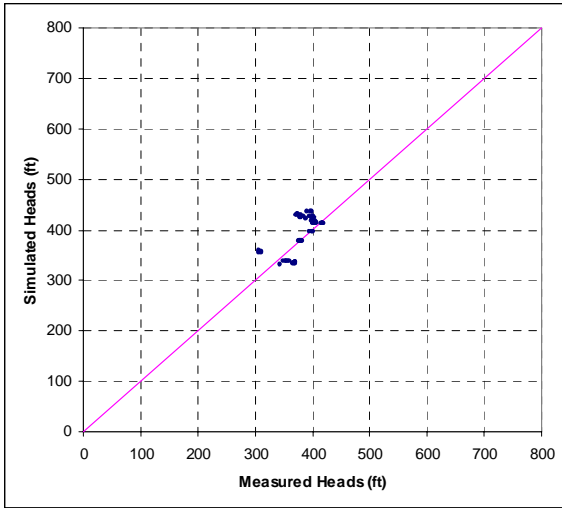


Middle Wilcox

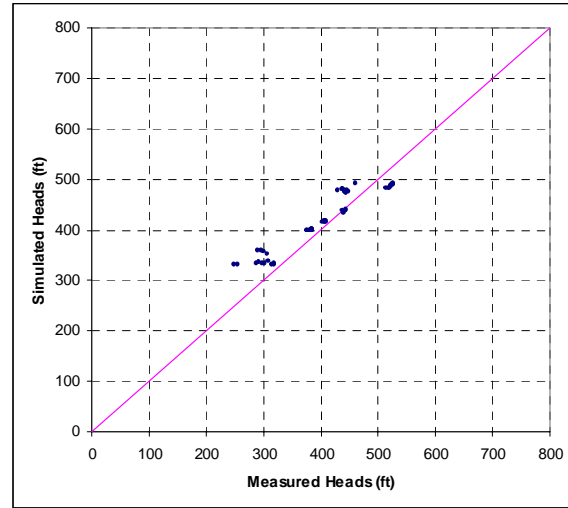


Lower Wilcox

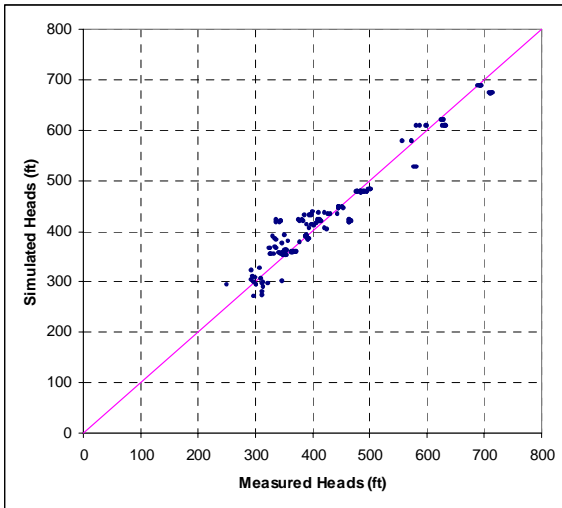
Figure 9.2.5 Calibration period crossplots for the calibrated transient model.



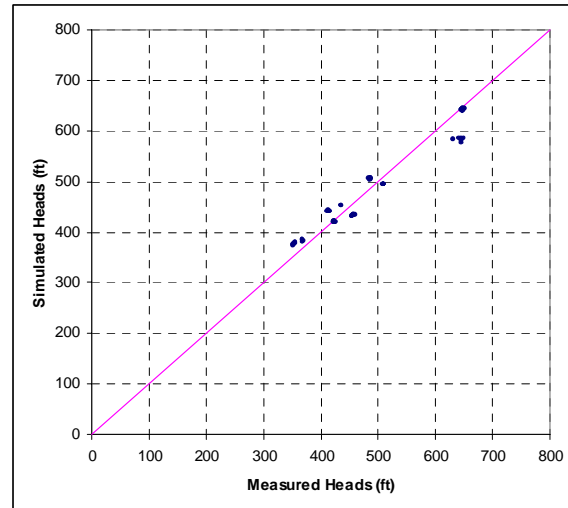
El Pico/Queen City



Upper Wilcox



Middle Wilcox



Lower Wilcox

Figure 9.2.6 Verification period crossplots for the calibrated transient model.

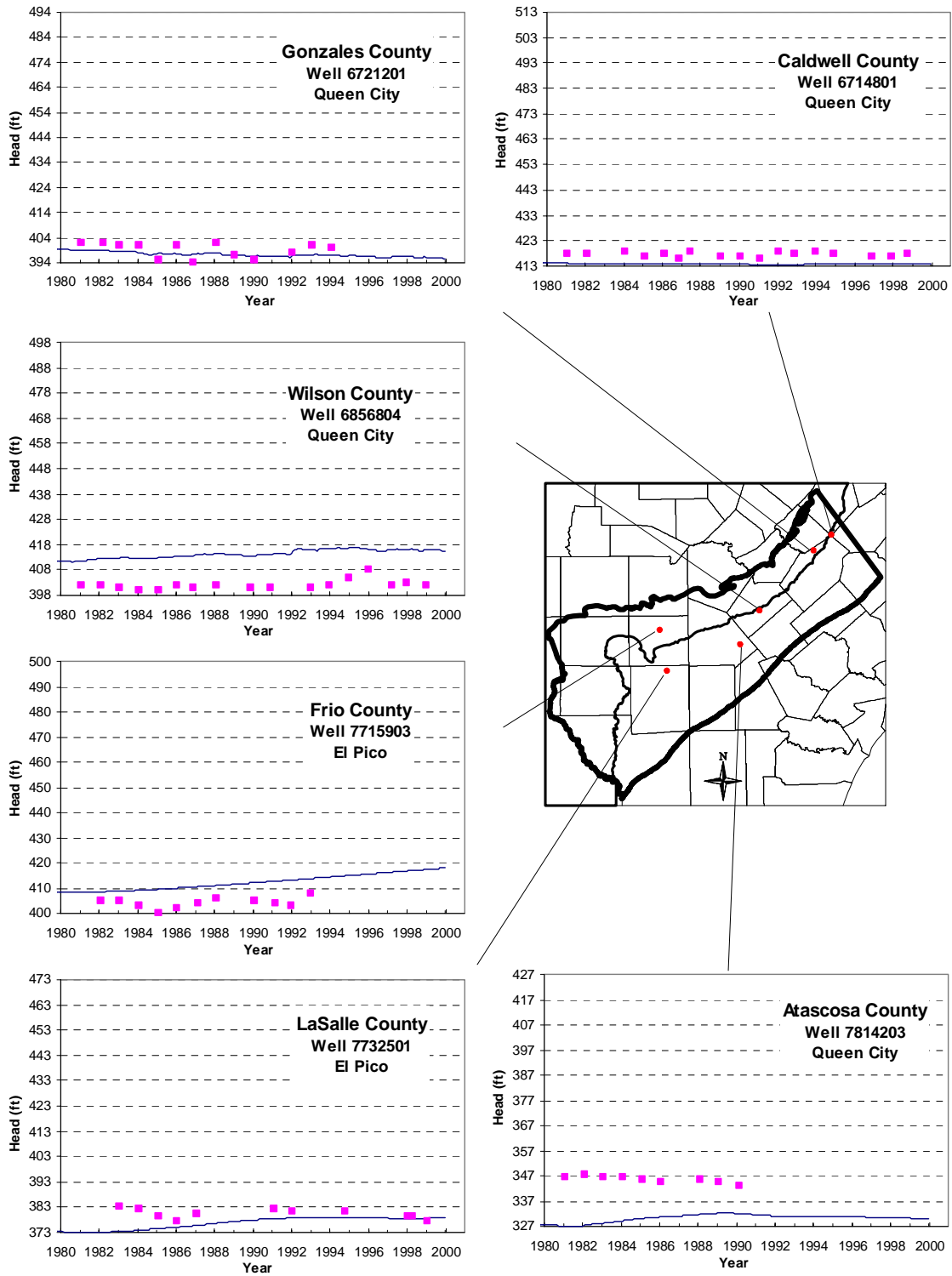


Figure 9.2.7 Transient model hydrographs from the Queen City/El Pico (Layer 1).

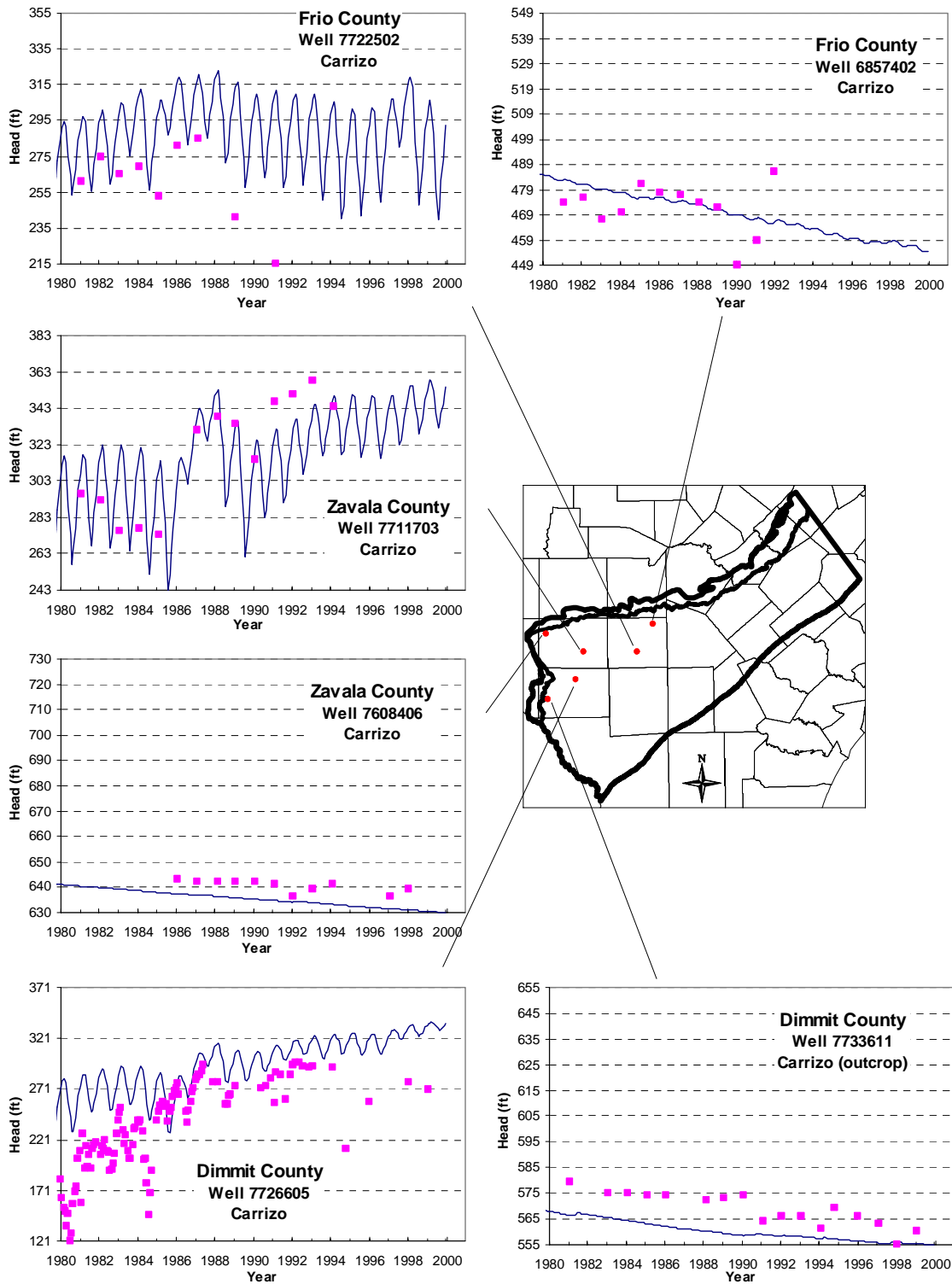


Figure 9.2.8 Transient model hydrographs from the Carrizo (Layer 3), West.

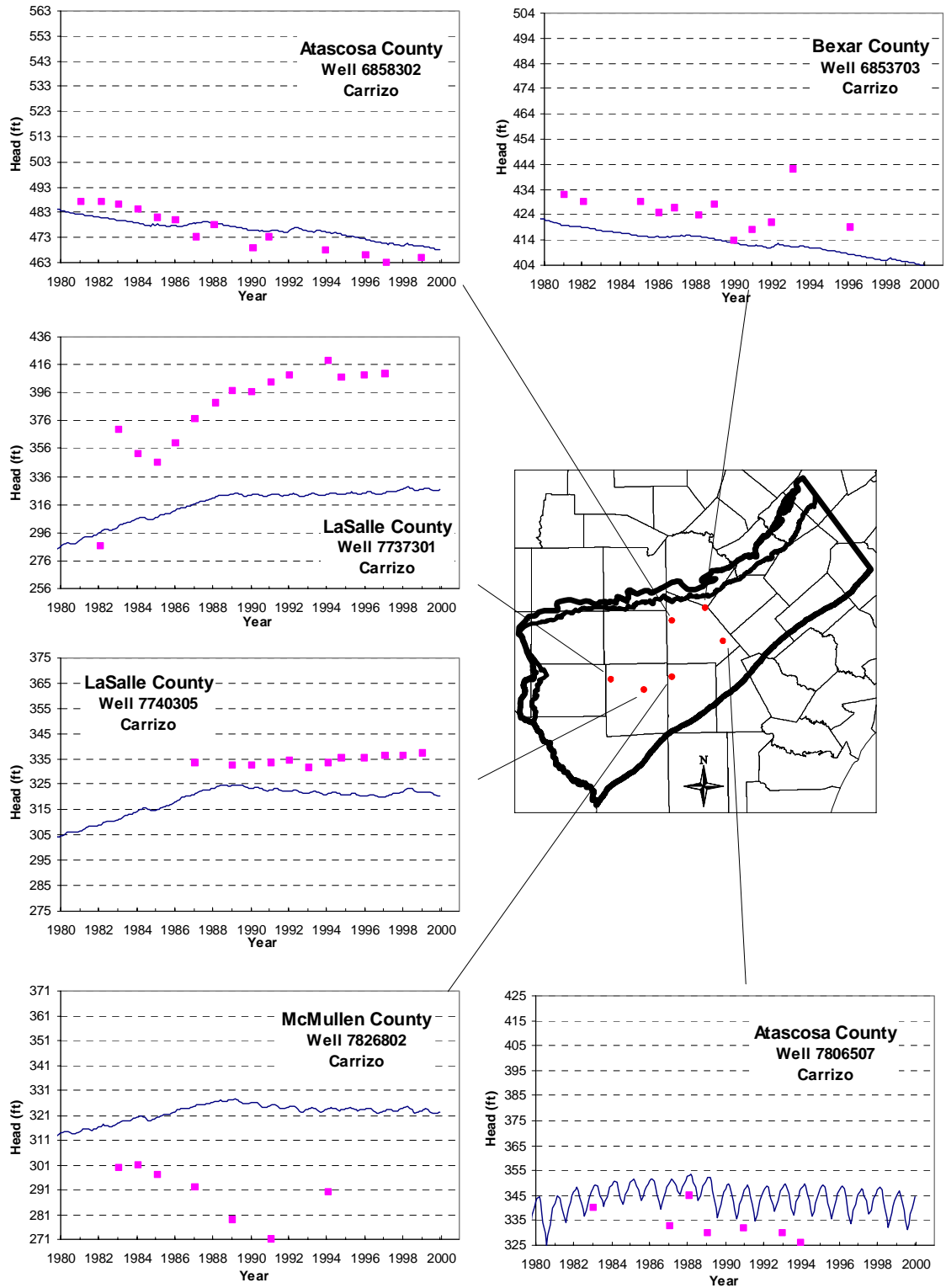


Figure 9.2.9 Transient model hydrographs from the Carrizo (Layer 3), Central.

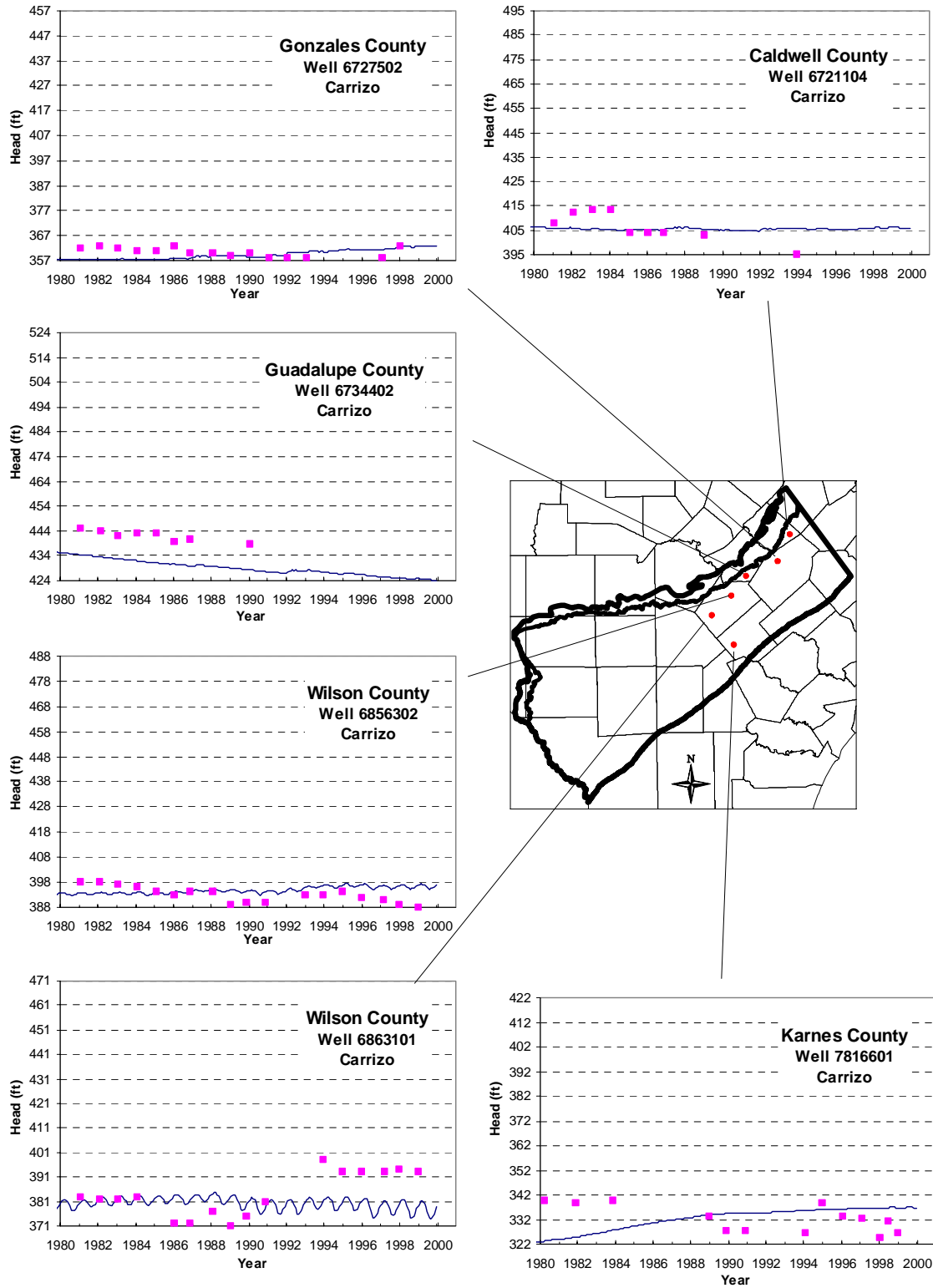


Figure 9.2.10 Transient model hydrographs from the Carrizo (Layer 3), East.

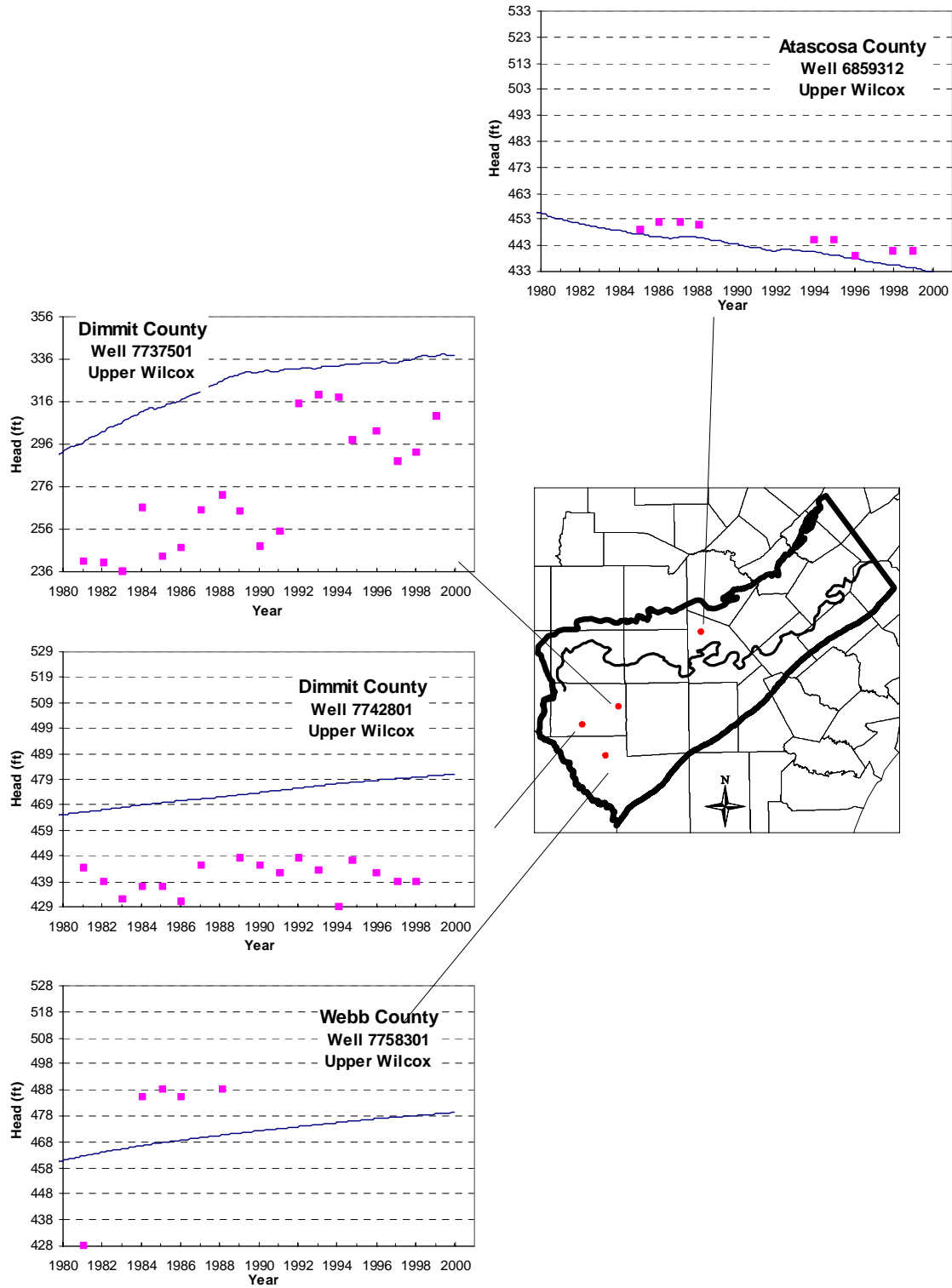


Figure 9.2.11 Transient model hydrographs from the upper Wilcox (Layer 4).

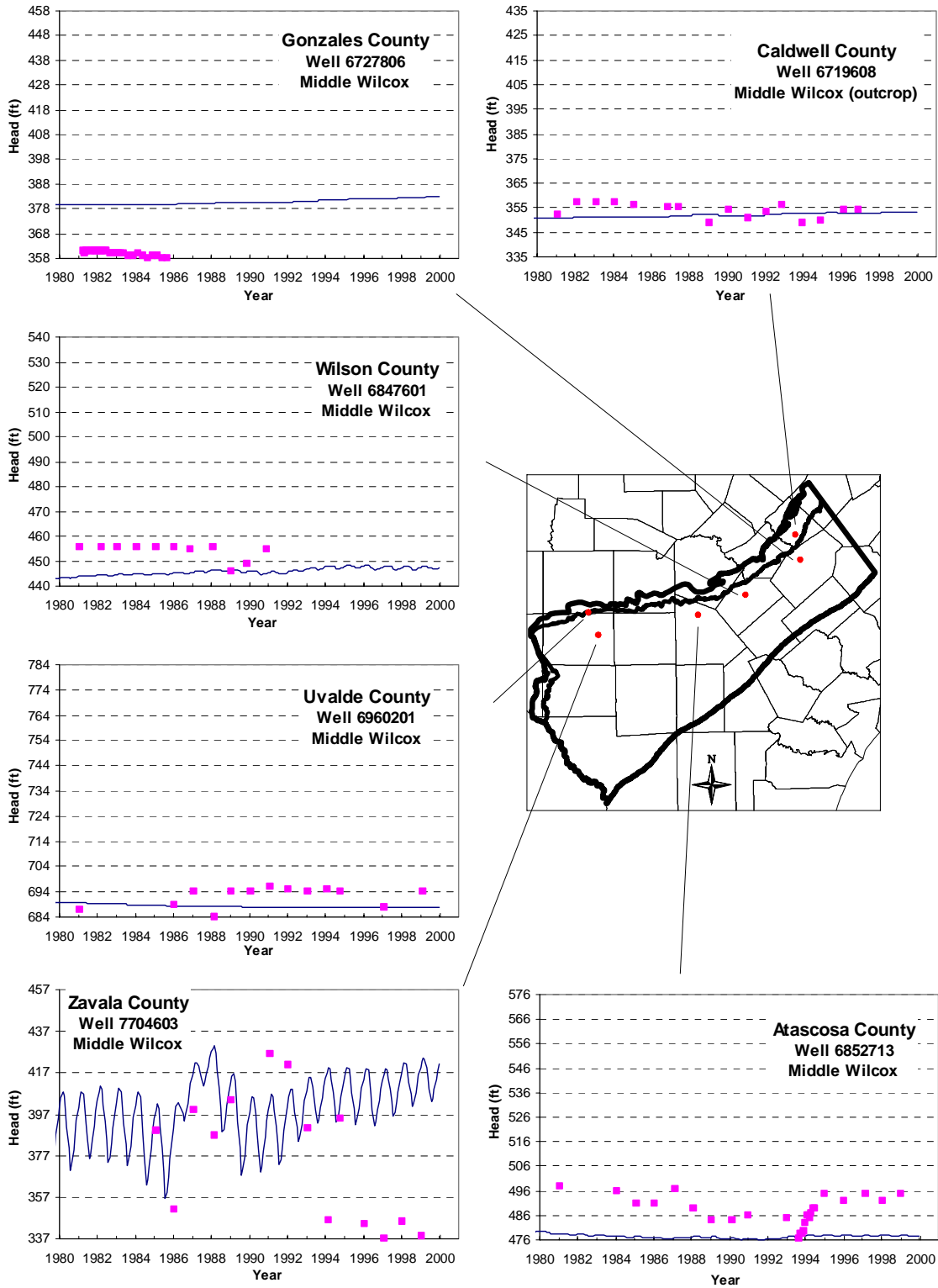


Figure 9.2.12 Transient model hydrographs from the middle Wilcox (Layer 5).

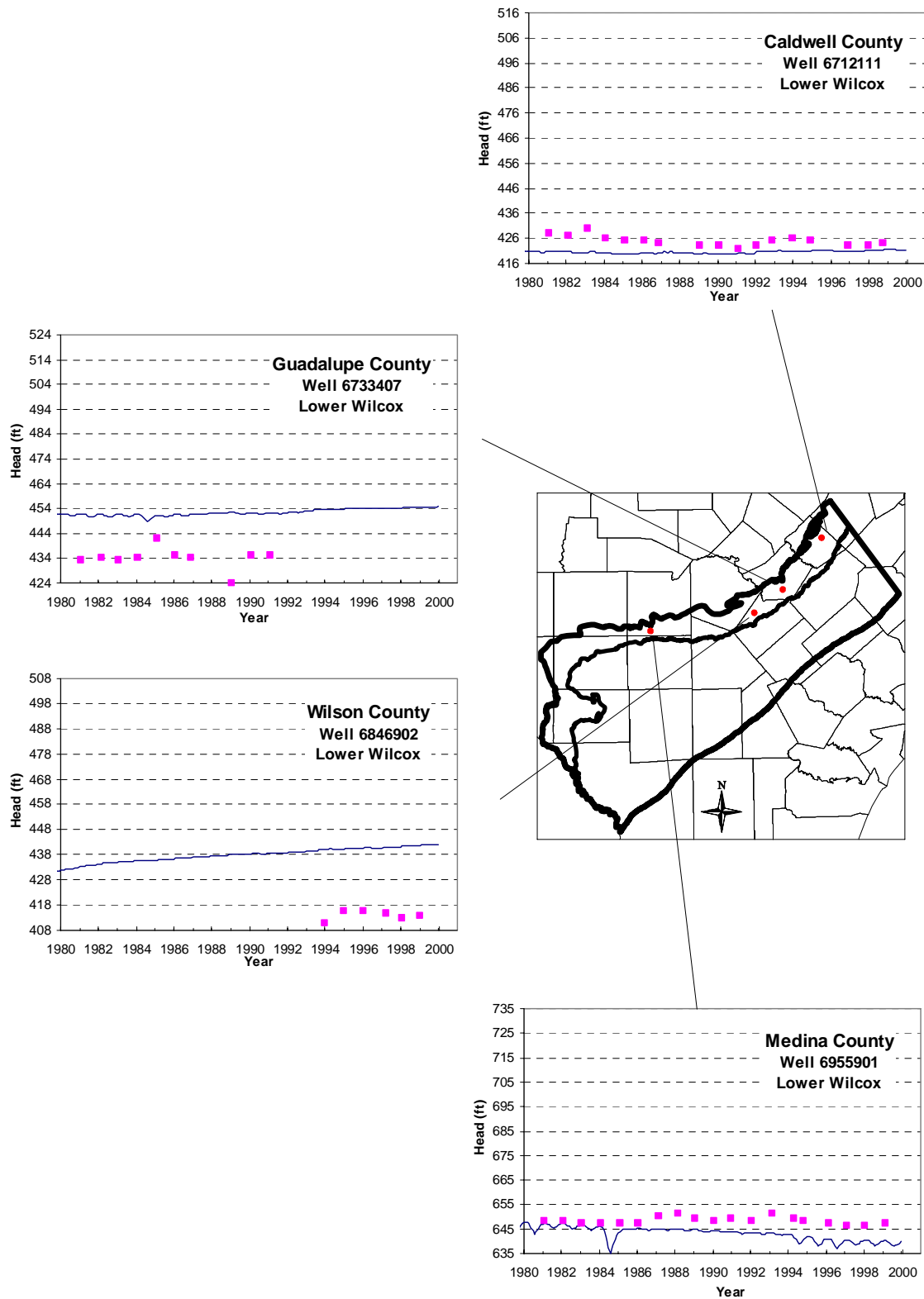


Figure 9.2.13 Transient model hydrographs from the lower Wilcox (Layer 6).

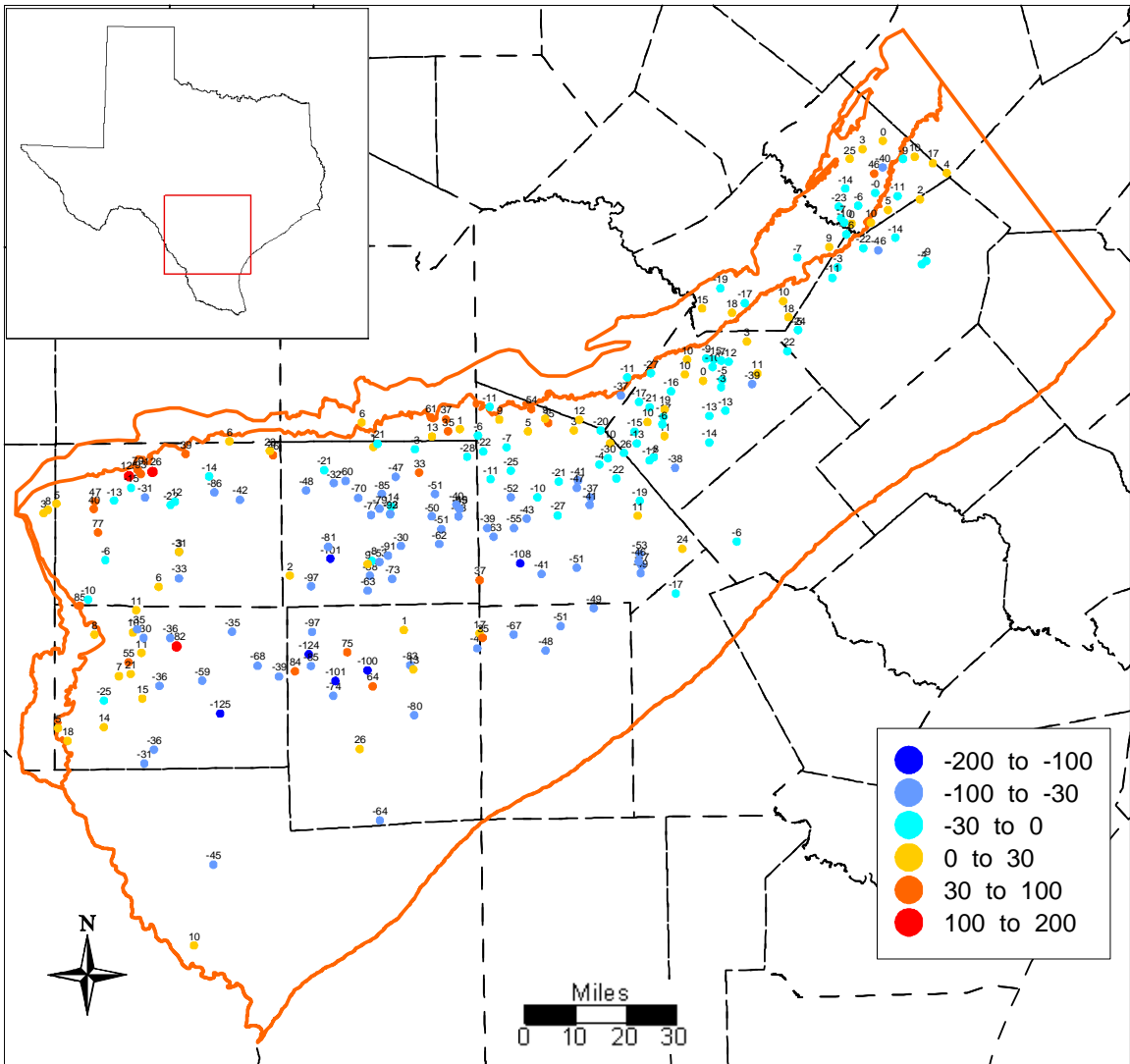


Figure 9.2.14 Average residuals for the verification period (1990-1999) in the Carrizo Formation (Layer 3).

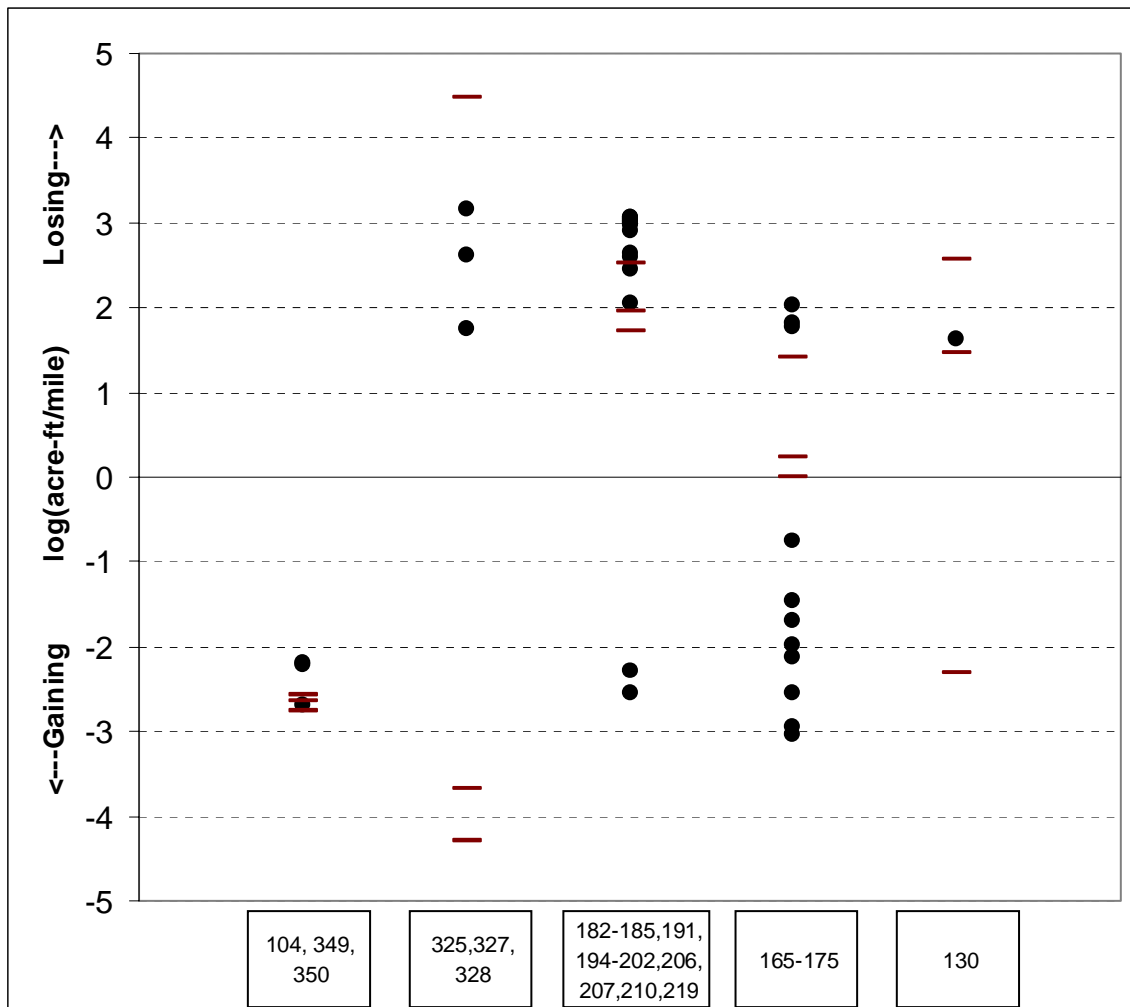


Figure 9.2.15 Comparison of Slade et al. (2002) with average simulated stream gain/loss.

Note: The horizontal lines represent the 10th, 50th, and 90th percentile simulated gains/losses, while the solid circles represent the Slade et al. (2002) measured values.

9.3 Sensitivity Analysis

Section 8.3 discusses the approach for the sensitivity analysis for the steady-state model. The sensitivity analysis for the transient model was performed similar to the steady-state model. However, some additional sensitivity simulations were added for the transient model to account for the addition of storage and pumping as model parameters.

Ten parameter sensitivity simulations were performed for the transient model. These are listed below.

1. Horizontal hydraulic conductivity, model-wide (K_h)
2. Vertical hydraulic conductivity in Layer 2 (K_v -Reklaw, model leakance between Layers 2 and 3)
3. Vertical hydraulic conductivity in Layers 4-6 (K_v -Wilcox, model leakance between layers 3-4, 4-5, and 5-6)
4. Recharge, model-wide
5. Streambed conductance, model-wide (K-Stream)
6. GHB conductance, model-wide (K-GHB)
7. Storativity in the Carrizo (S-Carrizo)
8. Specific yield, model-wide (S_y)
9. Pumping rate
10. Reservoir conductivity (K-Reservoir)

Equation 8-2 (varying linearly) was used for sensitivities 4, 8, and 9, and Equation 8-3 for the rest of the sensitivities listed above.

As with the steady-state model, we checked the difference between applying equation 8-4 at all grid blocks or only at grid blocks where targets were present. Figure 9.3.1 shows the transient sensitivity results for the Carrizo (Layer 3) calculated for the target gridblocks and Figure 9.3.2 shows the transient sensitivity results for the Carrizo (Layer 3) calculated at all gridblocks. As with the steady-state model, the order of the first four most sensitive parameters is the same for both methods. This indicates an adequate target coverage in this layer. Figure 9.3.2 shows that the most positively correlated parameter for the Carrizo is horizontal hydraulic conductivity. The most negatively correlated parameter for the Carrizo is pumping.

This is an important result because these parameters were changed very little during calibration (Section 9.2.1). The third most important parameter is the vertical hydraulic conductivity of the Reklaw/Bigford (Layer 2). This parameter was significantly adjusted during calibration. Contrast the results of this sensitivity with that of the steady-state model. In the steady-state model, recharge and GHB conductivity were the dominant parameters. In the transient model, hydraulic heads are much less sensitive to these parameters. This difference is another indication of the importance of calibrating to different hydrologic scenarios to improve the uniqueness of the calibrated parameter values.

Figure 9.3.3 shows the transient sensitivity results for Layer 1. The results are similar to the Carrizo, except that the GHB conductance has a significant *MD*. Since the GHBs are all attached directly to Layer 1, this is an expected result. Figure 9.3.4 shows the transient sensitivity results for the Reklaw/Bigford (Layer 2), which are similar to the Carrizo. Figures 9.3.5 and 9.3.6 show the transient sensitivity results for the upper Wilcox (Layer 4) and the middle Wilcox (Layer 5), which are also similar to the Carrizo. In the sensitivity results for the lower Wilcox (Layer 6), which are shown in Figure 9.3.7, the vertical conductivity of the Wilcox appears as a sensitive parameter with a significant *MD*. The lower Wilcox can only communicate with the rest of the model through the middle Wilcox, as the lower Wilcox is simulated as impermeable on the base of the formation at the Midway contact. So this sensitivity result is expected.

Figure 9.3.8 shows the sensitivity results for all layers, where horizontal hydraulic conductivity is varied. The layer with the greatest mean head difference is the Carrizo, indicating that this is the layer that is most affected by horizontal flow. We noted previously in this section that drawdowns in the Carrizo were most sensitive to pumping and horizontal hydraulic conductivity. During initial attempts at calibration, the Reklaw and Wilcox were more vertically conductive and heads in the Carrizo were far less sensitive to pumping or horizontal hydraulic conductivity. Reducing the vertical conductivity in the layers above and below the Carrizo brought the model to an inflection point with respect to its sensitivity to horizontal flow parameters. This sensitivity indicates that the model is currently better constrained than during initial calibration.

Figures 9.3.9 and 9.3.10 show the results for all layers for the recharge and specific yield sensitivities. Note that the maximum mean difference for both of these sensitivities is less than 1 ft. These figures indicate that recharge and specific yield, which should be most important in the outcrop, do not have a large overall effect on the heads in the model.

Figure 9.3.11 shows the effect of varying horizontal hydraulic conductivity on several Carrizo (Layer 3) hydrographs. In general, these hydrographs show a trend that is similar to Figure 9.3.8, i.e. hydraulic head decreases when horizontal hydraulic conductivity is decreased. This trend occurs where pumping is a significant stress. The hydrograph that is an exception to this trend is from Well 6858302 in Atascosa County. This hydrograph shows an increased head with decreased hydraulic conductivity. This trend is likely due to a combination of two factors: (1) head near this well is only weakly affected by pumping, and (2) the well is near the outcrop, where water flows in from recharge and losing streams, so decreasing horizontal hydraulic conductivity causes hydraulic head to build up. Figure 9.3.12 shows the effect of varying pumping rate on several Carrizo (Layer 3) hydrographs. All of these hydrographs display the trend of decreased hydraulic head with increased pumping. Hydrographs from wells in the western portion of the model show a larger change than hydrographs from wells in the eastern portion, simply due to the higher amount of pumping in the west during the simulated period.

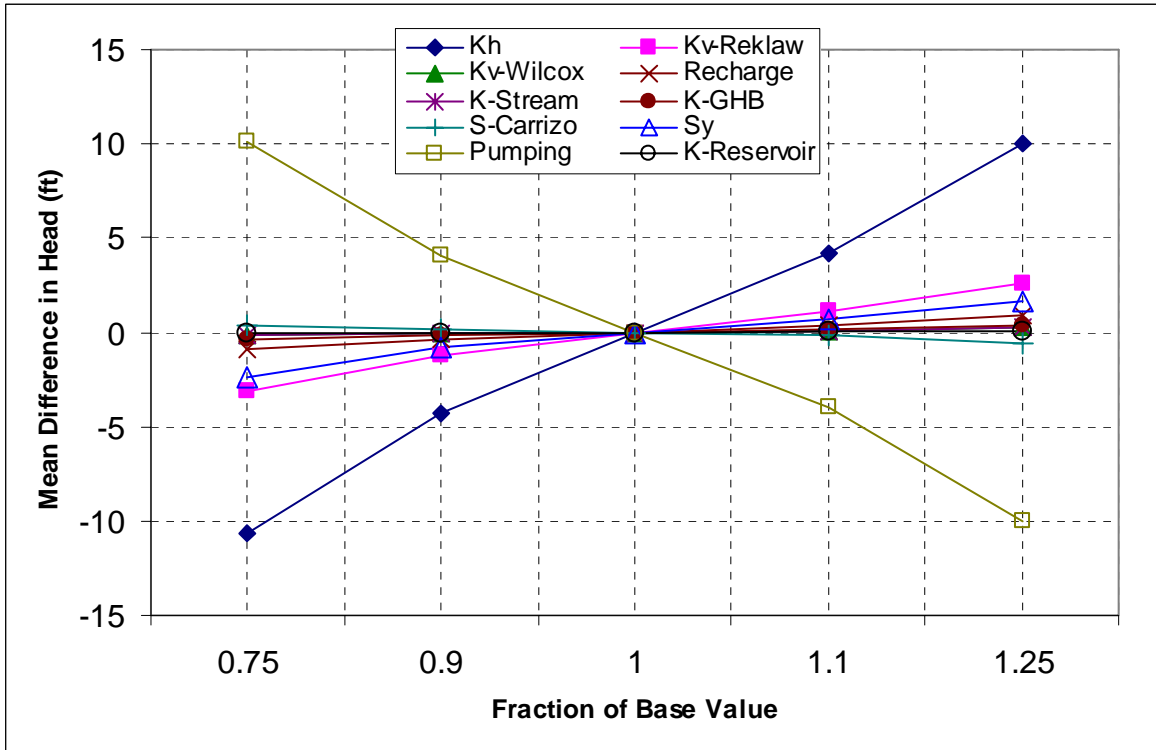


Figure 9.3.1 Transient sensitivity results for the Carrizo (Layer 3) using target locations.

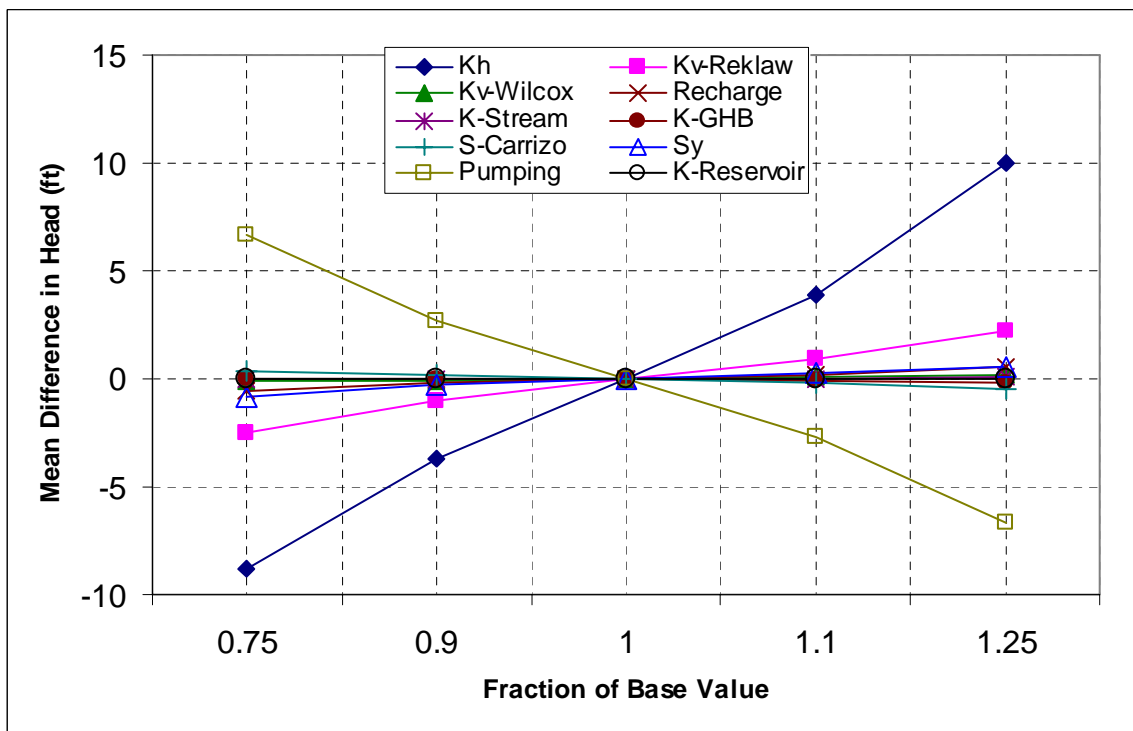


Figure 9.3.2 Transient sensitivity results for the Carrizo (Layer 3) using all active gridblocks.

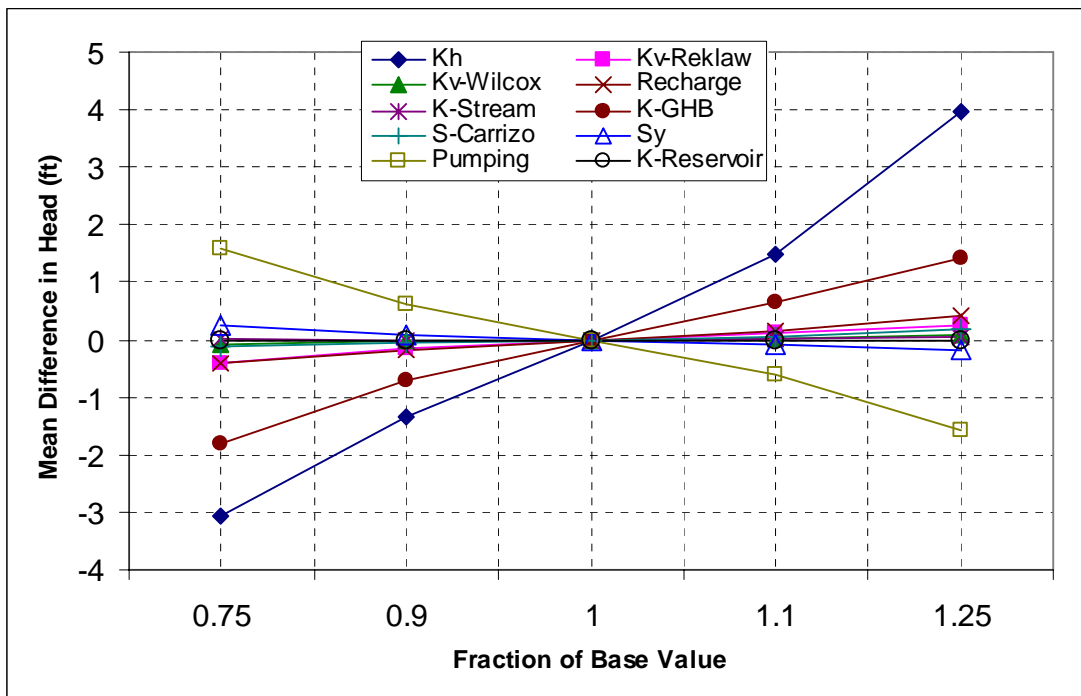


Figure 9.3.3 Transient sensitivity results for the Queen City/El Pico (Layer 1) using all active gridblocks.

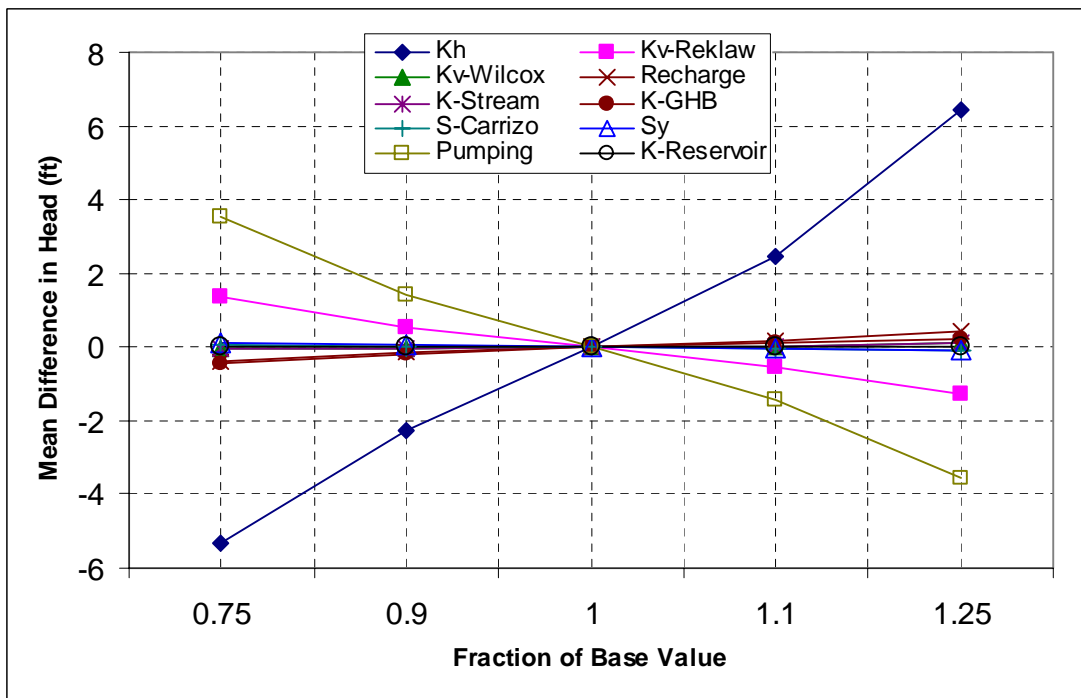


Figure 9.3.4 Transient sensitivity results for the Reklaw/Bigford (Layer 2) using all active gridblocks.

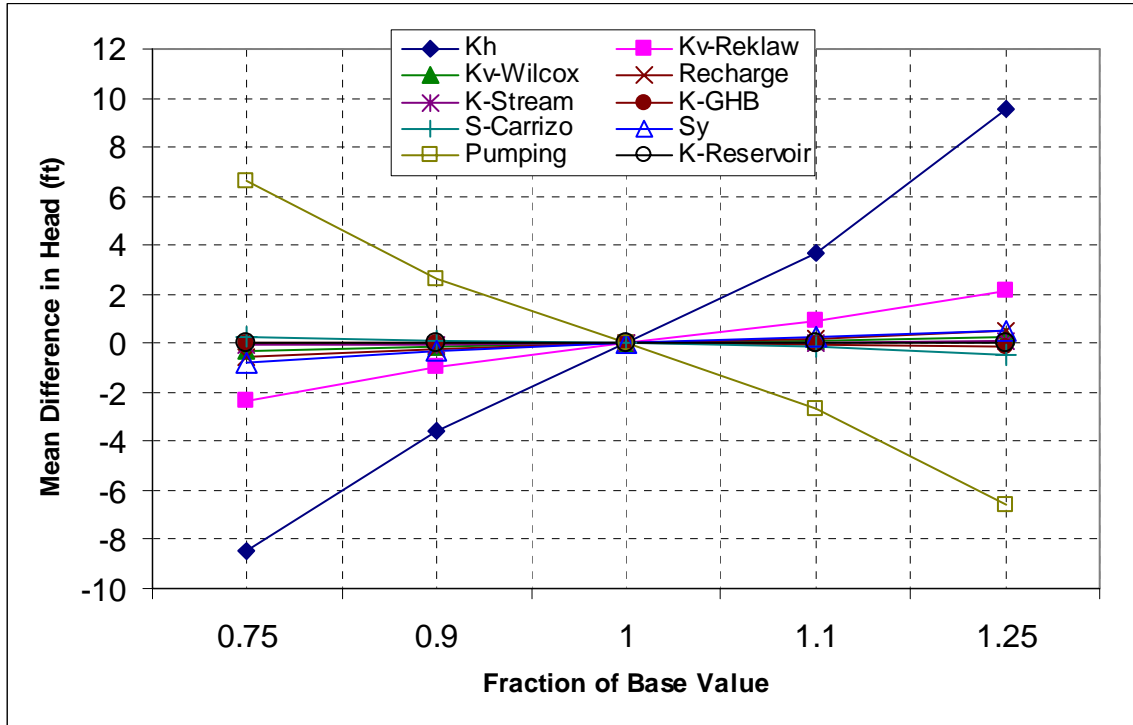


Figure 9.3.5 Transient sensitivity results for the upper Wilcox (Layer 4) using all active gridblocks.

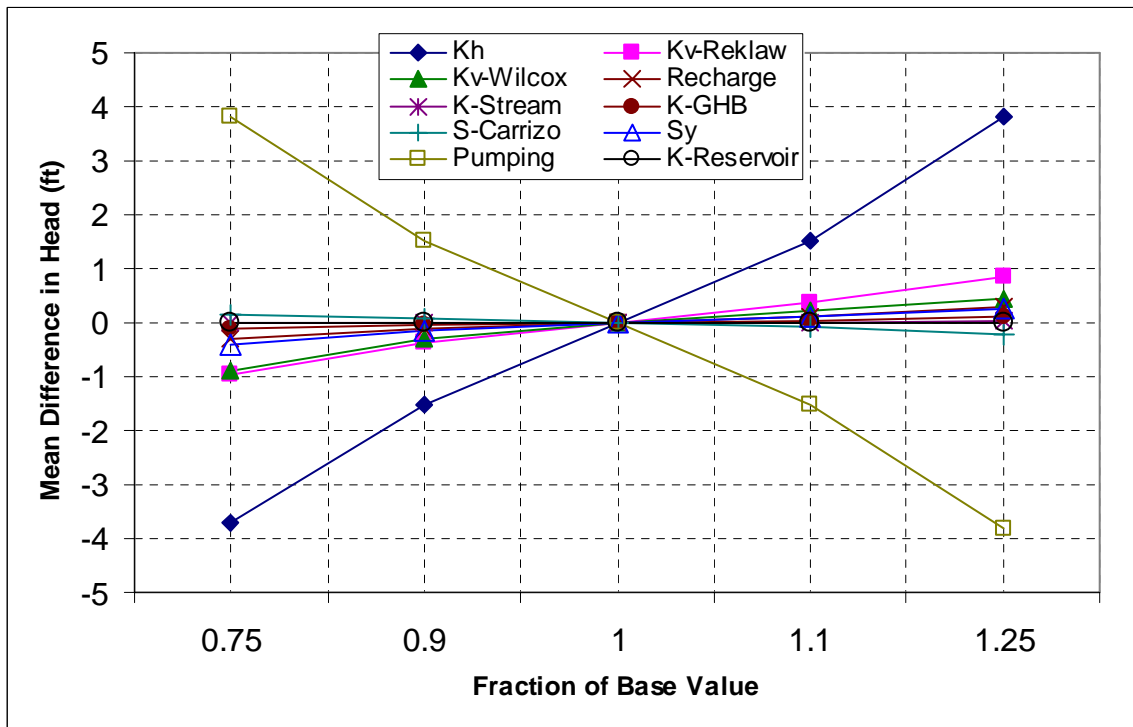


Figure 9.3.6 Transient sensitivity results for the middle Wilcox (Layer 5) using all active gridblocks.

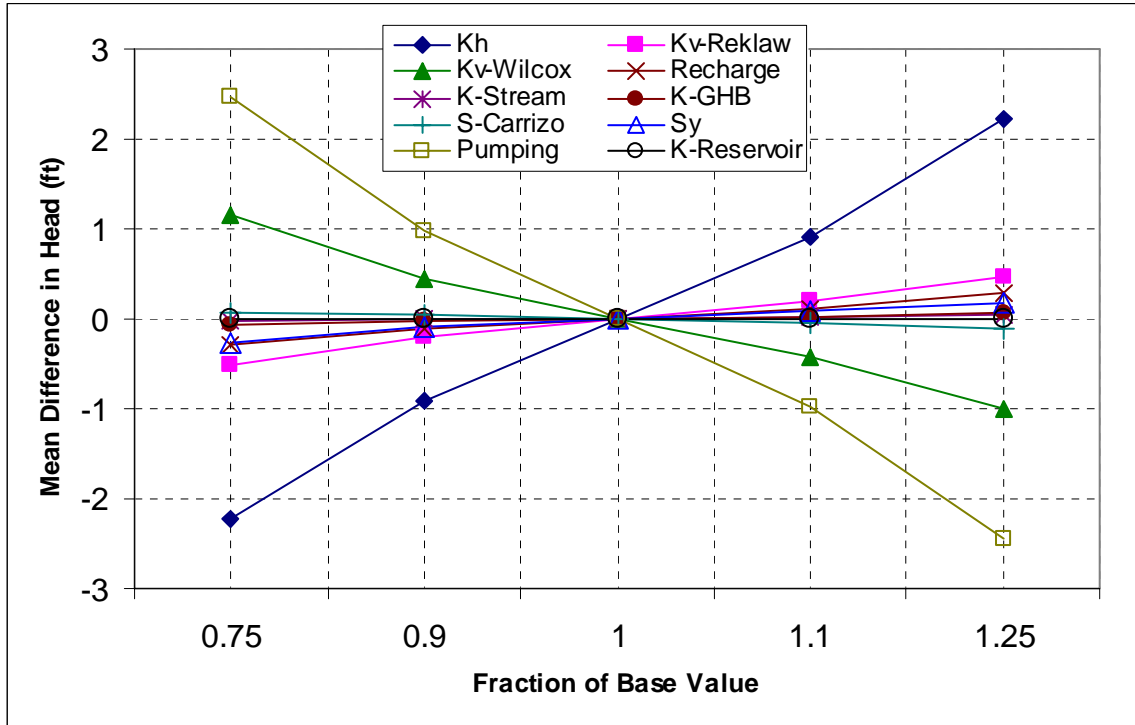


Figure 9.3.7 Transient sensitivity results for the lower Wilcox (Layer 6) using all active gridblocks.

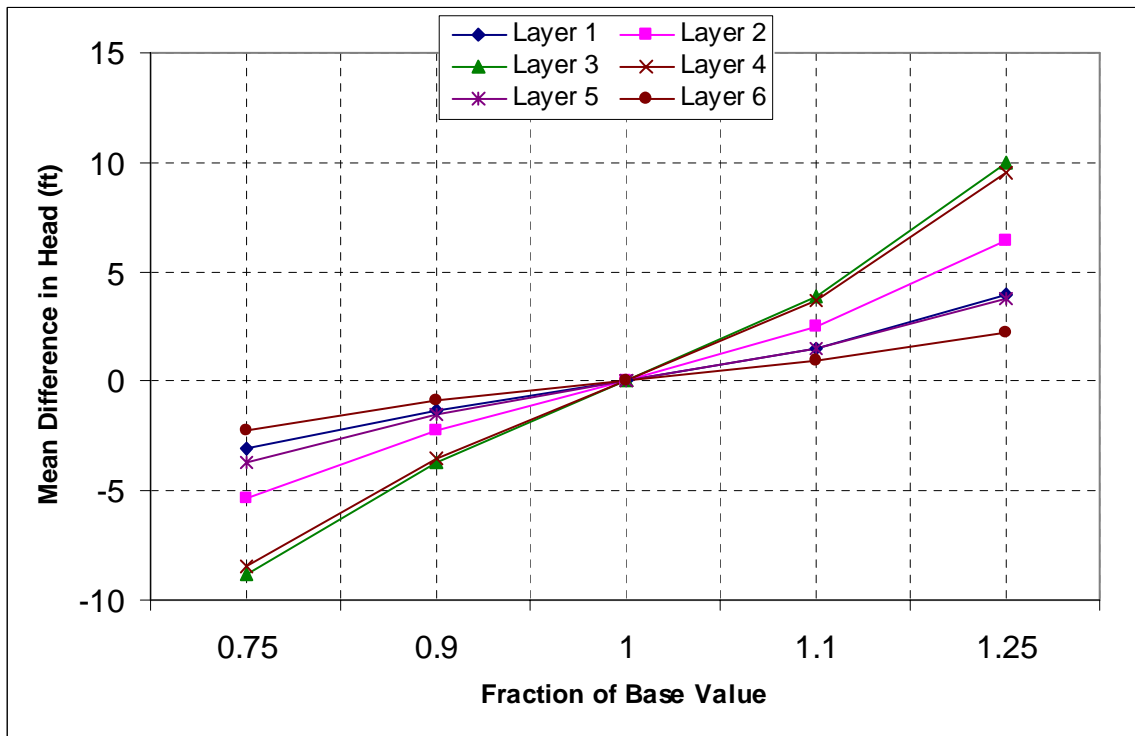


Figure 9.3.8 Transient sensitivity results where the horizontal hydraulic conductivities for all layers are varied.

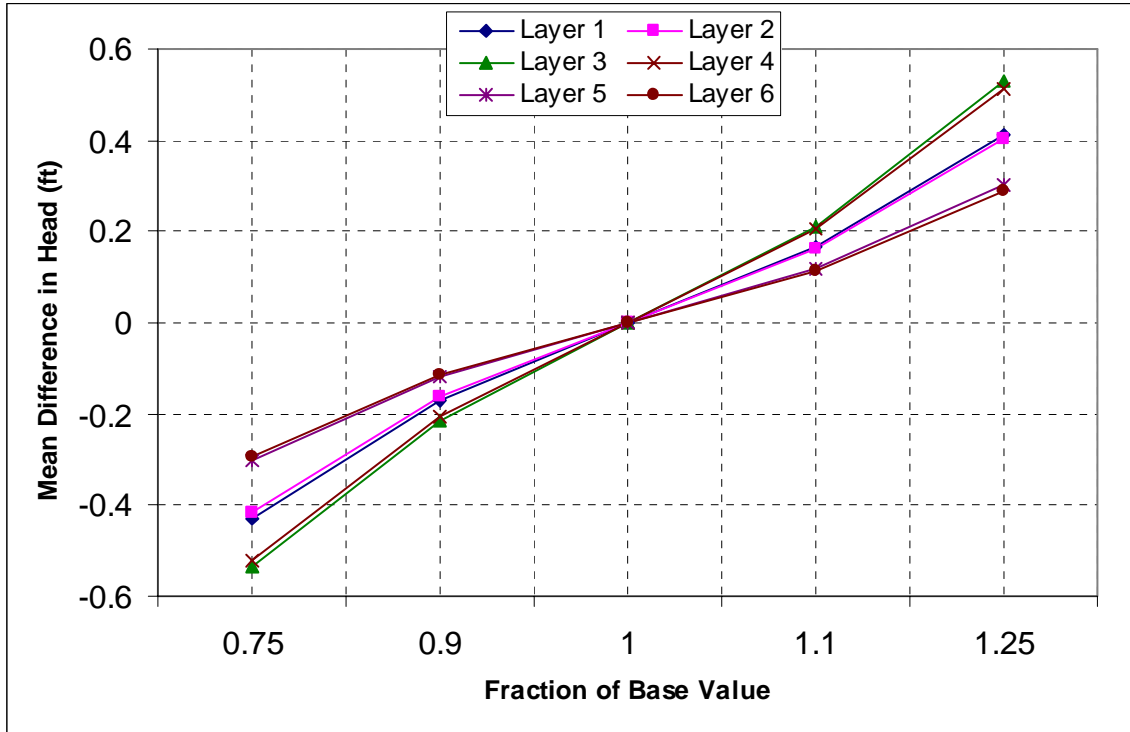


Figure 9.3.9 Transient sensitivity results where recharge is varied.

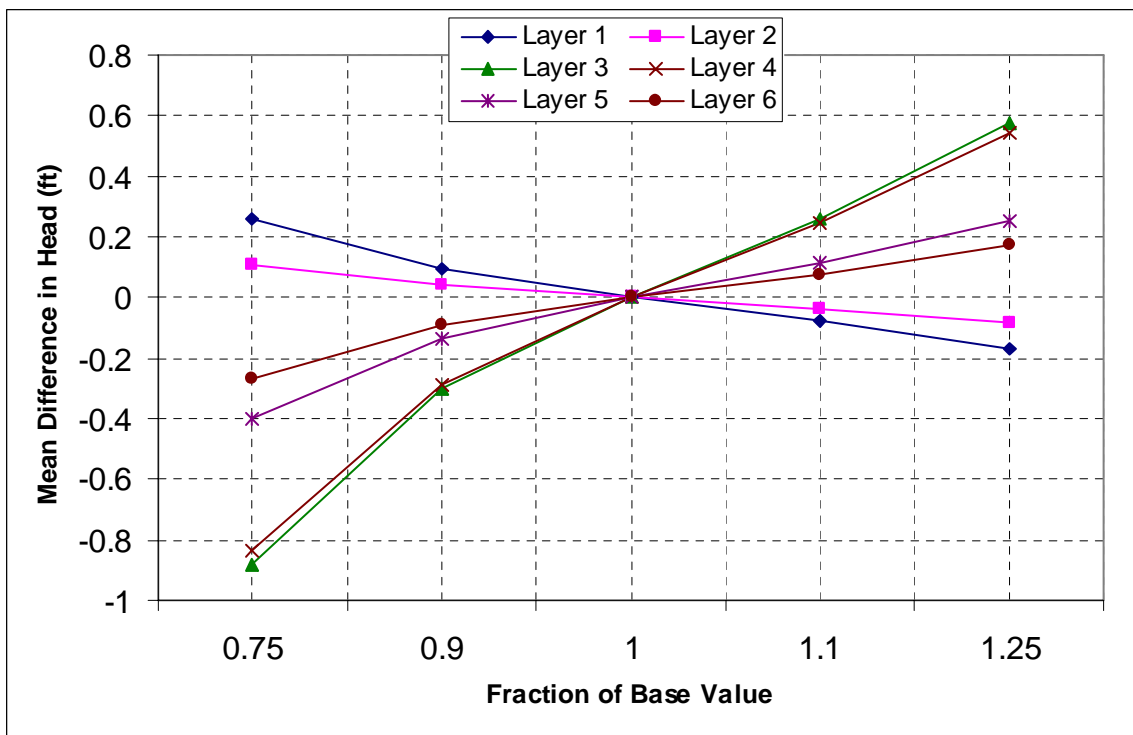


Figure 9.3.10 Transient sensitivity results where specific yield is varied.

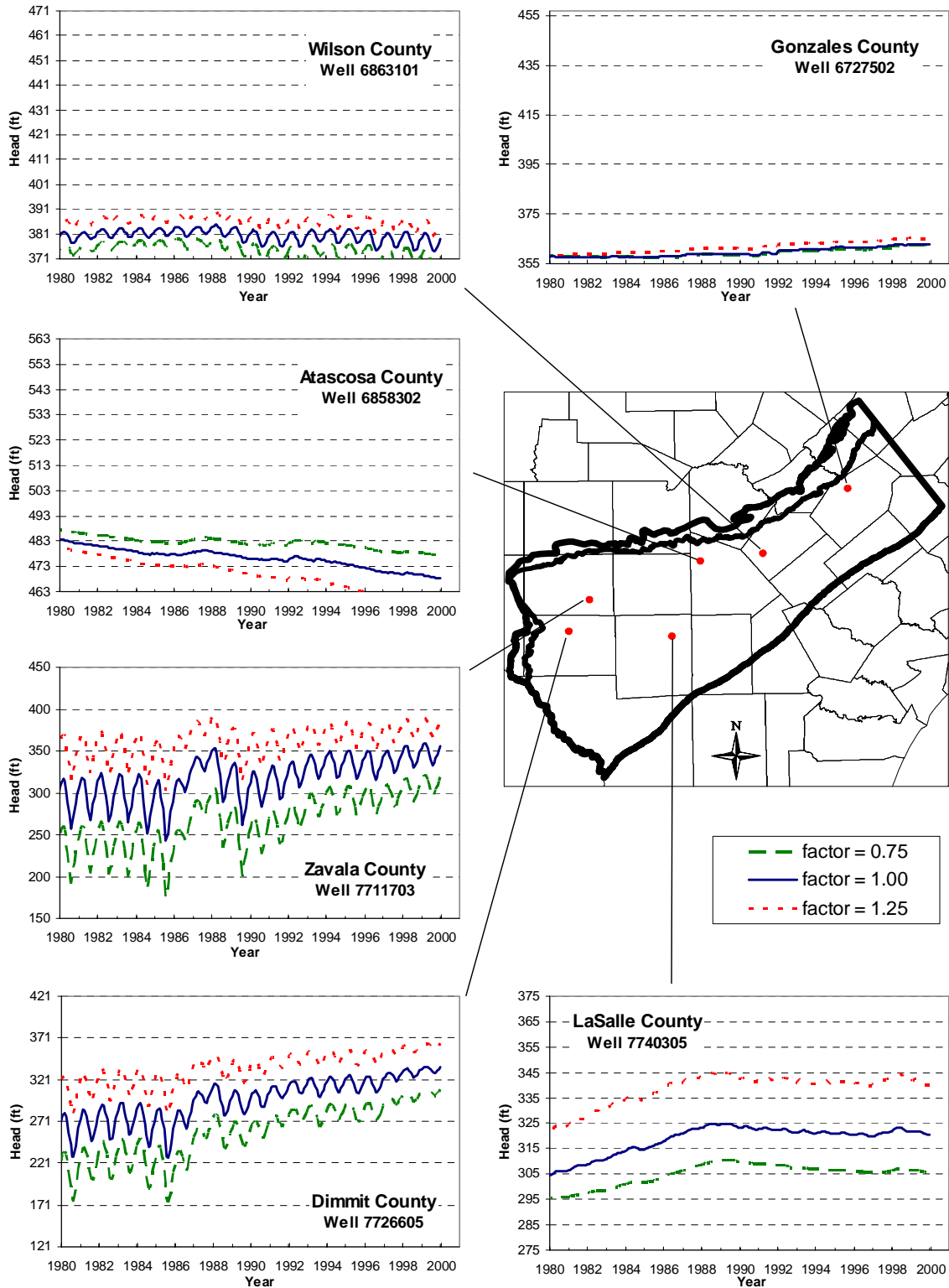


Figure 9.3.11 Transient sensitivity hydrographs from the Carrizo (Layer 3) where the horizontal hydraulic conductivities for all layers are varied.

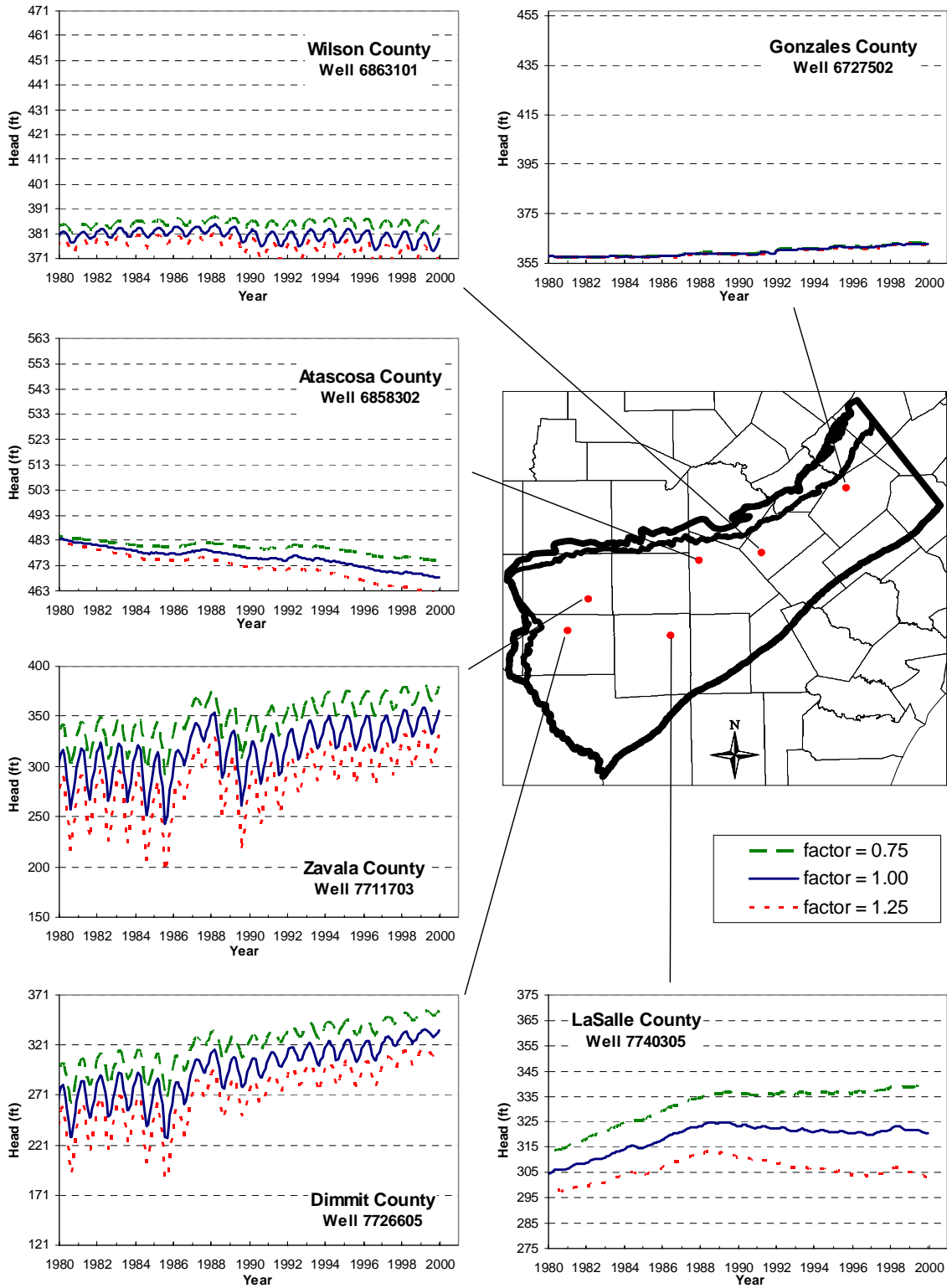


Figure 9.3.12 Transient sensitivity hydrographs from the Carrizo (Layer 3) where pumping rate is varied.

10.0 MODEL PREDICTIVE SIMULATIONS

The purpose of the GAM is to assess groundwater availability within the modeled Southern Carrizo-Wilcox GAM region over a 50-year planning period (2000-2050) using Regional Water Planning Group (RWPG) water-demand projections under drought-of-record (DOR) conditions. The GAM will be used to predict changes in regional groundwater water levels (heads) and fluxes related to baseflow to major streams and rivers, springs, and cross-formational flow.

Six basic predictive model runs are presented and documented: (1) average recharge ending with the DOR in 2010, (2) average recharge ending with the DOR in 2020, (3) average recharge ending with the DOR in 2030, (4) average recharge ending with the DOR in 2040, (5) average recharge ending with the DOR in 2050, and (6) average recharge through 2050 without including the DOR. In addition, a model run to 2010 that includes an estimated implementation of the Twin Forks project (7) is presented.

To complete the predictive simulations, estimates of pumping, recharge and groundwater evapotranspiration (ET), and streamflow must be completed for both an average future condition and a DOR. Predictive pumping demands from the RWPGs are used in the predictive simulations assuming that the pumping distribution (as determined in Appendix C) for the year 1999 applies in the future (2000-2050). Section 6.3.4 discusses the estimation of recharge and ET for the future conditions. In short, transient estimates from the calibration/verification period were averaged by month to maintain seasonality and used for the predictive simulations. For the DOR, additional SWAT runs were made over the time of the DOR to determine recharge and ET. Additional streamflow estimates (Section 6.3.3) were also made using gage records from the time period of the DOR. The following discusses the development of a DOR.

10.1 Drought of Record

GAM specifications require that the DOR used for model predictions be representative for the past 100 years and be defined by severity and duration. Drought is considered a normal, recurring climatic event. It is conceptually defined by the National Drought Mitigation Center as a protracted period of deficient precipitation resulting in extensive damage to crops with loss of yield. Operational definitions of drought are typically used to define the beginning, end, and

severity of a drought over a given historical period. Operational definitions typically quantify the departure of precipitation, or some other climatic variable, from average conditions over a defined time window (typically 30 years).

Drought indices are quantitative measures that assimilate raw data into a single value that defines how precipitation has varied from a specific norm. As discussed above, drought is a phenomenon related directly to available moisture from precipitation. Precipitation is the primary variable controlling recharge in the model region. Accordingly, we used precipitation data as the raw data for defining the DOR in the Southern Carrizo-Wilcox GAM region.

There are many drought indices available to measure the degree that precipitation has deviated from historical norms. The typical measure is “percent of normal”, which is calculated by dividing the measured annual precipitation depth by the average annual precipitation depth and multiplying by 100. This calculation could be performed over a range of time scales but is typically annualized. The average annual precipitation depth is usually a long-term arithmetic mean. The available precipitation records within the model domain were analyzed to calculate the percent of normal as an indicator of drought. Figure 2.12 shows a select set of long-term annual precipitation records in the model region. Inspection of these shows particularly dry periods in 1917 and 1954 and 1956. The drought of 1917 is consistently measured by the nine available gages at that time and 1917 represents yearly minimum precipitation depths for five out the nine available gages. The average precipitation, as measured in percent of normal averaged across all available gages in the model area was equal to 42% in 1917 and 66% for the three year period from 1915 to 1917.

The 1950’s represents a period of historical drought in Texas and the Rio Grande Basin including the region being modeled. The drought peaked in 1954 and continued through 1956. By the 1950s the available number of rain gages in the model area increased to 38. The severe drought conditions in the 1950s were consistently recorded by the model region precipitation gage records with 27 of 38 gages recording their period of record low annual precipitation depths between 1954 and 1956. The average precipitation, as measured in percent of normal averaged across all available gages in the model area, is equal to 70% from 1950 through 1956. The same metric calculated for the peak drought years from 1954 through 1956 is 56% of normal.

A secondary drought index that can be used to quantify the DOR is the Standardized Precipitation Index (SPI). This index was developed to define precipitation deficits over multiple time scales (McKee et al., 1993). The SPI is calculated based upon the precipitation record for a given location. The long-term precipitation record is fitted to a general probability distribution (typically the Gamma distribution). This distribution is then normally transformed and standardized so that the mean SPI for that location over the time period of interest is equal to zero. When the SPI is equal to zero, it signifies median precipitation conditions for that location based upon the time integration window specified (Edwards and McKee, 1997). Because the index is normalized, comparison of SPI values between locations (i.e., across our model domain) is simplified in that an SPI of -1 represents a similar magnitude deficit for all stations. Monthly precipitation averages are used as the raw data for the SPI calculation. A one-month SPI would represent normalized precipitation data without temporal averaging. The SPI is backward-averaged over some user-specified duration, typically between six months and three years. By lengthening this time integration window, one investigates longer term precipitation trends less subject to short-term variations. Short-term deficit conditions or anomalies are of less concern for predicting groundwater conditions. Figure 10.1.1 shows the SPI for precipitation gage 412458 in Frio County calculated using one year, two year, and three year averaging windows. Current SPI index maps are available online for the State of Texas for multiple time averaging periods from one month through three years at the following URL: <http://www.txwin.net/Monitoring/Meteorological/Drought/spi.htm>

McKee et al. (1993) defined a classification system for defining drought conditions using the SPI. This classification is taken from (Hayes, 2001) and presented in the table below. McKee et al. (1993) defined a drought event as any time period over which the SPI is continuously negative and reaches a magnitude of -1.0 or less.

Table 10.1 SPI Precipitation Deficit Classification System (Hayes, 2001).

SPI Value	Precipitation Deficit Condition
2.0 and above	Extremely wet
1.5 to 1.99	Very wet
1.0 to 1.49	Moderately wet
-0.99 to 0.99	Near normal
-1.0 to -1.49	Moderately dry
-1.5 to -1.99	Severely dry
-2.0 and less	Extremely dry

Figure 10.1.2 plots SPI curves for five representative long-term precipitation gages in the model area. A two year time window was used for the analysis. Drought occurs most consistently in these gages in the period from 1915 to 1920 and in the 1950s. The drought in the 1950s is of longer duration, and is supported by more available data. The SPI analysis gives a consistent result to the analysis of percent normal. The DOR is, therefore, considered to have occurred in the mid-1950s.

With the DOR picked to occur in the mid-1950s, we next reviewed the monthly data to define the month the DOR began and ended. For picking the beginning and end of the DOR, one would like to use a measure that represents climate conditions across the entire model domain. To meet this need, records from all of the precipitation stations in the model area were averaged for each month to provide input to a “model-wide” SPI. Figure 10.1.3 shows the SPI calculated for this average dataset for several time integration windows. The longer duration (2- and 3-year) integration windows dip well below -1 starting in July 1954. However, the monthly data show that the below-average precipitation that started this downward trend began in October 1953. The consistently below-normal precipitation continued until February 1957, when a wet-dry-wet period occurred, followed by more normal precipitation trends. Therefore, we chose the DOR to have occurred between October 1953 and February 1957 for this model region.

To implement the drought of record in the predictive scenarios, we replaced the end of the scenario with the drought of record data, while maintaining the seasonality of the dataset. For instance, for the 2010 scenario, September 2006 marks the end of the averaged predictive dataset. From that point, climatic data calculated for October 1953 through February 1957 were used for the remainder of the simulation to estimate recharge. The simulation then ends in February 2010.

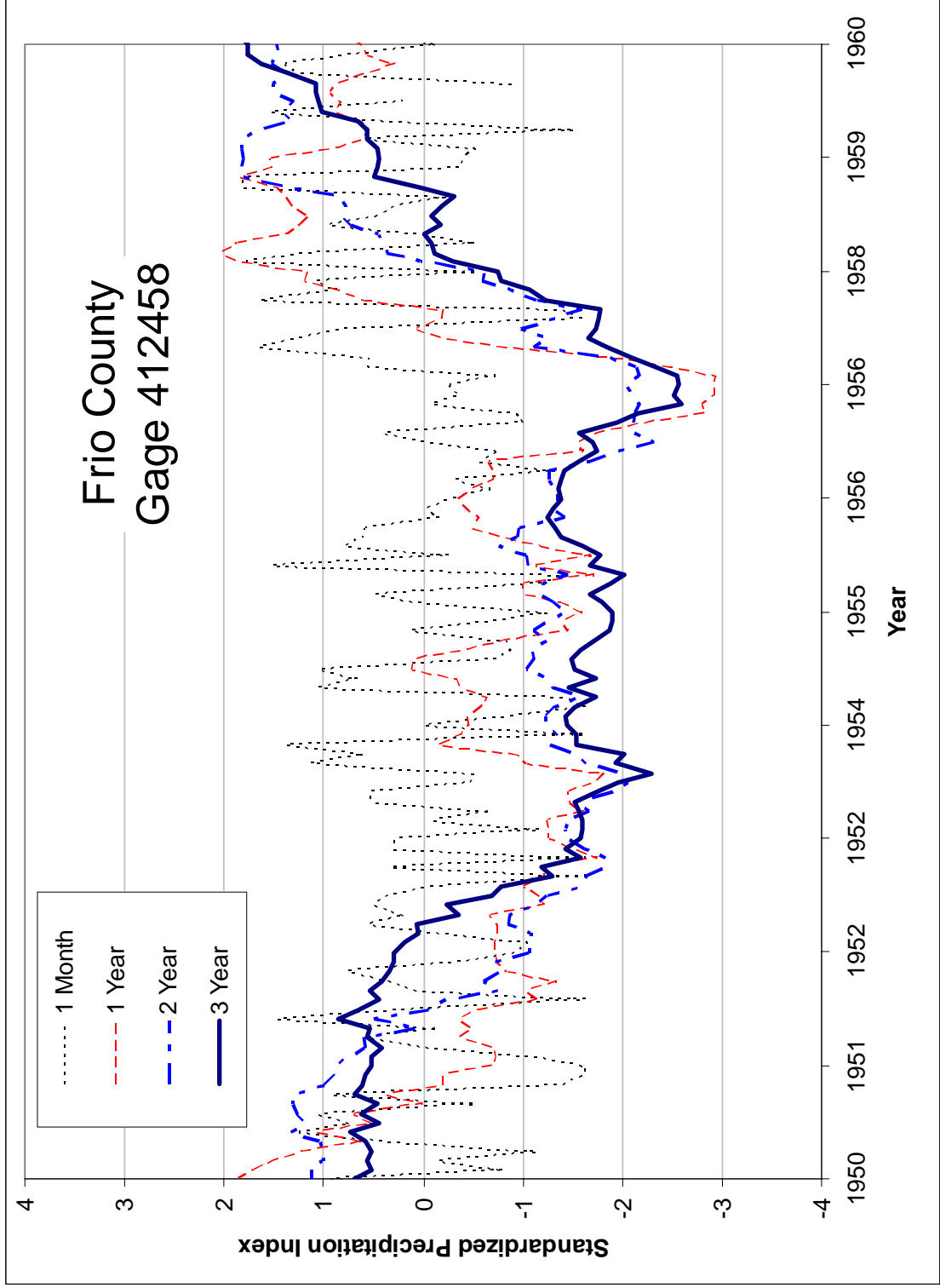


Figure 10.1.1 Standard precipitation index (SPI) curves for the Dilley rain gage (#412458-Frio Co.) for 1 month, 1 year, 2 year, and 3 year time periods.

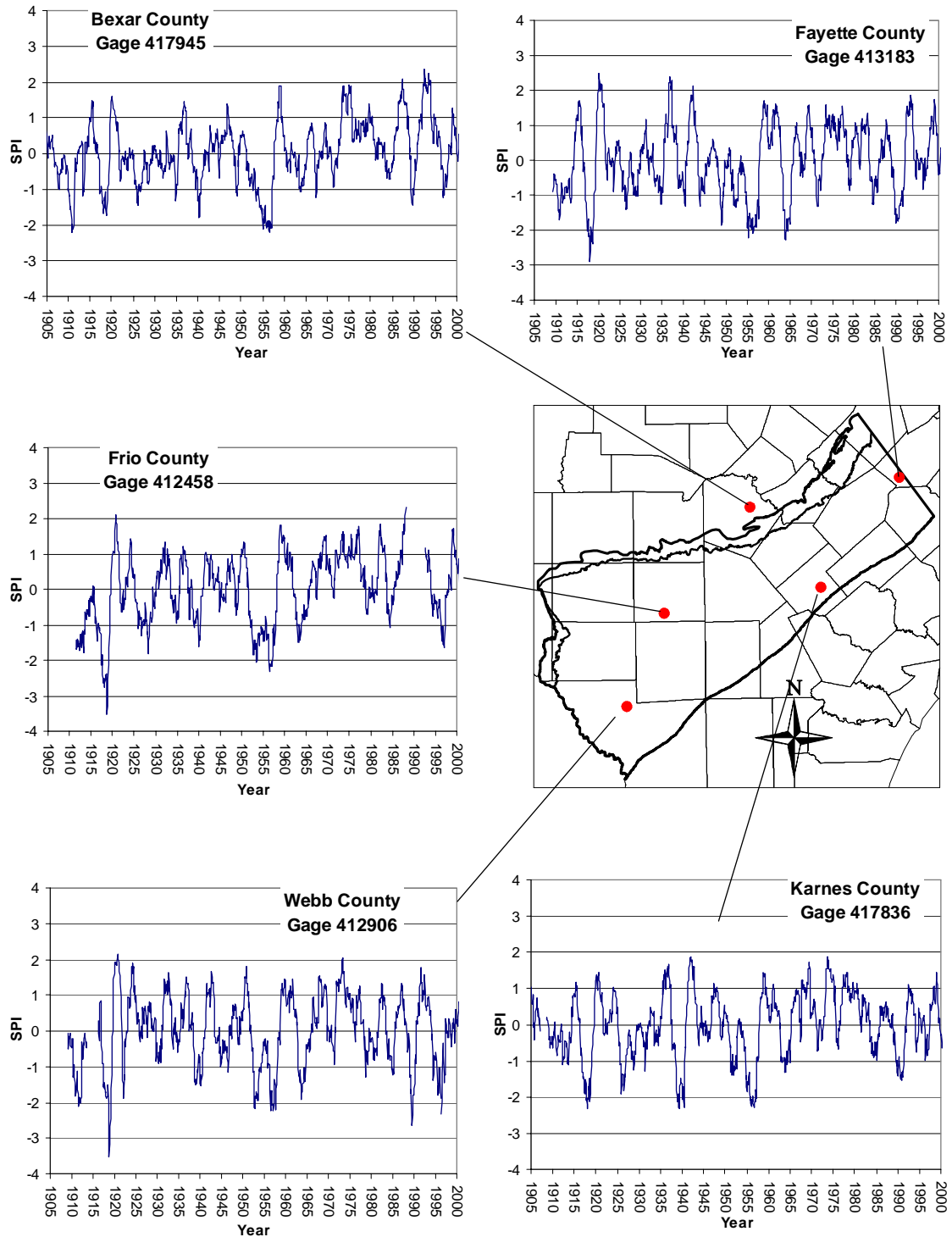


Figure 10.1.2 Standardized precipitation indices for precipitation gages in the region.

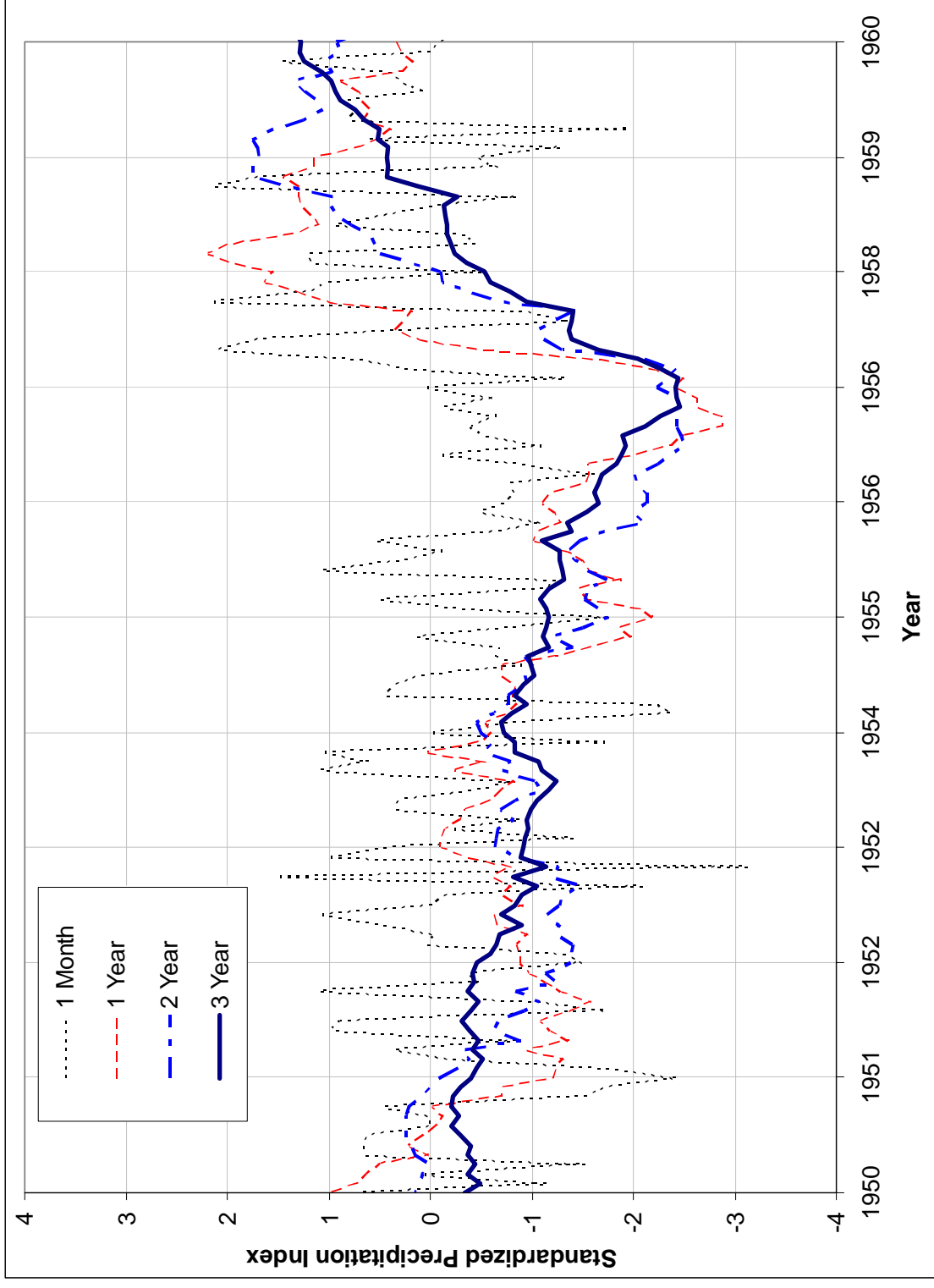


Figure 10.1.3 Standardized precipitation index averaged for all gages in the region from 1950-1960.

10.2 Predictive Simulation Results

In this section, we present the head and drawdown surfaces from the predictive simulation results. We also discuss a comparison between the average recharge condition simulation and the simulation with a drought of record (DOR).

Figure 10.2.1 shows the simulated 2000 and 2050 head surfaces for Layer 1. The direction of the gradient does not change significantly from 2000 to 2050. The contour lines have smoothed somewhat in the western portion of the model, with not as pronounced a depression in LaSalle county as had previously been present. Figure 10.2.2 shows that heads decreased slightly in the eastern portion of the model, but increased more than 25 ft in a region that includes parts of Frio, Atascosa, LaSalle, and McMullen counties.

Figure 10.2.3 shows the simulated 2000 and 2050 head surfaces for the Carrizo (Layer 3). This figure shows that the most pronounced drawdown has moved from between Frio and LaSalle counties down to northern Webb county. This drawdown is the result of including pumping for one of the options in the Rio Grande region (Region M) water plan for the City of Laredo. This option is a groundwater development project in the Carrizo aquifer in northern Webb County that would serve the city of Laredo in southern Webb County. The drawdown plot in Figure 10.2.4 shows the two main phenomena occurring over the simulated time period, the increase in heads in the Wintergarden area primarily due to relocated or decreased pumping, and the drawdown in northwest Webb County. Also, some drawdown occurred in the eastern portion of the model, where pumping is projected to increase over time. What is shown in this figure is the projected trend of shifting pumping from the west to the east in this region.

Figure 10.2.5 shows the simulated 2000 and 2050 head surfaces for the upper Wilcox (Layer 4). The upper Wilcox is strongly affected by heads in the Carrizo, so it mimics many of the changes occurring in the Carrizo that directly overlies it. The drawdown plot for the upper Wilcox (Layer 4) shown in Figure 10.2.6 demonstrates this, with increasing heads in the Wintergarden area and decreasing heads in northern Webb County. Figure 10.2.7 shows the simulated 2000 and 2050 head surfaces for the middle Wilcox (Layer 5). This figure illustrates the change in gradient direction occurring over the simulated period. In the 2000 head surface in the western portion of the model, gradients are primarily south with Dimmitt, Webb, and

southern La Salle counties showing a northeast gradient, as everything feeds into the depression in the Wintergarden area that continues downdip to the growth faults. By 2050, the rebound in heads has changed the gradients to predominantly southeast, directly downdip. Along the western boundary, the gradients have shifted to the east. The drawdown plot shown in Figure 10.2.8 indicates that in the middle Wilcox (Layer 5) heads are increasing in the Wintergarden area. The drawdown in the eastern portion of the model that was seen in the shallow layers is not evident in the middle Wilcox. Figure 10.2.9 shows the simulated 2000 and 2050 head surfaces for the lower Wilcox (Layer 6). Because the lower Wilcox is hydrologically separated from the rest of the model by the middle Wilcox, which has a low vertical hydraulic conductivity, many of the effects seen in the shallower layers are dampened in the lower Wilcox. This figure indicates that the direction of flow has not changed much in the lower Wilcox, although Figure 10.2.10, which shows the drawdown plot, does indicate more than 50 ft of head increase beneath the Wintergarden region.

Figures 10.2.11 through 10.2.14 show the simulated head results in the Carrizo for the remaining predictive runs. These simulations ended with a drought of record in 2010, 2020, 2030, and 2040, respectively. These figures show a consistent trend of drawdown in northern Webb County, increasing heads in the Wintergarden area, and slight decreases in heads in the eastern region of the model. Figures 10.2.15 through 10.2.19 show the 2010, 2020, 2030, and 2040 simulated head surfaces for the upper and middle Wilcox layers. The head surfaces for the Queen City and Lower Wilcox layers are not shown for all cases because the change in head in these layers is small (less than about 50 ft) at 2050. In all layers, we examined the drawdowns with respect to the assumed boundary conditions in the model (Section 6.3.1). Drawdowns at the lateral no-flow boundaries to the northeast, southwest, and downdip are within estimated model head error, so the boundaries are considered appropriate for the predictive simulations. In one investigative simulation, we found that replacing the northeast no-flow boundary with a general head boundary had little effect on the resulting head surfaces, further validating the suitability of the northeast no-flow boundary.

The trends in the simulated Carrizo hydraulic heads through time are further exemplified in Figure 10.2.19 which shows selected hydrographs from the predictive simulation from 2000 to 2050 ending with the drought of record. In the eastern region of the model, illustrated by the hydrographs from Wilson and Gonzales counties, the trend after 2000 is a slight decrease in

head. In the Gonzales County hydrograph, the decrease is steady over time. In the Wilson County hydrograph, the decrease is most evident in the first few predictive years, (i.e. 2000-2010), then the heads level off for the rest of the simulation period. In both cases, the decrease in heads is not dramatic. The previous figures 10.2.11 and 10.2.14 also show the trend from Wilson County where there is slight drawdown in 2010 which has not increased significantly by 2040. The hydrograph for Atascosa County shown in Figure 10.2.19 shows the increase in heads that results from decreased pumping in the area. The effect is more dramatic if the well is near an area of historically greater pumping than in the predictive simulation period (2000-2050). This is evident in the hydrograph for Frio County. In 2000, the amplitude of the seasonal cycling decreases dramatically and the head increases more than 50 feet over the simulated period. See Table 4.7.1 for a summary of the predictive and historical pumping by county. The hydrograph from Dimmit County shows a steady downward trend throughout the simulation, from the calibration/verification period through the predictive period. This is likely the result of the increased pumping in the northern Webb County area.

Figures 10.2.20 through 10.2.22 show the differences between the simulated head surfaces for 2050 with average recharge and the simulated head surfaces for 2050 with the DOR for the Carrizo through the lower Wilcox (Layers 3 through 6). In all of these layers there is a maximum head difference of less than 10 ft. All of the simulated head difference is in or near the outcrop, where recharge has the most impact. These figures emphasize an important point about the hydrology of this aquifer system. Recharge does not have a significant impact on downdip heads over the timescale of these simulations. One aspect of these simulations that is misleading is that simulated pumping does not increase during the DOR. The DOR only impacts climate data and subsequently, recharge and ET. Therefore, the effect of a DOR will be seen predominantly in the updip and outcrop areas. The hydrographs for Gonzales and Wilson counties (Figure 10.2.19) show a slight effect of the drought of record for heads near the outcrop. The slight increase in negative slope of the hydrograph in the last years of the simulation is concurrent with the drought of record.

Figures 10.2.23 and 10.2.24 show the saturated thickness in the outcrop for 2000 and 2050, respectively. Note that the figures show the saturated thickness for each layer outcrop, without combining any layers. The Carrizo-Wilcox aquifer is primarily confined and the layers are thin in the narrow outcrop region, so the model does not provide great resolution for

saturated thickness. These figures indicate that little change has occurred in the saturated thickness between years 2000 and 2050.

An additional predictive simulation was performed to add the expected pumping associated with the Twin Oaks Project in southern Bexar County. Approximately 14,000 AFY of pumping was added to a 5 square mile area in southern Bexar County. The simulation was identical to the 2010 predictive simulation, except that the additional pumping was started in 2003. Figure 10.2.25 shows the difference between the base 2010 simulation and the simulation that includes the Twin Oaks Project. The additional pumping causes a maximum of about 20 ft of drawdown in southern Bexar County.

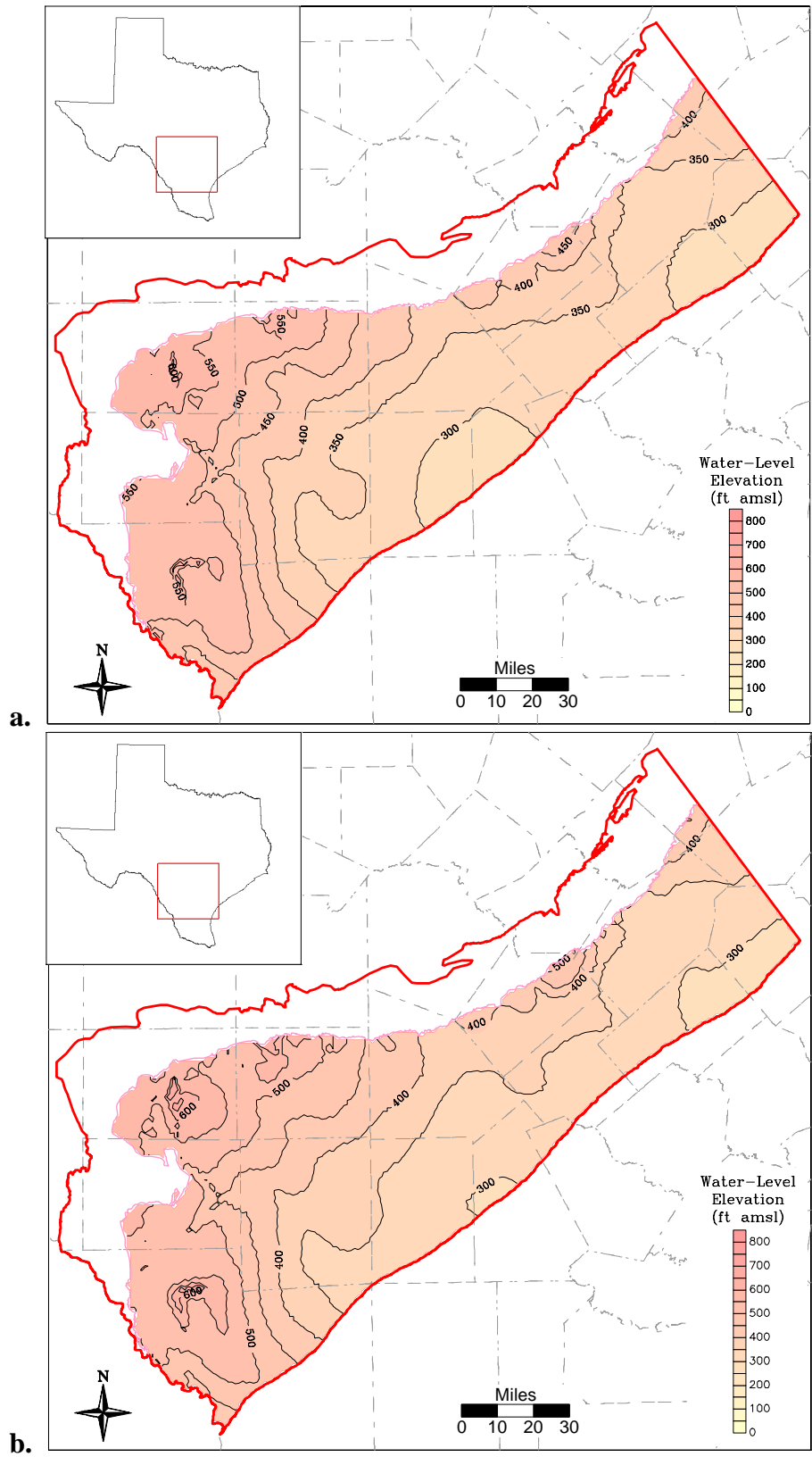


Figure 10.2.1 Simulated 2000 (a) and 2050 (b) head surfaces, Queen City/El Pico (Layer 1).

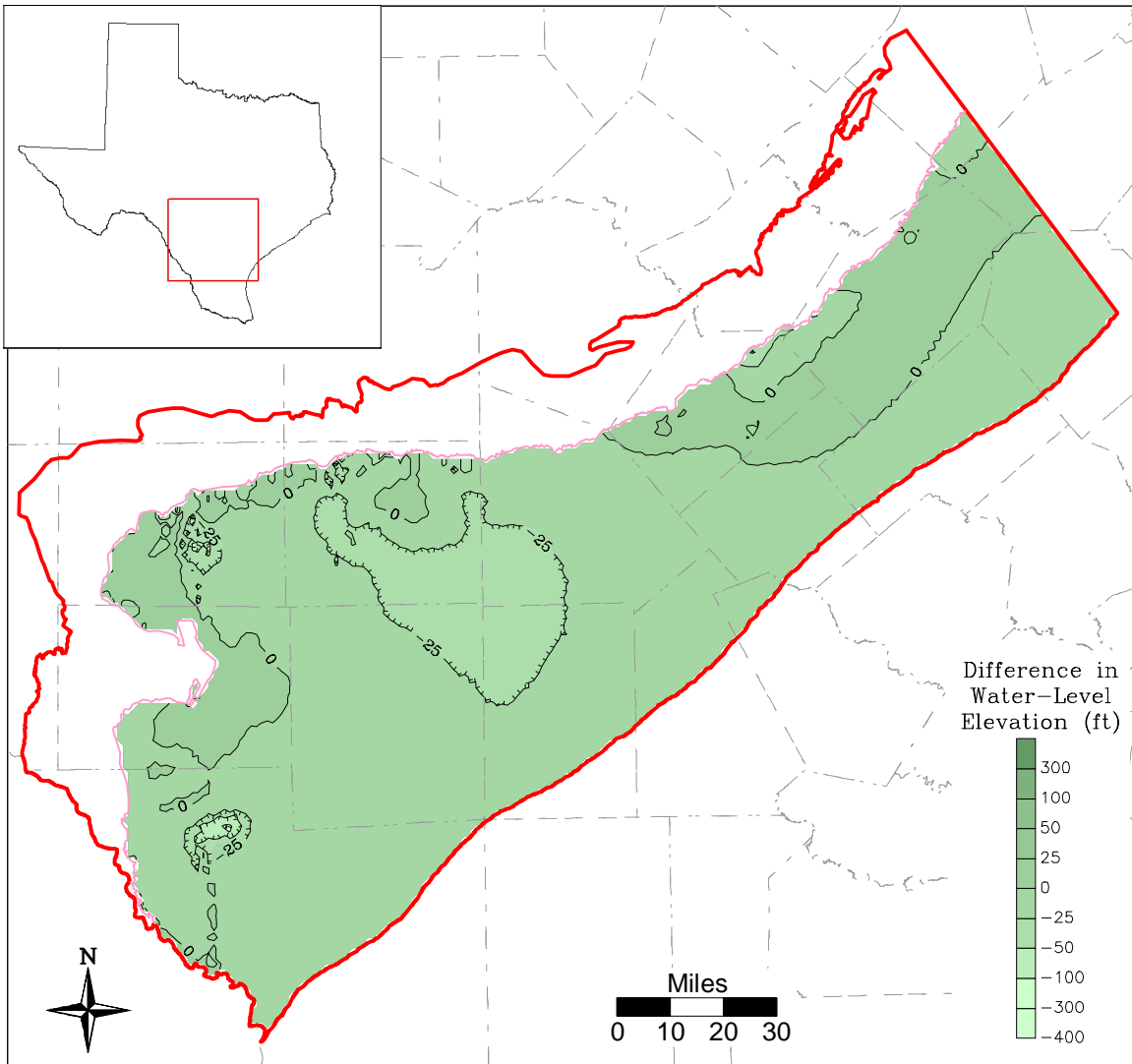


Figure 10.2.2 Difference between 2000 and 2050 simulated head surfaces, Queen City/El Pico (Layer 1).

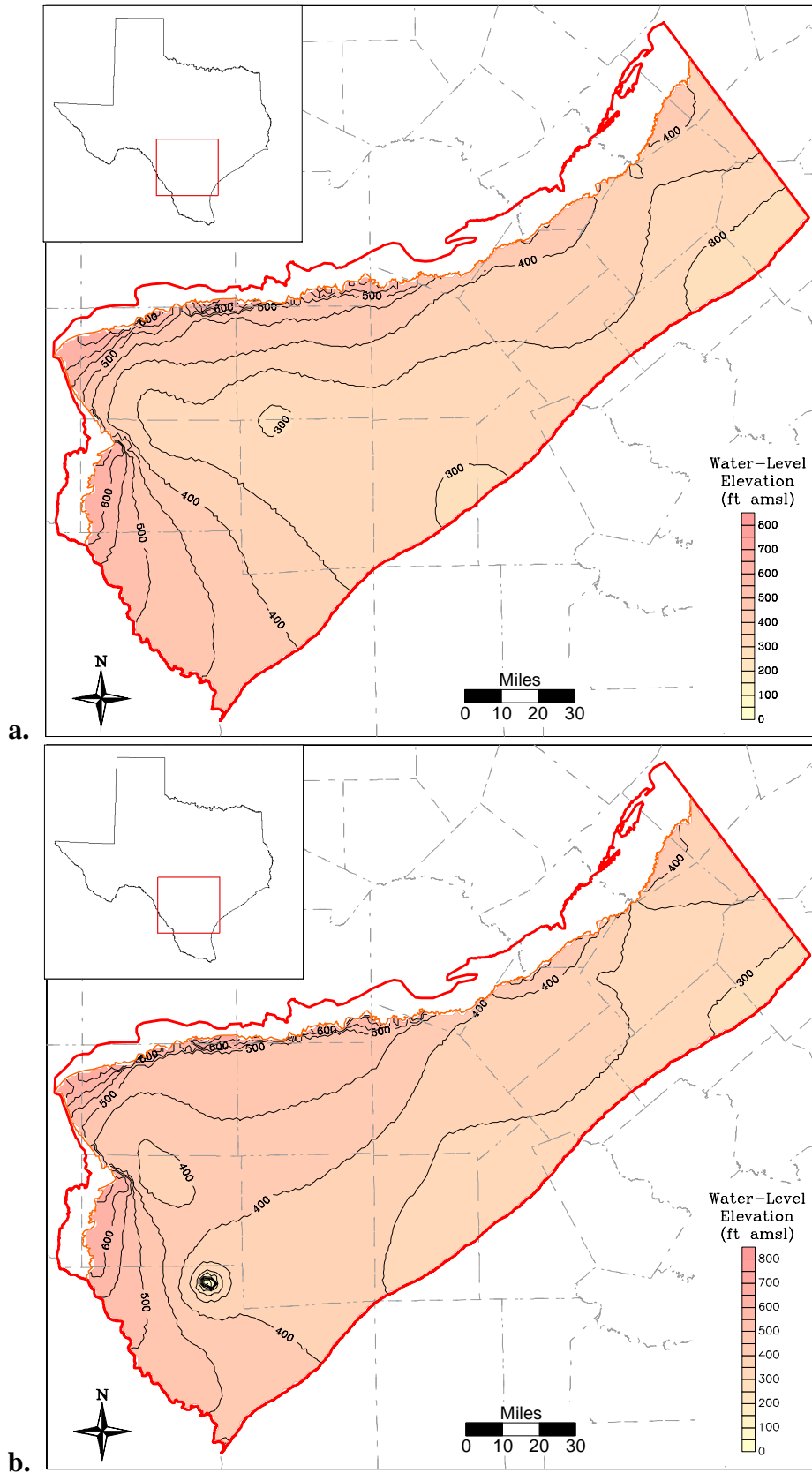


Figure 10.2.3 Simulated 2000 (a) and 2050 (b) head surfaces, Carrizo (Layer 3).

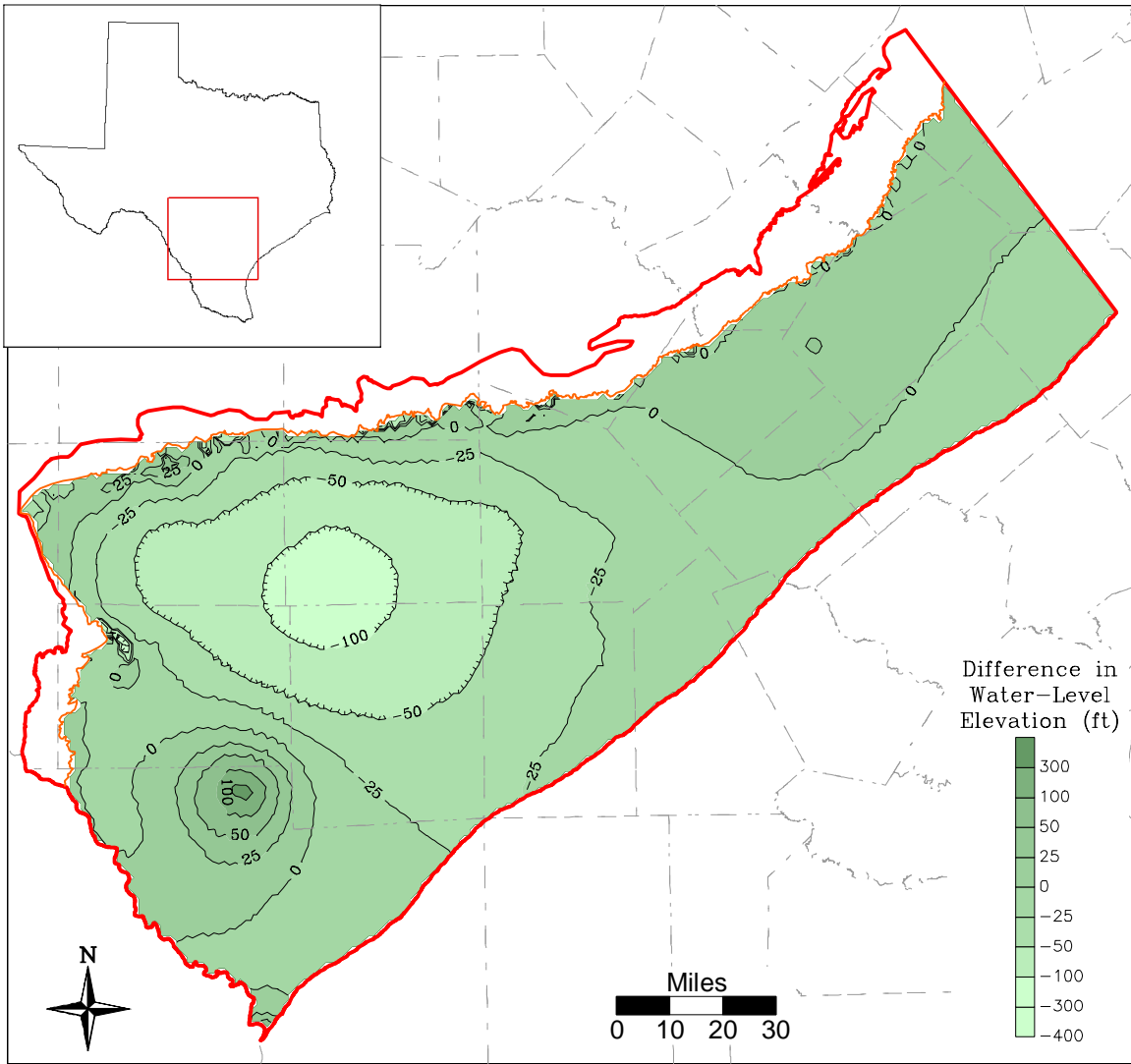


Figure 10.2.4 Difference between 2000 and 2050 simulated head surfaces, Carrizo (Layer 3).

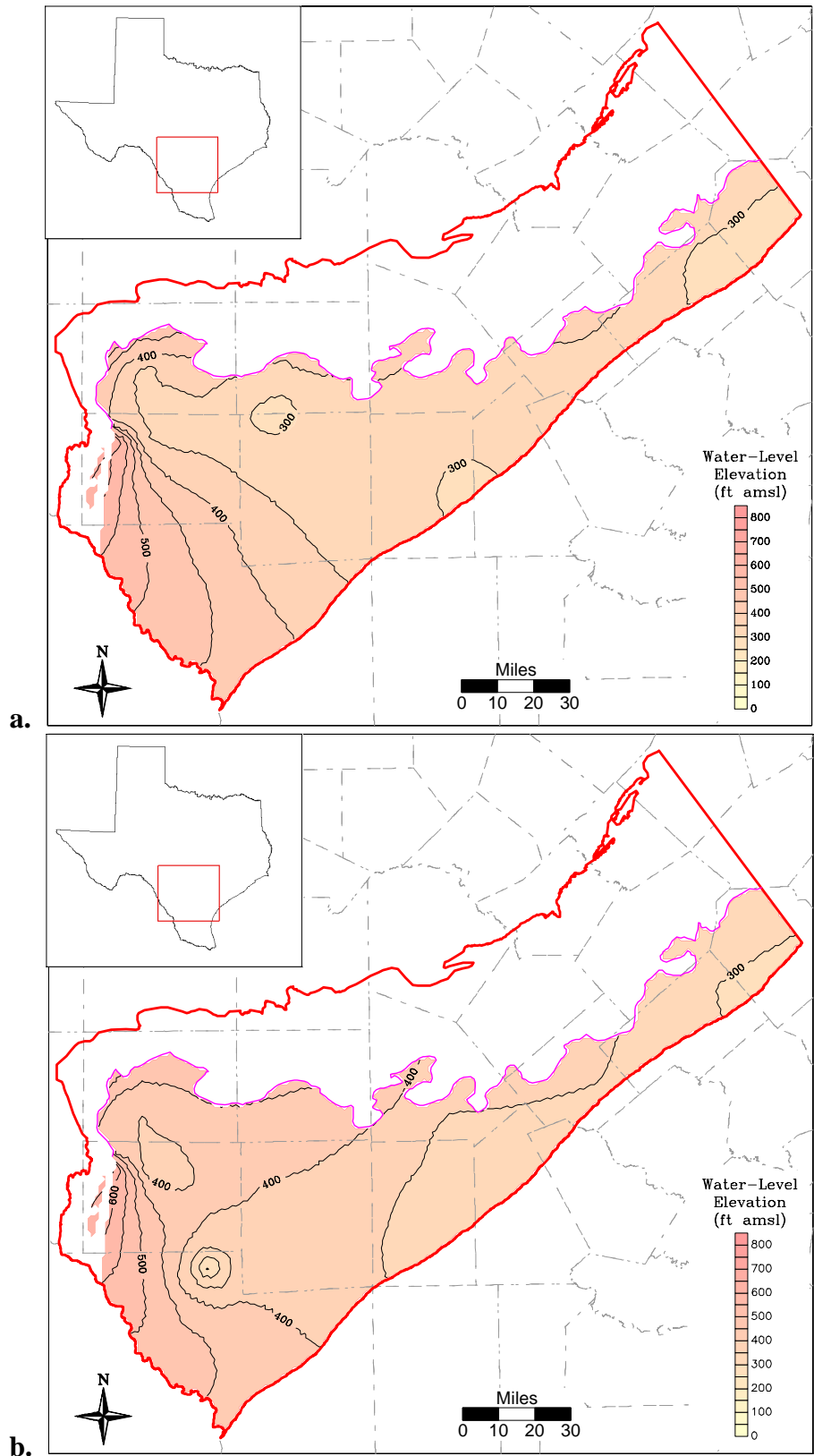


Figure 10.2.5 Simulated 2000 (a) and 2050 (b) head surfaces, upper Wilcox (Layer 4).

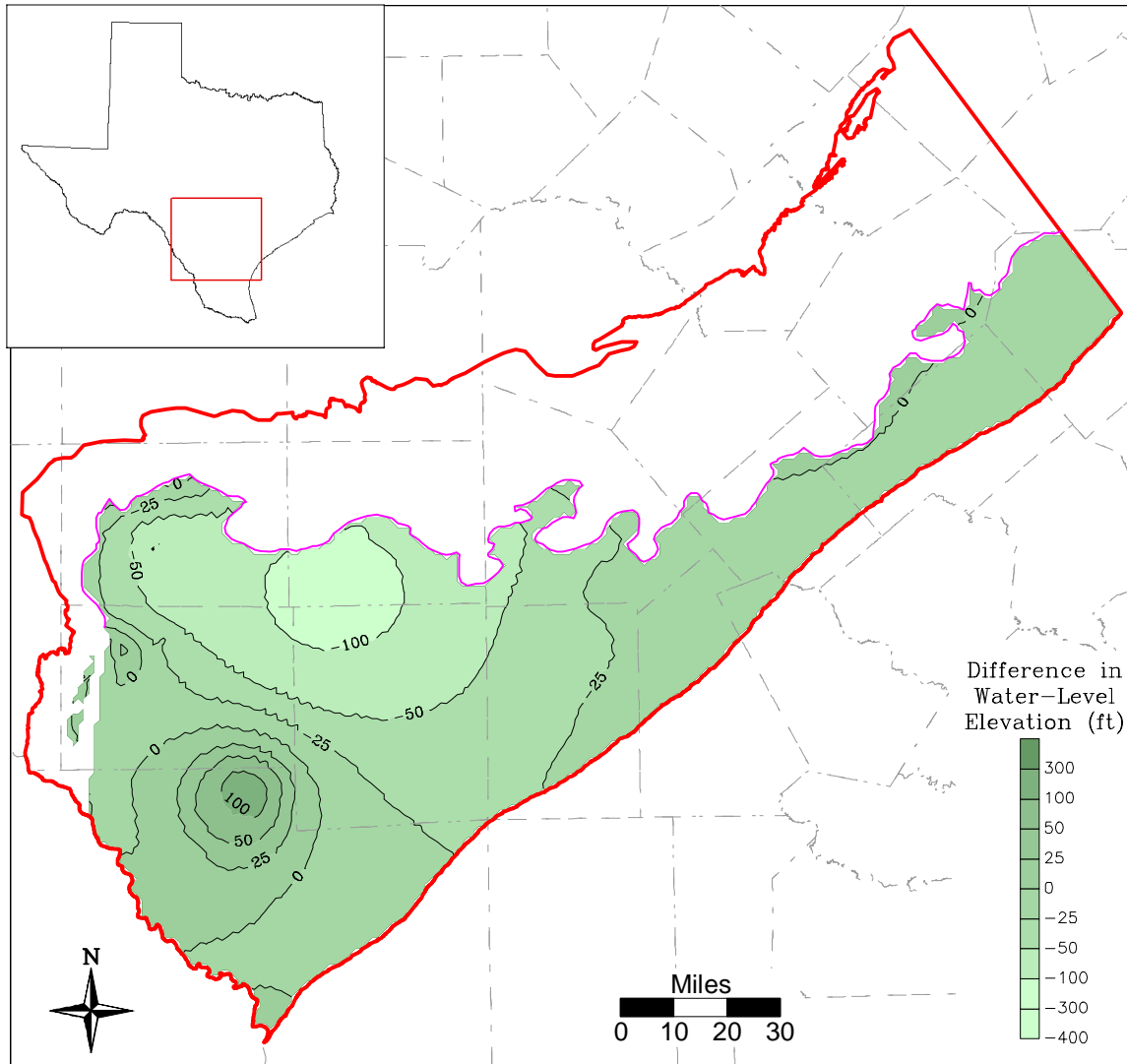


Figure 10.2.6 Difference between 2000 and 2050 simulated head surfaces, upper Wilcox (Layer 4).

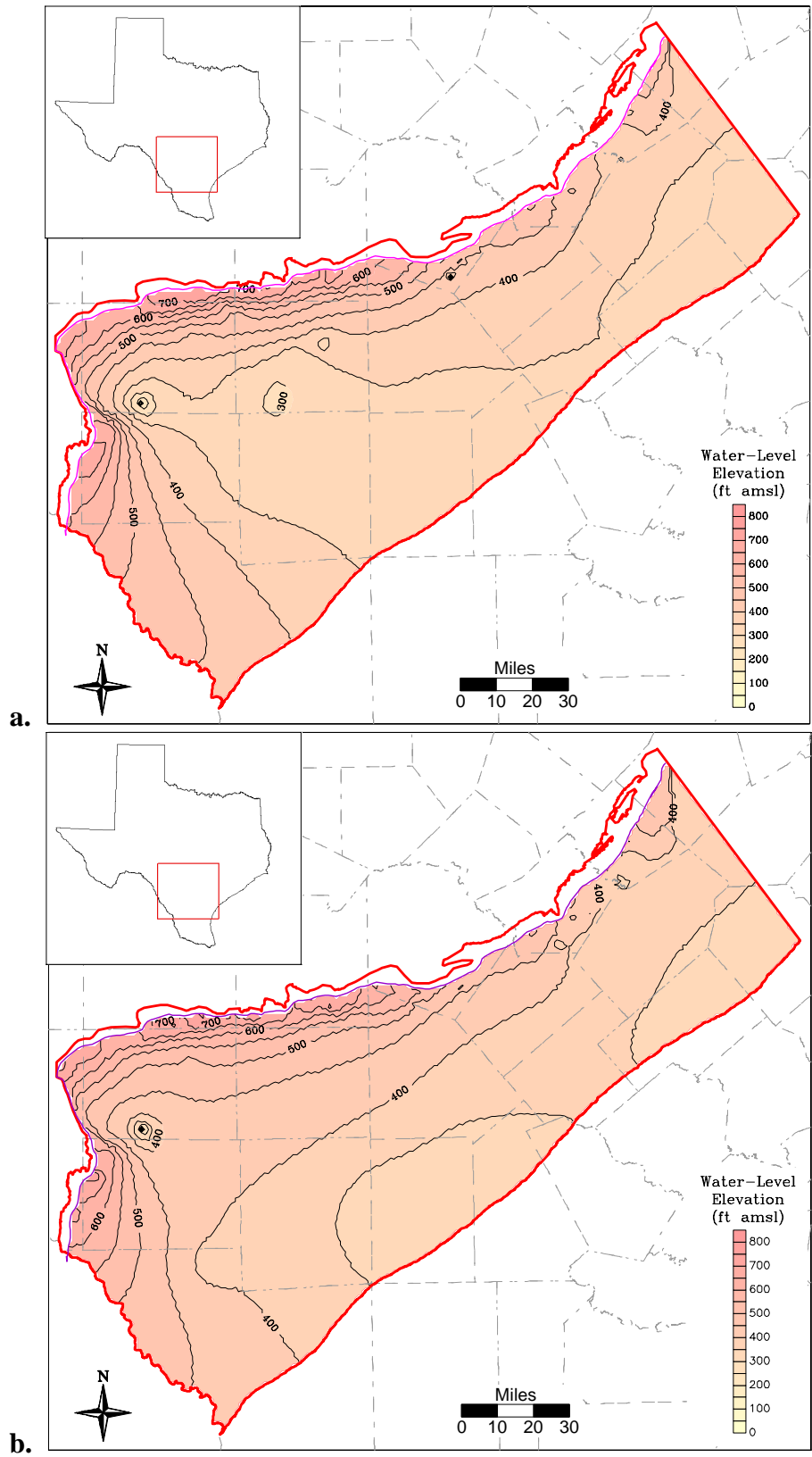


Figure 10.2.7 Simulated 2000 (a) and 2050 (b) head surfaces, middle Wilcox (Layer 5).

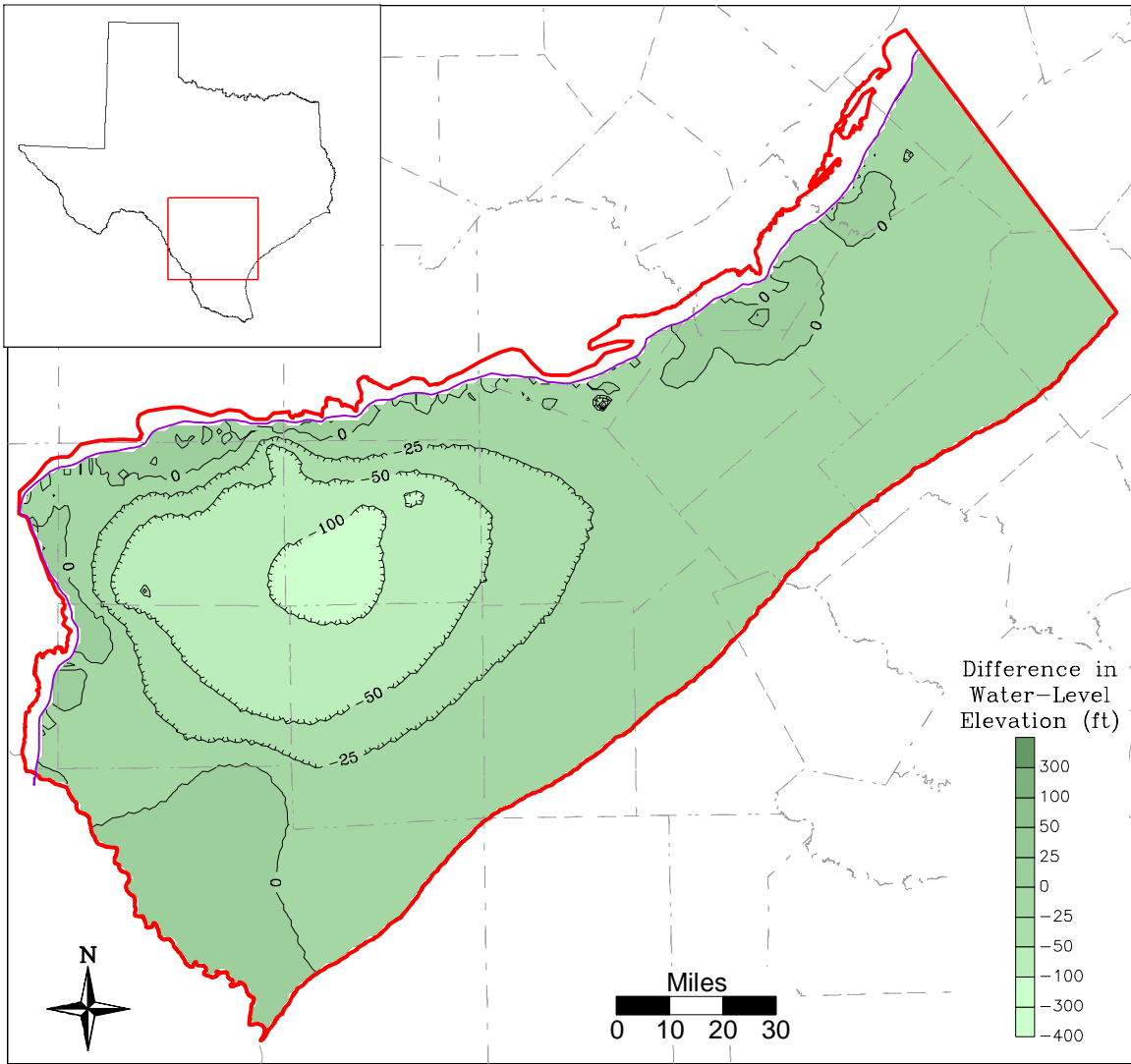


Figure 10.2.8 Difference between 2000 and 2050 simulated head surfaces, middle Wilcox (Layer 5).

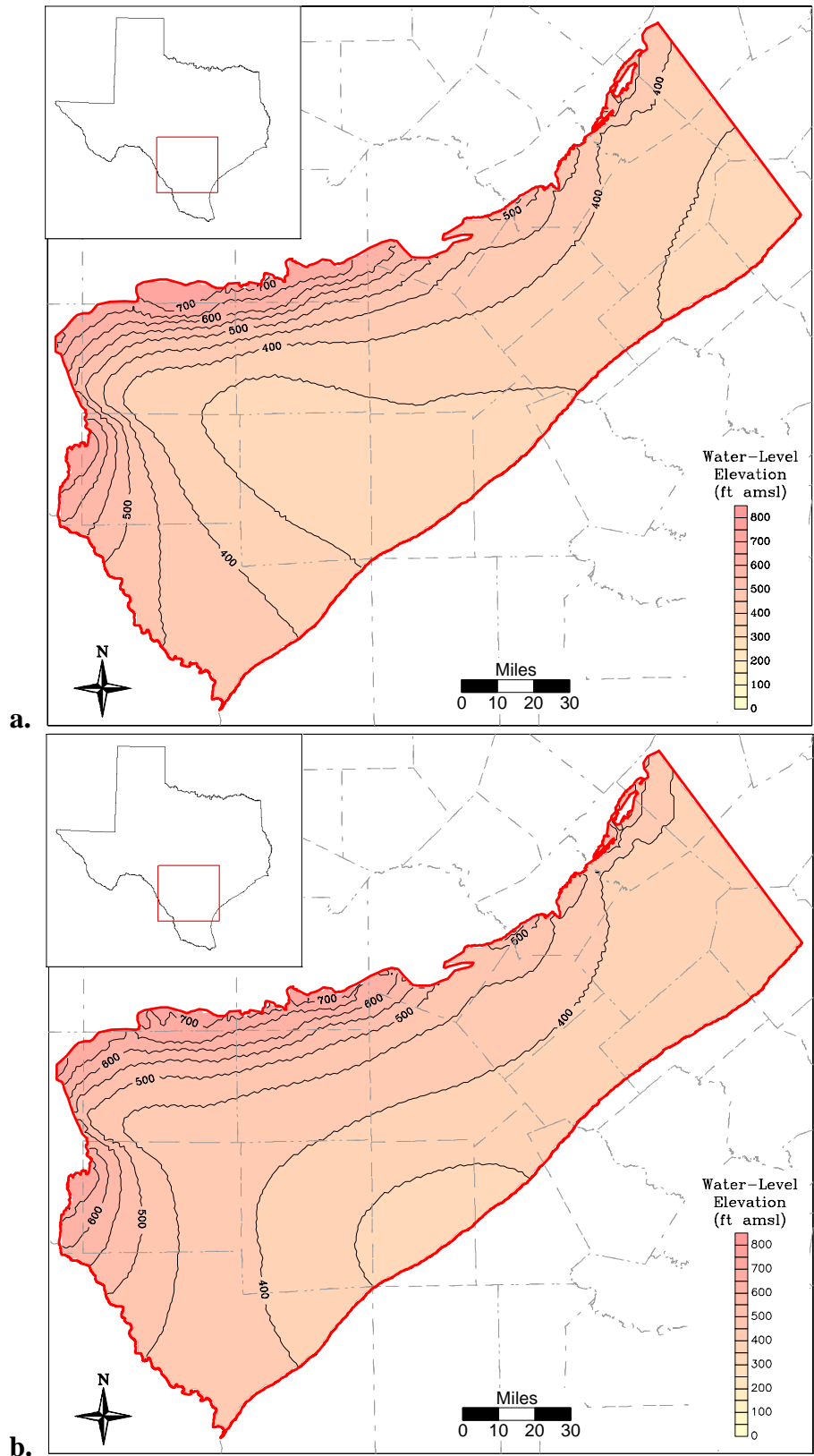


Figure 10.2.9 Simulated 2000 (a) and 2050 (b) head surfaces, lower Wilcox (Layer 6).

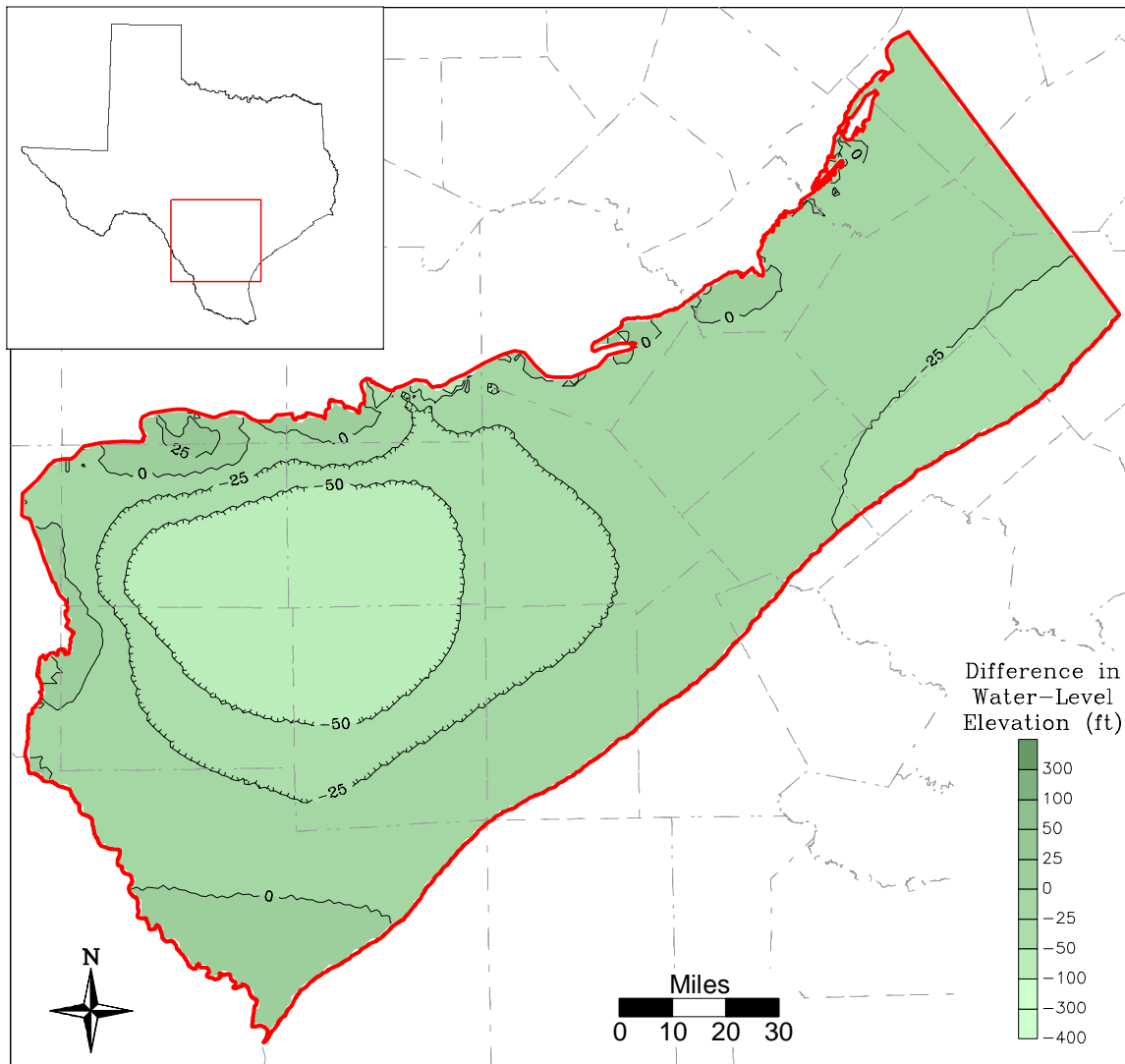


Figure 10.2.10 Difference between 2000 and 2050 simulated head surfaces, lower Wilcox (Layer 6).

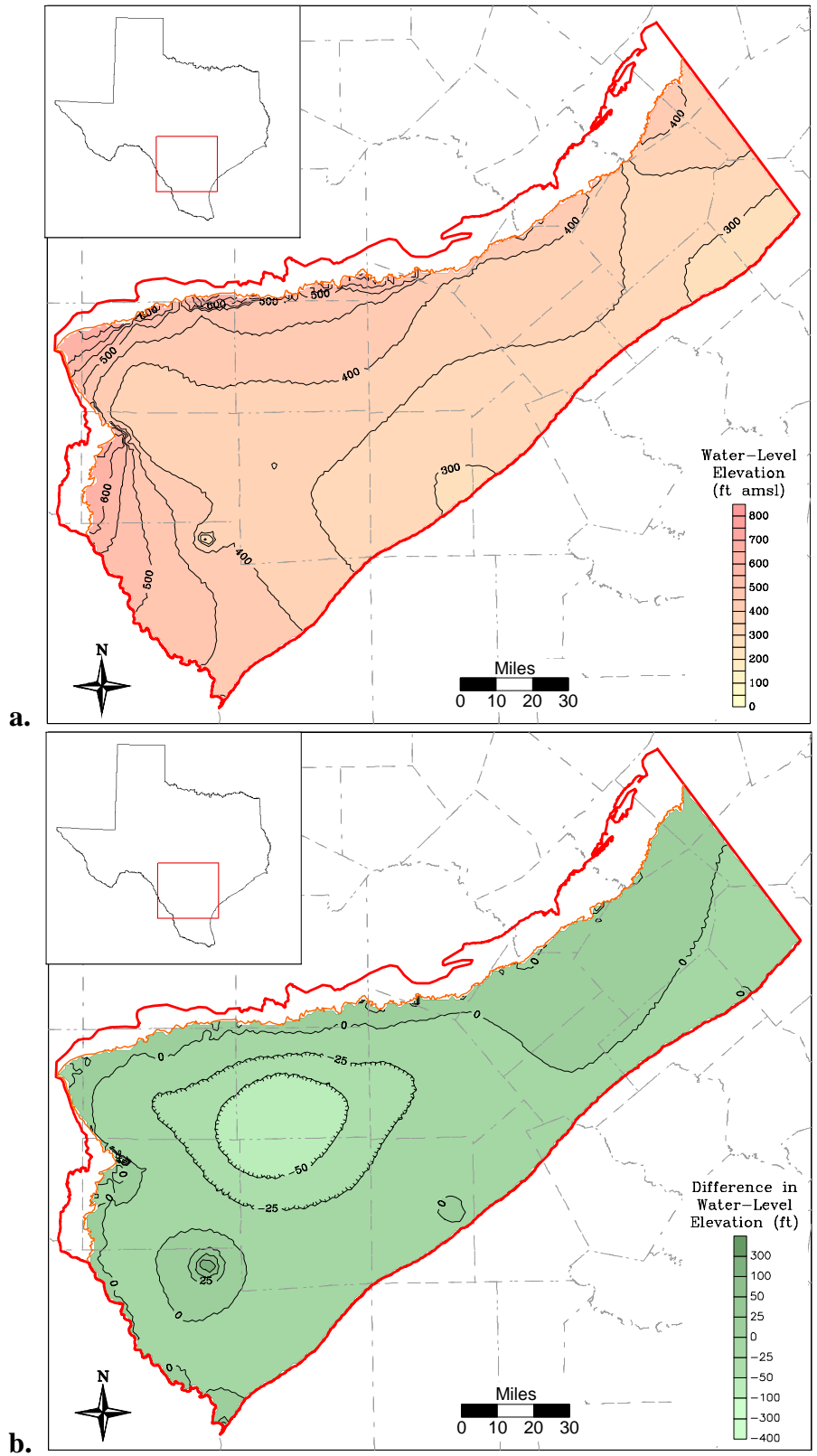


Figure 10.2.11 Simulated 2010 head surface (a) and drawdown from 2000 (b) for the Carrizo (Layer 3).

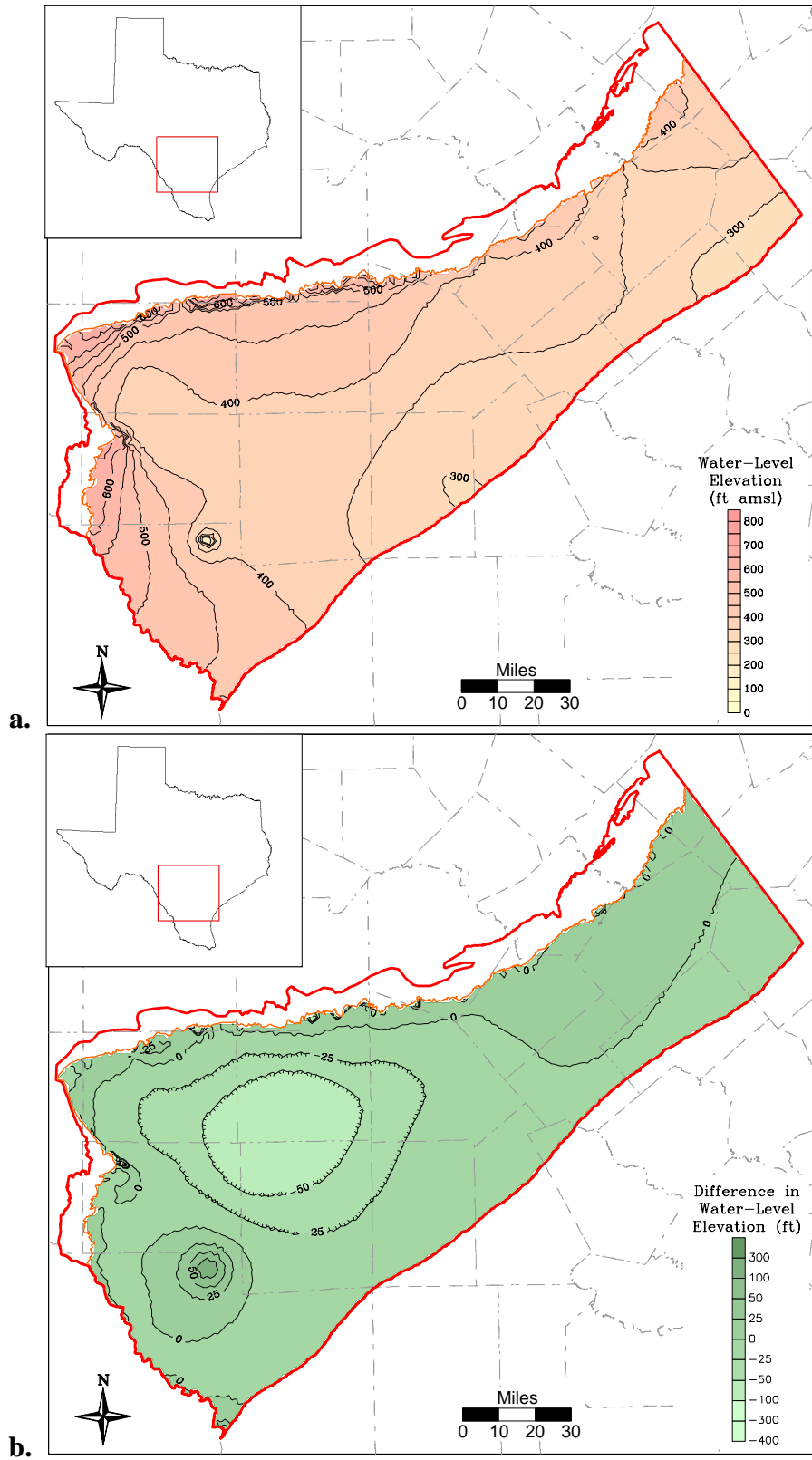


Figure 10.2.12 Simulated 2020 head surface (a) and drawdown from 2000 (b) for the Carrizo (Layer 3).

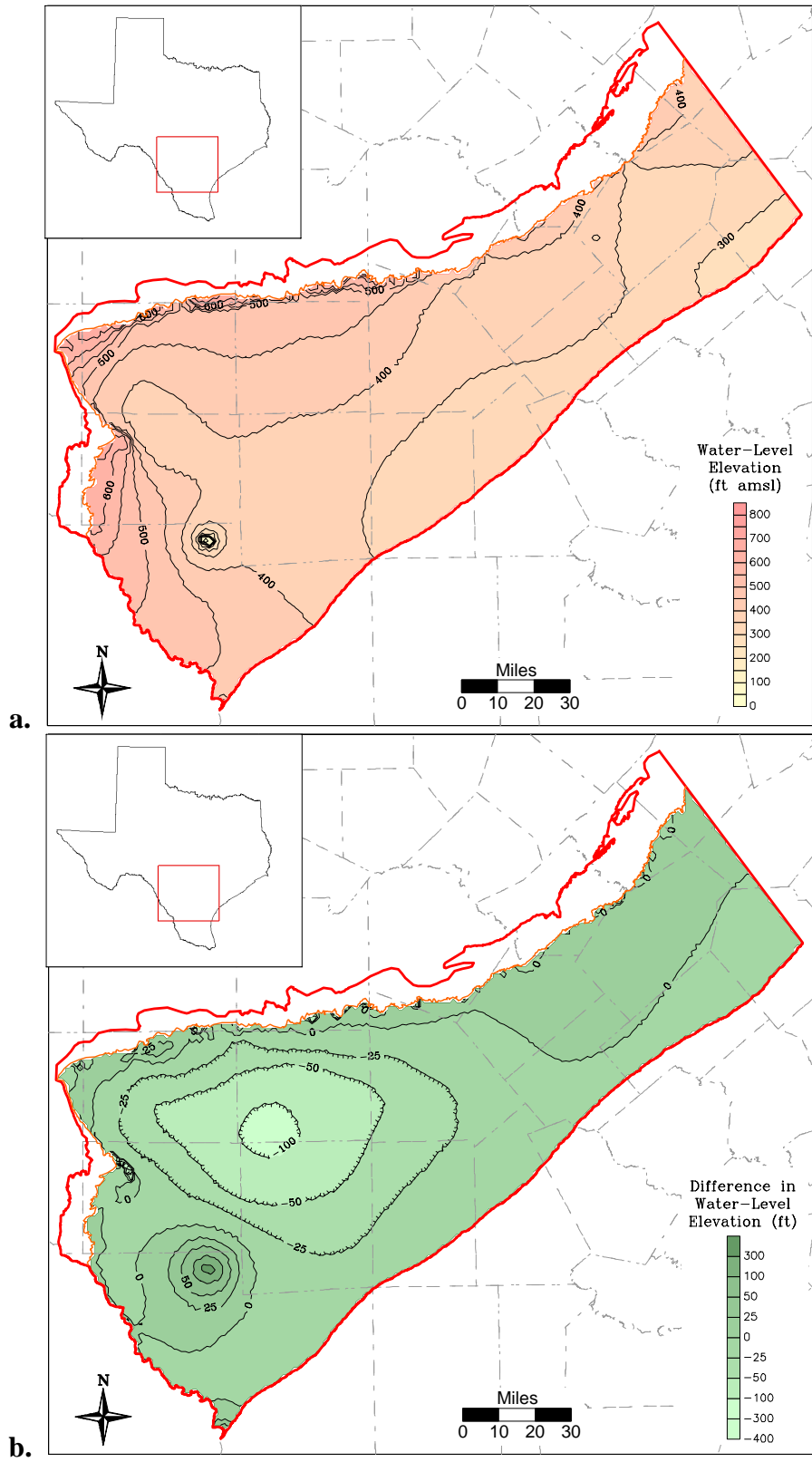


Figure 10.2.13 Simulated 2030 head surface (a) and drawdown from 2000 (b) for the Carrizo (Layer 3).

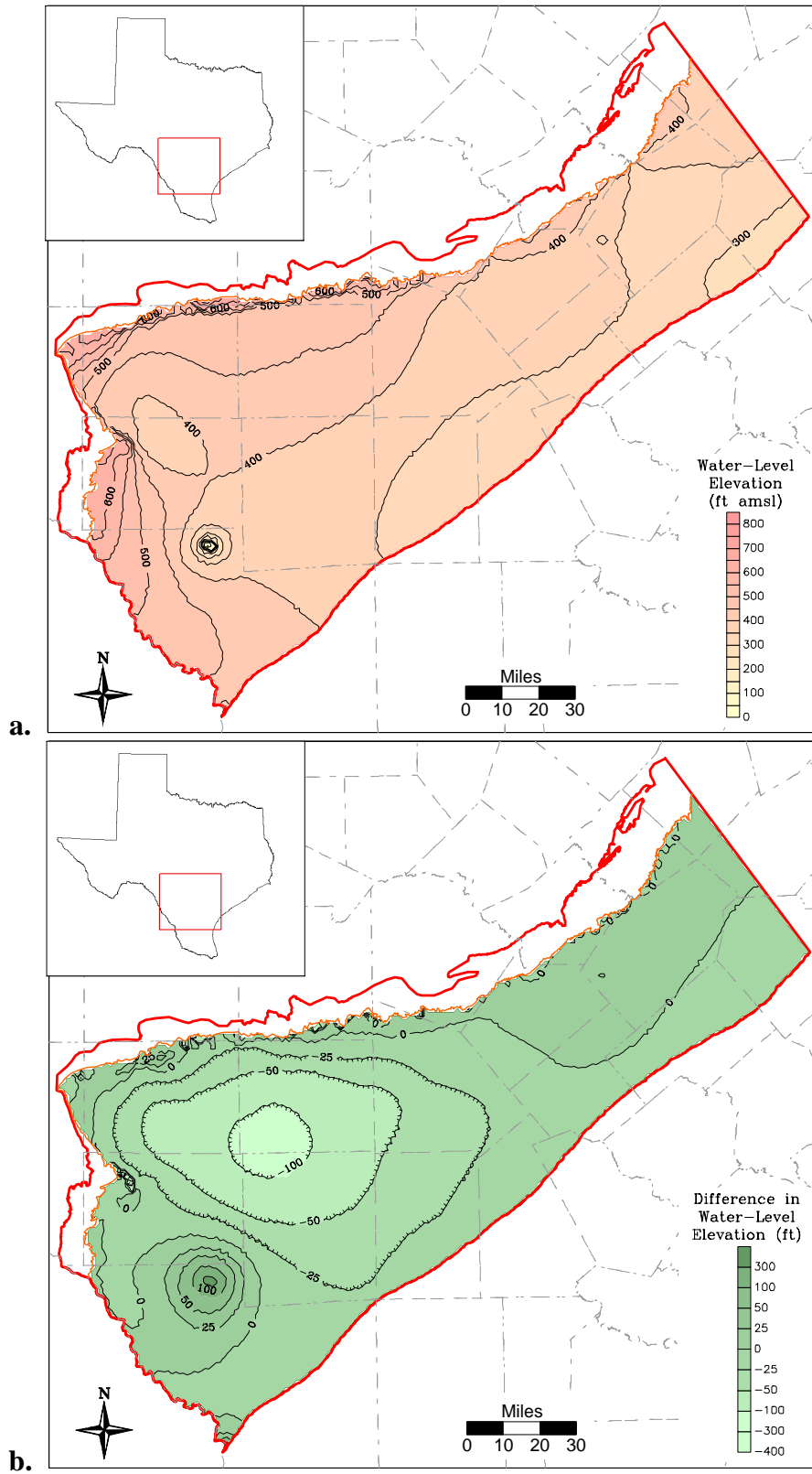


Figure 10.2.14 Simulated 2040 head surface (a) and drawdown from 2000 (b) for the Carrizo (Layer 3).

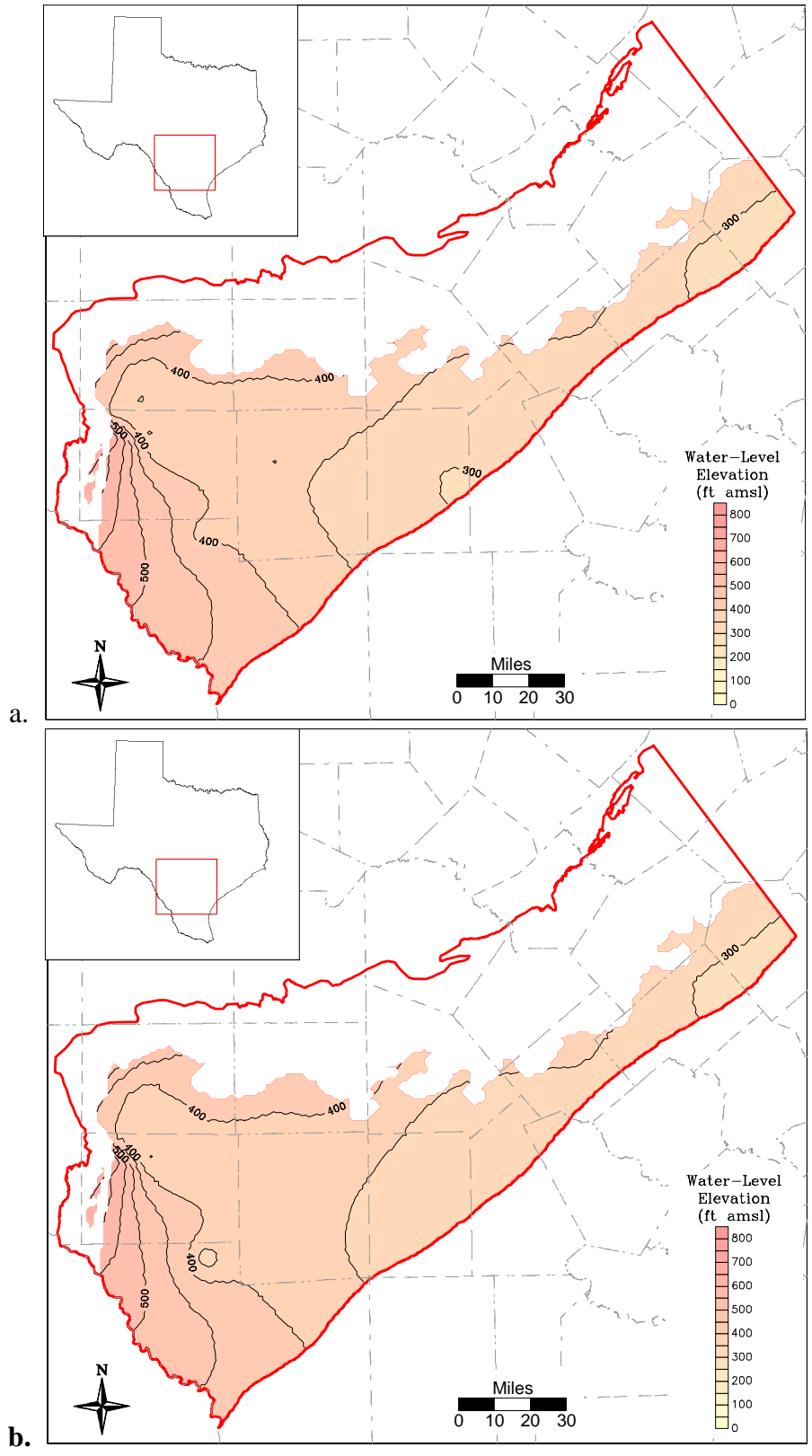


Figure 10.2.15 Simulated 2010 (a) and 2020 (b) head surface, upper Wilcox (Layer 4).

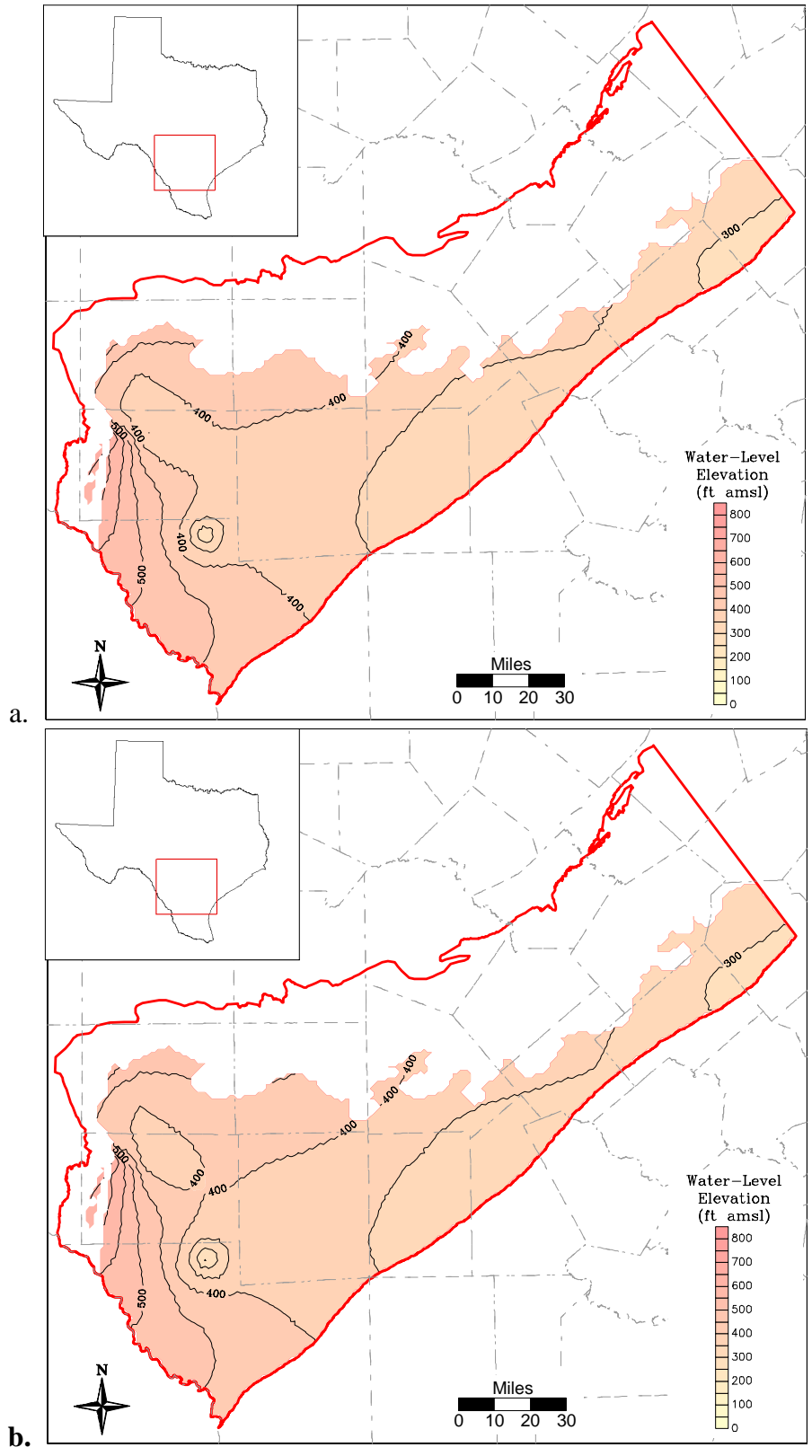


Figure 10.2.16 Simulated 2030 (a) and 2040 (b) head surface, upper Wilcox (Layer 4).

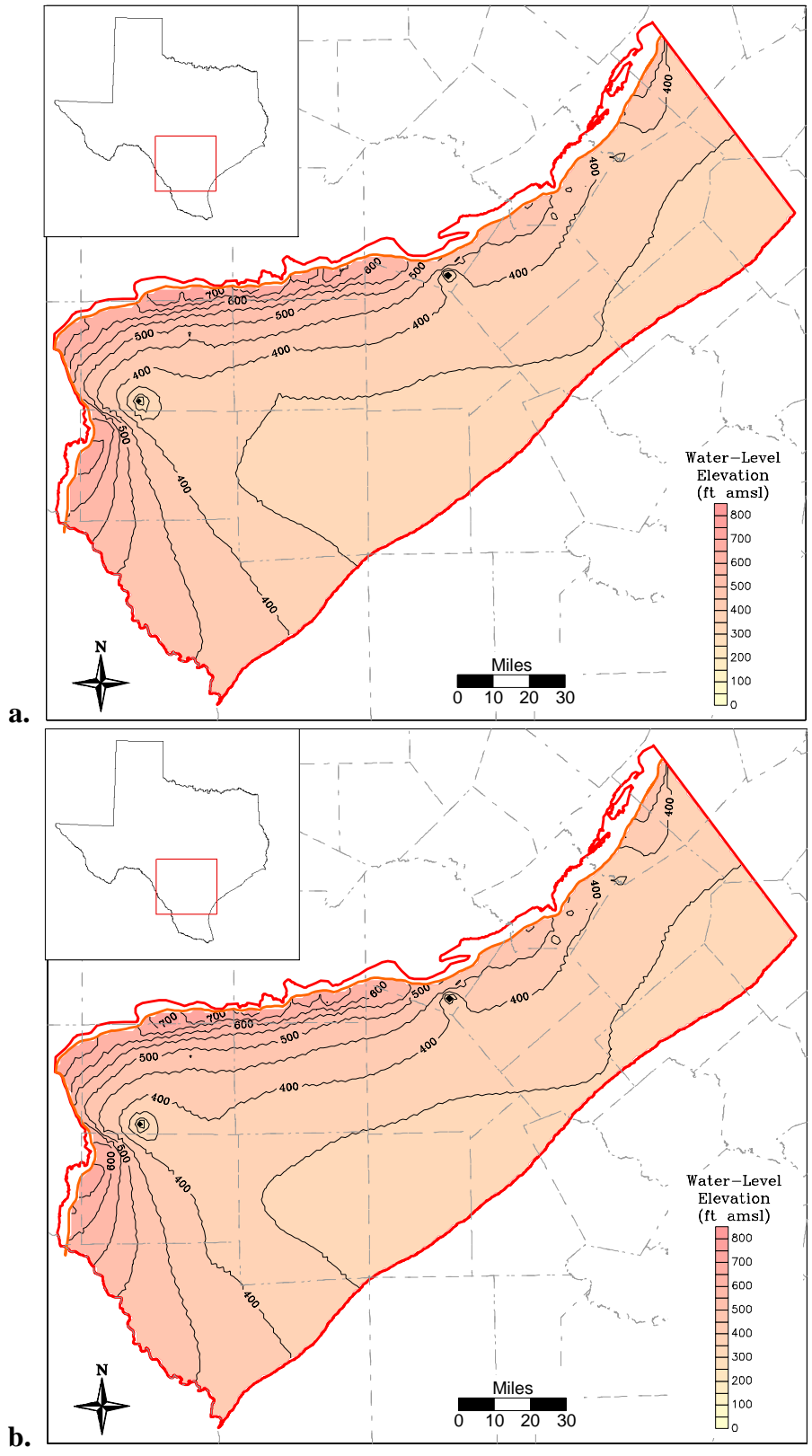


Figure 10.2.17 Simulated 2010 (a) and 2020 (b) head surface, middle Wilcox (Layer 5).

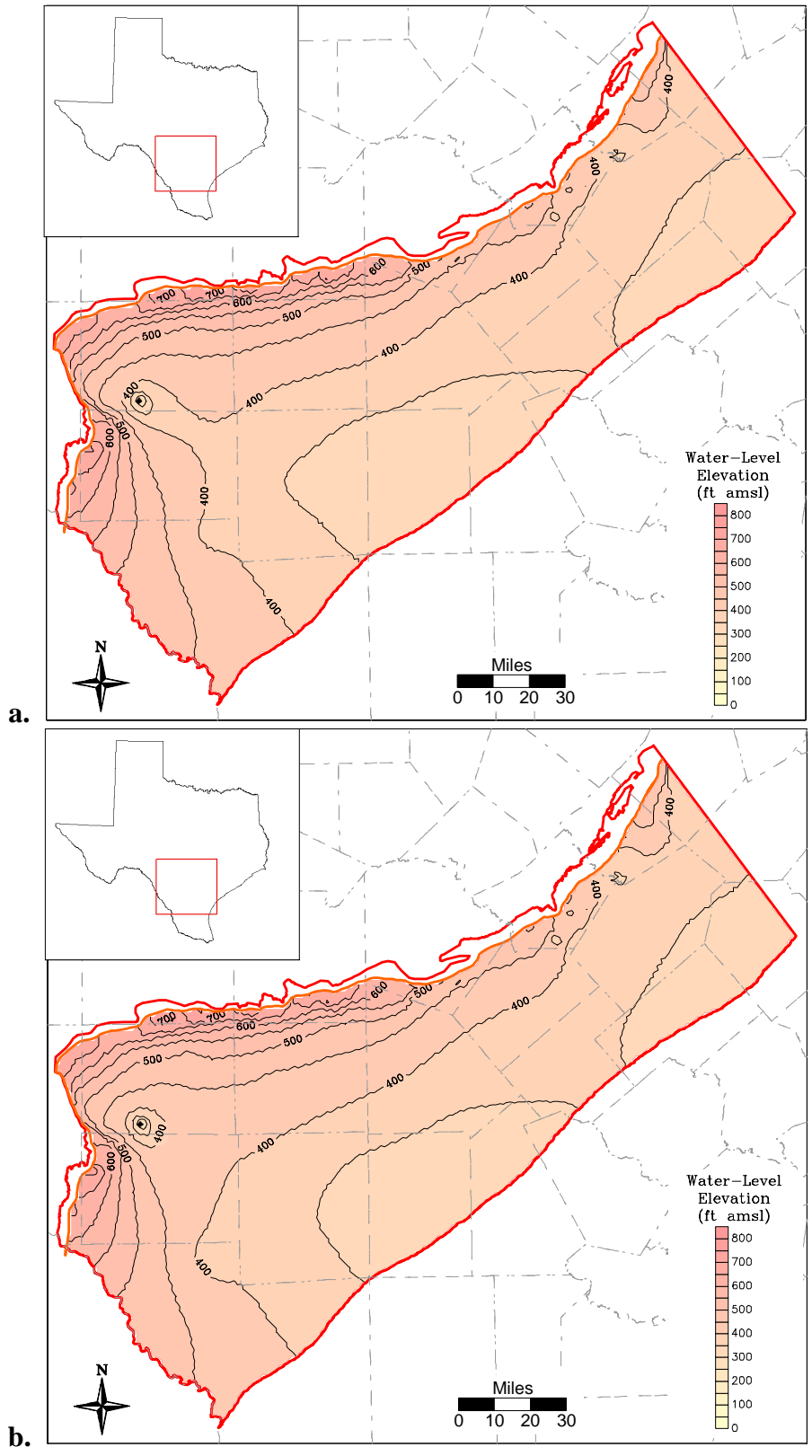


Figure 10.2.18 Simulated 2030 (a) and 2040 (b) head surface, middle Wilcox (Layer 5).

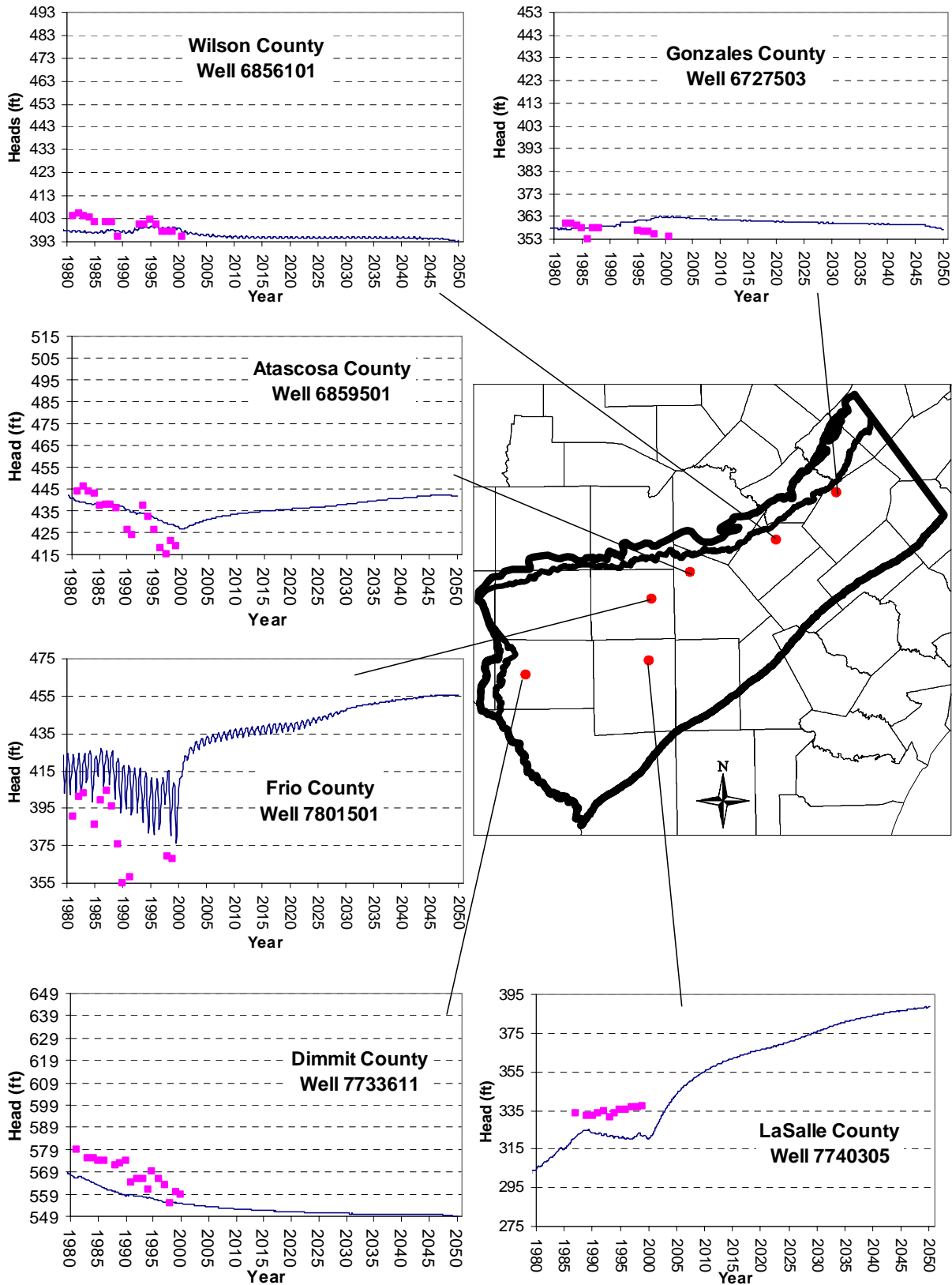


Figure 10.2.19 Selected hydrographs from predictive simulation to 2050 with the DOR.

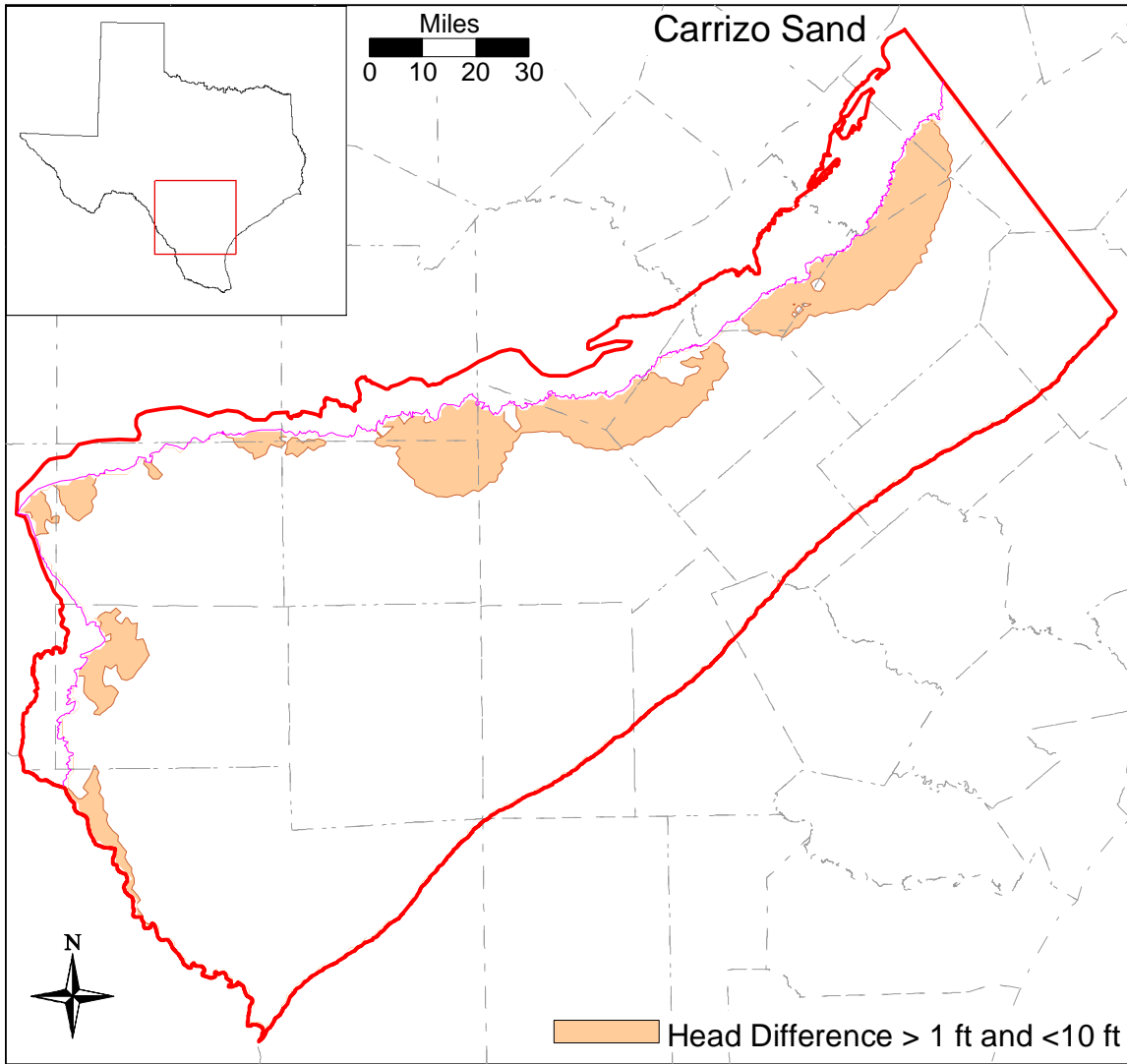


Figure 10.2.20 Simulated difference in head surfaces for the Carrizo between the average condition 2050 simulation and the drought of record 2050 simulation.

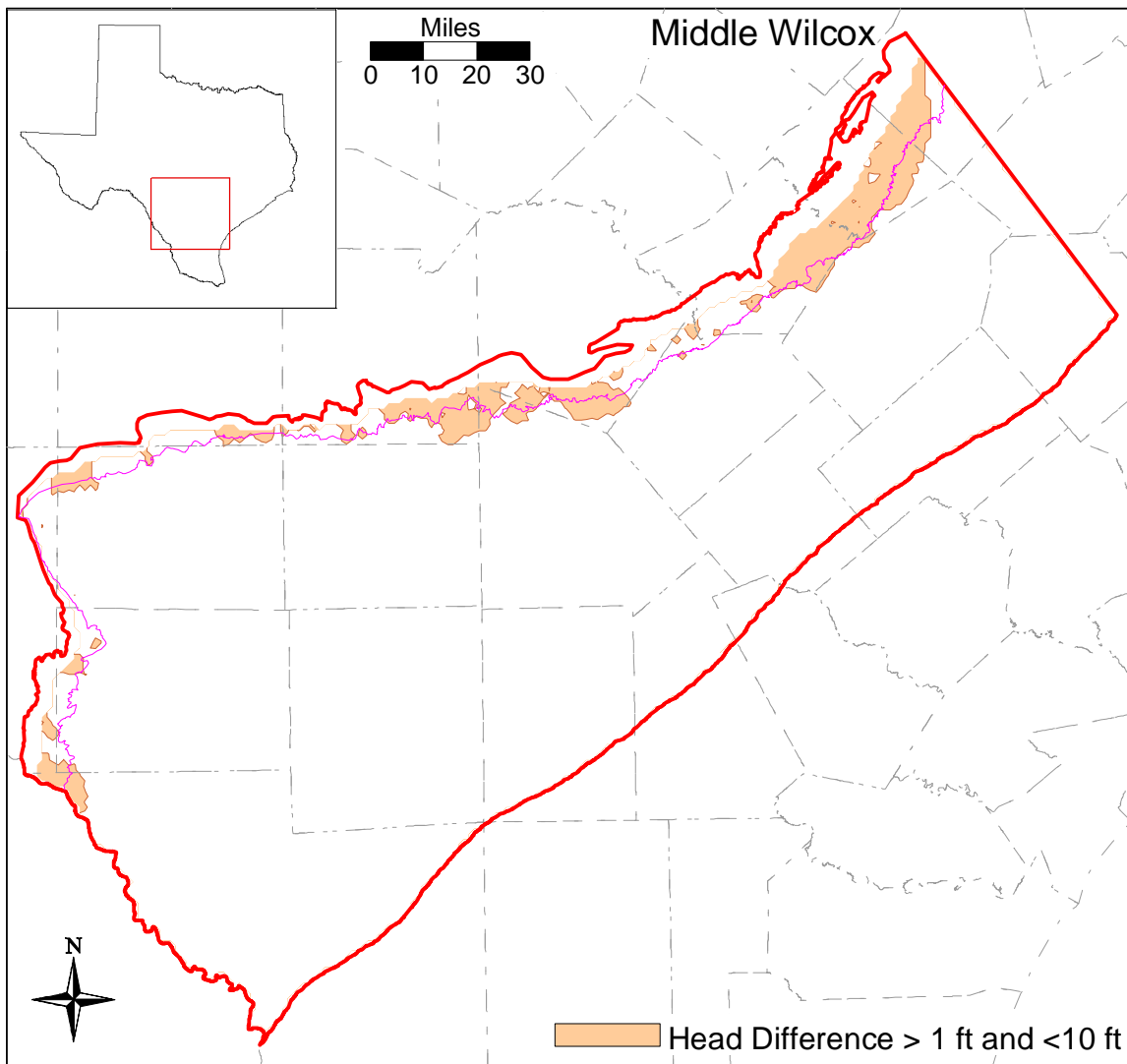


Figure 10.2.21 Simulated difference in head surfaces for the middle Wilcox between the average condition 2050 simulation and the drought of record 2050 simulation.

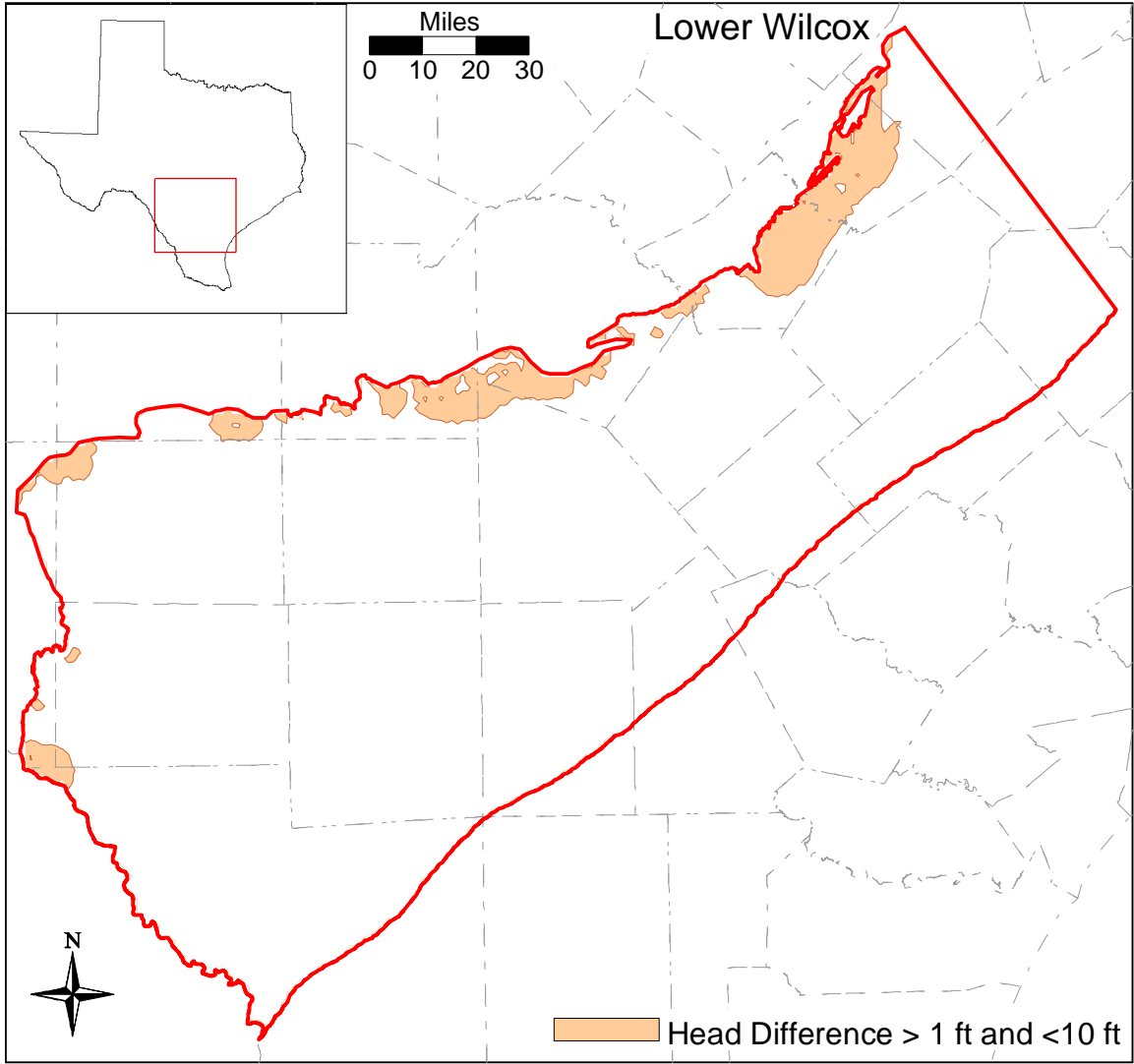


Figure 10.2.22 Simulated difference in head surfaces for the lower Wilcox between the average condition 2050 simulation and the drought of record 2050 simulation.

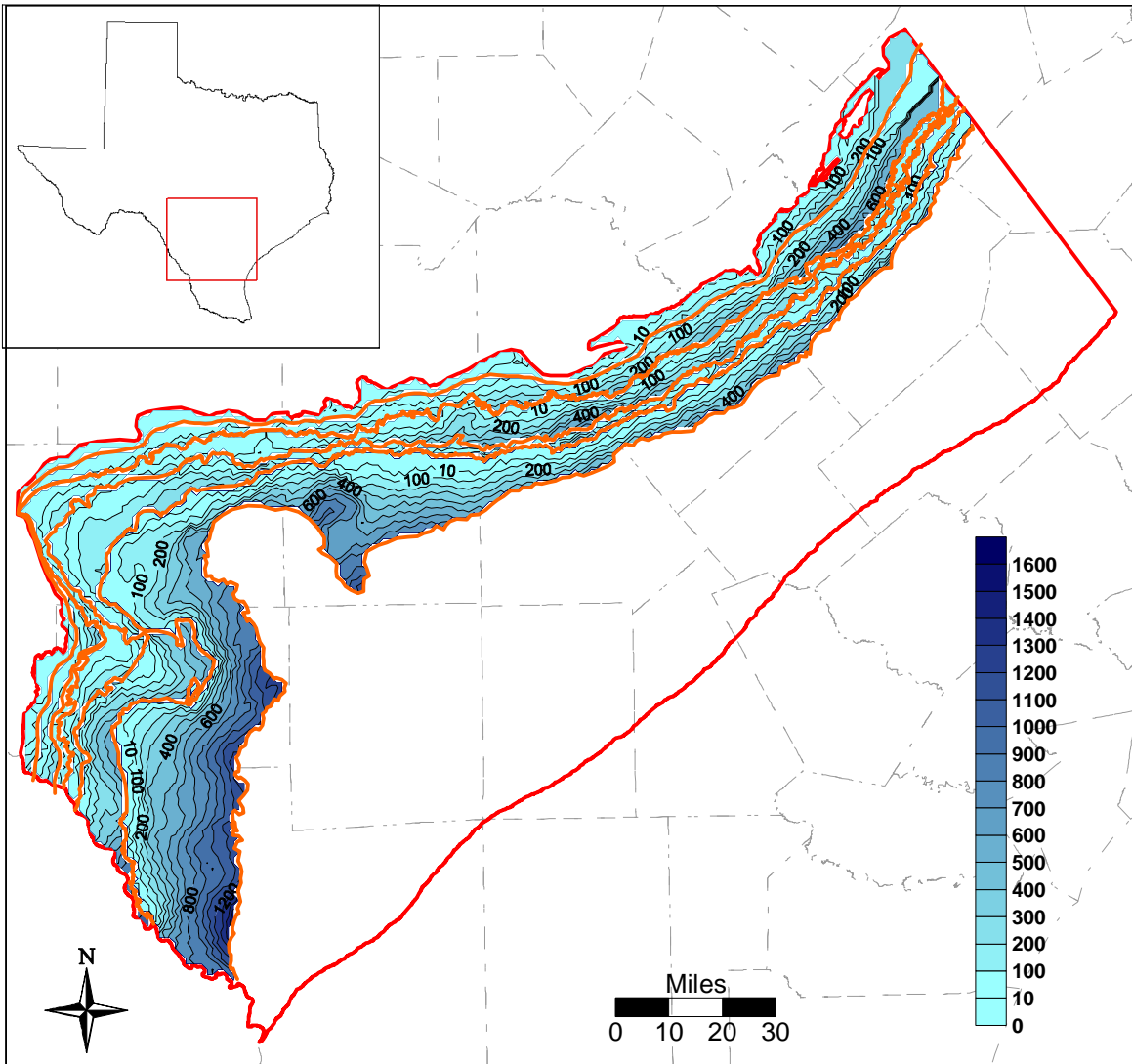


Figure 10.2.23 Simulated saturated thickness in the outcrop at year 2000.

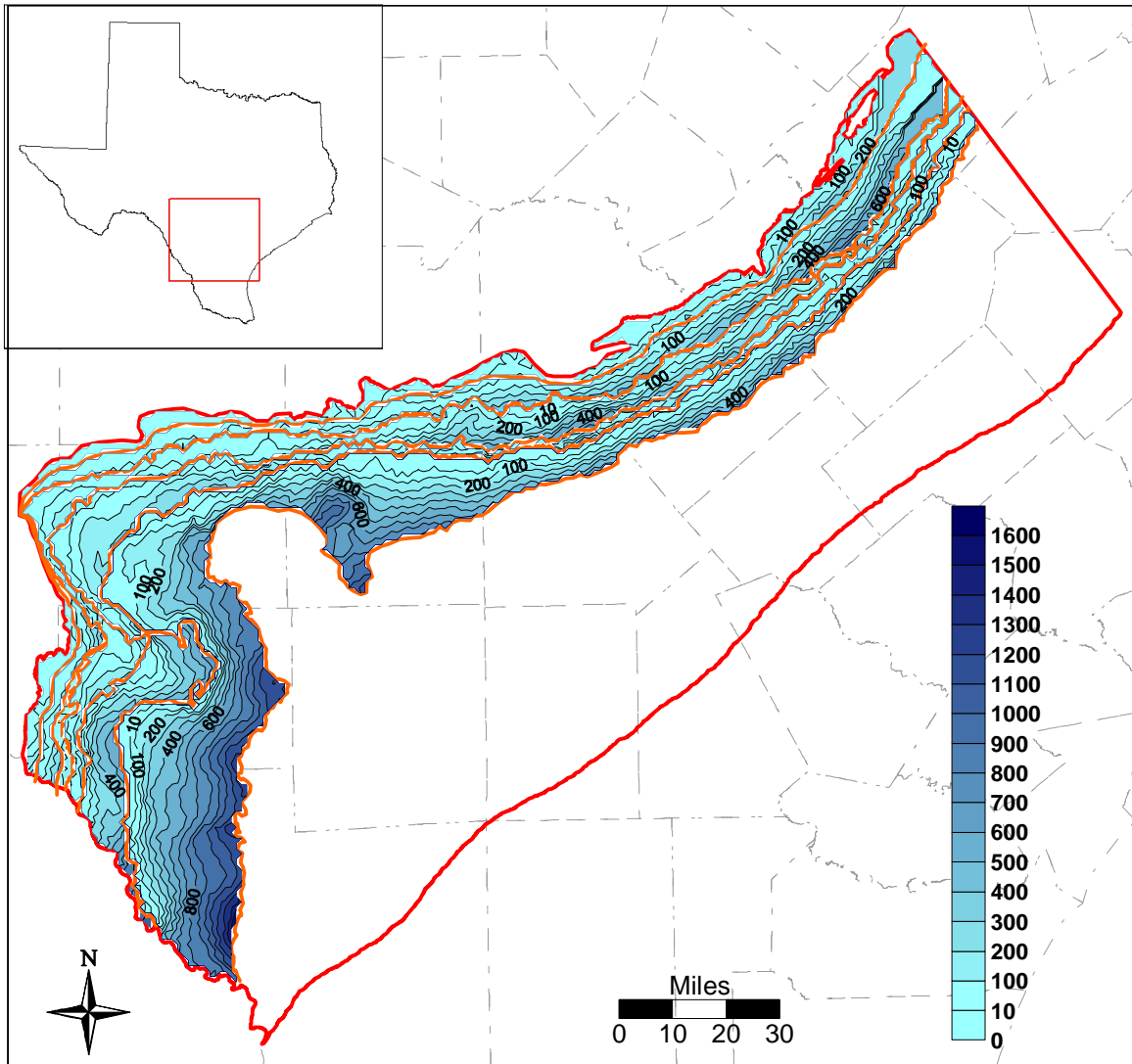


Figure 10.2.24 Simulated saturated thickness in the outcrop at year 2050.

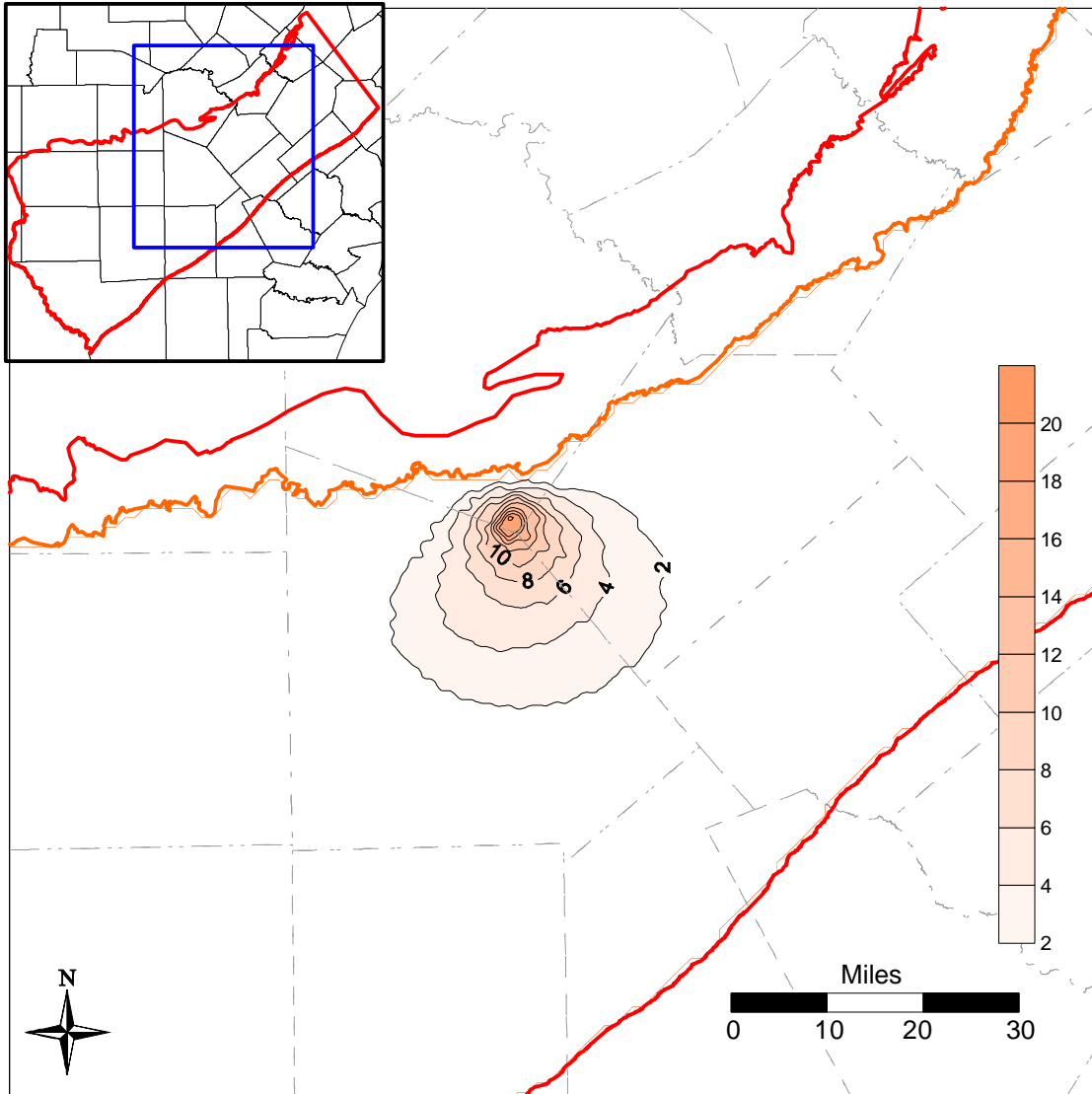


Figure 10.2.25 Difference between the 2010 base simulation and the 2010 simulation including the Twin Oaks Project in Bexar County.

10.3 Predictive Simulation Water Budget

Table 10.3.1 shows the water budget for the predictive simulations. The table shows the water budget for the final year of each of the predictive simulations. Because the simulations ended in February (defined by the drought of record), these balances are from February of the previous year to February of the given year. For example, the water budget for 2010 extends from February 2009 to February 2010. In general, the predictive simulation water budget shows similar trends to that of the calibration/verification simulations. However, a major difference in the predictive simulations is the decrease in pumping. Table 10.3.1 shows that the pumping decreases by 44% from 1990 to 2010. The pumping decreases further to 130,427 AFY in 2030 and is relatively stable for the remainder of the simulation. Most of the increase in heads seen in the predictive simulations, discussed in the previous section, can be attributed to this decrease in pumping. The most significant pumping decreases are in the Carrizo, where historically most of the pumping has occurred. As with the calibration/verification simulations, the amount of leakage from the streams varied significantly through the predictive period. In all years shown in the table, the streams are gaining more water than they are losing. As discussed in Section 9.2.3, this is likely due to the drought of record which has decreased the amount of flow in the streams to the point where the losing streams are not contributing as significantly to the aquifer. Note that in the 2050 run with average recharge (i.e., no DOR), the net gain of the streams is at least an order of magnitude less than in all of the drought years. Also, comparing the 2050 run with average recharge to the DOR years shows the difference between average and drought condition recharge, which in the case of the 2050 simulation is approximately 232,000 AFY, or more than half of the average recharge. Groundwater evapotranspiration is also higher in the 2050 DOR simulation than in the 2050 average condition simulation.

The Carrizo aquifer behaves similarly in the predictive runs, with most of the outflow from the aquifer due to pumping. However, as pumping decreases in the predictive simulations, less water is directed across the Reklaw Formation into the Carrizo. For example, in 1990, when pumping is 303,154 AFY, 50,412 AFY of water comes into the Carrizo from the Reklaw. In 2010, when pumping is 170,747 AFY, 29,817 AFY flows in through the top. So, as pumping decreases, the gradient across the Reklaw decreases, and by 2050 the inflow from the top seems stable at approximately 25,000 AFY.

Table 10.3.1 Water budget for predictive simulations, AFY.

Year	Layer	GHBs	Reservoirs	Wells	ET	Top	Bottom	Recharge	Streams	Storage
1990	1	21,575	0	-7,228	-31,897	0	-54,422	102,478	-97,276	64,941
	2	0	0	-13,989	-1,742	54,422	-50,412	21,747	-31,279	19,029
	3	0	0	-223,628	-20	50,412	-16,618	25,865	4,246	159,753
	4	0	0	-29,546	-10	16,618	7,338	5,676	-1,783	1,569
	5	0	4,925	-17,754	-4,210	-7,338	3,002	24,736	-24,670	21,288
	6	0	0	-11,009	-3,144	-3,002	0	17,914	-7,972	7,204
	Sum	21,575	4,925	-303,154	-41,023	111,112	-111,112	198,416	-158,734	273,785
2000	1	16,185	0	-7,884	-24,002	0	-60,693	116,840	-231,968	191,441
	2	0	0	-10,030	-3,339	60,693	-61,387	27,310	-237,867	224,480
	3	0	0	-200,091	-119	61,387	-8,705	36,551	-28,422	139,411
	4	0	0	-19,299	-36	8,705	9,778	4,192	-19,224	15,879
	5	0	2,255	-15,077	-2,193	-9,778	2,984	30,349	-57,843	49,289
	6	0	0	-11,671	-1,660	-2,984	0	20,006	-45,922	42,224
	Sum	16,185	2,255	-264,053	-31,348	118,023	-118,023	235,247	-621,245	662,723
2010	1	6,854	0	-6,885	-57,704	0	-39,843	89,581	-135,466	142,334
	2	0	0	-6,227	-4,241	39,843	-29,817	13,514	-111,055	96,531
	3	0	0	-104,592	-118	29,817	-6,119	15,994	-1,414	66,498
	4	0	0	-13,145	-745	6,119	6,370	531	-7,670	8,398
	5	0	3,104	-22,516	-2,607	-6,370	1,129	22,721	-33,354	37,871
	6	0	0	-17,382	-3,436	-1,129	0	10,460	-17,167	28,640
	Sum	6,854	3,104	-170,747	-68,851	68,280	-68,280	152,800	-306,126	380,271
2020	1	618	0	-6,382	-57,799	0	-38,111	90,806	-138,703	148,050
	2	0	0	-6,147	-4,317	38,111	-31,967	12,525	-111,428	101,777
	3	0	0	-110,559	-120	31,967	-2,125	15,954	-1,356	66,251
	4	0	0	-13,191	-861	2,125	8,968	474	-8,329	10,728
	5	0	2,992	-23,850	-2,631	-8,968	1,949	22,973	-33,488	41,000
	6	0	0	-17,871	-3,521	-1,949	0	10,388	-17,468	30,406
	Sum	618	2,992	-178,000	-69,250	61,287	-61,287	153,121	-310,772	398,212

Table 10.3.1 (continued)

Year	Layer	GHBs	Reservoirs	Wells	ET	Top	Bottom	Recharge	Streams	Storage
2030	1	-4,638	0	-5,525	-58,092	0	-33,062	92,518	-140,031	147,217
	2	0	0	-2,890	-4,261	33,062	-24,283	10,814	-111,355	97,469
	3	0	0	-84,017	-130	24,283	1,452	16,110	-1,353	43,667
	4	0	0	-9,342	-862	-1,452	9,663	318	-8,637	10,224
	5	0	2,874	-14,650	-2,411	-9,663	1,942	23,009	-34,422	33,299
	6	0	0	-14,004	-3,616	-1,942	0	10,492	-17,923	26,980
	Sum	-4,638	2,874	-130,427	-69,372	44,289	-44,289	153,260	-313,722	358,856
2040	1	-9,713	0	-5,394	-58,564	0	-30,820	92,519	-142,424	152,682
	2	0	0	-2,964	-4,308	30,820	-21,910	10,813	-111,353	97,458
	3	0	0	-85,455	-153	21,910	3,578	16,111	-1,413	45,460
	4	0	0	-9,002	-862	-3,578	11,019	398	-8,796	10,706
	5	0	2,763	-15,250	-2,603	-11,019	2,577	23,336	-34,925	35,101
	6	0	0	-14,005	-3,981	-2,577	0	10,156	-18,270	28,662
	Sum	-9,713	2,763	-132,070	-70,471	35,556	-35,556	153,333	-317,180	370,069
2050	1	-11,981	0	-5,344	-59,587	0	-32,606	92,542	-144,405	160,299
	2	0	0	-4,386	-4,267	32,606	-24,137	10,791	-111,439	99,389
	3	0	0	-93,093	-175	24,137	5,275	16,265	-1,377	49,083
	4	0	0	-9,089	-862	-5,275	11,985	461	-8,891	11,479
	5	0	2,667	-15,596	-2,838	-11,985	3,154	23,117	-35,340	36,800
	6	0	0	-13,335	-4,314	-3,154	0	11,671	-18,670	27,786
	Sum	-11,981	2,667	-140,843	-72,042	36,330	-36,330	154,848	-320,122	384,836
2050*	1	-12,348	0	-5,344	-32,694	0	-33,043	164,603	-27,664	-53,501
	2	0	0	-4,386	-2,448	33,043	-25,186	41,870	17,274	-60,173
	3	0	0	-93,094	-408	25,186	3,985	73,466	7,881	-16,919
	4	0	0	-9,089	-429	-3,985	11,597	4,927	230	-3,323
	5	0	2,367	-15,596	-2,743	-11,597	2,412	61,866	-18,258	-18,456
	6	0	0	-13,383	-3,635	-2,412	0	40,471	-1,114	-19,924
	Sum	-12,348	2,367	-140,893	-42,357	40,235	-40,235	387,203	-21,651	-172,295

* Does not include DOR.

11.0 LIMITATIONS OF THE MODEL

A model can be defined as a representation of reality that attempts to explain the behavior of some aspect of it, but is always less complex than the real system it represents (Domenico, 1972). As a result, limitations are intrinsic to models. Model limitations can be grouped into several categories including: (1) limitations in the data supporting a model, (2) limitations in the implementation of a model which may include assumptions inherent to the model application, and (3) limitations regarding model applicability. The limitations of this modeling study are discussed in the following consistent with the grouping provided above.

11.1 Limitations of Supporting Data

Developing the supporting database for a regional model at this scale and with this large number of grid cells is a challenge. An adequate database was available from published sources for estimation of the structural surfaces for the Carrizo-Wilcox aquifer at the scale of the model. Because the model is at a regional scale, structural data will not have every bend and discontinuity found at a local scale. However, we did find that the regional projection of our structure through a smaller scale structural data set made available by the Gonzales Underground Water Conservation District showed very good agreement even at the local scale.

Our discussion will now focus on the parameters which were found to be important in the sensitivity analyses and the quality of the targets used to assess calibration and verification. For the steady-state model, the primary parameters controlling model behavior are recharge and vertical conductivity. For the transient model, the primary parameters controlling model behavior are pumping and the horizontal hydraulic conductivity. Recharge in the Carrizo-Wilcox aquifer has been studied by many and Scanlon et al. (2002) provide a good summary of the available recharge estimates in the study area. Estimates of recharge for the Carrizo-Wilcox vary from less than an inch per year to up to five inches per year. The Southern Carrizo-Wilcox GAM steady-state model provides a good means for estimating viable recharge estimates for the aquifer. However, because of the correlation between recharge and vertical conductance of the formations, recharge cannot be uniquely determined. The vertical conductance of the modeled aquifers can only be estimated regionally by models such as this GAM. The conundrum is that in the steady-state model, the vertical conductance of the aquifers is inversely related to recharge

which means that unique determination of these two parameters is not possible. To take advantage of this, we estimated recharge with a forward model (SWAT), and considered the recharge to be fixed, for the most part, during calibration. Estimates of recharge are important to the GAM modeling process because they provide a means of constraining the vertical conductance terms in the model especially when calibrating to steady-state and transient conditions. Recharge studies should be continued in the Carrizo-Wilcox aquifer.

For the transient model, the most important parameter through the calibration process was the vertical conductivity of the Carrizo-Wilcox aquifer and the Reklaw/Bigford formations. At the end of calibration, the sensitivity analysis showed that the most important parameters at the final calibration state were pumping and the horizontal hydraulic conductivity. The pumping estimates were derived through a detailed process (see Appendices B and C), however they must be considered uncertain. Because the southern Carrizo-Wilcox aquifer is most heavily developed in the confined portion of the aquifer, errors in pumping rates make a significant impact on simulated water levels. Not unlike the situation with recharge and vertical conductance in the steady-state model, horizontal hydraulic conductivity and pumping are correlated parameters and unique determination of them is not possible. We were reticent to adjust the horizontal conductivities and could not find good evidence for adjusting/moving pumping.

Pumping estimates in the Wintergarden area should be revisited relative to the results of this model and the LBG-Guyton and HDR (1998) model. Likewise, applicability of aquifer test data to estimate regional effective hydraulic conductivity in the Wintergarden area should be further investigated. At this time, we do not know if our lack of model performance in the Wintergarden area is a result of pumping or horizontal hydraulic conductivity. This issue must be addressed to improve model predictions in that local area of the model.

The model also lacks horizontal hydraulic conductivity data for the Queen City/El Pico and the Wilcox Group. This is especially true in the downdip confined portions of the aquifer where there is a total lack of data. Hydraulic conductivity data for the Carrizo is also lacking in the deeper portions of the aquifer. The model was not strongly sensitive to the Wilcox hydraulic conductivity but this is probably because of a general lack of Wilcox head targets. With improved control on hydraulic conductivity data in the confined portions of the aquifer, estimates

of vertical conductance in the aquifer system would be better constrained. Carrizo hydraulic conductivity data would be of great benefit in the area of the model north of Laredo where development of the Carrizo-Wilcox is being considered. There is little hydraulic conductivity data available to support predictions in that area of the model.

The primary type of calibration target is hydraulic head. There is a general lack of heads representative of the predevelopment for all model layers. However, we believe the steady-state model is important to the constraint of the model calibration and accept the uncertainty in predevelopment conditions. Head calibration targets for the transient (historical model) are also lacking in the Wilcox and in the eastern Carrizo for the confined portions of the model. The model calibration could be improved by an increased density of head targets in these areas. Many of the groundwater conservation districts have implemented or are in the process of implementing monitoring programs. This effort should be continued and supported.

The other type of calibration target used was stream gain/loss estimates. There are limited stream gain/loss estimates in the model area. There were also a limited number of stream gages in the outcrop that were amenable to estimation of losses or gains through the study region. Because the MODFLOW stream routing package does not model runoff, direct comparison to stream gages is problematic. It would be beneficial if publicly available surface water models were developed for the outcrop regions in the study area. These would provide better estimates of the hydrography of the area and could be coupled with MODFLOW.

11.2 Limiting Assumptions

There are several assumptions that are key to the model regarding construction, calibration, and prediction. These are briefly discussed below with a discussion of the potential limitations of the assumption.

We modeled the lower boundary of the model as a no-flow boundary at the base of the Wilcox Group. This assumption is consistent with other regional models in the area and is probably a good assumption for the model in the overall sense. However, as the model moves to the outcrop, the no-flow nature of the base of the lower Wilcox creates some problems with recharge rates where the lower Wilcox is thin. This is not considered a significant limitation to the model since it causes only limited-area edge effects.

The lateral model boundaries were also modeled as no-flow boundaries. The western model boundary is the Rio Grande and probably does not limit the models performance in the west. The east boundary is in a region where significant pumping could occur in the future. We used a no-flow boundary because we assumed that the boundary provided a conservative reflective boundary as long as pumping east of the boundary was equal to or less than pumping west of the boundary. We reviewed the Central Carrizo-Wilcox GAM transient heads and concluded that drawdowns were not significant enough (less than 30 feet) to use a transient boundary condition for the historical period.

Another assumption used in our model is that the recharge estimated from SWAT was applicable to the region. As discussed earlier, we made few modifications to the SWAT output. We believe that the model provided defensible regional estimates of recharge in the model region using physical models and parameters representative of the area. We did not model the interflow zone in SWAT. We used MODFLOW to reject recharge to the stream networks. We consider this approach successful in this region because rejected recharge is less important to the model region as a whole than it would be in the eastern part of Texas.

In the predictive simulations, we assumed (in accordance with TWDB's GAM requirements) that the pumping estimates available from the Regional Water Planning Group database tables were representative of the future demands. This resulted in a 100,000 AFY decrease in pumping at the juncture between 1999 and 2000, prompting a significant head recovery in the Wintergarden area. The State Water Plan (TWDB, 2002) estimates that Region L, which is not entirely coincident with our model area, will meet 25 percent of their water needs in 2050 with new groundwater (approximately 200,000 AFY). This is in addition to 157,000 AFY from existing groundwater in 2050. The region is looking to the Carrizo-Wilcox aquifer as a source for water (strategies CZ-10C and CZ-10D). The current predictive simulations do not appear to bracket a worst case scenario of demand for the region. However, this does not limit the models applicability.

Finally, predictive pumping demand estimates provided by the RWPGs are based upon DOR conditions. As a result, pumping does not increase at the end of each predictive simulation when the DOR occurs. It is expected that we would see greater water level declines in the

aquifer system as a whole if the pumping and climate (recharge) were impacted as a result of the DOR.

11.3 Limits for Model Applicability

The model was developed on a regional scale and is only capable of predicting aquifer conditions at the regional scale. The model is applicable for assessing regional aquifer conditions resulting from groundwater development over a fifty-year time period.

The model itself was developed at a grid-scale of one square mile. The model is not capable of being used in its current state to predict aquifer responses at specific points such as a particular well at a particular municipality. The aquifer is accurate at the scale of tens of miles which is adequate for understanding groundwater availability at the scale of the southern Carrizo-Wilcox aquifer.

The model is ideal for refinement for more local scale issues related to specific water resource questions. Questions regarding local drawdown to a well should be based upon analytical solutions to the diffusion equation or a refined numerical model. The GAM produces water levels representative of large volumes of aquifer (e.g., 5,280 ft X 5,280 ft X aquifer thickness in feet). The model was built to determine how regional water levels will respond to water resource development in an area smaller than a county and larger than a square mile.

The GAM model provides a first-order approach to coupling surface water to groundwater which is adequate for the GAM model purposes and for the scale of application. However, this model does not provide a rigorous solution to surface water modeling in the region and should not be used as a surface water modeling tool in isolation.

The GAM model as developed does not simulate the transport of solute (water quality). As a result, the model cannot be used in its current form to explicitly address water-quality issues. The study and model did not delineate specific regions within the Carrizo-Wilcox aquifer having poorer water quality and thus potentially not being suitable as a groundwater resource. The study only documents a limited assessment of water quality in the study area.

12.0 FUTURE IMPROVEMENTS

To use models to predict future conditions requires a commitment to improve the model as new data becomes available or when modeling assumptions or implementation issues change. This GAM model is no different. Through the modeling process one generally learns what can be done to improve the model's performance or what data would help better constrain the model calibration. Future improvements to the model will be discussed below.

12.1 Supporting Data

Several types of data could be collected to better support the GAM model development process. These include recharge studies, surface water-groundwater studies and basic addition of stream gages, and water level monitoring in the confined portion of the Carrizo-Wilcox aquifer.

Estimates of recharge are important to the GAM modeling process because they provide a means of constraining the vertical hydraulic conductivity of the aquifer system when calibrating to steady-state and transient conditions. Studies should be continued into the nature of recharge in the Carrizo-Wilcox aquifer.

Characterization of surface water groundwater interaction requires a good coverage of stream gages in the model outcrop areas, preferably immediately upstream and downstream of the outcrop areas. The model predicts that stream-aquifer interaction is significant in the model region. It would be beneficial if publicly available surface water models were developed for the outcrop regions in the study area. These would provide better estimates of the hydrography of the area and could be coupled with MODFLOW in future model improvement.

Additional water-level monitoring in the Wilcox Group and downdip portions of the Carrizo Formation is also important for future model development. Nearly all available Wilcox water-level measurements are from the outcrop regions of the aquifer. Although the Wilcox may be non-potable in portions of the confined section, it is still advantageous to monitor these deep areas to improve aquifer understanding and to implement those improvements into the model. It is also important to increase water-level monitoring in areas that are potential areas of future development but which are currently not greatly developed. Two regions that fit this description in the model area are northern Webb County and the Gonzales, Wilson, and southern Bexar County area. These areas have not been heavily produced in the past. If monitoring begins prior

to increased development, the GAM can be calibrated against the aquifer response to improve model predictive capability in those regions.

Currently, horizontal hydraulic conductivity data are lacking for the Queen City/El Pico and the Wilcox Group in the model area. This is especially true in the downdip confined portions of the aquifer where there is a total lack of data. Hydraulic conductivity data for the Carrizo is also lacking in the deeper, more confined portions of the aquifer. Any additional hydraulic conductivity estimates and storativity estimates from pump tests will further help parameterize future improvements to this model.

12.2 Future Model Improvements

Pumping estimates in the Wintergarden area should be revisited relative to the results of this model and the LBG-Guyton and HDR (1998) model. Likewise, applicability of aquifer test data to estimate regional effective hydraulic conductivity in the Wintergarden area should be further investigated. The model exhibits a poorer fit in the largest drawdown cones in the Wintergarden area. At this time, we do not know if this is the result of errors in historical pumping or horizontal hydraulic conductivity, or both. This issue should be addressed in future model improvements.

The lateral model boundaries were modeled as no-flow boundaries. The east boundary is in a region where significant pumping could occur in the future. We used a no-flow boundary because we assumed that the boundary provided a conservative reflective boundary as long as pumping east of the boundary was equal to or less than pumping west of the boundary. The applicability of the eastern boundary should be reviewed with the finalization of the Central and Southern Carrizo-Wilcox GAMs. If the boundary condition should be transiently applied as a head-dependent flow boundary, these changes can be made when the Queen City-Sparta aquifers are added to the model.

The current predictive simulations, although based upon pumping in the Regional Water Planning Group tables, do not appear to bracket a worst case scenario of demand for the region. An upper-end estimate of pumping should be developed in cooperation with the TWDB and the RWPGs and run with the Southern Carrizo-Wilcox GAM model.

13.0 CONCLUSIONS

This report documents a three-dimensional groundwater model developed for the southern Carrizo-Wilcox aquifer to the GAM standards defined by the TWDB. This regional-scale model was developed using MODFLOW with the stream-routing package to simulate stream-aquifer interaction and the reservoir package to model groundwater interaction with lakes and reservoirs. The model divides the Carrizo-Wilcox aquifer into four layers: the Carrizo, and the upper, middle, and lower Wilcox. The Reklaw/Bigford formations and the Queen City/El Pico formations are also modeled as individual model layers.

The purpose of this GAM is to provide predictions of groundwater availability through the year 2050 based on current projections of groundwater demands during drought-of-record conditions. This GAM provides an integrated tool for the assessment of water management strategies to directly benefit state planners, Regional Water Planning Groups (RWPGs), and Groundwater Conservation Districts (GCDs).

This GAM has been developed using a modeling protocol which is standard to the groundwater model industry. This protocol includes: (1) the development of a conceptual model for groundwater flow in the aquifer, (2) model design, (3) model calibration, (4) model verification, (5) sensitivity analysis, (6) model prediction, and (7) reporting.

The model has been calibrated to predevelopment conditions (prior to significant resource use) which are considered to be at steady state. The steady-state model reproduces the predevelopment aquifer heads well and within the uncertainty in the head estimates. The median recharge rate estimated for the steady-state model was 0.51 inches per year. In the predevelopment model, recharge accounted for approximately 87% of the aquifer inflow and streams and ET discharged approximately 43% and 30% of aquifer flow, respectively. Approximately 27% of the aquifer inflowing water passed from the outcrop through to the confined aquifer and exited vertically through the GHBs attached to the confined portion of the Queen City/El Pico. A sensitivity analysis was performed to determine which parameters had the most influence on aquifer performance and calibration. The two most sensitive parameters for the steady-state model were recharge and vertical hydraulic conductivity of all units younger (overlying) the Carrizo.

The model was also satisfactorily calibrated to transient aquifer conditions from 1980 through December 1989. The model did a good job of reproducing aquifer heads and available estimates of aquifer-stream interaction. The transient-calibrated model was verified by simulating to aquifer conditions from 1990 through December 1999. Again, the model satisfactorily simulated observed conditions. However, the model did have problems matching the very low heads in the Wintergarden area which has experienced extreme water level declines. This issue is considered to be either the result of lower hydraulic conductivities in the area than are measured or the result of an inadequate accounting of pumping in the area. Regionally, the model reproduces model heads to within head target errors. A sensitivity analysis was performed on the transient model. The two most sensitive parameters for the transient model were pumping and the Carrizo horizontal hydraulic conductivity.

Model predictions were performed to estimate aquifer conditions for the next 50 years based upon projected pumping demands under DOR conditions as developed by the Regional Water Planning Groups. The pumping demand estimates developed from the regional water plans predicted a significant decline in Carrizo-Wilcox pumping starting in 2000. This decline is approximately 100,000 AFY. As a result of the significant pumping declines predicted, the Carrizo-Wilcox rebounds significantly in the western model region where groundwater pumping was predicted to decrease. The eastern portion of the model showed a slight gradual water level decline as pumping demand generally increased in that part of the model. Pumping associated with potential future Laredo development (14,000 AFY) of the Carrizo-Wilcox in northern Webb County created a significant local drawdown of over 100 feet by 2050.

This model, like all models, has limitations and can be improved. However, this calibrated GAM provides a documented, publicly-available tool for the assessment of future groundwater availability in the southern Carrizo-Wilcox region. The GAM is capable of reproducing the natural (predevelopment) and historical conditions of the aquifer measured by multiple calibration measures.

14.0 ACKNOWLEDGEMENTS

The Southern Carrizo-Wilcox GAM was developed with the participation of a committed group of stakeholders representing varied interests within the model region. Interaction with these stakeholders was performed through a series of Stakeholder Advisory Forums (SAF) held across the model region. In these meetings, stakeholders were solicited for data and were provided updates on a regular basis. The model described in this report has benefited from the stakeholders involvement and interest. In addition, we would like to specifically thank those members of the SAF who have hosted meetings across the model region, including: Barry Miller at the Gonzales Underground Water Conservation District, Steve Raabe and Ronnie Hernandez at the San Antonio River Authority, Mike Mahoney at the Evergreen Underground Water Conservation District, and Ed Walker at the Wintergarden Underground Water Conservation District.

We would also like to thank the TWDB GAM staff led by Robert Mace for their support during this modeling exercise. We would like to thank Ted Angle who has managed our contract with professionalism. We would also like to thank Grant Snyder of URS Corporation and Bill Klemt of LBG-Guyton and Associates for providing aquifer test results and data in the study region. We would also like to thank Rick Hay from Texas A&M Corpus for his help in understanding previous modeling studies in the area.

We would like to thank our senior technical reviewers for this project; Dr. Steve Gorelick (Stanford University) and Dr. Graham Fogg (University of California, Davis). The model was greatly improved by their recommendations. We would also like to thank Jeannie Gibbs of INTERA for her efforts in compiling and organizing the tremendous amount of data collected for this study and her GIS support. Finally, we would like to thank Judy Ratto of INTERA for her efforts above and beyond the call of duty in developing this report.

15.0 REFERENCES

- Alexander, W.H., Jr., B.N. Myers, and O.C. Dale, 1964. Reconnaissance investigation of the ground-water resources of the Guadalupe, San Antonio, and Nueces River Basins, Texas. Texas Water Commission, Bulletin 6409.
- Alexander, W.H., and White, D.E., 1966. Ground-water resources of Atascosa and Frio Counties, Texas: Texas Water Development Board Report 32, 99 p.
- Anders, R.B., 1960. Ground-water geology of Karnes County, Texas. Texas Board of Water Engineers, Bulletin 6007.
- Anders, R.B., and E.T. Baker, Jr., 1961. Ground-Water Geology of Live Oak County, Texas. Texas Board of Water Engineers, Bulletin 6105.
- Anders, R.B., 1967. Ground-water resources of Sabine and San Augustine Counties, Texas: Texas Water Development Board Report 37, 115 p.
- Ashworth J.B., and J. Hopkins, 1995. Aquifers of Texas. Texas Water Development Board, Report 345.
- Anderson. M.P., and W.W. Woessner, 1992. *Applied Groundwater Modeling*. Academic Press, San Diego, CA, 381 p.
- Ayers, W.B., Jr., and A.H. Lewis, 1985. The Wilcox Group and Carrizo Sand (Paleogene) in East-Central Texas: Depositional Systems and Deep-Basin Lignite: The University of Texas at Austin, Bureau of Economic Geology Special Publication, 19p., 30 pls.
- Bebout, D.G., B.R. Weise, A.R. Gregory, and M.B. Edwards, 1982. Wilcox Sandstone reservoirs in the deep subsurface along the Texas Gulf Coast; their potential for production of geopressed geothermal energy: : The University of Texas at Austin, Bureau of Economic Geology Report of Investigations No. 117, 125 p.
- Borrelli, J., C.B Fedler, and J.M. Gregory, 1998. Mean Crop Consumptive Use and Free-Water Evaporation for Texas. Report for TWDB Grant 95-483-137. Feb. 1, 1998.
- Broom, M.E., 1968. Ground-water resources of Wood County, Texas: Texas Water Development Board Report 79, 84 p.

- Broom, M.E., and B.N. Myers, 1966. Ground-water resources of Harrison County, Texas: Texas Water Development Board Report, 27, 73 p.
- Broom, M.E., W.H. Alexander, Jr., and B.N. Myers, 1965. Ground-water resources of Camp, Franklin, Morris, and Titus Counties, Texas: Texas Water Development Board Bulletin 6517, 153 p.
- Brune, G., 1975. Springs of Texas, Volume I. Branch-Smith, Inc., Texas.
- Bureau of Economic Geology, 1996. River Basin Map of Texas. Bureau of Economic Geology, The University of Texas at Austin.
- Chiang, W.-H., and W. Kinzelbach, 1998. Processing Modflow- A simulation system for modeling groundwater flow and pollution: software manual, 325 p.
- de Marsily, G., 1986. Quantitative Hydrogeology, Groundwater Hydrology for Engineers. Academic Press, Orlando, FL, p. 440.
- Domenico, P.A., 1972. Concepts and Models in Groundwater Hydrology, McGraw Hill, New York, 405 pp.
- Domenico, P. A., and Schwartz, F. W., 1990. Physical and chemical hydrology: John Wiley & Sons, New York, 824 p.
- Duffin, G.L., and G.R. Elder, 1979. Variations in specific yield in the outcrop of the Carrizo Sand in South Texas as estimated by seismic refraction. Texas Department of Water Resources, Report 229.
- Dutton A.R., 1999. Groundwater availability in the Carrizo-Wilcox aquifer in Central Texas – numerical simulations of 2000 through 2050 withdrawal projections. The University of Texas at Austin, Bureau of Economic Geology, Report of Investigations No. 256.
- Edwards, D.C., and T.B. McKee, 1997. Characteristics of 20th Century drought in the United States at multiple time scales. Climatology Report Number 97-2, Colorado State University, Fort Collins, Colorado.
- Fenske, J.P., S.A. Leake, and D.E. Prudic, 1996. Documentation of a computer program (RESI) to simulate leakage from reservoirs using the modular finite-difference ground-water flow model (MODFLOW). U.S. Geological Survey, Open-File Report 96-364.

- Fisher W.L., and J.H. McGowen, 1967. Depositional systems in the Wilcox Group of Texas and their relationship to occurrence of oil and gas. Transactions-Gulf Coast Association of Geological Societies, Vol. XVII.
- Fogg, G.E., 1989. Stochastic analysis of aquifer interconnectedness: Wilcox Group, Trawick area, East Texas: The University of Texas at Austin, Bureau of Economic Geology, Report of Investigations No. 189, 68 p.
- Fogg, G.E., 1986. Groundwater flow and sand-body interconnectedness in a thick, multiple-aquifer system: Water Resources Research, v. 22, no. 5, p. 679-694.
- Fogg, G.E., and W.R. Kaiser, 1986. Regional hydrogeologic considerations for deep-basin lignite development in Texas, *in* Kaiser, W. R., and others, Geology and ground-water hydrology of deep-basin lignite in the Wilcox Group of East Texas: The University of Texas at Austin, Bureau of Economic Geology Special Publication, p. 57-59.
- Fogg, G.E., and C.W. Kreitler, 1982. Ground-water hydraulics and hydrochemical facies in Eocene aquifers of the East Texas Basin: The University of Texas at Austin, Bureau of Economic Geology Report of Investigations No. 127, 75 p.
- Fogg, G.E., S.J. Seni, and C.W. Kreitler, 1983. Three-dimensional ground-water modeling in depositional systems, Wilcox Group, Oakwood salt dome area, east Texas. The University of Texas at Austin, Bureau of Economic Geology Report of Investigations No. 133, 55 p.
- Follett, C.R., 1966. Ground-Water Resources of Caldwell County, Texas. Texas Water Development Board, Report 12.
- Follett, C.R., 1970. Ground-Water Resources of Bastrop County, Texas. Texas Water Development Board, Report 109.
- Freeze, R.A., 1969. The mechanism of natural ground-water recharge and discharge. 1. One-dimensional, vertical, unsteady, unsaturated flow above a recharging or discharging ground-water flow system: Water Resources Research, Vol. 5, No. 1, p. 153-171.
- Freeze, R.A., 1971. Three-dimensional, transient, saturated-unsaturated flow in a groundwater basin: Water Resources Research, Vol. 7, No. 2, p. 347-366.

- Freeze, R.A., 1975. A stochastic-conceptual analysis of one-dimensional ground-water flow in nonuniform homogeneous media: *Water resources Research*, Vol. 11, No. 5, p. 679-694.
- Freeze, R.A., and J.A. Cherry, 1979. *Groundwater*: Prentice-Hall, Inc., New Jersey, 604 p.
- Galloway, W.E., X. Liu, D. Travis-Neuberger, and L. Xue, 1994. References high-resolution correlation cross sections, paleogene section, Texas Coastal Plain. The University of Texas at Austin, Bureau of Economic Geology.
- Gelhar, L.W., and C.L. Axness, 1983. Three-dimensional stochastic analysis of macrodispersion in aquifers: *Water Resources Research*, v. 19, no. 1, p. 161-180.
- Grubb, H.F., 1997. Summary of hydrology of the regional aquifer systems, Gulf Coastal Plain, south-central United States. U.S. Geological Survey, Professional Paper 1416-A.
- Gutjahr, A.L., L.W. Gelhar, A.A. Bakr, and J.R. MacMillan, 1978. Stochastic analysis of spatial variability in subsurface flows-2, Evaluation and application. *Water Resources Research*, v. 14, no. 5, p. 953-959.
- Hamlin, H.S., 1988. Depositional and ground-water flow systems of the Carrizo-Upper Wilcox, South Texas. The University of Texas at Austin, Bureau of Economic Geology, Report of Investigations No. 175.
- Harbaugh, A.W., and M.G. McDonald, 1996. User's documentation for MODFLOW-96, an update to the U.S. Geological Survey modular finite-difference ground-water flow model: U.S. Geological Survey Open-File Report 96-485, 56 p.
- Harden and Associates, Inc., 2000. Brazos G Regional Water Planning Area, Carrizo-Wilcox ground water flow model and simulations results.
- Harris, H.B., 1965. Ground-Water Resources of La Salle and McMullen counties, Texas. Texas Water Commission, Bulletin 6520.
- Hayes, M., 2001. Drought Indices. National Drought Mitigation Center, Available online at <http://enso.unl.edu/ndmc/enigma/indices.htm>.
- HDR Engineering, Inc., 2000. Preliminary feasibility options to deliver ALCOA/CPS groundwater to Bexar County: technical report prepared for San Antonio Water Systems, variously paginated.

- Helm, D.C., 1976. One-dimensional simulation of aquifer system compaction near Pixley, California-2, Stress-dependent parameters, *Water Resources Research*, Vol. 12, No. 3, p. 375-391.
- Henry, C.D., J.M. Basciano, and T.W. Duex, 1980. Hydrology and water quality of the Eocene Wilcox Group; significance for lignite development in East Texas: The University of Texas at Austin, Bureau of Economic Geology Geological Circular 80-3,9p.
- Hibbs, B.J., and J.M. Sharp, Jr., 1991. Evaluation of underflow and the potential for instream flow depletion of the lower Colorado River by high capacity wells in adjoining alluvial systems : final report for the Lower Colorado River Authority, Water Resources Division, 126p.
- Isaaks, E.H., and R.M. Srivastava, 1989. *An Introduction to Applied Geostatistics*. Oxford University Press, New York.
- Kaiser, W.R., 1990. The Wilcox Group (Paleocene-Eocene) in the Sabine Uplift area, Texas: Depositional systems and deep-basin lignite: The University of Texas at Austin, Bureau of Economic Geology Special Publication, 20p.
- Kaiser, W.R., M.L. Ambrose, W.B. Ayers, Jr., P.E. Blanchard, G.F. Collins, G.E. Fogg, D.L. Gower, C.L. Ho, C.S. Holland, M.L. W. Jackson, C.M. Jones, A.H., Lewis, G.L. Macpherson, C.A. Mahan, A.H. Mullin, D.A. Prouty, S.J. Tewalt, and S.W. Tweedy, 1986. Geology and ground-water hydrology of deep-basin lignite in the Wilcox Group of East Texas: The University of Texas at Austin, Bureau of Economic Geology Special Publication, 182 p.
- Kaiser, W.R., 1974. Texas lignite: near-surface and deep-basin resources: The University of Texas at Austin, Bureau of Economic Geology Report of Investigations No. 79, 70 p.
- Kaiser, W.R., 1978. Depositional systems in the Wilcox Group (Eocene) of east-central Texas and the occurrence of lignite, *in* Kaiser, W.R., ed., *Proceedings, 1976 Gulf Coast Lignite Conference: geology, utilization, and environmental aspects*. The University of Texas at Austin, Bureau of Economic Geology, Report of Investigations No. 90.

- Klemt, W.B., G.L. Duffin, and G.R. Elder, 1976. Ground-water resources of the Carrizo aquifer in the Winter Garden area of Texas, Volume 1: Texas Water Development Board, Report 210.
- Kreitler, C.W., 1979. Ground-water hydrology of depositional systems, *in* Galloway, W.E., and others, Depositional and ground-water flow systems in the exploration for uranium, a research colloquium. The University of Texas at Austin, Bureau of Economic Geology.
- Kuiper, L.K., 1985. Documentation of a numerical code for the simulation of variable density ground-water flow in three dimensions. U.S. Geological Survey, Water-Resources Investigations Report 84-4302.
- LBG-Guyton Associates and HDR Engineering Inc., 1998. Interaction between ground water and surface water in the Carrizo-Wilcox aquifer.
- Mace, R.E., R.C. Smyth, L. Xu, and J. Liang, 2000a. Transmissivity, hydraulic conductivity, and storativity of the Carrizo-Wilcox Aquifer in Texas, The University of Texas at Austin, Bureau of Economic Geology Final Report submitted to the Texas Water Development Report, 76p.
- Mace, R.E., A.H. Chowdhury, R. Anaya, and S.C. Way, 2000b. Groundwater availability of the Middle Trinity aquifer in the Hill Country area of Texas – Numerical simulations through 2050: Texas Water Development Board Report, 174p.
- Maidment, D.R., 1992. Handbook of Hydrology. McGraw-Hill, Inc.
- Mason, C.C., 1960. Geology and ground-water resources of Dimmit County, Texas. Texas Board of Water Engineers, Bulletin 6003.
- McDonald, M.G., and A.W. Harbaugh, 1988. A modular three-dimensional finite-difference ground-water flow model. U.S. Geological Survey, Techniques of Water-Resources Investigations, book 6, chapter A1.
- McKee, T.B., N.J. Doesken, and J. Kleist, 1993. The relationship of drought frequency and duration to time scales. Preprints, 8th Conference on Applied Climatology, 17-22 January, Anaheim, CA, pp. 179-184.

- Moulder, E.A., 1957. Development of Ground Water from the Carrizo Sand and Wilcox Group in Dimmit, Zavala, Maverick, Frio, Atascosa, Medina, Bexar, Live Oak, McMullen, La Salle, and Webb counties, Texas. USGS Open-File Report.
- Opfel, W.J., and G.R. Elder, 1978. Results of an infiltration study on the Carrizo Sand outcrop in Atascosa County, Texas. Texas Department of Water Resources, LP-61.
- Payne, J.N., 1975. Geohydrologic significance of lithofacies of the Carrizo Sand of Arkansas, Louisiana, and Texas and the Meridian Sand of Mississippi: U.S. Geological Survey Professional Paper, P 0569-D, 11p.
- Pearson, F.J., Jr., and D.E. White, 1967. Carbon 14 ages and flow rates of water in Carrizo Sand, Atascosa County, Texas, Water Resources Research, Vol. 3, No. 1, p. 251-261.
- Prudic, D.E., 1988. Documentation of a computer program to simulate stream-aquifer relations using a modular, finite-difference, ground-water flow model, U.S. Geological Survey, Open-File Report 88-729, Carson City, Nevada.
- Prudic, D.E., 1991. Estimates of hydraulic conductivity from aquifer-test analyses and specific capacity data, gulf coast regional aquifer systems, south-central United States., U.S. Geological Survey, Water- Resources Investigation Report 90-4121, Austin, Texas.
- Ritchey, J.D. and J.O. Rumbaugh, 1996. Subsurface fluid flow (ground-water and vadose zone) modeling. ASTM Special Technical Publication 1288.
- Ryder, P.D., 1988. Hydrogeology and Predevelopment Flow in the Texas Gulf Coast Aquifer Systems. USGS Water-Resources Investigations Report 87-4248.
- Ryder, P.D., and A.F. Ardis, 1991. Hydrology of the Texas Gulf Coast aquifer systems. U.S. Geological Survey, Open-File Report 91-64.
- Sandeen, W.M., 1987. Ground-water resources of Rusk County, Texas: Texas Water Development Board Report 297, 121 p.
- Scanlon, B.R., A. Dutton, and M. Sophocleus, 2002. Groundwater recharge in Texas.
- Shafer, G.H., 1965. Ground-water resources of Gonzales County, Texas. Texas Water Development Board, Report 4

- Slade, R.M., Jr., J.T. Bentley, and D. Michaud, 2002. Results of streamflow gain-loss studies in Texas, with emphasis on gains from and losses to major and minor aquifers, Texas, 2000. U.S. Geological Survey, Open-File Report 02-068.
- Texas Water Development Board (TWBD), 1972. Survey of the subsurface saline water of Texas, Report 157.
- Texas Water Development Board (TWBD), 1997. Water for Texas, A Consensus-Based Update to the State Water Plan, Volume II, Technical Planning Appendix, August 1997, Document No. GP-6-2.
- Texas Water Development Board (TWBD), 2002. Water for Texas – 2002, January, 2002, 155 p.
- Theis, C.V., 1940. The source of water derived from wells - essential factors controlling the response of an aquifer to development: Civil Engineering, American Society of Civil Engineers, p. 277-280.
- Thompson, G.L., 1972. Ground-water resources of Navarro County, Texas: Texas Water Development Board Report 160, 63 p.
- Thorkildsen, D, R. Quincy, and R. Preston, 1989. A digital model of the Carrizo-Wilcox aquifer within the Colorado River Basin of Texas. Texas Water Development Board, Report 332.
- Thorkildsen, D., and Price, R.D., 1991. Ground-water resources of the Carrizo-Wilcox aquifer in the Central Texas Region: Texas Water Development Board Report 332, 59p.
- Turner, S.F., T.W. Robinson, and W.N. White., revised by D.E. Outlaw, W.O. George, and others, 1960. Geology and Ground-Water Resources of the Winter Garden District Texas, 1948. USGS Water-Supply Paper 1481.
- Warren, J.E., and H.S. Price, 1961. Flow in heterogeneous porous media, Society of Petroleum Engineers Journal, Vol. 1, p. 153-169.
- White, D.E., 1973. Ground-water resources of Rains and Van Zandt counties, Texas. Texas Water Development Board, Report 169.

- White, W.N., and O.E. Meinzer, 1931. Ground-Water in the Winter Garden and Adjacent Districts in Southwestern Texas. USGS Open-File Report.
- Williams, T.A., and A.K. Williamson, 1989. Estimating water-table altitudes for regional ground-water flow modeling. U.S. Gulf Coast: National Water Well Association, Ground Water, v. 27, no. 3, p. 333-340.
- Williamson, A.K., H.F. Grubb, and J.S. Weiss, 1990. Ground-water flow in the Gulf Coast aquifer systems, South Central United States – A preliminary analysis. U.S. Geological Survey, Water-Resources Investigations Report 89-4071.
- Wilson, T.A., and R.L. Hossman, 1988. Geophysical well-log data base for the gulf coast aquifer systems, south-central United States. U.S. Geological Survey, Open-File Report 87-677.

APPENDIX A

Brief Summary of the Development of the Carrizo-Wilcox Aquifer in Each County and List of Reviewed Reports

This appendix provides a review of Carrizo-Wilcox aquifer development in the counties within the study area. The review will summarize the available literature on a county basis. A brief introduction will describe the history of development and the magnitude of water level declines using long-term historical water levels (hydrographs).

Development of groundwater from the Carrizo Sand and Wilcox Group began in the early 1900s in parts of the study area. The first flowing well was drilled in 1884 at Carrizo Springs in Dimmit County (Turner et al., 1960). Successful crop growth and available transport to market via railroads resulted in the rapid development of Carrizo and Wilcox waters in parts of the Wintergarden as early as 1910 (Moulder, 1957). Irrigation was greatest in Dimmit and Zavala Counties. White and Meinzer (1931) investigated groundwater conditions in southwestern Texas and show that the original extent of flowing wells was substantially reduced by 1930 in these two counties.

Our analysis of predevelopment conditions (Section 4.4.1 in the main body of this report) has shown that the largest water-level declines are in the western part of the study area with water-level declines of greater than 150 ft throughout the Wintergarden. Figure A.1 plots select long-term hydrographs in the western part of the study area including the Wintergarden area. In general, water-level declines are greatest in the confined portions of the aquifer. In LaSalle County we see the influence of a reduction of pumping in the early 1980's at the selected hydrograph. This is in contrast to the hydrographs from Frio, Zavala, Dimmit, McMullen, and Medina counties. Figure A.2 plots select hydrographs from the central and eastern portion of the study area. In general, historical water-level declines have been less severe in the eastern study area with the least amount of decline observed in Gonzales and Caldwell counties.

A discussion of Carrizo-Wilcox groundwater development for each county in the study area will follow.

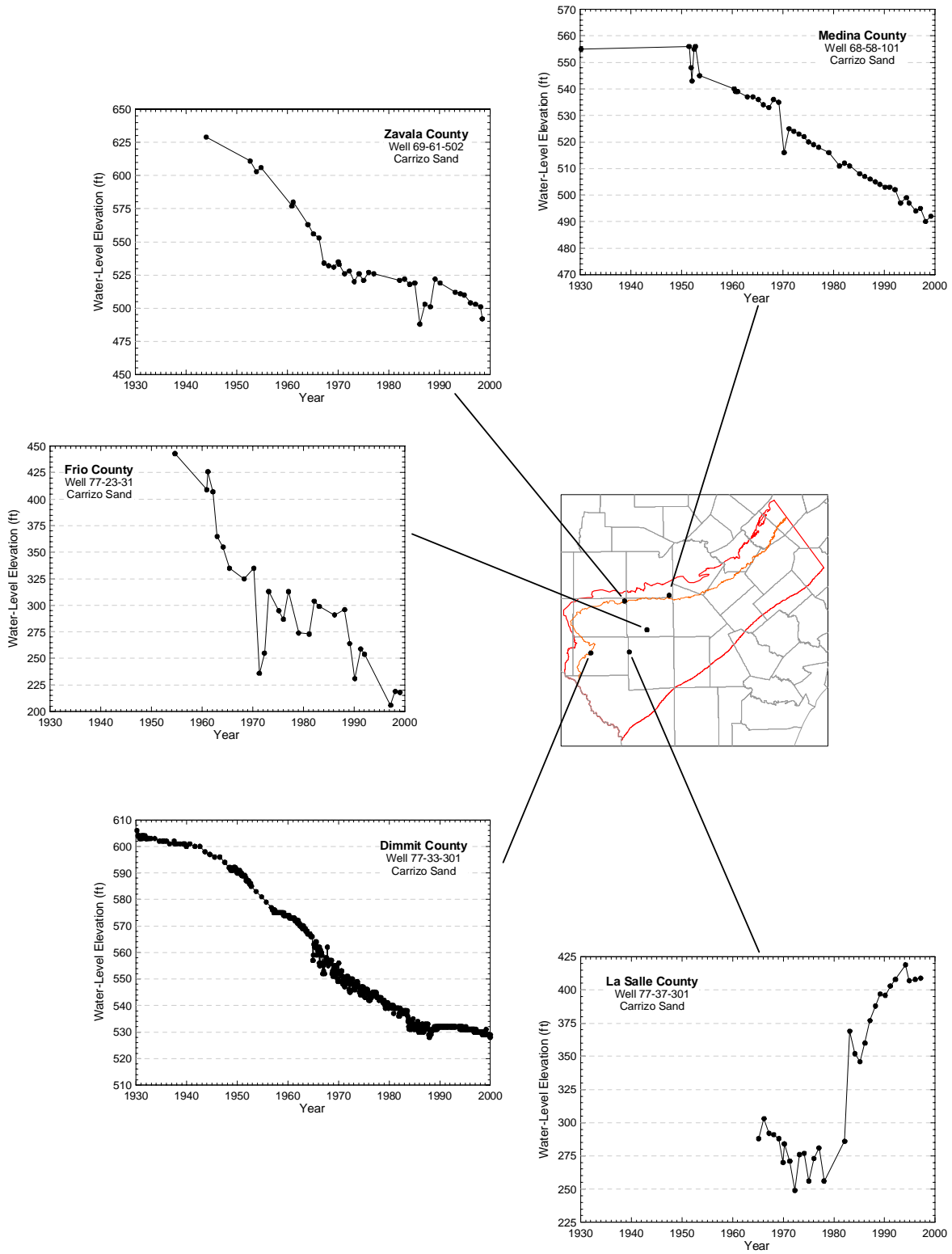


Figure A.1 Select long-term hydrographs in the western study area.

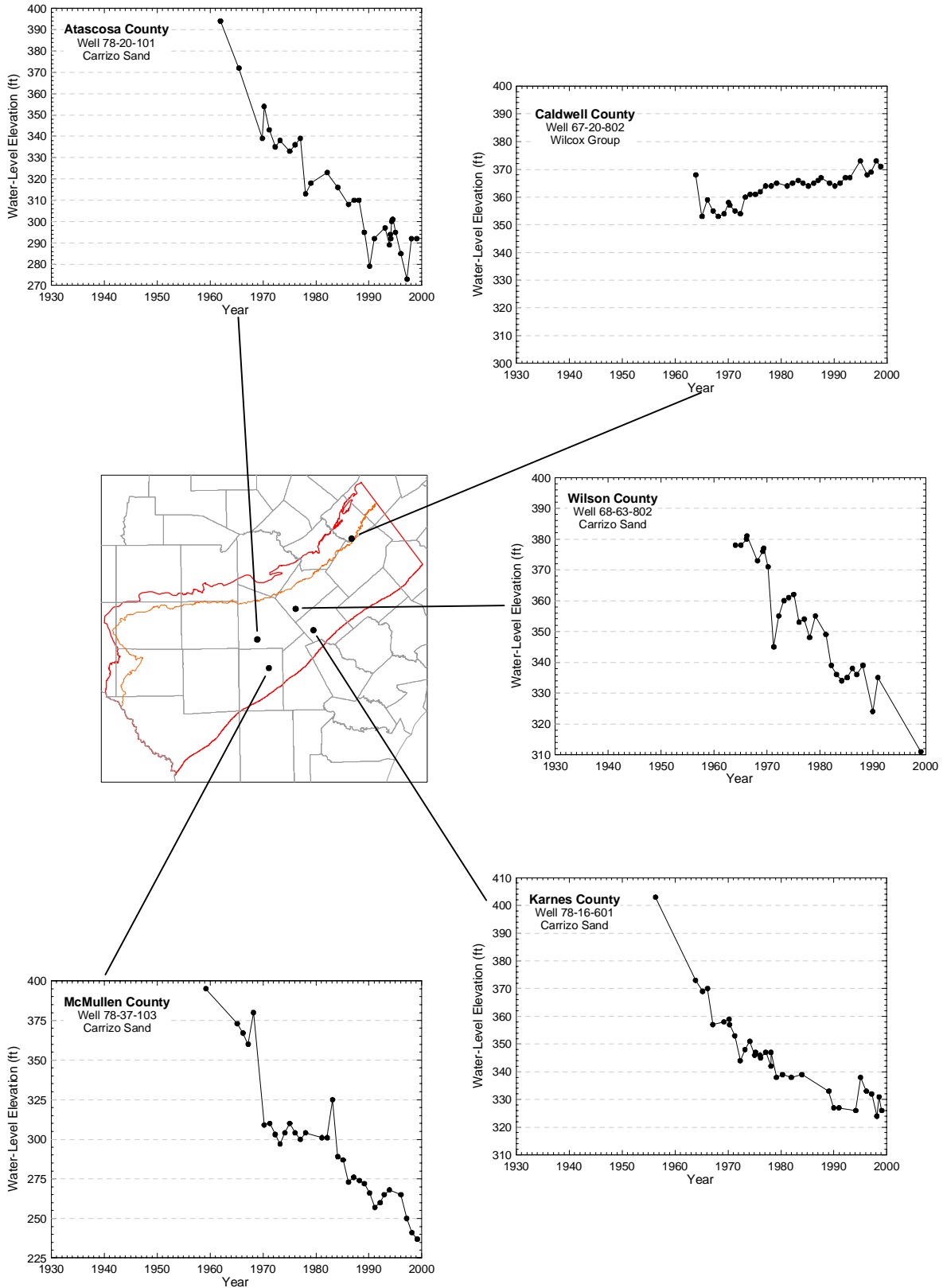


Figure A.2 Select long-term hydrographs in the eastern study area.

Atascosa County

The information regarding the history of development of the Carrizo Sand and Wilcox Group in Atascosa County comes from Lonsdale (1935). The following discussion is taken from that report. The Carrizo Sand is the principal aquifer in Atascosa County. Water from the Wilcox Group is fresh only in the area in and near the outcrop. Initial development in Atascosa County occurred near Poteet, Texas, which is located near the center of the county. The first well in that area was drilled in 1904. Nine additional wells were drilled by 1910 and another 40 wells by 1932. Most of the wells originally flowed. Lansdale (1935) estimates about a 25 ft drop in head in the Carrizo in the Poteet, Texas area between 1904 and 1932. Both Lansdale (1935) and Sundstrom and Follett (1950) indicate that uncontrolled flowing wells in the county wasted large volumes of water from the Carrizo. Sundstrom and Follett (1950) state, "From 1932 to 1944, withdrawals of water have increased materially and artesian pressures have declined in most of the county." They also say that total withdrawal from the Carrizo increased by 63 percent from 1929-1930 to 1944-1945. The earliest water-level measurements found in the county reports and on the TWDB website are from 1908, 1909, and 1910. These three measurements were considered to be fairly representative of predevelopment conditions.

Bastrop County

Little information related to historical development of the Carrizo Sand and Wilcox Group in Bastrop County was found during the literature review. In Bastrop County, the Carrizo Sand and Wilcox Group act as a single aquifer (Follett, 1970). Follett (1970) states that the Carrizo-Wilcox aquifer has not been significantly developed in the county due to (1) little need for water because of the sparse population of the county in and southeast of the outcrop area, and (2) the presence of good water in the overlying Queen City Sand/Bigford Formation and younger aquifers. Water-level measurements for Bastrop County used to generate the predevelopment water-level elevations were taken in 1925 and 1950.

Bee County

Myers and Dale (1966) state that "The Carrizo Sand of Eocene age is not tapped by water wells in Bee County; however, electric logs indicate that slightly saline water (1000 to 2000 ppm dissolved solids) may be obtained from the Carrizo in an area of about 10 square miles in the extreme northwestern part of the county at a depth of about 6000 ft."

Bexar County and San Antonio, Texas Area

The principal aquifer underlying Bexar County is the Edwards Limestone. Consequently, little historical information related to the development of the Carrizo Sand and Wilcox Group in Bexar County was found during the literature review. No water-level measurements from this county were used in generation of the predevelopment water-level elevations for the Carrizo-Wilcox aquifer.

Caldwell County

Little historical information related to the development of the Carrizo Sand and Wilcox Group in Caldwell County was found during the literature review. The Carrizo Sand and Wilcox Group act as a single aquifer in this county (Follett, 1966). Data on the TWDB website indicate wells were completed into the Carrizo-Wilcox aquifer as early as 1870. The first public use of Carrizo-Wilcox waters began in 1926 (Follett, 1966). At this time, approximately 30 wells tapped the Carrizo-Wilcox aquifer (TWDB, website). The two earliest water-level measurements for Carrizo-Wilcox wells in Caldwell County were taken in 1906 and 1923 (TWDB, website). These two measurements were not consistent, and only the higher value from 1923 was used to generate the predevelopment contours.

De Witt, County

The Carrizo Sand and the sands of the Wilcox Group are not listed by Follett and Gabrysch (1965) in De Witt County.

Dimmit County

Unless stated otherwise, the historical information given here regarding development of the Carrizo Sand and Wilcox Group in Dimmit County comes from Mason (1960). The Carrizo Sand is the principal water-bearing unit in this county. Some water is withdrawn from the Wilcox Group for domestic and stock purposes in the outcrop area. Downdip of the outcrop, the waters of the Wilcox group are highly mineralized. The first flowing well was drilled in 1884 at Carrizo Springs, Texas. Sixty flowing wells were being used for irrigation and stock watering by 1907. The use of Carrizo waters for irrigation increased rapidly in the county. Between Dimmit and Zavala Counties, 250 irrigation wells were active by 1910. Of those, 35 flowed (Turner et al., 1960). Until about 1947, irrigation was wide-spread throughout the northern one-half of the

county. After that time, irrigation was concentrated in a few locations in the northern half of the county.

The quantity of water removed from the Carrizo aquifer became a concern of some county residents as early as the 1920s. Mason (1960) estimates that between 1929 and 1957 the decline in water levels was approximately 1.1 ft/yr in the outcrop and as much as 230 ft total in the artesian section of the aquifer. In the outcrop areas, withdrawal from the Carrizo aquifer has exceeded recharge since 1929 (Mason, 1960). White and Meinzer (1931) provides a graphic showing that in the northern half of Dimmit County all wells originally flowed and that the area of flowing wells was drastically reduced by 1930.

The earliest water-level measurements for the Carrizo aquifer were taken in 1913 as given on the TWDB website. These measured depths to water yield water-level elevations that are below ground surface in the northern part of the county where it is known that wells originally flowed. Because none of the earliest water-level measurements reflected flowing conditions, the values for selected measurements were increased until the calculated water-level elevation was above ground surface. Those increased values were then used to generate the predevelopment water-level elevation contours (see Table 4.4-1).

Fayette County

Fresh to slightly saline water can be found in the Carrizo Sand and sands of the Wilcox Group in Fayette County (Rogers, 1967). However, the occurrence of fresh water in aquifers located at shallower depths has limited development of the Carrizo Sand and Wilcox Group in this county. Currently, two wells are completed to the Carrizo Sand in Fayette County (TWDB, website). The first was completed in 1917 and the second in 1980. The first recorded water level was measured in 1966 (TWDB, website). Due to the long period of time between the completion date and the date of the first water-level measurement, that measurement is not considered to represent predevelopment conditions.

Frio County

Unless stated otherwise, the following discussion regarding the history of development of the Carrizo Sand and the Wilcox Group in Frio County comes from Lonsdale (1935). The Carrizo Sand is the principal aquifer in Frio County. Water from the Wilcox Group is fresh only

in the area in and near the outcrop. The first flowing well completed in the Carrizo was drilled in 1905. This well continued to flow until 1915 (Alexander and White, 1966). Between 1905 and 1932, 12 additional wells were drilled in the county; 10 for irrigation purposes and two for use as municipal supply wells. Water levels in all of the wells had declined by 1932 and some of the wells that originally flowed had stopped flowing by that time. Frio County experienced an increase in the use of Carrizo water for irrigation during the drought of 1950 to 1956. The earliest water-level measurements found for the county on the TWDB website were taken in 1928 and 1929. Several of those early measurements were used in generation of the predevelopment water-level elevation contours.

Gonzales County

Little information related to historical development of the Carrizo Sand and Wilcox Group in Gonzales County was found during the literature review. Shafer (1965) states that the Carrizo Sand is a major aquifer in Gonzales County and usable water for most purposes can be obtained from the Wilcox Group only in and near the outcrop area. Data on the TWDB website indicate wells were completed into the Carrizo aquifer as early as 1900. The two earliest water-levels measurements for Carrizo wells in Gonzales County were taken in 1901 and 1931 (TWDB, website). These two measurements were not consistent, and only the higher value from 1931 and another measurement from 1940 were used to generate the predevelopment contours.

Guadalupe County

Little information related to historical development of the Carrizo Sand and Wilcox Group in Guadalupe County was found during the literature review. At locations in the county where the Wilcox Group is overlain by the Carrizo Sand, the two are considered to be a single hydrologic unit (Shafer, 1966). Data on the TWDB website indicate wells were completed into the Carrizo-Wilcox aquifer as early as 1892. The two earliest water-levels measurements for Carrizo-Wilcox wells in Guadalupe County were taken in 1936 (TWDB, website). Several of the 1936 measurements, along with high measurements taken in 1982 and 2000, were used to generate the predevelopment water-level elevation contours for the Carrizo-Wilcox aquifer.

Karnes County

Little information related to historical development of the Carrizo Sand and Wilcox Group in Karnes County was found during the literature review. Due to the moderate to very

high salinity of the water in the Wilcox Group, the undifferentiated sands and clays of the Wilcox Group are not considered to be an aquifer in Karnes County (Anders, 1960). Data on the TWDB website indicate that the first wells developed in the Carrizo aquifer were drilled in the 1940s. The first water-level measurement was taken in 1956 (TWDB, website). That measurement was used to generate the predevelopment water-level elevation contours for the Carrizo aquifer.

Lavaca County

The Carrizo Sand and the sands of the Wilcox Group are not sources of fresh water in Lavaca County (Loskot et al., 1982).

LaSalle County

Little information related to historical development of the Carrizo Sand and Wilcox Group in LaSalle County was found during the literature review. The Carrizo Sand is the principal aquifer in this county. Harris (1965) states that the Wilcox Group is "...not known to yield water to wells..." in this county. Development of the Carrizo aquifer for irrigation purposes occurred rapidly until 1920 (Moulder, 1957). At that time, the poor quality of the water and the high cost of drilling deep wells ended the drilling of irrigation wells in the Carrizo (Moulder, 1957). Moulder (1957) states, "The withdrawals from LaSalle County [for irrigation purposes] were considerably less in 1955 than in 1913." Some of the wells in LaSalle County show a rise in water level during 1959 to 1960 due to increased precipitation and decreased irrigation pumpage (Harris, 1965). Data on the TWDB website indicate that the first well developed in the Carrizo aquifer was drilled in 1909. The first water-level measurement was taken in 1942 (TWDB, website). This earliest measurements reflects the effects of pumpage. Therefore, water-level measurements taken during 1959 and 1960, when precipitation was high and irrigation pumping was low, were used in generation of the predevelopment contours. The depth to water for the 1960 measurement yields a water-level elevation below ground surface in the northwestern part of the county where it is known that wells originally flowed. Because this water-level measurement does not reflect flowing conditions, the measured value was increased until the calculated water-level elevation was above ground surface. That increased value, along with a 1959 measurement, was used to generate the predevelopment water-level elevation contours.

Live Oak County

Little information related to historical development of the Carrizo Sand and Wilcox Group in Live Oak County was found during the literature review. The Carrizo Sand is an aquifer for fresh to slightly saline water in this county. However, most of the water in this aquifer is found at depths greater than 4000 ft and is “too deeply buried to be economically developed for most uses” (Anders and Baker, 1961). Most ground-water in this county is obtained from younger, shallower aquifers. Data on the TWDB website list two Carrizo wells in Live Oak County. Both were drilled in 1948. Only one water-level measurement from 1965 is given for one of the wells. The other well has measurements of water levels from 1970 to 1996. Generation of the predevelopment water-level elevations did not use any water-level measurements for this county.

Maverick County

Little historical information related to the development of the Carrizo Sand and Wilcox Group in Maverick County was found during the literature review. Moulder (1957) states, “The Carrizo Sand and sands of the Wilcox age have not been extensively developed [for irrigation purposes] in Maverick...Count[y] because only a small part of the area is underlain by the sands [and] yields from wells have been small...”. Withdrawal for irrigation was less in 1937-1938 than in 1929-1930, but more than doubled from 1938 to 1948 (Moulder, 1957). Taylor (1907) states, “So far as can be ascertained there are no artesian wells in Maverick County”. Data on the TWDB website indicate that the earliest well completed into the Carrizo aquifer was drilled in 1900. The earliest water-levels measurements for Carrizo wells were taken in 1930 (TWDB, website). No water-level measurements from Maverick County were used to generate the predevelopment contours.

McMullen County

Little information related to historical development of the Carrizo Sand and Wilcox Group in McMullen County was found during the literature review. The Carrizo Sand is the principal aquifer in this county. Harris (1965) states that the Wilcox Group is “...not known to yield water to wells...” in this county. Little early development of the Carrizo aquifer for irrigation purposes occurred due to the poor quality of the water and the depth at which the water was located (Moulder, 1957). A rapid increase in development for irrigation occurred from 1949

to 1954 (Moulder, 1957). Some of the wells in McMullen County show a rise in water level during 1959 to 1960 due to increased precipitation and decreased irrigation pumpage (Harris, 1965). Data on the TWDB website indicate that the first wells developed in the Carrizo aquifer were drilled in the 1940s. The first water-level measurement was taken in 1958 (TWDB, website). Two water-level measurements taken during 1959, when precipitation was high and irrigation pumping was low, were used in generation of the predevelopment contours.

Medina County

Little historical information related to the development of the Carrizo Sand and Wilcox Group in Medina County was found during the literature review. In the southern portion of the county, enough water can be obtained from the Carrizo Sand for domestic and stock purposes. As of 1936, there were no irrigation wells completed in the Carrizo Sand or Wilcox Group in this county (Sayre, 1936). Data on the TWDB website indicate that the earliest well completed into the Carrizo aquifer was drilled in 1875. The earliest water-levels measurements for Carrizo wells were taken in 1930 (TWDB, website). Two of the 1930 water-level measurements were used to generate the predevelopment contours.

Uvalde County

Little historical information related to the development of the Carrizo Sand and Wilcox Group in Uvalde County was found during the literature review. The principal aquifer in this county is the Edwards and associated limestones (Welder and Reeves (1962). In the southern portion of the county, enough water can be obtained from the Carrizo Sand for domestic and stock purposes. As of 1936, there were no irrigation wells completed in the Carrizo Sand or Wilcox Group in this county (Sayre, 1936). The only Carrizo or Wilcox well listed in on the TWDB website as having a drilled date was drilled in 1984. The first recorded water-level measurement given on the TWDB website was taken in 1970. No water-level measurements from Uvalde County were used to generate the predevelopment contours.

Webb County

Little historical information related to the development of the Carrizo Sand and Wilcox Group in Webb County was found during the literature review. By 1932, there were four Carrizo wells in the outcrop and 10 Carrizo wells (non-flowing) east of the outcrop (Lonsdale and Day, 1937). The Carrizo Sand is a chief water-bearing unit in the county although it has not been as

extensively developed as the shallower Cook Mountain Formation (Lonsdale and Day, 1937). Data on the TWDB website indicate that the earliest wells completed into the Carrizo Sand or Wilcox Group were drilled to the Carrizo Sand in 1908 and 1915. The earliest water-level measurements for Carrizo wells were taken in 1947 (TWDB, website). The county report by Lonsdale and Day (1937) gives 13 water-level measurements for 1931. Because these 1931 data appeared to be effected by pumpage, no water-level data from Webb County was used to generate the predevelopment contours.

Wilson County

Little historical information related to the development of the Carrizo Sand and Wilcox Group in Wilson County was found during the literature review. The Carrizo Sand is the principal aquifer in Wilson County and the Wilcox Group is an aquifer of less importance in the county (Anders, 1957). Data on the TWDB website indicate that the earliest wells completed into the Carrizo Sand and Wilcox Group were drilled in 1900. The earliest water-level measurement for a Carrizo well was taken in 1910 (TWDB, website). Water-levels were then measured in both Carrizo and Wilcox wells in 1936. The 1910 water-level measurement from the Carrizo was used in generation of the predevelopment contours.

Zavala County

The historical information presented below regarding development of the Carrizo Sand and Wilcox Group in Zavala County comes from Moulder (1957) unless otherwise stated. It appears that the Carrizo Sand and Wilcox Group are hydraulically connected to some extent in this county. The use of Carrizo waters for irrigation developed rapidly in the early 1900s. Between Dimmit and Zavala Counties, 250 irrigation wells were active by 1910. Of those, 35 flowed (Turner et al., 1960). Until 1949, irrigation development was greater in Zavala County than in any other county in the Wintergarden District. The withdrawal of water for irrigation purposes was less in 1937-1938 than in 1929-1930. During the ten year period from 1938 to 1948, the amount of ground water withdrawn for the purposes of irrigation doubled in the county. Historically, the use of ground water for irrigation was greater in Zavala County than in any other county in the Wintergarden District. Data on the TWDB website indicate that the earliest wells completed to the Carrizo Sand or the Wilcox Group were drilled in 1904 and 1905. The earliest water-level measurements for Carrizo and Wilcox wells were taken in 1928 and

1929 (TWDB, website). The measured depths to water for the wells located in the southern portion of the county, where it is known that wells originally flowed, yield water-level elevations that are below ground surface in. Because none of the earliest water-level measurements in the southern part of the county reflected flowing conditions, the value for one measurement was increased until the calculated water-level elevation was above ground surface. That increased values was then used to generate the predevelopment water-level elevation contours. The actual values for several other water-level measurements taken in 1929 and 1931 in the northern portion of the county were also used in generation of the predevelopment contours.

Reviewed Reports

- Alexander, W.H., Jr., and D.E. White. 1966. Ground-Water Resources of Atascosa and Frio Counties, Texas. Texas Water Development Board, Report 32.
- Anders, R.B. 1957. Ground-Water Geology of Wilson County, Texas. Texas Board of Water Engineers, Bulletin 5710.
- Anders, R.B. 1960. Ground-Water Geology of Karnes County, Texas. Texas Board of Water Engineers, Bulletin 6007.
- Anders, R.B., and E.T. Baker, Jr. 1961. Ground-Water Geology of Live Oak County, Texas. Texas Board of Water Engineers, Bulletin 6105.
- Deussen, A., and R.B. Dole. 1916. Ground Water in La Salle and McMullen Counties, Texas. USGS Water-Supply Paper 375.
- Follett, C.R. 1966. Ground-Water Resources of Caldwell County, Texas. Texas Water Development Board, Report 12.
- Follett, C.R. 1970. Ground-Water Resources of Bastrop County, Texas. Texas Water Development Board, Report 109.
- Follett, C.R., and R.K. Gabrysch. 1965. Ground-Water Resources of De Witt County, Texas. Texas Water Commission, Bulletin 6518.
- Harris, H.B. 1965. Ground-Water Resources of La Salle and McMullen Counties, Texas. Texas Water Commission, Bulletin 6520.
- Hutson, W.F. 1898. Irrigation Systems in Texas. USGS Water-Supply Paper 13.

- Lang, J.W. 1954. Ground-Water Resources of the San Antonio Area, Texas: A Progress Report of Current Studies. Texas Board of Water Engineers, Bulletin 5412.
- Lonsdale, J.T. 1935. Geology and Ground-Water Resources of Atascosa and Frio Counties, Texas. USGS Water-Supply Paper 676.
- Lonsdale, J.T., and J.R. Day. 1937. Geology and Ground-Water Resources of Webb County, Texas. USGS Water-Supply Paper 778.
- Loskot, C.L., W.M. Sandeen, and C.R. Follett. 1982. Ground-Water Resources of Colorado, Lavaca, and Wharton Counties, Texas. Texas Department of Water Resources, Report 270.
- Mason, C.C. 1960. Geology and Ground-Water Resources of Dimmit County, Texas. Texas Board of Water Engineers, Bulletin 6003.
- Moulder, E.A. 1957. Development of Ground Water from the Carrizo Sand and Wilcox Group in Dimmit, Zavala, Maverick, Frio, Atascosa, Medina, Bexar, Live Oak, McMullen, La Salle, and Webb Counties, Texas. USGS Open-File Report.
- Myers, B.N., and O.C. Dale. 1966. Ground-Water Resources of Bee County, Texas. Texas Water Development Board, Report 17.
- Rogers, L.T. 1967. Availability and Quality of Ground Water in Fayette County, Texas. Texas Water Development Board, Report 56.
- Sayre, A.N. 1936. Geology and Ground-Water Resources of Uvalde and Medina Counties, Texas. USGS Water-Supply Paper 678.
- Shafer, G.H. 1965. Ground-Water Resources of Gonzales County, Texas. Texas Water Development Board, Report 4.
- Shafer, G.H. 1966. Ground-Water Resources of Guadalupe County, Texas. Texas Water Development Board, Report 19.
- Stearman, J. 1960. Water Levels in Observation Wells in Atascosa and Frio Counties, Texas 1955-1960. Texas Board of Water Engineers, Bulletin 6015.
- Sundstrom, R.W., and C.R. Follett. 1950. Ground-Water Resources of Atascosa County, Texas. USGS Water-Supply Paper 1079-C.

Taylor, T. U. 1902. Irrigation Systems in Texas. USGS Water-Supply and Irrigation Paper No. 71.

Taylor, T. U. 1907. Underground Waters of Coastal Plain of Texas. USGS Water-Supply and Irrigation Paper No. 90.

Turner, S.F., T.W. Robinson, and W.N. White., revised by D.E. Outlaw, W.O. George, and others. 1960. Geology and Ground-Water Resources of the Winter Garden District Texas, 1948. USGS Water-Supply Paper 1481.

Welder, F.A., and R.D. Reeves. 1962. Geology and Ground-Water Resources of Uvalde County, Texas. Texas Water Commission, Bulletin 6212.

White, W.N., and O.E. Meinzer. 1931. Ground-Water in the Winter Garden and Adjacent Districts in Southwestern Texas. USGS Open-File Report.

APPENDIX B

Standard Operating Procedures (SOPs) for Processing Historical Pumpage Data TWDB Groundwater Availability Modeling (GAM) Projects

**Standard Operating Procedures (SOPs)
for Processing Historical Pumpage Data
TWDB Groundwater Availability Modeling (GAM) Projects**

TABLE OF CONTENTS

1. Groundwater Use Source Data	1
1.1 Pumpage by Major Aquifer 1980-1997	1
1.2 RawDataMUN_WaterUseSurvey	1
1.3 RawDataMFG_WaterUseSurvey.....	1
1.4 RuralDomestic_Master_Post1980_021502.xls	1
2. Initial Processing.....	1
2.1. Completion of monthly pumpage estimates for MUN, MFG, PWR, and MIN uses.....	1
2.2 Predicting historical pumpage for 1981-83 and 1997-1999.....	2
2.3 Selecting pumpage within the model domain.....	3
2.4 Preparing a county-basin Arcview shapefile and associating model grid cells with a county-basin	4
3. Matching Pumpage to Specific Wells.....	5
3.1 Create All Wells Table.....	5
3.2 Linking water use data to the state well database.....	6
3.3 Locating unmatched pumpage 1	6
3.4 Locating unmatched pumpage 2	6
3.5 Locating unmatched pumpage 3	6
3.6 Locating unmatched pumpage 4.....	6
3.7 Count wells matched.....	7
3.8 Apportion water use between matched wells	7
3.9 Calculate additional fields	7

3.10 Append out-of-state data	7
3.11 Summarize well-specific matching completeness	8
4. Spatial Allocation of Groundwater Pumpage to the Model Grid	8
4.1 Spatial allocation of well-specific groundwater pumpage	8
4.2 Spatial allocation of irrigation groundwater pumpage.....	9
4.3 Spatial allocation of livestock groundwater pumpage	12
4.4 Spatial allocation of rural domestic (C-O) groundwater pumpage.....	14
4.5 Vertical distribution of groundwater pumpage (all uses).....	16
5. Temporal Distribution of Rural Domestic, Livestock, and Irrigation Groundwater Use	19
5.1. Temporal distribution of livestock pumpage.....	20
5.2 Temporal distribution of irrigation (IRR) pumpage	20
5.3 Temporal distribution of rural domestic (C-O) pumpage	21
6. Summarize Pumpage Information	22
6.1 Summary queries	22
6.2 Join pumpage queries to Arcview shapefile	25
Appendix 1. Vertical Distribution Avenue Script	26
Appendix 2. Script to Return Land Surface Elevation for a Well from a DEM Grid	31

1. Groundwater use source data - Groundwater use data is derived from three tables provided by the Texas Water Development Board (TWDB) in a MS Access 97 database and one spreadsheet provided in MS Excel format:
 - 1.1. **PumpagebyMajorAquifer1980-1997** – This table contains water use summaries, in acre-feet/year) from each major aquifer, county, and basin for the years 1980 and 1984-1997 for the water use categories:
 - IRR – irrigation
 - STK – livestock
 - MIN - mineral extraction
 - MFG – manufacturing
 - PWR – power generation
 - MUN – municipal water supply, and
 - C-O – county-other (rural domestic) use.
 - 1.2. **RawDataMUN_WaterUseSurvey** – This table contains reported annual and monthly self-generated groundwater use totals, in gallons, from each municipal water user for the years 1980-1999. Monthly totals are missing in many cases. The data originate from the annual water use surveys. The county, basin, and major aquifer of origin are reported, as well as the water user group ID, alphanumeric code of the water user, and line 1 of the address of the water user. The number of wells from which the water was pumped is reported in most cases.
 - 1.3. **RawDataMFG_WaterUseSurvey** – This table contains reported annual and monthly self-generated groundwater use totals, in gallons, from each manufacturing, power generation, or mining water user for the years 1980-1999. Monthly totals are missing in many cases. The data originate from the annual water use surveys. The county, basin, and major aquifer of origin are reported, as well as the water user group ID, alphanumeric code of the water user, and line 1 of the address of the water user. The number of wells from which the water was pumped is reported in most cases.
 - 1.4. **RuralDomestic_Master_Post1980_021502.xls** – This Excel spreadsheet contains summaries of annual rural domestic water use, by county-basin, from 1980 to 1997.
2. Initial Processing
 - 2.1. Completion of Monthly Pumpage Estimates for MUN, MFG, PWR, and MIN Uses - In the tables **RawDataMUN_WaterUseSurvey** and **RawDataMFG_WaterUseSurvey**, monthly pumpage estimates are reported for the majority, but not all, of the water users. For other users, only the annual total pumpage is reported. It is necessary to estimate the

monthly pumpage totals for some water users via the following procedure.

- 2.1.1. First, export the tables **RawDataMFG_WaterUseSurvey** and **RawDataMUN_WaterUseSurvey** to Microsoft Excel. Append the records from the latter file to the former. Delete records with reported annual total water use (in gallons) of “0”.
 - 2.1.2. In Excel, calculate the monthly fractions of annual total water use for each record for which monthly pumpage was reported. As an example, a monthly distribution factor of 1/12, or 0.0833, would result from a uniform annual distribution.
 - 2.1.3. Calculate the average monthly distribution factor for each county-basin and water use category. Statistically review these average monthly fractions for outliers. Generally, monthly distribution factors fall within the range 0.035 to 0.15.
 - 2.1.4. Next, for those water use records that contain an annual total water use but no monthly value, calculate estimated monthly water use values by multiplying annual total pumpage by the average monthly distribution factor for the same water use category (MUN, MFG, PWR, MIN) in the county-basin within which it was located. If the monthly distribution factor for its county basin and water use category was an outlier, usually due to the fact that only one or two water users were located in the county-basin, use the monthly distribution factor from the nearest adjacent county-basin. (Note: For Louisiana and Arkansas parishes/counties, for which no monthly values are available, use the values from the nearest Texas counties.)
 - 2.1.5. Add an additional field, “Monthly Calculated” to the spreadsheet, with “N” entered in those records containing original, reported monthly pumpage values, and “Y” for those records with calculated monthly pumpage values.
 - 2.1.6. Finally, re-import the Excel spreadsheet into the Access database as a table **MUN+MFG_WaterUseSurvey**.
- 2.2. Predicting historical pumpage for 1981-83 and 1997-1999 - In the table **PumpagebyMajorAquifer1980-1997**, groundwater use summaries were reported for the years 1980 and 1984-1997 for the categories MIN, MFG, PWR, STK, IRR, and MUN (actually MUN + C-O) for each major aquifer and county-basin. Water use summaries for the years 1981-1983 and 1998-1999 were not reported. In the spreadsheet **RuralDomestic_Master_Post1980_021502.xls**, water use is not reported for 1998 and 1999. The groundwater use for these years must be obtained by interpolation from existing data.
- 2.2.1. First, import the tables **PumpagebyMajorAquifer1980-1997** and **RuralDomestic_Master_Post1980_021502.xls** into SAS datasets.
 - 2.2.2. Import into a SAS dataset the weather parameters “average annual temperature” and “total annual precipitation” for 1980-1999 from National Weather Service cooperative weather stations. Delete those stations that have valid measurements in less than 16 of the 20 years. Also, delete data from any stations that do not have

valid measurements for at least 4 of the 5 years 1981, 1982, 1983, 1998, and 1999.

2.2.3. In Arcview, identify the weather station (with valid data for at least 16 of the 20 years) closest to each county-basin. Create a look-up table in SAS to link each county-basin with the closest weather station.

2.2.4. In SAS, apply linear regression in Proc REG with stepwise selection, to regress annual pumpage (dependent variable) vs. 1) year, 2) average annual temperature and 3) total annual precipitation from the nearest weather station, for each county-basin, major aquifer, and water use category, for the years 1980 and 1984-97. Select the best valid regression equation based on the statistic Mallows' Cp, which balances the improvement in regression fit as independent variables are added to the regression with the increasing uncertainty in the resulting dependent variable estimates. Transformations (e.g., natural logarithms) of the independent variables may yield a better regression equation. There should be a regression equation for each county-basin, and water use category.

2.2.5. Using the regression equations and weather data for the years 1981, 1982, 1983, 1998, and 1999, in SAS, calculate predicted pumping for these years each county-basin and water use category. If predicted values are less than zero, a value of zero is entered. Append the predicted water use for these five years to the reported water use for 1980 and 1984-1997. Export this table, then import it into the Access database as **PumpagebyMajorAquifer1980-1999**.

2.2.6. In general, this regression procedure is appropriate for pumpage changes that might be expected based on gradual annual changes (e.g., population) or year-to-year weather variability. It may not make good predictions when pumpage changes rapidly for non-weather-related factors. Review and inspect the regression-based pumpage estimates for 1981-83 and 1998-99 versus the TWBD-provided pumpage estimates for 1984-1997. Carefully inspect all between-year pumpage differences of more than 20%. Subjectively, if the predicted pumpage estimates do not make sense, replace the regression-based estimate with the TWDB pumpage estimate for the previous year.

2.2.7. Add a new column "Annual Source" to the table, and enter in it "Reported" for those years for which annual water use was reported, and "Regression" or "Previous Year" for those years for which pumpage sums were predicted from regression or previous years.

2.3. (OPTIONAL) Selecting Pumpage within the model domain – The tables contain pumpage estimates for the entire state, or the entire aquifer of interest. Ultimately, pumpage originating within the model domain will be made during attribution of data to model grid cells. To speed the analysis, it may be beneficial to create a subset of data for pumpage that will encompass the model domain, with a buffer. **WARNING:** Pumpage sometimes originates (e.g., wells exist) in a different geographic area from where water is used and reported. Be careful that this procedure does not exclude any reported pumpage!

- 2.3.1. Once the model domain has been identified by the modelers, it is overlain on the county GIS layer in Arcview, and all counties containing, or very near to, any part of the model domain are selected.
- 2.3.2. Next, in MS Access, a new field “Domain?” is added to the table **Reference_Countyname_number_FIPS**. A value of “Y” is entered in this field for records of counties within the model domain.
- 2.3.3. Using this table, in a select query with other tables or queries joined by county name, number, or FIPS (federal information processing system) code, one can specify “Domain='Y’ as a condition to limit queries to those counties within the model domain.
- 2.4. Preparing a County-basin Arcview Shapefile and Associating Model Grid Cells with a County-Basin – Much of the reported pumpage is spatially divided into county-basin units, which consist of the area in the same county and river basin. Many counties are split between two or more river basins, thus, county-basins are smaller than counties.
 - 2.4.1. To create a county-basin Arcview shapefile, in Arcview, load GIS shapefiles of counties and river basins in GAM projection. Intersect these two layers using the Geoprocessing Wizard to create a new shapefile **countybasins.shp**.
 - 2.4.2. Associate each model grid cell with the county-basin it falls primarily within. This will be useful when we need to determine monthly distribution factors and water user group IDs (WUG IDs) for non-well-specific pumpage categories (IRR, STK, C-O). These monthly distribution factors are estimated as averages within a county-basin. **Note:** The primary county-basin is not used to spatially distribute pumpage among grid cells because it is inexact. A grid cell may be part of multiple county-basins. For spatial distribution purposes, this grid cell should be split by county-basin – then later aggregated.
 - 2.4.2.1. Load the model grid shapefile in GAM projection. Union this shapefile with countybasins.shp using the Geoprocessing Wizard. Add a numeric field “fr_grdarea” to the attribute table, and use the field calculator function to enter its values ($fr_grdarea = shape.returnarea/27878400$). Here, 27878400 is the area, in square feet, of each grid cell. Export the table as a dbf file.
 - 2.4.2.2. Import the dbf file into MS Access as a new table - **Table1**. Our goal is to identify, for each grid cell, the county-basin with which it is primarily associated.
 - 2.4.2.3. Select by query the records with no value for the field “CountyBasin.” Delete these records, as they are grid cells over Mexico or the ocean.
 - 2.4.2.4. Run a make table query, sorting the table1 records by grid_id (ascending) and fr_grd_area (descending) to create a new table, **Table2**.
 - 2.4.2.5. Copy **Table2**, and paste only the table structure as a new table –

Grid_countybasin.

2.4.2.6. In design view, make the field “grid_id” a primary key in the table **Grid_countybasin**.

2.4.2.7. Run an append query, to append all fields of the records from table 2 to **Grid_countybasin**. When the warning window comes up, say yes to proceed with the query. This appends only the first record for each grid_id to **Grid_countybasin**, leaving one record for each grid cell with the county basin with the largest value of “fr_grdarea”. The resulting table should have one record for each grid cell in the model grid, and the county-basin name for that model grid cell.

3. Matching Pumpage to Specific Wells

Historical groundwater use from the categories MUN, MIN, MFG, and PWR is to be matched with specific wells from which it was pumped. Reported groundwater use for these uses, from the annual water use surveys, is contained in the table **MUN+MFG_WaterUseSurvey**. For MUN, MFG, MIN, and PWR, water use is reported for each year from 1980 to 1999. These tables report total annual use and, in most cases, monthly use, for each water user. The water user is identified by a unique alphanumeric code “alphanum.” The tables also list the county and river basin, as well as their water user group ID, their regional water planning group, their water use category, the major aquifer from which the groundwater was pumped, and the number of wells from which the water was pumped. These tables do not indicate the specific location of the wells, well elevation, well depth, a specific aquifer name, or other information needed for groundwater modeling. This information must be retrieved from other sources. The primary source of well information is the state well database maintained by the TWDB. Secondary sources include well data found in the TNRCC public water supply database, and the USGS site inventory. A final source is the follow-up survey provided by the TWDB in October 2001.

3.1. Create **All_wells** table –

3.1.1. Download the state well database as a table **wellda.txt** for the entire state (under the menu “all counties combined”) from the TWDB web site <http://www.twdb.state.tx.us/publications/reports/GroundWaterReports/GWDatabaseReports/GWdatabaserpt.htm>. Import this table into MS Access as a new table **All_Wells**.

3.1.2. The TNRCC public water supply database includes data for some wells that are not found in the TWDB state well database. Retrieve this database from the TNRCC. Create a query to link the required well data, and append the well data to **All_wells**, exercising care to match fields appropriately.

3.1.3. The USGS site inventory <http://waterdata.usgs.gov/tx/nwis/inventory> contains data for wells that may not be found from other sources. Run a query for the state of Texas with site type = ‘ground water’ to download the well data and append it to **All_wells**. Be careful to match fields appropriately.

- 3.1.4. Delete any oil, gas, geothermal, or observation wells, anodes, drains, or springs after a query of the attribute table on the fields “GW_type_cd” or “Site_use1_cd”.
- 3.2. Linking water use data to the state well database – Using a make-table query to create a new table **MUN+MFG_linkedwithwellinfo**, all fields from the water use survey are merged with all fields from the state well database by joining the field “alphanum,” in the table **MUN+MFG_WaterUseSurvey**, to the field “user code econ,” in the state well database table **All_wells**. In many cases, several different wells may have the same “user code econ,” making a one-to-many match (this is expected, since one city may own multiple wells). Add a field “Location Source” to the table **MUN+MFG_linkedwithwellinfo**. For the pumpage records with one or more matched well, enter the text “state well database” in this field.
- 3.3. Locating unmatched pumpage 1 – Identify the pumpage records without a matching well using a **Find Unmatched** query. Check the field “alphanum” in unmatched pumpage records of the table **MUN+MFG_WaterUseSurvey**, and “user_code_econ” in the table **All_Wells** for obvious errors that prevent automatic matching, and correct any found and repeat the steps to make the table above. Next, manually search the **All Wells** table for wells in the same county and basin, for which the user name field “owner_1” matches the field “line1” in **MUN+MFG_WaterUseSurvey**. When a match is found, add a field to the well table, and copy the “alphanum” field from the water use survey, to facilitate match-merging. Next, match this new field in the well database to “alphanum” of the water use survey, and append these matched records to the table **MUN+MFG_linkedwithwellinfo**. Enter “state well database manual match” for the field “Location Source” for these new appended records.
- 3.4. Locating unmatched pumpage 2 – For those pumpage records not matched via the above procedures, open the TNRCC public water supply database and attempt to manually match the water user to specific wells based on the county, aquifer_id, and owner name - “A1Name.” When a match is found, add a field to the well table, copy the “alphanum” field from the water use survey, perform a match-merging query, and update these new matched records to the table **MUN+MFG_linkedwithwellinfo**. Enter “TNRCC PWS database” for the field “Location Source” for these new appended records.
- 3.5. Locating unmatched pumpage 3 - For those pumpage records, if any, still not matched in the above procedures, manually search the TWDB follow-up survey data. When a match is found, this data must be manually copied to the table **MUN+MFG_linkedwithwellinfo** because the table format is substantially different. Enter “TWDB followup survey” for the field “Location Source” for these new appended records.
- 3.6. Locating unmatched pumpage 4 - For those pumpage records, if any, still not matched in the above procedures, it may be possible to identify an approximate well location via the EPA’s Envirofacts facility database. In an internet browser, go to http://www.epa.gov/enviro/html/fii/fii_query_java.html and perform a facility information query using a characteristic part of the facility name in the query field “facility site name.” If a single facility of matching name is located in the same county,

copy the facility latitude and longitude, in degrees, minutes, seconds into the appropriate fields of the table **MUN+MFG_linkedwithwellinfo**. Enter “facility centroid” in the field “Location Source” if Envirofacts lists that as the source of the latitude and longitude, or “facility zip code centroid” if Envirofacts lists that as the source of the latitude and longitude. Note that the median size of a zip code in Texas is approximately 5.5 square miles. Thus, pumpage located based on a zip code centroid may be very uncertain, especially in rural areas, and should be used with caution. However, it was felt that having an approximate location was better than leaving them out of the model. Note: Because this step is labor-intensive, it may be acceptable to perform this procedure for only the “major” water users, as indicated by volume used.

3.7. Count wells matched - Count the number of wells matched to each pumpage record via a crosstab query on **MUN+MFG_linkedwithwellinfo**.

3.8. Apportion water use between matched wells –

3.8.1. For that water use matched to more than one well, compare the number of matched wells to the number of wells reported as used in the water use survey. If the number of matched wells exceeds the number reportedly used, inspect the well data, including the county, basin, aquifer_id, well_type, drill_date, and other fields to see if some of the wells can be excluded from consideration as the source from which the water was reportedly pumped. If so, remove that well from the table.

3.8.2. Next, we need to apportion the reported pumpage among the wells matched. Since we don’t have data indicating otherwise, pumpage will be divided equally between wells. Create a new query that 1) adds a column “Num Wells Matched” indicating the number of wells matched (based on the aforementioned crosstab query) to the table **MUN+MFG_linkedwithwellinfo**, and 2) if one or more wells are matched, divides the reported pumpage in the fields “annual total in gallons” and “jan” – “dec” by the number of wells matched. Add another field “Corrected for Numwells” with a value of “Y” if the original pumpage sum for the water user was divided by two or more wells, and “N” otherwise.

3.8.3. Quality control check – In a query, summarize total annual water use by county-basin-year in the table **MUN+MFG_linkedwithwellinfo**. Make sure that these match the corresponding totals from the original table **MUN+MFG_WaterUseSurvey**. If not, correct the situation, which may occur by double-matching some water use records to wells.

3.9. Calculate Additional Fields - In a new make-table query, create the table **Well-specific_pumpage** based on **MUN+MFG_linkedwithwellinfo**, calculate latitude and longitude as decimal degrees from degrees-minutes-seconds in new fields “lat_dd” and “long_dd.” Also in the same query, calculate water use in acre-feet from gallons in new fields “Annual total in acre-ft”, “JAN in acre-ft”, “FEB in acre-ft”,.....,”DEC in acre-ft.”

3.10. Append Out-of-State Data - Append the well-specific Louisiana and Arkansas water use, in acre-ft, from LADEQ and USGS, to the table **Well-specific_pumpage**.

- 3.11. Summarize well-specific matching completeness – Perform queries to calculate the sum of matched water use by county-basin-year, and the total water use (matched and unmatched) by county-basin-year. Based on these queries, calculate the volumetric percent completeness of matching by county, basin, and year. Completeness should be high (e.g., >80%) to facilitate accurate accounting for water use in the model.
4. Spatial Allocation of Groundwater Pumpage to the Model Grid - The model grid is comprised of an equal-spaced grid with a size of one mile by one mile. The grid has 3 dimensions- row, column, and model layer. Each cell of the model grid is labeled with a 7-digit integer “grid_id”. The first digit represents the model layer. Digits 2 through 4 represent the row number. Digits 5 through 7 represent the column. The model grid is represented in a MS Access table linked to an Arcview shapefile via the field “grid_id”.
 - 4.1. Spatial allocation of well-specific groundwater pumpage from the categories MUN, MFG, MIN, and PWR
 - 4.1.1. Distribute pumpage into grid cells
 - 4.1.1.1. In MS Access, verify that all records in the table **Well-specific_pumpage** have x,y coordinates in decimal degrees.
 - 4.1.1.2. In Access, add a new autonumbered, long integer field “Unique ID” to the table **Well-specific_pumpage**.
 - 4.1.1.3. In Arcview, enable the Database Access extension. Add a new table **PtSrcTbl** to an ArcView project via SQL connect, including only the fields “unique_id”, “well_depth”, “lat_dd”, and “long_dd”. To perform an SQL connect, select the “SQL connect” menu item under the Project menu. Then navigate to the correct database and select the table **Well-specific_pumpage**.
 - 4.1.1.4. Add **PtSrcTbl** as an event theme named **Wellpts** to a view based on lat/long coordinates. To do this, from the view menu, select the “add event theme” menu item, and choose long_dd for x field and lat_dd for y field in the dialog. Re-project the view to GAM projection using the View->Properties dialog box according to GAM Technical Memo 01-01 (rev A), then save it as a shapefile **Wellpts.shp**. Load **Wellpts.shp** and the model grid, also as a shapefile in GAM projection, into a new view.
 - 4.1.1.5. Spatially join the model Grid table to the **WellPts** table. To do this make the “shape” fields of each table active, and with the **WellPts** table active, choose “join” from the table menu. This will join the 1 mile grid cell records to all of the **WellPts** records that are contained with that grid cell.
 - 4.1.1.6. Migrate the GridId to the **WellPts** table. Do this by first adding a new 7-digit, no decimal, field to the **WellPts** table called “Grid_Id”. Then, with the new field active, using the field calculator button make the new field equal to the “GridId” field from the joined table.

- 4.1.1.7. Delete those pumpage records outside the model domain with a “Grid_ID” of “0”.
- 4.1.1.8. Vertical Distribution: Follow procedures outlined in sections 4.5.
- 4.1.2. Import the Arcview attribute table **Wellpts.dbf** to the MS Access database. Change the data type for the fields “Unique ID” and “Grid_ID” back to long integer if they were converted to double length real numbers during the import operation.
- 4.1.3. Run an update query to update the empty values of “Grid ID” in the table **Well-specific_pumpage** with the “Grid_ID” values from the table **Wellpts**, using an inner join on the field “Unique ID.”
- 4.1.4. The table **Well-specific_pumpage** now has only the grid_id of the upper model, i.e., the first digit is 1. The actual vertical distribution data is in the fields “per1” to “perx” where x is the number of vertical layers (L) in the model. Copy the table x-1 times in an append query, incrementing the first digit of the grid id, to create a record for each model layer. There now should be L times the original number of records in the table. For example, for the northwestmost grid cells of a model with four layers, the following grid id’s should now exist: 1001001, 2001001, 3001001, and 4001001; whereas only 1001001 was in the original table.
- 4.1.5. Calculate for each year the actual pumpage for each record as the product of the pumpage for a given year multiplied by the percent of pumpage from that model layer (from the fields “per1” – “per4”, for a model with 4 layers).
- 4.1.6. Create a new summary query **gridsum_well_specific** to summarize the pumpage for each grid_id and year from the table **Well-specific_pumpage**.
- 4.2. Spatial allocation of irrigation groundwater pumpage – Irrigation pumpage is distributed between the USGS MRLC land use types 61 (orchard/vineyard), 82 (row crops), and 83 (small grains) within each county-basin based on area. The distribution is further weighted based on proximity to the irrigated farmlands mapped from the 1989 or 1994 irrigated farmlands survey. The weighting factor is the natural logarithm of distance in miles to an irrigated polygon. However, this weighting factor is manually constrained to be between 0.5 and 2, in order to limit the effect of weighting to a factor of 4. All grid cells further than roughly 7.4 miles from an irrigated polygon will have a weight of 0.5, while all grid cells nearer than 1.6 miles from an irrigated polygon will have a weight of 2.
 - 4.2.1. Create shapefile for MRLC land use categories 61, 82, and 83.
 - 4.2.1.1. In ArcView, load MRLC grid. Resample grid with a larger grid size to make the file more manageable (use x4 factor and set the analysis extent to the model domain). Select, in the new resampled grid, values 61, 82, and 83, and convert to shapefile. Call it “mrlc_irrigated.shp.”
 - 4.2.2. Create “distance grids” for the irrigated farmlands 89 and 94 shapefiles. These

will be grid files that contain the distance from each grid cell to the nearest irrigated farmlands polygon.

- 4.2.2.1. Add “irr_farms89.shp” to a view, and make it active. With Spatial Analyst extension activated, select “find distance” from the analysis menu. Choose a grid cell size of 1 mile, and set the extent to the model domain. This will generate a grid of distance values to the nearest irrigated farm. Repeat for “irr_farms94.shp.” Call them “dist_irryy.”
- 4.2.3. Using the Geoprocessing Wizard, intersect county-basin boundaries with “mrlc_irrigated.shp” to create “mrlc_cb.shp.” Create a unique id “cb_irr_id” so that, if necessary, these unique polygons can be queried.
- 4.2.4. Intersect “mrlc_cb.shp” with the 1 mi. sq. grid cells.
 - 4.2.4.1. Select only the 1 mile grid cells that are above the aquifer of concern’s extents (The county-basin irrigation pumpage totals are aquifer specific, so the pumpage should only be distributed where the proper underlying aquifer is present).
 - 4.2.4.2. It is also necessary to distribute across the entire county-basin area where the underlying aquifer is present, and not limited to the model domain in counties partly within the model domain. Therefore, if a county-basin is intersected by the model domain boundary, the pumpage total must be distributed across the entire county-basin so that only the proper percentage gets distributed inside the model domain. To insure that this happens, select the county-basins on the perimeter that get intersected by the model domain boundaries. With the Geoprocessing Wizard, intersect these county-basins with the subsurface aquifer boundaries, the resulting file will be county-basins above the aquifer. Clip out the areas that reside inside the model domain (Union with model domain and delete that which is inside). What is left, (county-basins above aquifer of concern and outside of model domain) can be dissolved into one polygon and merged with the 1 mile grid cells. Give this new polygon a grid_id of “9999999” (later when pumpage values are summed by grid id the “9999999” values will fall out).
 - 4.2.4.3. Add the new record “9999999” to the selected set from 4.3.4.1. Using Geoprocessing Wizard, intersect the selected 1 mile grid cells with the “mrlc_cb.shp” file. The result will be all of the irrigated land with the proper grid_id and county-basin name. Call it “mrlc_cb_grid.shp”.
 - 4.2.4.4. Add field “un_area_gd” and calculate the polygons’ areas in sq. miles using the field calculator (“un_area_gd” = [shape].returnarea/27878400).
- 4.2.5. Determine weighting factor for each polygon based on area and proximity with irrigated farms.
 - 4.2.5.1. Add fields “dist_irr89”, “dist_fact89”, “ardisfac89”, “sumcbfac89”,

“w_ar_dis89”.

- 4.2.5.2. Populate the distance to irrigated farmland field (“dist_irr89”) using the values from the “dist_irr89” grid file.
 - 4.2.5.3. Calculate the distance to irrigated farms factor using the field calculator (“dist_fact89”= $1/(1+[dist_irr89]).ln + 0.0001$). Select all values that are greater than 2 and change them to 2, and select all values that are less than 0.5 and change to 0.5 so that the range is 0.5 – 2.
 - 4.2.5.4. Calculate the area-distance factor using the field calculator (“ardisfac89” = “un_area_gd” * “dist_fact89”).
 - 4.2.5.5. Create a summary table by county-basin that summarizes the “ardisfac89” field. Link the summary table back up by county-basin and migrate the summed values into “sumcbfac89”.
 - 4.2.5.6. Calculate the distribution weighting factor for area of irrigated land (mrlc land use) and distance to irrigated farmland (farmland survey) using the field calculator (“w_ar_dis89” = “ardisfac89” / “sumcbfac89”). This is basically the fraction of the total county-basin pumpage that will be distributed to a specific polygon.
 - 4.2.5.7. Repeat section 4.3.5 for irrigated farmland 94.
- 4.2.6. Calculate unique pumpage values for 1 mile grid cells.
- 4.2.6.1. Create 20 new fields (1 for each year: “pmp_80” – “pmp_99”).
 - 4.2.6.2. Using SQL Connect, query the Access table **PumpagebyMajorAquifer1980-1999** for all years.
 - 4.2.6.3. Query the records (by the year column) for each year and specific aquifer (by aquifer code column) and export each query as a separate *.dbf file. “Pump_by_cb_yyyy_aquifer.dbf.” These tables will have a column for each use category, and can therefore also be used in livestock calculations for the same aquifer of concern.
 - 4.2.6.4. Join the table “pump_by_cb_1980_cw.dbf” to the attribute table “mrlc_cb_grid.shp” by countybasin. (make certain that all countybasin names are spelled the same).
 - 4.2.6.5. Calculate “pmp_80” using the field Calculator ($pmp_80 = w_ar_dis89 * irrigation$). Irrigation is the column of the joined table “pump_by_cb_1980” that contains the countybasin annual pumpage totals for irrigation use. Use “w_ar_dis89” for years 80-89 and use “w_ar_dis94” for years 90-99.
 - 4.2.6.6. Repeat 4.2.6.4 – 4.2.6.5 for all years.

- 4.2.7. Summarize all unique pumpage totals by grid cell id.
- 4.2.7.1. Summarize all the “pump_unyy” fields by grid cell id, by using the summarize button and adding “pmp_80” (sum) through “pmp_99” (sum) in the dialog box. Name this summary file **area_irr_pumpbygrid_80_99**. (i.e. **sw_irr_pumpbygrid_80_99.dbf**).
- 4.2.8. Vertical Distribution: Follow procedures outlined in sections 4.5.
- 4.2.9. Import irrigation pumpage table back into MS Access database as a table **area_irrigation_total**, e.g., **sw_irrigation_total**
- 4.2.9.1. In MS Access, import the attribute table for the Arcview shape file **grid_irr_yy.dbf** as a dbase file. This table should include one record for each possible Grid_ID, and at least the fields “Grid_ID”, “year”, and “pumpy_IRR.”
- 4.2.10. The table **area_irrigation_total** now has only the grid_id of the upper model, i.e., the first digit is 1. The actual vertical distribution data is in the fields “per1” to “perx” where x is the number of vertical layers in the model. Copy the table x-1 times in an append query, incrementing the first digit of the grid id, to create a record for each model layer. There now should be L times the original number of records in the table. For example, for the northwestmost grid cells of a model with four layers, the following grid id’s should now exist: 1001001, 2001001, 3001001, and 4001001; whereas only 1001001 was in the original table.
- 4.2.11. Calculate for each year the actual pumpage for each record as the product of the pumpage for a given year multiplied by the percent of pumpage from that model layer (from the fields “per1” – “per4”, for a model with 4 layers).
- 4.2.12. Create a new summary query **Irrigation_annual_area** to summarize the pumpage for each grid_id and year from the table **area_irrigation_total**.
- 4.3. Spatial allocation of livestock groundwater pumpage – Livestock groundwater use within each county-basin is distributed evenly to all rangeland, Anderson Level II land use codes 31 (herbaceous rangeland), 32 (shrub and brush rangeland), and 33 (mixed rangeland) of the USGS 1:250,000 land use land cover data set (http://edcwww.cr.usgs.gov/glis/hyper/guide/1_250_lulc).
- 4.3.1. Determine rangeland within each county-basin
- 4.3.1.1. In Arcview, create a rangeland-only land use shapefile by loading the USGS land use shapefiles by quadrangle, merging them as required to cover the model domain, selecting the land use codes 31, 32, and 33 in a query, then saving the theme as a new shapefile **Rangeland.shp**.

- 4.3.1.2. Using the Geoprocessing Wizard, intersect the Rangeland shapefile with the County-basin shapefile (make sure to use entire county basin areas, and not the “clipped to domain” version) to make a new intersection shapefile **range_countybasin.shp**.
- 4.3.1.3. Calculate the unique area (in square miles) of the new intersected polygons “area_un1” using the field calculator ($\text{area_un1} = \text{shape.returnarea} / 27878400$).
- 4.3.1.4. Summarize the unique area by county-basin (total area of rangeland within county-basin) using the summary button.
- 4.3.1.5. Link the summary table back to the range_countybasin shape file and migrate it into a new field “rg_cb_tot” using the field calculator.
- 4.3.1.6. Determine weighted area factor “w_area1” for each polygon using the field calculator ($\text{w_area1} = (\text{area_un1} / \text{rg_cb_tot})$). W_area1 is, for each rangeland polygon, the fraction of the total rangeland area within the county-basin.
- 4.3.2. Intersect the rangeland/countybasin polygons with the Model Grid and set up for unique pumpage calculations.
 - 4.3.2.1. Using the Geoprocessing Wizard, intersect the shapefiles range_countybasin and Model Grid to create a new shape file **rng_cb_mg.shp**.
 - 4.3.2.2. Calculate the unique area of “intersected” polygons (area_un_grid) using the field calculator ($\text{area_un_grid} = \text{shape.returnarea} / 27878400$). Double check that no values are greater than 1.
 - 4.3.2.3. Determine the weighted area factor ($\text{w_area_grid} = (\text{area_un_grid} / \text{area_un1})$).
- 4.3.3. Calculate unique pumpage “pump_un_yy” for the intersected polygons for every year (80-99).
 - 4.3.3.1. Add the fields “pump_un80” – “pump_un99” to the **rng_cb_mg** attribute table.
 - 4.3.3.2. Using SQL Connect, query the Access table **PumpagebyMajorAquifer1980-1999** for all years.
 - 4.3.3.3. Query the records (by the year column) for each year, and specific aquifer (by aquifer code column) and export each query as a separate .dbf file. “Pump_by_cb_yyyy_aquifer.dbf.” These tables will have a column for each use category, and can therefore be used in the irrigation calculations for the same aquifer of concern.
 - 4.3.3.4. Join the table “pump_by_cb_1980.dbf” to the attribute table “rng_cb_mg” by countybasin. (make certain that all countybasin names are spelled the same).

- 4.3.3.5. Calculate “pump_un80” using the field Calculator ($\text{pump_un80} = \text{w_area_grid} * (\text{w_area_1} * \text{livestock})$). (livestock is the column of the joined table “pump_by_cb_1980” that contains the countybasin annual pumpage totals for livestock use).
 - 4.3.3.6. Repeat 4.3.3.4 – 4.3.3.5 for all years.
 - 4.3.4. Summarize all unique pumpage totals by grid cell id.
 - 4.3.4.1. Summarize all the “pump_unyy” fields by grid cell id, by using the summarize button and adding “pump_un_80” (sum) through “pump_un_99” (sum) in the dialog box. Name this summary file “*area_stk_pumpbygrid_80_99.*” (i.e. *sw_stk_pumpbygrid_80_90.dbf*).
 - 4.3.5. Vertical Distribution: Follow procedures outlined in sections 4.5.
 - 4.3.6. Import livestock pumpage summary table back into MS Access database as a table **area_livestock_total**, e.g. **sw_livestock_total**.
 - 4.3.7. The table **area_livestock_total** now has only the grid_id of the upper model, i.e., the first digit is 1. The actual vertical distribution data is in the fields “per1” to “perx” where x is the number of vertical layers in the model. Copy the table x-1 times in an append query, incrementing the first digit of the grid id, to create a record for each model layer. There now should be L times the original number of records in the table. For example, for the northwestmost grid cells of a model with four layers, the following grid id’s should now exist: 1001001, 2001001, 3001001, and 4001001; whereas only 1001001 was in the original table.
 - 4.3.8. Calculate for each year the actual pumpage for each record as the product of the pumpage for a given year multiplied by the percent of pumpage from that model layer (from the fields “per1” – “per4”, for a model with 4 layers).
 - 4.3.9. Create a new summary query **Livestock_annual_area** to summarize the pumpage for each grid_id and year from the table **area_irrigation_total**.
- 4.4. Spatial allocation of rural domestic (C-O) groundwater pumpage.
 - 4.4.1. Calculate the Population in each 1 mile grid cell.
 - 4.4.1.1. In Arcview, load the 1990 block-level census population shapefile.
 - 4.4.1.2. Load Arcview polygon shapefiles for cities. Select census blocks that fall within city boundaries and delete those records so that rural domestic pumpage does not get distributed to cities. (Note: we’re assuming that city boundaries are good surrogates for the extent of the area served by public water supply systems, whose pumpage is reported under the category “MUN”).

Repeat this process for the reservoir areas.

- 4.4.1.3. Calculate the area of census blocks in sq. miles in a new field “blk_area” using the Field Calculator function ($\text{blk_area} = \text{shape.returnarea} / 27878400$).
 - 4.4.1.4. Load the model grid, model domain, and county-basins shapefile. Select all county-basins that are intersected by the model domain boundary. Union the selected county-basins with the model domain boundary. In the resulting shapefile, delete the polygons that are inside the model domain, leaving only areas of the county-basins that are outside of the model domain. Dissolve these polygons into one and merge with the model grid shapefile. Give this new record a grid_id of 9999999. (Adding this new area will insure that, when the county-basin total populations are calculated, the population outside of the model domain will be included).
 - 4.4.1.5. In the Geoprocessing Wizard, intersect the census block shapefile with the model grid shapefile to create a new shape file **intrsct90.shp**. (Note: Because the model grid size is 1 square mile, no intersected polygon (inside the model domain) should be larger than 1 square mile. Make sure that this is the case before proceeding).
 - 4.4.1.6. Calculate the unique area of all intersected polygons in square miles as a new field “area_un1” using the Field Calculator function ($\text{area_un1} = \text{shape.returnarea} / 27878400$). (so that one grid cell has an area of 1).
 - 4.4.1.7. Add a new numeric field “pop_un1” – the unique Population of the intersected polygons. Using the Field Calculator, calculate its value as ($\text{POP_un1} = \text{pop90} * \text{area_un1} / \text{blk_area}$) where pop90 is the block Population from the census file.
 - 4.4.1.8. Sum the field “pop_un1” by grid_id using the Field Summarize function to calculate the total population within each grid cell. Join this summary table to the original grid table by grid_id and copy value into new field “pop_90”.
 - 4.4.1.9. Repeat steps 4.5.1.1 – 4.5.1.8 (no need to repeat step 4.5.1.4, just use the grid file that was used for previous iteration).
- 4.4.2. Calculate the rural domestic pumpage for each 1 mile grid cell.
- 4.4.2.1. Intersect the county-basins shapefile with the model grid (which now has census populations for 1990 and 2000) to create a new shapefile **grid_cb_pop**.
 - 4.4.2.2. Create new field “area_un2” and calculate unique area using field calculator (“area_un2” = $[\text{shape}].\text{returnarea}/27878400$)
 - 4.4.2.3. Create two new fields “pop_un90” and “pop_un00”. Calculate using the field calculator (“pop_unyy” = $\text{“area_un2”}/\text{“pop_yy”}$)

- 4.4.2.4. Using SQL Connect, query the Access table **PumpagebyMajorAquifer1980-1999** for all years.
 - 4.4.2.5. Query the records (by the year column) for each year (because Rural Domestic pumpage data is not aquifer specific, there is no need to query by aquifer) and export each query as a separate .dbf file. “Pump_by_cb_yyyy.dbf.”
 - 4.4.2.6. Join table “pump_by_cb_1980.dbf” to grid_cb_pop.dbf by county-basin.
 - 4.4.2.7. Add field “pmp80.” Using field calculator, calculate “pmp80” (pmp80=CO*pop_un90/cb_pop90).
 - 4.4.2.8. Repeat steps 4.5.2.6 – 4.5.2.7 for each year. Use pop90 for years 1980-1989 and use pop00 for years 1990-1999.
 - 4.4.2.9. As a quality control check, sum the values of “rdom_pump” for each county-basin and make sure it matches the total for the county-basin from the Access table.
 - 4.4.2.10. Summarize pmp80 through pmp99 by grid id. Link summary back to model grid file and migrate pumpage values.
- 4.4.3. Vertical Distribution: Follow procedures outlined in section 4.5.
 - 4.4.4. Import the rural domestic pumpage table into the MS Access database as a table **area_rurdom_total**, e.g., **sw_rurdom_total**.
 - 4.4.5. The table **area_rurdom_total** now has only the grid_id of the upper model, i.e., the first digit is 1. The actual vertical distribution data is in the fields “per1” to “perx” where x is the number of vertical layers in the model. Copy the table x-1 times in an append query, incrementing the first digit of the grid id, to create a record for each model layer. There now should be L times the original number of records in the table. For example, for the northwestmost grid cells of a model with four layers, the following grid id’s should now exist: 1001001, 2001001, 3001001, and 4001001; whereas only 1001001 was in the original table.
 - 4.4.6. Calculate for each year the actual pumpage for each record as the product of the pumpage for a given year multiplied by the percent of pumpage from that model layer (from the fields “per1” – “per4”, for a model with 4 layers).
 - 4.4.7. Create a new summary query **Rurdom_annual_area** to summarize the pumpage for each grid_id and year from the table **area_rurdom_total**.
- 4.5. Vertical Distribution of groundwater pumpage. *Note: These procedures are for all use categories, and this section is referenced multiple times. Take care, and perform only

the operations that apply to that particular use.

- 4.5.1. Assign default well depths to model grid cells – Most, but not all, well-specific pumpage from the categories MUN, MFG, PWR, and MIN are associated with a reported well depth, screened interval, land surface elevation, which are used to attribute the pumpage to a specific vertical model layer. For those wells whose depth, screened interval, or land surface elevation is unknown, and for the non-well-specific pumpage in the categories C-O, STK, and IRR, it is necessary to interpolate these depths/elevations to assign the pumpage to a specific model layer. In this procedure, the approach is to interpolate on the basis of the depths of nearby (<10 miles) wells. On average, municipal, industrial, and irrigation water wells tend to be deeper than rural domestic or livestock wells. Thus, if there are nearby wells in the same water use category, the interpolation is based on these wells. In the absence of nearby wells of the same use category, the interpolation is based on nearby wells of any water use category. **The procedures outlined in section 4.5.1 cover all use categories, and therefore, only need to be done once per model area.*
- 4.5.1.1. In Arcview, using SQL Connect, query the MS Access database table **All_wells** for all wells in the major aquifer of concern (based on the field “aqfr_id_1”). Save this query as a table **AQ_wells**, where **AQ** is a 2-character code representing the aquifer of interest.
- 4.5.1.2. Load these wells in a View as an event theme, using the fields lat_dd as y-coordinate and long_dd as x-coordinate. Convert the event theme to GAM projection as per GAM Technical Memo 1-01, then save this theme as a shape file.
- 4.5.1.3. Query the shape file’s attribute table for all domestic water wells (water_use_1 = “domestic”).
- 4.5.1.4. Using Arcview Spatial Analyst, under the Analyst, Properties menu, set analysis extent and grid size to be equal to the GAM model grid.
- 4.5.1.5. Next, under the Surface menu, interpolate a grid with values of interpolated well depth, via the inverse distance weighting method, within a fixed radius of 10 miles, with a power of 2.
- 4.5.1.6. Repeat steps 4.5.1.3 – 4.5.1.5 to create an interpolated well depth grid for each of the other water use categories MUN, MFG, PWR, MIN, STK, and IRR, as well as a well depth grid for all water use categories combined.
- 4.5.1.7. When a depth was not reported for a well, these grid values can be used as an estimated well depth. A new text field “depth source” is added to the well table to indicate that the well depth was estimated by interpolation, not reported. This allows a hydrogeologist or modeler to review these wells to make sure they fall in the proper model layer. When a well depth is checked and corrected manually, a value of “manual” is entered in the field “depth source”. Valid values of depth source include “reported”, “interpolated”, or

“manual”.

- 4.5.2. Assign default screened intervals to wells – For wells with no reported screened interval, calculate the well screened interval. The lower boundary is the well depth, while the upper boundary of the screened interval is calculated as the well depth minus an estimated screen length. The default screen lengths will be estimated from other wells in the same aquifer for which the screened interval is known.
- 4.5.2.1. An Excel file *Screened_Interval.xls* is provided by the modelers. It contains the land surface elevation and depths to the top and bottom of the screen for each well. The screened interval is calculated as the difference between the top and bottom depths. This file is loaded in Arcview and joined to the *AQ_Wells* table by state well number. Next, under the Surface menu, interpolate a grid with values of interpolated screened interval, via the inverse distance weighting method, within a fixed radius of 10 miles, with a power of 2.
- 4.5.2.2. When a screened interval is not reported for a well, these grid values can be used to estimate the upper depth of the screened interval, assuming that the well depth is the bottom of the interval. A new text field “screen_source” is added to the well table to indicate that the well depth was estimated by interpolation, not reported. Valid values of screen source include “reported” or “interpolated”, or “manual”.
- 4.5.3. Assign land surface elevations to wells – For wells without a reported land surface elevation (in the field “elev of lsd”) a land surface elevation must be estimated. For this purpose, a 30-meter digital elevation model (DEM) grid is added to an Arcview project with the well data table. The Arcview script “getgridvalue” in Appendix 2 is run to return the value of the land surface elevation for the well.
- 4.5.4. Estimate the screened interval for non-well-specific pumpage - For the non-well-specific uses STK, IRR, and C-O, in order to distribute the pumpage vertically, each model grid cell may be treated as a well. Using the centroids of the model grid cells as if they were wells, copy the interpolated values of well depth, screened interval, and land surface elevation to each grid cell as described above.
- 4.5.5. Convert depths to elevations - In order to compare to model layers, which are reported as elevation (feet above mean sea level), it is necessary to convert the depths of the top and bottom of screened intervals to elevations. To do this, subtract the depths from the land surface elevation, in feet above mean sea level.
- 4.5.6. Determine vertical distribution of pumpage totals by comparing the elevations of the top and bottom of the well screened interval to model layer elevations. (For point source water use categories, this will be done for each specific well. For non-point source this will be done for each 1 mile grid cell).
- 4.5.7. Spatially join the flow layer structure (model grid cells with tops of aquifer elevations) to the wells. (for non-point source join by grid id).

- 4.5.8. Run vertical distribution avenue script on points (see appendix for code). This script will place a “pumpage percentage” in the flow layer percentage columns (per1 – per6). This value is actually the percentage of the total length of the screened interval that resides in each flow layer (possible 0 – 100).
- 4.5.9. Once script is successfully run, a series of QA checks must be run, and in certain cases percentage values must be altered manually. Field “calc_code” will be given a specific code for each case of manual alteration.
 - 4.5.9.1. Query records that have a value of “99999” for every layer elevation (i.e. layer doesn’t exist at that location). Set calc_code to “N”.
 - 4.5.9.2. Query records whose top of screen elevation is shallower than the top of the shallowest existing layer. (i.e. (top of layer 2 = 999999 and per2 > 0)). The script automatically puts a value in per2 if the top of screen is shallower than layer 3, but if layer 2 doesn’t exist there then per2 should be zero and the value should be shifted down. In this case, calc_code should be set to “S3”. This will tell someone that the screen is shallower than the shallowest layer which is layer 3.
 - 4.5.9.3. Query records whose depth is deeper than the bottom layer. (i.e. depth < bottom layer). Put the remainder of the pumpage that was lost below into the bottom layer and set calc_code to “D”.
 - 4.5.9.4. Query records whose screened interval spans layer 1 or 2 and enters layer 3 (Carrizo). (i.e. per3 > 0 and per2 > 0). It is assumed that if the screened interval reaches the Carrizo then all of the water is being taken from that layer and not the above layers of inferior quality. Set per1 and per2 to zero and add their values to per3. Set calc_code to “C”.
 - 4.5.9.5. Query records whose reported top of screen elevation is less than the bottom of screen elevation. Manually set the appropriate layer percentage to 100%. Set calc_code to “E”.
 - 4.5.9.6. Query records whose top of screen elevation exactly equals one of the layer top elevations. This is very rare, but if it happens, the percentage value must be manually entered. Set calc_code to “=”.
 - 4.5.9.7. Query records whose total percentage is less than 100% by less than .5%. Due to a program glitch values of 99.5% get rounded to 100% and the rest is left out. Manually set percentage value to 100%. Set calc_code to “R”.
 - 4.5.9.8. Query all other records (records that don’t have a calc_code value and whose tot_per = 100%). Set calc_code to “NP” for no problems.

5. Temporal Distribution of Rural Domestic, Livestock, and Irrigation Groundwater Use

5.1. Temporal distribution of livestock pumpage - Because we have only annual total groundwater pumpage estimates for STK, we need to derive monthly pumpage estimates. According to TWDB GAM Technical Memo 01-06, annual total livestock pumpage may be distributed uniformly to months since the water needs of livestock are not likely to vary significantly over the course of a year.

5.1.1. In the MS Access database, create a new table called Monthly Factors with the fields "countyname", "basinname", "countynumber", "basinnumber", "data_cat", "year", and "month". The table should include a record for every county-basin within the model domain, water use category "data_cat", year (1980-1999), and month (1-12), as well as an additional annual total record (month="0") for each county-basin, year, and water use category. Add 2 new fields "mfraction" and "Monthly distribution factor source" to the new table. The former is the numeric monthly distribution factor, while the latter is a text field indicating the source of the distribution factor. For all monthly livestock water use records (data_cat=STK, month in 1-12), enter an mfactor of "0.0833" (1/12) and a monthly distribution factor source of "Tech Memo 01-06". For all annual total water use records (data_cat=STK, month =0), enter an mfactor of "1" and a monthly distribution factor source of "NA".

5.2. Temporal distribution of irrigation (IRR) pumpage - Because we have only annual total groundwater pumpage estimates for IRR, we need to derive monthly pumpage estimates. Monthly distribution factors will be derived separately for rice-farming counties and non-rice-farming counties.

5.2.1. Temporal distribution of groundwater used for non-rice irrigation –

5.2.1.1. Record monthly crop evapotranspiration (ET), or total water demand, for each of the Texas Crop Reporting Districts (TCRDs) that occur within the model domain, from the report "Mean Crop Consumptive Use and Free-Water Evaporation for Texas" by J. Borrelli, C.B. Fedler, and J.M. Gregory, Feb. 1, 1998 (TWDB Grant No. 95-483-137). Use these values for all years.

5.2.1.2. Next, determine monthly precipitation (P) for the period 1980-1999 for the locale within each of the TCRDs that occur within the model domain.

5.2.1.3. Determine the monthly water deficit for each month of the two periods 1980-1989 and 1990-1999 by subtracting the P values from the ET values for each TCRD. Replace negative values with zero. Sum all water deficit values by month for each of the two periods, and divide by the number of months in each period to obtain an average non-rice monthly distribution factor for each month for the two periods 1980-89 and 1990-99.

5.2.2. Temporal distribution of groundwater used for rice irrigation –

5.2.2.1. First, identify the counties within the model area where rice is irrigated, using the 1989 and 1994 irrigation reports. Include only those counties in this analysis.

- 5.2.2.2. Next, using monthly pump power usage records provided by rice farmers, calculate monthly distribution factors for total annual power usage. Average all distribution factors within a county to get an average rice irrigation distribution factor.
- 5.2.3. Develop composite irrigation monthly distribution factors for each county and year based on the monthly factors for rice and non-rice irrigation, and the fraction of irrigation for rice in that county.
- 5.2.3.1. The TWDB irrigation survey data files Irr1989.xls and Irr1994.xls contain reported irrigation water use estimates for each crop and county. From these tables, calculate the fraction of irrigation water for rice in each county for the 1980s (based on 1989) and the 1990's (based on 1994).
- 5.2.3.2. Calculate the composite monthly distribution factor (MF_{comp}) for irrigation for each county as:
- $$MF_{comp} = MF_{rice} * X + MF_{non-rice} * (1 - X)$$
- where X is the fraction of water used for rice, and MF_{rice} and $MF_{non-rice}$ are the monthly distribution factors for rice and non-rice crops determined in steps 5.2.1 and 5.2.2, above.
- 5.2.4. For the county-basins where rice is not irrigated, enter the monthly distribution factors from step 5.2.3, above, in the table **Monthly Factors** for each year, county, basin, using "data_cat"="IRR", and "Monthly Distribution Factor Source"="ET/P Water Deficit Analysis."
- 5.2.5. For the county-basins where rice is irrigated, enter the monthly distribution factors from step 5.2.3, above, in the table **Monthly Factors** for each year, county, basin, using "data_cat"="IRR", and "Monthly Distribution Factor Source"="ET/P + Power Usage Analysis."
- 5.3. Temporal distribution of rural domestic (C-O) pumpage - Because we have only annual total groundwater pumpage estimates for C-O, we need to derive monthly pumpage estimates. According to TWDB GAM Technical Memo 01-06, annual rural domestic pumpage may be distributed based on the average monthly distribution of all municipal water use within the same county-basin.
- 5.3.1. In a MS Access query based on the table **RawDataMUN_linkedwithwellinfo**, calculate the sum of the fields "Annual total in gallons", "jan", "feb", ".....", "dec" for each county, basin, and year.
- 5.3.2. Next, calculate "mfraction," the fraction of the annual total for each month, by dividing the columns "sum of jan", "sum of feb", ".....", "sum of dec" by the "sum of annual total in gallons.". Transpose this table via a query to make a table with the following fields: "countyname", "basinname", "year", "month", "mfraction", "data_cat," and "monthly distribution factor source." A value of "C-O" should be

entered in the field “data_cat”, and the value of “monthly distribution factor source”=“this county-basin mun.”

5.3.3. The values of “mfraction” are statistically reviewed for outliers. Generally, monthly distribution factors fall within the range 0.035 to 0.15. Higher or lower values can be found when there is little municipal water use in a county-basin. In this case, substitute the values of “mfraction” from an adjacent county-basin, preferably from within the same county. Update the field “monthly distribution factor source” with the name of the county-basin used as a source.

5.3.4. For Louisiana and Arkansas parishes and counties, use the monthly distribution factors of the nearest Texas county-basin.

5.3.5. Add an annual total record for each county-basin-year, with “data_cat”=“C-O”, “month”=“0”, “mfraction”=“1”, and “monthly distribution factor source”=“NA.”

5.3.6. Using an append query, append these records to the table **Monthly Factors**.

6. Summarize Pumpage Information

6.1. Summary Queries

6.1.1. Queries for livestock - Create a new select query **MMMY_STK** to calculate pumpage for the month and year of interest by multiplying the monthly factor for that month, year, and water use category, in the table **Monthly Factors**, by each entry in the imported table **Livestock_annual_CGC**. For any specified month (MMM) and year (YY), the SQL for the query **MMMY_STK** is:

```
SELECT Livestock_annual_CGC.GRID_ID, Livestock_annual_CGC.DATA_CAT,  
Livestock_annual_CGC.Year, Livestock_annual_CGC.MODEL, [MONTHLY  
FACTORS].MONTH, [SumPumpageAF]*[mfraction] AS PumpageAF
```

```
FROM Livestock_annual_CGC LEFT JOIN [MONTHLY FACTORS] ON  
(Livestock_annual_CGC.Year = [MONTHLY FACTORS].YEAR) AND  
(Livestock_annual_CGC.DATA_CAT = [MONTHLY FACTORS].DATA_CAT)  
AND (Livestock_annual_CGC.basinum = [MONTHLY FACTORS].basinum)  
AND (Livestock_annual_CGC.CountyNumber = [MONTHLY  
FACTORS].countynum)
```

```
WHERE (((Livestock_annual_CGC.DATA_CAT)="STK") AND  
((Livestock_annual_CGC.Year)=1980) AND  
((Livestock_annual_CGC.MODEL)="CGC") AND (([MONTHLY  
FACTORS].MONTH)=1))
```

```
ORDER BY [SumPumpageAF]*[mfraction];
```

6.1.2. Queries for irrigation – Create a new select query **MMMY_IRR** to calculate pumpage for the month and year of interest by multiplying the monthly factor for

that month, year, and water use category, in the table **Monthly Factors**, by each entry in the imported table **Irrigation_annual_CGC**. For any specified month (MMM) and year(YY), the SQL for the query **MMMYY_IRR** is:

```
SELECT Irrigation_annual_CGC.GRID_ID, Irrigation_annual_CGC.DATA_CAT,  
Irrigation_annual_CGC.Year, Irrigation_annual_CGC.MODEL, [MONTHLY  
FACTORS].MONTH, [SumPumpageAF]*[mfraction] AS PumpageAF
```

```
FROM Irrigation_annual_CGC LEFT JOIN [MONTHLY FACTORS] ON  
(Irrigation_annual_CGC.basinum = [MONTHLY FACTORS].basinum) AND  
(Irrigation_annual_CGC.CountyNumber = [MONTHLY FACTORS].countynum)  
AND (Irrigation_annual_CGC.Year = [MONTHLY FACTORS].YEAR) AND  
(Irrigation_annual_CGC.DATA_CAT = [MONTHLY FACTORS].DATA_CAT)
```

```
WHERE (((Irrigation_annual_CGC.DATA_CAT)="IRR") AND  
((Irrigation_annual_CGC.Year)=1980) AND  
((Irrigation_annual_CGC.MODEL)="CGC") AND (([MONTHLY  
FACTORS].MONTH)=1))
```

```
ORDER BY [SumPumpageAF]*[mfraction];
```

- 6.1.3. Queries to summarize rural domestic (county-other) - Create a new select query **MMMYY_C-O** to calculate pumpage for the month and year of interest by multiplying the monthly factor for that month, year, and water use category, in the table **Monthly Factors**, by each entry in the imported table **Rurdom_annual_CGC**. For any selected month (MMM) and year(YY), the SQL for the query **MMMYY_C-O** is:

```
SELECT Rurdom_annual_CGC.GRID_ID, Rurdom_annual_CGC.DATA_CAT,  
Rurdom_annual_CGC.Year, Rurdom_annual_CGC.MODEL, [MONTHLY  
FACTORS].MONTH, [SumPumpageAF]*[mfraction] AS PumpageAF
```

```
FROM Rurdom_annual_CGC LEFT JOIN [MONTHLY FACTORS] ON  
(Rurdom_annual_CGC.DATA_CAT = [MONTHLY FACTORS].DATA_CAT)  
AND (Rurdom_annual_CGC.Year = [MONTHLY FACTORS].YEAR) AND  
(Rurdom_annual_CGC.CountyNumber = [MONTHLY FACTORS].countynum)  
AND (Rurdom_annual_CGC.basinum = [MONTHLY FACTORS].basinum)
```

```
WHERE (((Rurdom_annual_CGC.DATA_CAT)="C-O") AND  
((Rurdom_annual_CGC.Year)=1980) AND  
((Rurdom_annual_CGC.MODEL)="CGC") AND (([MONTHLY  
FACTORS].MONTH)=1))
```

```
ORDER BY [SumPumpageAF]*[mfraction];
```

- 6.1.4. Query to summarize well-specific pumpage - Create a new select query in MS Access **MMMYYWell-SpecificSum** to summarize the well-specific pumpage from all wells within a grid cell for the desired month or year. For any specified month

and year, the SQL query for well-specific pumpage would be:

```
SELECT CGC_gridsum_well_specific.GRID_ID, "WS" AS DATA_CAT,
CGC_gridsum_well_specific.year, CGC_gridsum_well_specific.Model,
CGC_gridsum_well_specific.month,
CGC_gridsum_well_specific.SumPumpage_af AS PumpageAF

FROM CGC_gridsum_well_specific

WHERE (((CGC_gridsum_well_specific.year)=[Enter year]) AND
((CGC_gridsum_well_specific.Model)="CGC") AND
((CGC_gridsum_well_specific.month)=[Enter month]))

ORDER BY CGC_gridsum_well_specific.SumPumpage_af;
```

6.1.5. In order to ensure that each grid cell is included in the final summary queries, even if there is no pumpage from the cell, we must create a full grid with values of zero.

6.1.5.1. Create a new table **Zero_grid_annual** in a make-table query based on the table **grid_lkup_area** with one record for each grid cell and year. For instance, a model with 212 rows, 180 columns, and 6 layers, for 20 years would be create a table with 212 x 180 x 6 x 20= 4,579,200 records. In the make-table query, add a field “SumPumpageAF” with a value of zero for each record.

6.1.5.2. Create a new query **MMMYZ_ZeroGrid** to provide zero values for each grid cell for each month. You can use any of the monthly factors, as all results will equal zero. As an example, the SQL query for January 1980 would be:

```
SELECT Zero_Grid_Annual.GRID_ID, Zero_Grid_Annual.DATA_CAT,
Zero_Grid_Annual.Year, Zero_Grid_Annual.MODEL, [MONTHLY
FACTORS].MONTH, Zero_Grid_Annual.SumPumpageAF

FROM Zero_Grid_Annual LEFT JOIN [MONTHLY FACTORS] ON
(Zero_Grid_Annual.basinum = [MONTHLY FACTORS].basinum) AND
(Zero_Grid_Annual.CountyNumber = [MONTHLY FACTORS].countynum)
AND (Zero_Grid_Annual.Year = [MONTHLY FACTORS].YEAR)

WHERE (((Zero_Grid_Annual.Year)=[Enter year]) AND (([MONTHLY
FACTORS].MONTH)=[Enter month]) AND (([MONTHLY
FACTORS].DATA_CAT)="IRR"))

ORDER BY Zero_Grid_Annual.GRID_ID;
```

6.1.6. In Access, create a new union query **MMMYZ_UnionofPumpage** to combine the domestic, livestock, rural domestic, and well-specific pumpage sums, as well as the

zero value, for each grid cell. As an example, the SQL for any given year and month is:

```
SELECT * FROM [MMMY_C-O] UNION ALL SELECT * FROM  
[MMMY_IRR] UNION ALL SELECT * FROM [MMMY_STK]  
UNION ALL SELECT * FROM [MMMY_ZeroGrid] UNION ALL  
SELECT * FROM [MMMYWell-specificSum];
```

- 6.1.7. Create a new select query **SumPumpageGrid_MMMYY** to summarize all pumpage by grid cell, grouping by grid_id, month, and year the pumpage from the above union query. As an example, the SQL for January 1980 is:

```
SELECT MMMYYUnionofPumpage.GRID_ID,  
MMMYUnionofPumpage.Year, MMMYYUnionofPumpage.MONTH,  
Sum(MMMYYUnionofPumpage.PumpageAF) AS SumOfPumpageAF,  
Sum([PumpageAF]*[MGDfromAF]) AS PumpageMGD  
  
FROM MMMYYUnionofPumpage LEFT JOIN UnitConversion ON  
MMMYUnionofPumpage.MONTH = UnitConversion.Month  
  
GROUP BY MMMYYUnionofPumpage.GRID_ID,  
MMMYUnionofPumpage.Year, MMMYYUnionofPumpage.MONTH  
  
ORDER BY MMMYYUnionofPumpage.GRID_ID;
```

- 6.2. Join pumpage queries to Arcview shapefile if visual display of the results for a month or year is desired.

- 6.2.1. In Arcview, import the MS Access query **SumPumpageGrid_MMMYY**, and join it to the model grid cells in the Arcview shapefile based on the field "Grid_ID."
- 6.2.2. In Arcview, import the MS Access queries **MMMY_STK**, **MMMY_IRR**, **MMMY_C-O**, and **Well-specificpumpage**. Link these tables to the model grid cells in the Arcview shapefile based on the field "Grid_ID" and, for well-specific pumpage, "year." Selection of a grid cell in Arcview will then also select the records in each of these tables that pump from the grid cell selected.

Appendix 1 - Vertical Distribution Avenue Script

```
theView = Av.GetActiveDoc
theTheme = theView.findTheme("wells")
theFtab = theTheme.GetFtab

'get elevation values for layers
theLay1Field = theFtab.findField("top_young")
theLay2Field = theFtab.findField("top_reklaw")
theLay3Field = theFtab.findField("top_carriz")
theLay4Field = theFtab.findField("top_uwilco")
theLay5Field = theFtab.findField("top_mwilco")
theLay6Field = theFtab.findField("top_lwilco")
theBottomField = theFtab.findField("bas_lwilco")

'get percentfield holders
thePer1Field = theFtab.findField("per1")
thePer2Field = theFtab.findField("per2")
thePer3Field = theFtab.findField("per3")
thePer4Field = theFtab.findField("per4")
thePer5Field = theFtab.findField("per5")
thePer6Field = theFtab.findField("per6")
theTotPerField = theFtab.findField("tot_per")

'get well values
theScreenField = theFtab.findField("Screen")
theDepthField = theFtab.findField("depth")

theSel = theFtab.GetSelection

for each rec in theSel
  ct = 0
  totPerVal = 0
  cumPerVal = 0
  theDepthVal = theFtab.ReturnValue(theDepthfield,rec)
  theScreenVal = theFtab.ReturnValue(theScreenfield,rec)
  screenLengthVal = (theScreenVal - theDepthVal).abs

  theLay1Val = theFtab.ReturnValue(theLay1field,rec)
  theLay2Val = theFtab.ReturnValue(theLay2field,rec)
  theLay3Val = theFtab.ReturnValue(theLay3field,rec)
  theLay4Val = theFtab.ReturnValue(theLay4field,rec)
  theLay5Val = theFtab.ReturnValue(theLay5field,rec)
  theLay6Val = theFtab.ReturnValue(theLay6field,rec)
  theBotVal = theFtab.ReturnValue(theBottomField,rec)

  if ((theScreenVal < theLay1Val ) And (theScreenVal > theLay2Val)) then
    if (theDepthVal < theLay2Val) then
      per1 = (((theLay2Val - theScreenVal) / screenLengthVal) * 100).abs
      theFtab.SetValue(thePer1field,rec,per1)
      cumPerVal = cumPerVal + per1
    else
      per1 = (100 - cumPerVal)
      cumPerVal = cumPerVal + per1
```

```
        theFtab.SetValue(thePer1field,rec,per1)
    end
else
    per1 = 0
    theFtab.SetValue(thePer1field,rec,per1)
end
'-----layer 2
if (cumperval.round = 100) then
    'continue
    ct=ct+1
    per2 = 0
    theFtab.SetValue(thePer2field,rec,per2)
else
    if ((theScreenVal < theLay2Val ) And (theScreenVal > theLay3Val)) then
        if (theDepthVal < theLay3Val) then
            per2 = (((theScreenVal - theLay3Val) / screenLengthVal) * 100).abs
            cumPerVal = cumPerVal + per2
            theFtab.SetValue(thePer2field,rec,per2)
        else
            per2 = (100 - cumPerVal)
            cumPerVal = cumPerVal + per2
            theFtab.SetValue(thePer2field,rec,per2)
        end
    end
else
    if (cumPerVal > 0) then 'if continuing
        if (theDepthVal < theLay3Val) then
            per2 = (((theLay3Val - theLay2Val) / screenLengthVal) * 100).abs
            cumPerVal = cumPerVal + per2
            theFtab.SetValue(thePer2field,rec,per2)
        else
            per2 = (((theDepthVal - theLay2Val) / screenLengthVal) * 100).abs
            cumPerVal = cumPerVal + per2
            theFtab.SetValue(thePer2field,rec,per2)
        end
    end
else
    per2 = 0
    theFtab.SetValue(thePer2field,rec,per2)
end
end
end
'-----layer 3
if (cumperval.round = 100) then
    'continue
    ct=ct+1
    per3 = 0
    theFtab.SetValue(thePer3field,rec,per3)
else
    if ((theScreenVal < theLay3Val ) And (theScreenVal > theLay4Val)) then
        if (theDepthVal < theLay4Val) then
            per3 = (((theScreenVal - theLay4Val) / screenLengthVal) * 100).abs
            cumPerVal = cumPerVal + per3
            theFtab.SetValue(thePer3field,rec,per3)
        else
            per3 = (100 - cumPerVal)
            cumPerVal = cumPerVal + per3
            theFtab.SetValue(thePer3field,rec,per3)
        end
    end
end
```

```

end
else
if (cumPerVal > 0) then 'if continuing
if (theDepthVal < theLay4Val) then
per3 = (((theLay4Val - theLay3Val) / screenLengthVal) * 100).abs
cumPerVal = cumPerVal + per3
theFtab.SetValue(thePer3field,rec,per3)
else
per3 = (((theDepthVal - theLay3Val) / screenLengthVal) * 100).abs
cumPerVal = cumPerVal + per3
theFtab.SetValue(thePer3field,rec,per3)
end
else
per3 = 0
theFtab.SetValue(thePer3field,rec,per3)
end
end
end
'-----layer 4
if (cumperval.round = 100) then
'continue
ct=ct+1
per4 = 0
theFtab.SetValue(thePer4field,rec,per4)
else
if ((theScreenVal < theLay4Val ) And (theScreenVal > theLay5Val)) then
if (theDepthVal < theLay5Val) then
per4 = (((theScreenVal - theLay5Val) / screenLengthVal) * 100).abs
cumPerVal = cumPerVal + per4
theFtab.SetValue(thePer4field,rec,per4)
else
per4 = (100 - cumPerVal)
cumPerVal = cumPerVal + per4
theFtab.SetValue(thePer4field,rec,per4)
end
else
if (cumPerVal > 0) then 'if continuing
if (theDepthVal < theLay5Val) then
per4 = (((theLay5Val - theLay4Val) / screenLengthVal) * 100).abs
cumPerVal = cumPerVal + per4
theFtab.SetValue(thePer4field,rec,per4)
else
per4 = (((theDepthVal - theLay4Val) / screenLengthVal) * 100).abs
cumPerVal = cumPerVal + per4
theFtab.SetValue(thePer4field,rec,per4)
end
else
per4 = 0
theFtab.SetValue(thePer4field,rec,per4)
end
end
end
'-----layer 5
if (cumperval.round = 100) then
'continue
ct = ct+1

```

```

per5 = 0
theFtab.SetValue(thePer5field,rec,per5)
else
if ((theScreenVal < theLay5Val ) And (theScreenVal > theLay6Val)) then
if (theDepthVal < theLay6Val) then
per5 = (((theScreenVal - theLay6Val) / screenLengthVal) * 100).abs
cumPerVal = cumPerVal + per5
theFtab.SetValue(thePer5field,rec,per5)
else
per5 = (100 - cumPerVal)
cumPerVal = cumPerVal + per5
theFtab.SetValue(thePer5field,rec,per5)
end
else
if (cumPerVal > 0) then 'if continuing
if (theDepthVal < theLay6Val) then
per5 = (((theLay6Val - theLay5Val) / screenLengthVal) * 100).abs
cumPerVal = cumPerVal + per5
theFtab.SetValue(thePer5field,rec,per5)
else
per5 = (((theDepthVal - theLay5Val) / screenLengthVal) * 100).abs
cumPerVal = cumPerVal + per5
theFtab.SetValue(thePer5field,rec,per5)
end
else
per5 = 0
theFtab.SetValue(thePer5field,rec,per5)
end
end
end
'-----layer 6
if (cumPerVal.round = 100) then
'continue
ct = ct+1
per6 = 0
theFtab.SetValue(thePer6field,rec,per6)
else
if ((theScreenVal < theLay6Val ) And (theScreenVal > theBotVal)) then
if (theDepthVal < theBotVal) then
per6 = (((theScreenVal - theBotVal) / screenLengthVal) * 100).abs
cumPerVal = cumPerVal + per6
theFtab.SetValue(thePer6field,rec,per6)
else
per6 = (100 - cumPerVal)
cumPerVal = cumPerVal + per6
theFtab.SetValue(thePer6field,rec,per6)
end
else
if (cumPerVal > 0) then 'if continuing
if (theDepthVal < theBotVal) then
per6 = (((theBotVal - theLay6Val) / screenLengthVal) * 100).abs
cumPerVal = cumPerVal + per6
theFtab.SetValue(thePer6field,rec,per6)
else
per6 = (((theDepthVal - theLay6Val) / screenLengthVal) * 100).abs
cumPerVal = cumPerVal + per6

```

```
        theFtab.SetValue(thePer6field,rec,per6)
    end
else
    per6 = 0
    theFtab.SetValue(thePer6field,rec,per6)
end
end
end
theFtab.SetValue(theTotPerField,rec,cumPerVal)
end 'end for loop
```

Appendix 2 – Arcview script to return land surface elevation for a well from a DEM grid

```
'-----  
' Name: getgridvalue.ave  
' Date: 991004  
'  
' Description: Moves copies values from a grid to a  
' feature theme. The values from the grid are placed  
' in a user defined field. If the feature theme isn't  
' a point theme, then the feature gets the grid value  
' from the value under it's centroid point.  
'  
' Requires: Spatial Analyst  
'  
' Author: Originally written by Mikael Elmquist (mikael@swegis.com), but later  
' modified by Jeremy Davies (jeremy.davies@noaa.gov)  
'-----  
  
theView = av.GetActiveDoc  
theThemes={ }  
  
'-----  
' Choose in theme  
'-----  
themeList = theView.GetThemes  
rep = 0  
stupid = 0  
while (rep = 0)  
  theTheme = MsgBox.ChoiceAsString(themeList,"Select theme that shall get values from the grid  
  theme.,"GetGridValue")  
  if (theTheme = NIL) then  
    exit  
  end  
  if (theTheme.Is(Ftheme).Not) then  
    stupid = stupid+1  
    if (stupid = 4) then  
      msgBox.Info("Dear ArcView GIS user. Try to select a valid theme","Problem?")  
    end  
    msgBox.Error("Not a valid theme","Error")  
  else  
    rep = 1  
    theFtab = theTheme.GetFtab  
  end  
end  
rep = 0  
stupid = 0  
  
theThemes={ }  
if (theFtab.CanEdit) then  
  theFtab.SetEditable(true)
```

```
if ((theFtab.CanAddFields).Not) then
  MsgBox.Info("Can't add fields to the table."+NL+"Check write permission.", "Can't add grid values")
  exit
end
else
  MsgBox.Info("Can't modify the feature table."+NL+"Check write permission.", "Can't add grid values")
  exit
end
```

```
'-----
'Choose grid theme
'-----
```

```
for each TargetTheme in theView.GetThemes
  if (TargetTheme.Is(Gtheme)) then
    theThemes.Add(TargetTheme)
  end
end
theGtheme = MsgBox.ChoiceAsString(theThemes, "Select grid that shall assign values to the point
theme.", "GetGridValue")
if (theGtheme = Nil) then
  exit
end
theGrid = theGtheme.Clone.GetGrid.Clone
thePrj = Prj.MakeNull
```

```
'-----
' Add the new field
'-----
```

```
'enter name of new field name and parameters
newField = MsgBox.Input( "Enter new field name:", "Value", "" )
fieldsize = MsgBox.Input( "Enter new field width:", "Value", "10" )
precision = MsgBox.Input( "Enter number of decimals places in new field:", "Value", "4" )
```

```
gridvalueField = Field.Make (newField,#FIELD_DECIMAL,fieldsize.asNumber,precision.asNumber)
theShapeField = theFtab.FindField("shape")
theFtab.AddFields({ gridvalueField})
```

```
'-----
' Copy values
'-----
```

```
av.ShowMsg("Calculating values")
av.SetStatus(0)
sstatus = theFtab.GetNumRecords.Clone
for each aRec in theFtab
  av.SetStatus(aRec/sstatus*100)
  theValue = theGrid.CellValue(theFtab.returnValue(theShapeField,aRec).ReturnCenter,thePrj)
  av.SetStatus(aRec/sstatus*100)
  if (theValue<>Nil) then
    theFtab.SetValue(gridvalueField,aRec,theValue)
  end
end
```

end

'-----
'Reset arcview
'-----

theFtab.Flush
theFtab.Refresh
theFTab.SetEditable(False)
av.purgeobjects
av.ClearStatus
av.ClearMsg

APPENDIX C

Standard Operating Procedures (SOPs) for Processing Predictive Pumpage Data TWDB Groundwater Availability Modeling (GAM) Projects

**Standard Operating Procedures (SOPs)
for Processing Predictive Pumpage Data
TWDB Groundwater Availability Modeling (GAM) Projects**

TABLE OF CONTENTS

1. Background..... 1

2. Groundwater Use Source Data 1

3. Initial Processing..... 1

 3.1. Create a sub-set of data for the modeled aquifer and geographic area 2

 3.2. Split water use between surface and ground water..... 2

 3.3. Interpolate pumpage estimates for all years 2000-2050 2

4. Spatially distribute well-specific pumpage 2

 4.1. Identify locations of new wells 2

 4.2. Matching Predictive to Historical Locations by Alphanum..... 2

 4.3. Create new tables for each well-specific water use category 3

5. Spatially distribute non-well-specific pumpage 3

 5.1. Calculate the fraction of groundwater pumpage for “C-O” use from each grid cell within a county-basin from 1999 4

 5.2. Calculate the fraction of groundwater pumpage for “IRR” use from each grid cell within a county-basin from 1999 4

 5.3. Calculate the fraction of groundwater pumpage for “STK” use from each grid cell within a county-basin from 1999 4

 5.4. Note..... 5

6. Monthly Distribution of Annual Pumpage Totals. 5

7. Summarize Pumpage Information to Create Model Input Files..... 5

8. Handling Non-Texas Pumpage..... 5

1. Background – These procedures were developed to further implement the guidance provided by the Texas Water Development Board (TWDB) in their Technical Memorandum 02-01 “Development of Predictive Pumpage Data Set for GAM.” The information in that technical memorandum will not be repeated here, and readers should first consult that document.
2. Groundwater Use Source Data - To the extent possible, procedures for predictive pumpage distribution among model grid cells mimicked the procedures for historical pumpage data. Predicted future groundwater use estimates are derived from one spreadsheet (**GAMPredictivePumpage_2002SWP.xls**) provided by the Texas Water Development Board (TWDB), as well as the previously developed historical pumpage datasets. This spreadsheet contains water use estimates from the state water plans for each water user group for the years 2000, 2010, 2020, 2030, 2040, and 2050. Water user groups are generally assigned for each water user category (IRR, STK, MIN, MFG, PWR, MUN, and C-O) in each county-basin. However, individual municipal water supplies within a county-basin are assigned identified as separate water user groups. The water use categories are listed below:

- IRR – irrigation
- STK – livestock
- MIN - mineral extraction
- MFG – manufacturing
- PWR – power generation
- MUN – municipal water supply, and
- C-O – county-other (rural domestic) use.

Historical groundwater use records from the categories MIN, MFG, PWR, and MUN are available for each specific water user, each assigned an alphanumeric water user code (aka “alphanum”) in historical water use data tables. Specific locations and wells from which this groundwater was pumped were identified in historical pumpage records. These are known as “well-specific” water use categories. However, the particular locations of historical groundwater pumpage were generally not known for the use categories IRR, STK, and C-O. These categories are known as “non-well-specific” water use categories. This pumpage was distributed spatially based on population density, land use, and other factors.

The spreadsheet **GAMPredictivePumpage_2002SWP.xls** was downloaded from the TWDB web site. The spreadsheet file was then imported into a new Microsoft Access database file **Predictive Pumpage**.

3. Initial Processing

- 3.1. Create a sub-set of data for the modeled aquifer and geographic area – The table

Predictive Pumpage_2002SWP was queried for water use in the aquifer of interest based on the aquifer’s major aquifer code, as well as the code “99.” Other records were deleted. Next, the table was queried for those records within source county ID’s found in the modeling domain. Records for water pumpage outside the model domain were deleted.

- 3.2. Split water use between surface and ground water – Some records contain an aggregate of surface and ground water use, as indicated by a value of “04” in the field “SO_TYPE_ID_NEW.” A new field “PERCENT GROUNDWATER” was added to the table and assigned a value from 0 to 1 based on information in the field “ADDTL COMMENTS.”
- 3.3. Interpolate pumpage estimates for all years 2000-2050 – The table **Predictive Pumpage_2002SWP** only contains water use estimates for the years 2000, 2010, 2020, 2030, 2040, and 2050. Water use estimates for the intervening years are calculated by linear interpolation. This can be calculated in a query as for example:

$$\text{Pumpage}_{2001} = \text{Pumpage}_{2000} + \text{modulus}(2001,10)*[(\text{Pumpage}_{2010}-\text{Pumpage}_{2000})/10]$$

4. Spatially distribute well-specific pumpage –

- 4.1. Identify locations of new wells – If the field “Possible_New_Wells” contained a flag “NW”, it was necessary to identify the location of the new wells. The Regional Water Plan was consulted to identify the location of the new wells (a map showing the projected locations of the new wells was available). Using Arcview, the latitude and longitude of the well(s) were estimated and copied into a new field “KD_comment.” This latitude and longitude were used to identify the model grid_id(s) from which the well was expected to pump. These grid_id’s were copied into a new field “grid_id” in the predictive pumpage table.
- 4.2. Matching Predictive to Historical Locations by “Alphanum” - We assumed that a water user would tend to pump water in the future from the same locations from which they had pumped groundwater historically. A specific water user can best be identified in the TWDB predictive pumpage data using the field “WUG_Prime_Alpha”, or, if the water was purchased, the field “Seller Alpha.”
 - 4.2.1. A new field “Source_Alpha” was created and populated with the value from the field “WUG_Prime_Alpha” or, if available, the value from the field “Seller Alpha.”
 - 4.2.2. In many cases, no value of alpha_num was provided in the table for a well-specific WUG_ID, typically for MIN, MFG, and PWR. Therefore, the value(s) of “alphanum” associated with that WUG_ID in the historical pumpage table was copied to the predictive pumpage table.

In the case that multiple values of “alphanum” were identified for a given “WUG_ID” in the historical data, we first made replicate copies of the record in the predictive pumpage table for each value of alphanum, copied each alphanum into

the field “Source_Alpha”, and entered in the field “percent groundwater” the fraction of pumpage for each alphanum for the period 1995-1999 from the historical table. An explanation was entered in the field “KD_comment.”

- 4.2.3. The value of “Source_Alpha” was matched manually to the field “alphanum” in the historical pumpage datasets, and the model grid_id identified for this water user in historical pumpage distribution was manually copied to the field “Grid_ID” in the predictive pumpage table.

In many cases, more than one grid was associated with a given “alphanum”. The predictive pumpage for each alphanum was distributed among multiple Grid ID’s in an identical manner as the average for the period 1995-1999. Additional copies of predictive pumpage records were added to equal the number of grid_id’s, and a field “grid_frac” was added to the predictive pumpage table, and assigned a value from 0 to 1, calculated as the average of the 1995-1999 fraction of pumpage from that grid_id for that alphanum in the historical pumpage dataset. The values of grid_frac summed to 1 for each “source_alpha.”

4.3. Create new tables for each well-specific water use category –

- 4.3.1. Create a new table or query for the water use category MUN containing a value of MUN pumpage for each grid_id for each year from 2000 to 2050. The pumpage for each record is calculated as the total pumpage for the year of interest multiplied by the fields “grid_frac” and “percent groundwater.”
- 4.3.2. Create a new table or query for the water use category MFG containing a value of MFG pumpage for each grid_id for each year from 2000 to 2050. The pumpage for each record is calculated as the total pumpage for the year of interest multiplied by the fields “grid_frac” and “percent groundwater.”
- 4.3.3. Create a new table or query for the water use category MIN containing a value of MIN pumpage for each grid_id for each year from 2000 to 2050. The pumpage for each record is calculated as the total pumpage for the year of interest multiplied by the fields “grid_frac” and “percent groundwater.”
- 4.3.4. Create a new table or query for the water use category PWR containing a value of PWR pumpage for each grid_id for each year from 2000 to 2050. The pumpage for each record is calculated as the total pumpage for the year of interest multiplied by the fields “grid_frac” and “percent groundwater.”

5. Spatially distribute non-well-specific pumpage – We assume that groundwater pumpage in the future would be distributed within each county-basin in a similar way that it has been done in the recent past. While we do not discount the impact of changes in population and land use due to urban growth, sprawl, and other factors, we cannot reliably predict the spatial locations of these changes.

- 5.1. Calculate the fraction of groundwater pumpage for “C-O” use from each grid cell within

a county-basin from 1999.

- 5.1.1. Run a query to summarize “C-O” groundwater pumpage in 1999 for each county-basin within the model domain.
 - 5.1.2. For each `grid_id` within each county-basin, divide the “C-O” pumpage value for the year 1999 by the total “C-O” pumpage for that county-basin. Save this as a new field “`Fr_pumpage`” for each `grid_id`.
 - 5.1.3. As a quality check, sum the values of “`Fr_pumpage`” for C-O by county-basin to ensure they sum to 1.
 - 5.1.4. Create a new table or query for the water use category “C-O” containing a value of C-O pumpage for each `grid_id` for each year from 2000 to 2050. The pumpage for each record is calculated as the total pumpage for the year of interest (from the TWDB-provided table **GAMPredictivePumpage_2002SWP.xls**, with interpolated values for intervening years) multiplied by the fields “percent groundwater” (from the same table) and the field “`Fr_pumpage`” from the previous three steps.
- 5.2. Calculate the fraction of groundwater pumpage for “IRR” use from each grid cell within a county-basin from 1999.
- 5.2.1. Run a query to summarize “IRR” groundwater pumpage in 1999 for each county-basin within the model domain.
 - 5.2.2. For each `grid_id` within each county-basin, divide the “IRR” pumpage value for the year 1999 by the total “IRR” pumpage for that county-basin. Save this as a new field “`Fr_pumpage`” for each `grid_id`.
 - 5.2.3. As a quality check, sum the values of “`Fr_pumpage`” for IRR by county-basin to ensure they sum to 1.
 - 5.2.4. Create a new table or query for the water use category “IRR” containing a value of IRR pumpage for each `grid_id` for each year from 2000 to 2050. The pumpage for each record is calculated as the total pumpage for the year of interest (from the TWDB-provided table **GAMPredictivePumpage_2002SWP.xls**, with interpolated values for intervening years) multiplied by the fields “percent groundwater” (from the same table) and the field “`Fr_pumpage`” from the previous three steps.
- 5.3. Calculate the fraction of groundwater pumpage for “STK” use from each grid cell within a county-basin from 1999.
- 5.3.1. Run a query to summarize “STK” groundwater pumpage in 1999 for each county-basin within the model domain.
 - 5.3.2. For each `grid_id` within each county-basin, divide the “STK” pumpage value for the year 1999 by the total “STK” pumpage for that county-basin. Save this as a new field “`Fr_pumpage`” for each `grid_id`.

-
- 5.3.3. As a quality check, sum the values of “Fr_pumpage” for STK by county-basin to ensure they sum to 1.
 - 5.3.4. Create a new table or query for the water use category “STK” containing a value of STK pumpage for each grid_id for each year from 2000 to 2050. The pumpage for each record is calculated as the total pumpage for the year of interest (from the TWDB-provided table **GAMPredictivePumpage_2002SWP.xls**, with interpolated values for intervening years) multiplied by the fields “percent groundwater” (from the same table) and the field “Fr_pumpage” from the previous three steps.
 - 5.4. Note: The result of this step should be three tables (or queries), one each for C-O, IRR, and STK. Each should contain, at a minimum, the fields “Grid_ID”, “county_name”, “basin_name”, “year”, “data_cat”, and “pumpage.”
 6. Monthly Distribution of Annual Pumpage Totals - We assume that the historical average of monthly water use distribution is a valid predictor of future monthly distribution.

Monthly factors are calculated for each county-basin and data_cat as the average of mfraction for the period 1995-1999 (in the historical pumpage table “MONTHLY FACTORS”) in a new table **PredictiveMonthlyFactors**. There should be a monthly factor for each combination of the seven water use categories and county-basin. If no monthly factor can be calculated because there was no historical pumpage, then the monthly factor for that data_cat in the nearest other county-basin should be used.
 7. Summarize Pumpage Information to Create Model Input Files - Summary queries for a given year and/or month should be performed as described in the SOP for historical pumpage data.
 8. Handling Non-Texas Pumpage – Predictions of future pumpage for portions of the model domain outside of Texas are not available from the Texas Regional Water Plans. In this case, we will assume that the average pumpage for the period 1995-1999 is the best estimate of future pumpage for the water use categories MFG, MIN, PWR, STK, and IRR. Because population projections are available, however, we can project future water use for MUN and C-O based on the 1990 water use for each county or parish and the ratio of projected future county/parish population to its 1990 population.
 - 8.1. Download from the respective state census data center or the U.S. census bureau population estimates from each county or parish through 2050. Linearly interpolate values for intervening years if necessary.
 - 8.2. For each year from 2000 to 2050, calculate the ratio of projected population for each year to that in 2000 for each county or parish.
 - 8.3. Multiply the historical pumpage value from C-O or MUN out-of-Texas records in 1999 by the factor to obtain a projected pumpage estimate for that year.
-

APPENDIX D1

Tabulated Groundwater Withdrawal Estimates for the Carrizo-Wilcox for 1980, 1990, 2000, 2010, 2020, 2030, 2040, and 2050

Table D1.1
Rate of groundwater withdrawal (acre-feet per year) from flow layer 1 of the
Carrizo-Wilcox aquifer for counties within the study area

Municipal and Industrial*

COUNTY	1980	1990	2000	2010	2020	2030	2040	2050
ATASCOSA	0	0	0	0	0	0	0	0
BASTROP	0	0	0	0	0	0	0	0
BEE	0	0	0	0	0	0	0	0
BEXAR	0	0	0	0	0	0	0	0
CALDWELL	0	0	0	0	0	0	0	0
DEWITT	0	0	0	0	0	0	0	0
DIMITT	0	0	0	0	0	0	0	0
FAYETTE	0	0	0	0	0	0	0	0
FRIO	0	0	0	0	0	0	0	0
GONZALES	0	0	0	0	0	0	0	0
GUADALUPE	0	0	584	651	697	739	803	867
KARNES	0	0	1296	1214	1241	1315	1376	1446
LA SALLE	0	0	0	0	0	0	0	0
LAVACA	0	0	0	0	0	0	0	0
LIVE OAK	0	0	0	0	0	0	0	0
MAVERICK	0	0	0	0	0	0	0	0
MCMULLEN	0	0	0	0	0	0	0	0
MEDINA	0	0	0	0	0	0	0	0
UVALDE	0	0	0	0	0	0	0	0
WEBB	0	0	288	209	145	100	79	82
WILSON	0	0	0	0	0	0	0	0
ZAVALA	0	0	0	0	0	0	0	0

*industrial includes manufacturing, mining, and power generation

County – Other (Non-reported Domestic)

COUNTY	1980	1990	2000	2010	2020	2030	2040	2050
ATASCOSA	163	200	175	196	231	170	199	209
BASTROP	9	18	56	67	77	89	103	128
BEE	0	0	80	81	80	82	84	88
BEXAR	0	0	0	0	0	0	0	0
CALDWELL	1	1	2	2	3	2	2	2
DEWITT	3	4	0	0	0	0	0	0
DIMITT	0	0	0	0	0	0	0	0
FAYETTE	80	100	0	0	0	0	0	0
FRIO	269	372	410	415	415	306	315	321
GONZALES	716	918	631	601	580	563	566	573
GUADALUPE	0	0	0	0	0	0	0	0
KARNES	478	545	762	701	704	625	655	663
LA SALLE	152	182	325	334	340	319	324	320
LAVACA	1	1	0	0	0	0	0	0
LIVE OAK	1	3	0	0	0	0	0	0
MAVERICK	0	0	0	0	0	0	0	0
MCMULLEN	45	32	30	27	21	14	10	7
MEDINA	0	0	0	0	0	0	0	0
UVALDE	0	0	0	0	0	0	0	0
WEBB	142	404	75	80	81	81	81	81
WILSON	250	305	413	521	569	600	717	835
ZAVALA	110	72	41	48	50	54	69	93

Table D1.1 (continued)

Livestock

COUNTY	1980	1990	2000	2010	2020	2030	2040	2050
ATASCOSA	74	66	0	0	0	0	0	0
BASTROP	21	20	0	0	0	0	0	0
BEE	0	0	0	0	0	0	0	0
BEXAR	0	0	0	0	0	0	0	0
CALDWELL	1	0	0	0	0	0	0	0
DEWITT	5	1	0	0	0	0	0	0
DIMITT	70	81	0	0	0	0	0	0
FAYETTE	4	2	0	0	0	0	0	0
FRIO	28	14	0	0	0	0	0	0
GONZALES	756	157	0	0	0	0	0	0
GUADALUPE	0	0	0	0	0	0	0	0
KARNES	58	46	0	0	0	0	0	0
LA SALLE	53	44	0	0	0	0	0	0
LAVACA	3	1	0	0	0	0	0	0
LIVE OAK	1	1	0	0	0	0	0	0
MAVERICK	0	0	0	0	0	0	0	0
MCMULLEN	43	23	307	307	307	307	307	307
MEDINA	0	0	0	0	0	0	0	0
UVALDE	0	0	0	0	0	0	0	0
WEBB	34	33	442	442	442	439	439	439
WILSON	100	70	0	0	0	0	0	0
ZAVALA	12	2	0	0	0	0	0	0

Irrigation

COUNTY	1980	1990	2000	2010	2020	2030	2040	2050
ATASCOSA	1813	1229	94	93	91	0	0	0
BASTROP	0	0	0	0	0	0	0	0
BEE	0	0	0	0	0	0	0	0
BEXAR	0	0	0	0	0	0	0	0
CALDWELL	0	0	0	0	0	0	0	0
DEWITT	1	4	0	0	0	0	0	0
DIMITT	0	0	0	0	0	0	0	0
FAYETTE	2	2	8	8	7	7	6	6
FRIO	228	282	59	59	59	7	7	7
GONZALES	275	1107	671	579	499	423	365	315
GUADALUPE	0	0	0	0	0	0	0	0
KARNES	8	15	902	726	567	424	294	176
LA SALLE	50	37	22	20	19	17	15	14
LAVACA	0	0	0	0	0	0	0	0
LIVE OAK	114	77	171	171	171	171	171	171
MAVERICK	0	0	0	0	0	0	0	0
MCMULLEN	0	0	0	0	0	0	0	0
MEDINA	0	0	0	0	0	0	0	0
UVALDE	0	0	0	0	0	0	0	0
WEBB	0	1	3	3	3	2	2	2
WILSON	976	1886	1585	1399	1048	777	699	637
ZAVALA	0	0	0	0	0	0	0	0

Table D1.2
Rate of groundwater withdrawal (acre-feet per year) from flow layer 2 of the
Carrizo-Wilcox aquifer for counties within the study area

Municipal and Industrial*

COUNTY	1980	1990	2000	2010	2020	2030	2040	2050
ATASCOSA	0	0	1564	1564	1564	76	403	1798
BASTROP	0	0	0	0	0	0	0	0
BEE	0	0	0	0	0	0	0	0
BEXAR	0	0	0	0	0	0	0	0
CALDWELL	0	0	0	0	0	0	0	0
DEWITT	0	0	0	0	0	0	0	0
DIMITT	0	0	0	0	0	0	0	0
FAYETTE	0	0	0	0	0	0	0	0
FRIO	0	0	0	0	0	0	0	0
GONZALES	0	0	0	0	0	0	0	0
GUADALUPE	0	0	0	0	0	0	0	0
KARNES	1101	52	21	9	4	2	1	1
LA SALLE	0	0	0	0	0	0	0	0
LAVACA	0	0	0	0	0	0	0	0
LIVE OAK	0	0	0	0	0	0	0	0
MAVERICK	0	0	0	0	0	0	0	0
MCMULLEN	73	1207	0	0	0	0	0	0
MEDINA	0	0	0	0	0	0	0	0
UVALDE	0	0	0	0	0	0	0	0
WEBB	0	0	0	0	0	0	0	0
WILSON	0	0	0	0	0	0	0	0
ZAVALA	0	0	0	0	0	0	0	0

*industrial includes manufacturing, mining, and power generation

County – Other (Non-reported Domestic)

COUNTY	1980	1990	2000	2010	2020	2030	2040	2050
ATASCOSA	260	348	307	343	405	298	349	366
BASTROP	11	24	36	42	49	56	65	81
BEE	0	0	0	0	0	0	0	0
BEXAR	1	1	2	3	3	2	2	1
CALDWELL	10	14	37	39	40	38	35	31
DEWITT	0	0	0	0	0	0	0	0
DIMITT	16	14	9	8	8	8	9	10
FAYETTE	0	0	0	0	0	0	0	0
FRIO	66	53	58	59	59	43	45	46
GONZALES	54	66	46	43	42	41	41	41
GUADALUPE	0	0	0	0	0	0	0	0
KARNES	0	0	0	0	0	0	0	0
LA SALLE	29	11	19	19	20	18	19	18
LAVACA	0	0	0	0	0	0	0	0
LIVE OAK	0	0	0	0	0	0	0	0
MAVERICK	0	0	0	0	0	0	0	0
MCMULLEN	6	3	3	3	2	1	1	1
MEDINA	0	0	0	0	0	0	0	0
UVALDE	0	0	0	0	0	0	0	0
WEBB	80	21	4	4	4	4	4	4
WILSON	129	194	270	345	379	405	487	568
ZAVALA	157	230	130	154	161	172	220	296

Table D1.2 (continued)

Livestock

COUNTY	1980	1990	2000	2010	2020	2030	2040	2050
ATASCOSA	24	21	0	0	0	0	0	0
BASTROP	12	11	0	0	0	0	0	0
BEE	0	0	0	0	0	0	0	0
BEXAR	0	0	0	0	0	0	0	0
CALDWELL	5	0	0	0	0	0	0	0
DEWITT	0	0	0	0	0	0	0	0
DIMMIT	208	243	0	0	0	0	0	0
FAYETTE	0	0	0	0	0	0	0	0
FRIO	101	51	0	0	0	0	0	0
GONZALES	91	19	0	0	0	0	0	0
GUADALUPE	0	0	0	0	0	0	0	0
KARNES	0	0	0	0	0	0	0	0
LA SALLE	21	18	0	0	0	0	0	0
LAVACA	0	0	0	0	0	0	0	0
LIVE OAK	0	0	0	0	0	0	0	0
MAVERICK	0	0	0	0	0	0	0	0
MCMULLEN	1	0	5	5	5	5	5	5
MEDINA	0	0	0	0	0	0	0	0
UVALDE	0	0	0	0	0	0	0	0
WEBB	20	19	217	217	217	215	215	215
WILSON	46	32	0	0	0	0	0	0
ZAVALA	174	32	0	0	0	0	0	0

Irrigation

COUNTY	1980	1990	2000	2010	2020	2030	2040	2050
ATASCOSA	1752	1094	83	83	81	0	0	0
BASTROP	4	2	0	0	0	0	0	0
BEE	0	0	0	0	0	0	0	0
BEXAR	0	0	0	0	0	0	0	0
CALDWELL	0	5	11	10	9	8	7	6
DEWITT	0	0	0	0	0	0	0	0
DIMMIT	284	97	105	99	95	93	87	80
FAYETTE	0	0	0	0	0	0	0	0
FRIO	2116	2246	470	472	473	53	53	54
GONZALES	55	206	126	109	94	80	69	59
GUADALUPE	0	0	0	0	0	0	0	0
KARNES	3	5	0	0	0	0	0	0
LA SALLE	880	538	310	292	275	237	222	208
LAVACA	0	0	0	0	0	0	0	0
LIVE OAK	0	0	0	0	0	0	0	0
MAVERICK	0	0	0	0	0	0	0	0
MCMULLEN	0	0	0	0	0	0	0	0
MEDINA	0	0	0	0	0	0	0	0
UVALDE	0	0	0	0	0	0	0	0
WEBB	7	146	445	422	403	234	255	280
WILSON	494	895	662	584	454	332	297	269
ZAVALA	5025	4708	1389	1393	1394	195	196	196

Table D1.3
Rate of groundwater withdrawal (acre-feet per year) from flow layer 3 of the
Carrizo-Wilcox aquifer for counties within the study area

Municipal and Industrial*

COUNTY	1980	1990	2000	2010	2020	2030	2040	2050
ATASCOSA	3102	8712	12265	12559	12874	7351	9242	15331
BASTROP	0	0	0	0	0	0	0	0
BEE	0	0	0	0	0	0	0	0
BEXAR	0	0	17013	17576	18046	18325	18614	18914
CALDWELL	0	0	0	0	0	0	0	0
DEWITT	0	0	0	0	0	0	0	0
DIMITT	1652	1322	1695	1821	1947	2207	2468	2766
FAYETTE	0	0	0	0	0	0	0	0
FRIO	3179	2717	3205	3234	3265	3283	3375	3449
GONZALES	996	1207	1179	1191	1202	1213	1268	1320
GUADALUPE	0	0	8041	8284	8426	9335	10294	11321
KARNES	0	176	319	280	264	223	229	244
LA SALLE	636	673	612	609	599	609	625	642
LAVACA	0	0	0	0	0	0	0	0
LIVE OAK	0	0	0	0	0	0	0	0
MAVERICK	0	0	0	0	0	0	0	0
MCMULLEN	259	290	226	154	121	99	78	63
MEDINA	0	0	397	408	422	440	452	464
UVALDE	0	0	0	0	0	0	0	0
WEBB	0	0	100	118	135	164	159	155
WILSON	1454	1785	2243	2262	2323	2424	2553	2721
ZAVALA	1127	1291	1308	1227	1145	1162	1154	1151

*industrial includes manufacturing, mining, and power generation

County – Other (Non-reported Domestic)

COUNTY	1980	1990	2000	2010	2020	2030	2040	2050
ATASCOSA	559	837	736	825	973	716	839	880
BASTROP	14	31	156	185	215	246	286	356
BEE	0	0	0	0	0	0	0	0
BEXAR	340	714	2110	2365	2285	1333	1336	1077
CALDWELL	9	15	41	43	45	42	39	35
DEWITT	0	0	0	0	0	0	0	0
DIMITT	130	117	72	67	64	70	78	85
FAYETTE	0	0	0	0	0	0	0	0
FRIO	106	69	76	77	77	57	59	60
GONZALES	117	131	91	87	84	81	82	82
GUADALUPE	36	74	198	274	346	407	438	467
KARNES	2	1	2	2	2	2	2	2
LA SALLE	7	5	9	9	9	9	9	9
LAVACA	0	0	0	0	0	0	0	0
LIVE OAK	0	0	0	0	0	0	0	0
MAVERICK	3	1	2	2	2	2	2	2
MCMULLEN	3	2	2	2	2	1	1	1
MEDINA	171	272	451	469	477	438	453	481
UVALDE	0	0	0	0	0	0	0	0
WEBB	18	6	2	2	2	2	2	2
WILSON	377	675	1019	1355	1498	1655	2019	2372
ZAVALA	69	96	56	66	68	73	94	126

Table D1.3 (continued)

Livestock

COUNTY	1980	1990	2000	2010	2020	2030	2040	2050
ATASCOSA	34	30	0	0	0	0	0	0
BASTROP	24	22	0	0	0	0	0	0
BEE	0	0	0	0	0	0	0	0
BEXAR	2	1	0	0	0	0	0	0
CALDWELL	5	0	0	0	0	0	0	0
DEWITT	0	0	0	0	0	0	0	0
DIMMIT	197	230	0	0	0	0	0	0
FAYETTE	0	0	0	0	0	0	0	0
FRIO	43	22	0	0	0	0	0	0
GONZALES	215	45	0	0	0	0	0	0
GUADALUPE	4	2	0	0	0	0	0	0
KARNES	0	0	0	0	0	0	0	0
LA SALLE	12	10	0	0	0	0	0	0
LAVACA	0	0	0	0	0	0	0	0
LIVE OAK	0	0	0	0	0	0	0	0
MAVERICK	4	4	15	15	15	10	10	10
MCMULLEN	1	0	5	5	5	5	5	5
MEDINA	14	9	0	0	0	0	0	0
UVALDE	0	0	0	0	0	0	0	0
WEBB	17	17	163	163	163	161	161	161
WILSON	81	57	0	0	0	0	0	0
ZAVALA	97	19	0	0	0	0	0	0

Irrigation

COUNTY	1980	1990	2000	2010	2020	2030	2040	2050
ATASCOSA	61657	40811	3108	3094	3028	0	0	0
BASTROP	7	3	0	0	0	0	0	0
BEE	0	0	0	0	0	0	0	0
BEXAR	1156	678	0	0	0	0	0	0
CALDWELL	2	20	47	41	36	32	28	24
DEWITT	0	0	0	0	0	0	0	0
DIMMIT	7638	2616	2691	2544	2432	2389	2224	2054
FAYETTE	0	0	0	0	0	0	0	0
FRIO	64338	70106	14672	14730	14751	1666	1669	1672
GONZALES	197	681	417	360	310	263	227	196
GUADALUPE	5	7	0	0	0	0	0	0
KARNES	0	0	0	0	0	0	0	0
LA SALLE	4373	3440	2020	1903	1790	1545	1448	1353
LAVACA	0	0	0	0	0	0	0	0
LIVE OAK	0	0	0	0	0	0	0	0
MAVERICK	482	1509	16	245	474	458	399	346
MCMULLEN	2	2	0	0	0	0	0	0
MEDINA	2096	344	1460	1464	1464	208	208	207
UVALDE	0	0	0	0	0	0	0	0
WEBB	0	36	112	106	101	59	64	70
WILSON	5161	8321	5590	4935	3937	2854	2549	2296
ZAVALA	54968	51345	15151	15188	15199	2131	2135	2136

Table D1.4
Rate of groundwater withdrawal (acre-feet per year) from flow layer 4 of the
Carrizo-Wilcox aquifer for counties within the study area

Municipal and Industrial*

COUNTY	1980	1990	2000	2010	2020	2030	2040	2050
ATASCOSA	93	0	0	0	0	0	0	0
BASTROP	0	0	0	0	0	0	0	0
BEE	0	0	0	0	0	0	0	0
BEXAR	0	0	0	0	0	0	0	0
CALDWELL	0	0	0	0	0	0	0	0
DEWITT	0	0	0	0	0	0	0	0
DIMITT	951	805	2003	1924	2116	2305	2497	2726
FAYETTE	0	0	0	0	0	0	0	0
FRIO	0	0	0	0	0	0	0	0
GONZALES	0	0	0	0	0	0	0	0
GUADALUPE	0	0	251	242	232	254	272	277
KARNES	0	0	0	0	0	0	0	0
LA SALLE	175	185	389	400	404	416	431	446
LAVACA	0	0	0	0	0	0	0	0
LIVE OAK	0	0	0	0	0	0	0	0
MAVERICK	0	0	0	0	0	0	0	0
MCMULLEN	0	0	0	0	0	0	0	0
MEDINA	0	0	0	0	0	0	0	0
UVALDE	0	0	0	0	0	0	0	0
WEBB	0	0	2	5477	7213	10951	10951	10951
WILSON	0	0	0	0	0	0	0	0
ZAVALA	681	781	1017	974	925	954	951	954

*industrial includes manufacturing, mining, and power generation

County – Other (Non-reported Domestic)

COUNTY	1980	1990	2000	2010	2020	2030	2040	2050
ATASCOSA	10	11	9	10	12	9	11	11
BASTROP	2	3	16	19	22	25	29	37
BEE	0	0	0	0	0	0	0	0
BEXAR	16	31	94	95	85	51	51	39
CALDWELL	0	1	2	2	2	2	2	2
DEWITT	0	0	0	0	0	0	0	0
DIMITT	172	246	149	139	133	145	163	176
FAYETTE	0	0	0	0	0	0	0	0
FRIO	1	0	0	0	0	0	0	0
GONZALES	4	2	1	1	1	1	1	1
GUADALUPE	2	5	12	17	22	27	29	31
KARNES	0	0	0	0	0	0	0	0
LA SALLE	0	0	0	0	0	0	0	0
LAVACA	0	0	0	0	0	0	0	0
LIVE OAK	0	0	0	0	0	0	0	0
MAVERICK	1	0	1	1	1	1	1	1
MCMULLEN	0	0	0	0	0	0	0	0
MEDINA	9	12	20	21	22	20	20	22
UVALDE	0	0	0	0	0	0	0	0
WEBB	12	13	2	2	2	2	2	2
WILSON	38	92	139	185	205	227	277	326
ZAVALA	42	99	56	67	69	74	95	128

Table D1.4 (continued)

Livestock

COUNTY	1980	1990	2000	2010	2020	2030	2040	2050
ATASCOSA	0	0	0	0	0	0	0	0
BASTROP	1	1	0	0	0	0	0	0
BEE	0	0	0	0	0	0	0	0
BEXAR	0	0	0	0	0	0	0	0
CALDWELL	0	0	0	0	0	0	0	0
DEWITT	0	0	0	0	0	0	0	0
DIMMIT	122	143	0	0	0	0	0	0
FAYETTE	0	0	0	0	0	0	0	0
FRIO	1	0	0	0	0	0	0	0
GONZALES	2	0	0	0	0	0	0	0
GUADALUPE	0	0	0	0	0	0	0	0
KARNES	0	0	0	0	0	0	0	0
LA SALLE	0	0	0	0	0	0	0	0
LAVACA	0	0	0	0	0	0	0	0
LIVE OAK	0	0	0	0	0	0	0	0
MAVERICK	1	1	4	4	4	2	2	2
MCMULLEN	1	0	5	5	5	5	5	5
MEDINA	3	2	0	0	0	0	0	0
UVALDE	0	0	0	0	0	0	0	0
WEBB	15	14	164	164	164	163	163	163
WILSON	1	1	0	0	0	0	0	0
ZAVALA	27	6	0	0	0	0	0	0

Irrigation

COUNTY	1980	1990	2000	2010	2020	2030	2040	2050
ATASCOSA	50	33	3	2	2	0	0	0
BASTROP	0	0	0	0	0	0	0	0
BEE	0	0	0	0	0	0	0	0
BEXAR	1	1	0	0	0	0	0	0
CALDWELL	0	0	1	1	1	1	1	1
DEWITT	0	0	0	0	0	0	0	0
DIMMIT	8938	2693	2863	2707	2588	2542	2366	2180
FAYETTE	0	0	0	0	0	0	0	0
FRIO	4186	4554	953	957	958	108	108	109
GONZALES	1	3	2	2	2	1	1	1
GUADALUPE	0	1	0	0	0	0	0	0
KARNES	0	0	0	0	0	0	0	0
LA SALLE	2679	2176	1235	1164	1095	945	885	827
LAVACA	0	0	0	0	0	0	0	0
LIVE OAK	0	0	0	0	0	0	0	0
MAVERICK	224	721	7	117	226	219	191	165
MCMULLEN	0	0	0	0	0	0	0	0
MEDINA	62	5	38	38	38	5	5	5
UVALDE	0	0	0	0	0	0	0	0
WEBB	0	0	0	0	0	0	0	0
WILSON	19	36	30	27	20	15	13	12
ZAVALA	14442	13416	3952	3962	3965	556	557	557

Table D1.5
Rate of groundwater withdrawal (acre-feet per year) from flow layer 5 of the
Carrizo-Wilcox aquifer for counties within the study area

Municipal and Industrial*

COUNTY	1980	1990	2000	2010	2020	2030	2040	2050
ATASCOSA	0	0	0	0	0	0	0	0
BASTROP	0	0	0	0	0	0	0	0
BEE	0	0	0	0	0	0	0	0
BEXAR	26	36	5034	5205	6088	5896	6129	6122
CALDWELL	270	347	1763	2001	2224	2538	2806	3101
DEWITT	0	0	0	0	0	0	0	0
DIMITT	0	0	0	0	0	0	0	0
FAYETTE	0	0	0	0	0	0	0	0
FRIO	0	0	0	0	0	0	0	0
GONZALES	0	0	0	0	0	0	0	0
GUADALUPE	0	0	0	0	0	0	0	0
KARNES	0	0	0	0	0	0	0	0
LA SALLE	0	0	0	0	0	0	0	0
LAVACA	0	0	0	0	0	0	0	0
LIVE OAK	0	0	0	0	0	0	0	0
MAVERICK	0	0	11	5	3	1	0	0
MCMULLEN	0	0	0	0	0	0	0	0
MEDINA	0	0	0	0	0	0	0	0
UVALDE	0	0	241	232	270	173	200	233
WEBB	0	0	0	0	0	0	0	0
WILSON	26	36	56	58	59	64	69	72
ZAVALA	1242	1523	1566	1657	1729	1795	1939	2071

*industrial includes manufacturing, mining, and power generation

County – Other (Non-reported Domestic)

COUNTY	1980	1990	2000	2010	2020	2030	2040	2050
ATASCOSA	95	190	185	203	230	197	223	229
BASTROP	115	225	1441	1709	1976	2267	2634	3284
BEE	0	0	0	0	0	0	0	0
BEXAR	921	1095	3356	3406	3068	1826	1838	1410
CALDWELL	210	259	716	748	772	733	679	609
DEWITT	0	0	0	0	0	0	0	0
DIMITT	15	22	13	12	11	12	14	15
FAYETTE	0	0	0	0	0	0	0	0
FRIO	7	19	21	22	22	16	16	17
GONZALES	18	19	13	13	12	12	12	12
GUADALUPE	212	371	1001	1381	1785	2141	2366	2469
KARNES	0	0	0	0	0	0	0	0
LA SALLE	0	0	0	0	0	0	0	0
LAVACA	0	0	0	0	0	0	0	0
LIVE OAK	0	0	0	0	0	0	0	0
MAVERICK	1	0	0	0	1	0	0	0
MCMULLEN	0	0	0	0	0	0	0	0
MEDINA	171	258	428	445	453	416	430	457
UVALDE	5	1	3	3	2	1	1	1
WEBB	0	0	0	0	0	0	0	0
WILSON	314	564	854	1138	1259	1395	1704	2003
ZAVALA	10	9	5	7	7	7	9	12

Table D1.5 (continued)

Livestock

COUNTY	1980	1990	2000	2010	2020	2030	2040	2050
ATASCOSA	2	1	0	0	0	0	0	0
BASTROP	95	88	0	0	0	0	0	0
BEE	0	0	0	0	0	0	0	0
BEXAR	1	1	0	0	0	0	0	0
CALDWELL	43	3	0	0	0	0	0	0
DEWITT	0	0	0	0	0	0	0	0
DIMMIT	38	44	0	0	0	0	0	0
FAYETTE	0	0	0	0	0	0	0	0
FRIO	3	2	0	0	0	0	0	0
GONZALES	12	3	0	0	0	0	0	0
GUADALUPE	38	24	0	0	0	0	0	0
KARNES	0	0	0	0	0	0	0	0
LA SALLE	0	0	0	0	0	0	0	0
LAVACA	0	0	0	0	0	0	0	0
LIVE OAK	0	0	0	0	0	0	0	0
MAVERICK	4	3	14	14	14	9	9	9
MCMULLEN	0	0	3	3	3	3	3	3
MEDINA	26	16	0	0	0	0	0	0
UVALDE	1	1	0	0	0	0	0	0
WEBB	2	2	18	18	18	18	18	18
WILSON	16	12	0	0	0	0	0	0
ZAVALA	27	5	0	0	0	0	0	0

Irrigation

COUNTY	1980	1990	2000	2010	2020	2030	2040	2050
ATASCOSA	612	507	52	52	52	0	0	0
BASTROP	30	13	0	0	0	0	0	0
BEE	0	0	0	0	0	0	0	0
BEXAR	47	48	0	0	0	0	0	0
CALDWELL	16	136	313	276	243	213	187	163
DEWITT	0	0	0	0	0	0	0	0
DIMMIT	1684	583	737	697	666	654	609	563
FAYETTE	0	0	0	0	0	0	0	0
FRIO	2830	3068	642	645	646	73	73	73
GONZALES	7	25	15	13	11	10	8	7
GUADALUPE	219	212	144	138	131	125	119	113
KARNES	0	0	0	0	0	0	0	0
LA SALLE	0	0	0	0	0	0	0	0
LAVACA	0	0	0	0	0	0	0	0
LIVE OAK	0	0	0	0	0	0	0	0
MAVERICK	107	348	4	56	109	105	92	80
MCMULLEN	0	0	0	0	0	0	0	0
MEDINA	774	79	483	485	485	69	69	69
UVALDE	173	55	1789	1794	1775	560	547	531
WEBB	0	0	0	0	0	0	0	0
WILSON	194	357	302	267	199	148	133	121
ZAVALA	6506	5956	1750	1754	1755	246	247	247

Table D1.6
Rate of groundwater withdrawal (acre-feet per year) from flow layer 6 of the
Carrizo-Wilcox aquifer for counties within the study area

Municipal and Industrial*

COUNTY	1980	1990	2000	2010	2020	2030	2040	2050
ATASCOSA	0	0	0	0	0	0	0	0
BASTROP	0	0	0	0	0	0	0	0
BEE	0	0	0	0	0	0	0	0
BEXAR	51	72	155	146	139	131	124	121
CALDWELL	1223	1497	2075	2266	2444	2684	2725	2750
DEWITT	0	0	0	0	0	0	0	0
DIMITT	0	0	0	0	0	0	0	0
FAYETTE	0	0	0	0	0	0	0	0
FRIO	0	0	0	0	0	0	0	0
GONZALES	0	0	0	0	0	0	0	0
GUADALUPE	0	0	0	0	0	0	0	0
KARNES	0	0	0	0	0	0	0	0
LA SALLE	0	0	0	0	0	0	0	0
LAVACA	0	0	0	0	0	0	0	0
LIVE OAK	0	0	0	0	0	0	0	0
MAVERICK	0	0	0	0	0	0	0	0
MCMULLEN	0	0	0	0	0	0	0	0
MEDINA	0	0	68	54	53	45	46	47
UVALDE	0	0	0	0	0	0	0	0
WEBB	0	0	0	0	0	0	0	0
WILSON	79	107	169	173	176	191	207	215
ZAVALA	0	0	97	42	25	8	2	0

*industrial includes manufacturing, mining, and power generation

County – Other (Non-reported Domestic)

COUNTY	1980	1990	2000	2010	2020	2030	2040	2050
ATASCOSA	56	84	81	89	100	87	98	101
BASTROP	275	607	3907	4633	5359	6146	7142	8906
BEE	0	0	0	0	0	0	0	0
BEXAR	3125	2974	8834	8903	7975	4754	4788	3657
CALDWELL	2872	528	1470	1540	1593	1526	1420	1286
DEWITT	0	0	0	0	0	0	0	0
DIMITT	8	1	1	1	1	1	1	1
FAYETTE	0	0	0	0	0	0	0	0
FRIO	0	0	0	0	0	0	0	0
GONZALES	0	0	0	0	0	0	0	0
GUADALUPE	476	807	2189	3015	3965	4816	5408	5567
KARNES	0	0	0	0	0	0	0	0
LA SALLE	0	0	0	0	0	0	0	0
LAVACA	0	0	0	0	0	0	0	0
LIVE OAK	0	0	0	0	0	0	0	0
MAVERICK	6	12	320	322	323	318	319	322
MCMULLEN	0	0	0	0	0	0	0	0
MEDINA	172	234	402	417	425	382	395	420
UVALDE	160	232	509	450	408	214	203	182
WEBB	0	0	0	0	0	0	0	0
WILSON	5	9	12	16	18	20	24	29
ZAVALA	5	2	1	1	2	2	2	3

Table D1.6 (continued)

Livestock

COUNTY	1980	1990	2000	2010	2020	2030	2040	2050
ATASCOSA	7	6	0	0	0	0	0	0
BASTROP	151	139	0	0	0	0	0	0
BEE	0	0	0	0	0	0	0	0
BEXAR	28	37	0	0	0	0	0	0
CALDWELL	73	10	0	0	0	0	0	0
DEWITT	0	0	0	0	0	0	0	0
DIMMIT	34	39	0	0	0	0	0	0
FAYETTE	0	0	0	0	0	0	0	0
FRIO	1	0	0	0	0	0	0	0
GONZALES	0	0	0	0	0	0	0	0
GUADALUPE	77	49	0	0	0	0	0	0
KARNES	0	0	0	0	0	0	0	0
LA SALLE	0	0	0	0	0	0	0	0
LAVACA	0	0	0	0	0	0	0	0
LIVE OAK	0	0	0	0	0	0	0	0
MAVERICK	45	33	119	119	119	79	79	79
MCMULLEN	0	0	1	1	1	1	1	1
MEDINA	47	30	0	0	0	0	0	0
UVALDE	30	19	0	0	0	0	0	0
WEBB	0	0	2	2	2	2	2	2
WILSON	10	7	0	0	0	0	0	0
ZAVALA	60	11	0	0	0	0	0	0

Irrigation

COUNTY	1980	1990	2000	2010	2020	2030	2040	2050
ATASCOSA	0	2312	2283	276	275	273	0	0
BASTROP	60	26	0	0	0	0	0	0
BEE	0	0	0	0	0	0	0	0
BEXAR	1944	993	0	0	0	0	0	0
CALDWELL	33	327	726	639	562	494	433	379
DEWITT	0	0	0	0	0	0	0	0
DIMMIT	166	54	54	51	49	48	45	41
FAYETTE	0	0	0	0	0	0	0	0
FRIO	46	48	10	10	10	1	1	1
GONZALES	0	0	0	0	0	0	0	0
GUADALUPE	989	1129	782	173	165	157	149	142
KARNES	0	0	0	0	0	0	0	0
LA SALLE	0	0	0	0	0	0	0	0
LAVACA	0	0	0	0	0	0	0	0
LIVE OAK	0	0	0	0	0	0	0	0
MAVERICK	326	992	10	161	312	301	262	227
MCMULLEN	0	0	0	0	0	0	0	0
MEDINA	4888	369	2802	2811	2811	400	399	398
UVALDE	4372	58	1906	1910	1890	896	582	565
WEBB	0	0	0	0	0	0	0	0
WILSON	262	439	347	306	229	170	153	139
ZAVALA	961	845	249	250	250	35	35	35

APPENDIX D2

Post Plots of Groundwater Withdrawal Estimates for the Carrizo-Wilcox for 1980, 1990, 2000, 2010, 2020, 2030, 2040, and 2050

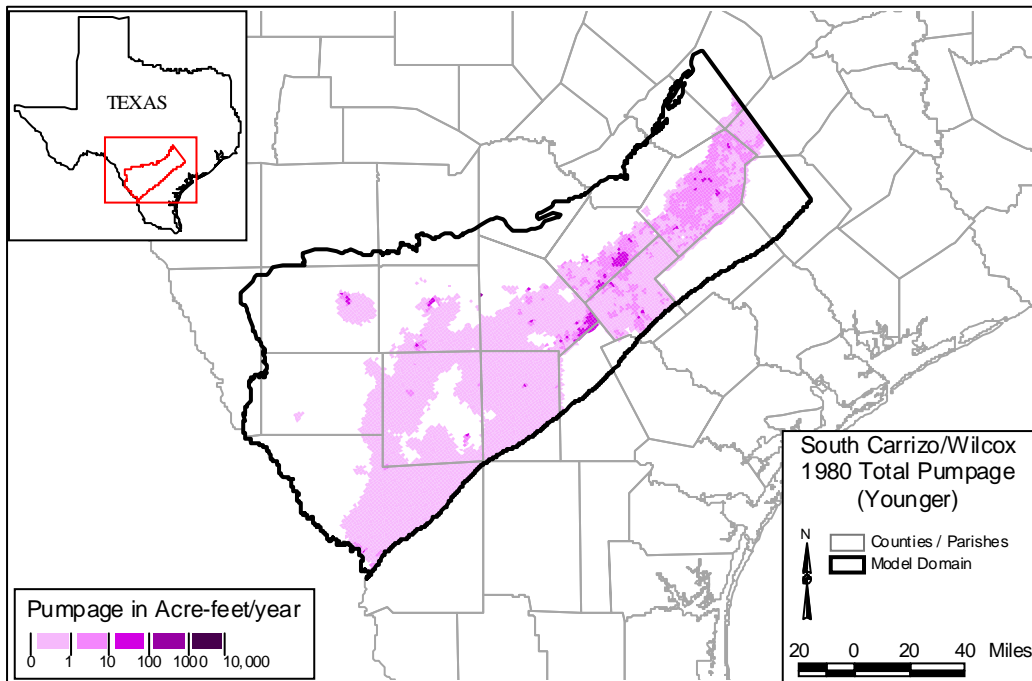


Figure D.2.1 Younger (Layer 1) Pumpage, 1980 (AFY)

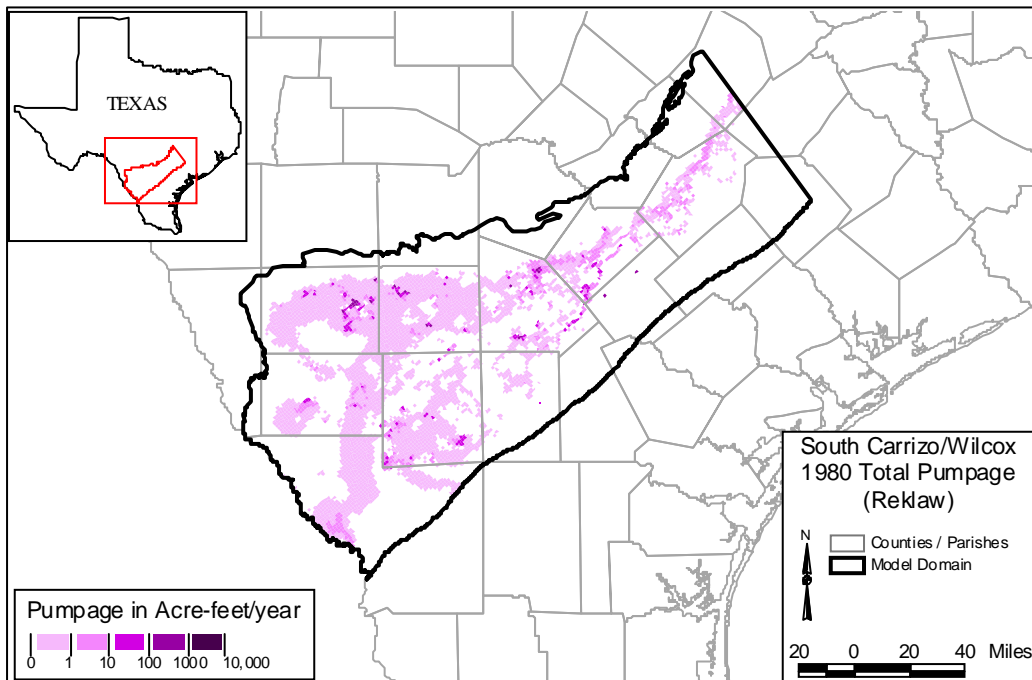


Figure D.2.2 Reklaw (Layer 2) Pumpage, 1980 (AFY)

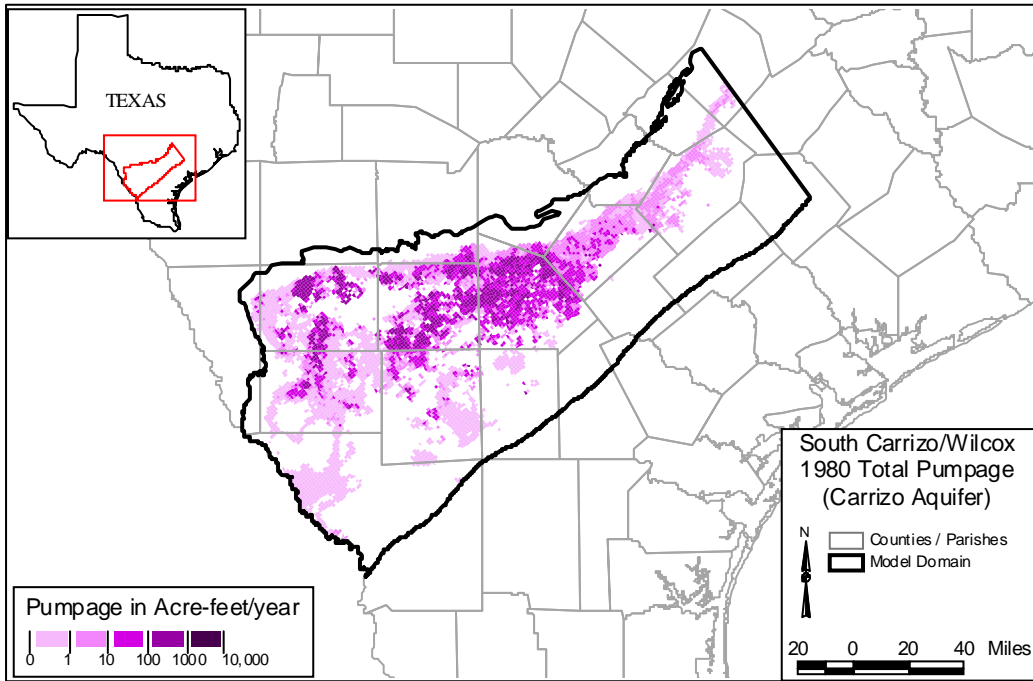


Figure D.2.3 Carrizo (Layer 3) Pumpage, 1980 (AFY)

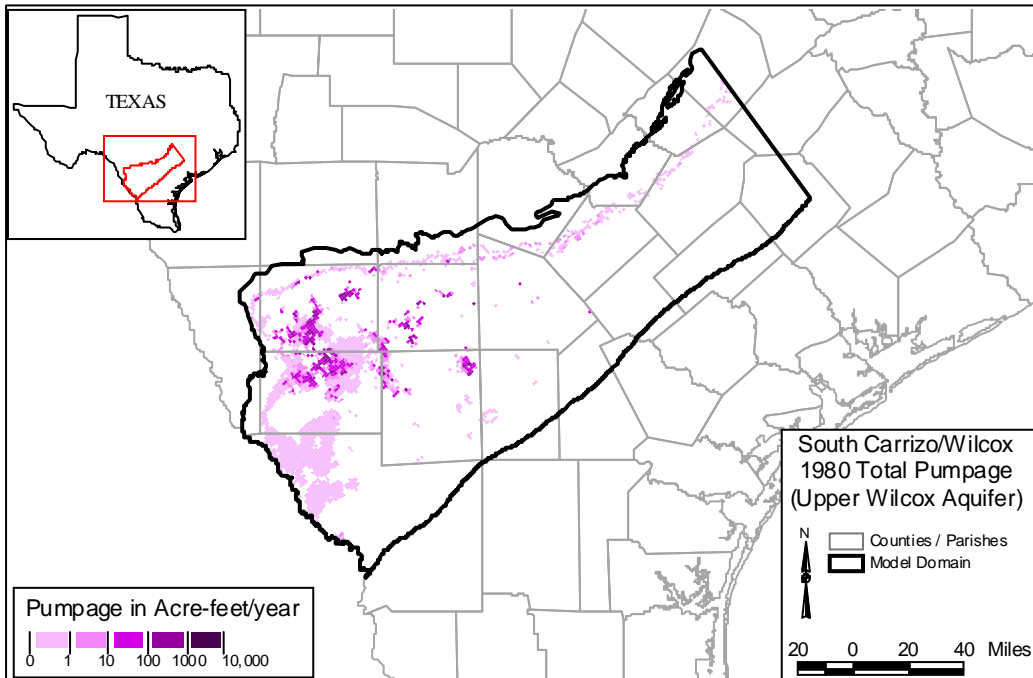


Figure D.2.4 Upper Wilcox (Layer 4) Pumpage, 1980 (AFY)

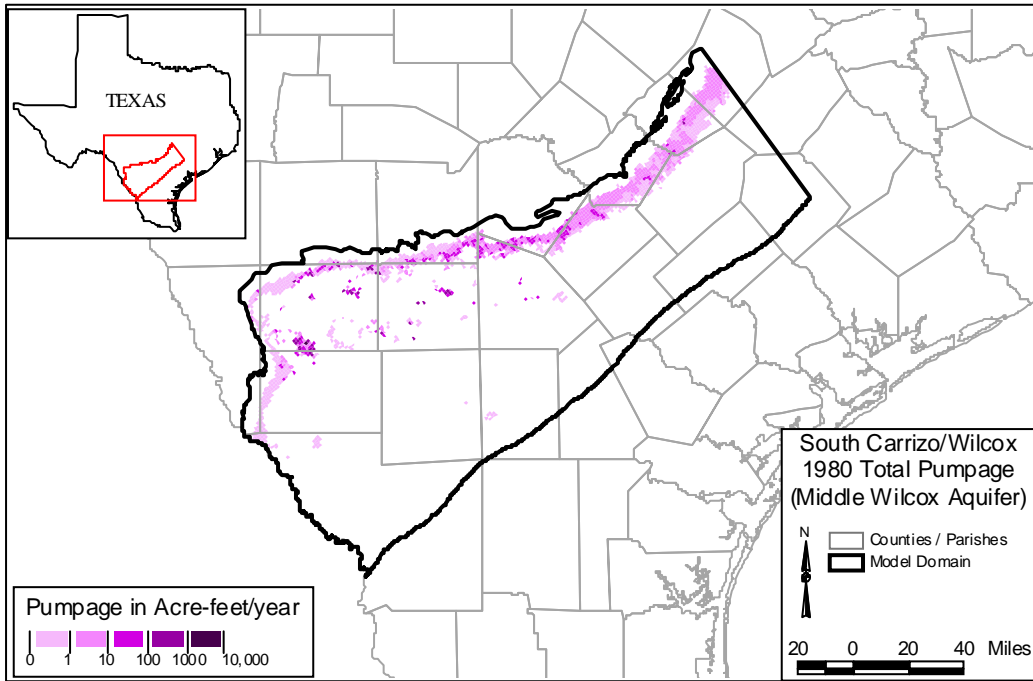


Figure D.2.5 Middle Wilcox (Layer 5) Pumpage, 1990 (AFY)

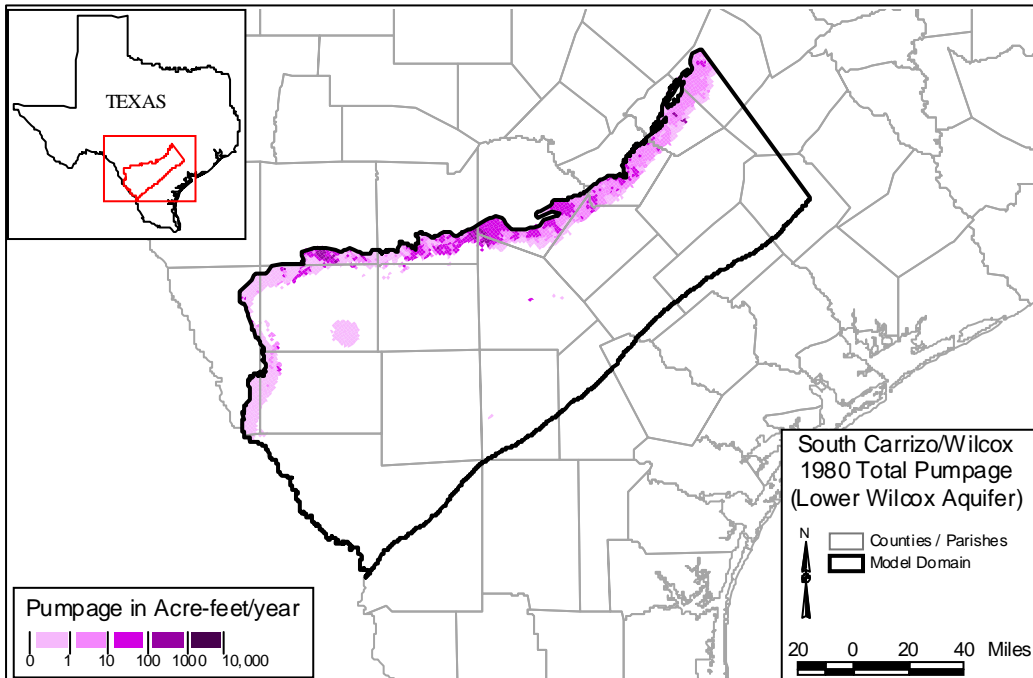


Figure D.2.6 Lower Wilcox (Layer 6) Pumpage, 1990 (AFY)

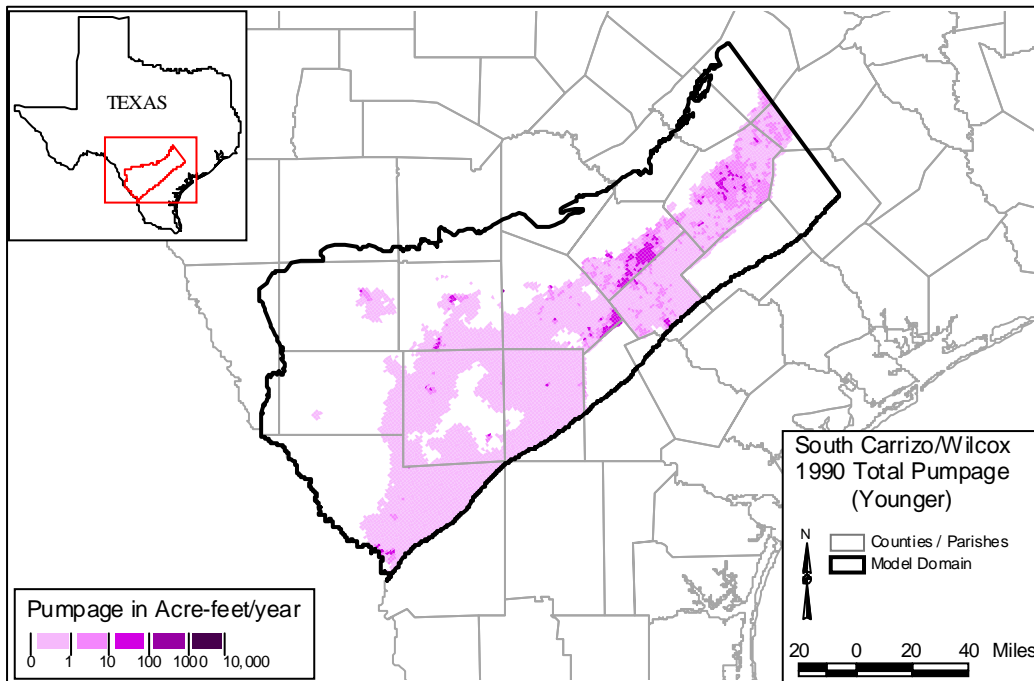


Figure D.2.7 Younger (Layer 1) Pumpage, 1990 (AFY)

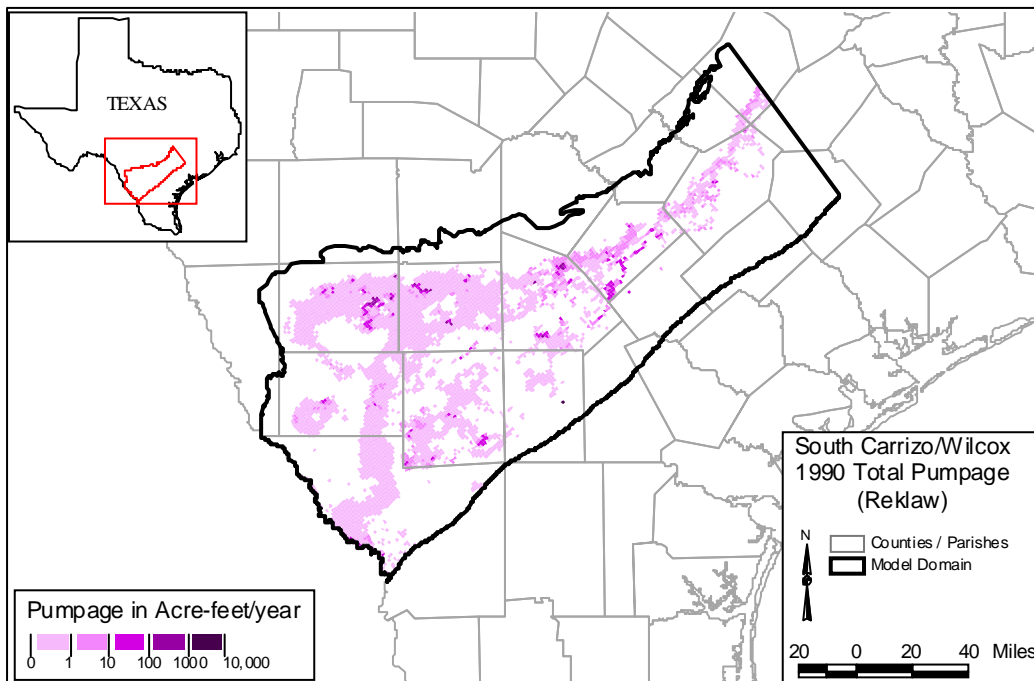


Figure D.2.8 Reklaw (Layer 2) Pumpage, 1990 (AFY)

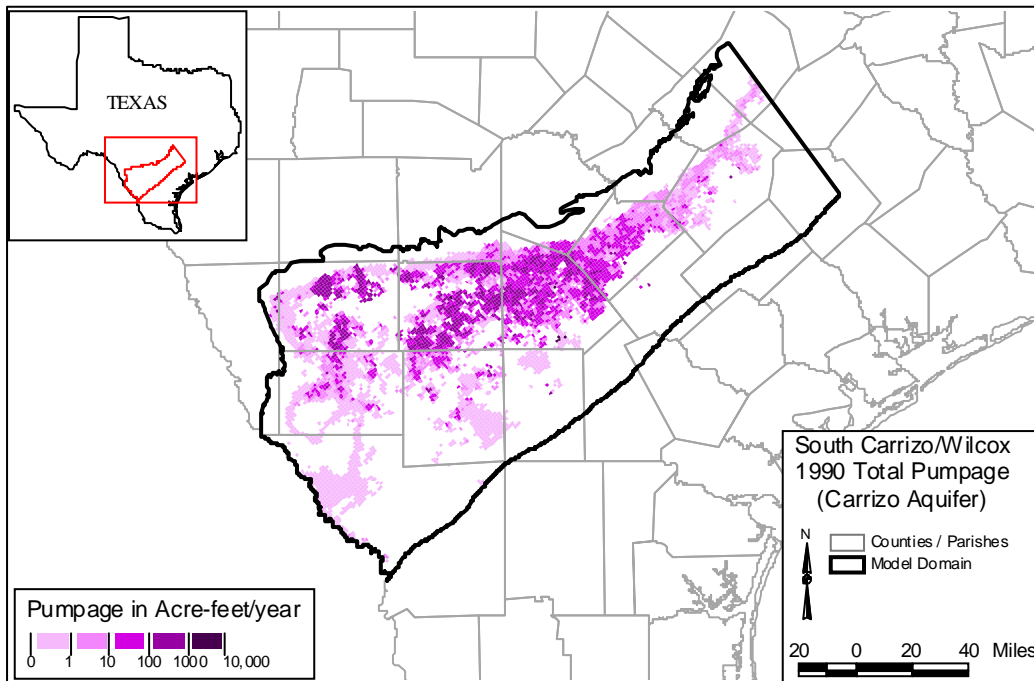


Figure D.2.9 Carrizo (Layer 3) Pumpage, 1990 (AFY)

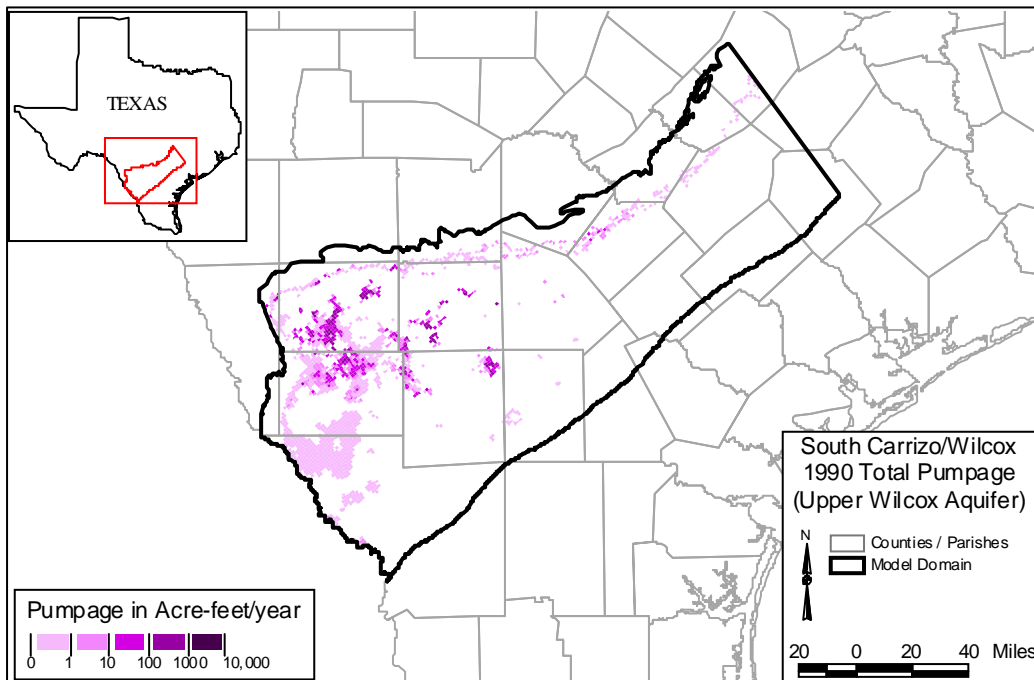


Figure D.2.10 Upper Wilcox (Layer 4) Pumpage, 1990 (AFY)

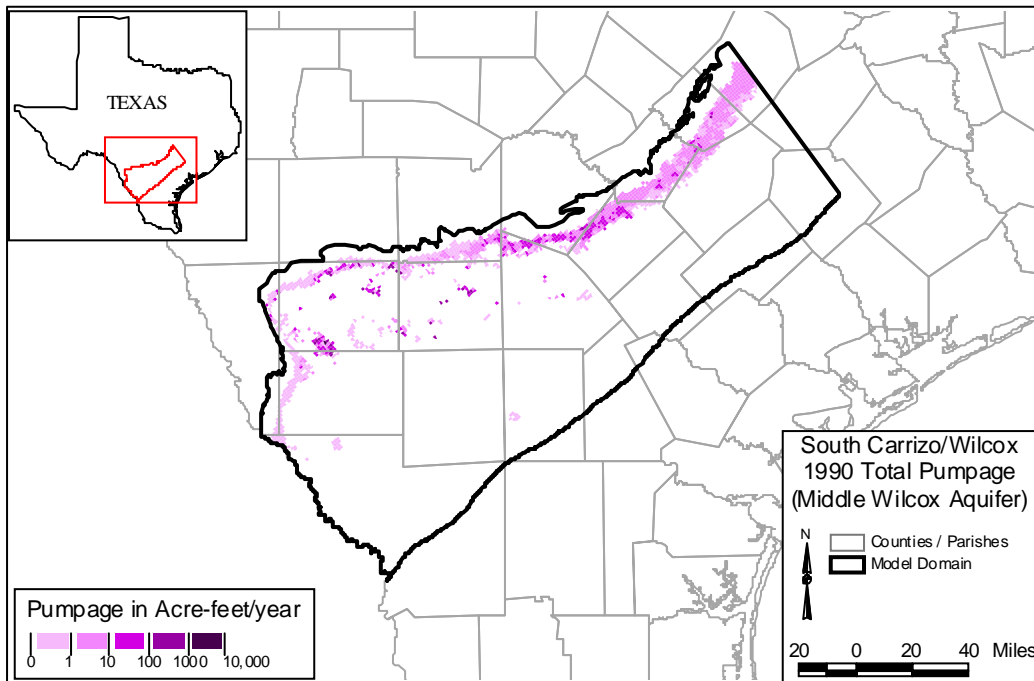


Figure D.2.11 Middle Wilcox (Layer 5) Pumpage, 1990 (AFY)

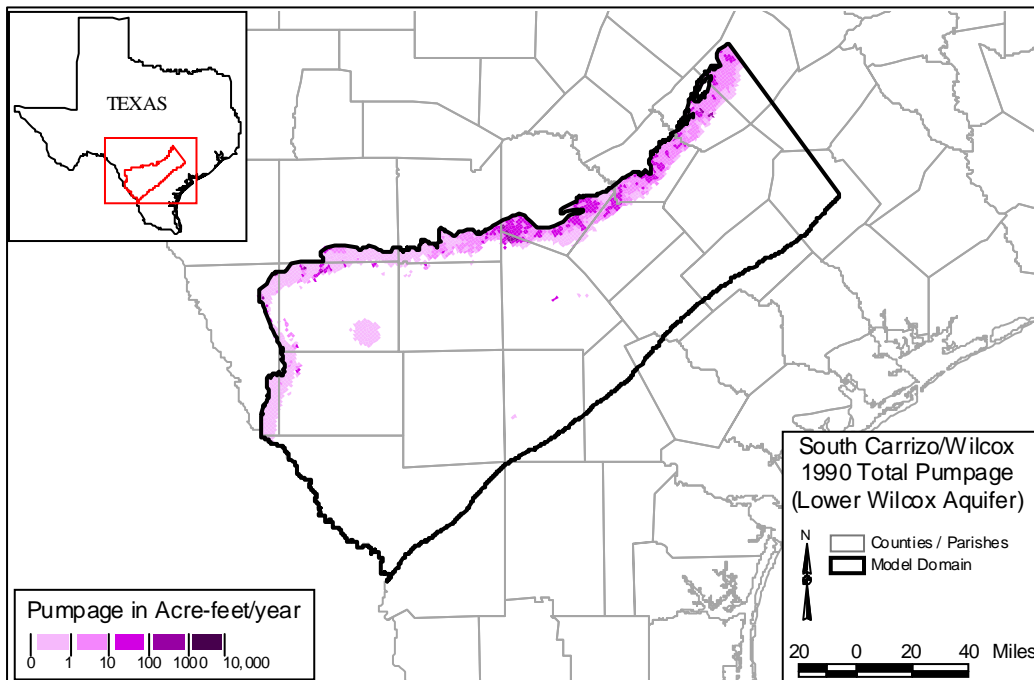


Figure D.2.12 Lower Wilcox (Layer 6) Pumpage, 1990 (AFY)

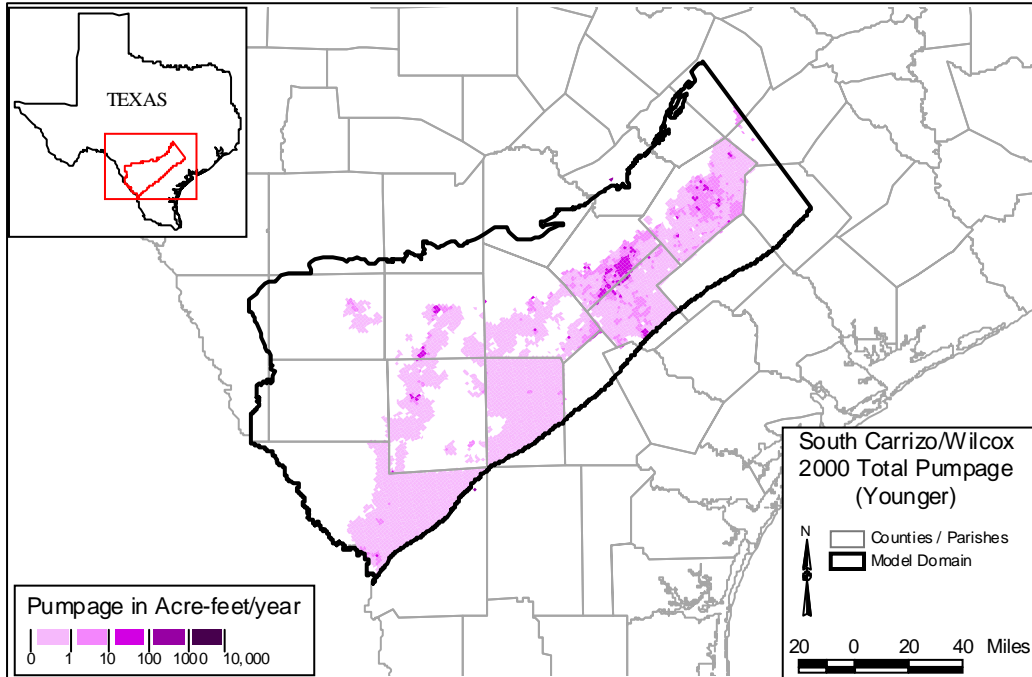


Figure D.2.13 Younger (Layer 1) Pumpage, 2000 (AFY)

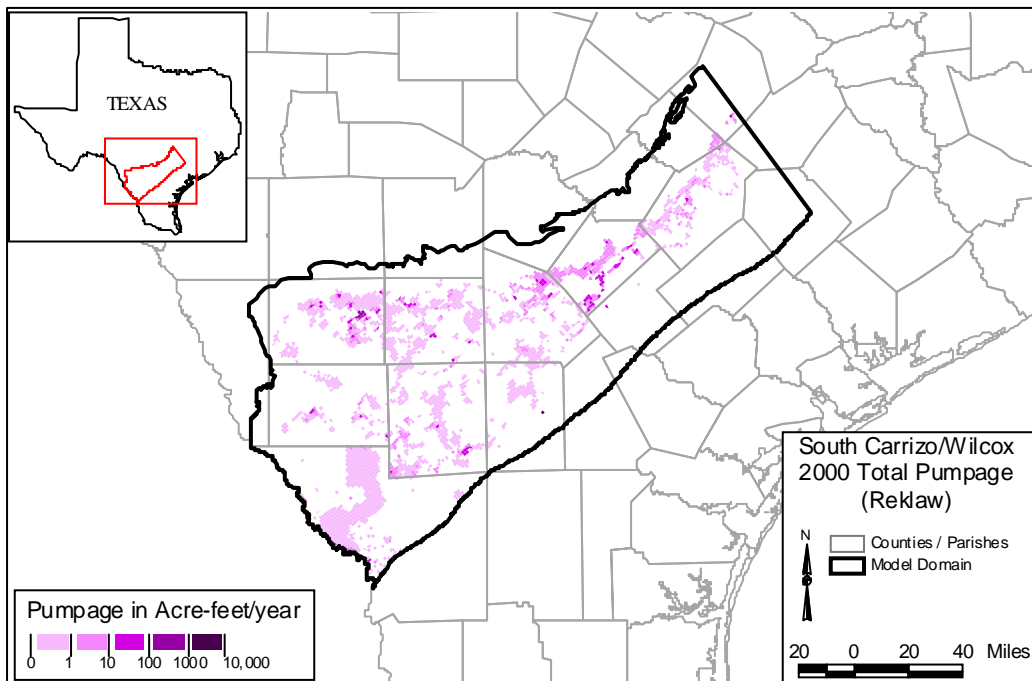


Figure D.2.14 Reklaw (Layer 2) Pumpage, 2000 (AFY)

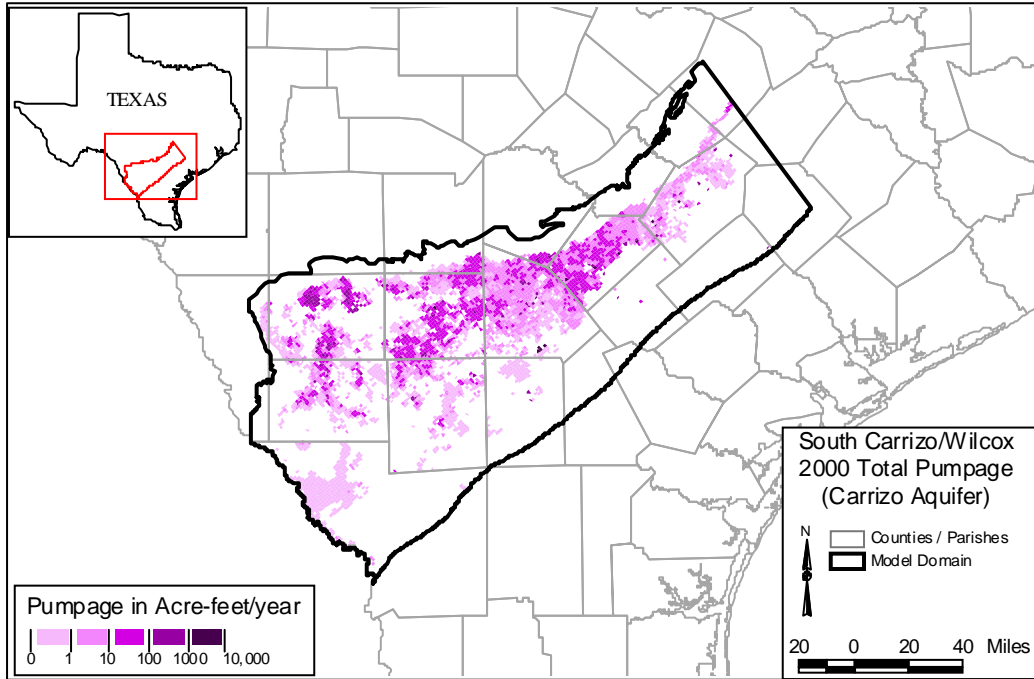


Figure D.2.15 Carrizo (Layer 3) Pumpage, 2000 (AFY)

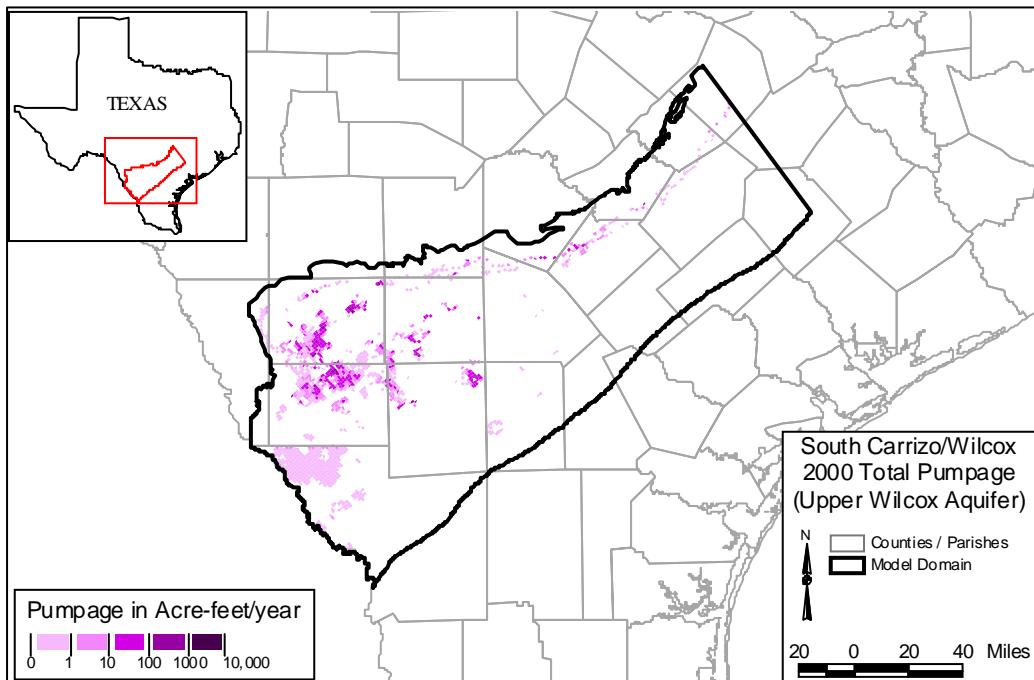


Figure D.2.16 Upper Wilcox (Layer 4) Pumpage, 2000 (AFY)

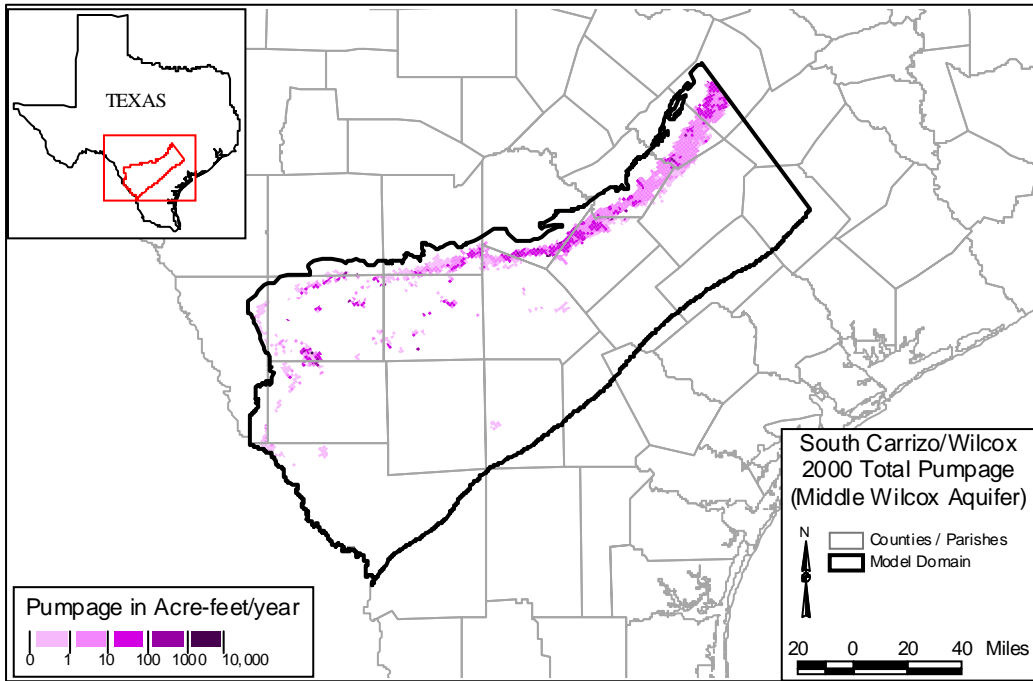


Figure D.2.17 Middle Wilcox (Layer 5) Pumpage, 2000 (AFY)

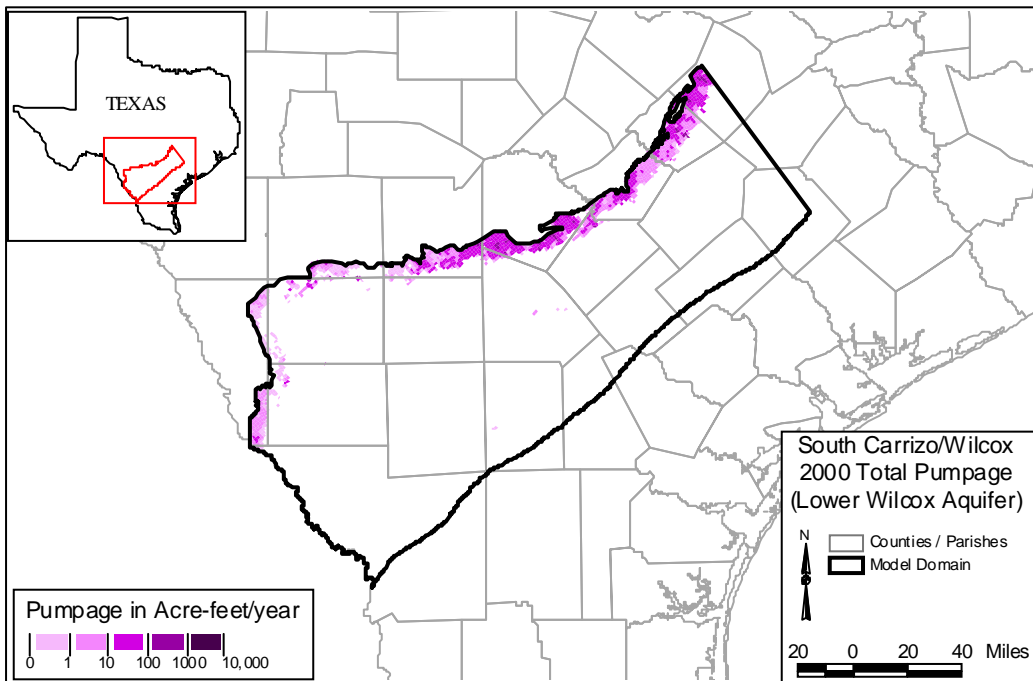


Figure D.2.18 Lower Wilcox (Layer 6) Pumpage, 2000 (AFY)

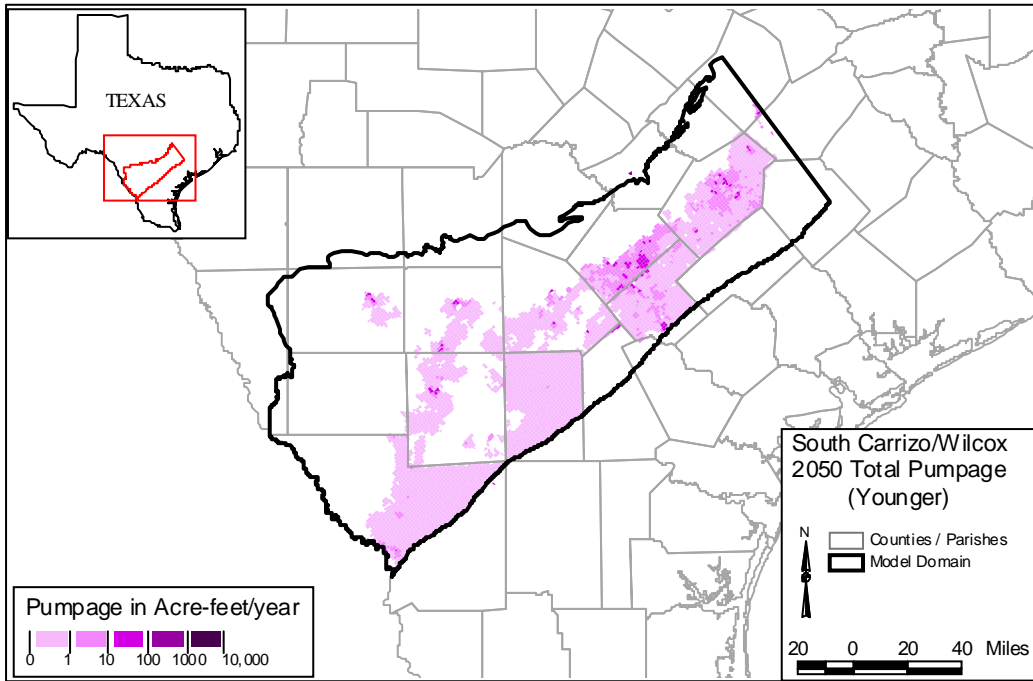


Figure D.2.19 Younger (Layer 1) Pumpage, 2050 (AFY)

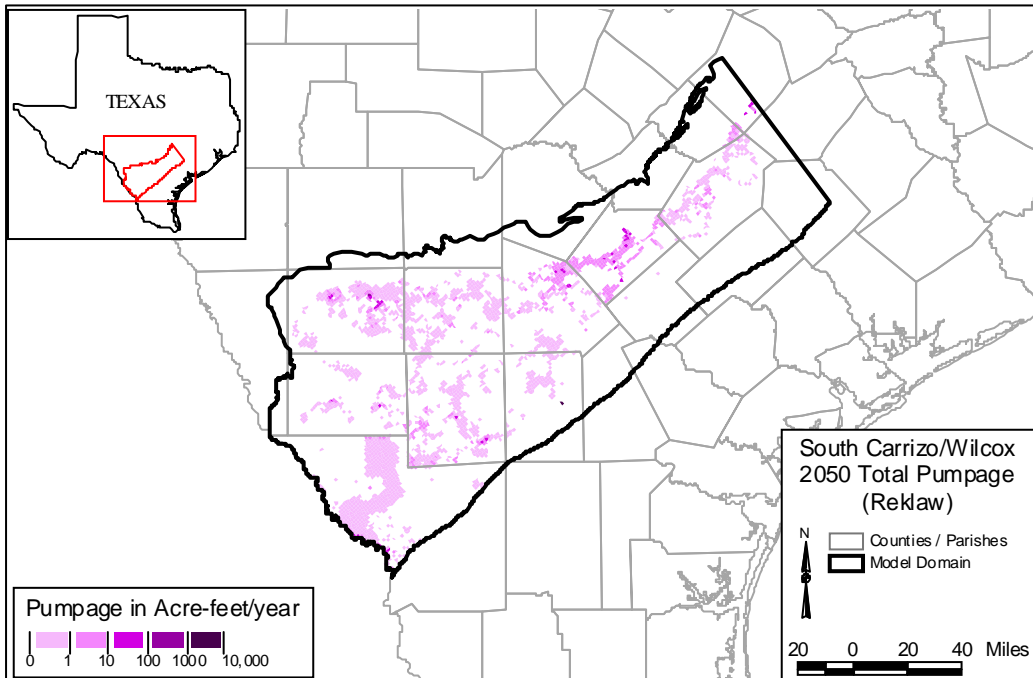


Figure D.2.20 Reklaw (Layer 2) Pumpage, 2050 (AFY)

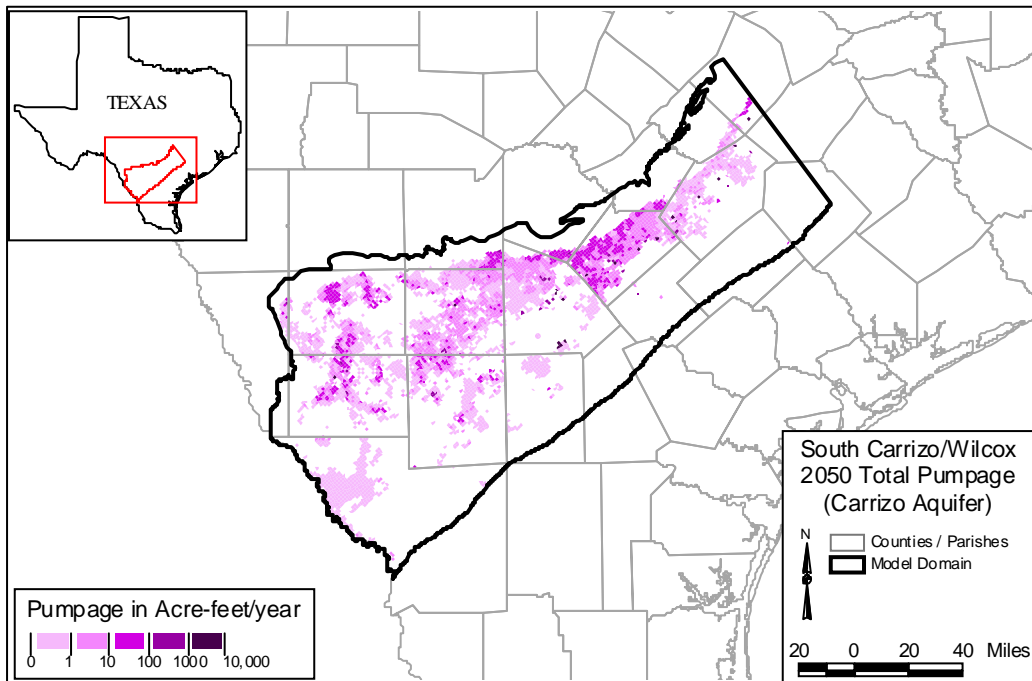


Figure D.2.21 Carrizo (Layer 3) Pumpage, 2050 (AFY)

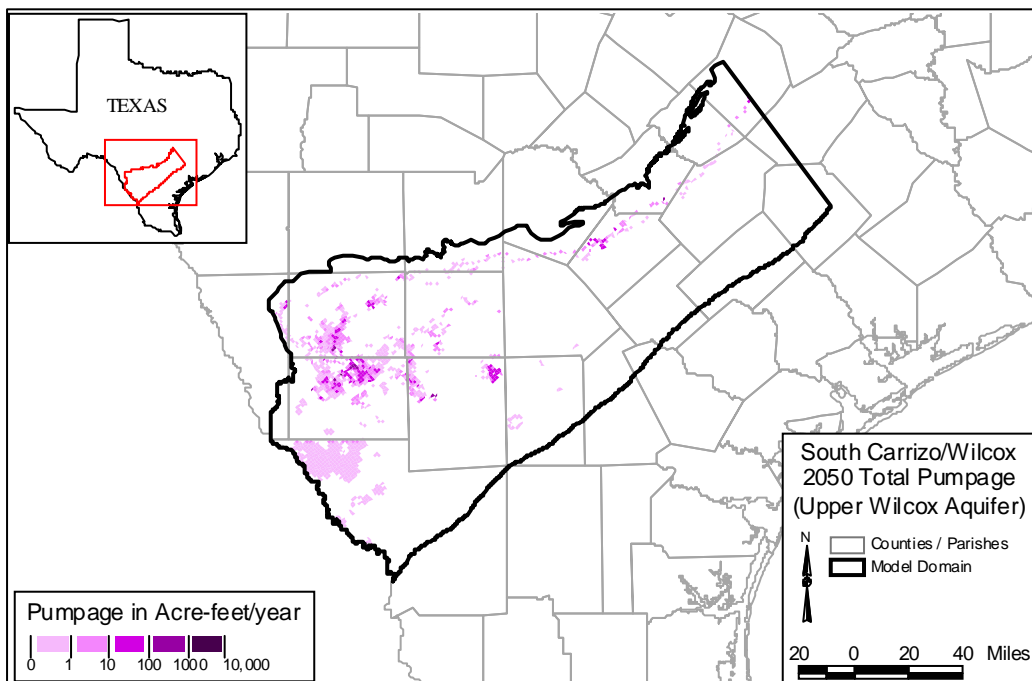


Figure D.2.22 Upper Wilcox (Layer 4) Pumpage, 2050 (AFY)

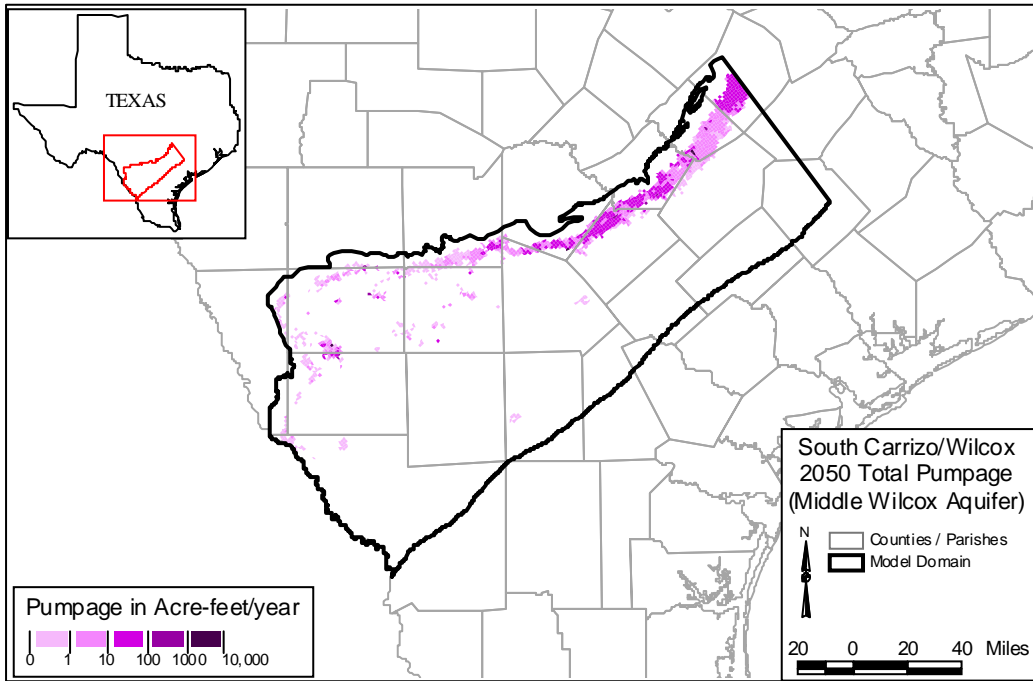


Figure D.2.23 Upper Wilcox (Layer 5) Pumpage, 2050 (AFY)

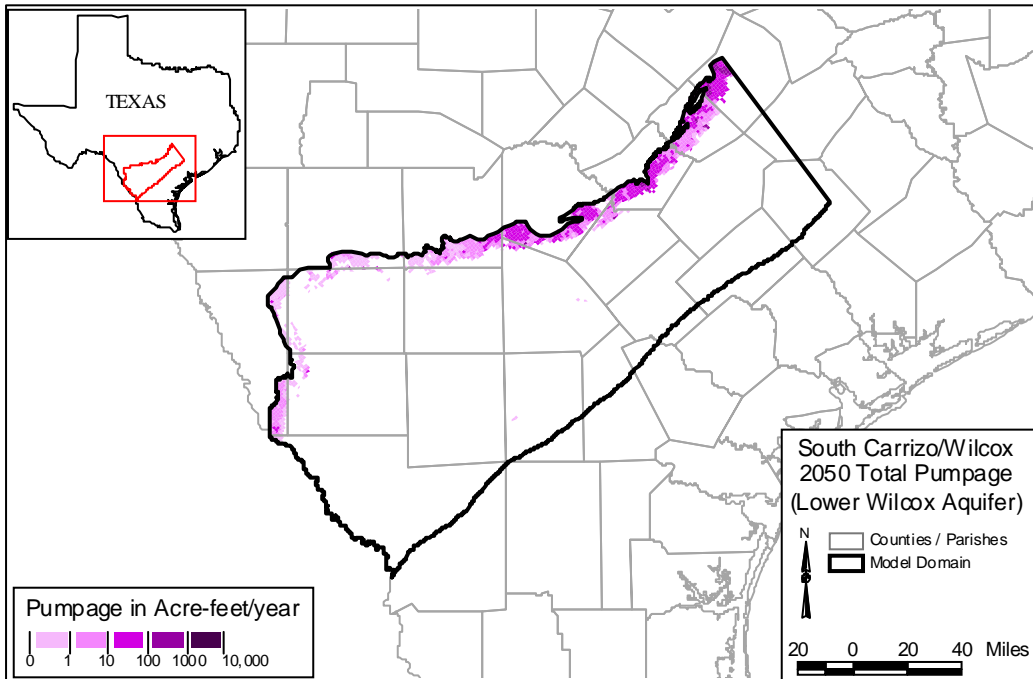
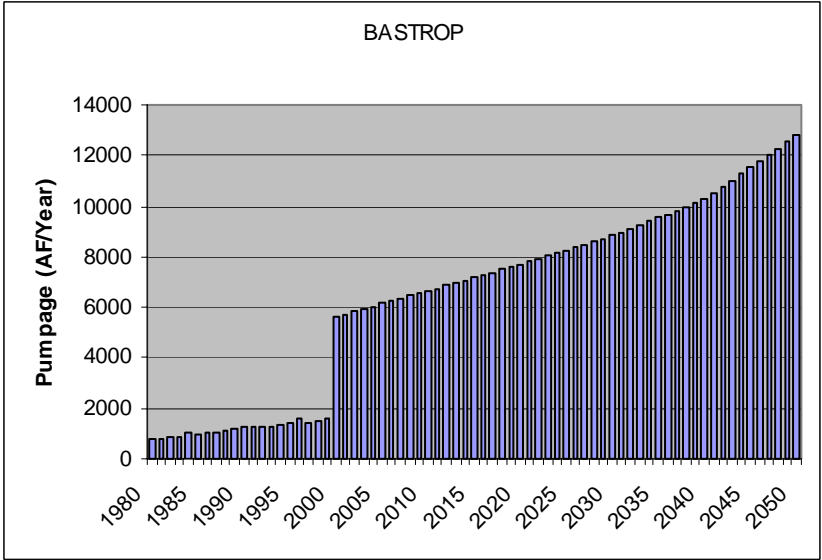
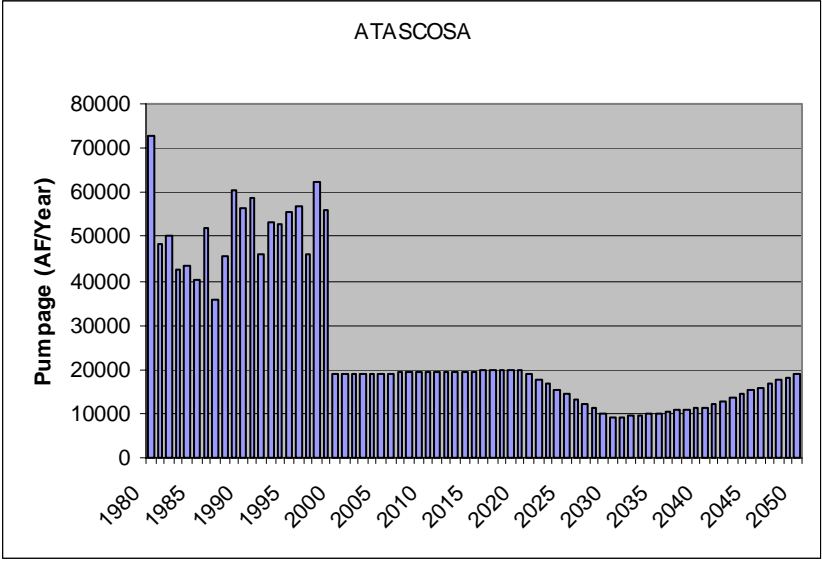
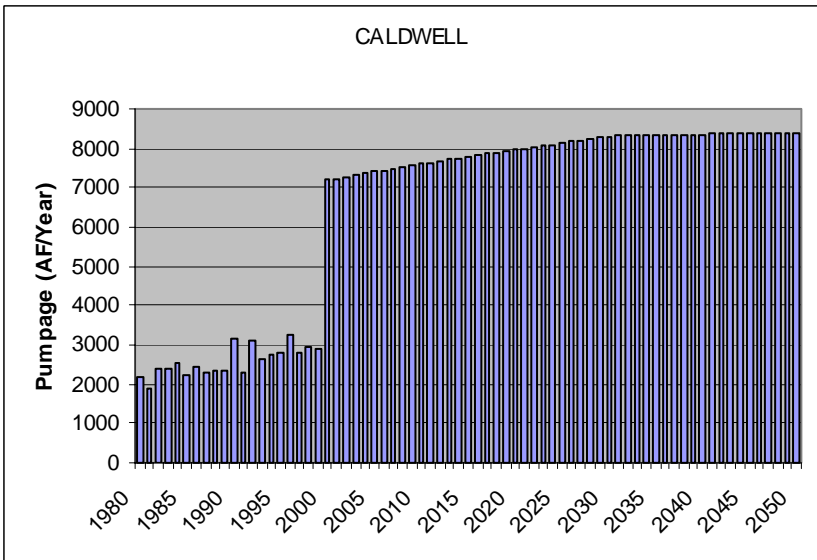
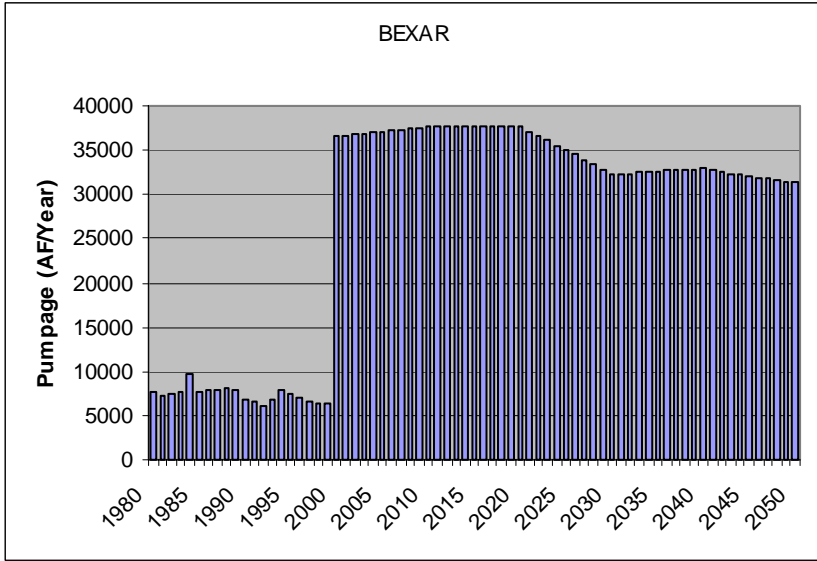


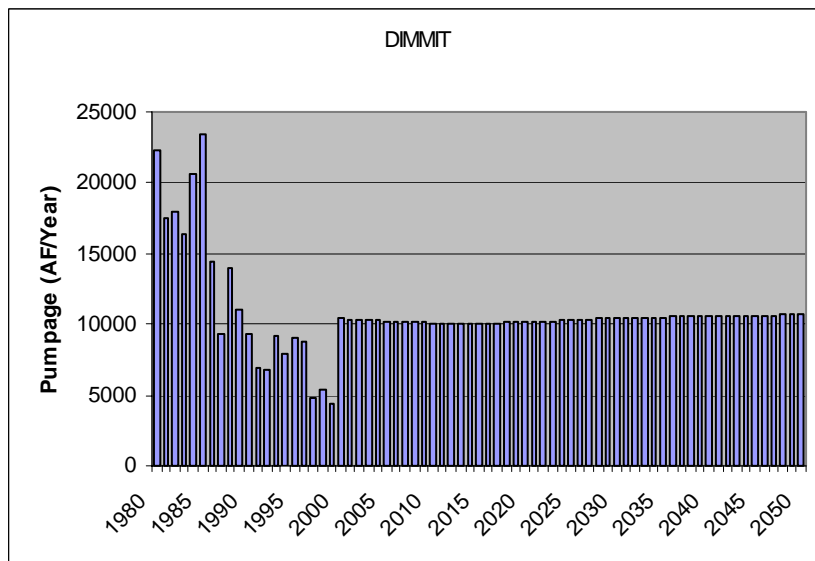
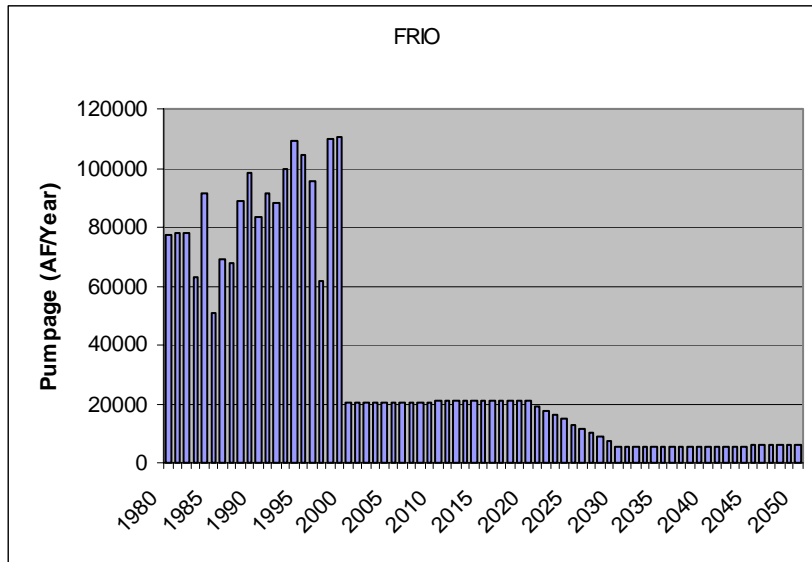
Figure D.2.24 Lower Wilcox (Layer 6) Pumpage, 2050 (AFY)

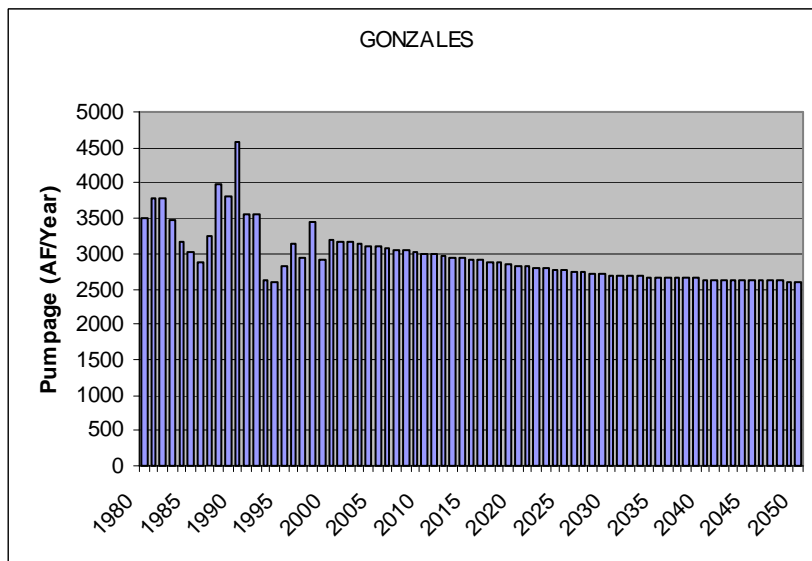
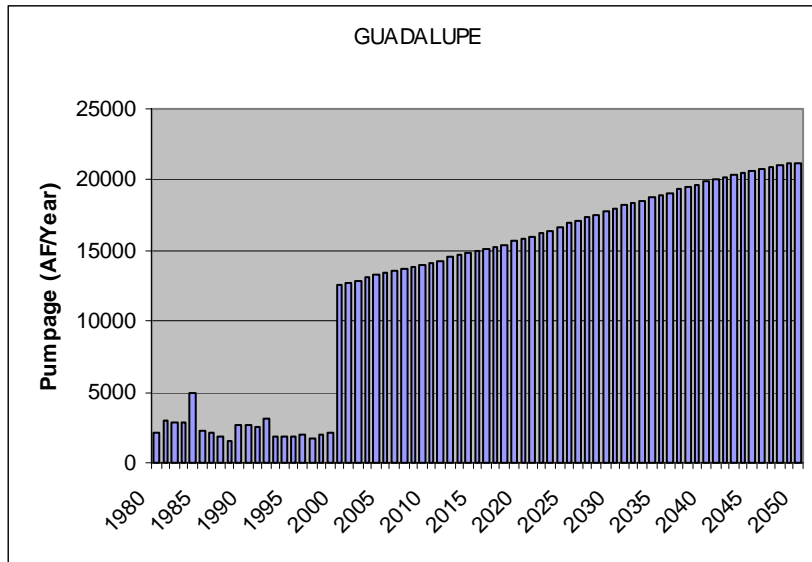
APPENDIX D3

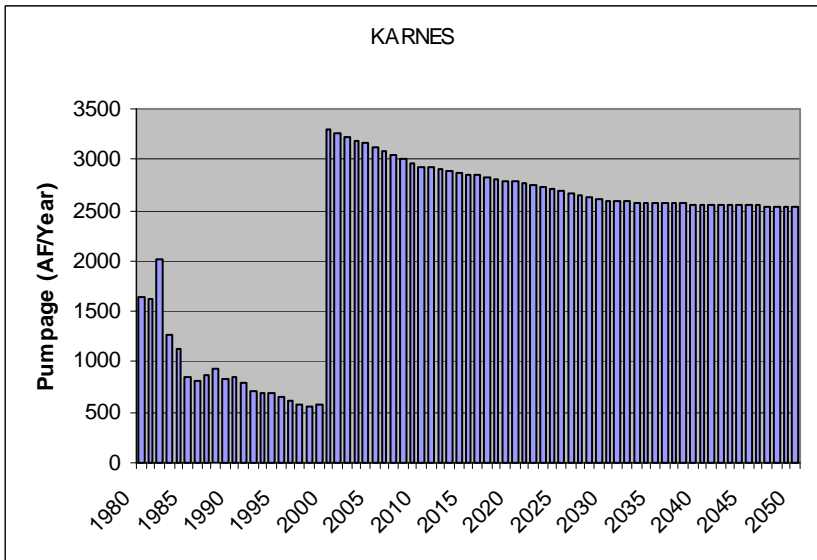
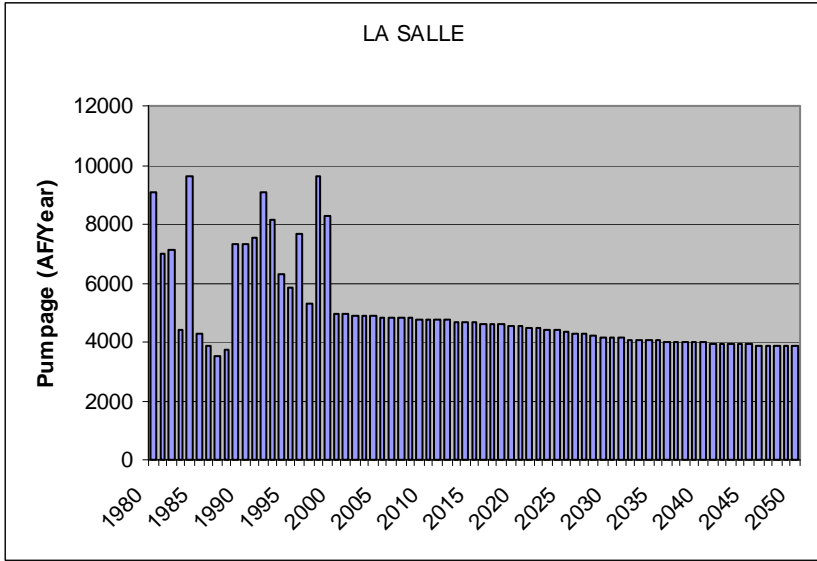
**Carrizo-Wilcox Groundwater
Withdrawal Distributions by County**

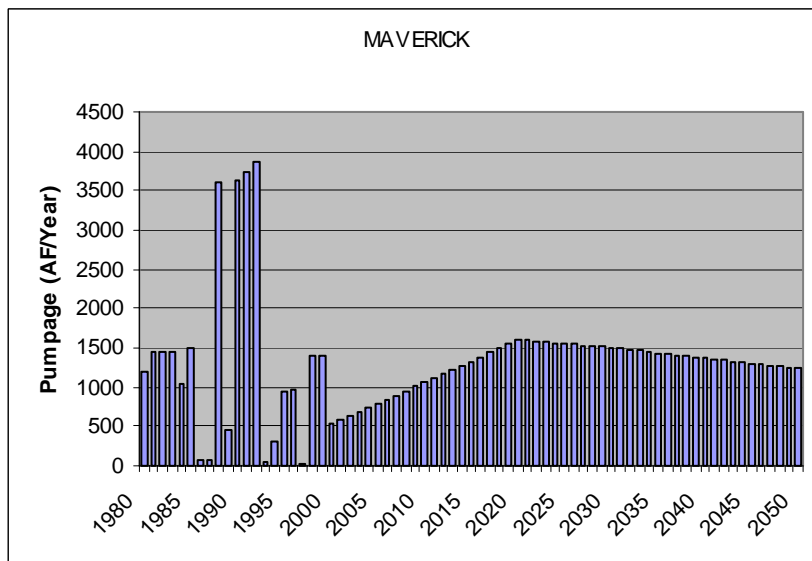
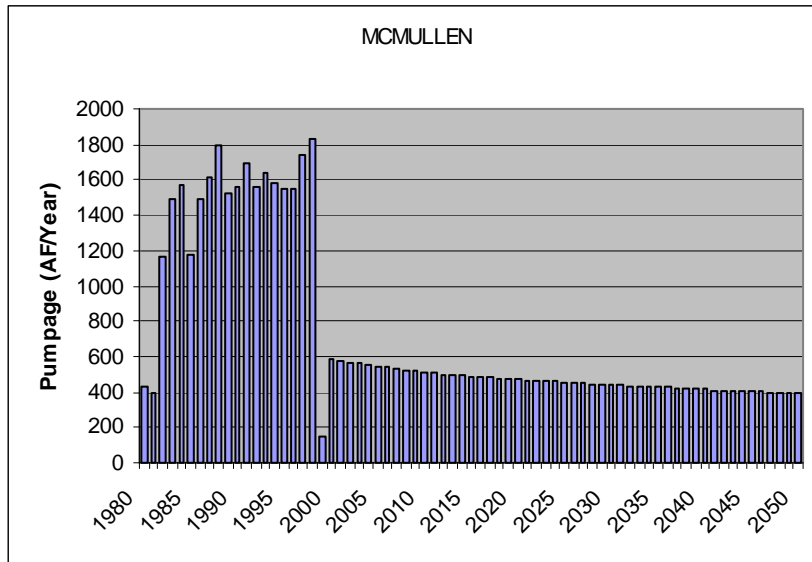


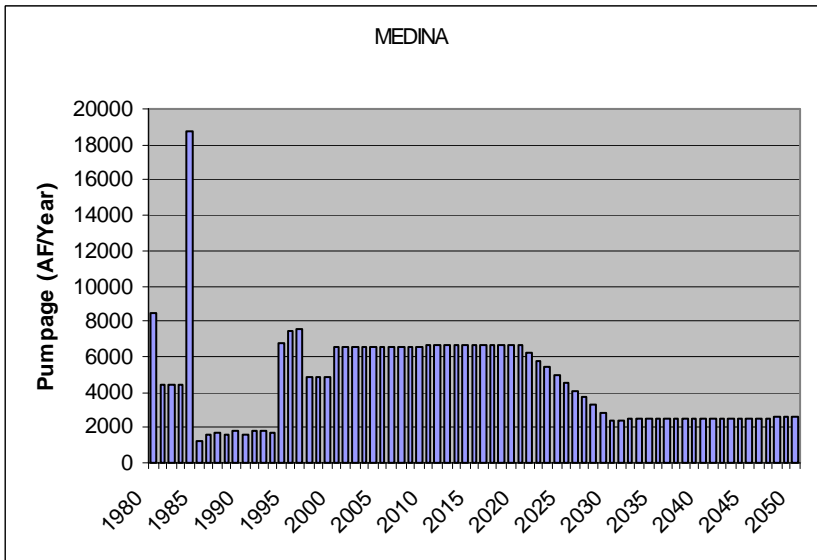
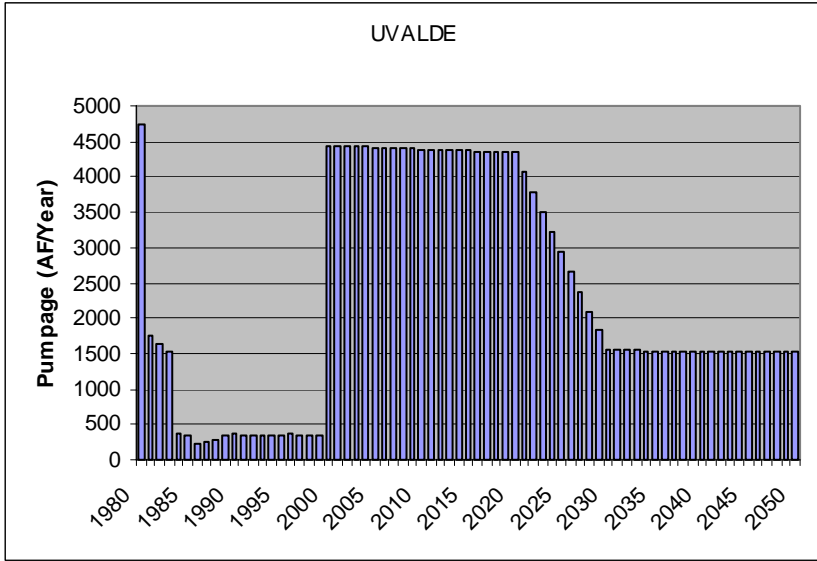


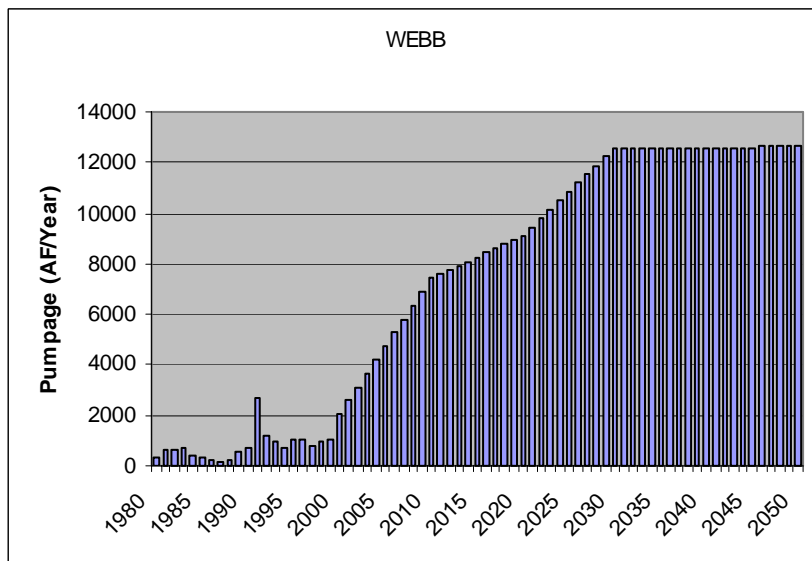
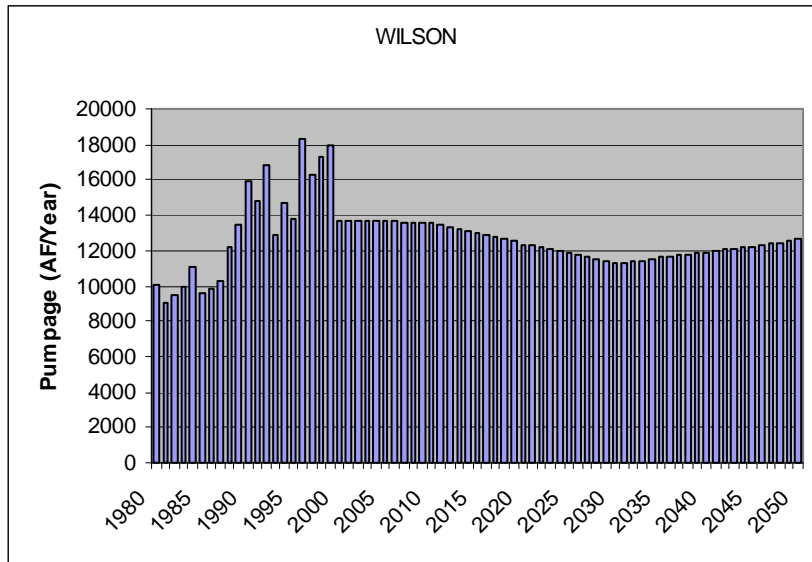


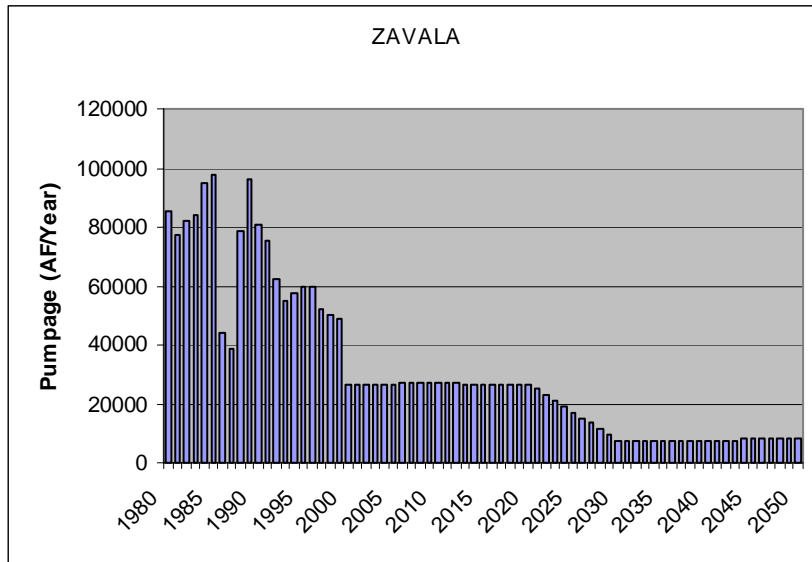












APPENDIX E

Using SWAT with MODFLOW in a Decoupled Environment

Appendix E Using SWAT with MODFLOW in a Decoupled Environment

Background:

Our goal is to use the recharge/evapotranspiration estimates from a SWAT simulation to estimate recharge/evapotranspiration inputs to a MODFLOW simulation. We do not want to do any iteration and are not allowed real-time updating between the two.

The following is a general description of how these physical processes are implemented in the two models.

Recharge/Evapotranspiration in MODFLOW:

In MODFLOW, recharge is input in length/time units. This rate of water is added directly to the uppermost active layer during each stress period. The rate can be varied spatially for each grid block, and temporally for each stress period.

In MODFLOW, evapotranspiration removes water directly from the uppermost saturated layer. When the water table is at or above a specified elevation (called the “ET surface”), water is removed at the specified maximum rate. If the water table is below the ET surface, but above a specified extinction depth, then water is removed at a rate that decreases linearly from a maximum at the ET surface to zero at the extinction depth. Below the extinction depth, no water is removed. Figure 1 illustrates this approach.

Recharge/Evapotranspiration in SWAT:

In SWAT, basically

$$\text{Change in Soil Water} = \text{Infiltration} - \text{Evapotranspiration} - \text{Recharge}$$

where

$$\text{Infiltration} = \text{Precipitation} - \text{Runoff}$$

A running soil water balance is calculated during the simulation. Precipitation is separated into infiltration and runoff using the SCS Curve Number method. Evapotranspiration requires more complex calculations. The following is a summary of how evapotranspiration is calculated in SWAT (skipping some of the minor details):

First, a potential (or more correctly, “reference”) evapotranspiration, $E_{t,0}$, is calculated, typically using some flavor of the Penman approach. This reference evapotranspiration is that which would occur for some reference grass with no soil water limitation. Three separate steps are required to estimate an actual evapotranspiration from this potential evapotranspiration.

Step 1: Account for vegetative differences -- since not all vegetation is reference grass, differences in growing cycles, size, and water use are accounted for by correlating the maximum daily transpiration with the leaf area index (LAI) of the plant, i.e.

$$E_{t,max} = \frac{(LAI)(E_{t,0})}{3.0} \quad 0 < LAI < 3.0$$

$$E_{t,max} = E_{t,0} \quad LAI > 3.0$$

The LAI changes with plant type, growth cycle, growing conditions, etc.

Step 2: Account for decreasing potential with increasing root zone depth -- root density is assumed to be greatest near the soil surface, and decreases with depth. With default SWAT parameters, about 50% of the water uptake occurs in the top 6% of the root zone.

Step 3: Account for soil water limitation -- plants cannot remove water from the soil if the soil water content is at the plant wilting point. So the $E_{t,max}$ that is calculated in Step 1 has to be limited by soil water.

Without writing down all of the equations, we just note that

$$E_{t,actual} = f(E_{t,max}, depth, soil\ moisture)$$

Note that this explanation applies to the unsaturated zone only. SWAT does allow for calculation of groundwater transpiration (called “revap” in SWAT). However, SWAT has a very crude implementation of groundwater modeling, so the relative height of the water table is unlikely to be consistent. Therefore, we do not calculate groundwater evapotranspiration in SWAT.

The Approach

So if we apply the recharge from SWAT directly MODFLOW, we neglect groundwater transpiration. The greatest error will occur when SWAT is predicting dry soil conditions and MODFLOW is predicting a near-surface water table (i.e. within the root zone). When these conditions occur, SWAT will underpredict actual ET.

What we will do to rectify this is to apply the “unused” ET (that is, the difference between maximum ET and actual ET) as ET in MODFLOW. In MODFLOW, we set

$$\begin{aligned} \text{Recharge} &= \text{Recharge from SWAT} \\ \text{ET} &= (E_{t,max} - E_{t,actual}) \text{ from SWAT} \end{aligned}$$

The four main scenarios are discussed below:

Scenario 1: Infiltration > Evapotranspiration, water table below extinction depth

This scenario should be fine, with no MODFLOW ET (since the water table is below the extinction depth), but with recharge being estimated by SWAT. The SWAT estimate does not include groundwater ET of course, but with the water table below the extinction depth, there should be no groundwater ET.

Scenario 2: Infiltration > Evapotranspiration, water table above extinction depth

In this scenario, MODFLOW starts to draw water from the water table based on the difference between the maximum transpiration and the actual transpiration estimated by SWAT. However, the MODFLOW ET shouldn't have much impact in this case because with infiltration occurring, soil moisture should be high, $E_{t,actual}$ will be similar to $E_{t,max}$, and the difference will be near zero.

Scenario 3: Infiltration < Evapotranspiration, water table below extinction depth

In this scenario, there will be no recharge, and MODFLOW will have shut down ET.

Scenario 4: Infiltration < Evapotranspiration, water table above extinction depth

In this scenario, SWAT will have set recharge to zero, and will not remove water from the soil profile below the wilting point. SWAT will not account for the fact that the groundwater evapotranspiration should be occurring. However, the ET in MODFLOW will be pulling water off of the water table at a rate near $E_{t,max}$, (since $E_{t,actual}$ will be small due to low soil moisture) which is a good estimate for this situation.

Figure 2 shows an example of preliminary SWAT results from a deciduous forest area for the year 1975 in the northern model region. Note that actual evapotranspiration is primarily due to soil evaporation in the winter months. In the spring and summer, transpiration begins to dominate the ET, and when soil water is high, actual transpiration is similar to maximum potential transpiration. Note that in late summer, the precipitation is inconsistent and soil water is decreasing, so the difference between maximum and actual transpiration is significant on some days.

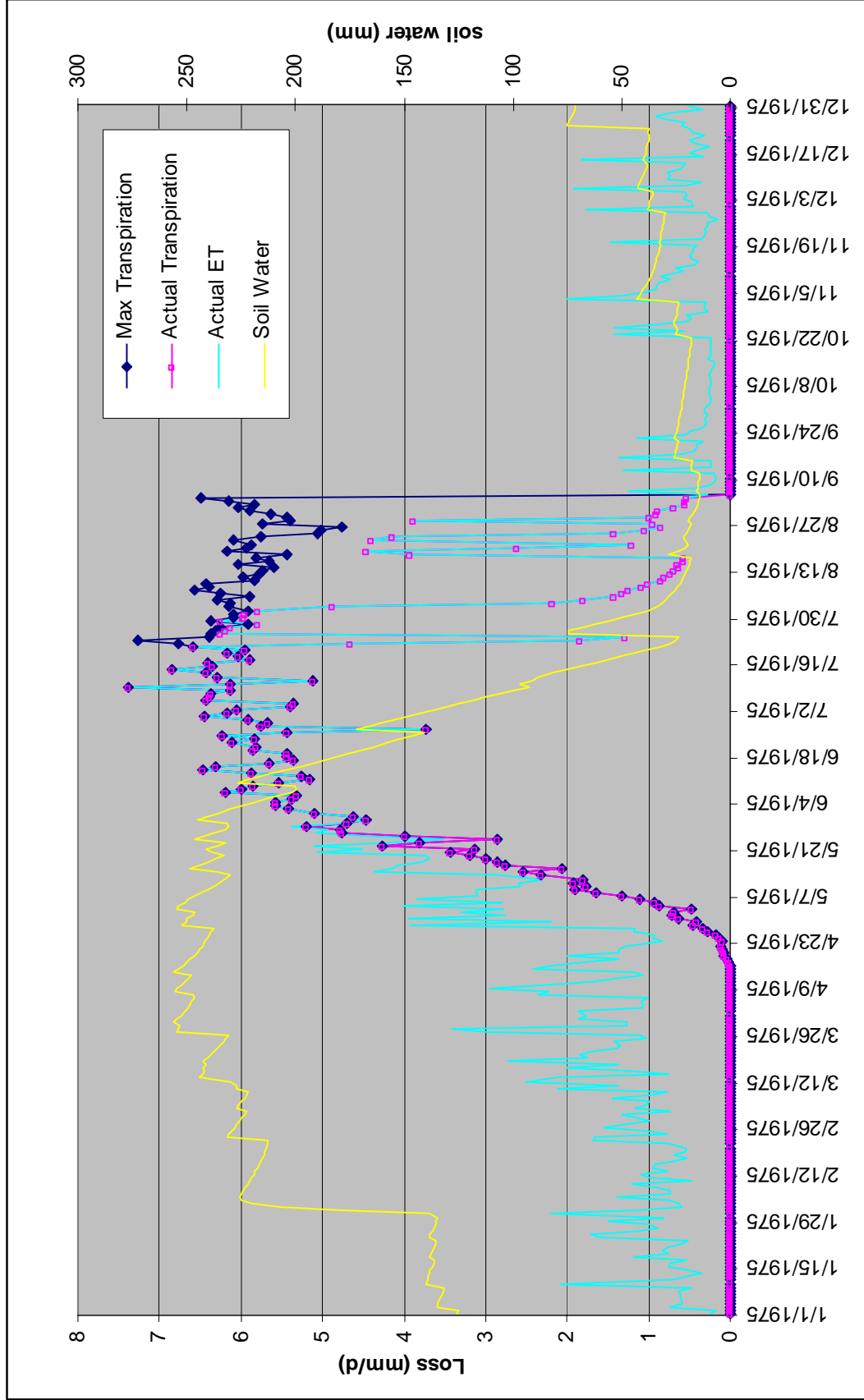


Figure E.1 Example SWAT results

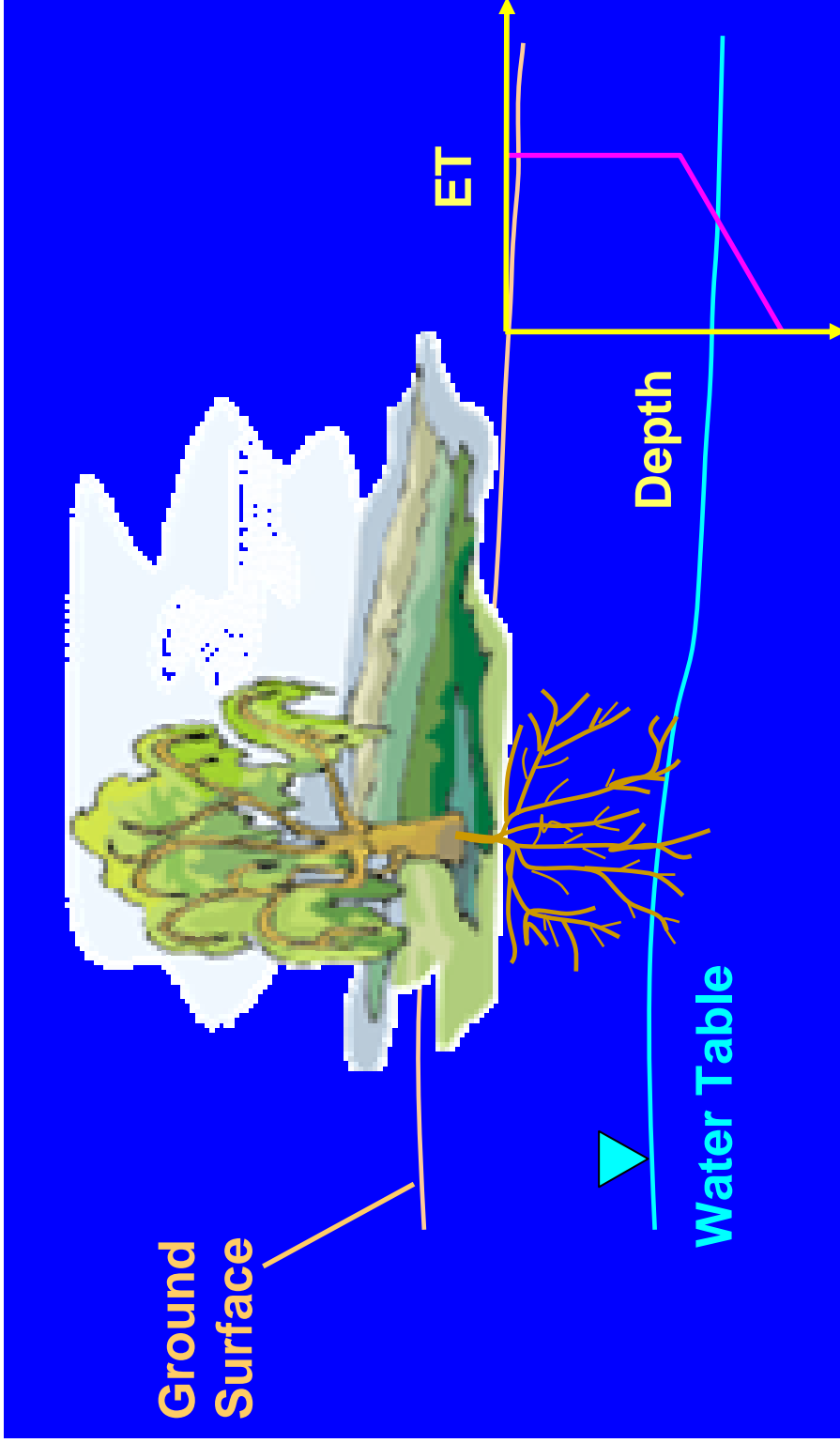


Figure E.2 MODFLOW approach to groundwater evapotranspiration

APPENDIX F
Water Quality

Appendix F

Water Quality

Ground water in the southern Carrizo-Wilcox aquifer was evaluated for its quality as a drinking water supply, for irrigation of crops, and for industrial purposes, by comparing the measured chemical and physical properties of the water to screening levels. Water quality measurements were retrieved for the entire available historical record, from about 1920 through 2001, from databases maintained by the Texas Water Development Board, the U.S. Geological Survey, and the Texas Commission on Environmental Quality's Public Water System. The percentages of wells in the aquifer with one or more measurements exceeding individual screening levels are illustrated in Table F.1. Table F.2 indicates the percentage of wells in the southern Carrizo-Wilcox aquifer from each county that exceeded at least one screening level for drinking water, irrigation, or industrial uses.

Concentration levels of selected constituents were evaluated for well data from the identified databases. They are presented in Figures F.1 through F.7 for radium, alpha activity, nitrate nitrogen, iron, sodium hazard, total dissolved solids, and hardness, respectively. Each column in the figures reflects the highest observed measurement in a single well. The height of the column, and its color, represent the magnitude of the concentration. A general discussion of drinking, irrigation, and industrial water quality within the southern Carrizo-Wilcox GAM area is presented below.

Drinking Water Quality - Screening levels for drinking water supply are based on the maximum contaminant levels (MCLs) established in National Primary Drinking Water Regulations and National Secondary Drinking Water Regulations. National Primary Drinking Water Regulations are legally enforceable standards that apply to public water systems to protect human health from contaminants in drinking water. National Secondary Drinking Water Regulations are non-enforceable guidelines for drinking water contaminants that may cause aesthetic effects (taste, color, odor, foaming), cosmetic effects (skin or tooth discoloration), and technical effects (e.g., corrosivity, expensive water treatment, plumbing fixture staining, scaling, and sediment).

Total dissolved solids (TDS) is a measure of water saltiness, the sum of concentrations of all dissolved ions (such as sodium, calcium, magnesium, potassium, chloride, sulfate, carbonates) plus silica. Some dissolved solids, such as calcium, give water a pleasant taste, but most make water taste salty, bitter, or metallic. Dissolved solids can also increase its corrosiveness. TDS levels have exceeded the secondary MCL, the maximum contaminant level allowed in National Secondary Drinking Water Standards) in approximately 44% of the wells in the southern Carrizo-Wilcox aquifer. There are zones in the aquifer (Webb, LaSalle, Dimmit, Zavalla counties) that consistently have concentrations of total dissolved solids that exceed 1,000 mg/L and chlorides that exceed 300 mg/L.

Elevated levels of iron and manganese adversely impact water quality in approximately 30% of the wells in the southern Carrizo-Wilcox aquifer. Water containing iron in excess of the secondary MCL of 0.3 mg/L and manganese in excess of 0.05 mg/L may cause reddish-brown or

blackish-gray stains on laundry, utensils, and plumbing fixtures, as well as color, taste and odor problems.

Radium is a naturally-occurring radionuclide with two radioactive isotopes that can cause cancer. While there have been few measurements historically of radium activity, approximately 20% of these have exceeded the primary MCL of 5 picoCuries per liter (pCi/L). These wells were primarily located in Medina, Frio, Zavala, and Dimmit counties.

Alpha particles are one type of naturally-occurring radionuclide that can cause cancer. Alpha activity that exceeds the primary MCL of 15 pCi/L was recorded in approximately 7% of the wells. The greatest percentages of radioactive MCL exceedances were found in the Carrizo sand in Zavala County.

High concentrations of nitrate nitrogen can cause serious illness in infants younger than 6 months old. Nitrate nitrogen levels that exceed the primary MCL of 10 mg/L were detected in about 6% of the wells. The greatest percentage of nitrate nitrogen MCL exceedances was found in Uvalde and Medina counties.

Fluoride is a naturally-occurring element found in most rocks. At very low concentrations, fluoride is a beneficial nutrient. At a concentration of 1 mg/L, fluoride helps to prevent dental cavities. However, at concentrations above the secondary MCL of 2 mg/L, fluoride can stain children's teeth. Approximately 3% of wells in the southern Carrizo-Wilcox aquifer have exceeded this level. At concentrations above the primary MCL of 4 mg/L, fluoride can cause a type of bone disease. Less than 1% of wells have exceeded 4 mg/L fluoride.

Overall, approximately 8% of the wells in the southern Carrizo-Wilcox aquifer are deemed to have unsuitable drinking water quality for health reasons, and approximately 40% of the wells have water that may be unpalatable for drinking, cause stains to teeth, plumbing fixtures, and laundry, or cause scaling or corrosion in plumbing without prior treatment.

Irrigation Water Quality - The utility of groundwater for crop irrigation was evaluated based on the concentrations of boron, chloride, and total dissolved solids, as well as the salinity hazard, the sodium hazard, and the sodium absorption ratio. Various soils and plants differ in their tolerance of salts. This tolerance is also affected by the abundance of rainfall and frequency of irrigation. In the absence of consensus standards for water quality for irrigation, we attempted to identify thresholds that would be unsuitable for long-term use on most types of plants and soils.

Boron may cause toxicity to many plants at levels above 2 mg/L (van der Leeden et al., 1990). Boron levels in the southern Carrizo-Wilcox aquifer exceed this level in approximately 5% of wells. Most crops cannot tolerate chloride levels above 1000 mg/L for an extended period of time (Tanji, 1990), a level exceeded in about 2% of wells in the southern Carrizo-Wilcox aquifer.

Salinity, as measured by total dissolved solids (TDS) or electrical conductivity, can also be toxic to plants by making plants unable to take up water. James et al. (1982) consider TDS levels above 2100 unsuitable for most irrigation. The salinity hazard classification system of the U.S. Salinity Laboratory (1954) indicates that waters with electrical conductivity over 750 micromhos present a high salinity hazard, and those with electrical conductivity over 2250 micromhos present a very high salinity hazard. Irrigation water containing large amounts of sodium cause a

breakdown in the physical structure of soil such that movement of water through the soil is restricted. The sodium absorption ratio (SAR) is an indication of the sodium hazard to soils. An SAR of greater than 18 is generally considered unsuitable for continuous use in irrigation, but the sodium hazard depends on both the SAR and water salinity. The sodium hazard was calculated based on the classification system developed by the U.S. Salinity Laboratory (1954).

Overall, approximately 20% of the wells in the southern Carrizo-Wilcox aquifer are deemed to have unsuitable water quality for irrigation of many types of crops.

Industrial Water Quality - The quality of water for most industrial purposes is indicated by the content of dissolved solids, as well as its corrosivity and tendency to form scale and sediment in boilers and cooling systems. Some constituents responsible for scaling are hardness (calcium and magnesium), silica, and iron. Water temperature and pH also have a direct effect on how quickly and severely these constituents cause scaling or corrosion. pH values below 6.5 may enhance corrosion, while pH values above 8.5 will contribute to scaling and sediment. Waters with a silica concentration of 40 mg/L or higher are considered unsuitable for use in most steam boilers. Waters with a hardness of 180 mg/L (as calcium carbonate) or higher are considered very hard, and are unsuitable for many industrial purposes because water softening becomes uneconomical.

Overall, approximately 63% of the wells in the southern Carrizo-Wilcox aquifer are deemed to have unsuitable water quality for many industrial purposes without substantial pre-treatment, such as water softening.

Literature Cited

- James, D.W., R.J. Hanks, and J.H. Jurinak. 1982. *Modern Irrigated Soils*. John Wiley and Sons, New York.
- Shafer, G.H. 1968. *Ground-water Resources of Nueces and San Patricio Counties, Texas*. Report 73. Texas Water Development Board, Austin, Texas
- Tanji, K.K. 1990. *Agricultural Salinity Assessment and Management*. American Society of Civil Engineers. *Manuals and Reports on Engineering Practice* Number 71.
- U.S. Salinity Laboratory Staff. 1954. *Diagnosis and Improvement of Saline and Alkali Soils*. U.S. Department of Agriculture, Agricultural. Handbook 60.
- Van der Leeden, F., F.L. Troise, and D.K. Todd. 1990. *The Water Encyclopedia*. Lewis Publishers.

Table F.1 Occurrence and levels of some commonly-measured groundwater quality constituents in the southern Carrizo-Wilcox aquifer.

Constituent	Number Of Wells	Screening Level (mg/L)	Type	Percent Of Wells Exceeding Screening Level*
Radium 226+228 Activity, pCi/L	66	5	1° MCL	20%
Alpha Activity, pCi/L	197	15	1° MCL	7.1%
Nitrate Nitrogen	1521	10	1° MCL	6.4%
Chromium	311	0.1	1° MCL	1.0%
Selenium	319	0.05	1° MCL	0.6%
Arsenic	318	0.01	1° MCL	0.6%
Beta Activity, pCi/L	189	50	1° MCL	0.5%
Fluoride	1442	4	1° MCL	0.5%
Lead	319	0.015	1° MCL	0.3%
Beryllium	201	0.004	1° MCL	0.0%
Cadmium	311	0.005	1° MCL	0.0%
Barium	318	2	1° MCL	0.0%
Copper	318	1.3	1° MCL	0.0%
Antimony	201	0.006	1° MCL	0.0%
Mercury	210	0.002	1° MCL	0.0%
Nitrite Nitrogen	195	1	1° MCL	0.0%
Thallium	193	0.002	1° MCL	0.0%
Total Dissolved Solids	1624	500	2° MCL	44%
Iron	553	0.3	2° MCL	31%
Manganese	387	0.05	2° MCL	27%
Chloride	1659	250	2° MCL	15%
Sulfate	1626	250	2° MCL	11%
Fluoride	1442	2	2° MCL	2.8%
Aluminum	291	0.2	2° MCL	1.0%
Zinc	318	5	2° MCL	0.0%
Copper	318	1.0	2° MCL	0.0%
Silver	209	0.1	2° MCL	0.0%
Salinity Hazard	1499	Very High (Sp. Cond. >2250)	Irrigation	12%
		High Or Very High (Sp. Cond. > 750)	Irrigation	53%
Sodium (Alkali) Hazard	1596	Very High (SAR>26)	Irrigation	15%
		High Or Very High (SAR>18)	Irrigation	17%
Boron	575	2	Irrigation	5.2%
Total Dissolved Solids	1624	2100	Irrigation	5.2%
Chloride	1659	1000	Irrigation	2.4%
Hardness	1783	180	Industrial	50%
PH	1525	<6.5 OR >8.5	Industrial	15%
Silica	1529	40	Industrial	9.1%

* percentage of wells with one or more measurements of the parameter that exceeded the screening level.

Table F.2 County-level water quality in the southern Carrizo-Wilcox aquifer.

County Name	RWPG	Wells Sampled	% of Wells Exceeding One or More Screening Levels			
			PMCL	SMCL	Irrigation	Industrial
Atascosa	L	249	2%	29%	12%	50%
Bastrop	K	190	6%	46%	9%	73%
Bexar	L	22	5%	77%	9%	95%
Caldwell	L	177	11%	46%	28%	81%
Dimmit	L	166	7%	28%	15%	42%
Fayette	K	2	0%	100%	100%	100%
Frio	L	169	4%	27%	8%	86%
Gonzales	L	78	4%	42%	21%	25%
Guadalupe	L	84	22%	46%	20%	89%
Karnes	L	11	11%	70%	90%	45%
La Salle	L	66	3%	38%	63%	14%
Live Oak	N	1	0%	100%	100%	0%
Maverick	M	20	22%	61%	44%	85%
McMullen	N	17	0%	76%	100%	59%
Medina	L	61	32%	48%	26%	92%
Uvalde	L	2	50%	0%	0%	100%
Webb	M	32	10%	63%	83%	47%
Williamson	G	4	0%	25%	25%	75%
Wilson	L	119	0%	33%	8%	46%
Zavala	L	179	16%	25%	13%	88%
Grand Total		1649	8%	39%	20%	63%

Figure F.1 Maximum observed radium levels.

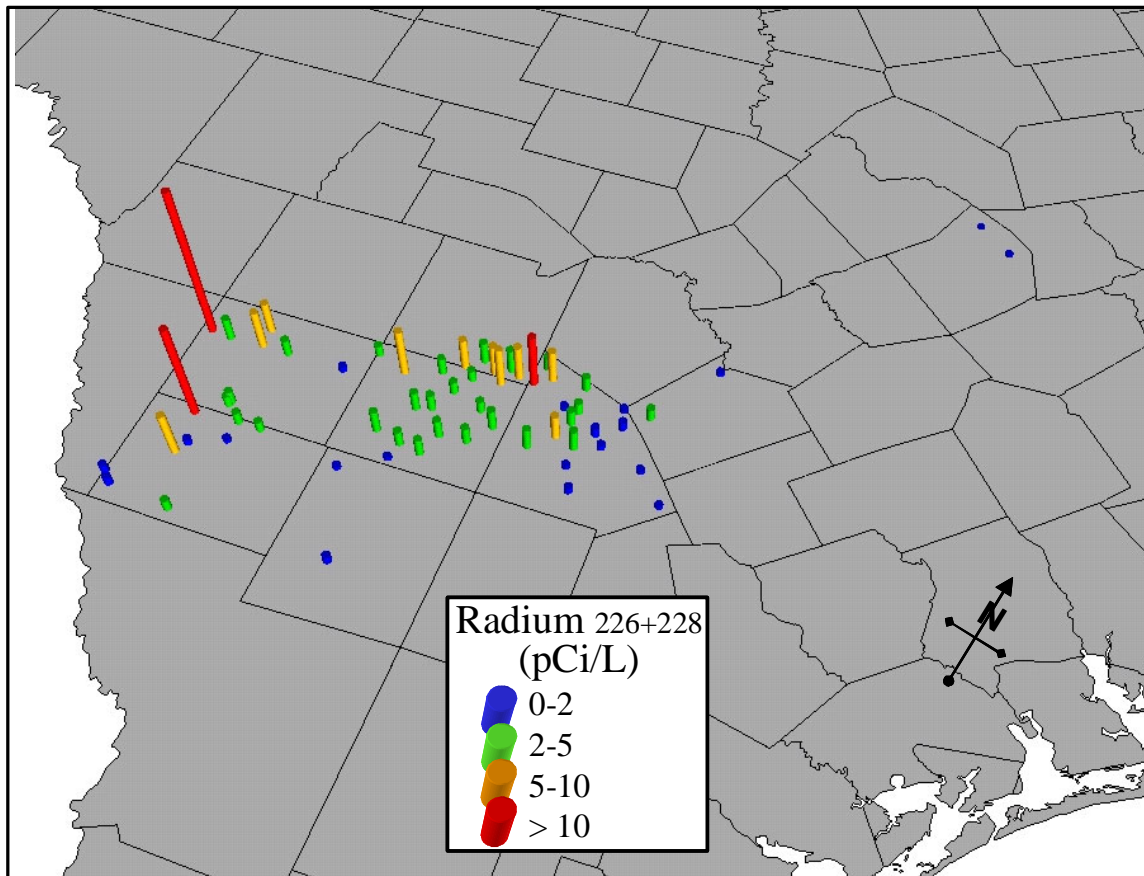


Figure F.2 Maximum observed alpha activity levels.

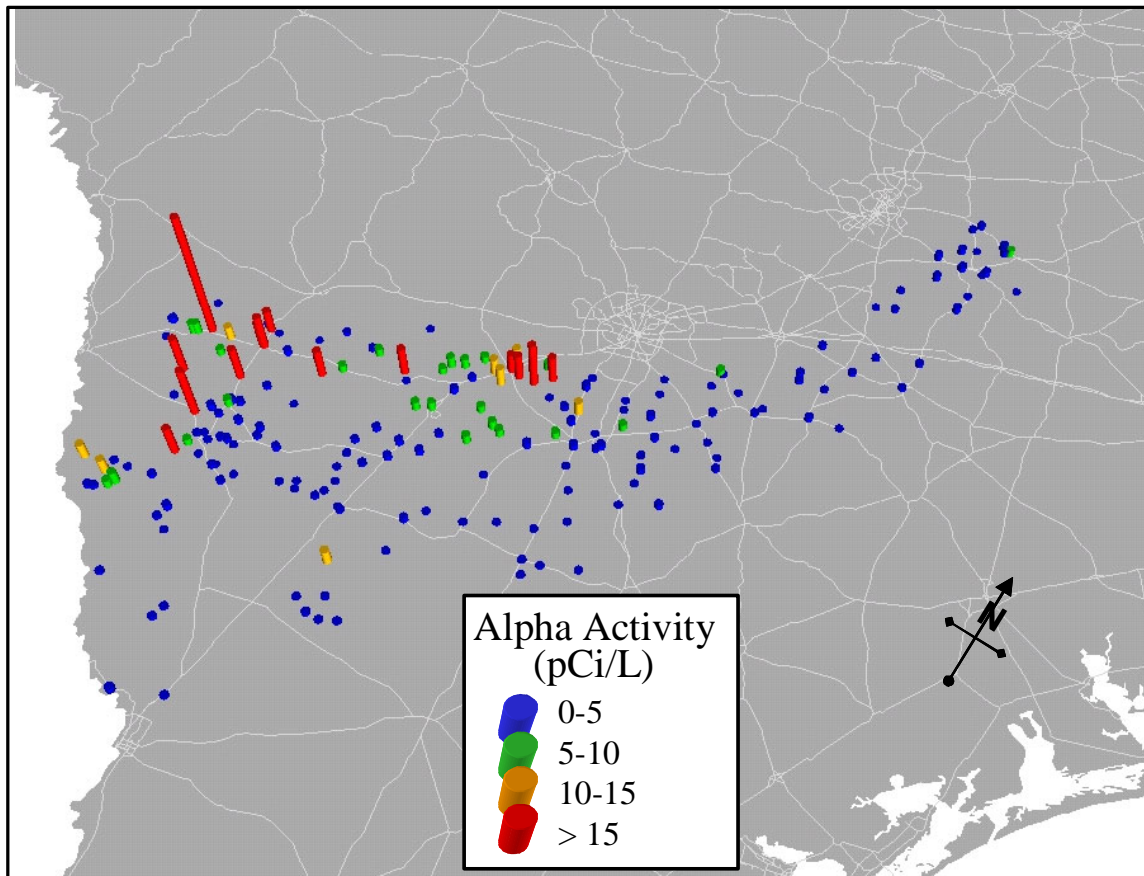


Figure F.3 Maximum observed nitrate nitrogen levels.

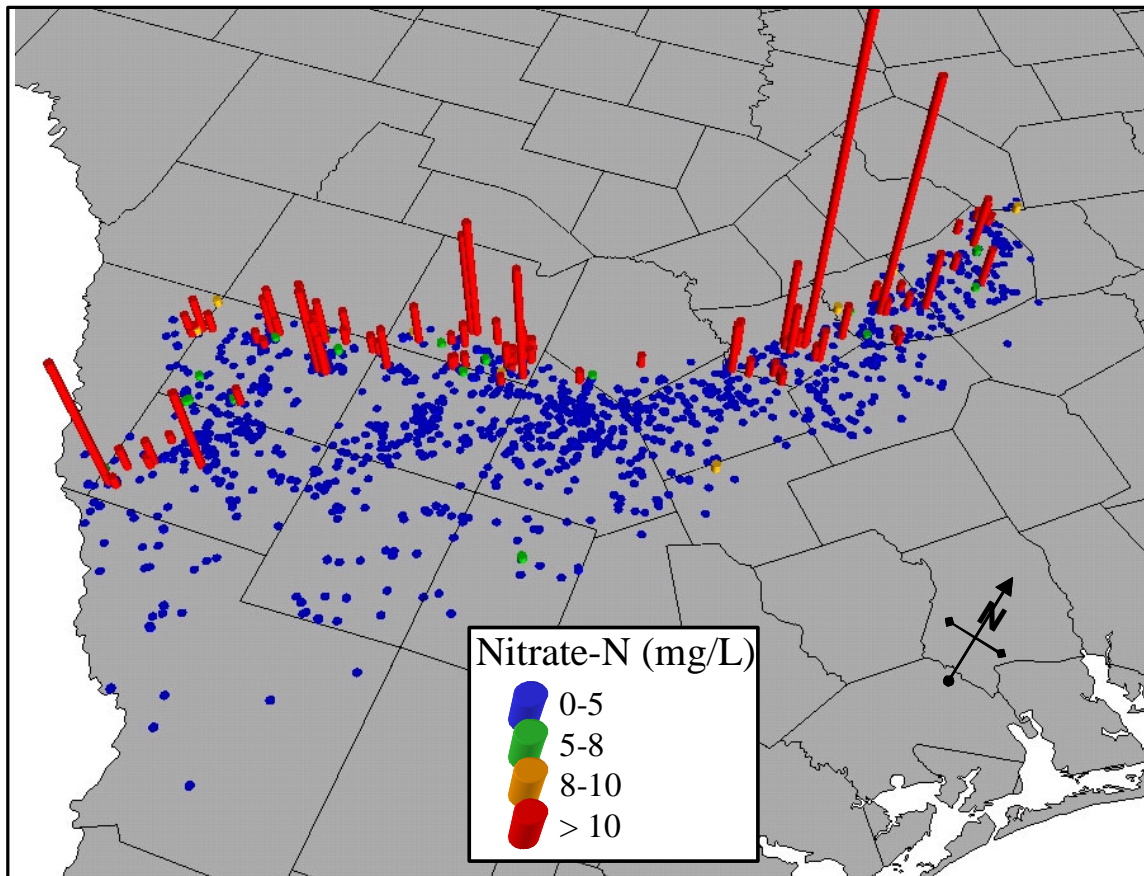


Figure F.4 Maximum observed iron levels.

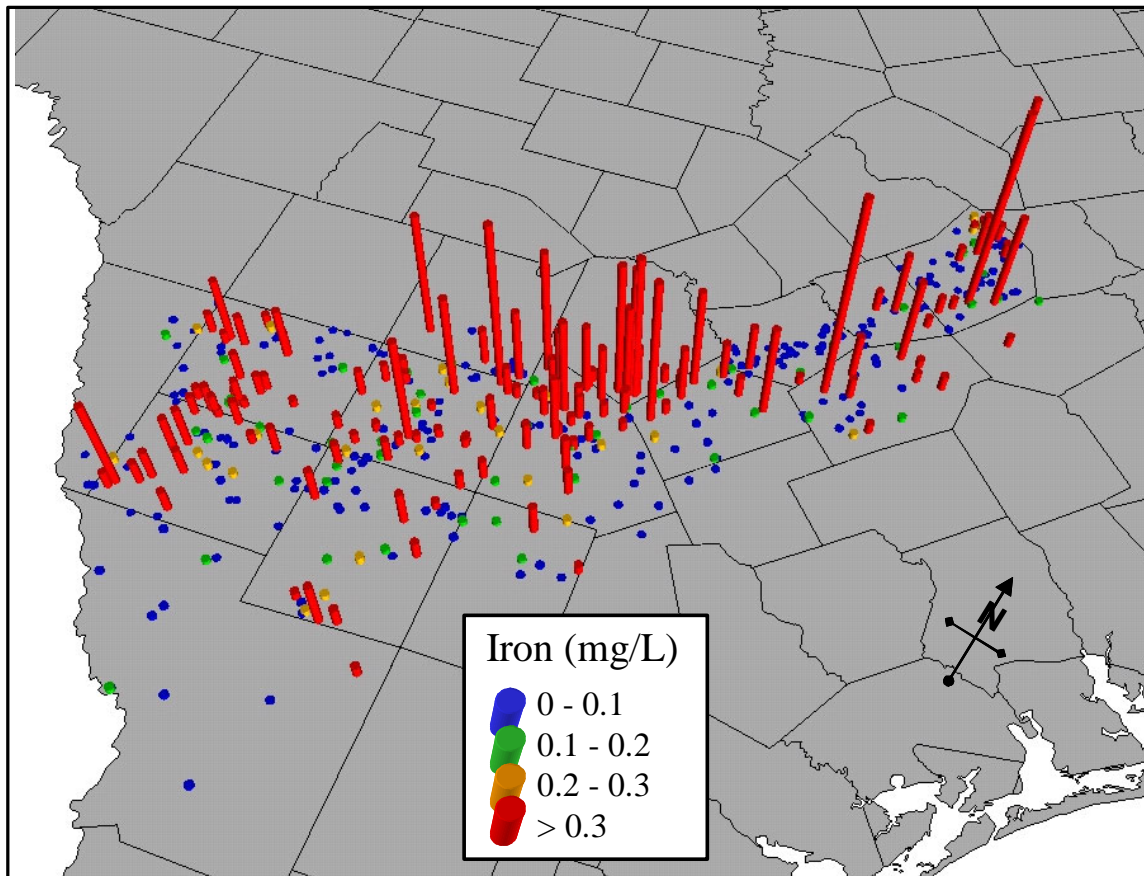


Figure F.5 Maximum observed sodium hazard levels.

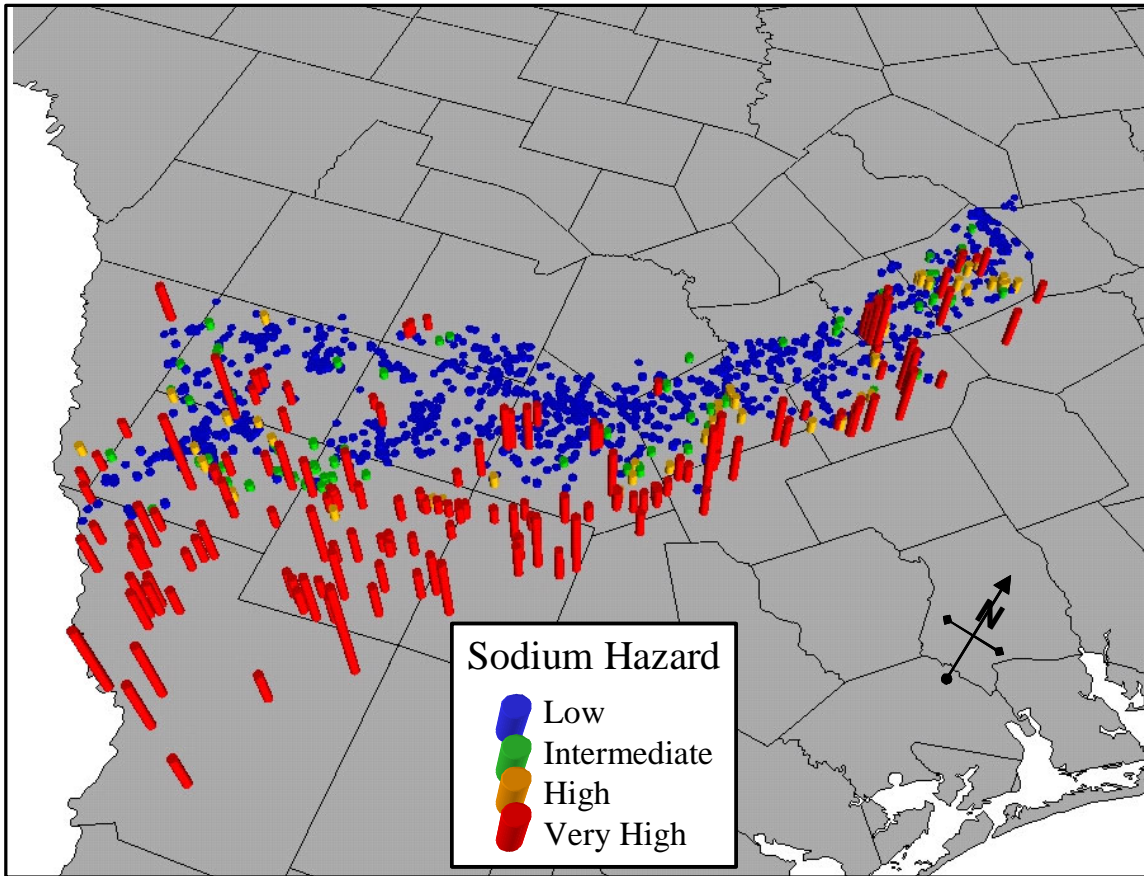


Figure F.6 Maximum observed total dissolved solids levels.

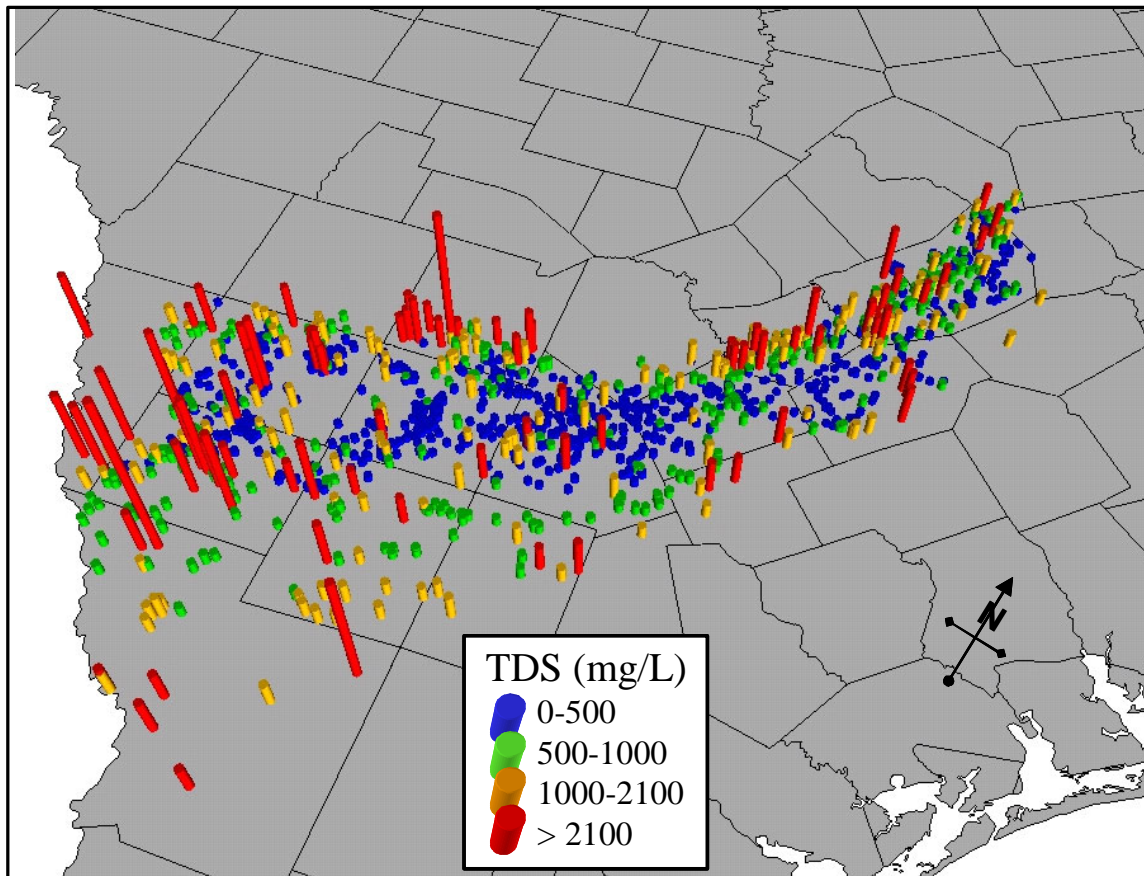
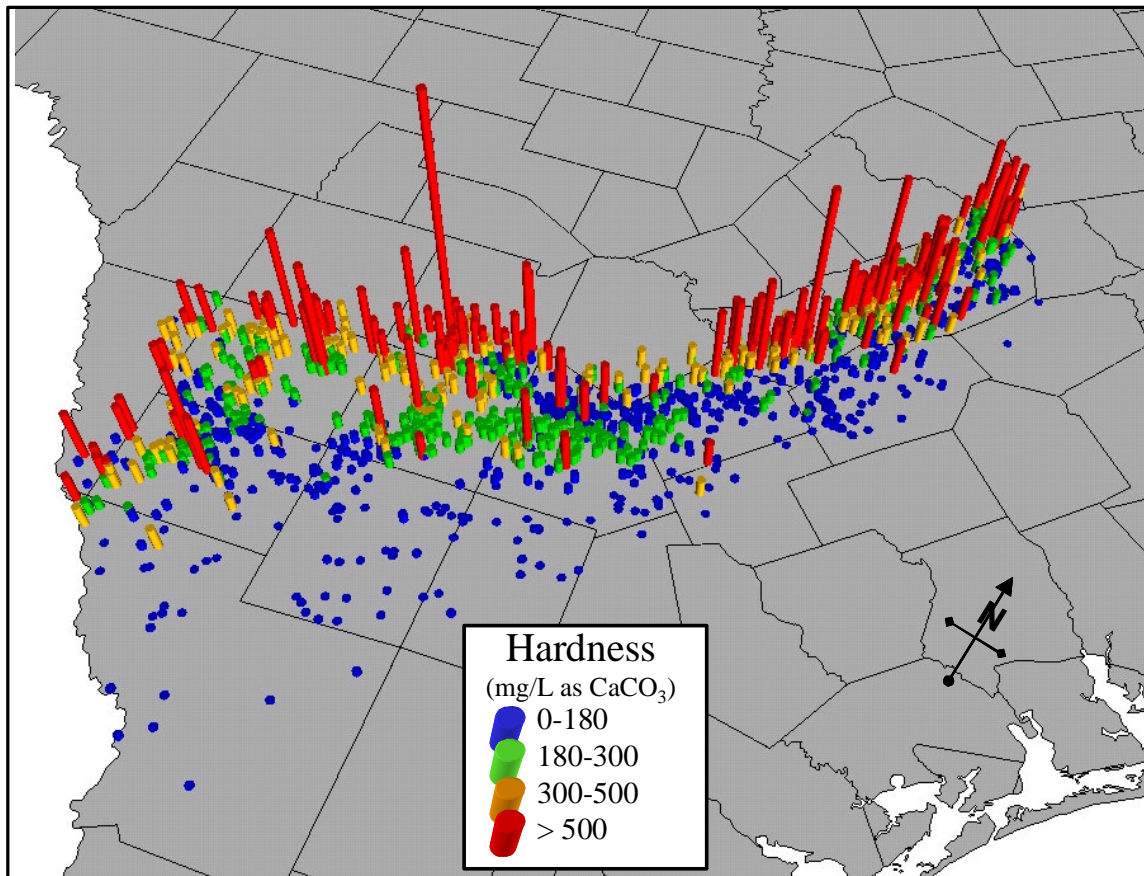


Figure F.7 Maximum observed hardness levels.



APPENDIX G
Draft Report Comments and Responses

TEXAS WATER DEVELOPMENT BOARD
Review of the Draft Final Report: Contract No. 2001-483-381
" Groundwater Availability Model for the Southern Carrizo-Wilcox Aquifer"

DRAFT REPORT TECHNICAL/ADMINISTRATIVE COMMENTS:

GENERAL

Consider using higher resolution graphics. Many of the graphics are pixelated and therefore difficult to understand.

Completed.

Include an authorship list.

Completed. See authorship list.

DRAFT REPORT - SECTION 2: STUDY AREA

1. Section 2.1 Please briefly discuss river basins and tabulate or list basin areas (Figure 2.6).

Completed. See text at bottom of page 2-2 and Table 2.1.

2. Figure 2.12 Surface Geology. This map is unreadable in black and white.
Due to the size of the model area and the detail presented in this figure, it will not be possible to make this figure readable in black and white at the model scale required for an 8.5x11 figure. The TWDB agreed that this figure would not have to be legible in black in white.

3. Page 2-1, second paragraph, line 6, list of counties in model area, add Bastrop, Fayette, Duval, Lavaca and Medina counties to the list.

Completed. See page 2-1, second paragraph.

4. Page 2-7, Figure 2.5 EAA district boundaries need to be corrected. The boundary of EAA covers all of Bexar, Medina and Uvalde counties.

Completed. See Figure 2.5.

5. Page 2-6, first paragraph, add to the list of GCDs in the model area, Pecan Valley, Lavaca County and Fayette County, GCDs.

Completed See page 2-2, first paragraph.

DRAFT REPORT - SECTION 4: HYDROLOGIC SETTING

1. Section 4.3.3: Spatial Distribution of Hydraulic Property Data: Please explain how K was kriged. The distribution does not look like a simple-kriged distribution.

Completed. See page 4-28, last paragraph. The following text has been added, “. . . is then produced by ordinary kriging”.

2. Section 4.3.3: Spatial Distribution of Hydraulic Property Data: Please include a discussion on horizontal anisotropy.

Completed. See page 4-28, first paragraph.

3. Section 4.5: Recharge: Please discuss possible temporal variations in recharge.
Completed. See page 4-86, second paragraph.
4. Section 4.0: Hydrogeologic Setting: Please include a sub-section on the water quality work done for the project.
Completed. See section 4.8.
5. Section 4.3: Please discuss information about anisotropy of horizontal hydraulic conductivity. ((See RFP Appendix 1, page 8/40, Section 3.1.8)
See #2 above. It is redundant to include this text here also.
6. Section 4.3.4: In addition to sand map of Carrizo please include map for upper Wilcox.
Completed. See figure 4.3.11.
7. Section 4.2: Please briefly discuss structural and tectonic history.
Completed. See page 4-5, first paragraph.
8. Section 4.2: Were USGS DEM's used for land surface elevation and top of outcrop? If so, please explicitly state this. If not, explain what was used and why.
Completed. See page 4-5, last paragraph.
9. Section 4.4.4: Extend period for some hydrographs further back than 1978.
Completed. See page 4-50, last paragraph which refers to Appendix A.
10. Section 4.6: Were results from TCEQ's (formerly TNRCC) WAM model incorporated into surface-water/groundwater interaction analysis? If yes please discuss. If not, please explain why not. (See RFP Appendix 1, page 7/40, Section 3.1.7).
The TCEQ WAM models were reviewed for use in the GAM studies. Because the WAM models are appropriation models that have to do with routing, they held little information that could be exploited in the GAMs. The underlying assumptions for the WAMs were unrepresentative of actual stream flow conditions at times or conditions needed in the GAM models. This explanation is limited to the comments and was not added to the text.
11. Section 4.7: Please include the map of rural population density used to distribute the county-other water use.
Completed. See figure 4.7.1.

DRAFT REPORT- SECTION 5: CONCEPTUAL MODEL

1. Page 5-1, 1st paragraph: Please clarify the last sentence about additional arrows in Figure 5.1.
Completed. See page 5-1, first paragraph.

DRAFT REPORT - SECTION 6: MODEL DESIGN

1. Page 6-15, 2nd paragraph: Please briefly explain the SCS Curve Number Method, Hargreaves Method and the NRCS curve-number method.
The purposes of the NRCS (SCS) curve number method for estimating runoff and infiltration, and the Hargreaves method for estimating reference evapotranspiration are given in the report (see page 6-10, first paragraph) The theory behind these methods is beyond the scope of this report, but can be readily found in the SWAT references.

2. Page 6-15, 3rd paragraph: This is the only time in the report that the ramp-up period (1975-1980) is mentioned. It should also be discussed in Section 9.0 along with a discussion of the initial conditions used for the transient simulation.
Completed. Text added to sections 7.1 and 9.0 regarding “ramp up” period.

DRAFT REPORT - SECTION 8: STEADY-STATE MODEL

1. Section 8.2 Simulation Results: Please include MAE and ME along with RMS.
Completed. See table 8.2.1.
2. Section 8.2.2 Streams: Please include an assessment of how well simulated stream baseflow matches measured streamflow.
Completed. See section 8.2.2.
3. Please include a detailed water budget for:
 - steady-state
Please see Tables 8.2.1 and 8.2.2.
 - beginning of calibration period
Please see Table 9.2.3.
 - the drought of the calibration period
Completed. Added to Table 9.2.3.
 - end of the calibration period
Please see Table 9.2.3.
 - end of the verification period
Please see Table 9.2.3.
 - end of 2000, 2010, 2020,2030,2040, and 2050.
Please see Table 10.3.1.
4. Page 8-18, 4th paragraph, 5th line down: “...cross-formational flow through the top of the Reklaw”? Shouldn't it be through the bottom of the Reklaw?
Completed See page 8-18, last paragraph..
5. Figure 8.2.8: Large 20 on the figure. Is this supposed to be 20,000 years? Please clarify in caption or on figure.
Completed. See figure 8.2.9.
6. Sections 8.2.1 and 9.2.1: Please, in addition to the RMS, also report the mean absolute error and the mean error (See RFP Appendix 1, page 13/40, Section 3.3).
Completed See table 8.2.1 and table 9.2.1.
7. Section 8.2.1: For at least layer 3 please compare observed head surface with simulated rather than just posting residuals.
Completed. See figure 8.2.4.
8. Sections 8.2.3 and 9.2.3: Please report the difference between simulated net inflow and simulated net outflow as a percent.
Completed. See page 8-18, last paragraph.

9. Sections 8.3 and 9.3: Please add sensitivity of assigned hydraulic head on ghb's to sensitivity analysis. (See RFP Appendix 1, page 16/40, Section 3.3).
Head values assigned to GHBs were set to water table elevations as estimated using the regression equations of Williams and Williamson (1989). We feel that varying these estimated water table elevations would not be appropriate since it could result in heads above ground surface or unreasonably deep for the model area. This explanation is found at page 8-32, second paragraph.

DRAFT REPORT- SECTION 9: TRANSIENT MODEL

1. Section 9.2 Simulation Results: Please include MAE and ME along with RMS.
Completed. See table 9.2.1.
2. Figure 9.2.4: The calibration of the Carrizo layer is drifting with time. This is a concern because the Carrizo aquifer is the primary aquifer in the area. Page 9-7 points out the issue but does not indicate what may be causing the divergence or what you did to keep it from happening.
Heads are initialized to be representative of 1980 conditions. In the Wintergarden Area, drawdowns are very large and the model has difficulty sustaining the deepest drawdown in the area. Our approach to dealing with this considered a two-tiered approach. First, we lowered the vertical hydraulic conductivity of the overlying and underlying formations to limit cross-formational flow and pressure support. In the initial stages of calibration, the model was most sensitive to vertical hydraulic conductivity. Once we got the vertical resistance low enough to be close to the model target RMS, we then re-visited our initialization to see if we could find evidence to suggest that the Carrizo was initialized at heads too low. This step resulted in very little model improvement. At the current calibrated condition, the transient model is most sensitive to horizontal hydraulic conductivity and pumping. Further adjustment of one, or both of these parameters may improve model fit. However, because both of these parameters are uncertain at the model scale and the model currently meets calibration metrics, we felt it was best to identify the need for further study in determining which parameter (conductivity or pumping) is best used to improve calibration. We believe our approach is consistent with the RFP which requests that model not be over-calibrated. This explanation is provided in the text, in sections 9.1 and 9.2.1. It is also discussed in section 11, model limitations.
3. Please include in the appendix all of the transient plots comparing simulated to measured for the model. The reader should also be able to identify where these plots spatially relate to.
This comment was amended upon discussion with TWDB. All hydrographs are part of the data model.
4. Page 9-8, 3rd paragraph, 3rd line from bottom: Are the percentiles for statistics of spatial stream loss/gain or temporal stream loss/gain over the simulation period or both? Please clarify.
Completed. See page 9-9, first paragraph.
5. Section 9: The initial conditions for the transient simulation should be discussed. According to the RFP (Appendix 1, page 15/40 the steady-state model should be contained within the transient with a very long stress period). Please explain what the transient initial conditions were and if the steady-state heads were not used please explain why.

Additional discussion of initial conditions for the transient model were added (see sections 4.4, 7.1, and parts of 9. As discussed with the TWDB early in the development of the conceptual model, we implemented predevelopment conditions in the steady-state model. Since significant drawdown occurred between predevelopment (early 1900's) and 1980, estimates of pumping rates prior to 1980 would be necessary to use the steady-state heads as initial conditions. Because this pumping information is not available, we chose to initialize the model using TWDB head data for the time period between 1977 and 1983.

The stated purpose of including the steady-state model within the transient model was to ensure that any changes made to the model during transient calibration would propagate to the steady-state model (RFP Appendix 1, pages 15 and 16). As noted in the report, we accomplished this goal through an iterative approach to calibration.

6. Section 9.2.1: Please give RMS of hydrograph fits. (See RFP Appendix 1, page 15/40, Section 3.3)
Completed. See table 9.2.2.
7. Section 9.2.2: Please explain why fluxes were not a calibrated parameters and give some quantitative comparison between stream loss/gain and other studies. (See RFP Appendix 1, page 14/40, Section 3.3)
Slade et al. (2002) note that the potential error in stream flow measurements is typically about 5 to 8 percent. Since this error is possible at both ends of a gain/loss subreach, the potential error in gain/loss can equal a significant fraction of the total flow in the subreach. Comparing the available gain/loss values to mean stream flows from the EPA River Reach data set shows that almost all of the gain/loss values are less than 5 percent of the mean stream flow. This suggests that the gain/loss values are uncertain and can be only used qualitatively. Figure 9.2.15 shows the comparison between field measured and simulated gain/loss. Table 9.2.3 shows a comparison to the LBG-Guyton and HDR (1998) model.
8. Sections 9.2.3 and 10.3: Please discuss the number of cells that go dry during the simulation period. Also explain how the dry cells were handled. (See RFP Appendix 1, page 15/40, Section 3.3).
Completed. See page 9-8, last paragraph.
9. Section 9.2.3: Please include a water budget for the estimated end-time of the 1980s drought ~ mid 1980s.
Completed. See table 9.2.4.
10. Section 9.3: Please include impact of sensitivity analyses on several hydrographs. (See RFP Appendix 1, page 16/40, Section 3.3).
Completed. See figures 9.3.11 and 9.3.12.

DRAFT REPORT - SECTION 10: PREDICTIONS

1. Section 10.2: Please also include head surfaces for all layers for simulations in 2010, 2020, 2030, 2040 with no drought of record.
This comment was amended upon discussion with TWDB. Head surfaces for layers with >50 ft of drawdown are shown. See additional figures 10.2.15-10.2.18.

2. Section 10.2: Please include saturated thickness maps for 2010, 2020, 2030, 2040, 2050 for the DOR and no DOR scenarios. (See RFP Appendix 1, page 27/40, Section 5.4).

This comment was amended upon discussion with the TWDB. Saturated thickness maps for 2000 and 2050 are shown in figures 10.2.23 and 10.2.24.

3. Section 10.2: Please include some discussion of predictive modeling results on assumed boundary conditions. (See RFP Appendix 1, page 23/40, Section 5.4).
Completed. See page 10-9, second paragraph.

DRAFT REPORT - APPENDICES

Appendix C: Water Levels

1. Appendices C and D: Please briefly explain how pumpage that is exported to another region was determined and included in the modeled pumping. (e.g. through consultation with RWPGs).

Basically, this work was already done for us by the TWDB (Cindy Ridgeway) when they put together the predictive pumpage data sets (GAMPredictivePumpage_2002SWP.xls). This spreadsheet lists the water user group ID, county, basin, and RWPG of the water source as well as the water user. The pumping SOP utilized the water source for the spatial distribution of pumpage, not the water user, when distributing predicted pumpage.

The use of the "source county ID" and "source alpha" for matching to well locations from historical pumpage data was explicitly stated in the SOP. Also, paragraph 1 of the SOP stated that the purpose of the SOP was only to provide additional procedures to implement the TWDB guidance in Tech Memo 2-1, and would not re-state the info in Tech Memo 2-1. Tech Memo 2-1 instructed to roll water sold by one water user group to another to the seller's water use for spatial distribution, which is what we did. This explanation is limited to the comments and was not added to the text.

DRAFT REPORT EDITORIAL COMMENTS:

Page ix (Abstract): 7th line from bottom: Suggest changing "significant pumping declines predicted" to "significant decrease in pumping"

Completed.

DRAFT REPORT- SECTION 1: INTRODUCTION

1. Page 1-2 1st paragraph, 8th line from bottom: "steady-state and transient models" "s" missing.

Completed See page 1-2, first paragraph.

DRAFT REPORT - SECTION 2: STUDY AREA

1. Page 2-1 1st paragraph, 4th line down: "Carrizo-Wilcox", hyphen missing.

Completed. See page 2-1, first paragraph.

2. Page 2-1 2nd paragraph, 4th line down: Suggest changing "These models possess" to "These models have".

Completed. See page 2-1, second paragraph.

3. Page 2-13, second paragraph, line 12: change “ syndepositional gravity tectonics and halokinesis” to “growth faults and salt dome development”.
Completed. See page 2-18, first paragraph.
4. Figure 2.2: Photocopies poorly in black and white (re: Attachment 1 of RFP page 25/40).
Completed (acceptable from black and white laser printer). See figure 2.2.
5. Figure 2.3: Photocopies poorly in black and white (re: Attachment 1 of RFP page 25/40).
Completed (acceptable from black and white laser printer). See figure 2.3.
6. Figure 2.7: Photocopies poorly in black and white (re: Attachment 1 of RFP page 25/40).
Due to the size of the model area and the detail presented in this figure, it will not be possible to make this figure readable in black and white at the model scale required for an 8.5x11 figure. TWDB agreed to allow this figure to be legible only in color.
7. Figure 2.9: Photocopies poorly in black and white (re: Attachment 1 of RFP page 25/40).
Completed (acceptable from black and white laser printer). Resolution enhanced, see figure 2.10.
8. Page 2-13 2nd paragraph end: Suggest language be rewritten for a non-geologist audience. (e.g., halokinesis ?)
Completed. See page 2-18, first paragraph.
9. Figure 2.10: Photocopies poorly in black and white (re: Attachment 1 of RFP page 25/40).
Completed (acceptable from black and white laser printer). See figure 2.11.
10. Figure 2.12: Photocopies poorly in black and white (re: Attachment 1 of RFP page 25/40).
Due to the size of the model area and the detail presented in this figure, it will not be possible to make this figure readable in black and white at the model scale required for an 8.5x11 figure.

DRAFT REPORT - SECTION 3: PREVIOUS WORK

1. Page 3-1 1st paragraph: Suggest changing first sentence to “...by many investigators and numerous groundwater bulletins have been developed ...”
Completed. See page 3-1, first paragraph.
2. Figure 3.1: What does SW in SW GAM Model refer to? It is called the southern GAM model everywhere else.
Completed SW was changed to Southern. See figure 3-1.
3. Page 3-3 2nd paragraph, last sentence: “as documented in the TWDB State Water Plan of the time.” Please give specific year of plan referred to.
Completed. See page 3-2, second paragraph.

DRAFT REPORT - SECTION 4: HYDROLOGIC SETTING

1. Figure 4.2.2 caption: space missing between “the” and “Wilcox”.
Completed. See figure 4.2.2.
2. Figure 4.2.9 – 4.2.15: Contour labels in dark regions do not photocopy well.
Completed (acceptable from black and white laser printer).
3. Figure 4.3.3 – 4.3.9: Photocopies poorly in black and white (re: Attachment 1 of RFP page 25/40).
Completed (acceptable from black and white laser printer). Now figures 4.3.4-4.3.10.
4. Page 4-36, 1st paragraph, 2nd line: Suggest “more transmissive zones” rather than “higher transmissive zones”
Completed. See page 4-30, second paragraph.
5. Figures 4.3.7 and 4.3.8 captions 1st line: Carrizo misspelled.
Completed. Now figures 4.3.8 and 4.3.9.
6. Page 4-42 3rd paragraph: Freeze and Cherry reference date is 1979 not 1975.
Completed. See page 4-33, first paragraph.
7. Figures 4.4.2 and 4.4.3 and page 4-46 2nd paragraph: Legend says elevations from DEM, but the text says it’s from the TWDB database?
Completed. Text changed to indicate DEM data used. See page 4-48, second paragraph.
8. Figures 4.4.5 and 4.4.6: Pink and gray are not readable when photocopied (re: Attachment 1 of RFP page 25/40).
Completed (acceptable from black and white laser printer).
9. Figures 4.4.8: Photocopies poorly in black and white (re: Attachment 1 of RFP page 25/40).
Completed (acceptable from black and white laser printer).
10. Tables 4.4.3 and 4.4.4: Missing parenthesis on title (continued”).
Completed.
11. Page 4-89, 2nd paragraph, 5th sentence from bottom: Suggest, “...with stream loss occurring more in summer and stream gain occurring more in winter.”
Completed. See page 4-93, first paragraph.
12. Figure 4.6.1 and 4.6.2: Photocopy poorly in black and white (re: Attachment 1 of RFP page 25/40).
Completed (acceptable from black and white laser printer).
13. Tables 4.6.1: Missing parenthesis on title (continued”).
Completed.
14. Figures 4.7.1 - 4.7.6: Photocopies poorly in black and white (re: Attachment 1 of RFP page.
Completed (acceptable from black and white laser printer).

15. Page 4-14, 4th paragraph from the top: “Gonzales County underground water conservation District” should be “Gonzales County Underground Water Conservation District”.

Completed. See page 4-6, last paragraph.

DRAFT REPORT- SECTION 5: CONCEPTUAL MODEL

1. Page 5-2, last line: typo “...is offset by a decrease...” not “at decrease”.
Completed. See page 5-3, first paragraph.
2. Page 5-3, 4th paragraph: “...is generally downdip “ rather than “...is generally to the downdip”.
Completed. See page 5-3, last paragraph.
3. Page 5-4, 1st paragraph, 1st line: “...where the dip of the strata increase” not “increased.”
Completed. See page 5-4, first paragraph.
4. Page 5-4, 1st paragraph, 3rd line: “...(TDS) southeast of the strike-oriented faults...”
Completed. See page 5-4, first paragraph.
5. Page 5-4, 1st paragraph, last line: “...in the study area...”
Completed. See page 5-4, first paragraph.

DRAFT REPORT - SECTION 6: MODEL DESIGN

1. Page 6-2, last line: “.... The model grid at the county scale”.
Completed See page 6-3, first paragraph..
2. Page 6-14, last paragraph, 3rd line from bottom: “a really” should be “areally”.
Completed. See page 6-9, third paragraph.
3. Page 6-17, 1st paragraph: “...provided in Section 4.7” (not 5.7).
Completed See page 6-11, last paragraph..
4. Page 6-17, 1st paragraph, 2nd line: “For details of how the...”
Completed. See page 6-11, last paragraph.
5. Page 6-19, 1st paragraph, last sentence: “...we considered the decreasing...” and “data are not available”
Completed. See page 6-19, third paragraph.
6. Page 6-21, last sentence: “....In storativity ~~parameters~~ from 2×10^{-4}”.
Completed. See page 6-22, first paragraph.

DRAFT REPORT - SECTION 8: STEADY-STATE MODEL

1. Page 8-1, 1st paragraph, 2nd line: “....Streams is ~~being~~ balanced...”
Completed. See page 8-1, first paragraph.
2. Page 8-1, 2nd paragraph: “...steady-state model is described below.”
Completed. See page 8-1, second paragraph.

3. Page 8-5, 2nd paragraph, 4th line from bottom: River misspelled.
Completed.
4. Figures 8.1.1 – 8.1.10: Photocopies poorly in black and white (re: Attachment 1 of RFP page 25/40).
Completed (acceptable from black and white laser printer).
5. Page 8-18, 4th paragraph, 4th line down: predevelopment misspelled.
Completed.
6. Figure 8.2.3, mislabeled as 8.2.2: (page 8-23).
Completed.

DRAFT REPORT- SECTION 9: TRANSIENT MODEL

1. Page 9-2, 2nd paragraph: Reference to Figures 9.1.2 and 9.1.3 should be switched in text.
Completed.
2. Figure 9.1.3: Photocopies poorly in black and white (re: Attachment 1 of RFP page 25/40).
Completed (acceptable from black and white laser printer).
3. Figure 9.2.14: Photocopies poorly in black and white (re: Attachment 1 of RFP page 25/40).
Completed (acceptable from black and white laser printer).

DRAFT MODEL RUNS:

This review addresses three questions:

1. Were all model files included?
2. Does the model run?
3. Do the results of the model match what is in the draft report?

Question 1:

All model files were included for running the steady-state simulation, 1975 – 1999 transient simulation, and 2000 – 2050 predictive simulations. However, borehole files *.bor were not included for comparing simulated and observed water levels at well locations.

Question 2:

Both the steady-state, transient, and predictive models run and converge with no errors.

Question 3:

Three items were evaluated to compare the model output with the results presented in the draft report – i) head surface maps, ii) hydrographs (transient only) and iii) groundwater budget.

For the steady-state model, both the water budget and the head surface maps of all six model layers exactly match what is presented in the draft report.

For the 1975 – 1999 transient model two head surface maps were presented in the draft report. The Carrizo (model layer 3) in 1989 and 1999. The model output at 180 stress periods (assumed to be 1989) and 300 stress periods (assumed to be 1999) match the results in Figures 9.2.1 and 9.2.2. One stress period is equal to one month in the model simulation.

Five boreholes were added to PMWIN data set and hydrographs at the five wells were compared for the period 1980 – 1999. The simulated results match the simulated hydrographs presented in the report (Figures 9.2.7 – 9.2.13).

The groundwater budget also matched that presented in the report for 1999 (Table 9.2.3).

Head surfaces for the predictive 2050 simulations were compared against Figures 10.2.1 (layer 1), 10.2.3 (layer 3), 10.2.5 (layer 4), 10.2.7 (layer 5), and 10.2.9 (layer 6), the results match those Figures. Figures 10.2.11 and 10.2.13 (layer 3 at 2010 and 2030) were also compared to simulation results and they match. A borehole file containing the six wells in Figure 10.2.15 was created and the simulation results match Figure 10.2.15.

Finally the groundwater budget was compared for the 2050 and the results match those in Table 10.3.1.

In summary,

- All model files were included, except borehole or observations well files.
Borehole and observation files were added to the data model.
- All models, steady-state, transient, and predictive converge and run with no errors.

The model results including head surfaces, groundwater budgets and hydrographs match those in the report for the steady-state, transient, and predictive simulations.

DRAFT DATA SOURCE FILES COMMENTS:

GENERAL

All files need to be in Access97. We are unable to evaluate data because the format is incorrect.

Did we get all of the data files we requested? NO
Is the data organized in the way we requested? YES

Review Summary:

The data provided by the contractor is missing some required data sets as listed in sections below. File lists are needed within each folder/directory listing all file names or groups of file names and their contents.

File descriptions were added where necessary.

The contractor did follow the requirements as set forth in Attachments 1 & 2 of the RFP for the most part. However a few of the metadata files had incorrect spatial reference information or missing altogether.

Existing metadata was checked and some added to the data model.

Furthermore, the SWAT model and all data used within the SWAT model must be provided in a separate folder/directory tree structure if used to calculate parameters for the ET, streamflow-routing, and/or recharge packages of MODFLOW.

SWAT model input/output datasets were added to the data model under a separate directory.

DRIVE:\CZWX_s\grddata\input\hydraul

Unable to evaluate data because Access file format not compatible with Access97.
Must make Access database file compatible with Access97 as stated in Attachments 1 and 2 of RFP.

Access database file converted to Access97.

DRIVE:\CZWX_s\grddata\input\ibnd

Unable to evaluate data because Access file format not compatible with Access97.
Must make Access database file compatible with Access97 as stated in Attachments 1 and 2 of RFP.

Access database file converted to Access97.

DRIVE:\CZWX_s\grddata\input\stress\ststate\drns

Unable to evaluate data because Access file format not compatible with Access97.
Must make Access database file compatible with Access97 as stated in Attachments 1 and 2 of RFP.

n/a.

DRIVE:\CZWX_s\grddata\input\stress\ststate\levt

Unable to evaluate data because Access file format not compatible with Access97.
Must make Access database file compatible with Access97 as stated in Attachments 1 and 2 of RFP.

Access97 table added.

DRIVE:\CZWX_s\grddata\input\stress\ststate\rech

Unable to evaluate data because Access file format not compatible with Access97.
Must make Access database file compatible with Access97 as stated in Attachments 1 and 2 of RFP.

Access database file converted to Access97.

DRIVE:\CZWX_s\grddata\input\stress\ststate\res

Unable to evaluate data because Access file format not compatible with Access97.
Must make Access database file compatible with Access97 as stated in Attachments 1 and 2 of RFP.

n/a.

DRIVE:\CZWX_s\grddata\input\stress\ststate\strm

Unable to evaluate data because Access file format not compatible with Access97.
Must make Access database file compatible with Access97 as stated in Attachments 1 and 2 of RFP.

Access97 tables added.

DRIVE:\CZWX_s\grddata\input\storage

Unable to evaluate data because Access file format not compatible with Access97.
Must make Access database file compatible with Access97 as stated in Attachments 1 and 2 of RFP.

Access97 tables added.

DRIVE:\CZWX_s\grddata\input\stress\ststate\well

Unable to evaluate data because Access file format not compatible with Access97.
Must make Access database file compatible with Access97 as stated in Attachments 1 and 2 of RFP.

Access97 tables added.

DRIVE:\CZWX_s\grddata\input\stress\trans\drns

Unable to evaluate data because Access file format not compatible with Access97.
Must make Access database file compatible with Access97 as stated in Attachments 1 and 2 of RFP.

n/a.

DRIVE:\CZWX_s\grddata\input\stress\trans\levt

Unable to evaluate data because Access file format not compatible with Access97.
Must make Access database file compatible with Access97 as stated in Attachments 1 and 2 of RFP.

Access97 tables added.

DRIVE:\CZWX_s\grddata\input\stress\trans\rech

Unable to evaluate data because Access file format not compatible with Access97.
Must make Access database file compatible with Access97 as stated in Attachments 1 and 2 of RFP.

Access97 tables added.

DRIVE:\CZWX_s\grddata\input\stress\trans\res

Unable to evaluate data because Access file format not compatible with Access97. Must make Access database file compatible with Access97 as stated in Attachments 1 and 2 of RFP.

Access97 tables added.

DRIVE:\CZWX_s\grddata\input\stress\trans\strm

Unable to evaluate data because Access file format not compatible with Access97. Must make Access database file compatible with Access97 as stated in Attachments 1 and 2 of RFP.

Access97 tables added.

DRIVE:\CZWX_s\grddata\input\stress\trans\well

Unable to evaluate data because Access file format not compatible with Access97. Must make Access database file compatible with Access97 as stated in Attachments 1 and 2 of RFP.

Access97 tables added.

DRIVE:\CZWX_s\grddata\input\struct

Unable to evaluate data because Access file format not compatible with Access97. Must make Access database file compatible with Access97 as stated in Attachments 1 and 2 of RFP.

Access database file converted to Access97.

DRIVE:\CZWX_s\modflow\modfl_96\input\ststate

These files are acceptable.

DRIVE:\CZWX_s\modflow\modfl_96\input\trans

These files are acceptable.

DRIVE:\CZWX_s\modflow\pmwin_50\input\ststate

These files are acceptable except for missing calibration borehole file.

boreholes.bor and observations.obs files added

DRIVE:\CZWX_s\modflow\pmwin_50\input\trans

These files are acceptable except for missing calibration borehole file.

boreholes.bor and observations.obs files added

DRIVE:\CZWX_s\modflow\pmwin_50\refdx

These files are acceptable.

DRIVE:\CZWX_s\scrdata\bndy

Need a file listing name of each file or grouped set of files and their contents or purpose.

Descriptors added.

Aquifers and groundwater conservation districts coverages have incorrect spatial reference in metadata file and SW_Boundary coverage has no metadata file.

Metadata edited. SW_Boundary was added in error to the draft model. This coverage was subsequently removed.

DRIVE:\CZWX_s\scrdata\clim

Need a file listing name of each file or grouped set of files and their contents or purpose.

Descriptors added.

All coverages need a completed metadata file.

Metadata added.

The monthly precipitation Access database must be compatible with Access97.

Access database file converted to Access97.

DRIVE:\CZWX_s\scrdata\cnsv

Need a file listing name of each file or grouped set of files and their contents or purpose.

Descriptors added.

DRIVE:\CZWX_s\scrdata\geol

Need a file listing name of each file or grouped set of files and their contents or purpose.

Descriptors added.

The outcrop delineations coverages and net sand coverages need metadata file or readme document describing the metadata and purpose of the coverages.

Descriptors added.

Must make Access database files compatible with Access97 as stated in Attachments 1 and 2 of RFP.

Access database file converted to Access97.

No cross-sections used in study? If yes, cross-sections must be provided under this folder.

n/a.

DRIVE:\CZWX_s\scrdata\geom

Need a file listing name of each file or grouped set of files and their contents or purpose.

Descriptors added.

The DEM needs a completed metadata file and must be in units of feet rather than meters.

Coverage converted. Metadata file added.

A physiography coverage is required by RFP.

Coverage added.

DRIVE:\CZWX_s\scrdata\geop

NO DATA FOUND – geophysical data should go here if used in study.

n/a.

DRIVE:\CZWX_s\scrdata\soil

Need a file listing name of each file or grouped set of files and their contents or purpose.

Descriptors added.

No spatial reference information for soils coverage metadata file.

Metadata added.

The runoff raster data for Texas needs a metadata file.

Coverage added to draft data model in error. Coverage was subsequently removed.

DRIVE:\CZWX_s\scrdata\subhyd

Need a file listing name of each file or grouped set of files and their contents or purpose.

Descriptors added.

Except for Predictive Pumpage data set, unable to evaluate most data because Access file formats not compatible with Access97. Must make Access database file compatible with Access97 as stated in Attachments 1 and 2 of RFP.

Access database files converted to Access97.

Need metadata for all coverages and Access databases.

Metadata added.

Need source and intermediate derivative coverages used to spatially distribute pumpage data here.

Pumping databases added.

Need source and intermediate derivative coverages used to spatially distribute water level data here.

Water level databases added.

Need source and intermediate derivative coverages used to spatially distribute conductivity data here.

Previously in place.

Need source and intermediate derivative coverages used to spatially distribute specific yield and porosity if available.

n/a.

Need point coverage of calibration target boreholes and hydrographs.

Coverage added.

DRIVE:\CZWX_s\scrdata\surhyd

Need a file listing name of each file or grouped set of files and their contents or purpose.

Descriptors added.

Must make Access database files compatible with Access97 as stated in Attachments 1 and 2 of RFP.

Access database files converted to Access97.

DRIVE:\CZWX_s\scrdata\tran

Need a file listing name of each file or grouped set of files and their contents or purpose otherwise, these files are acceptable.

Descriptors added.